Lecture Notes in Physics

B. Apagyi G. Endrédi P. Lévay (Eds.)

Inverse and Algebraic Quantum Scattering Theory

Proceedings,
Lake Balaton,
Hungary 1996

Springer

Lecture Notes in Physics

Springer-Verlag Berlin Heidelberg GmbH

The Editorial Policy for Proceedings

The series Lecture Notes in Physics reports new developments in physical research and teaching – quickly, informally, and at a high level. The proceedings to be considered for publication in this series should be limited to only a few areas of research, and these should be closely related to each other. The contributions should be of a high standard and should avoid lengthy redraftings of papers already published or about to be published elsewhere. As a whole, the proceedings should aim for a balanced presentation of the theme of the conference including a description of the techniques used and enough motivation for a broad readership. It should not be assumed that the published proceedings must reflect the conference in its entirety. (A listing or abstracts of papers presented at the meeting but not included in the proceedings could be added as an appendix.)

When applying for publication in the series Lecture Notes in Physics the volume's editor(s) should submit sufficient material to enable the series editors and their referees to make a fairly accurate evaluation (e.g. a complete list of speakers and titles of papers to be presented and abstracts). If, based on this information, the proceedings are (tentatively) accepted, the volume's editor(s), whose name(s) will appear on the title pages, should select the papers suitable for publication and have them refereed (as for a journal) when appropriate. As a rule discussions will not be accepted. The series editors and Springer-Verlag will normally not interfere with the detailed editing except in fairly obvious cases or on technical matters.

Final acceptance is expressed by the series editor in charge, in consultation with Springer-Verlag only after receiving the complete manuscript. It might help to send a copy of the authors' manuscripts in advance to the editor in charge to discuss possible revisions with him. As a general rule, the series editor will confirm his tentative acceptance if the final manuscript corresponds to the original concept discussed, if the quality of the contribution meets the requirements of the series, and if the final size of the manuscript does not greatly exceed the number of pages originally agreed upon. The manuscript should be forwarded to Springer-Verlag shortly after the meeting. In cases of extreme delay (more than six months after the conference) the series editors will check once more the timeliness of the papers. Therefore, the volume's editor(s) should establish strict deadlines, or collect the articles during the conference and have them revised on the spot. If a delay is unavoidable, one should encourage the authors to update their contributions if appropriate. The editors of proceedings are strongly advised to inform contributors about these points at an early stage.

The final manuscript should contain a table of contents and an informative introduction accessible also to readers not particularly familiar with the topic of the conference. The contributions should be in English. The volume's editor(s) should check the contributions for the correct use of language. At Springer-Verlag only the prefaces will be checked by a copy-editor for language and style. Grave linguistic or technical shortcomings may lead to the rejection of contributions by the series editors. A conference report should not exceed a total of 500 pages. Keeping the size within this bound should be achieved by a stricter selection of articles and not by imposing an upper limit to the length of the individual papers. Editors receive jointly 30 complimentary copies of their book. They are entitled to purchase further copies of their book at a reduced rate. As a rule no reprints of individual contributions can be supplied. No royalty is paid on Lecture Notes in Physics volumes. Commitment to publish is made by letter of interest rather than by signing a formal contract. Springer-Verlag secures the copyright for each volume.

The Production Process

The books are hardbound, and the publisher will select quality paper appropriate to the needs of the author(s). Publication time is about ten weeks. More than twenty years of experience guarantee authors the best possible service. To reach the goal of rapid publication at a low price the technique of photographic reproduction from a camera-ready manuscript was chosen. This process shifts the main responsibility for the technical quality considerably from the publisher to the authors. We therefore urge all authors and editors of proceedings to observe very carefully the essentials for the preparation of camera-ready manuscripts, which we will supply on request. This applies especially to the quality of figures and halftones submitted for publication. In addition, it might be useful to look at some of the volumes already published. As a special service, we offer free of charge LaTeX and TeX macro packages to format the text according to Springer-Verlag's quality requirements. We strongly recommend that you make use of this offer, since the result will be a book of considerably improved technical quality. To avoid mistakes and time-consuming correspondence during the production period the conference editors should request special instructions from the publisher well before the beginning of the conference. Manuscripts not meeting the technical standard of the series will have to be returned for improvement.

For further information please contact Springer-Verlag, Physics Editorial Department II, Tiergartenstrasse 17, D-69121 Heidelberg, Germany

Barnabás Apagyi Gábor Endrédi Péter Lévay (Eds.)

Inverse and Algebraic Quantum Scattering Theory

Proceedings of a Conference
Held at Lake Balaton, Hungary,
3–7 September 1996

Springer

Editors

Barnabás Apagyi
Gábor Endrédi
Péter Lévay
Department of Theoretical Physics
Technical University of Budapest
Budafoki út 8
H-1111 Budapest, Hungary

Cataloging-in-Publication Data applied for.

Die Deutsche Bibliothek - CIP-Einheitsaufnahme

Inverse and algebraic quantum scattering theory : proceedings of a conference held at Lake Balaton, Hungary, 3 - 7 September 1996 / Barnabás Apagyi ... (ed.).
Barcelona ; Budapest ; Hong Kong ; London ; Milan ; Paris ; Santa Clara ; Singapore ; Tokyo : Springer, 1997
(Lecture notes in physics ; Vol. 488)
ISBN 978-3-662-14147-2

ISSN 0075-8450
ISBN 978-3-662-14147-2 ISBN 978-3-662-14145-8 (eBook)
DOI 10.1007/978-3-662-14145-8

Originally published by Springer-Verlag Berlin Heidelberg New York in 1997
Softcover reprint of the hardcover 1st edition 1997

Typesetting: Camera-ready by the authors/editors
Cover design: *design & production* GmbH, Heidelberg
SPIN: 10550730 55/3144-543210 - Printed on acid-free paper

Preface

Inverse quantum scattering theory has proved to be one of the most fruitful discoveries in physics. It provides model-independent microscopical interactions in quantum physics and supplies fundamental theoretical tools to solve problems in nonlinear physics. Founded in the 1950s, inverse quantum scattering theory has originated from the spectral theory of the Schrödinger equation or, more precisely, the Sturm-Liouville operator. It soon became the heart of the inverse scattering transform, enabling tremendous technical applications such as wave propagation, light transmission through optical fibres, and so on. However, its original goal to derive quantum potentials from observables has been reached only in recent decades by suitable modifications of the theory. Also, other quantum inversion schemes have been developed. One of the purposes of this volume is to give an account of this progress.

Algebraic quantum scattering theory is a relatively new topic. It is capable of deriving scattering phase shifts (S-matrix elements) via specifying a noncompact dynamical symmetry group characterizing the colliding system. Those phase shifts can then be inverted into potentials or, alternatively, a special realization of the group generators can be chosen to get analytically known (exact) potentials. This is achieved by using a functional relation between the Casimir operators and the Hamiltonian of the system exhibiting the underlying symmetry. On the other hand, supersymmetrical quantum mechanics generates also exactly solvable (analytical) models and its basic equations can formally be cast into a form which is in correspondence with those of the quantum inverse scattering theory. Thus these three subjects turn out to be intimately connected with each other. The other purpose of this volume is to manifest this connection explicitly.

Distinguished scientists, mathematicians, and physicists from all over the world, came together at Lake Balaton to discuss current developments and problems of inverse and algebraic quantum scattering theory including supersymmetrical quantum mechanics, and to present new contributions in these beautiful topics of quantum scattering theory. The financial help of the sponsors (bme, otka, nefim, omfb, fefa, ictp) greatly contributed to the pleasant and fruitful atmosphere of the conference. The participants have decided to meet regularly every three years and to dedicate this volume to the memory

of the late Professor Harry Fiedeldey whose research work covered almost all the topics of the conference.

Budapest, April 1997

B. Apagyi
G. Endrédi
P. Lévay

In Memory of Harry Fiedeldey [1932-1994]

These conference proceedings are dedicated to the memory of Professor Harry Fiedeldey, an outstanding contributor to the area covered by this conference, namely inverse and algebraic quantum scattering theory.

Harry Fiedeldey passed away unexpectedly on 16th, September 1994 from a heart attack. He was born in Indonesia on 17th, December 1932. His elementary school education was interrupted by World War II and he miraculously survived several years in a Japanese concentration camp, being held captive until the end of the war. His schooling "continued" in Holland where he managed to make up the lost years and then finish his first degree in physics at Groningen University in 1954. Thereafter he emigrated to South Africa where he obtained his MSc degree at Pretoria University and his DSc at the University of Stellenbosch under the supervision of Prof. W. E. Frahn.

His acuteness of mind, his strong motivation, his infectious enthusiasm, and, most of all, the quality and quantity of his contributions, have made Harry Fiedeldey a recognized authority in all the fields he has worked in. The creativeness of his mind and the depth and range of his knowledge was astonishing. His research work covered a wide range of topics in nuclear physics, few-body physics, and inverse and algebraic quantum scattering theory.

While topics in nuclear and few-body physics were always on Harry Fiedeldey's agenda, the inverse scattering problem was one of his life-long interests and an area in which he was considered a pioneer. In collaboration with others he developed new inversion methods which have been applied to quantum processes in few-body physics, nuclear physics, atomic physics, and condensed matter physics. The fixed-energy inversion methods he pioneered with Professor Reiner Lipperheide (analogous to those for the fixed angular momentum Bargmann potentials and based on rational or nonrational forms of the scattering function) are perhaps the most successful inverse scattering methods in nuclear physics. Further examples of his invaluable contributions in the field are his early work on inversion with separable potentials and later for more general nonlocal potentials, the role of regularization in inversion and his investigations of supersymmetry with respect to a generalization of Levin-

son's theorem and its consequences for a variety of physical systems such as the three-quark and α-α systems. Harry Fiedeldey also published several important papers in algebraic scattering theory and its application to heavy-ion scattering.

In the field of inverse scattering theory he did some of his most original and seminal work. Here are but few of the highlights of his contributions in the field:

- The introduction of the fixed-energy inversion method based on algebraic rational and nonrational scattering functions having exactly solvable potentials and the corresponding transformations for the solution of the inverse scattering problem. This allows the application of inversion methods to realistic situations, which has led to the determination of a large variety of scattering and optical potentials in atomic and nuclear physics. Such algebraic methods were later also applied to the investigation of surface profiles of solid and liquid matter via neutron and x-ray specular reflection.
- The simultaneous application of inversion methods to two- and three-body problems, for which a specific transformation was introduced. This allowed the determination of quark-quark forces from baryon spectra.
- The clarification of the "phase problem" in neutron specular reflection through a combination of a logarithmic dispersion relation between reflectivity and reflection phase with the Darboux inversion scheme.
- Proposals for an experimental method to measure the reflection phase directly. In one method the phase is determined by the dwell time of the neutron in the sample, which can be obtained via absorption measurements. In another method, the interaction of the neutron spin with an external magnetic field is used to determine the reflection phase via the interference of the reflections from the external magnetic field and from the scattering profile of the sample.

The untimely death of Harry Fiedeldey at the height of his scientific career is a great loss to the quantum inverse scattering community. The work of this exceptional man and his unbounded love for scientific endeavour was, and will continue to be, a constant source of inspiration to all who had the privilege of knowing him and learning from him.

List of Participants

R.G. Airapetyan airapetyan@main1.jinr.dubna.su
Joint Institute for Nuclear Research, LCTA, Dubna, Moscow Region, Russia, 141980

L.J. Allen lja@physics.unimelb.edu.au
School of Physics, University of Melbourne, Parkville, Victoria 3052, Australia

K. Amos amos@higgs.ph.unimelb.edu.au
School of Physics, University of Melbourne, Parkville, Victoria 3052, Australia

B. Apagyi apagyi@phy.bme.hu
Technical University of Budapest, Department of Theoretical Physics, 1521 Budapest, Budafoki u. 8.

I. Barna barna@phy.bme.hu
Technical University of Budapest, Department of Theoretical Physics, 1521 Budapest, Budafoki u. 8.

D. Baye dbaye@ulb.ac.be
Universite Libre de Bruxelles, Physique Nucleaire Theorique et Physique Mathematique, Code Postal 229, Universite Libre de Bruxelles, Campus Plaine, B 1050 Bruxelles, Belgium

A. Boutet de Monvel anne@mathp7.jussieu.fr
University Paris VII, Laboratory of Mathematical Physics and Geometry, Mathematics, Tour 45, Boite postale 7012, 2 Place Jussieu, 75252 Paris Cedex 05

S.G. Cooper s.g.cooper@open.ac.uk
The Open University, UK, Physics Department, The Open University, Walton Hall, Milton Keynes, MK7 6AA, UK

J. Cseh csehj@tigris.klte.hu
MTA ATOMKI, Pf. 51. 4010 Debrecen

M. Eberspächer Matthias.Eberspaecher@theo.physik.uni-giessen.de
Institut für Theoretische Physik der Justus-Liebig-Universität Gießen, Germany

G. Endrédi endredi@ns.c3.hu
Computer Center of Eötvös University, ELTE, Budapest, Hungary

H.V. von Geramb I04GER@DSYIBM.DESY.DE
Theoretische Kernphysik, Universität Hamburg, Luruper Chaussee 149, D-22761 Hamburg, Germany

P.O. Hess hess@roxanne.nuclecu.unam.mx
Instituto de Ciencias Nucleares, UNAM, Circuito Exterior, C.U.A.P. 70-543, 04510 Mexico D.F., Mexico

H. Huber huber@ap1.kph.tuwien.ac.at
Institut für Kernphysik, Technische Universität Wien, Wiedner Hauptstr. 8-10/142, A-1040 Wien, Austria

L. Jäde I04GER@DSYIBM.DESY.DE
Theoretische Kernphysik, Universität Hamburg, Luruper Chaussee 149, D-22761 Hamburg, Germany

S. Jena jena@utkal.ernet.in
Department of Physics, Utkal University, Bhubabeswar-751004, India

F. Korinek korinek@is1.kph.tuwien.ac.at
Institut für Kernphysik, Technische Universität Wien, Wiedner Hauptsrasse 8-10/142, A-1040 Vienna, Austria

H. Leeb leeb@is1.kph.tuwien.ac.at
Institut für Kernphysik, Technische Universität Wien, Wiedner Hauptstrasse 8-10/142, A-1040 Vienna, Austria

G. Lévai levaig@tigris.klte.hu
Institute of Nuclear Research of the Hungarian Academy of Sciences (ATOMKI), 4010 Debrecen

P. Lévay levay@phy.bme.hu
Technical University of Budapest, Department of Theoretical Physics, 1521 Budapest, Budafoki u. 8.

B.M. Levitan spivak@Physics.SPA.UMN.EDU
School of Mathematics, University of Minnesota, 206 Church street, Minneapolis, MN 55455-0436, USA

R. Lipperheide lipperheide@hmi.de
Hahn-Meitner-Institut, Glienicker Straße 100, D-14109 Berlin, PO-Box 39 01 28, D14091 Berlin

I. Lovas LOVAS@rmk530.rmki.kfki.hu
University of Lajos Kossuth KLTE Debrecen

V.A. Marchenko marchenko@ilt.kharkov.ua
Institute for Low Temperature, Mathematical Division, 47 Lenin Avenue, 310164 Kharkov, Ukraine

A. Melin melin@maths.lth.se
Department of Mathematics, Lund Institute of Technology, Lund

Z. Papp pz@indigo.atomki.hu
Institute of Nuclear Research of the Hungarian Academy of Sciences (ATOMKI), 4010 Debrecen

A.G. Ramm Ramm@math.ksu.edu
Math. Dept. Kansas St. Univ., Manhattan, KS 66506-2602, USA

M. Sander I04GER@DSYIBM.DESY.DE
Theoretische Kernphysik, Universität Hamburg, Luruper Chaussee 149, D-22761 Hamburg, Germany
W. Scheid Werner.Scheid@theo.physik.uni-giessen.de
Institut für Theoretische Physik der Justus-Liebig-Universität Gießen, Germany
S.A. Sofianos sofiasa@risc3.unisa.ac.za
Univ. of South Africa, Physics Department, Unisa, PO Box 392, Pretoria, 0001, South Africa
J.M. Sparenberg jmspar@ulb.ac.be
Universite Libre de Bruxelles, ULB, CP 229 Plaine, 1050 Bruxelles, Belgium
A. Suzko Suzko@Thsun1.JINR.DUBNA.SU
Bogoliubov Laboratory of Theoretical Physics, Joint Institute for Nuclear Research, 141980, Dubna, Moscow Region, Russia
R. de Swiniarski DESWINI@frcpn11.in2p3.fr
Grenoble, Institute of Nuclear Physics
J.Trlifaj trlifaj@karlin.mff.cuni.cz
Institute of Physics, Na Slovance 2, 180 40 Prague 8, Czech Republic
A. Ventura ventura@risc990.bologna.enea.it
Centro Dati Nucleari, ENEA, Bologna, Italy
B.N. Zakhariev Zakharev@tsun1.jinr.dubna.su
Laboratory of the Theoretical Physics, Joint Institute for Nuclear Research, Dubna, 141980, Russia
L. Zuffi zuffi@milano.infn.it
Dipartimento di Fisica dell' Universita and INFN, Milano, Italy

Contents

New Inverse Spectral Problem and Its Application

Anne Boutet de Monvel[1,2] and Vladimir Marchenko[2]

[1] Institut de Mathématiques de Jussieu, CNRS UMR 9994,
Laboratoire de Physique mathématique et Géométrie, case 7012,
Université Paris 7 Denis Diderot, 2 place Jussieu, F-75251 Paris Cedex 05
[2] B. Verkin Institute for Low temperature Physics,
47, Lenin Avenue, 310164, Kharkov, Ukraine

1

The origin of inverse spectral problems lies in natural science, but the problems themselves are purely mathematical. At the beginning these problems attracted attention of mathematicians by their nonstandard physical contents. But we think that today their place in mathematical physics is determined rather by the unexpected connection between inverse problems and nonlinear evolution equations which was discovered in 1967. This discovery was made in a famous paper by Gardner, Greene, Kruskal and Miura (1967). They found that the scattering data of a family $H(t)$ $(-\infty < t < \infty)$ (i.e. the reflection coefficients $r(k,t)$ and normalizing coefficients $m(\mathrm{i}k_l,t)$) of Schrödinger operators

$$H(t) = -\frac{\mathrm{d}^2}{\mathrm{d}x^2} + u(x,t)$$

satisfy linear differential equations

$$\dot{r}_t = 8\mathrm{i}k^3 r, \qquad \dot{m}_t = 8\mathrm{i}(\mathrm{i}k_l)^3 m$$

if the potentials $u(x,t)$ are rapidly decreasing solutions of the KdV equation

$$\dot{u}_t = 6uu_x - u_{xxx} \ . \tag{1}$$

This fact allows to solve the Cauchy problem

$$u(x,0) = q(x) \tag{2}$$

for the KdV equation using inverse scattering problem according to the following scheme:

$$\begin{aligned} q(x) &\to r(k,0), \ \ m(\mathrm{i}k_l,0) \\ &\to r(k,t) = r(k,0)\mathrm{e}^{8\mathrm{i}k^3 t}, \ \ m(\mathrm{i}k_l,t) = m(\mathrm{i}k_l,0)\mathrm{e}^{8\mathrm{i}k^3 t} \\ &\to u(x,t). \end{aligned}$$

The condition of rapid decrease of the initial function $q(x)$ is absolutely necessary for this method to apply, because all the notions of scattering theory (Jost solutions, reflection coefficients, normalizing coefficients, etc.) are defined only for operators with the potentials tending to zero when $|x| \to \infty$. We will generalize this method to initial functions $q(x)$ which do not vanish at infinity.

For this purpose we solve an inverse spectral problem different from the inverse scattering problem. This new inverse problem for the initial data $q(x)$ under consideration play the same role as does the inverse scattering problem for initial data vanishing at infinity.

2

Let us consider the one-dimensional Schrödinger operator

$$L = -\frac{\mathrm{d}^2}{\mathrm{d}x^2} + q(x) \qquad (-\infty < x < \infty)$$

with real continuous potential $q(x)$ and denote by $c(\lambda, x)$, $s(\lambda, x)$ the solutions of the equation

$$L[y] = \lambda^2 y \tag{3}$$

with initial data

$$c(\lambda, 0) = s'(\lambda, 0) = 1$$
$$c'(\lambda, 0) = s(\lambda, 0) = 0 \ .$$

According to Weyl's theorem for all nonreal z the equation

$$L[y] = zy$$

has solutions

$$\psi_\pm(z, x) = c(\sqrt{z}, x) + m_\pm(z) s(\sqrt{z}, x)$$

belonging to the Hilbert spaces $L_2(\mathbb{R}_\pm)$ ($\mathbb{R}_+ = (0, \infty)$, $\mathbb{R}_- = (-\infty, 0)$) respectively:

$$\psi_\pm(z, x) \in L_2(\mathbb{R}_\pm) \ .$$

The functions $m_\pm(z)$ are connected with the spectral functions $\rho_\pm(\mu, \infty)$ of the operators $L_\pm(\infty)$ generated in the spaces $L_2(\mathbb{R}_\pm)$ by the operator L and the boundary condition $y(0) = 0$. That is:

$$m_\pm(z) = \pm\left\{ a_\pm + \int_{-\infty}^{\infty} \left(\frac{1}{\mu - z} - \frac{\mu}{1 + \mu^2} \right) \mathrm{d}\rho_\pm(\mu, \infty) \right\} \tag{4}$$

where $a_\pm$ are some real numbers.

Instead of two functions $m_\pm(z)$ and two solutions $\psi_\pm(z, x)$ we introduce a single function

$$n(\lambda) = \begin{cases} m_+(\lambda^2) & \operatorname{Im}\lambda > 0 \\ m_-(\lambda^2) & \operatorname{Im}\lambda < 0 \end{cases} \tag{5}$$

and a solution of the equation (3)

$$\psi(\lambda, x) = c(\lambda, x) + n(\lambda)s(\lambda, x) = \begin{cases} \psi_+(\lambda^2, x) & \operatorname{Im}\lambda > 0 \\ \psi_-(\lambda^2, x) & \operatorname{Im}\lambda < 0 \end{cases}$$

which obviously belongs to the space $L_2(\mathbb{R}_+)$ when $\operatorname{Im}\lambda > 0$ and to the space $L_2(\mathbb{R}_-)$ when $\operatorname{Im}\lambda < 0$. The function $n(\lambda)$ and the solution $\psi(\lambda, x)$ will be called the Weyl function and the Weyl solution respectively.

The functions $m_\pm(z)$ are holomorphic outside of the real axis $\mathbb{R}$ and their sets of singularities respectively coincide with supports of the measures $\rho_\pm(\mu, \infty)$. From (4) it follows that the function $n(\lambda)$ is holomorphic outside of the real and the imaginary axes and its singularities which lie on the imaginary axis form a set

$$\Omega(\mathrm{i}) = \Omega_+ \cup \Omega_-$$

where

$$\Omega_\pm = \{\lambda \mid \pm\operatorname{Im}\lambda > 0,\ \lambda^2 \in \operatorname{supp}(d\rho_\pm(\mu, \infty))\} \ .$$

Since $c(\lambda, x)$ and $s(\lambda, x)$ are even entire functions of the variable λ for every fixed x the solution $\psi(\lambda, x)$ is holomorphic with respect to λ everywhere outside of the set $\Omega(\mathrm{i}) \cup \mathbb{R}$.

One of the key theorems is the following (Marchenko 1994)

Theorem 2.1 *For any $\varepsilon > 0$ the Weyl function $n(\lambda)$ and the Weyl solution $\psi(\lambda, x)$ are holomorphic in the domain*

$$\Lambda(\varepsilon) = \{\lambda \mid \operatorname{dist}(\lambda, \Omega(\mathrm{i}) \cup \mathbb{R}) \geq \varepsilon\}$$

and satisfy there the equalities

$$\begin{cases} \lim\limits_{|\lambda|\to\infty} (\mathrm{i}\lambda)^{-1} n(\lambda) = 1 \\ \lim\limits_{|\lambda|\to\infty} \mathrm{e}^{-\mathrm{i}\lambda x}\psi(\lambda, x) = 1 \ . \end{cases} \tag{6}$$

In general the equalities (6) may not be true when $\varepsilon = 0$. The necessary condition for this is the absolute continuity of the spectral functions $\rho_\pm(\mu, x)$ in the neighborhood of infinity. A simple sufficient condition is the following corollary of Theorem 1:

Corollary 1 *If*

(i) *the potential $q(x)$ is bounded from below:*

$$\inf_{-\infty<x<\infty} q(x) > -\infty \ ,$$

(ii) *the spectral functions $\rho_\pm(\mu, x)$ are twice differentiable in a neighborhood of $+\infty$ and for some $\delta > 0$*

$$\lim_{\mu\to+\infty} \mu^{\frac{1}{2}+\delta} \frac{\mathrm{d}^2}{\mathrm{d}\mu^2}\Big\{\rho_\pm(\mu,\infty) - \frac{2}{3\pi}\mu^{\frac{3}{2}}\Big\} = 0 \ ,$$

then the equalities (6) *hold for* $\varepsilon = 0$.

3

From (4) it follows that there exist nontangential limit values almost everywhere on the real axis

$$m_\pm(t+\mathrm{i}0) = \overline{m_\pm(t-\mathrm{i}0)} = \pm\{u_\pm(t) + \mathrm{i}v_\pm(t)\}$$

where

$$v_\pm(t) = \pi\frac{\mathrm{d}}{\mathrm{d}t}(\rho_\pm(t,\infty)) \geq 0 \ .$$

Therefore the function $n(\lambda)$ has nontangential limit values almost everywhere on the real and imaginary axes

$$\begin{aligned} n(t\pm\mathrm{i}0) &= \pm u_\pm(t^2) + \mathrm{i}\frac{t}{|t|}v_\pm(t^2), \qquad -\infty < t < \infty \\ n(\mathrm{i}t\pm 0) &= \begin{cases} u_+(-t^2) \pm \mathrm{i}v_+(-t^2) & 0 < t < \infty \\ -u_-(-t^2) \pm \mathrm{i}v_-(-t^2) & -\infty < t < 0 \ . \end{cases} \end{aligned} \tag{7}$$

In particular the solutions $\psi(t+\mathrm{i}0,x)$, $\psi(-t+\mathrm{i}0,x)$ are linearly independent if

$$\frac{\mathrm{d}}{\mathrm{d}\tau}\rho_+(\tau,\infty)\Big|_{\tau=t^2} > 0 \ , \qquad -\infty < t < \infty$$

and for such values of t we get

$$\psi(t-\mathrm{i}0,x) = A\psi(t+\mathrm{i}0,x) + B\psi(-t+\mathrm{i}0,x)$$

where the coefficients A, B can be computed using the following system of equations

$$\begin{cases} A + B = 1 \ , \\ A\,n(t+\mathrm{i}0) + B\,n(-t+\mathrm{i}0) = n(t-\mathrm{i}0) \ . \end{cases}$$

When we solve this system we find that

$$\begin{aligned} A &= \frac{n(t-\mathrm{i}0) - n(-t+\mathrm{i}0)}{n(t+\mathrm{i}0) - n(-t+\mathrm{i}0)} = -\frac{u_+(t^2) + u_-(t^2) - \mathrm{i}\frac{t}{|t|}[v_+(t^2) + v_-(t^2)]}{2\mathrm{i}\frac{t}{|t|}v_+(t^2)} \\ B &= \frac{n(t+\mathrm{i}0) - n(-t-\mathrm{i}0)}{n(t+\mathrm{i}0) - n(-t+\mathrm{i}0)} = \frac{u_+(t^2) + u_-(t^2) + \mathrm{i}\frac{t}{|t|}[v_+(t^2) - v_-(t^2)]}{2\mathrm{i}\frac{t}{|t|}v_+(t^2)} \ . \end{aligned}$$

Thus we arrive to

Lemma 3.1 *For all* $t \in (-\infty, \infty)$ *satisfying the condition*

$$\infty > \frac{\mathrm{d}}{\mathrm{d}\xi}\rho_{\pm}(\xi, \infty)\Big|_{\xi=t^2} > 0$$

the equality

$$A^{-1}(t)\psi(t - \mathrm{i}0, x) = \psi(t + \mathrm{i}0, x) + d(t)\psi(-t + \mathrm{i}0, x)$$

holds and $|d(t)| < 1$. *Here*

$$d(t) = \frac{B(t)}{A(t)} = -\frac{u_+(t^2) + u_-(t^2) + \mathrm{i}\frac{t}{|t|}[v_+(t^2) - v_-(t^2)]}{u_+(t^2) + u_-(t^2) - \mathrm{i}\frac{t}{|t|}[v_+(t^2) + v_-(t^2)]}$$

and

$$A^{-1}(t) = 1 + d(t) = \frac{2\mathrm{i}t}{n(t - \mathrm{i}0) - n(-t + \mathrm{i}0)} \times \frac{v_+(t^2)}{|t|} \ .$$

Setting

$$N(\lambda) = \frac{2\mathrm{i}\lambda}{n(\lambda) - n(-\lambda)} \tag{8}$$

we find that

$$A^{-1}(t) = 1 + d(t) = N(t - \mathrm{i}0)\frac{v_+(t^2)}{|t|} \ . \tag{9}$$

The main ingredient is a special factorization of the functions $N(\lambda)$ and $1 + d(t)$.

As it is known

$$\frac{1}{m_+(z) - m_-(z)} = -\int_{-\infty}^{\infty} \frac{\mathrm{d}\rho(\mu)}{\mu - z}$$

where the nondecreasing function $\rho(\mu)$ is the upper diagonal element of the spectral matrix-function of operator generated by L in the Hilbert space $L_2(-\infty, \infty)$.

This function has also another representation:

$$\frac{1}{m_+(z) - m_-(z)} = C\exp\left\{-\frac{1}{\pi}\int_{-\infty}^{\infty}\left(\frac{1}{t - z} - \frac{t}{1 + t^2}\right)\delta(t)\,\mathrm{d}t\right\}$$

where

$$\delta(t) = \arg\{m_+(t + \mathrm{i}0) - m_-(t + \mathrm{i}0)\}$$

and C is a positive number. According to (5) and (8) it follows from this that we have

$$N(\lambda) = -\frac{\operatorname{Im}\lambda}{|\operatorname{Im}\lambda|}\int_{-\infty}^{\infty}\frac{2i\lambda}{\mu-\lambda^2}\,d\rho(\mu) \tag{10}$$

$$N(\lambda) = C\exp\left\{\frac{1}{\pi}\int_{-\infty}^{\infty}\left(\frac{1}{t-\lambda^2}-\frac{t}{1+t^2}\right)\eta(t)\,dt\right\} \tag{11}$$

where

$$\eta(t) = \delta_0(t) - \delta(t)$$

and

$$\delta_0(t) = \arg(i\sqrt{t+i0}) = \begin{cases}\frac{\pi}{2} & 0 < t < \infty\\ \pi & -\infty < t < 0\end{cases}.$$

Let us divide the set $\Omega(i)$ into two disjoint subsets

$$\Omega_1 = \{\xi \mid \xi \in \Omega(i), -\xi \notin \Omega(i)\}$$
$$\Omega_2 = \{\xi \mid \xi \in \Omega(i), -\xi \in \Omega(i)\}\ .$$

Further we suppose that

A) The conditions of Corollary 1 hold.

B) $\operatorname{dist}(\Omega_1, \Omega_2) > 0$.

C) The set Ω_2 can be covered by a finite number of mutually disjoint intervals Δ_l on each of which

$$\sup_{t\in\Delta_l}\delta(t) - \inf_{t\in\Delta_l}\delta(t) < \pi\ .$$

Then without loss of generality we can assume that the functions $\rho_\pm(\mu,\infty)$ are twice differentiable on the whole positive semiaxis and

$$\infty > \frac{d}{d\xi}\rho_\pm(\xi,\infty) > 0 \qquad (0 < \xi < \infty)\ .$$

In this case $\eta(t) = 0$ in some neighborhood of $-\infty$ and the formula (11) can be transformed to the form

$$N(\lambda) = \exp\left\{\frac{1}{\pi}\int_{-\infty}^{\infty}\frac{\eta(t)}{t-\lambda^2}\,dt\right\}\ .$$

The set $(-\infty,0]\setminus\Omega_1^2$, where $\Omega_1^2 = \{\xi^2 \mid \xi\in\Omega_1\}$, consists of a finite or denumerable family of disjoint intervals $(-a_k^2, -b_k^2)$:

$$(-\infty,0]\setminus\Omega_1^2 = \bigcup_k(-a_k^2, -b_k^2)\ .$$

Lemma 3.2 *Each interval* $(-a_k^2, -b_k^2)$ *splits into two intervals* $(-a_k^2, -c_k^2)$, $(-c_k^2, -b_k^2)$ *so that*

$$\eta(t) = \begin{cases} 0 & t \in (-a_k^2, -c_k^2) \\ \pi & t \in (-c_k^2, -b_k^2) \end{cases}$$

($-c_k^2 \in [-a_k^2, -b_k^2]$ *and one of the intervals may be empty).*

Let us denote by $\chi_1(\xi)$, $\chi_2(\xi)$, $\chi_3(\xi)$ the characteristic functions of the sets Ω_1, Ω_2, $\bigcup_k(-c_k^2, -b_k^2)$ and by $\theta(\xi)$ the function

$$\theta(\xi) = \begin{cases} \frac{\xi}{\mathrm{i}|\xi|} & \operatorname{Re}\xi = 0 \\ \frac{\xi}{|\xi|} & \operatorname{Im}\xi = 0 \end{cases} .$$

Lemma 3.3 (factorization) *The function* $N(\lambda)$ *can be factorized as follows*

$$N(\lambda) = a(\lambda)a(-\lambda)$$

where

$$a(\lambda) = \prod_k \left(\frac{\mathrm{i}b_k - \lambda}{\mathrm{i}c_k - \lambda}\right) \exp \frac{1}{2\pi}\left\{ - \int_{-\mathrm{i}\infty}^{\mathrm{i}\infty} \frac{\varphi(\xi)\theta(\xi)}{\xi - \lambda}\,\mathrm{d}\xi + \int_{-\infty}^{\infty} \frac{\varphi(\xi)}{\xi - \lambda}\,\theta(\xi)\,\mathrm{d}\xi \right\}$$

$$\varphi(\xi) = \begin{cases} [2\chi_1(\xi) + \chi_2(\xi)]\eta(\xi^2) - \chi_2(\xi)\chi_3(\xi^2)\pi & \operatorname{Re}\xi = 0 \\ \eta(\xi^2) & \operatorname{Im}\xi = 0 \end{cases} .$$

From (9) and Lemma 3 it follows that for $t \in (-\infty, \infty)$ we have

$$A^{-1}(t) = 1 + d(t) = a(t - \mathrm{i}0)a(-t + \mathrm{i}0)\frac{v_+(t^2)}{|t|}$$

and because

$$\frac{a(t - \mathrm{i}0)}{a(t + \mathrm{i}0)} = \exp \frac{1}{2\pi} \int_{-\infty}^{\infty} \left(\frac{1}{\xi - t + \mathrm{i}0} - \frac{1}{\xi - t - \mathrm{i}0}\right) \varphi(\mathrm{i}\xi)\theta(\xi)\,\mathrm{d}\xi = \mathrm{e}^{-\mathrm{i}\eta(t^2)\theta(t)},$$

$$a(t + \mathrm{i}0)a(-t + \mathrm{i}0) > 0$$

then

$$1 + d(t) = \frac{a(t - \mathrm{i}0)}{a(t + \mathrm{i}0)}\, a(t + \mathrm{i}0)a(-t + \mathrm{i}0)\frac{v_+(t^2)}{|t|} = \mathrm{e}^{-\mathrm{i}\eta(t^2)\theta(t)}\,|1 + d(t)| .$$

Assuming

$$b(\lambda) = \exp \frac{\mathrm{i}}{2\pi} \int_{-\infty}^{\infty} \frac{\ln|1 + d(\xi)|}{\xi - \lambda}\,\mathrm{d}\xi$$

we find that

$$|1 + d(\xi)| = \frac{b(t - \mathrm{i}0)}{b(t + \mathrm{i}0)}$$

and

$$A^{-1}(t) = 1 + d(t) = \frac{a(t - \mathrm{i}0)b(t - \mathrm{i}0)}{a(t + \mathrm{i}0)b(t + \mathrm{i}0)} \ .$$

So we get the following result:

Theorem 3.1 *The function $A^{-1}(t) = 1 + d(t)$ has the following representation*

$$1 + d(t) = \frac{R(t - \mathrm{i}0)}{R(t + \mathrm{i}0)} \qquad (-\infty < t < \infty)$$

where

$$R(\lambda) = a(\lambda)b(\lambda) = \prod_k \left(\frac{\mathrm{i}b_k - \lambda}{\mathrm{i}c_k - \lambda}\right) \exp \frac{1}{2\pi}\left\{ \int_{-\infty}^{\infty} \frac{\eta(\xi^2)\theta(\xi) + \mathrm{i}\ln|1 + d(\xi)|}{\xi - \lambda}\,\mathrm{d}\xi \right.$$

$$\left. - \int_{-\mathrm{i}\infty}^{\mathrm{i}\infty} \frac{[2\chi_1(\xi) + \chi_2(\xi)]\eta(\xi^2) - \chi_2(\xi)\chi_3(\xi^2)\pi}{\xi - \lambda}\theta(\xi)\,\mathrm{d}\xi \right\} \ .$$

The singularities of the function $R(\lambda)$ lie in the set $\bigcup_k \{\mathrm{i}c_k\} \cup \Omega(\mathrm{i}) \cup \mathbb{R}$ and

$$|R(t + \mathrm{i}0)| = |R(-t + \mathrm{i}0)| \qquad (-\infty < t < \infty)$$
$$\lim_{|\lambda| \to \infty} R(\lambda) = 1 \ .$$

From Theorem 2 and Lemma 1 it follows that for all $t \in (-\infty, \infty)$

$$R(t - \mathrm{i}0)\psi(t - \mathrm{i}0, x) = R(t + \mathrm{i}0)\psi(t + \mathrm{i}0, x) + R(-t + \mathrm{i}0)\psi(-t + \mathrm{i}0)r(t) \quad (12)$$

where

$$r(t) = \frac{R(t + \mathrm{i}0)}{R(-t + \mathrm{i}0)}\,d(t)$$

and

$$|r(t)| = |d(t)| < 1 \ .$$

4

The function

$$g(\lambda) = g(\lambda, x) = \mathrm{e}^{-\mathrm{i}\lambda x} R(\lambda)\psi(\lambda, x)$$

is holomorphic outside of the real axis and of the set $\Omega(\mathrm{i}) \cup D$ (where $D = \bigcup_k \{\mathrm{i}c_k\}$) which lies on the imaginary axis.

Lemma 4.1 *The function $g(\lambda)$ satisfies the equality*

$$\lim_{|\lambda|\to\infty} g(\lambda) = 1 \tag{13}$$

in the whole complex plane and uniformly in every strip $|\operatorname{Re}\lambda| \le M$ it satisfies the equality

$$\lim_{|\operatorname{Im}\lambda|\to\infty} \mathrm{i}\lambda(g(\lambda)-1) = R(\infty) + \frac{1}{2}\int_0^x q(t)\,\mathrm{d}t \ , \tag{14}$$

where

$$R(\infty) = \lim_{|\operatorname{Im}\lambda|\to\infty} \mathrm{i}\lambda[R(\lambda)-1] \ .$$

As the function $g(\lambda)$ has continuous limit values $g(t \pm \mathrm{i}0)$ for all $t \in (-\infty,\infty)$ then from (13) and the integral Cauchy formula it follows that

$$g(\lambda) = 1 + \frac{1}{2\pi\mathrm{i}}\int_{-\infty}^{\infty} \frac{g(t+\mathrm{i}0)-g(t-i0)}{t-\lambda}\,\mathrm{d}t + \frac{1}{2\pi\mathrm{i}}\int_{\Gamma} \frac{g(\xi)}{\xi-\lambda}\,\mathrm{d}\xi$$

where the system of closed clockwise oriented contours Γ envelops the set $\Omega(\mathrm{i}) \cup D$. Because of $\Omega(\mathrm{i}) \cup D = \Omega_2 \cup (\Omega_1 \cup D)$ and $\operatorname{dist}(\Omega_2, \Omega_1 \cup D) > 0$ we can change the system Γ to two systems Γ_2 and Γ_1 of nonintersecting contours enveloping the sets Ω_2 and $\Omega_1 \cup D$ respectively. The conditions A), B), C) make it possible to shrink contours of the system Γ_2 to the set Ω_2 and as a result to obtain the equality

$$\frac{1}{2\pi\mathrm{i}}\int_{\Gamma_2} \frac{g(\xi)}{\xi-\lambda}\,\mathrm{d}\xi = \frac{1}{2\pi\mathrm{i}}\int_{-\mathrm{i}\infty}^{\mathrm{i}\infty} \frac{[g(\xi-0)-g(\xi+0)]\chi_2(\xi)}{\xi-\lambda}\,\mathrm{d}\xi \ .$$

From the equality

$$g(\xi) = \frac{\mathrm{e}^{-2\mathrm{i}\xi x}R(\xi)}{R(-\xi)}\,g(-\xi) + \mathrm{e}^{-\mathrm{i}\xi x}s(\xi,x)R(\xi)[n(\xi)-n(-\xi)]$$

and formula (11) it follows that

$$\frac{1}{2\pi\mathrm{i}}\int_{\Gamma_1} \frac{g(\xi)}{\xi-\lambda}\,\mathrm{d}\xi = \int_{-\mathrm{i}\infty}^{\mathrm{i}\infty} \frac{\mathrm{i}\theta(-t)\mathrm{e}^{-2\mathrm{i}tx}}{t-\lambda}\,g(-t)\chi_1(t)R(-t)^{-2}\,\mathrm{d}(\theta(-t)\rho(t^2)) \ .$$

From the equalities thus obtained and formula (12) it follows that

$$g(\lambda) = 1 - \frac{1}{2\pi \mathrm{i}} \int_{-\infty}^{\infty} \frac{g(-t+\mathrm{i}0)\mathrm{e}^{-2\mathrm{i}tx}}{t-\lambda} r(t)\,\mathrm{d}t$$
$$+ \int_{-\mathrm{i}\infty}^{\mathrm{i}\infty} \frac{\mathrm{i}\theta(-t)\mathrm{e}^{-2\mathrm{i}tx}}{t-\lambda} g(-t)\chi_1(t)R(-t)^{-2}\,\mathrm{d}(\theta(-t)\rho(t^2))$$
$$+ \frac{1}{2\pi \mathrm{i}} \int_{-\mathrm{i}\infty}^{\mathrm{i}\infty} \frac{g(t-0)-g(t+0)}{t-\lambda} \chi_2(t)\,\mathrm{d}t \qquad (15)$$

and

$$f(\xi) = 1 - \frac{1}{2\pi \mathrm{i}} \mathrm{vp} \int_{-\infty}^{\infty} \frac{g(-t+\mathrm{i}0)\mathrm{e}^{-2\mathrm{i}tx} r(t)}{t+\xi}\,\mathrm{d}\xi$$
$$- \int_{-\mathrm{i}\infty}^{\mathrm{i}\infty} \frac{\mathrm{i}g(-t)\mathrm{e}^{-2\mathrm{i}tx}\theta(t)}{t+\xi} \chi_2(t)\,\mathrm{d}t$$
$$+ \frac{1}{2\pi \mathrm{i}} \mathrm{vp} \int_{-\mathrm{i}\infty}^{\mathrm{i}\infty} \frac{g(t-0)-g(t+0)}{t+\xi} \chi_2(t)\,\mathrm{d}t \qquad (16)$$

where $f(\xi)$ denotes the half-sum of nontangent limit values of the function $g(-\lambda)$ when $\lambda \to \xi \in \Omega(\mathrm{i}) \cup (-\infty, \infty)$, and $\mathrm{vp}\int$ denotes the principal value of the integral.

As the function $g(-\lambda)$ is holomorphic on the set $\Omega_1 \cup D$ then

$$f(\xi) = \mathrm{e}^{\mathrm{i}\xi x} y_1(\xi)\ , \qquad y_1(\xi) = g(-\xi)\mathrm{e}^{-\mathrm{i}\xi x} \qquad (\xi \in \Omega_1 \cup D)$$

and from (12) and the equality $|r(\xi)|^2 = r(-\xi)r(\xi)$ it follows that

$$f(\xi) = \mathrm{e}^{\mathrm{i}\xi x} p_0(\xi)^{-1} \left[y_0(\xi) + \frac{1}{2}|r(|\xi|)|\, y_0(-\xi) \right] \quad (-\infty < \xi < \infty)$$

where

$$p_0(\xi) = \sqrt{r(\xi)}\ , \qquad y_0(\xi) = g(-\xi + \mathrm{i}0)\sqrt{r(\xi)}\mathrm{e}^{-\mathrm{i}\xi x}\ .$$

The following Lemma 5 is a direct consequence of (7) and Theorem 2:

Lemma 4.2 *The limit values of the function $g(\lambda)$ on the set Ω_2 are connected by the equality*

$$f(\xi) = \mathrm{e}^{\mathrm{i}\xi x} p_2(\xi)^{-1} \left[y_2(\xi) + \theta(\xi) m(\xi)^2 \right) y_2(-\xi)] \,,$$

where

$$y_2(\xi) = \frac{[g(\xi-0)-g(\xi+0)]}{2}\,\frac{\mathrm{i}\theta(\xi)\mathrm{e}^{\mathrm{i}\xi x}}{p_2(\xi)}$$

$$p_2(\xi) = \sqrt{\frac{|R(\xi)|}{|R(-\xi)|}\,\mathrm{e}^{\theta(\xi)\alpha(\xi^2)}\cosh\alpha(\xi^2)\tan\beta(\xi^2)}$$

$$m(\xi^2) = \sinh\alpha(\xi^2)\cos\chi_3(\xi^2)\pi$$

$$\alpha(\xi^2) = \frac{1}{2}\ln\frac{v_+(\xi^2)}{v_-(\xi^2)}$$

$$\beta(\xi^2) = \frac{1}{2}|\eta(\xi^2)-\chi_3(\xi^2)\pi| \ .$$

Let us introduce the functions

$$y(\xi) = y(\xi,x) = y_0(\xi)\chi_0(\xi) + y_1(\xi)\chi_1(\xi) + y_2(\xi)\chi_2(\xi)$$
$$p(\xi) = p_0(\xi)\chi_0(\xi) + \chi_1(\xi) + p_2(\xi)\chi_2(\xi)$$

and the measure

$$\mathrm{d}\mu(\xi) = \chi_0(\xi)\frac{\mathrm{d}\xi}{2\pi} + \chi_1(\xi)R(-\xi)^{-2}\,\mathrm{d}\left(\theta(-\xi)\rho(\xi^2)\right) + \chi_2(\xi)\frac{\mathrm{d}\xi}{\pi\mathrm{i}}$$

where $\chi_0(\xi)$ denotes the characteristic function of the set $(-\infty,\infty)$. Then we can write (15)–(16) in the form

$$g(\lambda) = 1 - \int \frac{y(\xi)p(\xi)\,\mathrm{e}^{-\mathrm{i}\xi x}}{\mathrm{i}(\xi-\lambda)}\left\{\chi_0(\xi) - \theta(\xi)(\chi_1(\xi)+\chi_2(\xi))\right\}\mathrm{d}\mu(\xi) \ ;$$

$$y(\xi) + \left\{\theta(\xi)m(\xi^2)\chi_2(\xi) + \frac{1}{2}|p(|\xi|)|\,\chi_0(\xi)\right\} y(-\xi) +$$

$$+\,\mathrm{vp}\int \frac{p(\xi)\mathrm{e}^{-\mathrm{i}(\xi+\eta)x}p(\eta)}{\mathrm{i}(\xi+\eta)}y(\eta)\left\{\chi_0(\eta) - \theta(\eta)(\chi_1(\eta)+\chi_2(\eta))\right\}\mathrm{d}\mu(\eta) =$$

$$= p(\xi)\,\mathrm{e}^{-\mathrm{i}\xi x} \ . \quad (17)$$

From the first equality and Lemma 4 it follows that

$$R(\infty) + \frac{1}{2}\int_0^x q(\xi)\,\mathrm{d}\xi = \int y(\xi,x)p(\xi)\,\mathrm{e}^{-\mathrm{i}\xi x}\left\{\chi_0(\xi) - \theta(\xi)(\chi_1(\xi)+\chi_2(\xi))\right\}\mathrm{d}\mu(\xi)$$

and

$$q(x) = 2\frac{\mathrm{d}}{\mathrm{d}x}\int y(\xi,x)p(\xi)\,\mathrm{e}^{-\mathrm{i}\xi x}\left\{\chi_0(\xi) - \theta(\xi)(\chi_1(\xi)+\chi_2(\xi))\right\}\mathrm{d}\mu(\xi) \ . \quad (18)$$

For every fixed $x \in (-\infty,\infty)$ the function $y(\xi) = y(\xi,x)$ belongs to the space $L_2(\mathrm{d}\mu(\xi))$ and satisfies equation (17), whose unique solvability can be proved in the same way as in (Marchenko 1987).

The functions $p(\xi)$, $m(\xi^2)$ and the measure $\mathrm{d}\mu(\xi)$ are called the spectral data of operator L. The above arguments thus give the following theorem:

Theorem 4.1 *The spectral data* $p(\xi)$, $m(\xi^2)$, $\mathrm{d}\mu(\xi)$ *define uniquely the operator* L. *The potential* $q(x)$ *can be reconstructed by the formula* (18) *where* $y(\xi) \in L_2(\mathrm{d}\mu(\xi))$ *is the solution of the equation* (17) *that is uniquely solvable in the space* $L_2(\mathrm{d}\mu(\xi))$.

5

The inverse problem we consider (reconstruction of the potential $q(x)$ by the spectral data $p(\xi)$, $m(\xi^2)$, $\mathrm{d}\mu(\xi)$) allows to solve the Cauchy problem (1)–(2) if operator L with the potential $q(x) = u(x,0)$ satisfies the conditions A), B), C). Replacing the function $p(\xi)$ in (17) by $p(\xi,t) = p(\xi)\,\mathrm{e}^{4\mathrm{i}\xi^3 t}$ we get a family of equations depending on the parameters x, t. It follows from the results of (Marchenko 1987) that for any real x, t the respective equation has a unique solution $y(\xi;x,t) = y(\xi) \in L_2(\mathrm{d}\mu(\xi))$ and the function

$$u(x,t) = 2\frac{\mathrm{d}}{\mathrm{d}x}\int y(\xi;x,t)p(\xi)\,\mathrm{e}^{-\mathrm{i}\xi(x-4\xi^2 t)}\{\chi_0(\xi) - \theta(\xi)(\chi_1(\xi)+\chi_2(\xi))\}\,\mathrm{d}\mu(\xi)$$

will satisfy KdV equation.

As $u(x,0) = q(x)$ according to Theorem 3 then the function $u(x,t)$ is the solution of Cauchy problem (1)–(2). So the scheme of solving the Cauchy problem remains the same

$$\begin{aligned} q(x) &\to m_+(z),\ m_-(z) \\ &\to p(\xi),\ m(\xi^2),\ \mathrm{d}\mu(\xi) \\ &\to p(\xi)\,\mathrm{e}^{4\mathrm{i}\xi^3 t},\ m(\xi^2),\ \mathrm{d}\mu(\xi) \\ &\to u(x,t)\ . \end{aligned}$$

References

Gardner C.S., Greene J..M., Kruskal M.D., Miura R.M. (1967): Method for solving the Korteweg–de Vries equation, Phys. Rev. Lett. **19**, 1095–1097

Marchenko V.A. (1987): *Nonlinear Equations and Operators Algebras* (D. Reidel, Dordrecht)

Marchenko V.A. (1994): Characterization of the Weyl Solutions, Letters in Math. Physics **31**, 179–193

Inverse Problem on the Entire Line and Some Connected Questions of Spectral Theory

B. M. Levitan

University of Minnesota

Abstract. In this paper we consider several separate questions for one-dimensional-Schrödinger operators on the entire line. The paper consists of an Introduction, seven short Sections and three Appendices. Each of these Sections and Appendices is almost independent.

0 Introduction

This paper contains several results on the spectral theory of Schrödinger (Sturm-Liouville) operators on the entire line:

$$-y'' + q(x)y = \lambda y, \qquad -\infty < x < +\infty. \tag{0.1}$$

In this paper, $q(x)$ is supposed continuous on $(-\infty, +\infty)$ and real.

In Section 1, we present some fundamental results in the theory of equation (0.1).

In Section 2, we consider a necessary and sufficient condition for the eveness of the potential $q(x)$. This condition can be expressed in a simple form:

$$d\rho_{12}(\lambda) = 0 \tag{0.2}$$

(for definition of $\rho_{12}(\lambda)$ see Section 1). The proof of the necessity of condition (0.2) is well known and is trivial. Unfortunately, we don't know an elementary proof of the sufficiency. Our proof of sufficiency of the condition (0.2) is based on the integral equation of the inverse problem for a one-dimensional Schrödinger operator on the entire line from the spectral matrix-function.

In Section 3, we consider the Cauchy problem

$$\frac{\partial^2 u}{\partial t^2} = \frac{\partial^2 u}{\partial x^2} - q(x)u \tag{0.3}$$

$$u|_{t=0} = f(x), \qquad \frac{\partial u}{\partial t}|_{t=0} = 0. \tag{0.4}$$

As it is known from the authors previous investigations, explicit formulas for the solutions of the problem (0.3)-(0.4) are very useful in different spectral problems for the equation (0.1).

In Section 4, we prove the asymptotic expansion of the function $w(x,t,x)$ for fixed x as $t \to 0$. The function $w(x,t,s)$ is crucial for solution of equation (0.3) and is defined in Section 3. The final result about asymptotic expansion of $w(x,t,x)$ isn't new, but the method seems to be new.

Section 5 is auxiliary for Sections 6 and 7. We give there a short introduction to the theory of finite gap potentials. Our method is based on the inverse problem on the entire line from the spectral matrix.The manifold of the finite gap potentials obtained by our method coincides with the manifolds obtained in the papers of S. Novikov [7], P. Lax [8], and J. Moser [9],by using other methods.

In Section 6, we introduce important functions which present a true generalization of the classical Floquet solutions. In the case of periodic finite gap potentials, the formula (6.1) is given in B. Dubrovin's paper [12].

In Section 7 is proved a general trace formula (7.4) for real finite gap potentials. A formula close to (7.4) was obtained earlier in the case of a periodic potential by McKean - Moerbeke ([13], corollary 1 and 2, page 257).

In Appendix I we discuss how trace formulas (7.5) and (7.6) can be used in studying the infinite gap potentials.

In Appendix II we compare the functions (6.1) with the classical Floquet solutions of the Hill equation.

Finally, in Appendix III we obtain the asymptotic formulas for the entries of the spectral matrix. Our proof is based on the formula (3.6) and special Tauberian theorems (see [10], [14]).

1 Necessary information about the spectral theory of the Schrödinger (Sturm-Liouville) operator on the entire line

All problems we study in this paper are connected with the spectral theory of the operator

$$l(y) = -y'' + q(x)y, \qquad -\infty < x < +\infty$$

in the space $\mathcal{L}^2(-\infty, \infty)$.

We suppose that $q(x)$ (the potential) is real and continuous in $(-\infty, \infty)$.

Denote (in this section and hereafter) by $\theta(x,\lambda)$ and $\varphi(x,\lambda)$ the solutions of equation

$$-y'' + q(x)y = \lambda y \qquad -\infty < x < +\infty \tag{1.1}$$

satisfying the initial conditions:

$$\theta(0,\lambda) = \varphi'(0,\lambda) = 1, \qquad \theta'(0,\lambda) = \varphi(0,\lambda) = 0.$$

According to a classical theorem of H. Weyl (see e. g. [1], [2]),there exist functions $m_1(\lambda)$ and $m_2(\lambda)$ regular in the upper half-plane such that for $\operatorname{Im}\lambda > 0$

$$\psi_1(x,\lambda) = \theta(x,\lambda) + m_1(\lambda)\varphi(x,\lambda) \in \mathcal{L}^2(-\infty, 0)$$
$$\psi_2(x,\lambda) = \theta(x,\lambda) + m_2(\lambda)\varphi(x,\lambda) \in \mathcal{L}^2(0, +\infty).$$

It is easy to see that

$$W(\psi_1, \psi_2) = \psi_1\psi_2' - \psi_2\psi_1' = m_2(\lambda) - m_1(\lambda).$$

The functions $m_1(\lambda)$ and $m_2(\lambda)$ are known as Weyl-Titchmarsh functions (coefficients). Troughout this paper we will suppose that the Weyl-Titchmarsh functions are unique (disregarding constant factors). This assumption is not necessary in our investigations, but leads to some simplifications. If $m_1(\lambda)$ and $m_2(\lambda)$ are unique, then the resolvent $R(x, Y; \lambda)$ of the operator $l = -D^2 + q(x)$ is also unique and has the form

$$R(x,y;\lambda) = \begin{cases} \frac{\psi_2(x,\lambda)\psi_1(y,\lambda)}{m_1(\lambda)-m_2(\lambda)}, \text{ if } y \le x \\ \\ \frac{\psi_1(x,\lambda)\psi_2(y,\lambda)}{m_1(\lambda)-m_2(\lambda)}, \text{ if } y > x \ . \end{cases}$$

The following theorem was proved by H. Weyl ([1], [2]):

To every equation (1.1) corresponds a symmetric nondecreasing matrix-function

$$\begin{pmatrix} \rho_{11}(\lambda) & \rho_{12}(\lambda) \\ \rho_{12}(\lambda) & \rho_{22}(\lambda) \end{pmatrix}, \quad (-\infty < \lambda < \infty)$$

such that for every smooth function $f(x)$ with compact support

$$f(x) = \int_{-\infty}^{\infty} \{F(\lambda)\theta(x,\lambda)d\rho_{11}(\lambda) + [F(\lambda)\varphi(x,\lambda) + G(\lambda)\theta(x,\lambda)]d\rho_{12}(\lambda) + G(\lambda)\varphi(x,\lambda)d\rho_{22}(\lambda)\}, \tag{1.2}$$

where

$$F(\lambda) = \int_{-\infty}^{\infty} f(x)\theta(x,\lambda)dx, \qquad G(\lambda) = \int_{-\infty}^{\infty} f(x)\varphi(x,\lambda)dx.$$

Remark 1.

As the matrix $\rho(\lambda)$ is symmetric and nondecreasing, the inequality

$$(\rho_{12}(\Delta))^2 \le \rho_{11}(\Delta)\rho_{22}(\Delta)$$

is valid. Here $\Delta = (\alpha, \beta), \rho_{jk}(\Delta) = \rho_{jk}(\beta) - \rho_{jk}(\alpha)$; α, β are points of continuity of the martix $\rho(\lambda)$.

Remark 2.

In many applications the following formulas are useful:

$$\rho_{jk}(\beta) - \rho_{jk}(\alpha) = \lim_{u \to 0} \frac{1}{\pi} \int_{\alpha}^{\beta} M_{jk}(x + iu)\, dx. \tag{1.3}$$

where

$$M_{11}(z) = (m_1(z) - m_2(z))^{-1},$$
$$M_{12}(z) = 1/2(m_1(z) + m_2(z))(m_1(z) - m_2(z))^{-1}$$
$$M_{22}(z) = \frac{m_1(z)m_2(z)}{m_1(z) - m_2(z)}.$$

Formulas (1.3) are colled Titchmarsh-Kodaira's formulas.

2 The evenness condition of the potential

Theorem. *The necessary and sufficient condition for evenness of the potential $q(x)$ is:*

$$d\rho_{12}(\lambda) = 0. \tag{2.1}$$

Proof. a) *Necessity.* Denote by $\mathcal{L}^2_+(-\infty,\infty)$ and $\mathcal{L}^2_-(-\infty,\infty)$ the subspaces of the Hilbert space $\mathcal{L}^2(-\infty,\infty)$ of even and odd functions. If $q(x)$ is even, then the subspaces $\mathcal{L}^2_+$ and $\mathcal{L}^1_-$ are invariant with respect to the operator $l = -D^2 + q(x)$. This proves the necessity.

b) *Sufficiency.* Our proof is based on the integral equation of the inverse problem on the entire line from the spectral matrix-function (see [3], [4]). This equation has the form:

$$\operatorname{sign} x\ K(x,y) + F(x,y) + \int_{-x}^{x} K(x,t)F(t,y)dt = 0, \quad 0 < |y| \le |x| < \infty \tag{2.2}$$

where

$$F(x,y) = F_1(x,y) + F_2(x,y) + F_3(x,y)$$

$$F_1(x,y) = \int_{-\infty}^{\infty} \cos\sqrt{\lambda}x \cos\sqrt{\lambda}y d\sigma_{11}(\lambda),$$

$$F_2(x,y) = \int_{-\infty}^{\infty} \frac{\sin\sqrt{\lambda}(x+y)}{\sqrt{\lambda}} d\rho_{12}(\lambda),$$

$$F_3(x,y) = \int_{-\infty}^{\infty} \frac{\sin\sqrt{\lambda}x \sin\sqrt{\lambda}y}{\lambda} d\sigma_{22}(\lambda).$$

Here

$$\sigma_{11}(\lambda) = \begin{cases} \rho_{11}(\lambda) - \frac{1}{\pi}\sqrt{\lambda}, & \lambda \ge 0, \\ \rho_{11}(\lambda), & \lambda < 0 \end{cases}$$

$$\sigma_{22}(\lambda) = \begin{cases} \rho_{22}(\lambda) - \frac{1}{3\pi}\lambda^{3/2}, & \lambda \ge 0, \\ \rho_{22}(\lambda), & \lambda < 0. \end{cases}$$

Independently of $\operatorname{sign} x$, the potential $q(x)$ is given by the formula

$$q(x) = 2\frac{d}{dx}K(x,x). \tag{2.3}$$

If $d\rho_{12}(\lambda) = 0$, then $F_2(x,y) = 0$ and

$$F(x,y) = \int_{-\infty}^{\infty} \cos\sqrt{\lambda}x \cos\sqrt{\lambda}y\ d\sigma_{11}(\lambda) + \int_{-\infty}^{\infty} \frac{\sin\sqrt{\lambda}x \sin\sqrt{\lambda}y}{\lambda}\ d\sigma_{22}(\lambda).$$

From the last equation follows:

$$F(-x,-y) = F(x,y).$$

Replacing x by $-x$, y by $-y$, and t by $-t$ in equation (2.2),we obtain

$$\operatorname{sign} x\,[-K(-x,-y)] + F(x,y) + \int_{-x}^{x} [-K(-x,-t)]F(t,y)\,dt = 0 \qquad (2.4)$$

If the integral equation (2.2) has an unique solution, we can obtain from (2.2) and (2.4):

$$-K(-x,-y) = K(x,y).$$

In particular, for $y = x$

$$K(-x,-x) = -K(x,x) \qquad (2.5)$$

From (2.3) and (2.5) follows: $q(-x) = q(x)$

Remark. If the growth points of spectral matrix $\rho(\lambda)$ have at least one finite limit-point, then the integral equation (2.1) has an unique solution.

3 The auxiliary wave equation

The integral representation of the solution of the Cauchy problem

$$\frac{\partial^2 u}{\partial t^2} = \frac{\partial^2 u}{\partial x^2} - q(x)u, \quad u|_{t=0} = f(x), \quad \frac{\partial u}{\partial t}|_{t=0} = 0 \qquad (3.1)$$

is useful in exploring many spectral properties of the equation(1.1) (see e. g. [5]).

The solution of the problem(3.1) can be obtained by two ways:

i) Using the spectral expansion (1.2), the solution can be expressed in the form

$$u(x,t) = \int_{-\infty}^{\infty} \cos\sqrt{\lambda}t\{F(\lambda)\theta(x,\lambda)\,d\rho_{11}(\lambda) +$$

$$+[F(\lambda)\varphi(x,\lambda) + G(\lambda)\theta(x,\lambda)]\,d\rho_{12}(\lambda) + G(\lambda)\varphi(x,\lambda)\,d\rho_{22}(\lambda)\} \qquad (3.2)$$

ii) Using Duhamel theorem and successive iteration, the solution can be expressed in the form

$$u(x,t) = \frac{1}{2}[f(x+t) + f(x-t)] + \frac{1}{2}\int_{x-t}^{x+t} w(x,t,s)f(s)\,ds. \qquad (3.3)$$

As the problem (3.1) has an unique solution, from (3.2) and (3.3) we obtain an important identity:

$$\int_{-\infty}^{\infty} \cos\sqrt{\lambda}t\{F(\lambda)\theta(x,\lambda)d\rho_{11}(\lambda) + [F(\lambda)\varphi(x,\lambda) + G(\lambda)\theta(x,\lambda)]d\rho_{12}(\lambda) +$$

$$+G(\lambda)\varphi(x,\lambda)d\rho_{22}\} = \frac{1}{2}[f(x+t)+f(x-t)] + \frac{1}{2}\int_{x-t}^{x+t} w(x,t,s)f(s)\,ds \qquad (3.4)$$

Choose now a function $g_\epsilon(t)$ with the properties

1) $g_\epsilon(t)$ is even,
2) $g_\epsilon(t)$ is smooth and has a compact support $\operatorname{supp} g_\epsilon(t) \subseteq (-\epsilon, \epsilon)$. Let

$$\tilde{g}_\epsilon(\mu) = \int_0^\epsilon g_\epsilon(t) \cos \mu t dt$$

be the cosine-Fourier transform of $g_\epsilon(t)$. As $g_\epsilon(t)$ is smooth, $\tilde{g}_\epsilon(\mu)$ decreases rapidly as $\mu \to \pm\infty$.Multiplying the identity (3.4) by $g_\epsilon(t)$ and integrating, after some simple calculations (see e. g. [5]) we obtain

$$\int_{-\infty}^{\infty} f(s)ds \int_{-\infty}^{\infty} \tilde{g}_\epsilon(\sqrt{\lambda})\{\theta(x,\lambda)\theta(s,\lambda)d\rho_{11}(\lambda)+$$

$$+[\varphi(x,\lambda)\theta(s,\lambda) + \theta(x,\lambda)\varphi(s,\lambda)]d\rho_{12}(\lambda) + \varphi(x,\lambda)\varphi(s,\lambda)d\rho_{22}(\lambda)\} =$$

$$= \frac{1}{2}\int_{x-\epsilon}^{x+\epsilon} g_\epsilon(s-x)f(s)ds + \frac{1}{2}\int_{x-\epsilon}^{x+\epsilon} f(s)ds \int_{|x-s|}^{\epsilon} w(x,t,s)g_\epsilon(t)dt.$$

As $f(s)$ is arbitrary, from the last equation follows

$$\int_{-\infty}^{\infty} \tilde{g}_\epsilon(\sqrt{\lambda})\{\theta(x,\lambda)\theta(s,\lambda)d\rho_{11}(\lambda)+$$

$$+[\theta(x,\lambda)\varphi(s,\lambda) + \theta(s,\lambda)\varphi(x,\lambda)]d\rho_{12}(\lambda) + \varphi(x,\lambda)\varphi(s,\lambda)d\rho_{22}(\lambda)\} =$$

$$= \begin{cases} \frac{1}{2}g_\epsilon(x-s) + \frac{1}{2}\int_{|x-s|}^{\epsilon} w(x,t,s)g_\epsilon(t)dt, & |x-s| \le \epsilon \\ 0 & |x-s| \ge \epsilon. \end{cases} \tag{3.5}$$

The case $s = x$ is of particular interest. In this case it follows from (3.5) that

$$\int_{-\infty}^{\infty} \tilde{g}_\epsilon(\sqrt{\lambda})[\theta^2(x,\lambda)d\rho_{11}(\lambda) + 2\theta(x,\lambda)\varphi(x,\lambda)d\rho_{12}(\lambda) + \varphi^2(x,\lambda)d\rho_{22}(\lambda)] =$$

$$= \frac{1}{2}g_\epsilon(0) + \frac{1}{2}\int_0^\epsilon w(x,t,x)g_\epsilon(t)dt. \tag{3.6}$$

4 The asymptotic expansion of $w(x,t,x)$

It is well known that a product of two solutions of the equation $-y'' + q(x)y = \lambda y$ is a solution of the equation

$$z''' - 4qz' - 2q'z = -4\lambda z' \tag{4.1}$$

Suppose that $g_\epsilon(0) = g_\epsilon''(0) = 0$. Applying to equation (3.6) the operator

$$\mathcal{L} = D^3 - 4qD - 2(Dq), \quad D = \frac{d}{dx}$$

and using equation (4.1), we obtain:

$$4\frac{\partial}{\partial x}\int_{-\infty}^{\infty} -\lambda\tilde{g}_\epsilon(\sqrt{\lambda})[\theta^2(x,\lambda)d\rho_{11}(\lambda) + 2\theta(x,\lambda)\varphi(x,\lambda)d\rho_{12}(\lambda)+$$

$$+\varphi^2(x,\lambda)d\rho_{22}(\lambda)] = \frac{1}{2}\int_0^\epsilon \mathcal{L}_x[w(x,t,x)]g_\epsilon(t)dt \tag{4.2}$$

As $-\lambda\tilde{g}_\epsilon(\sqrt{\lambda})$ is the cosine-Fourier transform of $g''_\epsilon(t)$, from (3.6) follows

$$\int_{-\infty}^{\infty} -\lambda\tilde{g}_\epsilon(\sqrt{\lambda})[\theta^2(x,\lambda)d\rho_{11}(\lambda)+2\theta(x,\lambda)\varphi(x,\lambda)d\rho_{12}(\lambda)+\varphi^2(x,\lambda)d\rho_{22}(\lambda)] =$$

$$= \frac{1}{2}\int_0^\epsilon w(x,t,x)g''_\epsilon(t)dt = \frac{1}{2}\int_0^\epsilon \frac{\partial^2}{\partial t^2}w(x,t,x)g_\epsilon(t)dt. \tag{4.3}$$

From (4.2) and (4.3) we get

$$\int_0^\epsilon \frac{\partial}{\partial x}\frac{\partial^2}{\partial t^2}w(x,t,x)g_\epsilon(t)dt = \frac{1}{4}\int_0^\epsilon \mathcal{L}_x[w(x,t,x)]g_\epsilon(t)dt. \tag{4.4}$$

As $g_\epsilon(t)$ is arbitrary, from (4.4) follows (for $0 \le t \le \epsilon$)

$$\frac{\partial}{\partial x}\frac{\partial^2}{\partial t^2}w(x,t,x) = \frac{1}{4}\mathcal{L}_x[w(x,t,x)] \tag{4.5}$$

Let [1]

$$w(x,t.x) = \sum_{k=0}^{\infty} t^{2k+1}A_k(x) \tag{4.6}$$

Substituting (4.6) in (4.5) and comparing the coefficients in terms with t^{2k+1}, we obtain the recurrence formula

$$\frac{\partial}{\partial x}A_{k+1}(x) = \frac{1}{4(2k+3)(2k+2)}\mathcal{L}_x[A_k(x)], \quad ; \; k = 0,1,2,\ldots$$

In particular, for $k = 0$

$$\frac{\partial}{\partial x}A_1(x) = \frac{1}{24}\mathcal{L}_x[A_0(x)] \tag{4.7}$$

It remains to calculate $A_0(x)$. From equation (3.4) with $f(s) = 1$ follows (using Taylor's formula)

$$u(x,t) = 1 + \frac{1}{2}\int_{x-t}^{x+t} w(x,t,s)ds$$

$$= 1 + tw(x,t,x) + \frac{1}{2}\frac{\partial w}{\partial s}|_{s=x}\int_{x-t}^{x+t}(s-x)ds + O(t^3) = 1 + tw(x,t,x) + O(t^3).$$

Differentiating this equation twice with respect to t, we obtain

[1] Existence of the asymptotic expansion (4.6) can be based on analyzing the successive approximation of $w(x,t,s)$.

$$\frac{\partial^2 u}{\partial t^2} = 2\dot{w} + t\ddot{w} + O(t). \tag{4.8}$$

From (4.8) and (3.1) for $t = 0$ we get

$$-q(x) = 2\frac{\partial}{\partial t} w|_{t=0}.$$

Using expansions (4.6) and (4.7), we obtain now

$$A_0(x) = -\frac{1}{2}q(x)$$

and from (4.7)

$$A_1(x) = \frac{1}{48}(-q''(x) + 3q^2(x)).$$

5 Necessary information about finite gap potentials

Let $-\infty < \lambda_0 < \lambda_1 < \mu_1 < \lambda_2, \mu_2 < \ldots < \lambda_n < \mu_n < +\infty$ be $2n+1$ arbitrary real numbers. In every interval $[\lambda_k, \mu_k]$, $k = 1, 2, \ldots, n$ choose an arbitrary point ξ_k and prescribe in it an arbitrary sign $\epsilon_k = \pm$. Define four polynomials:

$$\begin{aligned} R(\lambda) &= (\lambda - \lambda_0)(\lambda - \lambda_1)(\lambda - \mu_1)\ldots(\lambda - \lambda_n)(\lambda - \mu_n), \\ P(\lambda) &= (\lambda - \xi_1)(\lambda - \xi_2)\ldots(\lambda - \xi_n), \\ Q(\lambda) &= P(\lambda)\sum_{j=1}^{n} \epsilon_j \frac{[-R(\xi_j)]^{1/2}}{(\lambda - \xi_j)P'(\xi_j)} \\ S(\lambda) &= \frac{R(\lambda) + Q^2(\lambda)}{P(\lambda)}. \end{aligned} \tag{5.1}$$

It can be proved that $S(\lambda)$ is a polynomial of degree $n+1$ with leading coefficient equal to 1. The last equation in (5.1) can be written as

$$S(\lambda)P(\lambda) - Q^2(\lambda) = R(\lambda) \tag{5.2}$$

The intervals $[\lambda_k, \mu_k]$ are called gaps,because they are gaps in the spectrum of a Sturm-Liouville operator, which will be defined in the next theorem.

Intervals adjacent to gaps are called *permitted* intervals. Their union

$$\sigma = [\lambda_0, \lambda_1] \cup [\mu_1, \lambda_2] \cup \ldots \cup [\mu_{n-1}, \lambda_n] \cup [\mu_n, +\infty]$$

is the spectrum of the operator which we shall define below.

Using polynomials (5.1),define three functions:

$$\frac{d\rho_{11}(\lambda)}{d\lambda} = \begin{cases} \frac{1}{2\pi}\frac{P(\lambda)}{\pm\sqrt{R(\lambda)}}, & \lambda \in \sigma \\ 0, & \lambda \overline{\in} \sigma \end{cases}$$

$$\frac{d\rho_{12}(\lambda)}{d\lambda} = \begin{cases} \frac{1}{2\pi}\frac{Q(\lambda)}{\pm\sqrt{R(\lambda)}}, & \lambda \in \sigma \\ 0, & \lambda \overline{\in} \sigma \end{cases} \tag{5.3}$$

$$\frac{d\rho_{22}(\lambda)}{d\lambda} = \begin{cases} \frac{1}{2\pi}\frac{S(\lambda)}{\pm\sqrt{R(\lambda)}}, & \lambda \in \sigma \\ 0, & \lambda \overline{\in} \sigma. \end{cases}$$

These functions are entries of the spectral matrix of a Sturm-Liouville equation with a finite gap potential. The sign of the square root of $R(\lambda)$ is defined in the following way: on the first interval (λ_0, λ_1) of the spectrum $\frac{d\rho_{11}(\lambda)}{d\lambda}$ must be positive. On the following intervals of the spectrum the signs of $[R(\lambda)]^{1/2}$ are defined by analytic continuation.

Theorem.
Let

$$\rho(\lambda) = \begin{pmatrix} \rho_{11}(\lambda)\ \rho_{12}(\lambda) \\ \rho_{12}(\lambda)\ \rho_{22}(\lambda) \end{pmatrix}$$

where the functions $\rho_{jk}(\lambda)$ are defined by equations (5.3). There exists a unique equation of the form

$$-y'' + q(x)y = \lambda y \tag{5.4}$$

whose spectral matrix coincides with $\rho(\lambda)$.(For the proof of this theorem see [3], [6].)

The potential $q(x)$ in equation (5.4) is called a *finite gap potential.* This class of potentials coincides with the manifolds of finite gap potentials defined by S. Novikov [7], P. Lax [8], and J. Moser [9] independently and by different methods.

Let t be an arbitrary real number. Consider the equation

$$-y'' + q(x+t)y = \lambda y.$$

It can be proved that for every t the potential $q(x+t)$ is also a finite gap potential with the same gaps as in the case of potential $q(x)$, but the spectral parameters ξ_k and ϵ_k are moving with t :

$$\xi_k = \xi_k(t), \quad \epsilon_k = \epsilon_k(t).$$

It is convenient to exchange the places of x and t. Put

$$P(x,\lambda) = (\lambda - \xi_1(x))(\lambda - \xi_2(x)) \cdots (\lambda - \xi_n(x)),$$

$$Q(x,\lambda) = P(x,\lambda) \sum_{j=1}^{n} \frac{\epsilon_j(x)\{-R[\xi_j(x)]\}^{1/2}}{(\lambda - \xi_j(x))P'(\lambda)|_{\lambda=\xi_j(x)}},$$

$$S(x,\lambda) = \frac{R(\lambda) + Q^2(x,\lambda)}{P(x,\lambda)}.$$

It can be proved (see [3], [6]) that:

$$\begin{aligned} P(x,\lambda) &= P(\lambda)\theta^2(x,\lambda) + 2Q(\lambda)\theta(x,\lambda)\varphi(x,\lambda) + S(\lambda)\varphi^2(x,\lambda), \\ Q(x,\lambda) &= P(\lambda)\theta(x,\lambda)\theta'(x,\lambda) + Q(\lambda)[\theta'(x,\lambda)\varphi(x,\lambda) + \theta(x,\lambda)\varphi'(x,\lambda)] + \\ &\quad + S(\lambda)\varphi(x,\lambda)\varphi'(x,\lambda), \\ S(x,\lambda) &= P(\lambda)\theta'^2(x,\lambda) + 2Q(\lambda)\theta'(x,\lambda)\varphi'(x,\lambda) + S(\lambda)\varphi'^2(x,\lambda). \end{aligned} \tag{5.5}$$

The functions $\theta(x,\lambda)$ and $\varphi(x,\lambda)$ were defined in section 1.

Differentiating equations (5.5) in x and using equation (5.4), we obtain:

$$\begin{aligned} \frac{d}{dx}P(x,\lambda) &= 2Q(x,\lambda), \\ \frac{d}{dx}Q(x,\lambda) &= S(x,\lambda) + [q(x) - \lambda]P(x,\lambda), \\ \frac{d}{dx}S(x,\lambda) &= 2[q(x) - \lambda]Q(x,\lambda). \end{aligned} \tag{5.6}$$

The equations (5.6) play a crucial role in the next sections.

6 The generalized Floquet solutions

The functions

$$\psi_{\pm}(x,\lambda) = \left[\frac{P(x,\lambda)}{P(\lambda)}\right]^{1/2} \exp\left\{\pm i\sqrt{R(\lambda)}\int_0^x \frac{du}{P(u,\lambda)}\right\} \tag{6.1}$$

are generalizations of classical Floquet solutions of Hill's equation.

Theorem.

The functions $\psi_{\pm}(x,\lambda)$ are solutions of equation (5.4).

Proof. From (6.1) and the first equation in (5.6) we can obtain

$$\frac{d}{dx}\psi_{\pm}(x,\lambda) = \left[\frac{Q(x,\lambda)}{P(x,\lambda)} \pm i\frac{\sqrt{R(\lambda)}}{P(x,\lambda)}\right]\psi_{\pm}(x,\lambda). \tag{6.2}$$

As $\psi_{\pm}(0,\lambda) = 1$, from (6.2) it follows that

$$\psi'_{\pm}(0,\lambda) = \frac{Q(\lambda)}{P(\lambda)} \pm i\frac{\sqrt{R(\lambda)}}{P(\lambda)}.$$

Differentiating (6.2) and using (5.6), we obtain

$$\psi''_{\pm}(x,\lambda) = \frac{Q'P - QP' \mp i\sqrt{R}P'}{P^2}\psi_{\pm} + \left(\frac{Q}{P} \pm i\frac{\sqrt{R}}{P}\right)^2 \psi_{\pm}(x,\lambda) =$$

$$= \frac{(q(x)-\lambda)P^2 + SP - 2Q^2 \mp 2iQ\sqrt{R}}{P^2}\psi_{\pm} + \left[\frac{Q^2}{P^2} \pm 2i\frac{Q\sqrt{R}}{P^2} - \frac{R}{P^2}\right]\psi_{\pm} =$$

$$= \left\{[q(x)-\lambda] + \frac{SP - Q^2 - R}{P^2}\right\}\psi_{\pm} = [q(x)-\lambda]\psi_{\pm},$$

as $SP - Q^2 - R = 0$.

Thus

$$\psi''_{\pm} = [q(x)-\lambda]\psi_{\pm}$$

which coincides with equation (5.4).

7 Proof of the trace formula

We start from the equation (6.2) of the preceding section:

$$\psi'_{+}(x,\lambda) = \left[\frac{Q(x,\lambda)}{P(x,\lambda)} + i\frac{\sqrt{R(\lambda)}}{P(x,\lambda)}\right]\psi_{+}(x,\lambda)$$

Denote

$$\frac{\psi'_{+}(x,\lambda)}{\psi_{+}(x,\lambda)} = z(x,\lambda) = \frac{Q(x,\lambda)}{P(x,\lambda)} + i\frac{\sqrt{R(\lambda)}}{P(x,\lambda)}. \tag{7.1}$$

We obtain, by differentiating:

$$z' = \frac{\psi''_{+}\psi_{+} - \psi'^2_{+}}{\psi^2_{+}} = q(x) - \lambda - z^2,$$

or

$$z' + z^2 + \lambda - q(x) = 0. \tag{7.2}$$

Put $k = \sqrt{\lambda}$ and let

$$z(x,\lambda) = ik + \sum_{j=1}^{\infty}\frac{\sigma_j(x)}{(2ik)^j}. \tag{7.3}$$

Substituting (7.3) into (7.2), we get

$$\sum_{j=1}^{\infty}\frac{\sigma'_j(x)}{(2ik)^j} + \left[ik + \sum_{j=1}^{\infty}\frac{\sigma_j(x)}{(2ik)^j}\right]^2 + k^2 - q(x) = 0.$$

Equating to zero the coefficients of $(2ik)^{-n}$, $n = 0, 1, 2\ldots$, we obtain

$$\sigma_1(x) = q(x), \quad \sigma_2(x) = -\sigma_1'(x) = -q'(x), \quad \sigma_3(x) = q'' - q^2, \ldots.$$

The general formula is:

$$\sigma_n' + \sigma_{n+1} + \sigma_1\sigma_{n-1} + \cdots + \sigma_{n-1}\sigma_1 = 0, \quad n = 2, 3, \ldots.$$

From (7.3) and (7.1) it follows that

$$ik + \sum_{j=1}^{\infty} \frac{\sigma_j(x)}{(2ik)^j} = \frac{Q(x,\lambda)}{P(x,\lambda)} + i\frac{\sqrt{R(\lambda)}}{P(x,\lambda)}. \tag{7.4}$$

Separating the odd power of $k = \sqrt{\lambda}$ we get

$$ik + \sum_{j=0}^{\infty} \frac{\sigma_{2j+1}(x)}{(2ik)^{2j+1}} = ik - ik\sum_{j=0}^{\infty}(-1)^j \frac{\sigma_{2j+1}(x)}{2^{2j+1}\lambda^{j+1}} =$$

$$= i\frac{\sqrt{R(\lambda)}}{P(x,\lambda)} = ik\left(1 - \frac{\lambda_0}{\lambda}\right)^{1/2}\left[\frac{(1-\frac{\lambda_1}{\lambda})(1-\frac{\mu_1}{\lambda})\cdots(1-\frac{\lambda_n}{\lambda})(1-\frac{\mu_n}{\lambda})}{(1-\frac{\xi_1(x)}{\lambda})^2\cdots(1-\frac{\xi_n(x)}{\lambda})^2}\right]^{1/2}.$$

Dividing the last equation by ik and taking ln, we get

$$\frac{1}{2}\ln\left(1-\frac{\lambda_0}{\lambda}\right) + \frac{1}{2}\sum_{j=1}^{n}\left[\ln\left(1-\frac{\lambda_j}{\lambda}\right) + \ln\left(1-\frac{\mu_j}{\lambda}\right) - 2\ln\left(1-\frac{\xi_j(x)}{\lambda}\right)\right] =$$

$$= \ln\left[1 - \sum_{j=0}^{\infty}(-1)^j \frac{\sigma_{2j+1}(x)}{2^{2j+1}\lambda^{j+1}}\right].$$

Expanding ln in series we obtain:

$$\sum_{r=1}^{\infty}\frac{1}{r}(\frac{\lambda_0}{\lambda})^r + \sum_{j=1}^{n}\sum_{r=1}^{\infty}\frac{1}{r}\left[\left(\frac{\lambda_j}{\lambda}\right)^r + \left(\frac{\mu_j}{\lambda}\right)^r - 2\left(\frac{\xi_j(x)}{\lambda}\right)^r\right] =$$

$$= 2\sum_{n=1}^{\infty}\frac{1}{n}\left[\sum_{j=0}^{\infty}(-1)^j\frac{\sigma_{2j+1}(x)}{2^{2j+1}\lambda^{j+1}}\right]^n. \tag{7.4}$$

Comparing coefficients by the same power of λ^{-1}, we can obtain trace formulas of arbitrary order.

The first two trace formulas are:

$$\lambda_0 + \sum_{j=1}^{n}[\lambda_j + \mu_j - 2\xi_j(x)] = q(x) \tag{7.5}$$

$$\lambda_0^2 + \sum_{j=1}^{n}[\lambda_j^2 + \mu_j^2 - 2\xi_j^2(x)] = -\frac{1}{2}q''(x) + q^2(x). \tag{7.6}$$

8 Appendix I. Applications to infinite gap potentials

Formulas (7.5) and (7.6) permit us to obtain some information about infinite gap potentials. Let $\lambda_0 > -\infty$ be fixed and suppose that an infinite sequence of pairs of real numbers (λ_k, μ_k), $\mu_k > \lambda_k$, $k = 1, 2, \ldots$ is given on the right of λ_0 . Suppose also that the following conditions are fulfilled:

1) The pairs (λ_k, μ_k) are arranged in decreasing order, that is $(\mu_1 - \lambda_1) \geq (\mu_2 - \lambda_2) \geq \cdots$, and not overlapping.

2) There exist constant positive numbers a_1 and a_2 such that

$$|\lambda_0| + 2\sum_{n=1}^{\infty}(\mu_n - \lambda_n) = a_1, \quad \lambda_0^2 + 2\sum_{n=1}^{\infty}(\mu_n^2 - \lambda_n^2) = a_2.. \qquad (A.I.1)$$

Choosing an arbitrary number N we consider the intervals

$$(\lambda_1, \mu_1), (\lambda_2, \mu_2), \ldots (\lambda_N, \mu_N)$$

as gaps. In every gap let us choose an arbitrary point $\xi_k \in (\lambda_k, \mu_k)$ and let $\epsilon_k = \pm$ be chosen also arbitrarily. According to the results of Section 5, there exists a unique potential $q_N(x)$ with prescribed λ_0, prescribed gaps (λ_k, μ_k), $1 \leq k \leq N$ and prescribed ξ_k and ϵ_k.

The estimates

$$|q_N(x)| \leq a_1, \qquad |q_N''(x)| \leq 2(a_1^2 + a_2)$$

follow from the trace formulas(7.5), (7.6) and estimates (A.I.1).The first inequality means that the family $\{q_N(x)\}_{N=1}^{\infty}$ is uniformly bounded on the entire line.The second inequality means that the family $\{q_n''(x)\}_{N=1}^{\infty}$ is also bounded on the entire line. From a classical theorem follows that the family $\{f_N'(x)\}_1^N$ is also bounded. Therefore the family $\{f_N(x)\}$ is compact (in the sense of uniform convergence on every finite interval). Denote by $q(x)$ some limit point of the family $\{q_N(x)\}$ and consider the equation

$$-y'' + q(x)y = \lambda y, \quad -\infty < x < +\infty. \qquad (A.I.2)$$

The following question arises naturally:

Does the spectrum σ of equation (A.I.2) coincide with the limit of spectra σ_N of equations

$$-y'' + q_N(x)y = \lambda y?$$

In some simple cases the answer is positive, as in the case when the distances between the gaps are bounded below.

9 Appendix II. Some remarks about the analytic structure of the generalized Floquet solutions

In the case of finite gap potential with arbitrary gaps, the spectral parameters $\xi_j(x)$ as functions of x are almost periodic functions (quasi periodic with the same periods for all j, see e. g.[3]).

In order for $\xi_j(x)$ to be periodic, the gaps must be located in special positions. Consider now the formula (6.1). In this formula the factor $[P(x)]^{1/2}$, in general case is an almost periodic function. The situation is much more complicated for the function

$$\int_0^x \frac{du}{P(u,\lambda)}. \qquad (A.II.1)$$

If λ is outside the spectrum of equation (5.4), then $P(u,\lambda) \neq 0$ for all real u and is almost periodic. Therefore the function $1/P(u,\lambda)$ is also almost periodic.

The expression (A.II.1) is an indefinite integral of an almost periodic function. There exists a notable difference between the indefinite integrals of periodic and almost periodic functions. Let $f(x)$ be a periodic function with period a . Then

$$\int_0^x f(x)dx = c_0 x + \varphi(x) \qquad (A.II.2)$$

where

$$c_0 = \frac{1}{a}\int_0^a f(x)dx$$

and $\varphi(x)$ is periodic with the same period a.

In the case of almost periodic functions the formula (A.II.2) holds also, but now

$$c_0 = \lim_{T\to\infty} \frac{1}{T}\int_0^T f(x)dx,$$

and generally the function $\varphi(x)$ is not bounded and therefore not almost periodic.[2] There exist sufficient conditions for almost periodicity of the function $\varphi(x)$. For example, it is enough that the Fourier exponents of the almost periodic function $f(x)$ have a gap in some neighborhood of zero; nevertheless,it is hard to believe that this can happen for finite gap potentials.

[2] According to a classical theorem of H. Bohr for almost periodicity of an indefinite integral of an almost periodic function is necessary and sufficient the boundness of the integral.

10 Appendix III. Asymptotic behavior of the spectral matrix

Our starting point is the formula (3.6). Having in mind some simplifications, we suppose that the spectrum of equation (1.1) is non-negative. After substituting $\rho_{jk}(\lambda)$, $\theta(x,\lambda)$. $\varphi(x,\lambda)$ by $\rho_{jk}(\mu)$, $\theta(x,\mu)$, $\varphi(x,\mu)$, $\mu=\sqrt{\lambda}$, the formula (3.5) takes the form:

$$\int_0^\infty \tilde{g}_\epsilon(\mu)\{\theta(x,\mu)\theta(s,\mu)d\rho_{11}(\mu)+[\theta(x,\mu)\varphi(s,\mu)+\varphi(x,\mu)\theta(s,\mu)]d\rho_{12}(\mu)+$$

$$+\varphi(x,\mu)\varphi(s,\mu)d\rho_{22}(\mu)\}=$$

$$=\begin{cases}\frac{1}{2}g_\epsilon(x-s)+\frac{1}{2}\int_{|x-s|}^{\epsilon} w(x,t,s)g_\epsilon(t)dt, & |x-s|\le\epsilon,\\ 0 & |x-s|\ge\epsilon.\end{cases} \qquad (A.III.1)$$

The case $s=x$ has special interest. In this case

$$\int_0^\infty \tilde{g}_\epsilon(\mu)[\theta^2(x,\mu)d\rho_{11}(\mu)+2\theta(x,\mu)\varphi(x,\mu)d\rho_{12}(\mu)+\varphi^2(x,\mu)d\rho_{22}(\mu)]=$$

$$=\frac{1}{2}g_\epsilon(0)+\frac{1}{2}\int_0^\epsilon w(x,t,x)g_\epsilon(t)dt \qquad (A.III.2)$$

For $x=s=0$ formula (A.III.1) gives

$$\int_0^\infty \tilde{g}_\epsilon(\mu)d\rho_{11}(\mu)=\frac{1}{2}g_\epsilon(0)+\frac{1}{2}\int_0^\epsilon w(0,t,0)g_\epsilon(t)dt. \qquad (A.III.3)$$

Using (A.III.3) and the method described in detail in our paper [10], it can be proved that

1) the estimate $\rho_{11}(a+1)-\rho_{11}(a)=O(1)$, $a\to+\infty$,

2) The asymptotic formula

$$\xi(\mu)=\frac{1}{\pi}\mu+O(1), \quad \mu\to+\infty.$$

In order to obtain the asymptotic formula for $\rho_{22}(\mu)$ differentiate the equation(A.III.1) once with respect to x and once with respect to s. Putting then $x=s=0$, we obtain

$$\int_0^\infty \tilde{g}_\epsilon(\mu)d\rho_{22}(\mu)=-\frac{1}{2}g_\epsilon''(0)+\alpha g_\epsilon(0)+\int_0^\epsilon \beta(t)g_\epsilon(t)dt \qquad (A.III.4)$$

where α is a constant and $\beta(t)$ is a bounded function.Using the method of [10], we can obtain, from (A.III.4),

1) the estimate $\rho_{22}(a+1)-\rho_{22}(a)=O(a^2)$, $a\to+\infty$,

2) the asymptotic formula

$$\rho_{22}(\mu)=\frac{1}{3\pi}\mu^3+O(\mu^2), \quad \mu\to+\infty.$$

The asymptotic behavior of $\rho_{12}(\mu)$ cannot be obtained, because, as we have seen in Section 2, $d\rho_{12}(\mu)$ can be zero; nevertheless, a strong estimate of $\rho_{12}(\mu)$ can be found for $\mu \to \infty$. At first, we have to prove the estimate

$$Var_a^{a+1}\{\rho_{12}(\mu)\} = O(a), \quad \mu \to +\infty.$$

As the spectral expansion of the operator (2.1) on the entire line can be obtained as a limit of the expansions on finite intervals, we can suppose that the spectrum of (2.1)is discrete.In this case (see[11], chapter 2)

$$\rho_{11}(a+1) - \rho_{11}(a) = \sum_{a<\mu_k\le a+1} \alpha_k^2 = O(1),$$

$$\rho_{22}(a+1) - \rho_{22}(a) = \sum_{a<\mu_k\le a+1} \beta_k^2 = O(a^2),$$

$$\rho_{21}(a+1) - \rho_{21}(a) = \sum_{a<\mu_k\le a+1} \alpha_k\beta_k.$$

Therefore

$$Var_a^{a+1}\{\rho_{12}(\mu)\} \le \sum_{a<\mu\le a+1} |\alpha_k\beta_k| \le \left(\sum_{a<\mu_k\le a+1} \alpha_k^2\right)^{1/2} \left(\sum_{a<\mu\le a+1} \beta_k^2\right)^{1/2} =$$

$$= O(a). \qquad (A.III.4)$$

Differentiating equation (A.III.1) with respect to x and putting $x = 0$, $s = 0$, we have

$$\int_0^\infty \tilde{g}_\epsilon(\mu) d\rho_{12}(\mu) = \frac{1}{2}\int_0^\epsilon \alpha(t) g_\epsilon(t) dt \qquad (A.III.5)$$

where

$$\alpha(t) = \frac{\partial}{\partial x} w(x,t,s)|_{x=s=0}$$

From (A.III.4), (A.III.5) and the Tauberian theorem [10] follows the estimate:

$$|\rho_{12}(\mu)| = O(\mu), \quad \mu \to +\infty.$$

References

[1] H. Weyl, *Über gewöhnliche Differentialgleichungen mit Singularitäten und die zugehörigen Entwicklungen willkürlicher Funktionen.* Math. Ann. 68 (1910), 220-269.

[2] C. E. Titchmarsh, *Eigenfunctions expansions associated with second order differential equations.* Part I, Oxford 1946.

[3] B. M. Levitan, *Inverse Sturm-Liouville problems.* Utrecht, 1987.

[4] F. S. Rofe-Beketov, *The spectral matrix and the inverse Sturm-Liouville problem on the axis* $(-\infty, \infty)$ Theorya Funktsiy, Funkts. Anal. Prilozhenija, 4, (1967), 189-197. (in Russian)

[5] B. M. Levitan, *Some Special Tauberian Theorems for Fourier Type Integrals and Eigenfunction Expansion of Sturm-Liouville Equation on the Whole Line.* Math. Nachr. 176 (1995), 179-193.

[6] B. M. Levitan *The inverse Sturm-Liouville problem for finite-zone and infinite-zone potentials.* Trudy Mosk. Obshch. 45, (1982), 3-36. (in Russian)

[7] S. P. Novikov *A periodic problem for Korteveg-de-Vries equation.* Funct. Anal. Prilojenije, 8(3) (1974) 236-240 (in Russian).

[8] P. Lax, *Periodic solutions of the KdV equation.* Comm.Pure Appl. Math. 28 (1975), 141-188.

[9] J. Moser, *Integrable Hamiltonian Systems and Spectral Theory.* Accad. Naz. Lincei, Pisa (1981).

[10] B. M. Levitan, *On the asymptotic behaviour of the spectral function of a self-adjoint differential equation of second order.* Izv. Akad. Nauk SSSR, Serie Math. 16 (1952), 325-352. English translation: Amer. Math. Soc. Transl. (2) 101 (1973), 192-221.

[11] B. M. Levitan and I. S. Sargsjan *Introduction to Spectral Theory.* Transl. of Math. Monographs, Amer. Math. Soc. (1975)

[12] B. A. Dubrovin, *Periodic problems for the Korteveg-de-Vries eqation in the class of finite-band potentials.* Funt. Anal. Appl. 9 (1975), 215-223.

[13] H,McKean and P. Moerbek, *The spectrum of Hill's equation.* Invent. Math. 30(3) (1975) 217-274.

[14] B. M. Levitan. *On a special Tauberian theorem.* Izv. Akad. Nauk SSSR, Ser. Mat. 17 (1953), 269-284 (in Russian) English translation:Amer. Math. Soc. Transl. (2) (101) (1973), 222-238.

Qualitative Physics in Spectral, Scattering and Decay Control

Chabanov V.M., Zakhariev B.N.

Bogoliubov Laboratory of Theoretical Physics, Joint Institute for Nuclear Research
Dubna, 141980, Russia
e-mail Zakharev@thsun1.jinrc.dubna.su

Abstract. This report is a review of the qualitative theory of quantum design: about our discoveries of new features of quantum systems by visualizing all possible potential and wave function transformations for variations of a complete set of independent spectral and scattering parameters. Special attention is paid to recently revealed multichannel aspects of this theory.

1 Introduction

There was a break-through in the last years (see e.g. [1-4]) in our understanding of relations between interactions (shapes of potentials) and observables (spectral, scattering and decay data) which form the main contents of quantum mechanics. This progress was based on the achievements of mathematical formalism of the inverse problem (IP)[1] and supersymmetry (SUSY) [5-9].

From our point of view the main worth of IP and SUSY consists in providing us with wide classes of exactly solvable models (and often even complete sets of them). It is of a great importance that visualization of these models allows us to reveal universal and unexpected phenomena hidden before. And the results derived by using exact models will be valid for ever.

The qualitative theory of quantum design for one-dimensional and one-channel systems was almost completed: it is clear now which potential transformations are necessary for the desired changes of physical properties. There were discovered even elementary constituents ("bricks"), which these transformations are composed of [10].

In this report we shall remind the basic rules of one-channel spectral management and then emphasize the peculiarities of multi-channel generalization of our qualitative theory to more complicated quantum systems. This multichannel approach is important as universal way to reduce the multi-dimensional and many-body partial Schrödinger equations to a system of coupled ordinary differential equations.

[1] This report was made in the presence of fathers-creators of IP: mathematicians B.M.Levitan and V.A.Marchenko from whose shoulders we have seen new physical horizons.

2 Golden Rules of One-Channel Spectral Control

The rules of elementary one-channel transformations are also important constituents of the quantum design for more complicated objects. Now we can predict qualitatively, without analytic formulae and computers, the shape of potential transformations needed for energy shift of one arbitrary bound state level without moving all (!) other levels in accordance with the exact IP and SUSY formalism [1,5,7]. From the direct problem point of view it may seem impossible to satisfy an infinite number of these conditions. But for the IP and SUSY approach it is the simplest task.

Take into account that any quantum state which we want to transform is more sensitive to potential perturbations at the places of its increased concentration (intensity of wave), that is at the bumps of standing wave.

So, *for lifting (lowering) the chosen energy level we should push the corresponding state by partial potential peaks (wells) at the places of its bumps.* But these peaks (wells) will also shift all other states and we want only one state to be shifted. So, *there must be also compensating partial wells (peaks) at the places of knots of the chosen state* where this is less sensitive to potential changes. For example, to push up the Nth state, $\Delta V(x)$ should possess N repulsive peaks and N+1 attractive wells.

In the process of motion of the chosen level the eigenfunctions of all other states are somewhat transformed (although their energy levels remain stable). In Fig.1 [11] the transformation of an oscillator potential by 50 potential peaks and 51 partial wells which shift the 50-th energy level up is demonstrated . It is remarkable that the lower states are almost not perturbed in spite of a strong potential transformation (they coincide with the initial bound state standing waves on the PC screen as is shown in Fig.1). Only very high, near the 50th level where the oscillations of the perturbation $\Delta V(x)$ are "in resonance" with eigenfunction oscillations, there are more visible changes in bound state wave functions.

Besides the energy levels E_λ there are other fundamental parameters, namely, spectral weights $c_\lambda = \psi'_\lambda(0)$. They play the part of levers controlling the space location of corresponding states [1,5,7].

To move states in space, the universal and elementary building block ("brick") of potential transformations is a combination of one partial well and one barrier for every bump, see for the simplest example Fig.2 how the ground state is gathered to the origin for the initial infinite rectangular potential well [1,5,7,12]. For the motion to the right (left) the barriers should be from the left (right) side of wells. To move the Nth state $\Delta V(x)$ should possess N barriers and wells. During the motion all knots of the chosen state remain fixed in space. Only the distribution of bump sizes changes. And there is some recoil of all other states (tendency to separation of the chosen state from other ones). For very big (small) values of c_λ the last (first) bump in the chosen state can move far to the right (left) or be pressed into the infinite vertical potential wall that restricts the motion.

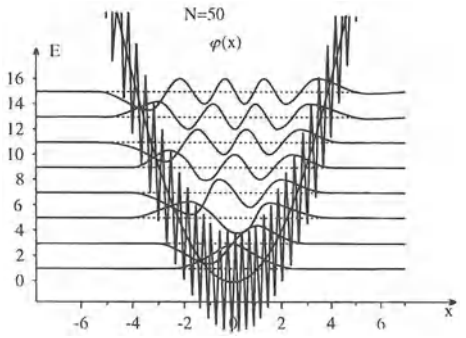

Fig. 1.

Fig. 1. Initial oscillator potential well was perturbed to shift up only the 50th energy level by 50 peaks at the positions of bound state wave bumps and 51 partial wells near its knots to keep all other levels exactly at the previous places [11]

The universality of these rules manifests itself both in creation of new states (energy levels) and in destruction of any chosen level of the initial spectrum. In the limit $c_{\lambda \to 0 \ or \ \pm\infty}$ there is effective annihilation of the state running to infinity or pressing into the infinite wall. Analogously, the creation of a new state (level) can be considered as being effectively brought from $\pm\infty$ by the potential perturbation with a relevant number of bricks. We can imagine in this case that this state is "returned after its removing" according to the above rules.

Our rules of the chosen state motion are valid even for *gathering scattering states into bound states* embedded into the continuum spectrum (BSEC) [10,13]. In this case an infinite number of these $\Delta V(x)$-bricks are naturally needed.

The same rules are applicable for variation of parameters of resonance (quasibound or decaying) states.

The qualitative theory of spectral control for waves on lattices (discrete quantum mechanics) and in periodic potentials was considered by us in [1,2]. In particular, there were investigated: spectral inversion, upside down barriers and wells, minimal nonlocal corrections to discrete soliton-like potentials to make them reflectionless, allowed and forbidden spectral zone managements. This theory can be useful for understanding the features of interchannel motion (over the discrete variable numbering mixed configurations).

Algorithms of spectral lacuna creation (tearing off or splitting continuous spectra at a relevant energy) were elaborated in [1,2].

3 Spectral Management and Multichannel Peculiarities

The system of coupled Schrödinger equations has the form:

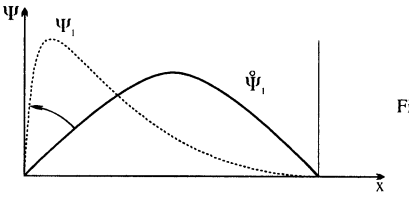

Fig. 2a.

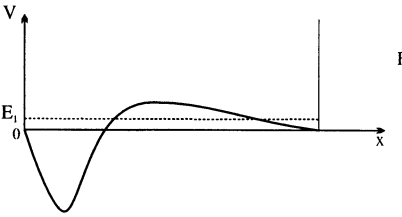

Fig. 2b.

Fig. 2. Gathering at the origin of the ground state wave function by increasing the spectral weight $c_{ground} = \psi'_{ground}(0)$ in the initial infinite rectangular well: a) wave functions, b) the potential. See the two-channel analogue of this phenomenon in Fig.3

$$-\psi_i''(x) + \sum_j V_{ij}(x)\psi_j(x) = E_i\psi_i(x) \tag{1}$$

where the channel waves $\psi_j(x)$ are the components of a wave vector, $E_i = E - \epsilon_i$ with the threshold energies ϵ_i.

Figure 3 exhibits the genuine multichannel phenomenon when by increasing only one ith component of the spectral weight vector (SWV) $c_{\lambda,i} = \psi_i'(0, E_\lambda)$ all other channel wave functions $\psi_{j\neq i}(x, E_\lambda)$ are partially transferred to the ith channel. The exact formulae that we have used here and in what follows have been given in [14]. It is a result of the channel connection ("as in communicating vessels"). So, the waves are gathering not only in the configurational, but also in the channel spaces. In the limit $|c_{\lambda,i}| \to \infty$ all components are completely sucked out by the chosen ith channel where they are pressed to the origin.

In the one-channel case in the limit $c_\lambda \to 0$ the corresponding bound state $\psi_\lambda(x)$ is pressed into the opposite (outer) potential wall. If $\psi'_\lambda(a) \to 0$ on the right boundary $x = a$, then $\psi_\lambda(x)$ is pressed into the outer potential wall. Unlike this, in the multichannel case the vanishing of partial $|c_{\lambda,i}|$ does not lead to pressing of the corresponding wave into the opposite wall. The wave is only partly shifted to the opposite wall and partly transferred (squeezed out) into the other channels. This is shown in Fig.4

In the process of variation of the spectral weight vector (SWV)-components there can (dis)appear knots in contrast with the one-channel case. This can be seen in Figs.3 and 5.

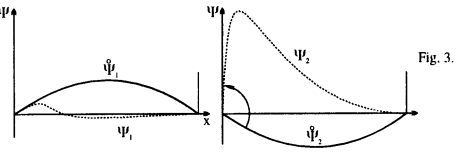

Fig. 3. Transformation of the components of the two-channel ground bound state wave function in the initial infinite rectangular well ($\overset{o}{V}_{11}(x) = \overset{o}{V}_{22}(x) = 0; \overset{o}{V}_{12}(x) = -0.3; [0 \leq x \leq \Pi]$ by a strong increasing of the derivative of the second component $\psi_{\lambda=1,2}(0)$ at the origin $x = 0$. As in the one-channel case, the wave $\psi_{\lambda=1,2}(x)$ is gathered to the origin, but also the first one $\psi_{\lambda=1,1}(x)$ is partly transferred into the first channel. There appears a knot in $\psi_{\lambda=1,1}(x)$ (see also Fig.5)

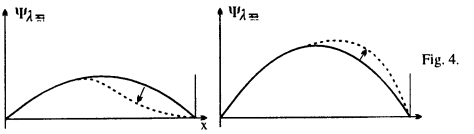

Fig. 4. Transformation of the components of the two-channel ground bound state wave function in the initial rectangular well of infinite depth ($\overset{o}{V}_{11}(x) = \overset{o}{V}_{22}(x) = 0; \overset{o}{V}_{12}(x) = -0.3; [0 \leq x \leq Pi]$ by making zero the derivative of the first component $\psi_1^I(a)$ on the right boundary $x = a$. In contrast with the one-channel case, the wave is not only slightly pressed to the opposite wall but also is partially transferred into the second channel

In the one-channel case we have found [4] the effective annihilation of two states when they approach one another (in the limit of degeneration of the levels). Unlike this, there is the allowed degeneration of M linearly independent bound states for M channels. By analogy with the one-channel case [4] there is the phenomenon of annihilation of degenerating bound multi-channel states with *linearly dependent* spectral weight vectors.

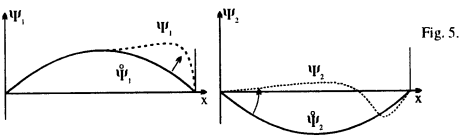

Fig. 5. The appearance of a knot in the second component $\psi_{\lambda=1,2}(x)$ of the ground state ($\lambda = 1$) wave function when the derivative of the second component $\psi'_{\lambda,2}(x)$ at the origin changes sign (from negative to positive). The initial interaction matrix elements are infinite rectangular wells with $\overset{o}{V}_{12}(x) = -0.3, V_{11}(x) = V_{22} = 0.3$, $[0 \leq x \leq Pi]$. See also Fig.3

As an example, we here consider the two-channel system with the rectangular interaction matrix of finite depth with $V_{11} = V_{22} = const$ $[0 \leq x \leq a]$ and achieve the degeneration of bound states by decreasing the channel coupling $V_{12} \to 0$. We have chosen equal SWV $\mathbf{c}_{\lambda;1,2}$ for two lowest states. In the process of approaching the levels, their bound state wave functions are divided into two parts one of which is going to infinity when $V_{12} \to 0$.

Rudiments of annihilation phenomena can be seen (Fig.6.) if we gradually change the SWV of the ith state whose energy is near some other $(i\pm1)$th level approaching $\mathbf{c}_{\lambda,i} \to \mathbf{c}_{\lambda,i\pm1}$ without shifting energy levels themselves. Similar states began to "break" in two pieces one of which has the trend to move away (the further the closer together are the levels). At the "crossing" point of $\mathbf{c}_{\lambda,i}$ with $\mathbf{c}_{\lambda,i\pm1}$ there occurs the "flip" (change of sign) of the repulsed (right) parts of the wave function components. The left bumps of the components do not change so much being fixed by given values of their derivatives (SWV) at the origin. So, Fig.6 also demonstrates the incompatibility of degeneration of states with the same SWV.

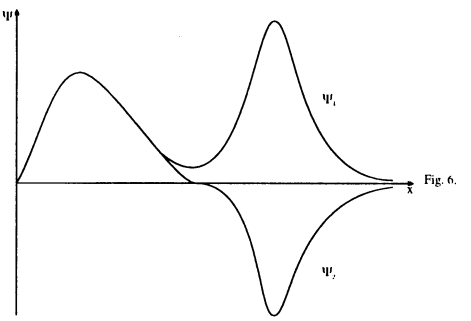

Fig. 6. The effect of "intolerance" of states which are close to each other in spectral parameters (energy levels $E_1 \approx E_2$ and similar SWV). The components of one function (of the two-channel ground bound state) are shown for the finite rectangular well interaction matrix. Pay attention to preparation of the effective annihilation of the "extra" state: the wave bumps on the right are teared off the original standing wave and pushed to the right (in the limit of degeneration and equal SWV these bumps are shifted to infinite x)

Consider a simple model of degeneration of three two-channel states which can be explained by one-channel analogies. The initial system consists of two *uncoupled* channels with infinite rectangular potential wells with different heights of their bottoms $V_{11} = 0, V_{22} = 3$. Linear combinations of the second state in the first well and the lowest state in the second well give two degenerated states with the energy levels $E_{2,3} = 4$ and orthogonal SWV. The initial ground state with $E_1 = 1$ and $c_{\lambda=1,2} = 0$ consists of the one-channel ground state in a deeper well and zero second component. The approximate triple

degeneration is produced by approaching E_1 to $E_{2,3} = 4$ with fixed SWV and $c_{\lambda=1,2} = 0$ so that the second component of the ground state remains zero and the channels remain uncoupled. All changes occur in one well V_{11} (in one channel as in [4]). The eigenfunction components in the first channel are teared into two pieces one of which (the right) is pressed to the right potential wall as in the ordinary one-channel case (preparation to effective annihilation). The left bumps are stabilized by fixed SWV values. Let us now increase $c_{\lambda=1,2}$ from its initial zero value to 1. This requires the wave transfer between channels. So, $V_{12}(x)$ appears to suck out some wave from the first channel as is shown in Fig.7. It has a big right side at the place of the right wave bump prepared for annihilation in the first channel. The shape of $V_{22}(x)$ provides the shift of the received wave to the left to make $c_{\lambda=1,2} = 1$. The interaction matrix element $V_{11}(x)$ has a barrier and a well which have pressed part of $\psi_{\lambda=1,1}(x)$ to the right wall.

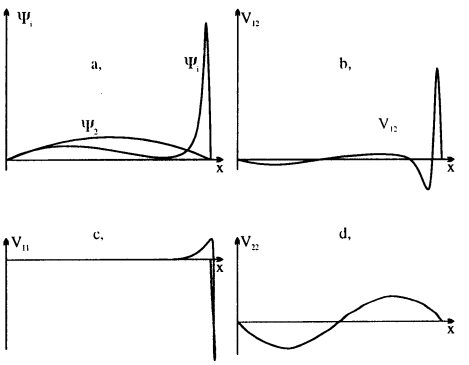

Fig. 7.

Fig. 7. Two-channel wave function components of the ground state (a), and interaction matrix elements (b, c, d) by approximate triple degeneration of three lower states. The initial system has uncoupled infinite rectangular potential wells with different heights of their bottoms $\overset{\circ}{V}_{12}=\overset{\circ}{V}_{11}= 0, \overset{\circ}{V}_{22}= 3$ and exactly degenerated second and third states. In the initial ground state SWV $\overset{\circ}{c}_{\lambda=1,2}= 0$. The initial system is transformed by lifting the ground state level up to neighboring exited states: $E_1 \to 3.9$, and making $c_{\lambda=1,2} = c_{\lambda=1,1} =$

It is well known that in the one-channel case the absolutely transparent potential is a soliton-like well and necessarily has one or more bound states. What could be expected when we transit from the one- to multi-channel case for transparent systems? It could seem that to the single-channel soliton-like potential there should correspond the interaction matrix with the soliton-like elements. Really, it is so in the case with identical thresholds in all channels. But in the general case there appear unexpected barriers in the interaction

matrix which are necessary for the reflectionless motion of waves [2]. Recently, we have obtained new classes of absolutely transparent multi-channel systems through the multi-channel generalization of SUSY transformation. Among them there are interaction matrices without bound states, which is impossible for one-channel systems (except the trivial case of free motion).

In Fig.8a an example of the two-channel interaction matrix reflectionless at any energy is shown without creation of a bound state. This resembles the picture of the absolutely transparent potential matrix bearing one bound state (Fig.8b) derived for the first time by the inverse problem technique in [5]. The difference is that in Fig.8a there is no potential well in the first channel, which results in the absence of a bound state. The SUSY-derived potential matrix without bound state depends on parameters ϵ,m_1,m_2 attributed to creation of the nonphysical state with the prescribed increasing asymptotic behavior.

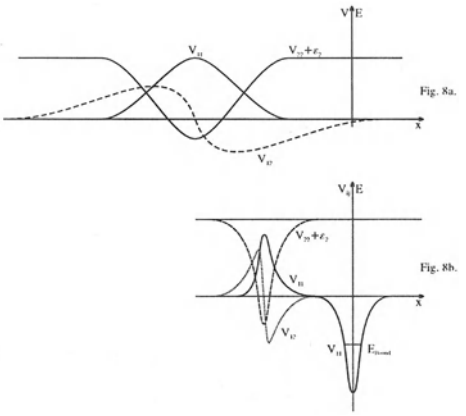

Fig. 8. Interaction matrix for a two-channel absolutely transparent system with different thresholds of channels: a) without and b) with creation of a bound state

A standard situation is when for the short-range interaction matrix $V_{ij}(x)$, different channels become disconnected at large distances and solutions there are combinations of the corresponding free waves. But even the weak coupling $V_{ij}(x)$ can suck out remaining waves from some open channels into other ones violating the standard asymptotic picture. For example, there can be an exponential decreasing function in the open channel. This happens for the multi-channel transparent interaction matrix when the wave incoming in one "α"-channel is distributed at first between other channels in the interaction region but then is concentrated again in the "α"-channel. This unnatural asymptotic disappearance of the wave in the open channel (which is unexpected because the motion there is not explicitly forbidden) due to

the coupling of channels even for rapidly decreasing $\Delta V_{ij}(x)$ is remarkable multichannel feature.

One of the wonderful possibilities of IP and SUSY transformations is the creation of bound states embedded into continuum (BSEC), see [1,7,13] and references therein. The corresponding standard one-channel potentials and BSEC wave functions have long-range oscillating tails (decreasing with r as $\sim 1/r$). Examples of short-range multichannel interaction matrices with BSEC below some threshold energies were considered in [7,15].

Now we have understood that it is of crucial importance for the construction of multichannel BSEC whether the spectral weight vector of the initial system without BSEC at the energy of creation of BSEC is changed by a scalar factor or different components of the vector weight are changed non-proportionally.

If the creation of BSEC does not violate the ratio of spectral vector components, then the transformation caused by the scalar factor in SWV does not hinder the cancellation of increasing waves in linear combination of regular solutions in closed channels under the integral in the denominator of the created state

$$\Psi_\alpha(x,E) = \frac{\sum_\beta c_\beta \overset{\circ}{\Phi}_{\alpha\beta}(x,E)}{1+\sum_\alpha \int_0^x \left[\sum_\beta c_\beta \overset{\circ}{\Phi}_{\alpha\beta}(y,E)\right]^2 dy}, \qquad (2)$$

where $\overset{\circ}{\Phi}_{\alpha\beta}(x,E)$ is matrix of the regular solutions of Schrödinger equations with initial $\overset{\circ}{V}_{\alpha\beta}(x)$ and obeying initial conditions

$$\overset{\circ}{\Phi}_{\alpha\beta}(0,E) = 0, \frac{d}{dx}\overset{\circ}{\Phi}_{\alpha\beta}(x=0,E) = \delta_{\alpha\beta};\ \epsilon_1 < E < \epsilon_2.$$

The denominator grows not faster than linearly with x. An example of such multichannel BSEC systems is shown in Fig.9. In the general case there appears an exponential suppression of BSEC wave functions and the interaction matrix.

We can predict that multi-BSECs will have properties analogous to the one-channel case of approximately linearly dependent and almost degenerated states and transformations caused by changing the spectral weight vector of one state by a scalar factor. But there are additional degrees of freedom of the independent variation of separate SWV-components.

We have considered the degeneration of one-channel BSEC states [18] and have.

In general, for M-channel equations it is possible to degenerate M BSEC with independent SWV and we expect annihilation of BSEC with linearly dependent SWV.

The system of coupled Schrödinger equations (1) can be considered as one equation for the function $\psi_i(x)$ of two variables: the continuous space coordinate "x" and discrete index "i" numbering the channels. The algorithms

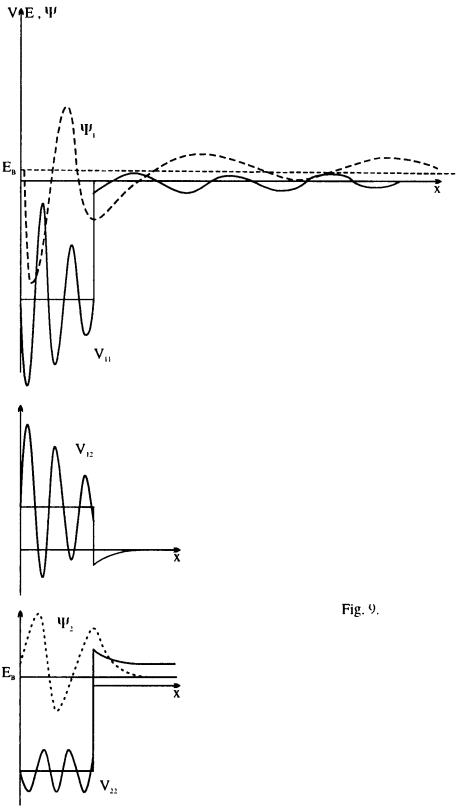

Fig. 9.

Fig. 9. Two-channel interaction matrix $V_{ij}(x)$ and components of wave function $\Psi^{I,II}(E_{BSEC}, x)$ for a bound state embedded into continuum spectrum (BSEC) between channel thresholds. This is a special case of the creation of BSEC by transformation of the SWV of the initial system by a scalar factor. Pay attention to the slowly decreasing potential and eigenfunction asymptotic tails in the open channel $(V_{11}(x), \Psi_1(x))$. The initial square well interaction matrix $\overset{o}{V}_{11}$ is also shown

of qualitative spectral, scattering and decay control for one-dimensional one-channel systems were elaborated by us separately for continuous and discrete variables [1,2]. The spectral management of (1) can be considered as a combination of these algorithms. In particular, in the simple two-channel case $V_{11}(x) = V_{22}(x)$; $V_{12} = const$ when the system (1) can be separated in two uncoupled equations for $\psi_{\pm}(x) = \psi_i(x) \pm \psi_i(x)$, we have found that the spectrum of (1) consists of multiplets of levels whose average positions are controlled exactly by the rules for continuous variable "x" and the position of levels inside the multiplets relative to their center can be managed by prescriptions of the discrete quantum mechanics [1,2].

The theory of qualitative quantum design [1-4] was based on freedom of considering not only real objects but all possibilities of the construction of quantum systems by arbitrary variation of independent spectral and scattering parameters. In the multi-dimensional case there appear additional constraints on the initial data of IP to except the extra variables in comparison with the number of variables in the potential. This excludes also the possibility of existence of exactly solvable models [1]. But including the potentials being nonlocal in part of variables allows us to get an equal number of variables in potential and spectral (scattering) data. In this case we again, as in one-dimensional space, obtain complete sets of exactly solvable models with independent spectral parameters. In principle, our investigations of multichannel quantum design is just the consideration of a convenient representation of such systems with nonlocal interactions (finite interaction matrices correspond in general to nonlocal potentials [1]).

Local potentials are a particular subset of nonlocal ones. So, we can approximate local systems by nonlocal models.

The unified theory of reactions suggested by Feshbach was generalized to arbitrary rearrangements of particles [16] and later this new formalism was used for a principal solution of the three- (and more) body inverse problem [19].

The multi-channel coupled equations can be treated as equations in discrete (numbering channels) and continuous (x) variables. The nondiagonal elements of interaction matrix $V_{ij}(x)$ represent the nonlocal interchannel coupling. Algorithms of spectral control are combinations of the corresponding rules separately for the wave management on lattices and in ordinary spaces.

Here it is very interesting to consider finite-difference Schrödinger equations of an order higher than 2 [1,2] (with multidiagonal Hamiltonians). There appears the phenomenon of spectrum folding and problems of control the number, positions and widths of the branches of spectra. It is worth mentioning that the potential nonlocality in discrete quantum mechanics has much in common with the effect of the corresponding difference operators and this makes discrete models a very convenient tool to elaborate quantum intuition concerning the nonlocality and interchannel coupling.

An analog of the two-spectrum theorem for the one-channel case is the M+1 spectrum multichannel theorem [1,2]. It would be interesting to consider the possibility to generalize these theorems to the wave motion on the half or the whole axis x including nonphysical (not L_2) eigenfunctions.

The inverse scattering problem for coupled channels with the modified Newton-Sabatier method (E=const approach) was considered at this Conference [17].

SUSY gives often new results in comparison with IP. Below we shall give the main formulae of exact multichannel models in the SUSY approach. They may be useful because we have not seen them in such a clear form.

4 Multichannel SUSY

In this approach the hamiltonian in Eq.(1) on the whole axis is represented in a factorized form

$$\hat{H}_- = \hat{A}^+ \hat{A}^- + \epsilon, \quad \epsilon < 0 \tag{3}$$

where ϵ is the so-called factorization energy. The operator $\hat{A}^-$ has the form

$$\hat{A}^- = -\frac{d}{dx} + \hat{W}(x), \tag{4}$$

where $\hat{W}(x)$ is a matrix to be found. The operator $\hat{A}^+$ is the hermitian conjugate of $\hat{A}^-$.

For definiteness, consider the case of two channels only. Furthermore, let the initial potential matrix $V_{ij}(x)$ be identically equal to zero on the whole axis. Let $\hat{\Psi}(x)$ be a matrix solution of the Schrödinger equation at the energy ϵ ($\hat{H}_-\hat{\Psi}(x) = \epsilon\hat{\Psi}(x)$). In particular, we can take

$$\hat{\Psi}(x) = \begin{pmatrix} m_1 e^{-\kappa_1 x} & c_1 e^{\kappa_1 x} \\ m_2 e^{-\kappa_2 x} & c_2 e^{\kappa_2 x} \end{pmatrix}, \tag{5}$$

$\kappa_i = \sqrt{\epsilon_i - \epsilon}$. We can easily obtain $\hat{W}(x)$ from the equation

$$\hat{A}^-\hat{\Psi}(x) = 0, \tag{6}$$

arising from the definition of $\hat{\Psi}(x)$. So, we have

$$\hat{W}(x) = \hat{\Psi}'(x)\hat{\Psi}(x)^{-1}. \tag{7}$$

Using (5) we rewrite this expression

$$\hat{W}(x) = \frac{1}{det\hat{\Psi}(x)} \begin{pmatrix} -\kappa_1 m_1 e^{-\kappa_1 x} & \kappa_1 c_1 e^{\kappa_1 x} \\ -\kappa_2 m_2 e^{-\kappa_2 x} & \kappa_2 c_2 e^{\kappa_2 x} \end{pmatrix} \begin{pmatrix} c_2 e^{\kappa_2 x} & -c_1 e^{\kappa_1 x} \\ -m_2 e^{-\kappa_2 x} & m_1 e^{-\kappa_1 x} \end{pmatrix} =$$

$$\begin{pmatrix} \frac{-\kappa_1[m_1 c_2 e^{(\kappa_2-\kappa_1)x} + m_2 c_1 e^{(\kappa_1-\kappa_2)x}]}{m_1 c_2 e^{(\kappa_2-\kappa_1)x} - m_2 c_1 e^{(\kappa_1-\kappa_2)x}} & \frac{2\kappa_1 c_1 m_1}{m_1 c_2 e^{(\kappa_2-\kappa_1)x} - m_2 c_1 e^{(\kappa_1-\kappa_2)x}} \\ \frac{-2\kappa_2 c_2 m_2}{m_1 c_2 e^{(\kappa_2-\kappa_1)x} - m_2 c_1 e^{(\kappa_1-\kappa_2)x}} & \frac{\kappa_2[m_2 c_1 e^{(\kappa_1-\kappa_2)x} + m_1 c_2 e^{(\kappa_2-\kappa_1)x}]}{m_1 c_2 e^{(\kappa_2-\kappa_1)x} - m_2 c_1 e^{(\kappa_1-\kappa_2)x}} \end{pmatrix}. \tag{8}$$

For $\hat{W}(x)$ to be hermitian, one should put $c_2 = -c_1 m_1 \kappa_1 / \kappa_2 m_2$. Then ($c_1$ is canceled in the numerator and denominator):

$$\hat{W}(x) =$$

$$\begin{pmatrix} \frac{\kappa_1[m_2^2\kappa_2 e^{(\kappa_1-\kappa_2)x} - m_1^2\kappa_1 e^{(\kappa_2-\kappa_1)x}]}{m_1^2\kappa_1 e^{(\kappa_2-\kappa_1)x} + m_2^2\kappa_2 e^{(\kappa_1-\kappa_2)x}} & -\frac{2\kappa_1 m_1 \kappa_2 m_2}{m_1^2\kappa_1 e^{(\kappa_2-\kappa_1)x} + m_2^2\kappa_2 e^{(\kappa_1-\kappa_2)x}} \\ -\frac{2\kappa_1 m_1 \kappa_2 m_2}{m_1^2\kappa_1 e^{(\kappa_2-\kappa_1)x} + m_2^2\kappa_2 e^{(\kappa_1-\kappa_2)x}} & \frac{\kappa_2[m_1^2\kappa_1 e^{(\kappa_2-\kappa_1)x} - m_2^2\kappa_2 e^{(\kappa_1-\kappa_2)x}]}{m_1^2\kappa_1 e^{(\kappa_2-\kappa_1)x} + m_2^2\kappa_2 e^{(\kappa_1-\kappa_2)x}} \end{pmatrix}. \tag{9}$$

The SUSY transformation itself is the permutation of operators $\hat{A}^-$ and $\hat{A}^+$ in (14). So, we get the transformed hamiltonian (supersymmetrical partner of $\hat{H}_-$)

$$\hat{H}_+ = \hat{A}^- \hat{A}^+ + \epsilon = \hat{H}_- - 2\hat{W}'(x). \tag{10}$$

It is easy to see that vector-column solutions of the Schrödinger equation with $\hat{H}_+$ have the form

$$\psi_+(x, E) = \hat{A}^- \psi_-(x, E). \tag{11}$$

Furthermore, it can be shown that these solutions have the same asymptotic behavior as the unperturbed ones, in other words, SUSY transformation does not change characteristics of the continuous spectrum (the reflection matrix remains unchanged and equals to zero identically). Unlike the one-channel case, the expression $\hat{\Psi}(x)^{-1}$ is not a solution at energy ϵ. Nevertheless, we can obtain four linearly independent vector-column solutions via formula (11), i. e. by the action of $\hat{A}^-$ on four linearly independent solutions for the initial hamiltonian $\hat{H}_-$ at $E = \epsilon$. It appears that the choice of $\hat{\Psi}(x)$ (5) corresponds to the case when the construction of a linear combination of the vector-column solutions with exponentially decreasing asymptotic is impossible. So we see that the bound state at energy ϵ is not created. We have a nontrivial potential transformation without affecting spectral characteristics. Of course, the choice of matrix solution (5) is not unique. This matrix may be composed of any two linearly independent vector-column solutions corresponding to the initial hamiltonian $\hat{H}_-$.

5 Conclusion

Hilbert once said that physics is too difficult for physicists. Maybe, Gell-Mann and Einstein expressed the same idea when they called quantum mechanics the "anti-intuitive discipline" and "bewitching calculus". But besides this there is a strong tendency of science simplification. There was a permanent remarkable growth in old good quantum physics from the very beginning. And one of the main points of the growth was the IP and SUSY theory. The exact models, some of which we have considered here, bridge direct and inverse problems, which will give us in future the renewed and unified quantum mechanics. The qualitative theory of Dubna school of the inverse problem is our contribution to enriching the algorithms of quantum intuition [1,2,7].

Quantum physics has already done very much for the progress of mankind. We expect from it much more in the future (the radical solution of energy problems, fantastic achievements in quantum electronics and due to them perfect technologies etc.). Now everybody knows the importance to save natural environment, but much more care is to be paid to our spiritual (informational) environment.

There are about $5\,10^9$ people on the Earth now. This means that there are about five million tons of brain matter. This is the most valuable thing (incomparable with oil, gold, etc. for which people so often involve one another in wars). But we treat this treasure nonrationally. Only a negligible part of this matter has satisfactory access to information which can tremendously increase creative power of the Earth population (millions of virtual Newtons, Lobachevskiis, Chaikovskiis ...).

Of course, every kilogram of the brain matter is egoistic, this is natural as well as the fact that we always retard relative to our contemporary possibilities. But egoism can be primitive (short-range) or clever (long-range). In the limit of global radius, egoism coincides with altruism that is really the most profitable strategy for everybody. Through possibilities of computer net connections of every person with another the mankind can sooner and deeper learn this truth. With memory elements of molecular size one quantum computer diskette can contain all what was written by people during the whole worlds history. This means that our quantum business helps us to make life on our Planet more spiritually comfortable, clever life.

6 Acknowledgments

Authors are grateful to RFFI (grant N 96-02-17383) for partial support.

7 References

References

1 Zakhariev B.N., *Lessons on Quantum Intuition*, JINR, Dubna, 1996.

2 Chabanov V.M., Zakhariev B.N., Phys.Rev.A49, 3159, 1994; **A50** 3948, 1994; Phys. Lett. **B319**, 13, 1993; Phys. El. Part. & Nucl. 21, N4, 1990; 23, N5, 1992; 25, N 6, 1994.

3 Serdyukova S.I., Zakhariev B.N., Phys.Rev., **A46**, 58, 1992; **A47**, 3518, 1993.

4 Chabanov V.M., Zakhariev B.N., Brandt S., Dahmen H.D., Stroh N., Phys.Rev. **A 52**, R3389, 1995; in Proc. Intern. Conf. "New Frontiers..." in Monteroduni (Italy), 1995.

5 Poshel J., Trubovitz E. *Inverse Spectral Theory*. Academic, New York, 1987.

6 Chadan K., Sabatier P. "Inverse Problems in Quantum Scattering Theory", Springer, Heidelberg 1989.

7 Zakhariev B.N., Suzko A.A., "Direct and Inverse Problems. Potentials in Quantum Scattering", (Springer-Verlag, Heidelberg, 1990).

8 Berezovoy V.P., Pashnev A.I. Z.Phys.C. 1991, v.51, p.525.

9 Baye D., J.Phys.1987.v.A.20.p.5529; Phys.Rev.Lett. 1987, v.58, p. 2738; Proc. Inverse Problems, p.127, Bad Honnef 1993, Springer, 1994.

10 Chabanov V.M., Zakhariev B.N., Sofianos S.A., Ann. der Phys. 1996

11 Stroh T., Zakhariev B.N., Phys. Scripta, (accepted for publication) 1996.

12 Zakhariev B.N., Mineev M.A. Preprint P4-96-280, JINR, Dubna (submitted to Phys.Rev.A).
13 WeberT.A., Pursey D.L., Phys.Rev. **A52**, 4255, 1995;
Stahlhofen et al. Phys. Scripta **50**, 9, 1994.
14 Amirkhanov I.V., Zakhariev B.N., et al in Proc.Conf. "Schrödinger Operator. Standart and Nonstandart" Dubna, 1988, World Scientific, 353, 1989.
15 Newton R.G. *Scattering Theory of Waves and Particles*, 2nd ed. NY, Springer, 1982.
16 Zhigunov V.P., Zakhariev B.N., *Methods of close coupling of channels in quantum scattering theory* (in Russian), Atomizdat, Moscow, 1974.
Efimenko T.G., Zhigunov V.P., Zakhariev B.N., Ann. Phys. (N.Y.),**47**, 275, 1968.
M. Eberspächer, B. Apagyi and W. Scheid in these Proc. Conf. "Inverse and Algebraic Quantum Scattering Theory" Lake Balaton 96-Balatonföldvar, 1996
18 Chabanov V.M., Stroh T., Zakhariev B.N., (to be published).
19 Zakhariev B.N., Few-Body Systems,**4**, 25, 1988.

Ambiguities in Inversion Potentials for Light Nuclear Ion Scattering

K. Amos and M. T. Bennett

School of Physics, University of Melbourne, Parkville, Victoria 3052 Australia.

1 Introduction

Understanding the nature and specifics of the potential energy of interaction between two colliding quantum systems, be they of nuclear, of atomic or of molecular type, is central in almost all studies of their possible reactions. Conventionally, elastic scattering data is used as a measure to assess the propriety or no of any candidate form one may specify for such (non–relativistic) interaction. Invariably also one considers that interaction to have local form which however may be complex and/or energy dependent.

There are two basic approaches by which quantitative information on the (effective, local) interaction between colliding quantal systems may be sought from measured, elastic scattering data. The first is the direct approach in which either a form for the interaction is assumed or its radial variation is determined by folding underlying component interactions with the density profiles of the colliding systems. The result is then used in the Schrödinger equations to specify the relative motion wave functions for the system. From those solutions, phase shifts are extracted and thence, by standard summations of Legendre polynomials, observables such as the differential cross sections are predicted. Frequently the procedure is modified to a numerical inverse method by adjusting values of parameters in the chosen form seeking a result that 'best fits' measured data [1].

Alternatively one can use global inverse scattering theories [1] with one of many methods of solution to determine candidate interactions from S functions (phase shifts) that have been determined by a (quality) fit to measured data. In so doing, there is essentially no *a priori* assumption made about the shape of the 'inversion' potentials. However, they are clearly linked to the chosen method of implementation, i.e. as one uses the Lipperheide–Fiedeldey, Newton–Sabatier, Marchenko or Gel'fand–Levitan equation to name a common set.

With either approach, central in the procedure is the scattering function, which for energy $E(=\hbar^2k^2/2\mu)$ is given in terms of the phase shifts by

$$S(\lambda, k) \equiv e^{2i\delta_\ell(k)}, \tag{1}$$

when the angular momentum variable (λ) are the real values $l + \frac{1}{2}$, as such gives the link

$$\left\{\frac{d\sigma}{d\Omega}\right\} \Leftrightarrow S(\lambda, k) \Leftrightarrow V(r, E) \tag{2}$$

Therein there are two possible spectral parameters, the energy and the angular momentum. But almost all studies, direct and inverse, have fixed one or the other. With inversion methods the fixed λ — variable energy approaches have led to new insights about the two nucleon interaction. But most experimental results suggest use of fixed E – variable angular momentum schemes. Typical data are differential cross sections measured at a single energy and for a set (often incomplete) of center of mass scattering angles. Such fixed energy data and their analyses are the subjects of this article, with particular emphasis placed upon the problems of the links between data and the inversion interactions via the S functions. The key problem in assessing a quantal scattering interaction is the definition of the physical S function. There are problems with the link between that physical S function and the interaction whether a direct or an inverse process is used. But it is worth noting that once the S function in the form suitable for use with an inversion method has been chosen, then the resulting potential is unique (to within any phase equivalent condition such as yield the so called 'transparent' additions or super–symmetric partners). With inversion schemes, the process of choosing the S function for a continuum of angular momentum values is ambiguous however. But equivalent ambiguities are present with analyses using direct methods in so far as the parametric specification is always ambiguous. Worse the direct process locks one into an *a priori* choice of form for the interaction; a choice that often has limited physical justification.

2 The process $\frac{d\sigma}{d\Omega} \Rightarrow S(\lambda)$

Consider the differential cross section of elastic scattering which, with θ being the scattering angle $(\hat{\mathbf{k}}_i \cdot \hat{\mathbf{k}}_f)$, is defined in terms of a complex, scattering amplitude by

$$\sigma(\theta) = \frac{d\sigma}{d\Omega}(\theta) = |f(\theta)|^2. \tag{3}$$

That scattering amplitude will be taken as

$$f(\theta) = \sqrt{\sigma(\theta)}\, e^{i\varphi(\theta)} \tag{4}$$

and in a partial wave expansion (with $S_\ell = S_\ell(k) = e^{2i\delta_\ell(k)}$)

$$f(\theta) = \sum_\ell f_l\, P_l(\theta) = \sum_\ell (2\ell+1)\frac{1}{2ik}\,[S_\ell - 1]\, P_\ell(\theta)\ , \tag{5}$$

whereby, if one can specify the phase $\varphi(\theta)$, and have the cross section at all scattering angles, then the S function at the physical values (ℓ) of the angular momentum variable $\lambda(=\ell+\frac{1}{2})$ are

$$S_\ell = 1 + ik \int_0^\pi f(\theta) P_\ell(\theta) \sin(\theta) d\theta. \tag{6}$$

This process seems of little value – indeed it is of none if the phase cannot be specified. We consider such questions further in another contribution to this issue wherein the constraint of unitarity is used to specify a nonlinear equation for that phase function and a method of solution specified and applied to both nuclear and atomic scattering data. But there are also uncertainties with any process of defining S_ℓ due to problems with the data sets, some of which are

(i) (large) statistical errors
(ii) systematic errors (both known and unknown), and
(iii) incomplete data requiring interpolation and extrapolation for $\theta = 0°$ to $180°$.

Of these, treatment of the systematic errors of data sets has been found to be particularly important in establishing what is and is not a statistical fit to that data set [2]. These matters are considered in brief in the next section. In addition there are ambiguities in the construction of the fixed energy S functions (or equivalently the phase shifts), some of which are

(i) layered ambiguities ($\delta_\ell \rightarrow \delta_\ell + n\pi$)
(ii) window ambiguities (limited data sets)
(iii) unknown bound state influences in $S(\lambda)$, and
(iv) phase symmetry condition ($\varphi \rightarrow 2\pi - \varphi$)

Such problems, and those created by loss of unitarity of the S function due to flux loss to other reaction channels, mean that functional forms for $S(\lambda)$ are taken usually. Therewith one also has the ambiguity of construction that is the prime consideration of this paper. The choice of S function form then is based upon its utility in effecting the inversion process. S functions having rational function form, viz.

$$S(\lambda) = e^{i\eta \ln(\lambda^2 + \lambda_c^2)} \prod_{n=1}^{N} \frac{(\lambda^2 - \beta_n^2)}{(\lambda^2 - \alpha_n^2)} , \tag{7}$$

where η is the Sommerfeld parameter, are particularly useful and are required for use with both the semi–classical WKB and fully quantal Lipperheide–Fiedeldey inversion schemes that have been of primary interest to us with analyses of electron–molecule, atom–atom and nuclear scattering cross sections [2].

3 Treatment of errors in data

The quality (and extent) of data is crucial in the determination of an S function. Such is reflected by the size of the statistical uncertainties with the quoted experimental values, by unknown systematic errors of any experiment and by known systematic errors such as the exact angle and acceptance of detectors. There is nothing a theorist can do about the count rates and the attendant statistical error but there are various techniques one may consider to estimate the effects of the systematic errors in defining S functions [2].

Smoothing splines provide 'nice' curves by which discrete noisy data can be smoothed and a particularly suitable process for smoothing cross–section data is that of generalized cross validation (GCV) [3]. Allowing that a measured N point data set consists of a smooth physical result plus white noise, the GCV process is a trade off between fidelity to the quoted data set (chisquare per data point, χ^2/N) and roughness of a selected $(2m-1)$ degree smoothing polynomial spline. That roughness is measured by the integrated square of the m^{th} derivative of the smoothing spline function. The end result is a new table of data (at the same scattering angles) whose differences from the original values one might consider to be an estimate of unknown systematic errors.

Even so, that does not guarantee that a new 'data set' will result against which an S function can be found to produce a fit of statistical significance; i.e. one for which the measure, chisquare per degree of freedom (χ^2/F; $F = M - N$) of the fit with N adjustable parameters and M data points, is of order 1.

In finding high quality fits to extensive cross–section data sets, one must consider also the known systematic errors and for differential cross sections that is usually an uncertainty with the angles at which the detector has been placed. We have taken such into account in a very simple manner. Specifically we have allowed each quoted experimental value to correspond to an angle in the range around the tabulated number. For heavy ion scattering, typically that angle uncertainty is $0.1°$. In a case studies recently, by 'angle shaking' each and every quoted experimental result, a relatively poor fit to the quoted cross section from ^{12}C–^{12}C scattering at 250 MeV actually became a statistically significant one to the 'angle shaken' values [2].

4 The nuclear isospin potential

That the interactions between nuclei are isospin dependent has been known recognized since the symmetry energy term in the Bethe–Weissäcker semi–empirical mass formula was established. Such a potential may be expressed by

$$V(r) = V_0(r) + V_{\rm iso}(r)[\boldsymbol{\tau}_p \cdot \boldsymbol{\tau}_t] \ ,$$

wherein $\boldsymbol{\tau}_i$ are the isospin operators for the projectile (p) and target (t) respectively. Analyses of scattering data from isobaric systems enable us to estimate both V_0 and $V_{\rm iso}$. Herein we report on such analyses of the cross-section data of Dem'yanova *et al.* [4] and for the systems ^{3}He from ^{14}C at 72 MeV and ^{14}C from ^{3}H at the matching energy of 334.4 MeV. With potentials, $V_{\rm H/He}(r)$ determined from fits to the separate differential cross sections, the central and isospin components follow from

$$V_{\rm H/He}(r) = aV_0(r) \pm \frac{1}{2}V_{\rm iso}(r) \ .$$

We have analysed these cross section data using both the global inverse method of Lipperheide–Fiedeldey (hereafter abbreviated as LF) and the numerical inverse method of a conventional optical model (OM) approach. In the LF approach, first we must ascertain S functions of the form,

$$S(\lambda) = S_{\rm ref}(\lambda) \prod_{n=1}^{N} \left(\frac{\lambda^2 - \beta_n^2}{\lambda^2 - \alpha_n^2} \right) \ ,$$

from fits to the data. The reference S function we took as

$$S_{\rm ref}(\lambda) = e^{i\eta \ln(\lambda^2 + \lambda_c^2)}$$

where η is the Sommerfeld parameter. Thus, with N complex pole/zero pairs, λ_c defines a $(4N + 1)$ parameter set for the S function. Both the 118 data points from the ^{14}C–^{3}H reaction and the 56 data points from the ^{3}He–^{14}C case were fit by using 21 parameter S functions giving, after the application of both the GCV smoothing and 'angle shaking', fits to the measure of 8.87 and 1.31 for χ^2/F respectively. The quoted experimental uncertainties were used in these analyses (not the typical 10% values usually considered in most studies) and an angle uncertainty of 0.1° was assumed for each datum as those were not quoted in the published results [4]. Of the 'smoothing techniques' used with our analyses, angle shaking had the most dramatic effect. But it did not suffice to bring the analysis of the data from the radioactive beam experiment (the ^{14}C–^{3}H scattering) to have a statistically significance, i.e. to have $\chi^2/F \sim 1$. But we note that one or two points give most of the contribution to the total value of χ^2 and if one may ignore them, then the result is very good. That is evident from the cross sections shown in Fig. 1. Therein the dashed curves give the best fits we have obtained to the GCV and angle shifted data using numerical inversion. The conventional complex OM potentials were used in those studies. With Woods–Saxon (WS) forms for the central real and imaginary attributes and a derivative WS form for a surface absorption term, the 10 parameter models gave fits that had values of 22.8 and 13.7 for χ^2/F. Note those values reduce to 3.41 and 1.94 if we allow 10% errors, as is often used in analyses instead of quoted experimental uncertainties.

The inversion potentials, in central and isospin form, are given in Fig. 2. The results obtained with the two approaches are quite different. The *LF* method has led to relatively weak refractive and even weaker absorptive interactions for both elements. The *OM* results, in contrast, give a weakly absorptive but strongly refractive central interaction and a repulsive, essentially real isospin component. But the quality of fit with the two approaches are not sufficiently similar, with only the *LF* method resulting in a fit of reasonably small error measure.

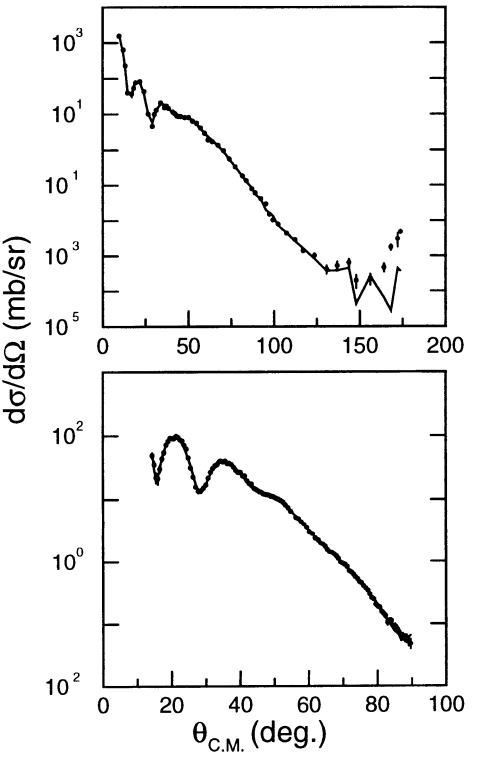

Fig. 1. The differential cross sections from the scattering of 334 MeV ^{14}C ions from ^{3}H (top) and from 72 MeV ^{3}He ions from ^{14}C (bottom) compared with fits by using the *LF* inversion potentials obtained from the rational *S* function forms (solid curves) and with those from optical model calculations (dashed curves).

The situation is different however with our analyses of some new data from the scattering of ^{7}Li ions. They are presented next.

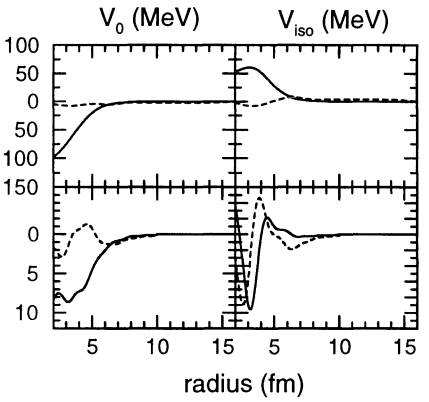

Fig. 2. The central and isospin potentials obtained from the LF inversion studies (bottom) compared with those obtained from the optical model analyses (top).

5 The *LF–OM* ambiguity — 350 MeV ^{7}Li–^{12}C and ^{7}Li–^{28}Si Scattering

In a recent publication [5], Nadasen *et al.* present high quality data from the elastic scattering of 350 MeV ^{7}Li ions off of ^{12}C and ^{28}Si to complement those they had measured previously at lower energies. They have analysed their data by numerical inversion with the standard OM approach finding what they term 'unique' OM potentials. The terminology is unfortunate even within the subclass of interactions of the OM approach. More to the point though, their high quality (^{12}C) data can be fit with both the LF global and OM numerical inversion methods and with comparable good fit measures. With the LF procedure, we have found excellent fits to the 350 MeV data by using 5 and 9 pole/zero pairs for the ^{12}C and ^{28}Si cases respectively. Likewise an excellent fit to the ^{12}C data has been found with the OM approach.

The cross section from the scattering of 350 MeV ^{7}Li ions off of ^{12}C is shown in Fig. 3. wherein the data are compared with the result (solid curve) of using the LF inversion potential to solve the Schrödinger equations for the scattering. The fit is excellent having a total χ^2 value of 50.1 and is therefore statistically significant as χ^2/F is 0.98. A similar, very good, LF inversion result has been obtained with the ^{7}Li–^{28}Si data ($\chi^2/F = 1.01$). But only with the ^{12}C data have we been able to find such a quality fit by numerical inversion. With a 7 parameter model consisting of a central real and imaginary WS form plus a Coulomb radius, the ^{12}C data has been fit with an end value of χ^2 of 69.4 and so χ^2/F of 1.07. For the ^{28}Si scattering, our best OM result has $\chi^2/F = 7.17$.

The S functions with which we find the best fits to the 350 MeV scattering data, are presented in Fig. 4. Therein, the phase has been plotted modulo π,

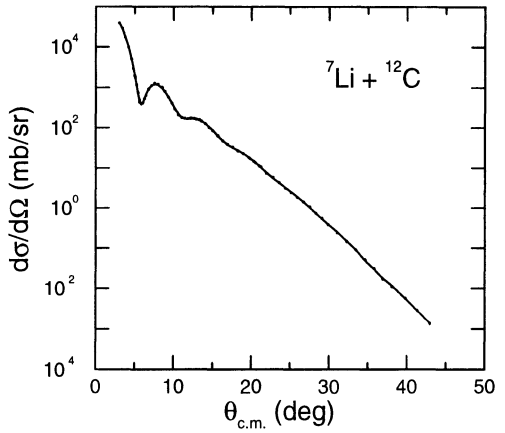

Fig. 3. The differential cross section from the scattering of 350 MeV ^{7}Li ions off of ^{12}C compared to the result calculated from the LF inversion potential. On this scale the OM result is indistinguishable.

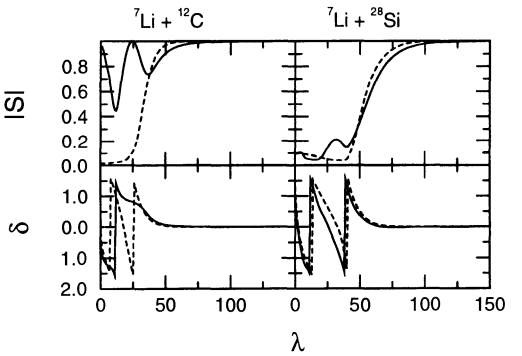

Fig. 4. The S functions for 350 MeV ^{7}Li on ^{12}C and ^{28}Si. The LF and OM results are displayed by the solid and dashed curves respectively and the phases are plotted modulo π.

hence the vertical segments shown. The solid curves portray the LF results while the dashed curves are the OM ones. Clearly the rational forms of the S function from the ^{12}C fit is quite different to that from the OM study. The LF result is very structured with $|S|$ being large, > 0.5 in fact, for all small partial waves. The LF and OM results from our analyses of the ^{28}Si data, in contrast, are quite similar and tend to the strong absorption model form. The variations in the S functions reflect in striking differences between the inversion potentials as is evident in Fig. 5. The top row contains the LF

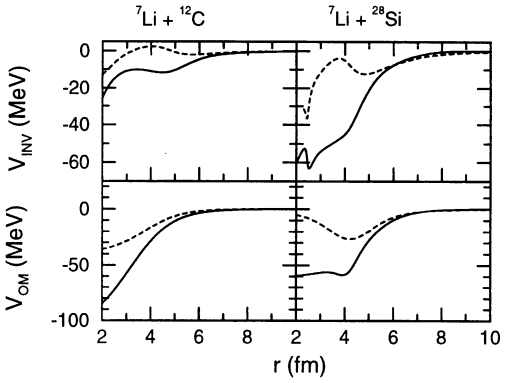

Fig. 5. The *LF* and *OM* potentials from the fits to the ^{7}Li scattering cross sections. The real and imaginary parts of the potentials are shown by the solid and dashed curves respectively.

inversion potentials, $V_{\rm INV}(r)$, for each system, while the bottom row shows the *OM* results, $V_{\rm OM}(r)$. In each case, the solid curves portray the real parts of the potentials while the dashed curves give the imaginary parts. A standard notch test revealed that the minimum radius of sensitivity is approximately 2 fm, hence the lower limit in the abscissa.

The differences between the *LF* and *OM* results are quite evident, and especially so for the ^{12}C scattering. But it is to be recalled that both interactions, when used in solving the scattering Schrödinger equations gave statistically significant fits to the data. Clearly some *a priori* bias has to be used to ascertain which is the most 'physical'.

References

[1] K. Chadan and P. S. Sabatier, *Inverse Problems in Quantum Scattering Theory* 2^{nd} Edition (Berlin, Springer, 1989); and references cited therein.

[2] M. T. Bennett, C. E. Steward, K. Amos, and L. J. Allen, Phys. Rev. C **54** (1996) in press; and references cited therein.

[3] P. Craven and G. Wahba, Numer. Math. **31**, 377 (1979).

[4] A. S. Dem'yanova *et al.*, Physica Scripta **T32**, 89 (1990); Nucl. Phys. **A553**, 727c (1993).

[5] A. Nadasen *et al.*, Phys. Rev. C **52**, 1894 (1995).

Coupled-Channel Marchenko Inversion in One Dimension with Thresholds

S. A. Sofianos[1], M. Braun[1], R. Lipperheide[1,2], and H. Leeb[3]

[1] Physics Department, University of South Africa, P.O.Box 392, Pretoria 0001, South Africa
[2] Hahn–Meitner–Institut Berlin and Freie Universität Berlin, D–14091 Berlin, Germany
[3] Institut für Kernphysik, Technische Universität Wien, Wiedner Hauptstraße 8-10/142, A-1040 Wien, Austria

Abstract. The one-dimensional coupled-channel Marchenko equation in the presence of thresholds is derived. Various aspects of this equation are discussed and a numerical algorithm for its solution is proposed. The efficiency of the algorithm is demonstrated using simulated scattering data.

1 Introduction

The inverse scattering problem on the line (i. e. in one dimension) has been formulated long ago (see, for example, Chadan and Sabatier (1982) and Calogero and Degasperis (1982)). Although its formal solution has become textbook knowledge, it is only recently that generally applicable and reliable *numerical* methods for solving it have been developed (Corvi (1992), Sacks (1993), Lipperheide et al. (1995a), Lipperheide et al. (1995b)). This may be attributed to the lack, so far, of a sufficiently complete set of scattering data to be used as input. In particular, the 'phase problem', i.e. the absence of information on the reflection phase, which is needed in addition to the reflectivity, has prevented the practical application of one-dimensional inverse scattering formalism, so that there was no urgency in developing viable numerical methods. Thus, the few one-dimensional inversions performed up to now in applications were concerned with model problems (Lipperheide et al. (1996)), or used parametrizations of the complex reflection coefficient which were fitted to the data ('phaseless inversion') (Pechenick and Cohen 1981, Jordan and Ladouceur 1987, Jordan and Lakshmanasamy 1989). However, in recent years the phase problem has received an increased attention, and various methods for obtaining empirical phase information have been proposed (Sivia et al. (1991), Fiedeldey et al. (1992), Gudkov et al. (1993), Majkrzak and Berk (1995), de Haan et al. (1995)).

In comparison with the single-channel inverse problem on the line, the corresponding coupled-, i.e. multiple-channel case has received less attention. Its radial counterpart in three-dimensional scattering has already been treated by Newton and Jost (1955), Agranovich and Marchenko (1963) and, more

recently, by Zakhariev and Suz'ko (1990, Chapter 5), and by Kohlhoff and von Geramb (1993). The one-dimensional case on the line, in which we are interested here, was considered by Wadati and Kamijo (1974) and Calogero and Degasperos (1977). In that work the threshold energies are assumed to be the same in all channels and set equal to zero. In such a case, the coupled-channel problem reduces to a straightforward matrix generalization of the single-channel inverse problem treated by Marchenko. When, however, account is taken of the existence of different thresholds, the problem becomes considerably more complicated. This is due to the fact that the reflection coefficient as a function of the incident momentum must be defined on a 2^{N-1}-fold Riemann surface, where N is the number of channels (cf. the work of Weidenmüller (1964) for the s-wave case in three-dimensional scattering).

The present work is devoted to the one-dimensional coupled-channel inverse problem in the presence of thresholds. The corresponding matrix form of the Marchenko equation is derived and discussed in Sec. 2. This equation is solved in Sec. 3 for a simulated two-channel example. Section 4 contains our conclusions. Some technical details of the algorithm used are given in the Appendix.

2 The Marchenko Method for Coupled Channels

2.1 The Jost Solutions

The coupled-channel Schrödinger equation in one dimension has the form (in appropriate units)

$$\left(-\frac{\partial^2}{\partial x^2} + \mathbf{V}(x) + \boldsymbol{\mathcal{E}}\right) \boldsymbol{\Psi} = k^2 \boldsymbol{\Psi}\,, \tag{1}$$

where $\mathbf{V}$ is a real symmetric $N \times N$ potential matrix with matrix elements v_{ij}, $i,j = 1,\cdots,N$, $\boldsymbol{\mathcal{E}}$ is a diagonal matrix containing the threshold energies ϵ_i, $i = 1,\cdots,N$, $\boldsymbol{\Psi}$ is a matrix whose columns are formed by the N linear independent solution vectors of (1), and k is the incident momentum. We arrange the threshold energies ϵ_i in increasing order and set the lowest, the 'elastic' threshold energy, equal to zero, $\epsilon_1 = 0$. We restrict ourselves to potential matrices with finite support; this effectively includes potentials which vanish more rapidly than any exponential (e.g. gaussian potentials). Moreover, we assume that the potential does not support bound states.

If the potential matrix vanishes identically, $\mathbf{V} = \mathbf{0}$, the solutions of (1) are the free solutions $\exp(\pm i\mathbf{K}x)$, where $\mathbf{K}$ is the diagonal matrix with

$$\mathbf{K}^2 = k^2\mathbf{1} - \boldsymbol{\mathcal{E}}\,. \tag{2}$$

The matrix $\mathbf{K}$ is defined on the physical sheet of the Riemann surface for the momentum variable k. This sheet has an $(N-1)$-fold branch cut on the

real axis on the upper rim of which the diagonal elements of $\mathbf{K}$ are defined as follows,

$$k_j = \begin{cases} \sqrt{k^2 - \epsilon_j}, & k \geq \sqrt{\epsilon_j}\,, \\ \mathrm{i}\sqrt{\epsilon_j - k^2}, & |k| < \sqrt{\epsilon_j}\,, \\ -\sqrt{k^2 - \epsilon_j}, & k \leq -\sqrt{\epsilon_j}\,, \end{cases} \tag{3}$$

for $j = 2, \cdots, N$ and $\epsilon_1 = 0$.

In generalization of the single-channel case we introduce the pairs of Jost solutions $\mathbf{F}_+(k,x)$, $\widetilde{\mathbf{F}}_+(k,x)$ and $\mathbf{F}_-(k,x)$, $\widetilde{\mathbf{F}}_-(k,x)$, which are solutions of (1) with the asymptotic form

$$\lim_{x\to+\infty} \exp(-\mathrm{i}\mathbf{K}x)\mathbf{F}_+(k,x) = \mathbf{1}\,, \qquad \lim_{x\to+\infty} \exp(+\mathrm{i}\mathbf{K}x)\widetilde{\mathbf{F}}_+(k,x) = \mathbf{1}\,, \tag{4}$$

$$\lim_{x\to-\infty} \exp(+\mathrm{i}\mathbf{K}x)\mathbf{F}_-(k,x) = \mathbf{1}\,, \qquad \lim_{x\to-\infty} \exp(-\mathrm{i}\mathbf{K}x)\widetilde{\mathbf{F}}_-(k,x) = \mathbf{1}\,. \tag{5}$$

Each pair represents a fundamental system of solution matrices.

The matrix $\widetilde{\mathbf{F}}_-(k,x)$ goes over into the diagonal incoming-wave matrix $\exp(+\mathrm{i}\mathbf{K}x)$ for $x \to -\infty$, that is, the Jost solution in the first column $\widetilde{\mathbf{F}}_-$ has an incoming wave with current density $k_1 = k$ in the first channel and none in the others, the one in the second column has an incoming wave with current density k_2 only in the second channel, and so on. The Jost solution matrix $\widetilde{\mathbf{F}}_-(k,x)$ therefore is the incoming component of the physical solution $\boldsymbol{\Psi}(k,x)$ for incidence from the left, to which we may add any linear combination of the outgoing Jost solution matrix $\mathbf{F}_-(k,x)$. On the other hand, in order to satisfy the physical boundary condition for $x \to \infty$, the physical solution must consist only of Jost solutions $\mathbf{F}_+(k,x)$. Therefore, we can write

$$\boldsymbol{\Psi}(k,x) = \mathbf{F}_+(k,x)\mathbf{T}(k) = \mathbf{F}_-(k,x)\mathbf{R}(k) + \widetilde{\mathbf{F}}_-(k,x)\,. \tag{6}$$

In view of the asymptotic conditions (4) and (5) the matrices $\mathbf{R}$ and $\mathbf{T}$ are recognized as the reflection and transmission matrices, respectively. A similar relation holds for incidence from the right.

As in the single-channel case the Jost solutions have the Levin representations (Chadan and Sabatier 1982)

$$\mathbf{F}_+(k,x) = \exp(+\mathrm{i}\mathbf{K}x) + \int_x^\infty \mathbf{G}_+(x,y)\exp(+\mathrm{i}\mathbf{K}y)dy\,, \tag{7}$$

$$\widetilde{\mathbf{F}}_+(k,x) = \exp(-\mathrm{i}\mathbf{K}x) + \int_x^\infty \mathbf{G}_+(x,y)\exp(-\mathrm{i}\mathbf{K}y)dy\,, \tag{8}$$

$$\mathbf{F}_-(k,x) = \exp(-\mathrm{i}\mathbf{K}x) + \int_{-\infty}^x \mathbf{G}_-(x,y)\exp(-\mathrm{i}\mathbf{K}y)dy\,, \tag{9}$$

$$\widetilde{\mathbf{F}}_-(k,x) = \exp(+\mathrm{i}\mathbf{K}x) + \int_{-\infty}^x \mathbf{G}_-(x,y)\exp(+\mathrm{i}\mathbf{K}y)dy\,. \tag{10}$$

Inserting these expressions into (1) one obtains, after some algebraic manipulations, the following differential equations for the kernels $\mathbf{G}_\pm(x,y)$:

$$\left(\frac{\partial^2}{\partial x^2} - \frac{\partial^2}{\partial y^2}\right) \mathbf{G}_{\pm}(x,y) = \mathbf{V}(x)\mathbf{G}_{\pm}(x,y) + [\boldsymbol{\mathcal{E}}, \mathbf{G}_{\pm}(x,y)] \; ; \qquad (11)$$

here we have introduced the commutator $[\mathbf{A},\mathbf{B}] = \mathbf{AB} - \mathbf{BA}$. The kernels satisfy the boundary conditions

$$\lim_{x,y\to\pm\infty} \mathbf{G}_{\pm}(x,y) = 0 \qquad (12)$$

and the potential matrix $\mathbf{V}(x)$ is related to either of the kernels $\mathbf{G}_{\pm}$ via

$$\mathbf{V}(x) = -2\frac{\partial}{\partial x}\mathbf{G}_{+}(x,x)\,, \qquad \mathbf{V}(x) = +2\frac{\partial}{\partial x}\mathbf{G}_{-}(x,x)\,. \qquad (13)$$

2.2 The Marchenko Inversion

The inverse scattering problem consists in determining the potential matrix $\mathbf{V}(x)$ from the knowledge of the reflection matrix $\mathbf{R}(k)$ as a function of the incident momentum k. This is done via the kernels $\mathbf{G}_{\pm}(x,y)$, which are calculated from the input reflection matrix $\mathbf{R}(k)$ with the help of the Marchenko matrix equation. The latter is obtained by inserting (12), (22) and (10) into (6), multiplying from the right by

$$\frac{1}{2\pi}\exp(-\mathrm{i}\mathbf{K}y)\frac{\partial \mathbf{K}}{\partial k} \equiv \frac{1}{2\pi}\exp(-\mathrm{i}\mathbf{K}y)\mathbf{K}^{-1}k$$

and integrating over k. The left-hand side of (6) yields, writing $\mathbf{T}(\mathbf{k}) = \mathbf{1} + \boldsymbol{\Gamma}(k)$,

$$\mathrm{LHS}(6) = \delta(x-y)\mathbf{1} + \mathbf{C}(x,y) + \mathbf{G}_{+}(x,y)H(y-x) + \int_x^{\infty} \mathbf{G}_{+}(x,z)\mathbf{C}(z,y)dz, \qquad (14)$$

where $H(x) = 1, 0$ $(x \gtrless 0)$ is the Heaviside function and

$$\mathbf{C}(x,y) = \frac{1}{2\pi}\int_{-\infty}^{+\infty} \exp(+\mathrm{i}\mathbf{K}x)\boldsymbol{\Gamma}(k)\exp(-\mathrm{i}\mathbf{K}y)\mathbf{K}^{-1}kdk\,. \qquad (15)$$

For the right-hand side of (6) we have

$$\mathrm{RHS}(6) = \delta(x-y)\mathbf{1} + \mathbf{B}(x,y) + \mathbf{G}_{-}(x,y)H(x-y) + \int_{-\infty}^{x} \mathbf{G}_{-}(x,z)\mathbf{B}(z,y)dz\,, \qquad (16)$$

where

$$\mathbf{B}(x,y) = \frac{1}{2\pi}\int_{-\infty}^{\infty} \exp(-\mathrm{i}\mathbf{K}x)\mathbf{R}(k)\exp(-\mathrm{i}\mathbf{K}y)\mathbf{K}^{-1}kdk\,. \qquad (17)$$

In the absence of bound states the matrix $\boldsymbol{\Gamma}(k)$ has no poles in the upper half-plane of k. If $x > y$ the contour for the integral (15) can be closed there

and we, therefore, find $\mathbf{C}(x,y) = 0$. Thus the expression (14) vanishes for $x > y$, and consequently the expression (16) yields

$$\mathbf{B}(x,y) + \mathbf{G}_-(x,y) + \int_{-\infty}^{x} \mathbf{G}_-(x,z)\mathbf{B}(z,y)dz = 0\,, \qquad x > y. \tag{18}$$

It is seen from the discussion above that, compared to the single-channel case (as well as to the no-threshold case), the new feature is the occurrence of the Jost solution matrices $\widetilde{\mathbf{F}}_+(k,x)$ and $\widetilde{\mathbf{F}}_-(k,x)$, which are no longer equal to $\mathbf{F}_+(-k,x)$ and $\mathbf{F}_-(-k,x)$, respectively. This is a consequence of the N-fold connectivity of the k-plane in the presence of thresholds. The kernel matrix $\mathbf{B}(x,y)$ now depends on the variables x and y separately, not just on the sum $x+y$, as in the former two cases.

Since $\mathbf{K}^{1/2}\mathbf{R}\mathbf{K}^{-1/2} = \mathbf{K}^{-1/2}\mathbf{R}^{\mathrm{T}}\mathbf{K}^{1/2}$ by the principle of micro-reversibility, we have $\mathbf{R}\mathbf{K}^{-1} = \mathbf{K}^{-1}\mathbf{R}^{\mathrm{T}}$. It follows that the kernel matrix $\mathbf{B}(x,y)$ has the symmetry property $\mathbf{B}(x,y) = \mathbf{B}^{\mathrm{T}}(y,x)$.

3 Numerical Solution of the Coupled-Channel Marchenko Equation

For a numerical test of the coupled-channel inversion procedure outlined above, we reconstruct a potential matrix $\mathbf{V}$ from simulated data calculated from that potential. Instead of solving the Schrödinger equation in the form (1), we found it convenient to consider the corresponding Riccati equation for the logarithmic derivative $\mathbf{Y}(k,x) = \boldsymbol{\Psi}'(k,x)\boldsymbol{\Psi}^{-1}(k,x) = \mathbf{F}'_+(k,x)\mathbf{F}_+^{-1}(k,x)$,

$$\mathbf{Y}' = \mathbf{V} + \boldsymbol{\mathcal{E}} - k^2\mathbf{1} - \mathbf{Y}^2\,. \tag{19}$$

This first-order differential equation is integrated from $x = x_{\mathrm{R}}$ to $x = x_{\mathrm{L}}$, where x_{R} and x_{L} are the right and left boundaries, respectively, of the region where the potential is nonvanishing. From (4) the boundary condition on $\mathbf{Y}(k,x)$ at $x = x_{\mathrm{R}}$ is

$$\mathbf{Y}(k,x_{\mathrm{R}}) = \mathrm{i}\mathbf{K}$$

and the reflection matrix $\mathbf{R}(k)$ can be expressed as

$$\mathbf{R}(k) = [\mathrm{i}\mathbf{K} + \mathbf{Y}(k,r_{\mathrm{L}})]^{-1}\,[\mathrm{i}\mathbf{K} - \mathbf{Y}(k,r_{\mathrm{L}})]\,. \tag{20}$$

With the reflection matrix $\mathbf{R}(k)$ given on a sufficiently fine equidistant grid of k-values up to a suitable $k_{\max}$, the integral in (17) can be accurately evaluated. After discretization of the variable y, the integral equation (18) can be solved as a matrix equation. The derivative in (13) is obtained using a Chebyshev interpolation (for more details cf. the Appendix).

As an example, we chose a potential matrix $\mathbf{V}(x)$ constructed from gaussians centered around $x = 2$ (cf. Fig. 1),

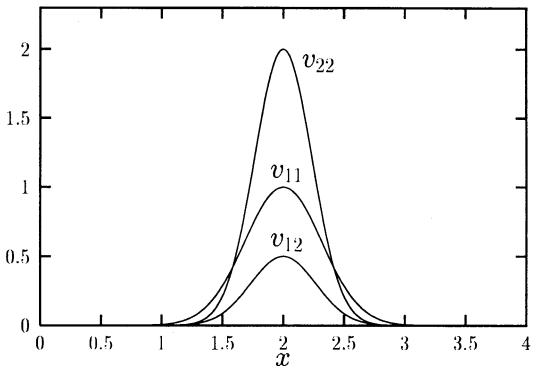

Fig. 1. The matrix elements of the potential $\mathbf{V}(x)$

$$\mathbf{V}(x) = \begin{pmatrix} 1.0\exp[-5(x-2)^2] & 0.5\exp[-7(x-2)^2] \\ 0.5\exp[-7(x-2)^2] & 2.0\exp[-9(x-2)^2] \end{pmatrix} . \tag{21}$$

The threshold energy of the second channel was chosen as $\epsilon_2 = 0.25$. We set $x_{\mathrm{L}} = 0$, $x_{\mathrm{R}} = 4$ and $k_{\max} = 10$. The reflectivities $|r_{11}(k)|^2$, $|r_{22}(k)|^2$ and $(k_2/k)|r_{21}(k)|^2$ corresponding to the reflection matrix $\mathbf{R}$ obtained for the potential (21) are shown in Fig. 2. The resulting kernel $\mathbf{B}(x, y)$ is shown in Fig. 3 as a function of the variables $u = x + y$ and $v = x - y$. We see that the kernel is nonzero only for $u = x + y > 0$, i.e. the lower limit of integration in the Marchenko equation becomes $-x$. Its dependence on the variable $v = x - y$ is relatively weak in the present example; it would disappear altogether if the threshold energies were all set equal to zero (cf. Wadati and Kamijo 1974).

The matrix Marchenko equation (18) was solved on the interval $[0, 4]$ using a bicubic spline interpolation (Press et al. 1992) for $\mathbf{B}(x, y)$. The reconstructed potential matrix resulting from the inversion coincides with the original one up to a difference whose absolute value does not exceed 2×10^{-3}.

In order to see the effect of the truncation in k-space we repeated the above calculation for $k_{\max} = 1.25, 2.5$, and 5. The results are shown in Fig. 4. It is seen that the cut-off momentum introduces spurious oscillations in the potential which disappear when $k_{\max} \geq 5$.

To study the sensitivity of the algorithm to experimental errors, we added numerically generated noise to the reflectivity for the test potential,

$$\mathbf{R}(k) \rightarrow \mathbf{R}(k) + \delta\mathbf{R}(k) , \tag{22}$$

where $\delta\mathbf{R}$ is a normally distributed random matrix with a standard deviation of 10^{-3} for the real and imaginary parts of all elements. The resulting error δV in the potential $\mathbf{V}_1$ (using $k_{\max} = 10$) is shown in Fig. 5. It appears that, in this example, the inversion is not very sensitive to experimental errors.

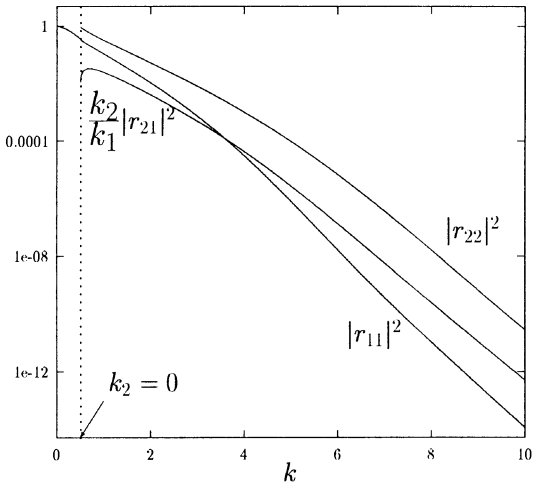

Fig. 2. The reflectivities $(k_i/k_j)|r_{ij}|^2$ corresponding to the reflection matrix $\mathbf{R}(k)$. The reflectivities in channel 2 are defined only above the threshold $k_2 = 0$.

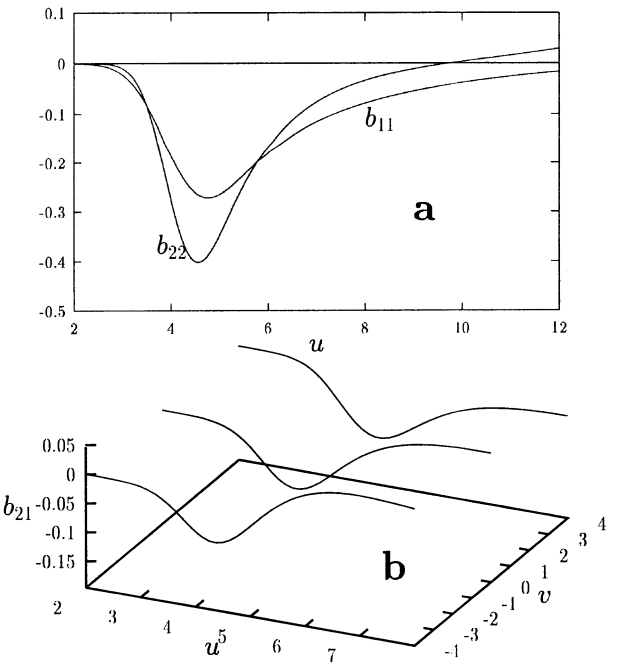

Fig. 3. The matrix elements of the kernel $\mathbf{B}(x, y)$ as functions of $u = x + y$ and $v = x - y$. a) The diagonal elements b_{11} and b_{22} as function of $u = x + y$, b) The nondiagonal element b_{21} as function of of $u = x + y$ and $v = x - y$.

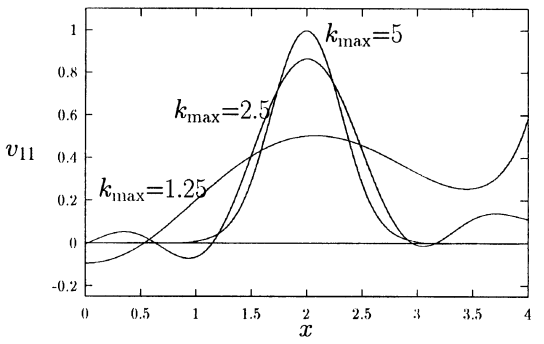

Fig. 4. The diagonal element v_{11} of the reconstructed potential $\mathbf{V}(x)$ for different values of the cutoff momentum k_{max}. For $k_{max} = 5$ the reconstructed v_{11} practically coincides with the original v_{11}.

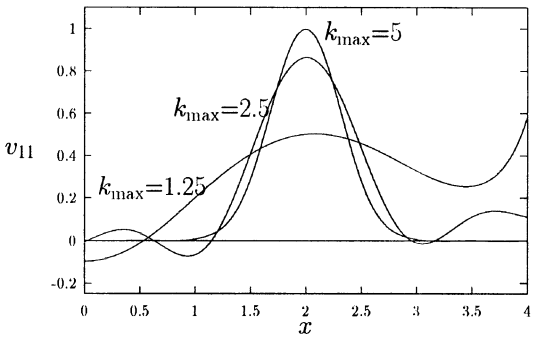

Fig. 5. The diagonal element v_{11} of the reconstructed potential $\mathbf{V}(x)$ for a reflection matrix with random noise (standard deviation) $5\,10^{-3}$. The results of four different runs are shown.

4 Concluding Remarks

We have derived the Marchenko integral equation for the coupled-channel inverse problem in one dimension in the presence of thresholds. These thresholds introduce specific features in the input for the Marchenko equation, so that the latter is appreciably different from what is done in the coupled-channel inverse problem without thresholds, which closely resembles the single-channel case. The Marchenko equation has been solved numerically for a simple two-channel test example, where the numerical algorithm has proved to be accurate and robust against random noise.

It remains to extend the formalism to include bound states, and to apply it to cases of physical relevance. Such applications are most likely to be found

in the field of nanostructure devices.

Acknowledgements

The authors gratefully acknowledge financial support from the the Foundation for Research Development, the University of South Africa, and the Hahn-Meitner Institut Berlin.

Appendix: Computational Procedure

To solve the Marchenko integral equation numerically, the integration over z is replaced by a summation over an equidistant grid and extrapolated in a similar manner as for the Romberg integration (Press et al. 1992). Discretization on the grid

$$y_m = -x + (m - 0.5)\frac{2x}{M}, \quad m = 1, \cdots, M$$

with the constant weight $2x/M$, i.e., according to the repeated mid-point rule, transforms the Marchenko integral equation into a system of linear equations,

$$b_{ij}(x, y_m) + g_{ij}(x, y_m) + \frac{2x}{M} \sum_{k=1}^{N} \sum_{m'=1}^{M} g_{ik}(x, y_{m'}) B_{kj}(y_{m'}, y_m) = 0\,. \qquad (A.1)$$

This can be written in a matrix form as

$$\mathcal{G}\mathcal{A} = \mathcal{B}$$

where $\mathcal{G}$ is an $N \times \widetilde{M}$–matrix ,

$$(\mathcal{G})_{i,(j-1)M+m} = g_{ij}(x, y_m)\,,$$

$\mathcal{A}$ an $\widetilde{M} \times \widetilde{M}$–matrix,

$$(\mathcal{A})_{(i-1)M+m,(j-1)M+m'} = \frac{2x}{M} b_{ij}(y_m, y_{m'}) + \delta_{ij}\delta_{mm'}\,,$$

and $\mathcal{B}$ an $N \times \widetilde{M}$–matrix,

$$(\mathcal{B})_{i,(j-1)M+m} = -b_{ij}(x, y_m)\,.$$

To solve this system we use the LU-decomposition of $\mathcal{A}$ followed by forward– and backward–substitution employing the relevant routines from LAPACK (Anderson et al. 1992).

To obtain $\mathbf{G}_-(x, y)$ when y is not a grid point, we use the Nystrom method (Press et al. 1992), i.e., we insert our solution for $\mathbf{G}_-$ in the discretized version of the integral equation, (A.1), with y_m replaced by y. In practice, we start with a relatively small value of M and double it until the Romberg-tableau has converged to a given precision ϵ.

In order to determine the potential matrix from (13) the function $\mathbf{G}_-(x,x)$ is interpolated on a Chebyshev grid in the interval $[x_{\min}, x_{\max}]$. The Chebyshev coefficients d_l for the derivative are then obtained from the coefficients c_l, $l = 0, 1, \cdots, L-1$, of the interpolating polynomial through a simple recursion relation (Press et al. 1992).

References

Agranovich Z. S. and Marchenko V. A. (1963), *The Inverse Problem in Scattering Theory*, Gordon and Breach, New York.

Anderson E. et al. (1992), *LAPACK Users Guide*, SIAM, Philadelphia.

Braun M., Sofianos S. A., and Lipperheide R. (1995), *Inverse Problems* **11**, L1.

Calogero F. and Degasperis D. (1982), *Spectral Transform and Solitons*, North–Holland, Amsterdam, Vol 1.

Chadan K. and Sabatier P. C. (1982), *Inverse Problems in Quantum Scattering Theory*, 2nd edition, Springer, Berlin.

Corvi M. (1992), *Numerical Algorithms for One–Dimensional Inverse Scattering and Imaging*, Bertero M. and Pike E. R., Eds., Hilger, Bristol, Philadelphia, New York, p. 411.

Fiedeldey H., Lipperheide R., Leeb H. and Sofianos S. A. (1992), *Phys. Lett.* **A179**, 347.

Ghosh Roy D. N. (1991), *Methods of Inverse Problems in Physics*, CRC Press, Boston.

Gudkov V. P., Opat G. I. and Klein A. G. (1994), *J. Phys.: Condensed Matter* **5**, 9013.

de Haan V. O., van Well A. A., Adenwalla S. and Felcher G. P. (1995), *Phys. Rev.* B **52** , 10831.

Jordan A. K. and Ladouceur H. D. (1987), *Phys. Rev.* A **36**, 4245.

Jordan A. K. and Lakshmanasamy S. (1989), *J. Opt. Soc. Am.* A **6**, 1206.

Kohlhoff H. and von Geramb H. V. (1993), in *Quantum Inversion: Theory and Applications*, Springer, Berlin, p.314.

Lipperheide R., Reiss G., Leeb H., Fiedeldey H., and Sofianos S. A. (1995), *Phys. Rev.* **B 51**, 11032.

Lipperheide R., Fiedeldey H., Leeb H., Reiss G., and Sofianos S. A. (1995), *Physica* **B213&214**, 914.

Lipperheide R., Reiss G., Leeb H. and Sofianos S. A. (1996), *Physica* **B221**, 514.

Majkrzak C. F. and Berk N. F. (1995), *Phys. Rev.* B **52**, 10827.

Newton R. G. and Jost R. (1955), *Nuovo Cimento* **1**, 590.

Pechenick K. R. and Cohen J. M. 1981, *Phys. Lett.* **82A**, 156.

Pechenick K. R. and Cohen J. M. (1983), *J. Math. Phys.* **24**(2), 406.

Press W. H., Teukolsky S. A., Vetterling W. T., and Flannery B. P. (1992), *Numerical Recipes in FORTRAN*, 2nd edition, Cambridge University Press.

Sacks P. E. (1993), *Wave Motion* **18**, 21.

Sivia D. S., Hamilton W. A. and Smith G. S. (1991), *Physica* **B173**, 121.

Wadati M. and Kamijo T. (1974), *Prog. Theor. Phys.* **52**, 397

Weidenmüller H. A. (1964), *Ann.Phys.* (N.Y.) **29**, 60.

Zakhariev B. N. and Suz'ko A. A. (1990), *Direct and Inverse Problems*, Springer, Berlin.

One-Dimensional Inversion in Neutron and X-Ray Reflection

R. Lipperheide[1], G. Reiss[1], and H. Leeb[2]

[1] Hahn–Meitner–Institut Berlin and Freie Universität Berlin, Postfach 390128, D–14091 Berlin, Germany
[2] Institut für Kernphysik, Technische Universität Wien, Wiedner Hauptstrasse 8-10/142, A-1040 Wien, Austria

Abstract. The application of the one-dimensional inverse scattering problem to neutron and x-ray specular reflection is discussed. Consideration is given to the problems of the numerical treatment as well as to the limitations on the input, in particular, the phase problem.

1 Introduction

The scattering of low-energy neutrons is described by neutron optics (cf. Sears (1989)) in the same fashion as the scattering of x-rays. Cold neutrons and x-rays are used to investigate the structure of surfaces and interfaces of samples in the nanometer range (cf. Russel (1990), Penfold and Thomas (1990), Kjaer and Als-Nielsen (1988)). Neutron and x-ray scattering supplement each other in many respects. However, from the theoretical point of view, their analysis is the same.

If the samples are planar we have to do with *specular* reflection and transmission. This is essentially quantal scattering by a one-dimensional potential barrier. The determination of this potential from the scattering information is, then, the *one-dimensional inverse scattering problem.* Usually one takes recourse to a simulation, i.e. one chooses a model for the potential whose parameters are adjusted via a fit to the data. However, for an unambiguous, model-independent answer one should solve the true inverse scattering problem [in x-ray and electron scattering this is often called the 'direct method' (!) (cf. Pendry et al. (1995)), which is to say that the solution of the inverse scattering problem is sought directly, not indirectly by simulation].

In the recent past working numerical procedures for solving the inverse scattering problem in specular reflection have been developed (cf. Corvi (1992), Sacks (1993), Lipperheide et al. (1995a)), and various methods for treating the phase problem have been proposed (cf. Ross et al. (1988), Sivia et al. (1991), Klibanov and Sacks (1992), Fiedeldey et al. (1992), Gudkov et al. (1993), Allman et al. (1994), Majkrzak and Berk (1995), de Haan et al. (1995)). Here we discuss the numerical solution of the Marchenko equation for a reconstruction of model potentials similar to those occurring in realistic situations (Sect. 2). We consider the direct solution of the integral equation

and the method of Padé approximants. The case of samples on thick substrates is troubled by rapid oscilations in the reflectivity; it is shown how this can be avoided by making use of inversion with a background potential for the substrate. In Section 3 we turn to the difficulties one encounters in actual applications. These arise, first, from the limitations on the accessible range of values of the incident momenta. Second, and more importantly, we are faced with the phase problem, i.e. the fact that, so far, the reflection phase cannot measured directly. It will be shown how this can be reduced to the problem of a discrete set of unknown parameters, and we remark on a number of proposals for an actual measurement of the reflection phase. Section 4 contains a summary.

2 Reconstruction of Realistic Model Potentials

2.1 Numerical Solution of the Marchenko Equation

Direct Solution. For a complex potential $V(x)$, with $V(x) = 0$ for $x < 0$ and in general $V(x) \to V_s$ for $x \to \infty$, the inverse problem is solved (cf. Kay (1960), Reiss (1995), Lipperheide et al. (1995a)) by inserting the Fourier transform $B(x)$ of the left reflection coefficient $R(q)$,

$$B(x) = \frac{1}{2\pi} \int_{-\infty}^{\infty} dq\, e^{-iqx} R(q) \quad \text{for} \quad x > 0, \tag{1}$$

$B(x) = 0$ for $x < 0$, in the Marchenko integral equation

$$K(x,y) + B(x+y) + \int_{-x}^{x} dz\; B(z+y)K(x,z) = 0 \quad \text{with} \quad x > y \tag{2}$$

and solving for $K(x,y)$; the potential is then given by

$$V(x) = 2dK(x,x)/dx \quad \text{for} \quad x > 0, \tag{3}$$

$V(x) = 0$ for $x < 0$. The solution is found numerically by the method of Galerkin using B-spline polynomials (cf. Reinhardt (1985)).

Padé Solution. When the range of integration is large, the direct solution of Eq. (2) becomes unstable, and it may be more convenient to use the method of Padé approximants,

$$\begin{aligned} K_0(x,y) &= -B(x+y) \\ K_n(x,y) &= -\int_{-x}^{x} dz K_{n-1}(x,z)B(z+y), \qquad n = 1,\ldots,M. \end{aligned} \tag{4}$$

This leads to

$$K(x,y) = \frac{\sum_{n=0}^{N} C_n(x,y)}{1 + \sum_{n=1}^{N} D_n(x,y)}, \tag{5}$$

where C_n and D_n are found from the equations

$$\sum_{m=1}^{N} K_{N+n-m}(x,y)D_m(x,y) = -K_{N+n}(x,y),$$
$$\sum_{m=0}^{N} K_{n-m}(x,y)D_m(x,y) = C_n(x,y), \tag{6}$$

with $C_0(x,y) = K_0(x,y)$, $D_0(x,y) = 1$ and $n = 1, \cdots, N$.

Example: Complex barrier with substrate. We present an example modelled on a realistic case, two double-layers of iron and silver on an infinitely thick glass substrate (cf. Fig. 1). In the numerical evaluation of the integral in Eq. (1) one must introduce a cut-off q_c. For a short cut-off, $q_c = 1$ nm^{-1}, the Marchenko solution and the potential obtained with the help of a (9,9)-Padé approximant are practically identical (cf. Fig. 1a); the expected oscillations of period $(\pi/q_c) = 3.14$ nm are visible in the real part. After averaging over these oscillations the Marchenko solution is seen to reproduce the original potential. For a long cut-off, $q_c = 6$ nm^{-1}, the Marchenko solution can only be found with adequate accuracy at high computational expense. However, when a (9,9)-Padé approximant is used, the reconstructed potential reproduces the original potential to good accuracy (cf. Fig. 1b).

2.2 Two-Step Inversion with Background Potential

For thick samples (compared to the wavelength) the reflection coefficient contains the rapid so-called Kiessig oscillations resulting from the interference of the waves reflected from the front and back sides. This applies also to thin samples mounted on a thick substrate, e.g. a silicon wafer. These oscillations make a numerical calculation of the integral (1) impossible; however, they can be taken into account analytically in the full reflection coefficient $R(q)$ via a known background scattering potential $V^0(x)$ representing the substrate.

We introduce the rapidly oscillating reflection coefficient for the substrate alone,

$$R_0(q) = -a\frac{1 - \exp(2\mathrm{i}\overline{q}d)}{1 - a^2\exp(2\mathrm{i}\overline{q}d)}, \tag{7}$$

where $a = a(q) = (\overline{q} - q)/(\overline{q} + q)$ is the Fresnel coefficient for the substrate, d is its thickness, and $\overline{q}$ is the wave number in the substrate. The exponential $\exp(2\mathrm{i}\overline{q}d)$ gives rise to Kiessig oscillations of period π/d. However, the difference

$$\widetilde{R}(q) = R(q) - R_0(q) \tag{8}$$

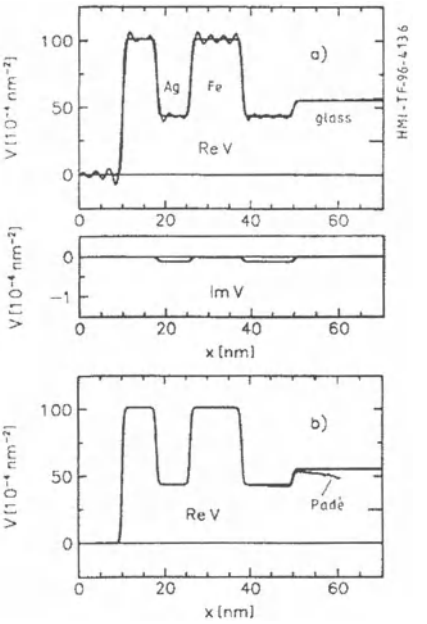

Fig. 1. Reconstruction of an iron-silver double-layer structure on a glass substrate. (a) The real and imaginary parts of the original potential (heavy curve) and their reconstruction by the Marchenko solution with the cut-off $q_c = 1\ \mathrm{nm}^{-1}$ (thin curve); the reconstruction via a (9,9) Padé approximant coincides with the Marchenko solution. (b) The real part of the original potential and its reconstruction via a (9,9) Padé approximant with the cut-off $q_c = 6\ \mathrm{nm}^{-1}$.

exhibits these oscillations only weakly.

The inversion formalism has been derived by Ghosh Roy (1991) and Reiss (1995). Instead of the Fourier transform (1) one defines

$$\widetilde{B}(x,y) = \frac{1}{2\pi} \int_{-\infty}^{\infty} dq f_0(q,x) f_0(q,y) \widetilde{R}(q), \tag{9}$$

where the function $f_0(q,x)$ is the Jost solution for the substrate. The quantity $\widetilde{B}(x,y)$ replaces $B(x,y)$ in the Marchenko equation (2), from whose solution $\widetilde{K}(x,t)$ one obtains the full potential in the form

$$V(x) = V^0(x) + 2d\widetilde{K}(x,x)/dx. \tag{10}$$

Example. An example of an inversion for a system consisting of a single layer on a substrate of finite thickness is shown in Fig. 2. The results of the

inversion with and without background potential coincide and reproduce the original potential in this example, where the substrate actually is rather thin (cf. Fig. 2a). However, the computing time in the first case is very much shorter than in the second. This has to do with the different structure of the input for the Marchenko equation: $\widetilde{R}(q)$ is smooth, whereas $R(q)$ is rapidly oscillating (cf. Fig. 2b). If we would consider a substrate with a realistic thickness of the order of a millimeter, the inversion with background potential could be carried out as easily as in the present case, but the inversion using the full reflection coefficient could not be done at all.

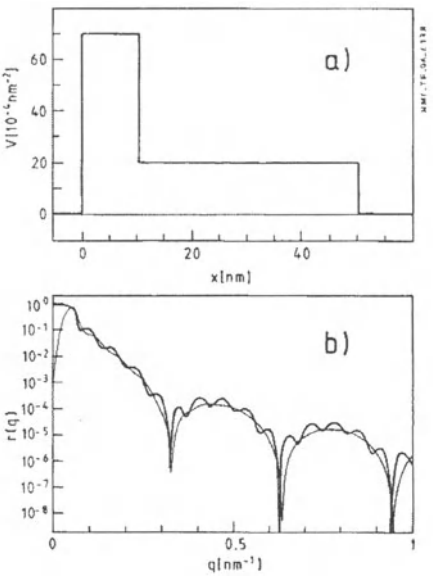

Fig. 2. Inversion with and without background potential. (a) The original potential for a single layer on a substrate of finite thickness; both types of inversion reproduce this potential. (b) The absolute square of the reflection coefficients $R(q)$ (heavy curve) and $\widetilde{R}(q)$ (thin curve).

3 Practical Applications and Their Problems

For the solution of the inverse scattering problem the complex reflection coefficient $R(q)$ must be known as a complex function of both positive and

negative values of the incident momentum q, cf. Eq. (1). On the other hand, usually only the reflectivity $|R(q)|^2$ for $0 < q < q_c$ is measured, where q_c generally is the cut-off momentum, for which the reflectivity has become too small to be measured. The input for negative values of q and the reflection phase must therefore be obtained from additional information.

3.1 The Input of Momenta

We begin with some remarks on the range of momenta. The effect of the cut-off q_c has already been discussed in Sect. 2.1. As to the reflection coefficient for negative values of q, it is, for real potentials, simply given by the complex conjugate of the reflection coefficient for positive values (cf. Chadan and Sabatier (1982)), $R(-q) = R^*(q)$, but for complex potentials this must be generalized to (cf. Lipperheide et al. (1996))

$$R(-q) = [R(q)R_R(q) - (\overline{q}/q)T^2(q)]^{-1}R_R(q), \tag{11}$$

where $R_R(q)$ is the reflection coefficient for incidence from the right, and $\overline{q}$ is the momentum of the transmitted wave. We see that information on transmission and on reflection from the right (for $q > 0$) is required in order to determine the left reflection coefficient $R(q)$ for $q < 0$.

3.2 The Phase Problem

The phase problem has plagued structure research by x-ray, electron- or neutron-scattering for decades (cf. Ross et al. (1988), Worcester (1991), Kramer (1991), Sivia et al. (1991), Klibanov and Sacks (1992), Fiedeldey et al. (1992), Pershan (1994), Lipperheide et al. (1995b)). The simulation approach represents the only means of determining potentials in the absence of phase information. In general it is non-unique, since different profiles may produce the same reflectivity. An inversion procedure, on the other hand, cannot even be started without phase information.

The Reduction of the Problem. Some insight into the phase problem can be gained by observing that the reflection phase is not strictly independent of the reflectivity owing to the analytic properties of the complex reflection coefficient. For a real potential which vanishes on the negative half-axis, $V(x) = 0$ for $x < 0$, and supports no bound states (this corresponds to most actual situations in neutron and x-ray reflectometry), the left reflection coefficient $R(q)$ is analytic in the upper q-plane (cf. Ross et al. (1988), Klibanov and Sacks (1992), Chadan and Sabatier (1982)). It can be written in the form

$$R(q) = \prod_{n=1}^{N} \left(\frac{q - a_n}{q - a_n^*} \frac{q + a_n^*}{q + a_n} \right) R_H(q) = A(q)R_H(q), \tag{12}$$

where we have introduced the Hilbert reflection coefficient

$$R_{\mathrm{H}}(q) = |R(q)| \exp[\mathrm{i}\,\phi_{\mathrm{H}}(q)] \tag{13}$$

with the 'Hilbert-phase' $\phi_{\mathrm{H}}(q)$ given, for real potentials, by

$$\phi_{\mathrm{H}}(q) = -\pi - \frac{2q}{\pi}\,\mathcal{P}\int_0^\infty \frac{\ln|R(q')|}{q'^2 - q^2}\,dq'. \tag{14}$$

Thus the Hilbert factor $R_{\mathrm{H}}(q)$ is completely determined by the reflectivity $|R(q)|^2$, whereas the rational phase factor $A(q)$ involving the zeros a_n of $R(q)$ in the upper half-plane is unknown in the absence of phase data.

The phase problem thus reduces to the problem of the zeros a_n, which represent the remaining ambiguity in the solution of the inverse scattering problem. Only a small number of them are expected to play a significant role.

It is convenient to treat only the Hilbert reflection coefficient $R_{\mathrm{H}}(q)$ in Eq. (12) by Marchenko inversion, yielding the Hilbert potential $V_{\mathrm{H}}(x)$. The rational phase factor $A(q)$ corresponds to a Darboux transformation, and leads to the full potential $V(x)$ via the iterative scheme (cf. Chadan and Sabatier (1982), Fiedeldey et al. (1992), Reiss and Lipperheide (1996))

$$\begin{aligned} V_0(x) &= V_{\mathrm{H}}(x), \\ V_n(x) &= V_{n-1}(x) - 2\frac{d^2}{dx^2} \ln \mathrm{Im}\,[f_{n-1}(a_n, x)\frac{d}{dx} f_{n-1}(-a_n^*, x)], \\ V(x) &= V_N(x), \end{aligned} \tag{15}$$

$n = 1, \ldots, N$. The function $f_{n-1}(q, x)$ is a Jost solution for the potential $V_{n-1}(x)$. The two potentials $V_{\mathrm{H}}(x)$ and $V(x)$ yield the same reflectivity but different reflection phases.

In order to illustrate the distribution of zeros, we consider neutron reflection by the two-step potential $V(x)$ shown in Fig. 3. (cf. Crowley et al. (1991)), which gives rise to the zeros $a_n \approx (2n+1)(\pi/4) + \mathrm{i}\,0.173$. Here the Hilbert potential $V_{\mathrm{H}}(x)$ arising from the inversion of the Hilbert reflection coefficient $R_{\mathrm{H}}(q)$ is not identical with the original potential $V(x)$ because of the presence of the zeros.

Including the first, the first two, and the first ten pairs of zeros in the inversion yields the potential curves labeled 1, 2, and 10 in Fig. 3. It is seen that supplementing the Hilbert reflection coefficient with the 'missing zeros' leads back to the original potential. The 'reflectivity-independent' phase information is vested in a finite number of complex zeros.

Example: X-ray reflection by liquid gallium. For an example we consider a recent analysis of the surface of liquid gallium using x-ray reflection (cf. Regan et al. (1995)). Here a peak of the reflectivity at incident momentum $q_{\mathrm{p}} \approx 12\ \mathrm{nm}^{-1}$ has been interpreted as a quasi-Bragg peak generated

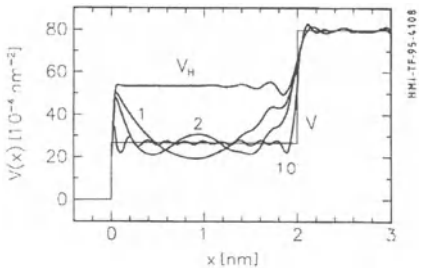

Fig. 3. A potential $V(x)$, the corresponding Hilbert potential $V_{\mathrm{H}}(x)$, and the potentials arising from the inclusion of the first, the first two, and first ten zeros of the reflection coefficient.

by a surface layering of the density with spacing $d = (\pi/q_{\mathrm{p}}) \approx 0.26$ nm. A good fit can be obtained using the potential represented by the thin curve in Fig. 4.

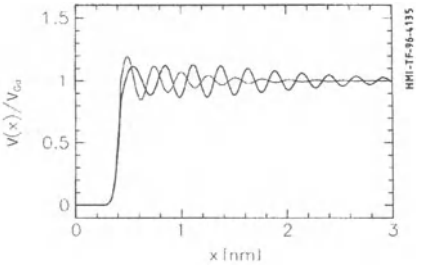

Fig. 4. The normalized potential profile for x-ray reflection by liquid gallium. Two profiles are shown which yield the same reflectivity. The profile represented by the thin curve is changed into that given by the heavy curve when the pair of zeros $(\pm 12.27 + \mathrm{i}\,0.73)$ is included in the reflection coefficient.

However, this potential is not unique. Taking the reflection coefficient calculated from it as $R(q)$, a new reflection coefficient $R^1(q)$ can be defined by applying relation (12) with a single pair of zeros $a = \pm 12.27 + \mathrm{i}\,0.73$. The profile corresponding to $R^1(q)$, as calculated by the procedure (15), has the form shown by the heavy curve in Fig. 4. It differs from the original profile in that it is shifted and less damped. Nevertheless, in the absence of any further physical arguments, it appears to be as acceptable as the original profile.

The scheme discussed above is useful for testing the 'physical uniqueness' of simulated profiles fitting measured reflectivities. It represents a step in the

direction of a systematic and complete investigation of the well-recognized but often somewhat recondite phase ambiguities. The complete phase problem can be resolved only with the help of actual measurements of the phase.

Measurement of the Phase. Several proposals have been made for measurement of the reflection phase. Sivia et al. (1991) and Gudkov et al. (1993) consider a reference layer method where the reflection phase is determined via the interference with the reflection from a known reference layer; this method is used in optics and can also be applied to neutron and x-ray scattering. Allman et al. (1994) propose a 'Lloyd's mirage' technique which makes use of the interference with a coherent reference beam. Finally, a method for neutron scattering has been investigated where the relation between the reflection phase and the 'dwell time' of the neutron in the sample (measured via absorption) is exploited (cf. Fiedeldey et al. (1992)).

In the following we examine a very promising method using polarized neutrons, which has recently been proposed by two groups (cf. Majkrzak and Berk (1995), de Haan et al. (1995)). We consider an arrangement (cf. Fig. 5) where the potential $V(x)$ of the sample (assumed to vanish for $x < a$) is super-imposed by the potential

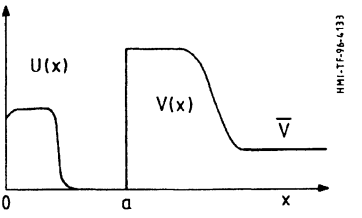

Fig. 5. An arrangement for measuring the complex reflection coefficient of the sample represented by the potential $V(x)$, super-imposed by a 'magnetic potential' $U(x)$. The substrate is represented by the potential $\overline{V}$.

$$U(x) \propto \boldsymbol{\sigma} \cdot \mathbf{B}(x), \tag{16}$$

$U(x) = 0$ for $x < 0$, generated by an external magnetic field $\mathbf{B}(x)$, and which depends on the polarization $\sigma_z = \pm 1$ of the incident neutron. The 'magnetic potential' may be due to a magnetic field in vacuum or to the magnetization in e.g. a cobalt layer in front of the sample. The total reflection coefficient for $\sigma_z = \pm 1$ and $\mathbf{B}(x) = |\mathbf{B}(x)|\,\hat{z}$ is

$$R_{\pm}(q) = \frac{\eta^{\pm}(q)R(q)\exp(2iaq) + \rho_{\mathrm{L}}^{\pm}(q)}{1 - R(q)\exp(2iaq)\rho_{\mathrm{R}}^{\pm}(q)} \tag{17}$$

where $R(q)$ is the reflection coefficient of the sample alone, $\rho_{\mathrm{L,R}}^{\pm}$ and $\tau_{\mathrm{L,R}}^{\pm}$ are the (left, right) reflection and transmission coefficients for the magnetic potential alone, and

$$\eta^{\pm}(q) = \tau_{\mathrm{L}}^{\pm}(q)\tau_{\mathrm{R}}^{\pm}(q) - \rho_{\mathrm{L}}^{\pm}(q)\rho_{\mathrm{R}}^{\pm}(q). \tag{18}$$

The measured total reflectivity is given by $|R_{\pm}(q)|^2$. Equation (16) then yields

$$|\eta^{\pm}(q)R(q)\exp(2iaq) + \rho_{\mathrm{L}}^{\pm}(q)|^2 = |1 - R(q)\exp(2iaq)\rho_{\mathrm{R}}^{\pm}(q)|^2|R_{\pm}(q)|^2, \tag{19}$$

and one can extract the complex reflection coefficient of the sample, $R(q)$, from measurements of $|R_{\pm}(q)|^2$ for three different magnetic fields $B(x)$ or shifts a.

This method has two limitations. For $q^2 < \overline{V}$, i.e. below the critical momentum of the substrate, one has $|R(q)| = |R_{\pm}(q)| = 1$. It can be shown that in this case Eq. (19) does not yield any information on the phase of $R(q)$. Second, the Kiessig oscillations associated with the exponential $\exp(2iaq)$ will destroy the phase information on $R(q)$ if a is larger than the inverse of the experimental error in q.

These limitations can be removed in principle when, instead of the reflectivities, one considers the polarisations of the reflected neutrons, and when the magnetic field is allowed to enclose the entire sample (cf. Leeb et al. (1996)).

4 Summary

The application of the one-dimensional inverse scattering problem to neutron and x-ray specular reflection has been discussed. A numerical algorithm is proposed which allows one to treat scattering samples on substrates. The phase problem is reduced to the problem of a discrete set of parameters, and proposals for measuring the reflection phase are critically examined. All these problems show promise of practical solution in the near future, so that analyses of reflection experiments by model-independent and unique inversion can hopefully be carried out in the near future.

References

Allman B. E., Klein A. G., Nugent K. A., and Opat G. I. (1994) *J. Appl. Opt.* **33** 1806. .

Chadan K. and Sabatier P. C. (1982), *Inverse Problems in Quantum Scattering Theory*, 2nd edition, Springer, Berlin.

Corvi M. (1992), in *Inverse Problems in Scattering and Imaging*, Bertero M. and Pike E. R., Eds., Hilger, Bristol, Philadelphia, New York, p. 411.

Crowley T. L., Lee E. M., Sinister E. A., and Thomas R. K. (1991), *Physica* **B 173**, 143.

de Haan V. O., van Well A. A., Adenwalla S. and Felcher G. P. (1995), *Phys. Rev.* **B 52**, 10831.

Fiedeldey H., Lipperheide R., Leeb H. and Sofianos S. A. (1992), *Phys. Lett.* **A 179**, 347.

Ghosh Roy D. N. (1991), *Methods of Inverse Problems in Physics*, CRC Press, Boston.

Gudkov V. P., Opat G. I. and Klein A. G. (1994), *J. Phys.: Condensed Matter* **5**, 9013.

Kay I. (1960), *Comm. Pure and Applied Math.* **13**, 371.

Kjaer K. and Als-Nielsen J. (1988), *Thin Solid Films* **159**, 17.

Klibanov M. V. and Sacks P. E. (1992), *J. Math. Phys.* **33**, 3813.

Kramer E. J. (1991), *Physica* **B 173**, 189.

Leeb H., Lipperheide R., and Kasper J. (1996), to be published.

Lipperheide R., Reiss G., Leeb H., Fiedeldey H., and Sofianos S. A. (1995a), *Phys. Rev.* **B 51**, 11032.

Lipperheide R., Fiedeldey H., Leeb H., Reiss G., and Sofianos S. A. (1995b), *Physica* **B 213&214**, 914.

Lipperheide R., Reiss G., Leeb H. and Sofianos S. A. (1996), *Physica* **B 221**, 514.

Majkrzak C. F. and Berk N. F. (1995), *Phys. Rev.* **B 52**, 10827.

Pendry J. B., Heinz K., and Oed W. (1988), *Phys. Rev. Lett.* **61**, 2953.

Penfold J. and Thomas R. K. (1990), *J. Phys. Cond. Matter* **2**, 1369.

Pershan P. S. (1994), *Phys. Rev.* **E 50**, 2369.

Pershan P. S. (1996), Proc. Materials Research Society, Boston, MA, ed. B. J. Wuensch (to appear in vol. 376 of the Materials Research Society).

Regan M. J., Kawamoto E. H., Lee S., Pershan P. S., Maskil N., Deutsch M., Magnussen O. M., Ocko B. M., and Berman L. E. (1995), *Phys. Rev. Lett.* **75**, 2498.

Reinhardt H.-J. (1985), *Analysis of Approximation Methods for Differential and Integral Equations*, Springer Ser. Appl. Math. Sci. **57**, Springer, Berlin.

Reiss G. (1995), Ph.D.-Thesis, Freie Universität Berlin.

Reiss G. and Lipperheide R. (1996), *Phys. Rev.* B **53**, 8157.

Ross G., Fiddy M. A., and Nieto-Vesperinas M. (1988), in *Inverse Scattering Problems in Optics*, Baltes H. P., Editor, Springer, Berlin.

Russel T. P. (1990), *Materials Science Reports* **5**, 171.

Sacks P. E., *Wave Motion* **18**, 21.

Sears V. F., *Neutron Optics*, Oxford University Press, Oxford, 1989.

Sivia D. S., Hamilton W. A. and Smith G. S. (1991), *Physica* **B173**, 121.

Worcester D. L. (1991), *Physica* B **173**, 139.

Non-standard Information in Optical Model Analyses

H. Leeb[1], H. Huber[1], B. Apagyi[2]

[1] Institut für Kernphysik, Technische Universität Wien, Wiedner Hauptstr. 8-10/142, A-1040 Wien, Austria
[2] Department of Theoretical Physics, Technical University of Budapest, Budafoki ut 8, Budapest, Hungary

Abstract. At the example of ^{12}C–^{12}C elastic scattering it is shown that the S-matrix at non-integer values of the orbital angular momentum quantum number contains valuable information which should be taken into account in the analysis of scattering data at fixed energy. The possibility of the available global inversion procedures to include such non-standard S-matrix values is discussed. Specifically, an extended Newton–Sabatier method based on the interpolation formulae of Sabatier is worked out and subsequently used to demonstrate the role of this information to reduce the inherent ambiguities of the inverse scattering problem at fixed energy.

1 Introduction

In the last two decades there has been considerable progress in the measurement and understanding of nuclear scattering processes. Nowadays, measurements of the elastic scattering cross sections can be performed with high accuracy (see e.g. [1]). A similar step forward has been achieved in the theoretical description of nuclear processes [2]. A basic tool of the theory is the optical potential which is a complex effective two-body interaction describing the elastic scattering explicitly.

Because of its basic role there has been many attempts to evaluate optical potentials microscopically [3]. The proper treatment of the multi-nucleon system, however, is rather difficult and our knowledge about the optical potential is far from being satisfactory. Among the various approaches the folding potentials based on different theoretically motivated nucleon-nucleon potentials are working best. In general they yield a satisfactory description of the gross structure but fail to reproduce details of the observed elastic cross sections.

An alternative way to determine optical potentials is the analysis of elastic scattering data. In the standard notation this is called an inverse problem at fixed energy. Most of this so-called optical model analyses are performed via simulation, where the parameters of a reasonable potential ansatz are adjusted in order to describe the experimental data. There exists a great variety of such simulations ranging from simple potential fits [5], [6] to rather

sophisticated procedures [7]. A common feature of all these methods is their uncontrollable trajectory in the parameter hyperspace and consequently their unknown dependence on the starting values. Hence, they are denoted as *local inversion procedures* [8].

An elegant and more fundamental way to determine optical potentials from scattering data is given by the use of *global inversion procedures.* They are characterized by an analytically known relationship between S-matrix and potential. In the fifties and sixties many solutions of various inverse problems in quantum scattering theory have been given by mathematical physicists [9], [10], [11], [12]. These solutions, however, are mathematically rather involved and the formulation of manageable numerical algorithms has only been started at the beginning of the eighties. In the last decade considerable progress has been achieved and many successful applications to experimental data underline the increasing importance of global inversion methods [13], [14], [15].

The determination of optical potentials from scattering data at a single energy is far from being unique. In principle there are two sources of ambiguities. The first one is related to the determination of the S-matrix from scattering data because the observables do not contain the complete phase information. The second source of ambiguity is the fact that observables at a single energy yield the S-matrix only at a finite number of integer values of the orbital angular momentum quantum number ℓ. From scattering theory it is well known that this is not sufficient to determine a unique potential [16].

In this paper we deal with the latter type of ambiguity which represents an inherent difficulty in all inverse scattering problems at fixed energy. In particular we will show in section 2 at the example of ^{12}C–^{12}C scattering that values of the S-matrix at non-integer ℓ–values contain important information on the potential. Such values of the S-matrix can easily be included in the global inversion scheme of Lipperheide and Fiedeldey [17] as well as in the semiclassical WKB-method. At present the standard matrix method of Newton–Sabatier [11] which is best suited for analyses at lower energies cannot include the S-matrices at non-integer ℓ-values. Therefore adapting properly the interpolation formulae of Sabatier [18] we present in section 3 an extended Newton–Sabatier method for central potentials which includes the S-matrix also at the half-integer ℓ-values. Section 4 is devoted to various applications of this method in order to demonstrate the importance of such non-standard S-matrix values. Finally, concluding remarks are given in section 5.

2 The inherent ambiguity of inversions at fixed energy

The inverse scattering problem in quantum mechanics at fixed energy deals with the determination of the potential from the knowledge of the associated S-matrix at a given energy. In principle it is a specific spectral problem based

on the radial Schrödinger equation,

$$\left\{\frac{d^2}{d\rho^2} - \frac{\lambda^2 - \frac{1}{4}}{\rho^2} + 1 - U(\rho)\right\} \Phi(\rho;\lambda) = 0\,, \tag{1}$$

where $\rho = kr$ with k being the wave number, $V(\rho/k) = EU(\rho)$ is the potential, E is the center of mass energy, and λ is related to the orbital angular momentum quantum number ℓ by $\lambda = \ell + \frac{1}{2}$. Since we are considering inverse scattering problems at fixed energy we will suppress the k– and E–dependence of the various functions in the following. For the description of scattering processes the so–called regular solution $\Phi(\rho;\lambda)$ of Eq. (1) is of interest. This solution vanishes at the origin and is therefore uniquely defined apart of its normalisation. At asymptotic distances the regular solution can be written as a superposition of regular and irregular Coulomb functions $F(\rho;\lambda,\eta)$ and $G(\rho;\lambda,\eta)$, respectively. Hence $\Phi(\rho;\lambda)$ takes the form

$$\Phi(\rho;\lambda) \underset{r\to\infty}{\longrightarrow} A(\lambda)\left[(S(\lambda)+1)\,F(\rho;\lambda,\eta) + (S(\lambda)-1)\,G(\rho;\lambda,\eta)\right]\,, \tag{2}$$

where η is the Sommerfeld parameter and $A(\lambda)$ is an arbitrary amplitude factor. The asymptotic behaviour of $\Phi(\rho;\lambda)$ is characterized by the S-matrix $S(\lambda)$. From the mathematical point of view there is no restriction on the values of λ and k and for arbitrary complex values of these quantities a regular solution can be given.

Optical model analyses aim at the determination of optical potentials from the knowledge of the scattering observables at a given energy. Let us assume that we can extract the corresponding values of the S-matrix uniquely. Thus the inverse scattering problem at fixed energy is reasonably posed and several solutions have been given in the literature [12]. An important question with regard to the central goal of the present paper is the question of uniqueness of the inverse problem at fixed energy. Already in 1968 Loeffel [16] could show that the potential is uniquely defined, if the S-matrix is known for $\mathrm{Re}\lambda \geq 0$.

The theorem of Loeffel reflects the mathematical structure of the radial Schrödinger equation but does not correspond to the situation of an analysis of scattering data at a given energy in terms of an optical potential. This can easily be seen from the calculations of cross sections in quantum mechanics. For simplicity we restrict ourselves again to the scattering of spinless particles with central interactions. In this case the scattering amplitude,

$$f(\theta) = \frac{1}{2ik}\sum_{\ell=0}^{\infty} 2\lambda\,[S(\lambda)-1]\,P_\ell(\cos(\theta))\,, \tag{3}$$

depends only on the scattering angle θ and the S-matrix at the half-integer values of λ. Hence, it is obvious that scattering observables yield information only on these specific values of the S-matrix which are often denoted as the standard or physical ones. The S-matrix at other values of the argument is

not directly accessible to experiment at the given energy and these values are therefore called, in what follows, non-standard or unphysical.

In practice elastic scattering data determine S-matrix values only at a finite number of half-integer λ-values. This is not sufficient to extract unique potentials from such analyses. Further assumptions about the S-matrix at non-standard λ-values are required to improve the situation and to associate a reliable potential with the scattering data. In a rather hidden and uncontrollable way this is done in local inversion procedures via the ansatz of a parametrized class of potentials. In global inversion procedures based on exactly solvable models [11], [17], [9] these assumptions become more evident because they yield classes of S-matrices defined on the whole complex λ-plane. The situation becomes particularly clear for the rational scheme [17], where parameters (α_i, β_i) of the explicitly given S-matrix,

$$S(\lambda) = S_0(\lambda) \prod_{i=1}^{N} \frac{(\lambda^2 - \beta_i^2)}{(\lambda^2 - \alpha_i^2)}, \tag{4}$$

are adjusted to reproduce the scattering data. Here $S_0(\lambda)$ is the S-matrix corresponding to an appropriately chosen background potential V_0. Because of the specific analytic form the values of the S-matrix at the half-integer λ-values determine the parameters (α_i, β_i) and thus the S-matrix in the complex λ-plane. Hence, the application of different exactly solvable models to the same scattering data can lead to different potentials.

In the following we give an example where this feature of exactly solvable models shows up. We consider the analysis of ^{12}C–^{12}C phase shift data which have been extracted from experimental cross sections measured by Ledoux et al. [20]. An extensive study of the associated potentials obtained in the so–called Newton–Sabatier inversion method has been given by May and Scheid [14]. In this system there is a quasi–molecular resonance which lead to a characteristic structure of the phase shifts. At $E_{cm} = 18.5$ MeV this resonance affects the behaviour of the phase shifts in the vicinity of $\ell = 11$ which, however, cannot be seen in experiment at this energy because of the identity of the colliding particles. Therefore, May and Scheid [14] employed the Newton–Sabatier inversion scheme assuming different values of the S-matrix at $\ell = 11$ and obtained the potentials denoted by MS in Fig. 1. For comparison we have used the same phase shift data in the mixed inversion scheme of Lipperheide and Fiedeldey (see e.g. [13]). In Fig. 1 the corresponding potentials are compared with the results of the Newton–Sabatier method of May and Scheid [14]. In the case of $\delta_{11} = 57.3$ degrees both methods lead to rather similar potentials. Under the assumption of $\delta_{11} = 174.2$ degrees a huge difference of the potentials is observed. Because the S-matrix at standard λ-values is equally reproduced by the potentials of both procedures this difference is related to the different behaviour of the phase shifts at non-standard λ-values.

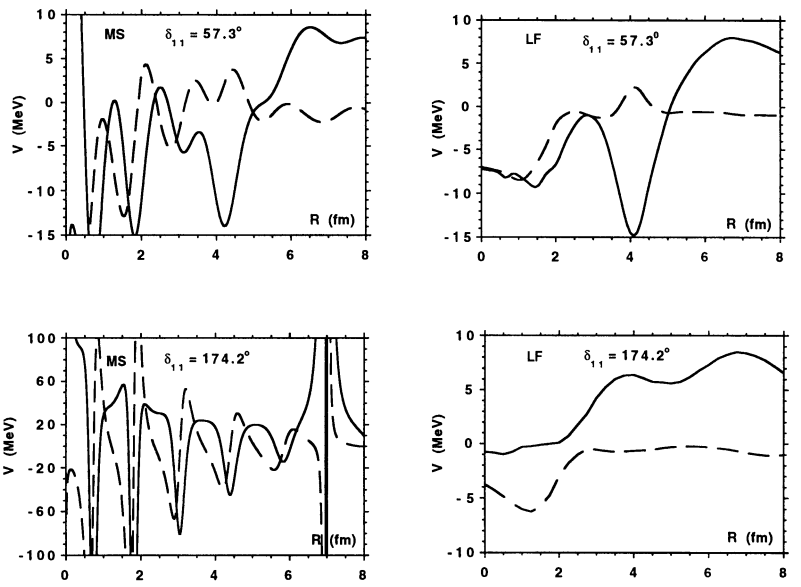

Fig. 1. Potentials obtained by inversion of ^{12}C–^{12}C phase shift data of Ledoux et al. [20] at $E_{c.m.} = 18.5$ MeV assuming different values of the phase shift at $\ell = 11$. The potentials of May and Scheid [14] are compared with those obtained by the mixed scheme of Lipperheide and Fiedeldey [17] .

3 Extended Newton–Sabatier method

The inclusion of additional information concerning the S-matrix at non half-integer λ-values into global inversion procedures will be an important step to gain reliability of the extracted potentials. As far as we know all applications of global inverse scattering methods to optical model analyses of experimental data are based either on semiclassical approximations or exactly solvable models. The latter are derived from Darboux transformations [9] of the radial Schrödinger equation and include the well known methods of Lipperheide and Fiedeldey [17] and the matrix method of Newton and Sabatier [11]. The rational and nonrational schemes of Lipperheide and Fiedeldey [17] are characterized by rather simple analytical forms of the S-matrix with open parameters. It is a straightforward extension to adjust these parameters to the S-matrix not only at the standard but also at non-standard λ-values. The same is true for the semiclassical WKB-potential [21] where an analytical form of the S-matrix is required to evaluate the associated quasi–potential.

Both methods work best at rather high energies but lead to difficulties in analyses of low energy data. At lower energies the matrix method of Newton

and Sabatier [11] is well suited and many successful applications of this procedure have been reported in the literature [22]. This method is based on the fundamental relation (see e.g. [12], chapters XI and XII)

$$\Phi(\rho;\lambda) = u(\rho;\lambda) - \int_0^\rho d\rho' K(\rho,\rho') u(\rho';\lambda)\,, \tag{5}$$

where $\Phi(\rho;\lambda)$ and $u(\rho;\lambda)$ are physical solutions associated with the interactions $U(\rho)$ and $U_0(\rho)$, respectively. The so-called transformation kernel $K(\rho,\rho')$ satisfies the integral equation

$$K(\rho,\rho') = Q(\rho,\rho') - \int_0^\rho ds s^{-2} K(\rho,s) Q(s,\rho') \tag{6}$$

and depends on the S-matrix of the unknown potential $U(\rho)$ via the spectral kernel $Q(\rho,\rho')$. The potential $U(\rho)$ can be obtained from $K(\rho,\rho')$ via,

$$U(\rho) = U_0(\rho) - \frac{2}{\rho}\frac{d}{d\rho}\left[\frac{1}{\rho}K(\rho,\rho)\right]\,, \tag{7}$$

thus solving the inverse scattering problem.

It is the basis of matrix methods [12], [9] to assume for the spectral kernel the separable form

$$Q(\rho,\rho') = \sum_{\lambda\in\Omega} c_\lambda u(\rho;\lambda) u(\rho';\lambda)\,, \tag{8}$$

where Ω may be any set of numbers in the half plane $\mathrm{Re}\lambda > -\frac{1}{2}$, provided that the summation of Eq. (8) exists. As can easily be seen from Eq. (6) this specific form of $Q(\rho,\rho')$ results in the separable transformation kernel

$$K(\rho,\rho') = \sum_{\lambda\in\Omega} c_\lambda \phi(\rho;\lambda) u(\rho';\lambda)\,. \tag{9}$$

Entering this expression in Eq. (5) yields reformulated equations for the wave functions

$$\Phi(\rho;\lambda) = u(\rho;\lambda) - \sum_{\lambda\in\Omega} c_\lambda L(\rho;\lambda,\lambda')\Phi(\rho;\lambda') \tag{10}$$

with

$$L(\rho;\lambda,\lambda') = \int_0^\rho ds s^{-2} u(s;\lambda) u(s;\lambda')\,. \tag{11}$$

This system of coupled equations, Eqs. (11,12), is used to determine the potential coefficients c_λ from the asymptotic behaviour of the wave function and thus from the S-matrix. For a set Ω with a finite number of elements it has been shown recently [9] that these matrix methods represent a subclass of Darboux transformations of Eq. (1).

The set Ω of the standard Newton–Sabatier method consists of all positive half–integer λ–values, $\Omega = \{\frac{1}{2}, \frac{3}{2}, \frac{5}{2}, \cdots\}$. Hence, only the S-matrix at so–called standard λ–values enter the (standard) Newton–Sabatier inversion.

To achieve our goal and to include the S-matrix also at non-standard values in a matrix inversion method we must extend the set Ω to contain also non-standard λ–values. In the following we consider the specific set Ω involving positive integers and half–integers which has been discussed by Sabatier [23].

The implementation of non-standard S-matrix values in the numerical procedure is performed analogously to the standard Newton–Sabatier method via Eqs. (2) and (11). In order to obtain a unique solution of Eq. (11) we employ the same modification as Münchow and Scheid [24] and assume that the potential for $r > r_0 = \rho_0/k$ either vanishes or is equal to the Coulomb potential from the scattering system. Consequently, the wave functions for $\rho > \rho_0$ are given by Eq. (2) and the system of coupled linear equations for the potential coefficients c_λ, Eq. (11), can be written down for several ρ–values with $\rho > \rho_0$. We solve this overdetermined system of equations for the potential coefficients c_λ by a least square method. The potential coefficients c_λ obtained are then used to evaluate $\phi(\rho;\lambda)$ and the potential $U(\rho)$ for $0 \leq \rho \leq \rho_0$.

In principle the method is a straightforward extension of the procedure of Münchow and Scheid [24]. We face the additional problem, however, that we must provide the Coulomb functions at non-standard λ–values. For this purpose the code COULFG [25], which has the required options, has been used for the examples discussed in section 4.

4 The importance of the S-matrix at non-standard λ-values

The possibility to include non-standard S-matrix values in global inversion procedures enables us to study the effect of this additional information on the potential. We are not aware of any calculations in the recent literature which has studied this specific aspect with respect to its applicablity in analyses of scattering data. We focus our interest to the extended Newton–Sabatier method because in this inversion procedure the inclusion of non-standard λ–values is less obvious compared to inversion algorithms with an explicitly given analytic form of the S-matrix.

First of all we perform a comparison of the standard and the extended Newton-Sabatier method by schematic examples. This is particularly interesting for the inversion of scattering data at rather low energies, where only very few partial waves with their corresponding S-matrix values can be extracted from experiment with reasonable accuracy. Consequently the input information for the standard Newton–Sabatier method is rather limited and

one cannot expect reliable inversion potentials. The situation improves significantly in the extended Newton–Sabatier method because the input information is doubled.

To show the effect of the additional information we consider a schematic example of n-α scattering below $E_{Lab} = 100$ MeV where the spin–orbit term as well as the imaginary part have been ignored. For the real part we assume a Woods–Saxon shape with the parameters $V_0 = -41.8$ MeV, $R_0 = 2.365$ fm, and $a_0 = 0.25$ fm corresponding to the n–α parameters of Satchler et al. [26] at $E_{Lab} = 1$ MeV. Because of the rather small radial range the number of significant partial waves is smaller than 10 even at $E_{Lab} = 100$ MeV. Using this potential the phase shifts at standard and non-standard λ–values have been evaluated at several energies. These values have been used in inversion procedures. The reconstructed potentials obtained by the standard and the extended Newton–Sabatier method are displayed in Fig. 2 together with the original one. A comparison of the results clearly exhibits the improvement of the reproduction by the use of non-standard S-matrix values. The improvements are most striking at lower energies where only few partial waves can be used.

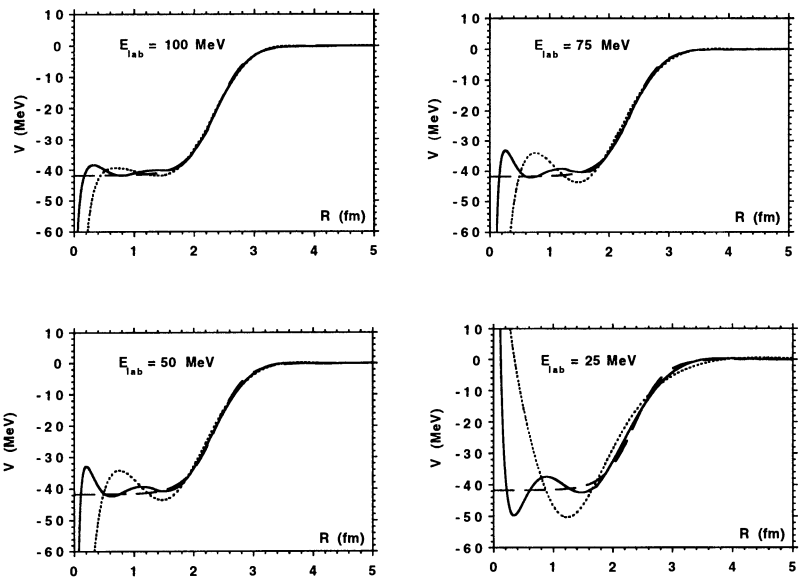

Fig. 2. Comparison of the reproduction of a schematic real n–α potential of Woods-Saxon form (dashed lines) from the phase shifts by inversion applying either the Newton-Sabatier method (dotted lines) or the extended Newton-Sabatier method (solid lines). The parameters of the original potential are given in the text.

The number of partial waves entering the analyses of heavy-ion scattering data is rather high even at low energies because of the large radial extension. One faces, however, the problem that the lowest partial waves are strongly absorbed and their phase shifts are not well determined from experiment. It is therefore worthwhile to study whether the additional information entering the extended Newton-Sabatier method will lead to an improved reconstruction of the potential also in this case. We consider therefore a schematic ^{12}C–^{12}C potential of Woods–Saxon form. The parameters have been chosen to be $V_R = 18.0$ MeV, $R_R = 2.315$ fm, $a_R = 0.73$ fm, $V_I = 2.5$ MeV, $R_I = 2.315$ and $a_I = 0.73$ which corresponds to the gross structure of the inversion potentials displayed in Fig. 1. Following the same procedure as above we apply the standard and the extended Newton-Sabatier method to the corresponding S-matrix. In this example sufficient scattering information is available and excellent reproduction is obtained by both inversion methods (Fig. 3). Considering the inversion potentials in detail the extended Newton-Sabatier method yields better results over the whole radial range. Both examples demonstrate the importance of additional S-matrix information to improve the reproduction of potentials. The suppression of the S-matrix at low ℓ-values by absorption does not change this finding.

The role of the information contained in the S-matrix at non-standard ℓ-values can easily be investigated by the extended Newton-Sabatier method. For this purpose we consider the example of ^{12}C–^{12} scattering at $E_{Lab} = 28$ MeV and assume slight modifications of the S-matrix at non-standard λ-values. To simplify the inversion calculations we restrict ourselves again to the Woods–Saxon potential with the parameters $V_R = 18.0$ MeV, $R_R = 2.315$ fm and $a_R = 0.73$ fm, $V_I = 2.5$ MeV, $R_I = 2.315$, $a_I = 0.73$, and the Coulomb radius $R_C = 3.7$ fm. This potential can reasonably be reproduced from the corresponding phase shift data by application of the standard as well as by the extended Newton–Sabatier method (Fig. 3). The modifications from the S-matrix $S_{WS}(\lambda)$ evaluated from the Woods–Saxon potential have been assumed as,

$$S_{mod}(\lambda) = S_{WS}(\lambda) \exp\left(2iA \sin((\lambda - \frac{1}{2})\pi) e^{-\frac{(\lambda-\lambda_0)^2}{\beta^2}}\right) \qquad (12)$$

where the parameters A, λ_0, and β determine the strength, the position and width of the modifications in λ-space. It is obvious that this specific form of the modifications does not change the S-matrix at integer ℓ-values, thus always leading to the same inversion potential in the standard Newton–Sabatier method. In order to demonstrate the effect of unphysical values we have fixed the parameters $\lambda_0 = 8$ and $\beta = 2$ and perform inversions by the extended Newton–Sabatier method varying the strength parameter A. The resulting potentials shown in Fig. 4 exhibit the strong dependence of the inversion potential on the so–called non-standard information. Thus it is obvious that reliable potentials via global inverse scattering procedures can only be obtained with inclusion of such additional information. This is particularly true

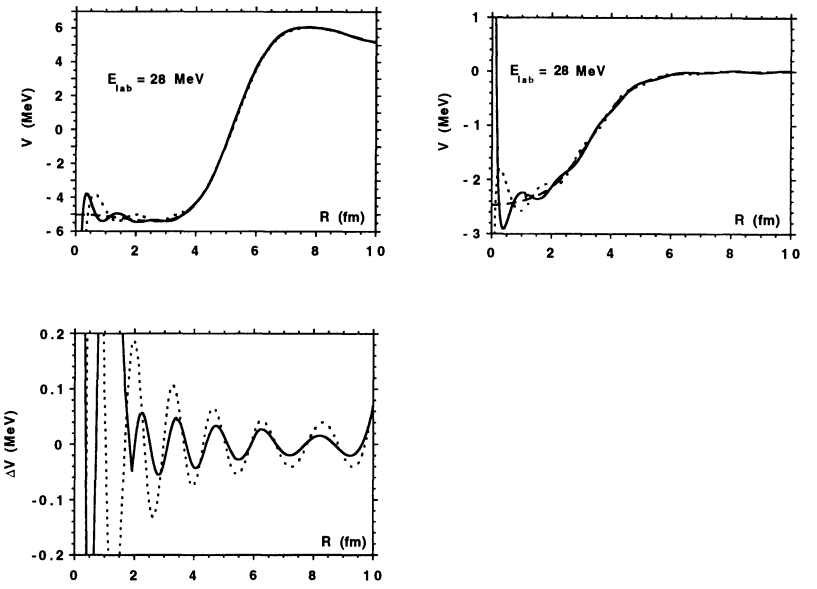

Fig. 3. Comparison of the reproduction of a complex ^{12}C–^{12}C potential of Woods-Saxon form (dashed lines) from the phase shifts at $E_{c.m.} = 28$ MeV by inversion applying either the Newton-Sabatier method (dotted lines) or the extended Newton-Sabatier method (solid lines). The parameters of the original potential are given in the text. The figure shows a) the real potential, b) the imaginary potential and c) the difference between the inverted and original real potentials.

for systems with identical particles where part of the usually accessible information is hidden by the symmetry properties of the scattering amplitude.

5 Conclusions

At the example of low energy ^{12}C–^{12}C scattering we have pointed out that the information contained in the S-matrix at non-standard λ-values is essential to determine uniquely potentials from phase shift data via inversion techniques. It is straightforward to include such S-matrix values into the WKB inversion method [21] as well as into the mixed inversion scheme of Lipperheide and Fiedeldey [17], which are best suited for applications at sufficiently high energies. At lower energies the Newton-Sabatier inversion method [11] has been successfully applied in the past, which in its standard version cannot take into account the behaviour of the S-matrix at non-standard λ-values.

To study the effect of additional information on the S-matrix at relatively low energies we have considered an extended Newton-Sabatier scheme which

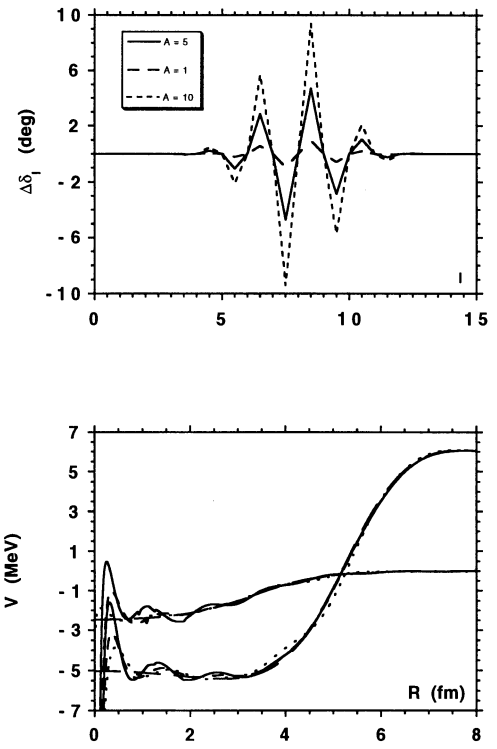

Fig. 4. Modification of the inversion potentials generated by changes of the ^{12}C–^{12}C scattering phase shifts at $E_{c.m.}$ = 28 MeV at non standard ℓ-values. The figure shows a) the modifications of the phase shifts, b) the inversion potentials.

is based on the knowledge of the S-matrix at integer and half-integer λ-values [23]. The application of this extended method is performed analogously to the inversion procedure introduced by Münchow and Scheid [24] assuming that the potential is known for large radii.

Although the method has already been given by Sabatier in 1967 we are not aware of any numerical application to nuclear scattering data. Our first calculations on schematic n–α- and ^{12}C–^{12}C-scattering data clearly indicate that there is an improved reproduction by the extended method compared to the standard one. In a further example we modified the S-matrix only at non-standard λ-values and applying the extended Newton-Sabatier procedure we could demonstrate the sensitivity of the potentials on this additional information.

Summarizing our results we can conclude that some knowledge about the behaviour of the S-matrix at non-standard λ-values is required to extract reliable optical potentials from scattering data at a single energy. This is particularly true for the theoretically formulated inversion method which takes into account central and spin-orbit terms [27]. Recently this method has been reformulated and implemented numerically [28] so that applications to optical potential analyses can be expected in the near future.

At this point there arises the important question, how to obtain reliable information on the S-matrix at non-standard λ-values. A promising way to gain this information seems to be a fit of a reasonably parametrized S-matrix to describe the cross sections at different energies simultaneously. Although only the S-matrix at half-integer λ-values enters into the fit at each energy one can expect to get a reliable interpolation for non-standard λ-values if cross section data at neighbouring energies are used. Because of the complex scattering phenomena in nuclear systems it is difficult to give a general form for the parametrisation of the S-matrix.

A severe problem will be the rather great sensitivity of the inversion potentials on the non-standard scattering information. Thus non suitable interpolations of the S-matrix may lead to oscillating potentials which are not useful for further calculations in nuclear physics. Apart from these difficulties the extended Newton-Sabatier method will be most valuable for low energies where only limited partial waves are significant.

Acknowledgements

This work was supported in part by Fonds zur Förderung der wissenschaftlichen Forschung in Österreich, project Nr. P10467-PHY, and by the partnership agreement between the Technical Universities of Budapest and Vienna. Support by OTKA (T17179) is also gratefully acknowledged.

References

[1] Stiliaris E., Bohlen H. G., Fröbrich P., Gebauer B., Kolbert D., Oertzen W. von, Wilpert M. and Wilpert Th. (1989) *Phys. Lett.* **B223**, 291.

[2] *Theoretical Nuclear Physics: Nuclear Physics*, John Wiley, New York 1992.

[3] Ray L., Hoffmann G. W. and Coker W. R. (1992) *Phys. Rep.* **212**, 223.

[5] Hodgson P., E., *The Optical Model of Elastic Scattering*, Clarendon Press, New York, 1962.

[6] Varner R. L. (1991), Phys. Rep. **201**, 57.

[7] Ioannides A. A. and Mackintosh R. S. (1987), *Nucl. Phys.* A **467**, 482.

[8] Sabatier P. C., in: *Advanced Methods in the Evaluation of Nuclear Scattering Data*, (Eds. H. J. Krappe and R. Lipperheide), (1985), *Lecture Notes in Physics* **236**, 1.

[9] Gel'fand I. M. and Levitan B. M. (1951), *Dokl. Akad. Nauk. USSR* **77**, 557, translated in (1955), *Am. Math. Soc. Transl. Ser.* **2**, 1, 253.
Marchenko V. A. (1955), *Dokl. Akad. Nauk. USSR* **104**, 695 translated (1956) in *Math. Rev.* **17**, 740.
[10] Burdet G., Giffon M., and Predazzi E. (1965), *Nuovo Cimento* **36**, 1337.
[11] Newton R. G. (1962), *J. Math. Phys.* **3**, 1, 75.
Newton R. G. (1967), *J. Math. Phys.* **8**, 8, 1566.
Sabatier P. C. (1966), *J. Math. Phys.* bf 7,8, 1515.
[12] Chadan K. and Sabatier P. C. (1982), *Inverse Problems in Quantum Scattering Theory*, 2nd edition, Springer, Berlin.
[13] Naidoo K., Fiedeldey H., Sofianos S. A. and Lipperheide R. (1984), *Nucl. Phys.* A **419**, 13.
Leeb H., Fiedeldey H. and Lipperheide R. (1985),*Phys. Rev.* **32**, 1223.
Allen L. J., Berge L., Steward C., Amos K., Fiedeldey H., Leeb H., Lipperheide R. and Fröbrich P. (1993), *Phys. Lett.* B **298**, 36.
[14] May K.-E. and Scheid W. (1987), *Nucl. Phys.* A **466**, 157.
[15] Kirst T., Amos K., Berge L., Coz M. and Geramb H. V. von (1989), *Phys. Rev.* C **40**, 940.
Leeb H. and Leidinger D. (1992), *Few-Body Systems Suppl.* **6**, 117.
[16] Loeffel J. J. (1968), *Ann. Inst. Henri Poincare* **8**, 339.
[17] Lipperheide R. and Fiedeldey H. (1978), *Z. Phys.* **286**, 45.
Lipperheide R. and Fiedeldey H. (1981), *Z. Phys.* **301**, 81.
[18] Sabatier P. C. (1968), *J. Math. Phys.* **9**, 1241.
[19] Schnizer W. A. and Leeb H. (1994),*J. Phys.* A **27**, 2605.
[20] Ledoux R. J., Bechara M. J., Ordonez C. E., Al-Juwair H. A. and Cosman E. R. (1983), *Phys. Rev.* C **27**, 1103.
[21] Vollmer G. (1967), *Z. Phys.* **226**, 423.
[22] N. Alexander, K. Amos, B. Apagyi, and D. R. Lun, Phys. Rev. **C53**, 88 (1996).
[23] Sabatier P. C. (1967), *J. Math. Phys.* **8**, 4, 905.
[24] Münchow M. and W. Scheid W. (1980), *Phys. Rev. Lett.* **44**, 1299.
[25] Thompson I. J. and Barnett A. R. (1985), *Comp. Phys. Comm.* **36**, 363.
[26] Satchler G. R., Owen L. W., Elwyn A. J., Morgan G. L. and Watson R. L. (1968), *Nucl. Phys.* A **112**, 1.
Ordonez C. E., Ledoux R. J. and Cosman E. R. (1986) *Phys. Lett.* B **173**, 39.
[27] Hooshyar M. A. (1975) *J. Math. Phys.* **16**, 257.
Hooshyar M. A. (1978) *J. Math. Phys.* **19**, 253.
[28] Huber H. and Leeb H., *An Exact Inversion Method for the Determination of Spin-Orbit Potentials from Scattering Data* (1996) preprint TU Wien.

Numerical Method for Solving the Inverse Problem of Quantum Scattering Theory

Ruben G. Airapetyan, Igor V. Puzynin, and Eugeni P. Zhidkov

Joint Institute for Nuclear Research, Laboratory of Computing Technics and Automation, Dubna, 141980, Russia

Abstract. We present a new numerical method for solving the problem of the reconstruction of interaction potential by a phase shift given on a set of closed intervals in (l,k)-plane, satisfying certain geometrical "Staircase Condition". The method is based on the Variable Phase Approach and on the modification of the Continuous Analogy of the Newton Method.

1 Introduction

The problem of the numerical reconstruction of potential by scattering data is well known and important from the mathematical point of view and for such physical applications as the analysis of a nuclear interaction potential by experimental data. The main approaches for theoretical investigations of the problem are well-known Gelfand-Levitan, Marchenko and Krein methods (Agranovich and Marchenko (1960), Marchenko (1977), Levitan (1984)), Chadan and Sabatier (1977,1989)). At the same time the development of the corresponding numerical methods is sufficiently complicated by the reason of the ill-posedness of the mentioned inverse problems.

In this report we consider a new statement of the inverse problem of the Quantum Scattering Theory and suggest the numerical method for its solving. To this end we describe the Newtonian Iterative Scheme with Simultaneous Iterations of the Inverse Derivative and formulate the theorem establishing its convergence. Then we use the method for the inverse problem for radial Schrödinger equation in more general statement than in Gelfand-Levitan-Marchenko-Krein Theory.

2 Statement of the Problem

The following Cauchy problem for the radial Schrödinger equation is considered:

$$\frac{\mathrm{d}^2}{\mathrm{d}r^2}\phi(l,k,r)+\left(k^2-\frac{l(l+1)}{r^2}\right)\phi(l,k,r)=V(r)\phi(l,k,r) \qquad (1)$$

$$\lim_{r\to 0}(2l+1)!!r^{-l-1}\phi(l,k,r)=1\ . \qquad (2)$$

It is well-known that for the potentials satisfying the condition

$$\int_0^\infty r|V(r)|dr < \infty \tag{3}$$

the wave function has the following asymptotic behaviour:

$$\phi(l,k,r) \sim \frac{|F(l,k)|}{k^{l+1}} \sin(kr - \frac{\pi l}{2} + \delta(l,k)) \quad r \to \infty \ , \tag{4}$$

where $F(l,k)$ is the Jost Function.

The Inverse Problem of the Quantum Scattering Theory is the problem of the reconstruction of an unknown potential $V(r)$ by some given information about phase shift $\delta(l,k)$.

Note. For details and complete bibliography we refer to Chadan and Sabatier (1977,1989), Ramm (1992), von Geramb (Ed.) (1994), Zakhariev and Suzko (1990), Zakhar'ev (1996) .

A potential in (1) is a function of one variable r so it is naturally to reconstruct a potential by a phase shift given on a certain one-dimensional submanifold of (l,k)-plane. The problem is well known and investigated in two important special cases: for the potentials given for fixed orbital momentum l ($\delta(k) = \delta_l(k)$) and for the potentials given for fixed energy (f.i. $\delta(l) = \delta_l(1)$). Geometrically these cases correspond to rays issuing from origin of the (l,k)-plane and parallel to the axes. At the same time there are very few results concerning the potential reconstruction by phase shifts given on another one-dimensional manifolds and all of them are obtained in the framework of the WKB or generalized WKB approaches (Vasilevsky and Zhirnov (1977), Bogdanov and Demkov (1982), Abramov (1984), Chadan and Sabatier (1977,1989)). The theoretical analysis of the problem is very difficult because there are no generalization of the Gelfand-Levitan-Marchenko-Krein Theory for such situations.

Our approach to the numerical investigation of these problems is based on the following Variable Phase Equation (Calogero (1967), Babikov (1968)):

$$\frac{\partial\delta(l,k,r)}{\partial r} = -k^{-1}V(r)[\cos(\delta(l,k,r))j_l(kr) - \sin(\delta(l,k,r))n_l(kr)]^2, \tag{5}$$

where

$$\delta(l,k,0) = 0, \quad \lim_{r\to\subset} \delta(l,k,r) = \delta(l,k), \tag{6}$$

and

$$j_l(z) = \sqrt{\frac{\pi z}{2}} J_{l+1/2}(z), \quad n_l(z) = \sqrt{\frac{\pi z}{2}} Y_{l+1/2}(z) \tag{7}$$

are Bessel-Ricatti functions.

Let us denote by Φ the nonlinear operator associating to a potential $V(r)$ corresponding phase shift $\delta(l,k)$. Then the inverse problem can be considered as a nonlinear equation

$$\Phi(V) = \delta \tag{8}$$

with respect to the unknown potential $V(r)$.

3 Continuous Analogy of Newton Method

First we describe the Continuous Analogy of Newton Method (CANM, Gavurin (1958),Zidkov and Puzynin (1967)).

Let H be a real or complex Hilbert space, $L(H)$ - the space of linear operators in H, $\varphi : H \to H$ - a nonlinear operator. The following nonlinear equation is considered:

$$\varphi(x) = 0 \ . \tag{9}$$

Denote by x_0 an initial approximation to the solution of the (1), by $\varphi'(x)$ - the Frechét derivative of the operator φ and by $\varphi''(x)$ - the Gateaux derivative of the operator $\varphi'(x)$, i.e. $\varphi''(x)$ for fixed x is a linear operator from H to $L(H)$, such that

$$\varphi'(x+\xi) - \varphi'(x) = \varphi''(x)\xi + \eta, \text{ and } ||\eta||\,||\xi||^{-1} \in 0, \text{ for } \xi \to 0 \ .$$

Now let us consider the following Cauchy problems in H:

$$x'(t) = -{\varphi'}^{-1}(x(t))\varphi(x(t)), \quad x(0) = x_0 \ . \tag{10}$$

For the problem the following convergence theorem holds.

Theorem 1. (Gavurin (1958)) *If there exists a positive number r such that the operators $\varphi'(x)$, ${\varphi'}^{-1}(x)$ and $\varphi''(x)$ exist in any point of the ball $B = \{x; ||x - x_0|| \le r||\varphi(x_0)||\}$, $\varphi''(x)$ is bounded in a neighborhood of every point of B, and for every $x \in B$*

$$||{\varphi'}^{-1}(x)|| \le r.$$

Then for $t \in [0, +\infty)$ there exists a solution $x(t)$ of the problem (2), $x(t) \in B$ for all $t \in [0, +\infty)$,

$$\lim_{t \in +\infty} x(t) = x^* \tag{11}$$

and x^* is the solution of the problem (1).

4 The Fréchet Derivative Operator $\Phi'(V)$

So the principal point for solving (8) by means of CANM is the inversion of the operator $\Phi'(V)$. The last one can be simply obtained:

$$(\Phi'(V)\xi)(l,k) = \int_0^\infty K(l,k,t)\xi(t)dt \ , \tag{12}$$

where

$$K(l,k,t) = -B(l,k,t)\exp\Big[\int_t^\infty V(s)A(l,k,s)ds\Big] \ , \tag{13}$$

$$A(l,k,r) = k^{-1}[\sin(2\delta(l,k,r))(j_l^2(kr) - n_l^2(kr)) +$$

$$+ \cos(2\delta(l,k,r))j_l(kr)n_l(kr)] \ , \tag{14}$$

$$B(l,k,r) = k^{-1}[\cos(\delta(l,k,r))j_l(kr) - \sin(\delta(l,k,r))n_l(kr)]^2 \ . \tag{15}$$

The inversion of the operator (12) is in fact a problem of solving the Fredholm integral equation of first kind. The last one is an ill-posed problem and needs some regularization. In (Vizner, Zhidkov and Lelek (1968)) the algorithm using Tikhonov regularization at every step of the Newtonian iterations was constructed in the particular case of the problem, when phase shift is given for zero orbital momentum (see also Vizner et al. (1978)). However such algorithm is unstable and has low accuracy.

Note. For another applications of CANM we refer to Vinitsky et al. (1990), Puzynin et al. (1993).

5 Continuous Analogy of Newton Method with the Simultaneous Inversion of the Fréchet Derivative

Now our aim is to consider a continuous Newton method with the simultaneous calculation of reciprocal to the operator $\varphi'(x)$. Let us consider the following system:

$$\begin{cases} \varphi(x) = 0 \\ \varphi'(x)Y - E = 0 \ , \end{cases} \tag{16}$$

where $Y \in L(H)$ and E is the identity operator. Let Y_0 be some approximation to $\varphi'(x_0)^{-1}$ and ρ is a positive number.

Let us consider the following Cauchy problem:

$$\begin{cases} x'(t) = -Y(t)\varphi(x(t)) \\ Y'(t) = -\rho^2((\varphi'(x(t))^*\varphi'(x(t))Y(t) + Y(t)\varphi'(x(t))(\varphi'(x(t)))^*) + \\ +2\rho^2(\varphi'(x(t)))^* \end{cases} \quad (17)$$

$$x(0) = x_0, \quad Y(0) = Y_0 \ .$$

Let us assume that the following condition holds.

Condition A. *There exist* $r > 0$ *and* $\epsilon > 0$ *such that*

1) Frechét derivative $\varphi'(x)$ *and Gateaux derivative* $\varphi''(x)$ *exist in* $B = B(x_0, r||\varphi(x_0)||)$, *moreover*

$$||\varphi''||_r = \sup_{x\in B} \sup_{\xi\in H,\, ||\xi||=1} ||(\varphi''(x)\xi||_{L(H)} < \infty \ ,$$

2) for any $x \in B$ *the operator* $(\varphi'^*(x))$ *is invertible and*

$$||\varphi'^{*-1}||_r = \sup_{x\in B} ||(\varphi'^*(x))^{-1}|| < \infty \ ,$$

3) the following inequality holds

$$0 < \frac{\max\{||Y_0||, ||\varphi'^{*-1}||_r\}}{1 - \max\{||\varphi'(x_0)Y_0 - E||, \epsilon\}} < r \ . \quad (18)$$

Denote

$$||\varphi||_r = \sup_{x\in B} ||\varphi(x)||$$

$$\rho_0 = \max\{||Y_0||, ||\varphi'^{*-1}||_r\}\, ||\varphi'^{-1}||_r \sqrt{\frac{||\varphi''||_r ||\varphi||_r}{2\epsilon}} \ . \quad (19)$$

The following theorem establishes the convergence of the method.

Theorem 2. (Airapetyan and Puzynin (1996)) *If the Condition A holds, then for every* $\rho > \rho_0$

1) the solution $(x(t), Y(t))$ *of the problem (4) exists for* $t \in [0, +\infty)$ *and*

$$x(t) \in B(x_0, r||\varphi(x_0)||) \ , \quad (20)$$

$$||\varphi'(x(t))Y(t) - E|| \le \max\{||\varphi'(x_0)Y_0 - E||, \epsilon\} \ ; \quad (21)$$

2) there exists

$$\lim_{t\in+\infty} x(t) = x^*$$

and x^* *is the solution of the problem (1).*

6 An Inversion of the Operator $\Phi'(0)$

So for the numerical solving of the inverse problem by means of the described method we must invert $\Phi'(V)$ only in the initial approximation point $V_0(r)$. As an initial approximation we use zero potential: $V_0(r) \equiv 0$. So we have to solve the following Fredholm equation of first kind:

$$(\Phi'(0)\xi)(l,k) = -\frac{1}{k}\int_0^\infty j_l^2(kr)\xi(r)dr = g(l,k) \ . \tag{22}$$

In the case $l = 0$, $g = g(k)$, $k \in [0, \subset)$ the operator $\Phi'(0)$ is very simple:

$$(\Phi'(0)\xi)(k) = -\frac{1}{k}\int_0^\infty \sin^2(kr)\xi(r)dr \tag{23}$$

and can be easy inversed by means of the Fourier sin-trasformation:

$$(\Phi'(0)^{-1}g)(r) = 2\pi\int_0^\infty \cos(2kr)g(k)kdk \ . \tag{24}$$

Now our goal is to inverse $\Phi'(0)$ for $g(l,k)$ given on more general subset. Let us denote

$$\eta(k) = \int_0^\infty \sin(kr)\xi(r)rdr \ .$$

From the recursion formulas for the Bessel-Ricatty functions

$$\frac{\mathrm{d}}{\mathrm{d}x}z_l(x) = \frac{2l+1}{x}z_l(x) - z_{l-1}(x) \quad l = 1,2,\dots \ ,$$

$$z_{l+1}(x) = z_{l-1}(x) - \frac{l}{x}z_l(x) \quad l = 1,2,\dots$$

we get the following relations:

$$\frac{\mathrm{d}}{\mathrm{d}k}[kg(0,k)] = -\eta(2k) \ , \tag{25}$$

$$\frac{\mathrm{d}}{\mathrm{d}k}[kg(l,k)] + \frac{2}{l}g(l,k) = 2\sum_{m=0}^{l-2}(-1)^m(2l-2m-1)g(l-m-1,k) +$$

$$+2(-1)^{l+1}g(0,k) + (-1)^{l+1}\eta(2k) \quad l = 1,2,\dots \ .$$

Therefore

$$\frac{\mathrm{d}}{\mathrm{d}k}[k(g(l,k)+g(l+1,k)] - \alpha_l[k(g(l,k)+g(l+1,k)] = (\beta_l - \alpha_l)g(l+1,k) \ ,$$

$$\frac{\mathrm{d}}{\mathrm{d}k}[k(g(l,k)+g(l+1,k)]-\beta_l[k(g(l,k)+g(l+1,k)]=(a_l-\beta_l)g(l,k)\ ,$$

where

$$\alpha_0=2,\quad \alpha_l=2\frac{(l+1)(2l-1)}{l},\quad \beta_0=-2,\quad \beta_l=-\frac{2}{(l+1)}\ .$$

So we obtain the following recursions:

$$g(l,k)=a^{1-\alpha_l}[g(l,a)+g(l+1,a)]k^{\alpha_l-1}+$$

$$+(\beta_l-\alpha_l)k^{\alpha_l-1}\int_a^k s^{-\alpha_l}g(l+1,s)ds-g(l+1,k)\ , \tag{26}$$

$$g(l+1,k)=a^{1-\beta_l}[g(l,a)+g(l+1,a)]k^{\beta_l-1}+$$

$$+(\alpha_l-\beta_l)k^{\beta_l-1}\int_a^k s^{-\beta_l}g(l,s)ds-g(l,k)\ . \tag{27}$$

Now let the two finite sequences of nonnegative numbers be given: the first one $\{l_1,l_2,\ldots,l_N\}$ consists of integers, and the second one $\{a_0,a_1,\ldots,a_{N-1}\}$ of real numbers, where $a_0=0$. Denote by I_N a finite set of closed intervals on the (l,k)-plane:

$$I_N=\bigcup_{j=1}^{N-1}\{(l,k);l=l_j,a_{j-1}\le k\le a_j\}\bigcup\{(l_N,k);a_{N-1}\le k<\infty\}\ . \tag{28}$$

Definition 1. *We say that the system I_N satisfies a "Staircase Condition" if there exist integers $0=n_1<n_2<\ldots<n_m<N$ such that for every i from 1 to m the following conditions hold*

a) $|l_{j+1}-l_j|=1$ for $j=n_i+1,n_i+2,\ldots,n_{i+1}-1$,

b) no less than one from the numbers $l_{n_i},l_{n_i+1},\ldots,l_{n_{i-1}-1}$ equal to zero.

From (26) and (27) the following lemma immediatly follows.

Lemma 1. *Let a continuous function $g(l,k)=\Phi'(0)\xi$ be given on a set of intervals I_N satisfying the "Staircase Condition". Then the corresponding function $g(0,k)$ is univalently determined on $[0,\infty)$ by recursion formulas (26) and (27).*

From Lemma 1 the recursion formula for the inversion of the operator $\Phi'(0)$ can be easy obtained for every set of intervals satisfying the "Staircase Condition".

7 Statement of the Problem and Numerical Example

Thus, now we can formulate the statement of the problem to which suggested Numerical Method could be applied.

Statement of the Problem. *To reconstruct the potential by means of the phase shift given on the set of the intervals satisfying the "Staircase Condition".*

For this problem there are no theorems establishing its well-posedness, so we are able only to examine it numerically. Let a phase shift $\delta(l,k)$ be given on the set

$$I_2 = \{(1,k); 0 \le k \le a_1\} \bigcup \{(0,k); a_1 \le k \le \infty\} \ . \tag{29}$$

Then from the formulas of Sect.6 we obtain the following relation:

$$(\Phi'^{-1}(0)g) = \pi(g(0,a)+g(1,a))[(ar^{-1} - \frac{1}{2}a^{-1}r^{-3})\sin(2ar) + r^{-2}\cos(2ar)] +$$

$$+2\pi \int_a^\infty g(0,k)\cos(2rk)kdk - 2\pi \int_0^a g(1,k) \times [(k - 2k^{-1}r^{-2})\cos(2rk) -$$

$$-(2r^{-1} + k^{-2}r^{-3})\sin(2rk)]dk \ . \tag{30}$$

Then using this inversion formula for initial approximation we apply the algorithm described in Sect.5. Below we bring some pictures illustrating the

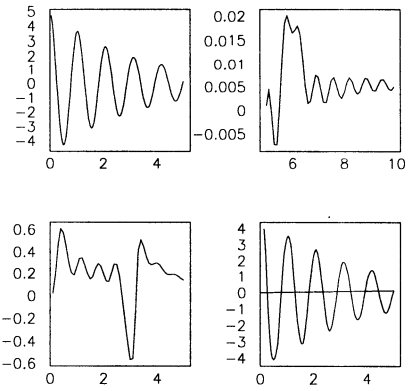

Fig. 1. In upper row the first figure displays V_n and second one – δ_0, in lower row the first figure displays δ_1 and second one – V_r

results of the numerical calculations based on this method. We start from the

known potential $V_n(r)$ on [0,10], then solve the direct problem and obtain phase shifts $\delta_0(k)$ on [5,10] and $\delta_1(k)$ on [0,5], and finally reconstruct the potential $V_r(r)$ on [0,10].

The results of numerical investigation show that the considered problem can be numerically solved with high accuracy and so such statement of a problem is reasonable. As seems to us, the interesting problem now is to prove the corresponding well-posedness theorem.

Acknowledgments. This work was supported by RFFI, grants 94-01-01119 and 95-01-01467a.

References

Abramov D.I. (1984): On a reconstruction of the interaction potential in quasiclassical scattering. Theor. Mat. Fiz. **58**, 244–253

Agranovich Z.S., Marchenko V.A. (1960): *Inverse Scattering Problem* (Kharkov)

Airapetyan R.G., Puzynin I.V. (to appear): Newtonian iterative scheme with simultaneous iterations of inverse derivative.

Babikov V.V., (1968): *The Method of Phase Functions in Quantum Mechanics* (Nauka, Moscow)

Bogdanov I.V., Demkov Yu.N. (1982): New classical inversion formula for centrally-symmetric electric and magnetic fields and the focussing potentials. Sov. Phys. JETP **82**, 1987–1806

Calogero F. (1967): *Variable Phase Approach to Potential Scattering* (Academic Press, New York, London)

Chadan K., Sabatier P.C. (1977,1989): *Inverse Problems in Quantum Scattering Theory* (Springer-Verlag)

Gavurin M.K. (1958): Nonlinear functional equations and continuous analogies of iterative methods. Izv. Vuzov. Ser. Matematika. **5**, 18–31

Von Geramb H.V. (Ed.) (1994): *Quantum Inversion Theory and Applications* (Springer-Verlag)

Krein M.G. (1955): On a determination of a potential of a particle by its S-function. DAN SSSR, **105**, 433–436

Levitan B.M. (1984): *Sturm-Liouville Inverse Problems* (Nauka, Moscow)

Marchenko V.A. (1977): *Sturm-Liouville Operators and their Applications* (Naukova Dumka, Kiev)

Puzynin I.V., Amirkhanov I.V., Puzynina T.P., Zemlyanaya E.V. (1993): The Newtonian iterative scheme with simultaneous calculating the inverse operator for the derivative of nonlinear function. JINR Rapid Comms. **62**, 63–73

Ramm A.G. (1992): *Multidimensional Inverse Scattering Problems* (Longman Group UK Limited, London)

Vasilevsky L.S., Zhirnov N.I. (1977): Construction of the potential from the phase-shifts in the generalized WKB method. J. Phys. B.: Atom. Molec. Phys. **10**, 1425–1435

Vinitsky S.I., Puzynin I.V., Smirnov Yu.S. (1990): The scattering problem solution using multiparameter Newton schemes. Single-channel scattering. J. Nucl. Phys. **52**, 1176–1189

Vizner Ya., Zidkov E.P., Lelek V. (1968): The method of a calculation of a potential by means of parameter introduction. (Dubna, JINR, P5-3895)

Vizner Ya., Zidkov E.P., Lelek V., Malyshev R.V., Khoromsky B.N., Hristov E.H., Ulegla I. (1978): Iterative methods of the solving of an inverse problem of scattering theory. Part. and Nucl. **9**, 710-768

Zakhar'ev B.N. (1996): *Lessons of Quantum Intuition* (JINR, Dubna)

Zakhar'ev B.N. Suz'ko A.A. (1985): *Potentials and Quantum Scattering: Direct and Inverse Problems* (Energoizdat, Moscow)

Zhidkov E.P., Puzynin I.V. (1967): The solving of boundary problems for second order nonlinear differential equations by means of the stabilization method. Soviet Math. Dokl. **8**, 614-616

The Inverse Scattering Problem for Coupled Channels with the Modified Newton–Sabatier Method

Matthias Eberspächer[1], Barnabás Apagyi[2], and Werner Scheid[1]

[1] Institut für Theoretische Physik, Justus-Liebig-Universität Gießen, Heinrich-Buff-Ring 16, D-35392 Gießen, Germany
[2] Department of Theoretical Physics, Technical University of Budapest, Budafoki út 8, H-1111 Budapest, Hungary

Abstract. The modified Newton-Sabatier method is extended to the inverse scattering problem for coupled channels at fixed energy. The coupled Schrödinger equations are assumed to depend on a potential matrix which couples the channels. This potential matrix is taken as independent on the angular coordinates of the relative motion. In order to test the inversion method it is applied to analytic S-matrices corresponding to potential matrices consisting of square well potentials. The scattered particles can be neutral or charged. In the latter case the S-matrix with the asymptotic Coulomb potential is transformed to the S-matrix with an asymptotic constant potential and then the inverse scattering problem for neutral particles is solved.

1 Introduction

The Inverse Scattering Problem (ISP) in quantum mechanics means the determination of the potential in the Schrödinger equation from the S-matrix. For elastic scattering the ISP at fixed energy was first solved by 1. 2 and 3 investigated this method in great detail which is named Newton-Sabatier method today. An extension of the work was given by 4 for practical applications by introducing the modified Newton method. This method assumes that the potential is known from a certain radius on up to infinity. Thus, the potential is unknown only in a finite interval. If one considers neutral particles for example, the potential vanishes from a certain radius. For charged particles it is the Coulomb potential. The Newton-Sabatier method and other inversion methods at fixed energy are reviewed in monographies (Chadan and Sabatier 1989, Newton 1982, Zakhariev and Suzko 1990).

In this paper we extend the modified Newton-Sabatier method from the problem of elastic scattering to the case of inelastic scattering at fixed energy. For solving this problem we assume that the channels are coupled by a potential matrix which does not depend on the angular coordinates of the relative motion. In section 2 we formulate the ISP for coupled channels. In section 3 we solve the ISP with the modified Newton-Sabatier method by using the S-matrix for a fixed energy. The special case of charged particles is reduced to

the case of neutral particles via a transformation given for elastic scattering by 7. Finally, in section 4 the new method is applied to potential matrices consisting of square well potentials which allow an analytical calculation of the S-matrix.

2 The ISP for coupled channels

We solve the ISP for a particular coupled channel problem. We assume that the Hamiltonian describing the scattering system of two colliding particles is given by

$$H = T(\mathbf{r}) + h(\xi) + W(r, \xi). \tag{1}$$

Here, T denotes the relative kinetic energy operator and h the Hamiltonian of the internal states of the two scattering partners. The interaction operator W between the relative and the intrinsic motion depends on the relative radial coordinate r and the intrinsic coordinates ξ. With this special choice, only monopole transitions can be described.

Due to this ansatz, the wavefunction of the system factorizes as

$$\Psi_{\ell m} = \left(\sum_{\alpha=1}^{N} R_\alpha^\ell(r) \chi_\alpha(\xi) \right) Y_{\ell m}(\theta, \phi) \tag{2}$$

with $R_\alpha^\ell(r)$ being the radial wavefunction, $Y_{\ell m}$ describing the orbital motion and $\chi_\alpha(\xi)$ solving the eigenvalue equation for the intrinsic motion:

$$h(\xi)\chi_\alpha(\xi) = \varepsilon_\alpha \chi_\alpha(\xi). \tag{3}$$

The eigenvalues ε_α are the intrinsic excitation energies.

Using the Schrödinger equation $H\Psi = E\Psi$ and introducing the potential matrix $V_{\alpha\beta} =< \chi_\alpha | W | \chi_\beta >$, we get the coupled equations for the radial wavefunctions:

$$\left[-\frac{\hbar^2}{2\mu} \frac{1}{r} \frac{d^2}{dr^2} r + \frac{\hbar^2}{2\mu} \frac{\ell(\ell+1)}{r^2} + \varepsilon_\alpha - E \right] R_{\alpha n}^\ell(r) + \sum_{\beta=1}^{N} V_{\alpha\beta}(r) R_{\beta n}^\ell(r) = 0. \tag{4}$$

The total number of channels is denoted by N. The reduced mass μ is independent of the channel α, as we do not consider transfer reactions. Because of our special choice of the interaction W, the potential matrix V does not depend on the quantum number ℓ of the orbital angular momentum of relative motion which means that it does not couple the orbital and intrinsic motions.

Equation (4) is a set of N linear homogeneous equations for the radial functions $R_{\alpha n}^\ell$. Thus, we can write the solutions of this system as vectors with N components:

$$\Psi_n(r) = \left(R^\ell_{1n}(r), R^\ell_{2n}(r), ..., R^\ell_{Nn}(r)\right), \quad \text{with } n = 1, 2, ...N. \tag{5}$$

These solutions are degenerate in the total energy E. For every channel α we have N linearly independent solutions. We will enumerate these solutions by the additional index n.

The ISP at fixed energy now consists of the calculation of the potential matrix $V_{\alpha\beta}(r)$ from the asymptotic radial solutions which depend on the S-matrix $S^\ell_{\alpha\beta}$. In order to solve this problem one needs the full matrix $S^\ell_{\alpha\beta}$ $(\alpha, \beta = 1, 2, ..., N)$ as function of the quantum number ℓ of angular momentum as input.

3 The modified Newton-Sabatier method for coupled channels

By introducing dimensionless coordinates and some abbreviations:

$$\rho = kr = \sqrt{\frac{2\mu E}{\hbar^2}}r, \quad \varphi^\ell_{\alpha n}(\rho) = \rho R^\ell_{\alpha n}(r), \quad U_{\alpha\beta}(\rho) = \frac{V_{\alpha\beta}(r)}{E}, \tag{6}$$

we can rewrite equation (4):

$$\sum_{\beta=1}^{N} D^U_{\alpha\beta}(\rho)\varphi^\ell_{\beta n}(\rho) = \ell(\ell+1)\varphi^\ell_{\alpha n}(\rho) \tag{7}$$

with the differential operator matrix given by:

$$D^U_{\alpha\beta}(\rho) = \rho^2 \left\{ \left[\frac{d^2}{d\rho^2} + \frac{E_\alpha}{E} \right] \delta_{\alpha\beta} - U_{\alpha\beta}(\rho) \right\}, \tag{8}$$

where $E_\alpha = E - \varepsilon_\alpha$ is the energy in channel α.

The first step in solving the ISP with the Newton-Sabatier method is to choose a reference potential matrix with $U^0_{\alpha\beta}(\rho) = U^0_{\beta\alpha}(\rho)$. The regular solutions $\varphi^{0\ell}_{\alpha n}(\rho)$ of the coupled channel problem with this reference potential matrix must be known:

$$\sum_{\beta=1}^{N} D^{U_0}_{\alpha\beta}(\rho)\varphi^{0\ell}_{\beta n}(\rho) = \ell(\ell+1)\varphi^{0\ell}_{\alpha n}(\rho) \tag{9}$$

with the reference differential operator

$$D^{U_0}_{\alpha\beta}(\rho) = \rho^2 \left\{ \left[\frac{d^2}{d\rho^2} + \frac{E_\alpha}{E} \right] \delta_{\alpha\beta} - U^0_{\alpha\beta}(\rho) \right\}. \tag{10}$$

Next, an ansatz for the yet unknown wavefunctions is made:

$$\varphi^\ell_{\alpha n}(\rho) = \varphi^{0\ell}_{\alpha n}(\rho) - \sum_{\beta=1}^{N} \int_0^\rho \frac{d\rho'}{\rho'^2} K^{UU_0}_{\alpha\beta}(\rho, \rho')\varphi^{0\ell}_{\beta n}(\rho'). \tag{11}$$

This is a generalization of the Povzner-Levitan representation to coupled channels (Chadan and Sabatier 1989). In this equation, the coupling between the different channels α and β is introduced by the kernel $K_{\alpha\beta}$. The potential matrix in terms of the kernel is obtained, if the kernel is a solution of the partial differential equations

$$\sum_{\beta=1}^{N} D^{U}_{\alpha\beta}(\rho) K^{UU_0}_{\beta\gamma}(\rho,\rho') = \sum_{\beta=1}^{N} D^{U_0}_{\gamma\beta}(\rho') K^{UU_0}_{\alpha\beta}(\rho,\rho') \tag{12}$$

with the boundary conditions:

$$K^{UU_0}_{\alpha\beta}(\rho=0,\rho') = 0, \quad K^{UU_0}_{\alpha\beta}(\rho,\rho'=0) = 0. \tag{13}$$

Under these conditions it can be shown that the potential matrix is given by

$$U_{\alpha\beta}(\rho) = U^0_{\alpha\beta}(\rho) - \frac{2}{\rho}\frac{d}{d\rho}\frac{K^{UU_0}_{\alpha\beta}(\rho,\rho)}{\rho}. \tag{14}$$

A solution of the kernel in terms of the wavefunctions φ and φ^0 can be written with yet unknown coefficients $c^{\ell}_{nn'}$:

$$K^{UU_0}_{\alpha\beta}(\rho,\rho') = \sum_{\ell=0}^{\infty}\sum_{n,n'=1}^{N} c^{\ell}_{nn'}\varphi^{\ell}_{\alpha n}(\rho)\varphi^{0\ell}_{\beta n'}(\rho'). \tag{15}$$

The kernel fulfills the above conditions (12) and (13). Inserting the kernel into equation (11) it is possible to calculate the coefficients $c^{\ell}_{nn'}$ and the wavefunctions $\varphi^{\ell}_{\alpha n}$ and then the potential matrix (14). If we extend the usual Newton-Sabatier method to coupled channels, the coefficients $c^{\ell}_{nn'}$ can be calculated by using the known asymptotic behaviour of the wavefunctions $\varphi^{\ell}_{\alpha n}$ depending on the S-matrix. In this paper we apply the modified Newton-Sabatier method which assumes that the potential matrix $U_{\alpha\beta}$ is known from some radius ρ_0 on. In this case the wavefunctions $\varphi^{\ell}_{\alpha n}$ are known for $\rho > \rho_0$ by their dependence through the S-matrix and the coefficients $c^{\ell}_{nn'}$ can be calculated by solving equation (11) for $\rho > \rho_0$. The modified Newton-Sabatier method yields an unique solution of the ISP in the class of potentials generated by the kernel (15).

3.1 Scattering of neutral particles

For neutral particles with short range interaction the potential matrix vanishes from a certain radial distance: $U_{\alpha\beta}(\rho > \rho_0) = 0$. In this case the simplest choice of the reference potential matrix U^0 is zero: $U^0_{\alpha\beta}(\rho) = 0$. Then, the regular reference solutions are:

$$\varphi^{0\ell}_{\alpha n}(\rho) = \rho T^{0\ell}_{\alpha n}(\rho) := \rho j_{\ell}(k_{\alpha}\rho)\delta_{\alpha n} \tag{16}$$

with $k_\alpha^2 = E_\alpha/E$.

The wavefunction φ in channel α is composed of a superposition of the degenerate solutions $T^\ell_{\alpha n}(\rho)$ in channel α with yet unknown coefficients $A^\ell_{n'n}$:

$$\varphi^\ell_{\alpha n}(\rho) = \sum_{n'=1}^{N} \rho T^\ell_{\alpha n'}(\rho) A^\ell_{n'n}. \tag{17}$$

The solutions $T^\ell_{\alpha n}(\rho)$ are asymptotically determined by the given S-matrix:

$$T^\ell_{\alpha n}(\rho > \rho_0) = \sqrt{k_\alpha}(\delta_{\alpha n} h^-_\ell(k_\alpha \rho) - S^\ell_{\alpha n} h^+_\ell(k_\alpha \rho)), \tag{18}$$

where $h^\pm_\ell$ are the spherical Hankel functions. By introducing the wavefunctions (16) and (17) together with the kernel (15) in the Povzner-Levitan representation (11) we obtain the set of coupled inhomogeneous equations

$$\sum_{n'=1}^{N} \left(T^\ell_{\alpha n'}(\rho) A^\ell_{n'n} + \sum_{\ell'=0}^{\ell_{\max}} T^{\ell'}_{\alpha n'}(\rho) b^{\ell'}_{n'n} L^{\ell'\ell}_n(\rho) \right) = T^{0\ell}_{\alpha n}(\rho) \tag{19}$$

with

$$L^{\ell'\ell}_n(\rho) = \int_0^\rho j_\ell(k_n \rho') j_{\ell'}(k_n \rho') d\rho', \quad b^\ell_{nn'} = \sum_{n''=1}^{N} A^\ell_{nn''} c^\ell_{n''n'}. \tag{20}$$

In order to get a set of finite coupled equations, we limit the summation over ℓ' to $\ell_{\max}$. The effect of this limitation will be discussed in the examples in section 4.

The known quantities in equation (19) are the reference solutions $T^{0\ell}$ and the matrix L. The solutions T^ℓ are only known in the outer region, where they depend on the S-matrix as given in equation (18). Further unknown quantities are the coefficients A and b. We will now use equation (19) two times to calculate these quantities.

In the first step, we solve equation (19) at two points $\rho_1, \rho_2 > \rho_0$ in the outer region. We then have $2 \times N \times N \times (\ell_{\max}+1)$ equations for the calculation of the coefficients $A^\ell_{nn'}$ and $b^\ell_{nn'}$ with the solutions T^ℓ depending on the S-matrix (18). In the second step we use these coefficients and solve equation (19) at discrete points ρ_i in the inner region $0 < \rho_i < \rho_0$ to get the solutions $T^\ell_{\alpha n}(\rho_i)$. We need to solve $N \times N \times (\ell_{\max}+1)$ equations at every radius ρ_i.

Now, knowing the coefficients and the wavefunctions, we can calculate the kernel (15) and the potential matrix (14). Thus, the ISP at fixed energy for the inelastic scattering of neutral particles is solved.

3.2 Scattering of charged particles

The asymptotic solutions for charged particles are given in terms of the Coulomb functions

$$T^{\ell}_{\alpha n}(\rho > \rho_0) = \sqrt{k_\alpha}(H^-_\ell(k_\alpha\rho)\delta_{\alpha n} - S^{\ell}_{\alpha n}H^+_\ell(k_\alpha\rho)) \tag{21}$$

with

$$H^{\pm}_{\ell}(k_\alpha\rho) = \frac{e^{i\sigma^{\ell}_{\alpha}}}{k_\alpha\rho}(G_\ell(k_\alpha\rho) \pm iF_\ell(k_\alpha\rho)), \tag{22}$$

where G_ℓ, F_ℓ are the irregular and regular Coulomb functions, respectively, and σ^{ℓ}_{α} are the Coulomb phases (Satchler 1983):

$$\sigma^{\ell}_{\alpha} = arg\Gamma(\ell + 1 + i\eta_\alpha), \quad \eta_\alpha = \frac{Z_p Z_t e^2 \mu}{\hbar^2 k k_\alpha}. \tag{23}$$

$Z_p e$ and $Z_t e$ are the projectile and target charges, respectively.

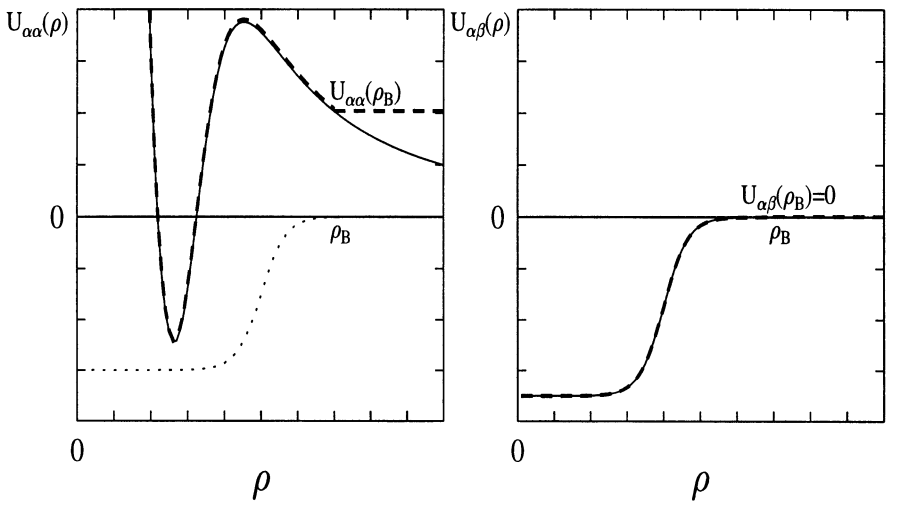

Fig. 1. The left diagram shows a diagonal element of the potential matrices $U_{\alpha\alpha}$ (Real part: —, Imaginary part: $\cdots$) and $U^{B}_{\alpha\alpha}$ (Real part: - - -, Imaginary part: $\cdots$), the right diagram gives an off-diagonal element. ρ_B is the transformation radius.

We could now choose the reference potential as a Coulomb potential and solve the ISP again as described above. We would get coupled equations of the type (19) where the solutions T^{ℓ} are of the form (21). However, the numerical calculation with Coulomb functions is much more time consuming than the calculation with spherical Hankel functions. Thus, we consider a transformation of the S-matrix from an asymptotic Coulomb potential to an asymptotic

constant potential. The procedure is an extension of the method described by 7 for the elastic scattering of charged particles to inelastic scattering.

The idea of the transformation can be seen in fig. 1. The wanted potential matrix (full curve) with an asymptotic Coulomb behaviour has the form

$$U_{\alpha\beta}(\rho) = \begin{cases} U_{\alpha\beta}(\rho) & , \quad \rho \leq \rho_0, \\ \delta_{\alpha\beta} \dfrac{Z_p Z_t e^2 k}{\rho E} & , \quad \rho > \rho_0. \end{cases} \tag{24}$$

We transform the S-matrix belonging to this potential matrix to another S-matrix of a potential matrix which has asymptotically constant elements ($\rho_B > \rho_0$)

$$U^B_{\alpha\beta}(\rho) = \delta_{\alpha\beta} \frac{Z_p Z_t e^2 k}{\rho_B E} \quad \text{for} \quad \rho > \rho_B, \tag{25}$$

and is identical to $U_{\alpha\beta}(\rho)$ in the inner region:

$$U^B_{\alpha\beta}(\rho) = U_{\alpha\beta}(\rho) \quad \text{for} \quad \rho < \rho_B. \tag{26}$$

The new S-matrix S^B describes the same potential matrix for $\rho < \rho_B$ as the original S-matrix.

The Schrödinger equations for the outer region of the Coulomb potential (24) are given by

$$\left(\frac{1}{\rho} \frac{d^2}{d\rho^2} \rho - \frac{\ell(\ell+1)}{\rho^2} + k_\alpha^2 - \frac{Z_p Z_t e^2 k}{\rho E} \right) T^\ell_{\alpha n}(\rho) = 0. \tag{27}$$

Their solutions are of the form (21). The Schrödinger equations for the outer region of the constant potential (25) are

$$\left(\frac{1}{\rho} \frac{d^2}{d\rho^2} \rho - \frac{\ell(\ell+1)}{\rho^2} + \left(k^B_\alpha\right)^2 \right) T^{\ell B}_{\alpha n}(\rho) = 0 \tag{28}$$

with the new notations

$$\left(k^B_\alpha\right)^2 = \frac{E_B - E_\alpha}{E}, \quad E_B = E - \frac{Z_p Z_t e^2 k}{\rho_B}. \tag{29}$$

The solutions of (28) can be written in a form similar to equation (18):

$$T^{\ell B}_{\alpha n}(\rho > \rho_B) = \sqrt{k^B_\alpha} (h^-_\ell(k^B_\alpha \rho)\delta_{\alpha n} - S^{\ell B}_{\alpha n} h^+_\ell(k^B_\alpha \rho)). \tag{30}$$

For the transformation of the S-matrix $S^\ell_{\alpha n} \rightarrow S^{\ell B}_{\alpha n}$, we use the continuity of the wavefunctions and their derivatives at $\rho = \rho_B$. The new wavefunctions (30) can then be used as input for the solution of the ISP for neutral particles. By transforming the S-matrix we have reduced the ISP for charged particles to the ISP for neutral particles. This transformation works for all potentials, to which the asymptotic solutions are known.

4 Application to coupled square well potentials

We now apply our method to the case of coupled square well potentials. For this problem, analytic formulas for the S-matrix were derived by 9 providing us with exact input data for the inversion procedure. For simplicity we restrict ourselves to two channels.

As a first application we consider a coupled square well potential for neutral particles. The input S-matrix was calculated for the potential matrix:

$$\mathbf{V}(r) = \begin{cases} \begin{pmatrix} -6-4i & -5 \\ -5 & -4-3i \end{pmatrix} MeV & , \quad r \leq 4fm, \\ \\ 0 \quad MeV & , \quad r > 4fm. \end{cases} \tag{31}$$

The excitation energy in the first channel is set to zero: $\varepsilon_1 = 0MeV$, in the second channel $\varepsilon_2 = 5MeV$. The reduced mass is chosen to model the scattering of a neutron on a ^{12}C-nucleus: $\mu = 859.85MeV/c^2$. For the calculation of the spectral coefficients A and b in equation (19) we take the points $r_1 = 4.1fm$ and $r_2 = 4.2fm$.

Fig. 2 shows the inverted potential matrix at three different energies. The diagrams at the top and bottom of fig. 2 are the diagonal elements V_{11} and V_{22}, respectively. The two diagrams in the middle correspond to the coupling potentials V_{12} and V_{21}. The left hand side shows the real part, the right one the imaginary part of the potential.

The energies are $E = 250, 150$ and $50MeV$ for the full, dashed, and dotted curves, respectively. The original potential is reproduced best for the highest energy, since more S-matrix elements can be taken into account with increasing energy. The following cut-off angular momenta $\ell_{\max}$ were chosen in equation (19): $\ell_{\max} = 15, 12, 7$ for $E = 250, 150$ and $50MeV$, respectively.

As can be seen from equations (14) and (15), the potentials are calculated with a finite superposition of wavefunctions. The greater $\ell_{\max}$ is chosen, the more wavefunctions contribute to the potential and the arising oscillations are diminished. This effect is best seen at the discontinuity at $r = r_0 = 4fm$, which is especially difficult to reproduce. Thus, we expect smoother results, when continuous potentials are inverted. As can be seen from equation (14), the inverted potential matrix has a singularity at the origin $r = 0$. This pole will arise also with other potentials.

The number of oscillations in the potential matrix depends on the energy. For $E = 50, 150$ and $250MeV$ we have three, five, and seven maxima, respectively.

At fixed energy and different choices of $\ell_{\max}$ the number of oscillations remains constant (see fig. 4).

Although the symmetry condition $U_{\alpha\beta} = U_{\beta\alpha}$ is not explicitly used in the method, the numerical procedure automatically provides the symmetry with high accuracy.

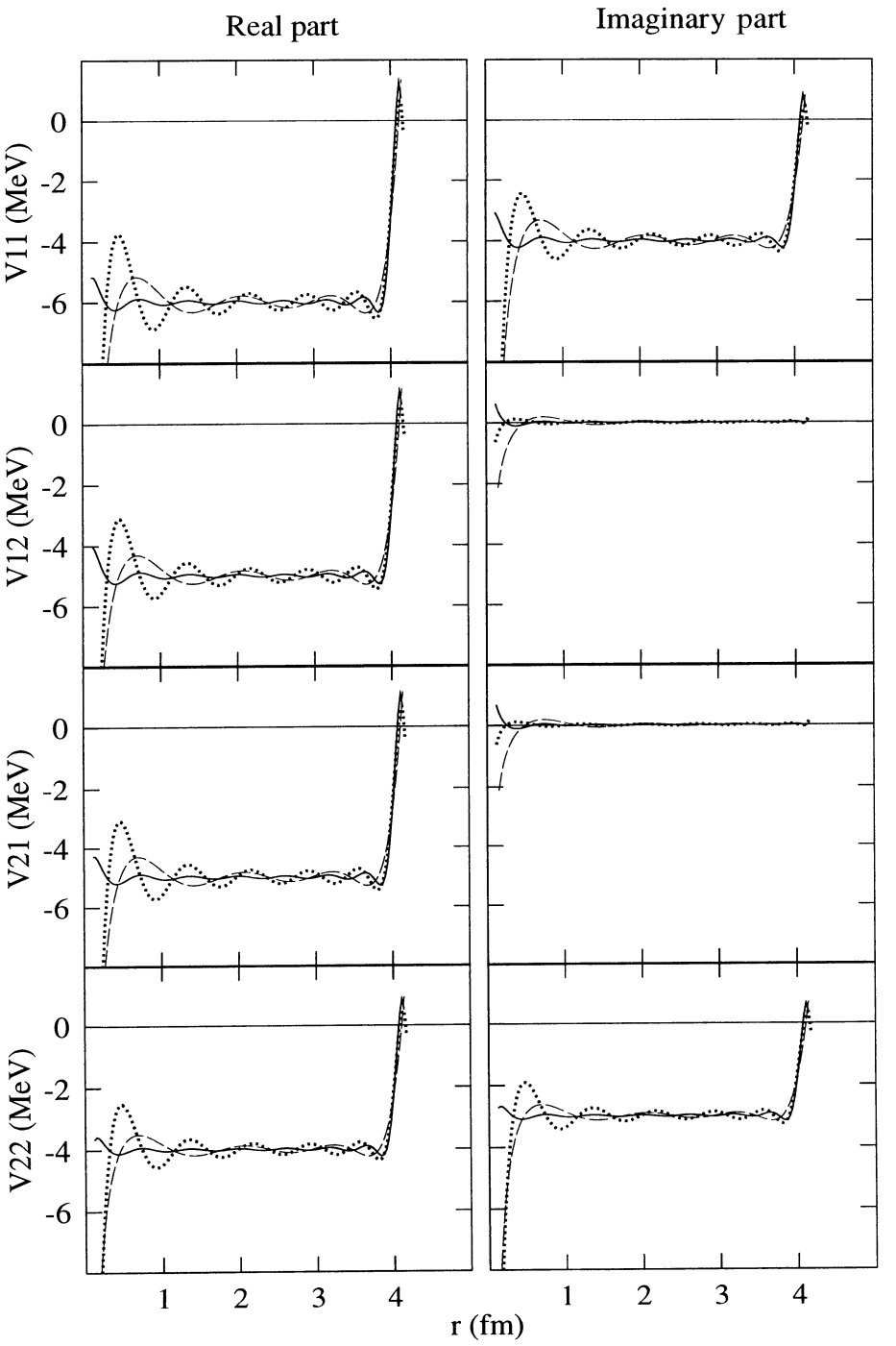

Fig. 2. Inverted potential matrix for neutral particles. $E = 250MeV$ (—), $E = 150MeV$ (- - -), $E = 50MeV$ (···).

In the second case we assume a potential matrix for two channels with charged particles:

$$\mathbf{V}(r) = \begin{cases} \begin{pmatrix} -6-4i & -5 \\ -5 & -4-3i \end{pmatrix} MeV & , \quad r \leq 5fm, \\ \dfrac{12e^2}{r} \quad MeV & , \quad r > 5fm. \end{cases} \tag{32}$$

The excitation energies are $\varepsilon_1 = 0MeV$ and $\varepsilon_2 = 5MeV$. The charge numbers and the reduced mass are chosen to model the scattering system ${}^4_2He + {}^{12}_6C$:$\mu = 2794.50MeV/c^2$.

The S-matrix corresponding to the asymptotic Coulomb potential is first transformed to the S-matrix of a constant asymptotic potential with $r_B = 6.5fm$. The radii for the calculation of the spectral coefficients A and b are $r_1 = 6.5fm$ and $r_2 = 6.6fm$.

Fig. 3 shows the inverted potential matrix at the same incident energies as in the first application. The following cut-off angular momenta $\ell_{\max}$ were chosen in equation (19): $\ell_{\max} = 30, 25, 16$ for $E = 250, 150$ and $50MeV$, respectively.

Let us now discuss the optimum choice of $\ell_{\max}$. Fig. 4 shows the inverted potential matrix for three different choices of $\ell_{\max}$: $\ell_{\max} = 27$ (dotted curve), 28 (dashed curve), and 35 (full curve). While the results for $\ell_{\max} = 27$ oscillate strongly, the potential matrix for the $\ell_{\max} = 28$ calculation already reproduces the original potential very good. This behaviour does not change significantly if $\ell_{\max}$ is further raised, as can be seen by comparisons with the $\ell_{\max} = 35$ calculation. It means, that a further improvement of the results can only be obtained by raising the numerical accuracy of the inversion program. A more detailed discussion of the optimization of the inversion procedures can be found in the diploma thesis of 10.

5 Summary and conclusions

We extended the modified Newton-Sabatier method from the one channel case to the case of N coupled channels. Due to the special choice of the Hamiltonian, the method is restricted to monopole transitions induced by the radial motion.

We need the full S-matrix as input data. This confronts us with the fundamental problem that the full S-matrix is usually not known from experimental data. In the experiment the particles are scattered in their ground state.

Thus, only one column of the S-matrix can be measured, describing the excitation from this state. In the case of only two channels and no absorption one might use the unitary condition for the S-matrix to calculate the missing matrix elements. The inversion method was derived for the scattering of neutral particles. Charged particles are treated by a transformation of the

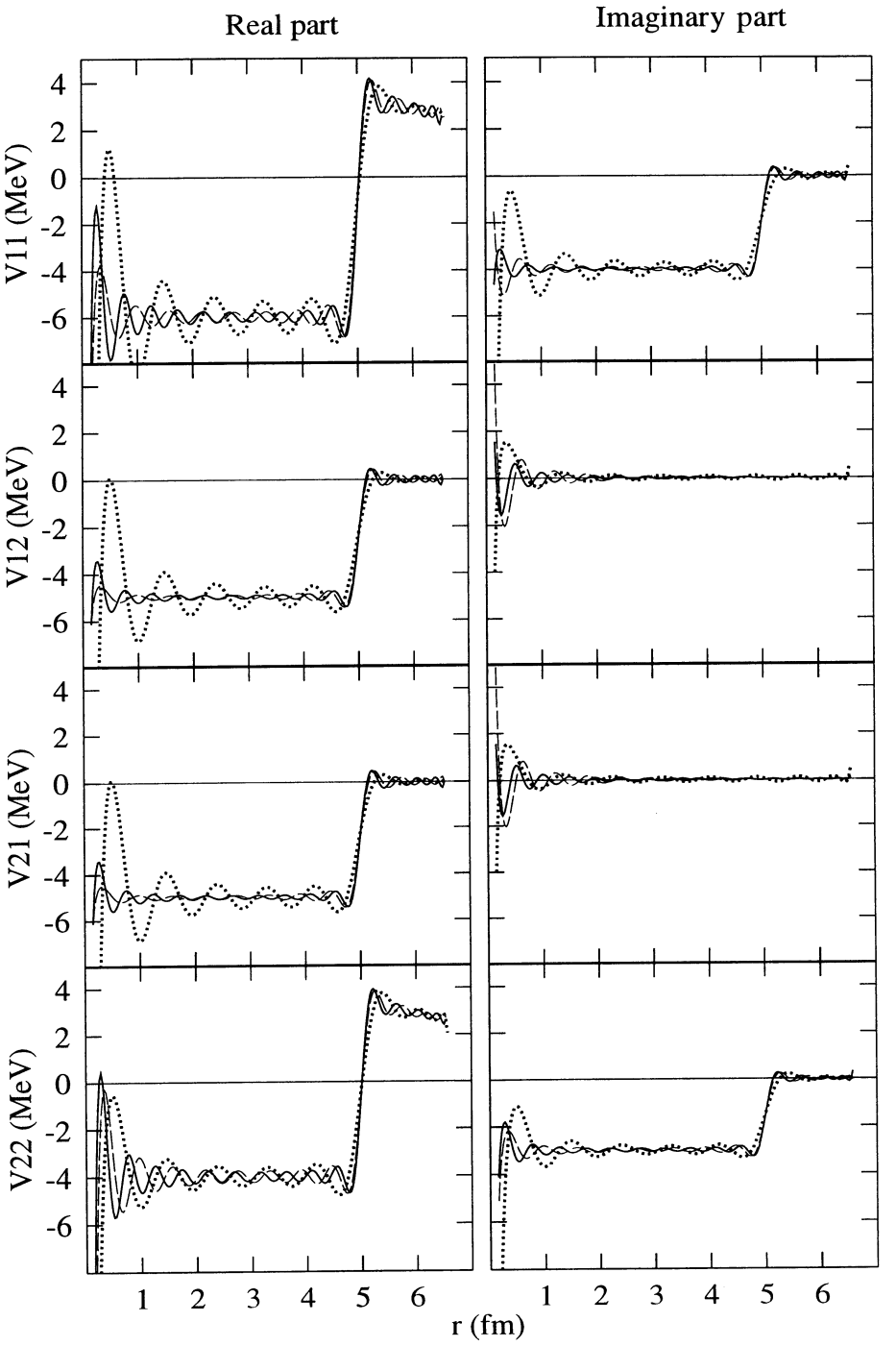

Fig. 3. Inverted potential matrix for charged particles. $E = 250MeV$ (—), $E = 150MeV$ (- - -), $E = 50MeV$ (···).

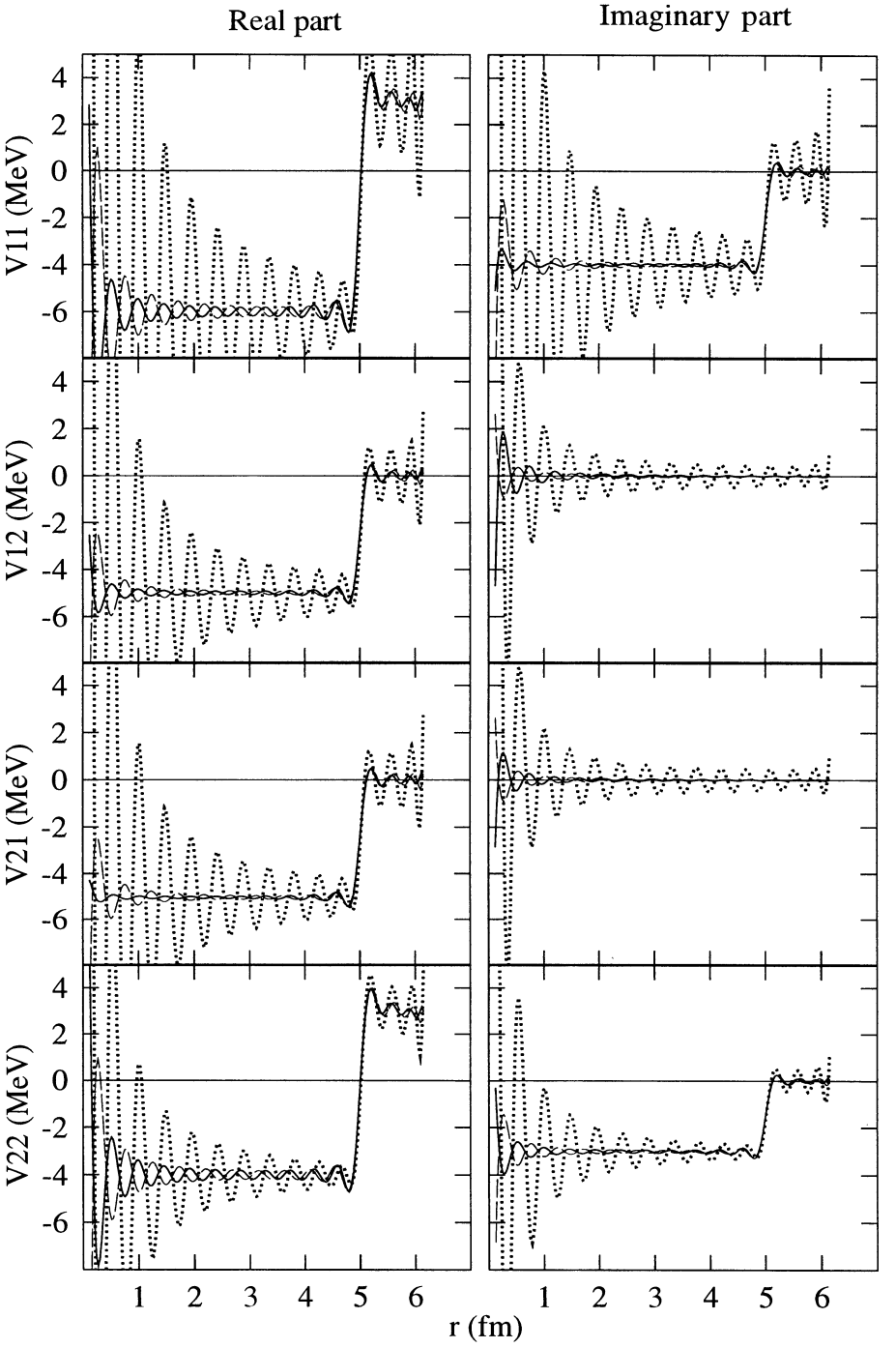

Fig. 4. Inverted potential matrix for different $\ell_{\max}$: $\ell_{\max} = 27$ (···), $\ell_{\max} = 28$ (- - -), $\ell_{\max} = 35$ (—).

S-matrix from an asymptotic Coulomb potential to an asymptotic constant potential. Then the transformed S-matrix serves as input for the inversion procedure for neutral particles.

The method was applied to an analytic S-matrix for the case of two coupled channels with a square well potential matrix for neutral and charged particles. For this case a good agreement with the initial potential matrix was found. Applications to more realistic potentials are in progress.

If we reconsider our procedure, we detect a relation of our method to the one of 11 who gave a solution of the ISP for coupled channels at fixed total angular momentum. In the case of Cox the S-matrix must be known as a function of the energy, whereas in the present method the S-matrix must be known as a function of the angular momentum of the relative motion. Therefore, in our case the angular momentum of relative motion at fixed total energy plays the same role as the energy at fixed total angular momentum in the method of Cox, and spans the space of functions in which the potential matrix is expanded. Hence, the resulting potential matrix can not depend on the angular momentum of the relative motion in our method and is not allowed to couple the orbital motion and the intrinsic dynamics of the scattered particles. In order to solve the ISP at fixed energy with a coupling between the orbital relative and the intrinsic motions, new ideas are needed.

Acknowledgements

The authors M.E. and W.S. are thankful to the Hungarian Academy of Sciences and to the DFG (Bonn) for their support in Hungary in September 1996. This work has been supported by DFG-MTA(76) and OTKA(T017179).

References

Chadan K. and Sabatier P.C. (1989): *Inverse Problems in Quantum Scattering Theory* (2nd Edition, Springer-Verlag, New York)

Cox J.R. (1967): On the determination of the many-channel potential matrix and S-matrix from a single function. Journ.Math.Phys. 8, **12**, 2327

Eberspächer M. (1996): Das Modifizierte Newton-Sabatier-Verfahren für das Inverse Streuproblem bei gekoppelten Kanälen. Diploma thesis, Gießen

Lovas R.G. (1972): Solution of coupled square well models. Atomki Közlemenyek **14**, 3, 161

May K.E., Münchow M. and Scheid W. (1984): The modified Newton method for the solution of the inverse scattering problem with charged particles at fixed energy. Phys.Lett. **141** B, 1

Münchow M. and Scheid W. (1980): Modification of the Newton Method for the Inverse-Scattering Problem at Fixed Energy. Phys.Rev.Lett **44** 1299

Newton R.G. (1962): Construction of potentials from the phase shifts at fixed energy. Journ. Math. Phys. **3**, 75

Newton R.G. (1982): *Scattering Theory of Waves and Particles* (2nd Edition, Springer Verlag, New York)

Sabatier P.C. (1966): Asymptotic Properties of the Potentials in The Inverse-Scattering Problem at Fixed Energy. Journ.Math.Phys. **7**, 1515

Satchler G.R. (1983): *Direct Nuclear Reactions* (Oxford University Press, New York)

Zakhariev B.N. and Suzko A.A. (1990): *Direct and Inverse Problems* (Springer Verlag, Berlin)

Energy-Dependent Potentials Obtained by IP Inversion

S.G. Cooper and R.S. Mackintosh

Physics Department, The Open University, Milton Keynes MK7 6AA
s.g.cooper@open.ac.uk, r.mackintosh@open.ac.uk

1 Introduction

The iterative-perturbative (IP) algorithm allows real or complex, central and spin-orbit potentials to be determined by inversion from the elastic S-matrix for both spin 0 and spin-1/2 scattering [1]. The procedure can also be applied to incomplete data sets, to data sets for a range of energies ("mixed case inversion") and to data sets containing experimental errors [2], [3]. Simple regularisation techniques are used to obtain the smoothest possible potentials where the data sets are incomplete. Although the method does not represent a rigorous mathematical solution of the inverse scattering problem, a considerable improvement over model independent fitting methods is obtained by using the Born approximation to obtain a rapidly convergent and computationally efficient solution. Similar techniques have been used by Kukulin, [4].

The IP procedure is easily further generalised for application to a wide range of cases, for example:

- Parity-dependent potentials can be established, which are necessary for a satisfactory description of p + α scattering for narrow energy ranges, [2].
- Potentials have been also determined from bound and resonant state energies for ^{3}He + α, [5].
- A recent extension of the procedure allows the determination of energy dependent potentials using an energy-independent form for the potential geometry, [6].

The last extension is the central subject of this report. It is particularly necessary for the inversion of phase shifts just above the inelastic threshold, where the imaginary potential has a strong energy dependence. In many cases a linear energy dependence in the real components provides both a sufficient and highly economical representation of the data over a wide energy range.

In this presentation, specific examples are presented to illustrate the application and limitations of this procedure for energy dependent inversion: Firstly we present a determination of p + α potentials from empirical S-matrices at energies both above and below the reaction threshold. These

potentials are compared with potentials determined from RGM phase shifts for energies up to $\sim$ 65 MeV. (The calculations are described in detail in a preprint, [6].) In the second case, an energy dependent potential is determined to reproduce $\alpha + {}^{16}\mathrm{O}$ RGM phase shifts and bound states.

2 The IP method for energy-dependent inversion

In the most general implementation of the IP procedure, bound state and resonance energies, are fitted simultaneously with phase shifts, permitting a consistent representation of bound and scattering states. The method is outlined in greater detail in a recent preprint, [6] and only a brief summary is given below.

Starting with a target set of N_κ complex S-matrix elements and N_b bound or resonant state energies, E_n, the inversion minimises,

$$\sigma^2 = \sum_\kappa w_\kappa^2 |S_\kappa^{\mathrm{tar}} - S_\kappa^{\mathrm{inv}}|^2 + W^2 \sum_n \left| \frac{\phi_2'^n}{\phi_2^n} - \frac{\phi_1'^n}{\phi_1^n} \right|^2_{r=R_{\mathrm{m}}} . \qquad (1)$$

The index, κ represent the l-value, the j-value for spins > 0 and the energy in mixed case inversion. The quantities w_κ and W are weighting factors, [6], although the w_κ might be determined from uncertainties generated in the phase shift fitting, [3]. The superscripts "tar" and "inv" refer to quantities either in the target data or determined from the inversion potential. The functions, ϕ_1^n and ϕ_2^n represent the two bound or resonant state wavefunctions, determined respectively for radial regions inside and outside the matching radius, R_{m} [5].

The procedure begins with a suitable starting reference potential, $V^{\mathrm{srp}}(r)$. In most cases a reasonable approximation is required only for the real central component. The potential determined by inversion may have imaginary and spin-orbit terms, for which each component, c, may take the parity dependent form, $V_1(r) + (-1)^l V_2(r)$. Energy dependence is introduced by expressing the components as, $V_c(r, E)) = U_c(r) F_c(E)$, where, for $V^{\mathrm{srp}}(r)$, $F_c(E) = 1$ for all c.

The value of σ^2 obtained from $V^{\mathrm{srp}}(r)$ (initially, the quantities labelled inv in Eq. 1 are calculated from $V^{\mathrm{srp}}(r)$) is decreased by adding perturbations separately to each component of $V^{\mathrm{srp}}(r)$. These perturbations are linear superpositions of suitable radial basis functions, $v_{ci}(r)$ and, optionally to establish energy dependence, a number of energy-dependent basis functions, $f_{ci}(E)$. The real components then have the form:

$$V_c^{\mathrm{inv}}(r, E) = \left[1 + \sum_{i=1}^{N_c^{\mathrm{E}}} \xi_{ci} f_{ci}(E) \right] \left[V^{\mathrm{srp}}(r) + \sum_{i=1}^{N_c^{\mathrm{b}}} \lambda_{ci} v_{ci}(r) \right] \qquad (2)$$

where ξ_{ci} and λ_{ci} are determined by inversion. The energy dependence in the imaginary components is chosen such that these components tend to zero at the inelastic threshold, i.e.,

$$F_c(E) = \left(\frac{E - E_0}{E'_{\rm ref} - E_0}\right)^p + \sum_i^{N_c^{\rm E}} \xi_{ci} g_{ci}(E - E'_{\rm ref}). \tag{3}$$

where p is a set positive value, and $E'_{\rm ref}$ is a chosen reference energy. In all applications considered here, only the first term in each energy expansion is found necessary to reproduce the phase shift data satisfactorily. For the real components we use $f_{ci}(E) = E$.

For a single perturbation, $\xi_{ci} f_{ci}(E) V_c^{\rm srp}(r)$, the approximate correction to S is given by,

$$\delta S_\kappa = \left(-\frac{i\mu\, C_c \xi_{ci} f_{ci}(E_\kappa)}{\hbar^2 k_\kappa}\right) \int_0^\infty V^{\rm srp}(r) \left(u_\kappa(r)\right)^2 \, {\rm d}r, \tag{4}$$

where $C_c = 1$ for the real central component and is suitably modified for the imaginary, spin-orbit or parity-dependent components, [6]. All other terms are as usually defined. A similar expression for δS_κ can be derived for the radial perturbation, $\lambda_{ci} v_{ci}(r)$, in which $V_c^{\rm srp}(r)$ is replaced by $v_{ci}(r)$ inside the integral and λ_{ci}, or $\lambda_{ci} F_c(E)$, replaces $\xi_{ci} f_{ci}(E_\kappa)$ outside.

The correction to $V^{\rm srp}(r)$ to fit the bound state energies is obtained by correcting the differences between the logarithmic derivatives of $\phi_1^n(R_{\rm m})$ and $\phi_2^n(R_{\rm m})$, i.e. for the perturbation, $\xi_{ci} f_{ci}(E_n^{\rm srp}) V_c^{\rm srp}(r)$, we get,

$$\xi_{ci} f_{ci}(E_n^{\rm srp}) C_c \left\{ \frac{1}{(\phi_1^n(R_{\rm m}))^2} \int_0^{R_{\rm m}} V_c^{\rm srp}(r) (\phi_1^n(r))^2 {\rm d}r + \frac{1}{(\phi_2^n(R_{\rm m}))^2} \int_{R_{\rm m}}^\infty V_c^{\rm srp}(r) (\phi_2^n(r))^2 {\rm d}r \right\} = \left(\frac{\phi_2'^n}{\phi_2^n} - \frac{\phi_1'^n}{\phi_1^n}\right)_{r=R_{\rm m}} \tag{5}$$

A similar expression is obtained for the radial perturbation, $\lambda_{ci} F_c(E) v_{ci}(r)$.

A least squares minimisation of σ^2, combined with Eqs 4 and 5, then produces a set of linear equations. These equations are solved using singular value decomposition, which, by using a suitable tolerance parameter, guarantees stabilisation of the inversion. Since the inversion equations represent only a first order approximation, the complete procedure must be repeated as an iterative process, with $V^{\rm inv}(r, E)$ replacing $V^{\rm srp}(r)$ in the above equations. However the method generally converges quickly, with close to the optimum σ^2 often obtained after two or three iterations. The complete IP procedure has been implemented in the code IMAGO.

The above method is capable of further generalisation. The scattering length at zero energy, $a^{\rm tar}$, can also be fitted simultaneously with phase shifts in the above procedure. For a potential, $V^{\rm inv}(r)$, the s-wave Schrödinger equation for $E = 0$ is integrated to obtain the radial wave functions, $u_{00}(r)$,

suitably normalised in the asymptotic region [7]. An approximation for the change in the s-wave scattering length at zero energy, δa, for a real central perturbation, $\lambda_{ci} F_c(E = 0) v_{ci}(r)$, is obtained similarly to Eqs. (4) and (5) as, [7], i.e.,

$$\delta a = \left(-\frac{\lambda_{ci} 2\mu C_c F_c(E=0)(a^{\text{inv}})^2}{\hbar^2} \right) \int_0^\infty v_{ci}(r) \left(u_{00}(r)\right)^2 \, \mathrm{d}r. \qquad (6)$$

In this case, a further term, $W_{\text{a}}(a^{\text{tar}} - a^{\text{inv}})^2$ must now be added to σ^2, where the weighting factor W_{a} establishes the relative accuracy to which the scattering length is reproduced.

The complete method can be directly applied to cases of higher spins if coupling can be neglected. Furthermore, Kukulin *et al* [4] have applied a very similar procedure to obtain potentials by direct inversion from elastic cross-section and polarisation data.

2.1 The uniqueness problem

In any problem with incomplete data, the resultant potential cannot be uniquely defined. The introduction of parity dependence increases this problem, although the extra degrees of freedom are only justified if the resultant potentials are markedly smoother than the best fitting parity independent potential, [8]. Regularisation is introduced into the IP procedure by restricting the radial basis used in the inversion and also by the use of singular value decomposition. The choice of the radial basis is then important, but the sensitivity of the solution to this choice is easily assessed by using different bases or a different choice of $V^{\text{srp}}(r)$. Bessel functions, gaussians or harmonic oscillator functions used by Kukulin may represent the functions, v_i.

The additional inclusion of energy dependence introduces further uncertainties since we consider only one out of the many possible definitions of energy dependence. A more explicit form of non-locality might be more appropriate.

3 The p-^{4}He potential up to $\sim$ 65 MeV

Before applying energy dependent inversion directly to empirical phase shifts, we first present a test of the energy dependence of the potential geometry. This test case is based on RGM phase shifts, [9], which have a smooth energy dependence. Strong similarities between the RGM potentials and empirical potentials have been previously established at subthreshold energies, [10]. In the present study, the inversion is based on "wide" energy bites, $E_{\text{cen}} \pm 1$ MeV, establishing potentials linearly dependent on energy for $E_{\text{cen}} = 10$, 30 and 50 MeV. These potentials, evaluated at $E = 0$, are shown in Fig. 1. Clearly there is little energy dependence in the potential shape for all but the

insignificant spin-orbit V_2 term. It is possibly of physical significance that the overall V_1/V_2 pattern persists almost unchanged as the range of contributing l-values changes markedly. However the coefficients ξ_{ci} decrease in magnitude with $E_{\rm cen}$, for both the central V_1 and V_2 terms, suggesting that non-linear terms in the energy-dependence are required to describe the complete energy range. In contrast, a similar analysis on the subthreshold empirical phase shifts confirms only the independence with energy of the potential shape and no predictions for a non-linear energy dependence can be deduced.

Fig 1

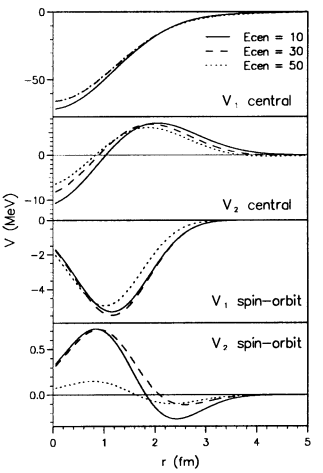

Fig. 1. For p + α, the real zero energy radial potentials $U_c(r)$ for the central and spin-orbit, V_1 and V_2 components obtained by inversion of RGM phase shifts over the energy bites, $E_{\rm cen} \pm 1$ MeV centred at the energies, $E_{\rm cen} = 10$ MeV (solid lines), $E_{\rm cen} = 30$ MeV (dashed) and $E_{\rm cen} = 50$ MeV (dotted).

For p + α at energies above the reaction threshold, energy dependent inversion has been applied to three phase shift analyses, described in detail in a recent preprint, [6]. Here we present only the potentials obtained from the S-matrices of Burzynski *et al* [11], covering the energy range from $\sim$ 30 to $\sim$70 MeV. This data set then avoids contributions from the $d_{3/2}$ resonance, which is not single particle in nature. In these inversion calculations, complex and parity dependent potentials are established, linearly dependent on energy for real $V(r)$.

Three forms of energy dependence in the imaginary potential, i.e. $p = 1$, 0.5 and 0, are used to give three inversion solutions, (1), (2) and (3) respectively. The $\arg(S_\kappa^{\rm inv})$ for these solutions are compared with the Burzynski $\arg(S_\kappa)$ in Fig. 2 and the comparison for $|S_\kappa|$ is presented in Fig. 3. The empirical data fluctuates considerably with energy so that, while the Burzynski

$\arg(S_\kappa)$ is well reproduced by the solutions, the values for $|S|$ are reproduced well only for certain partial waves.

Fig. 2

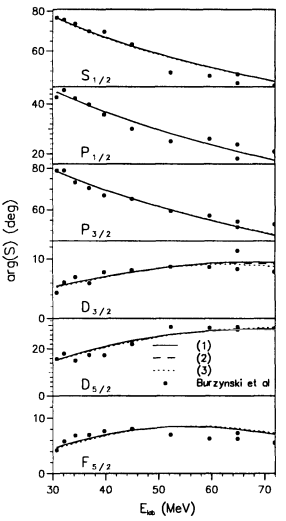

Fig. 2. For p + α above the inelastic threshold, $\arg(S_{lj})$ for $l \leq 3$ and $g_{7/2}$. The empirical values of Burzynski *et al* (solid dots) are compared with $\arg(S_{lj})$ for the three solutions described in the text, (1) solid lines, (2) dashed and (3) dotted.

The real potentials for solutions (1) and (3), extrapolated to $E = 0$, i.e. $V(r, E = 0)$ are shown in Fig. 4. This figure also includes two potentials (EF(1) and EF(2)) determined for subthreshold energies from the effective range phase shift parameterisation of Schwandt [12], and a potential determined by inversion of the complete tabulated energy range, 0 – 62 MeV, of the RGM phase shifts [9]. All these real components depend linearly on energy, and the parameters, ξ_1, are listed in Table 1.

The results presented in Fig. 4 and Table 1 reveal a remarkably consistent description, in the radial and energy dependence of most real empirical components, despite the large extrapolation in E made for the higher energy inversions. The real p + α potential may then be considered well-established up to $\sim$ 70 MeV. The parity dependence found at subthreshold energies is still significant at higher energies, although the energy gradient for the central $V_2(r)$ is notably larger than that of the central V_1 component. A good agreement is also found between the empirical and RGM potentials, particularly for $r > 3$ fm, in the radial shape, depth and energy dependence, despite the simplicity of the single channel RGM. We conclude that many features in the empirical potential relate directly to the effects of antisymmetrisation.

Fig. 3

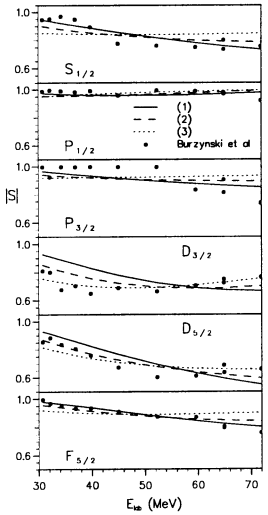

Fig. 3. As Fig. 2 for $|S_{lj}|$.

Fig. 4

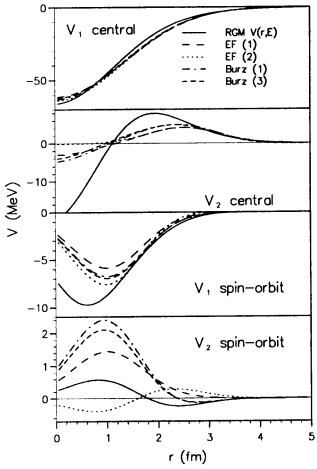

Fig. 4. For p + α real potentials linearly dependent on energy, evaluated at $E = 0$ (i.e. $U_c(r)$). The potentials are : solid line, RGM; long dashes, EF(1); dots, EF(2); dot-dash, Burzynski (1); and short dash, Burzynski (3).

The imaginary components of the three solutions for energies above the reaction threshold, are calculated for $E'_{\rm ref} = 30$ MeV and are shown in Fig. 5, evaluated at 30 MeV. These components are small in magnitude, but parity dependence is necessary to reproduce the phase shift data. However, due to the uncertainties in the empirical S-matrices, the exact radial form and energy dependence of the imaginary components cannot be well-determined.

Fig. 5

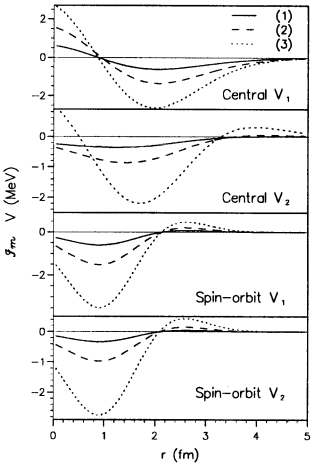

Fig. 5. For p + α above the inelastic threshold, the imaginary potentials evaluated at $E'_{\rm ref} = 30$ MeV for the three solutions resulting from inversion of the Burzynski S-matrix, (1) solid lines, (2) dashed and (3) dotted.

Table 1. The coefficients p (for cases above reaction threshold) and ξ_1 in MeV^{-1}, for potentials linearly dependent on energy determined from RGM, empirical sub-threshold phase shift parameterisations and from empirical S-matrices at energies above the inelastic threshold.

$\mathbf{S}^{\rm tar}$	p	ξ_1			
		Central V_1	Central V_2	Spin-orbit V_1	Spin-orbit V_2
Effective range (1)	-	−0.0043	−0.0119	0.0032	0.0344
Effective range (2)	-	−0.0045	−0.0123	0.0089	−0.00039
Burzynski (1)	1	−0.0054	−0.0109	0.0002	−0.0028
Burzynski (2)	0.5	−0.0053	−0.0109	0.0004	−0.0028
Burzynski (3)	0.0	−0.0053	−0.0108	0.0005	−0.0028
RGM	-	−0.0038	−0.0137	0.0024	−0.0086

4 $\alpha + {}^{16}O$ potential local equivalent to RGM

Here, as a preface to a wider analysis of empirical data for α–^{16}O, the IP procedure is applied to phase shifts and bound state energies obtained from single channel RGM calculations. Real phase shifts tabulated to 30 MeV (c.m.) and bound state energies for α–^{16}O calculated using the single channel RGM with all exchange terms, have been provided by Tang, (private communication). This idealised data set provides a test of the energy dependent inversion for higher mass systems.

An inversion of the bound and resonant state energies for the two lowest energy bands alone, 0_1^+ and 0^-, yields successful results using a parity and energy *independent* potential. The resulting energy values are listed in the first lines Table 2. The addition of a V_2 term leads to a decrease in σ^2 from 0.39 to 0.107, corresponding to a improvement in the reproduction of the energies for some states. Little improvement in σ^2 is gained by the addition of energy dependence.

Table 2. The bound and resonant state energies for the lowest energy bands obtained from RGM theory and compared with corresponding values obtained by IP inversion both with and without parity dependence.

$l=$	0	1	2	3	4	5	6	7	8
RGM	−4.72	1.26	−3.3	3.15	−0.06	6.8	5.2	12.75	11.65
V_1 only	−4.68	1.39	−3.32	3.25	−0.130	6.84	4.98	12.59	12.31
V_2 included	−4.77	1.25	−3.29	3.16	0.063	6.81	5.14	12.71	11.66
All data (V_1)	−4.92	1.52	−3.70	3.36	−0.77	6.90	3.99	12.57	10.94

Similar results are obtained from inversion of the complete data set, and a remarkable overall fit can be obtained without energy or parity dependence. In Fig 6, the resulting phase shifts are compared with the RGM values, showing how well the overall energy dependence is predicted. The last line of Table 2 lists the bound/resonant state energies obtained with this new potential and shows a satisfactory fit to the odd/even splitting of the resonances which is only slightly worse than that for the inversion of the bound/resonant state energies alone. However, only a slight improvement in the complete overall fit is found from the addition of a real V_2 term and, again, virtually no further improvement is found by allowing energy dependence in the potential depth.

Fixed energy inversion of the phase shifts is possible for α+^{16}O, and now a significantly lower value of σ^2 is obtained by including a V_2 term. Potentials, determined for energies of 10, 20, and 30 MeV (c.m.), are shown in Fig. 7. The parity dependent potential obtained from inversion of only

Fig. 6

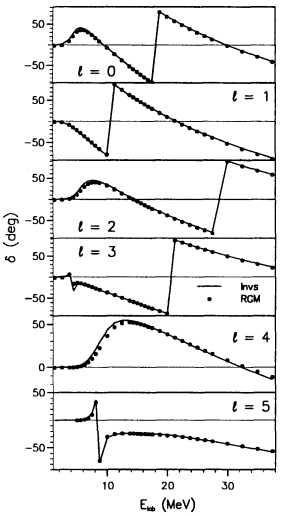

Fig. 6. For α+^{16}O, arg(S_{lj}) for $l = 0 - 6$, comparing values calculated using the RGM (filled circles) with values obtained by energy and parity independent inversion (solid lines).

the bound and resonant state energies is also shown. The V_1 component obtained from the fixed energy inversions is close in magnitude and depth to both the potential reproducing bound and resonant states only, as well as to the potential obtained by inversion of the complete data set (not shown). The fixed energy inversions show little energy dependence in the potential geometry of V_1, although the volume integrals increase slightly with energy. The small V_2 component is clearly less well defined, but significant changes are found in the geometry with increasing energy which will necessarily limit the accuracy of any mixed case inversion which does not accommodate this shape dependence.

5 Summary and outlook

We have presented the iterative perturbative inversion procedure in its most general form for determining energy and parity dependent potentials by inversion from both complex phase shifts and bound state energies. This method is a necessary extension of mixed case inversion techniques previously presented, which incorporate a wide range of data in order to reduce the ambiguities arising from inversion of incomplete data sets.

Fig. 7

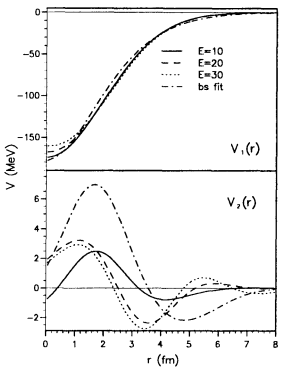

Fig. 7. For α+^{16}O, the real parity dependent potentials, $V(r)$ obtained by fixed energy inversion at the energies, $E = 10$ MeV (solid lines), $E = 20$ MeV (dashed lines) and $E = 30$ MeV (dotted lines) compared with that obtained by inversion from the bound and resonant states alone (dash-dot lines).

For the first time, inversion has established p + α potentials which describe the empirical complex phase shifts for a wide range of energies above the inelastic threshold. Combining these results with calculations for sub-threshold energies, a consistent energy dependent potential is obtained for the energy range, 0 ~70 MeV. For α + ^{16}O scattering, a good overall description of RGM phase shifts and bound state energies has been obtained with a local potential, without energy or parity dependence. However, an exact reproduction of the data requires inclusion of small energy dependent effects, which must include an energy dependence in the shape of the parity dependent term.

In the future we believe that the generalised IP procedure offers many advantages to facilitate the comparison between theory and experiment. Many empirical data sets contain too few l-values to allow fixed energy inversion although energy dependent potentials may be necessary. New descriptions of energy dependence, or more direct prescriptions of non-locality, must also be explored and the IP method should permit an easy comparison between different energy-dependent descriptions.

Acknowledgements

We are most grateful to the Science and Engineering Research Council of the UK, and its successor EPSRC, for grant GR/H00895 supporting Dr Cooper.

References

[1] A.A. Ioannides and R.S. Mackintosh, Nucl. Phys. **A467**, 482 (1987).
[2] S.G. Cooper and R.S. Mackintosh, Phys. Rev. C**43**, 1001 (1991).
[3] S.G. Cooper and R.S. Mackintosh, Inverse Problems, **5**, 707 (1989).
[4] V.I. Kukulin, V.N. Pomerantsev and S.V. Zuev, Phys. of Atomic Nuclei **59** 403 (1996)
[5] S.G. Cooper, Phys Rev C50 (1994) 359.
[6] S.G. Cooper and R.S. Mackintosh, OU preprint OUPD9602 (1996).
[7] J.D. Jackson and J.M. Blatt, Rev. Mod. Phys. **22**, 77 (1950).
[8] S.G. Cooper and R.S. Mackintosh, Z. Phys. A**337**, 357 (1990)
[9] I. Reichstein and Y.C. Tang, Nucl. Phys. **A158**, 529 (1970).
[10] S.G. Cooper, R.S. Mackintosh, A. Csótó, and R.G. Lovas, Phys. Rev.C **50**, 1308 (1994).
[11] S. Burzynski, J. Campbell, M. Hammans, R. Henneck, W. Lorenzon, M.A. Pickar, and I. Sick, Phys. Rev. C**39**, 56 (1989).
[12] P. Schwandt, T.B. Clegg, and W. Haeberli, Nucl. Phys. **A163**, 432 (1971).

Modeling of Nucleon–Nucleon Potentials, Quantum Inversion versus Meson Exchange Pictures

L. Jäde, M. Sander, and H. V. von Geramb

Theoretische Kernphysik, Universität Hamburg,
Luruper Chaussee 149, D–22761 Hamburg, Germany

Abstract. The notion of interacting elementary particles for low and medium energy nuclear physics is associated with definitions of potential operators which, inserted into a Lippmann–Schwinger equation, yield the scattering phase shifts and observables. In principle, this potential carries the rich substructure consisting of quarks and gluons and thus may be deduced from some microscopic model. In this spirit we propose a boson exchange potential from a nonlinear quantum field theory. Essentially, the meson propagators and form factors of conventional models are replaced by amplitudes derived from the dynamics of self–interacting mesons in terms of solitary fields. Contrary to deduction, we position the inversion approach. Using Gel'fand–Levitan and Marchenko inversion we compute local, energy–independent potentials from experimental phase shifts for various partial waves. Both potential models give excellent results for on–shell NN scattering data. In the off–shell domain we study both potential models in $(p, p\gamma)$ Bremsstrahlung, elastic nucleon–nucleus scattering and triton binding energy calculations. It remains surprising that for all observables the inversion and microscopic meson exchange potentials are equivalent in their reproduction of data. Finally, we look for another realm of elementary interactions where inversion and meson exchange models can be applied with the hope to find more sensitivity to discern substructure dynamics.

1 Introduction

In the last decade, the development of highly quantitative models for the nucleon–nucleon interaction was one of the major tasks of theoretical nuclear physicists. Based on Yukawa's pioneer work, potentials for NN forces mediated by the exchange of boson fields with masses below 1 GeV were invented and successfully applied to various problems in medium energy nuclear physics [1]. Despite of their remarkable ability to account for quantitative details of NN phenomenology, none of these models contains any reference to Quantum Chromodynamics QCD, which is believed to be the underlying microscopic theory of the strong interaction. There are a number of models which explicitly refer to QCD [2], but so far all of them fail to describe the nucleon–nucleon interaction comparable well as the phenomenological boson exchange potentials. Thus the major shortcomings of today's nucleon–nucleon potential models are the empirical character of the boson–exchange potentials

which arises from phenomenological usage of form factors without stringent connections to QCD and on the other side the failure of QCD inspired models to provide a quantitative description of nucleon–nucleon scattering data.

The goal of the Solitary Boson Exchange Potential, which will be described in detail in section 3 is to interpolate between these extreme positions [1]. Characteristic features of QCD inspired potential models, namely their nonlinear character, are taken into account using a nonlinear expansion of the Klein–Gordon equation as equation of motion for the boson fields. On the other hand, the solutions of this equation, called *solitary boson fields*, are used in a boson exchange potential which is in great analogy to the Bonn–B potential [4] to obtain a quantitative description of NN data comparable well as the phenomenological boson exchange potentials. It will turn out that the nonlinear character of the boson fields allows to substitute the phenomenological form factors of the Bonn potential. Simultaneously, an empirical scaling law is found which relates all meson parameters, as expected in a model based on QCD.

Contrary to the microscopic models, potentials obtained from quantum inversion were developed for various hadron–hadron interactions [5]. Using experimental phase shifts as input in the Gel'fand–Levitan and Marchenko inversion algorithm for the Sturm–Liouville equation yields local potential operators in coordinate space which are model–independent and reproduce the experimental data by construction.

As far as elastic NN data are concerned, inversion potentials evidently provide a precise description of the NN interaction. It is a nontrivial question, however, whether this accuracy remains in the application of inversion potentials to more complex problems. Since the scattering phase shifts, from which inversion potentials are obtained, only contain the *on–shell* information of the scattering amplitude, i.e. the absolute value of the incoming and outgoing nucleon momentum remains unchanged, it is questionable if such a potential can account for the description of reactions where the *off–shell* part of the t–matrix contributes. A sensitivity on details of the off–shell amplitude would provide the desired possibility to test possible effects of the substructure of potential models. In particular, we seek a signature in the data to confirm the assumptions which led to the Solitary–Boson–Exchange–Potential. To study this interesting point we apply boson exchange as well as inversion potentials to calculate the differential cross section for $(p, p\gamma)$ Bremsstrahlung and elastic nucleon–nucleus scattering as well as the triton binding energy. The astonishing outcome implies that inversion and boson exchange potentials yield equivalent results. Even more surprising, an improvement of the description of the on–shell data enhances the accuracy describing the off–shell data.

Before inversion and boson exchange potentials will be compared, we give a short reminder of the algorithms which are used to calculate inversion potentials from experimental phase shifts and show the typical structure of

boson exchange potentials outlining the basic ideas of our Solitary–Boson–Exchange–Potential model.

2 Nucleon–Nucleon Potentials from Inversion

Contrary to the direct path to obtain a potential for NN scattering from some microscopic model, the algorithm of quantum inversion can be applied using experimental phase shifts as input [5]. Nowadays, the inversion techniques for nucleon–nucleon quantum scattering have evolved up to almost perfection for scattering data below pion production threshold. Numerically, input phase shifts can be reproduced for single and coupled channels with a precision of 1/100 of a degree, which is much lower than the experimental uncertainty. This accuracy and the possibility to test the inversion potential 'online', i.e. inserting the potential into the scattering equation to reproduce the input phase shifts, makes them a reliable and easy–to–handle tool for highly quantitative medium energy nuclear physics. Guided by this spirit, the utmost aim of quantum inversion is to provide the most simple operator to reproduce the scattering data. This paradigm, however, proscribes to include any momentum dependence and thus any non–locality in the potential since this would open a box full of ambiguities which can not be associated with the goal of simplicity.

As a basis, the radial Schrödinger equation is assumed to be the relevant equation of motion for the two–particle system

$$\left\{-\frac{d^2}{dr^2}+\frac{\ell(\ell+1)}{r^2}+\frac{2\mu}{\hbar^2}V_\ell(r)\right\}\psi_\ell(k,r)=k^2\psi_\ell(k,r), \tag{1}$$

where $V_\ell(r)$ is a local, energy–independent operator in coordinate space. Substituting

$$q(r)=\frac{\ell(\ell+1)}{r^2}+\frac{2\mu}{\hbar^2}V_\ell(r) \qquad \text{and} \qquad \lambda=k^2, \tag{2}$$

one obtains the well–known Sturm–Liouville equation

$$\left[-\frac{d^2}{dx^2}+q(x)\right]y(x)=\lambda y(x). \tag{3}$$

The scattering phase shifts enter as boundary conditions for the physical solutions of (1) which read

$$\lim_{r\to\infty}\psi_\ell(k,r)=\exp(i\delta_\ell(k))\sin(kr-\frac{\ell\pi}{2}+\delta_\ell(k)) \tag{4}$$

There are two equivalent inversion algorithms for the Sturm–Liouville equation, the Marchenko and the Gel'fand–Levitan inversion, which will be outlined in the next sections for the case of uncoupled channels.

2.1 Marchenko Inversion

In the Marchenko inversion the experimental information enters via the S–matrix, which is related to the scattering phase shifts by the simple relation

$$S_\ell(k) = \exp(2i\delta_\ell(k)). \tag{5}$$

Inserting a rational representation of the S–matrix [5] into the integral equation for the input kernel

$$F_\ell(r,t) = -\frac{1}{2\pi}\int_{-\infty}^{+\infty} h_\ell^+(kr)\,[S_\ell(k)-1]\,h_\ell^+(kt)dk, \tag{6}$$

where $h_\ell^+(x)$ are the Riccati–Hankel functions, the Marchenko equation

$$A_\ell(r,t) + F_\ell(r,t) + \int_r^\infty A_\ell(r,s)F_\ell(s,t)ds = 0, \tag{7}$$

becomes an algebraic equation for the translation kernel $A_\ell(r,t)$. The potential is obtained by taking the derivative

$$V_\ell(r) = -2\frac{d}{dr}A_\ell(r,r). \tag{8}$$

2.2 Gel'fand–Levitan Inversion

Instead of the S–matrix in the Gel'fand–Levitan inversion the Jost–matrix carries the experimental input. The latter is related to the S–matrix by

$$S_\ell(k) = \frac{F_\ell(-k)}{F_\ell(k)}, \tag{9}$$

and leads to the input kernel

$$G_\ell(r,t) = \frac{2}{\pi}\int_0^\infty j_\ell(kr)\left[\frac{1}{|F_\ell(k)|^2}-1\right]j_\ell(kt)dk, \tag{10}$$

where $j_\ell(x)$ are the Riccati–Bessel functions. A rational representation of the spectral density [5] again yields an algebraic form for the Gel'fand–Levitan equation

$$K_\ell(r,t) + G_\ell(r,t) + \int_0^r K_\ell(r,s)G_\ell(s,t)ds = 0, \tag{11}$$

and the desired potential is obtained from

$$V_\ell(r) = 2\frac{d}{dr}K_\ell(r,r). \tag{12}$$

2.3 Coupled Channel Inversion

For coupled channels, i.e. transitions between states with different angular momentum ℓ_i, the Schrödinger equation (1) becomes a matrix equation.

$$\left\{-\frac{d^2}{dr^2}\mathbf{1}+\mathbf{V}(r)\right\}\Psi(r)=k^2\Psi(r), \tag{13}$$

where in the case of two coupled angular momentum the potential matrix reads

$$\mathbf{V}(r)=\begin{pmatrix} \dfrac{\ell_1(\ell_1+1)}{r^2}+\dfrac{2\mu}{\hbar^2}V_{\ell_1\ell_1}(r) & \dfrac{2\mu}{\hbar^2}V_{\ell_1\ell_2}(r) \\ \dfrac{2\mu}{\hbar^2}V_{\ell_2\ell_1}(r) & \dfrac{\ell_2(\ell_2+1)}{r^2}+\dfrac{2\mu}{\hbar^2}V_{\ell_2\ell_2}(r) \end{pmatrix}.$$

The input and translation kernels of the previous sections and in particular the S–matrix now generalize to matrices. Since it is cumbersome for coupled channel situations to solve the Riemann–Hilbert Problem (9) numerically we will focus on the Marchenko inversion which does not include any serious difficulty for the general case of coupled channels. Defining the diagonal matrix which contains the Riccati–Hankel functions by

$$\mathbf{H}(x)=\begin{pmatrix} h^+_{\ell_1}(x) & 0 \\ 0 & h^+_{\ell_2}(x) \end{pmatrix},$$

one gets as a generalization of (6) for the input kernel

$$\mathbf{F}(r,t)=-\frac{1}{2\pi}\int_{-\infty}^{+\infty}\mathbf{H}(kr)\left[\mathbf{S}(k)-\mathbf{1}\right]\mathbf{H}(kt)dk+\sum_{i=1}^{N_B}\mathbf{H}(k_ir)\mathbf{N}(k_i)\mathbf{H}(k_it), \tag{14}$$

where the matrix $\mathbf{N}(k_i)$ contains the asymptotic normalizations of the wave functions for the bound states at (imaginary) momentum k_i. The Marchenko fundamental equation (7) now reads

$$\mathbf{A}(r,t)+\mathbf{F}(r,t)+\int_r^{\infty}\mathbf{A}(r,s)\mathbf{F}(s,t)ds=0, \tag{15}$$

and the potential matrix is obtained from

$$\mathbf{V}(r)=-2\frac{d}{dr}\mathbf{A}(r,r). \tag{16}$$

3 The One–Solitary–Boson–Exchange Potential

In the following section, our Solitary–Meson–Exchange–Potential model is used to demonstrate the major problems in the modeling of nucleon–nucleon potentials using the boson exchange picture. As mentioned in the introduction today's models for NN interaction either refer to QCD but can not describe scattering data or — as is the case for the conventional boson exchange potentials — they contain empirical entities which must be fitted to experiment.

The One–Solitary–Boson–Exchange–Potential OSBEP which was recently developed by the Hamburg group [1] tries to interpolate between these extreme positions. Surprisingly, it turns out that the inclusion of typical features from QCD inspired models can account for the empirical parts of usual boson exchange potentials preserving the high accuracy in the description of NN data. Therefore, we take the OSBEP as an illustrative example of how a microscopic model is used to obtain a boson exchange potential for nucleon–nucleon interactions.

3.1 Solitary Mesons

Motivated by the nonlinear character of QCD we assume a nonlinear self–interaction for *all* mesons which enter the boson exchange potential. Doing so, we use the model of solitary mesons developed by Burt [6]. Here the decoupled meson field equation is parameterized by

$$\partial_\mu \partial^\mu \Phi + m^2 \Phi + \lambda_1 \Phi^{2p+1} + \lambda_2 \Phi^{4p+1} = 0, \tag{17}$$

where Φ is the operator to describe the self–interacting fields. For mesons with nonzero spin this operator is a vector in Minkowski space. The parameter p equals $1/2$ or 1 to yield odd or even powered nonlinearities. Using this parameterization, equation (17) can be solved analytically. The solutions are represented as a power series in φ [6]

$$\Phi = \sum_{n=0}^{\infty} C_n^{1/2p}(w)\, b^n\, \varphi^{2pn+1}, \tag{18}$$

where φ is a solution of the free Klein–Gordon equation with meson mass m. These special wavelike solutions of (17) are oscillating functions which propagate with constant shape and velocity. Corresponding to the classical theory of nonlinear waves they shall be called *solitary meson fields*. The coefficients $C_n^a(w)$ are Gegenbauer Polynomials, b and w are functions of the coupling constants and the order p of the self–interaction. To quantize the solitary fields we use free wave solutions of the Klein–Gordon equation in a finite volume V [7]

$$\varphi(x,k) := \frac{1}{\sqrt{2 D_k \omega_k V}}\, a(k)\, e^{-ikx}, \tag{19}$$

where the operator $a(k)$ annihilates and the hermitian adjoint $a^\dagger(k)$ creates quanta of positive energy

$$\omega_k^2 = \mathbf{k}^2 + m^2.$$

At this point it is important to notice that we added a factor D_k which is an arbitrary Lorentz invariant function of ω_k. As will become obvious later this constant is crucial for the proper normalization of solitary waves.

The probability for the propagation of an interacting field can now be defined as the amplitude to create an interacting system at some space–time point x which is annihilated into the vacuum at y. Since the intermediate state is not observable and the particles are not distinguishable a weighted sum over all intermediate states has to be performed [8]

$$\begin{aligned} iP(y-x) = & \\ & \sum_k \sum_{N=0}^{\infty} \frac{1}{N!} \Big[\langle 0|\Phi(y,k)|N_k\rangle\langle N_k|\Phi^\dagger(x,k)|0\rangle\theta(y_0 - x_0) \\ & + \langle 0|\Phi(x,k)|N_k\rangle\langle N_k|\Phi^\dagger(y,k)|0\rangle\theta(x_0 - y_0)\Big]. \end{aligned} \tag{20}$$

A straight forward calculation yields the desired amplitude in momentum space

$$\begin{aligned} iP(k^2,m) = & \sum_{n=0}^{\infty} \left[C_n^{1/2p}(w)\right]^2 \\ & \times \frac{b^{2n}}{(2V)^{2pn}} \frac{(2pn+1)^{2pn-2}}{D_k^{2pn+1}(\mathbf{k}^2 + M_n^2)^{pn}}\, i\Delta_F(k^2, M_n), \end{aligned} \tag{21}$$

with the Feynman propagator

$$i\Delta_F(k^2, M_n) = \frac{i}{k_\mu k^\mu - M_n^2}, \tag{22}$$

and a mass–spectrum

$$M_n = (2pn+1)m.$$

Since $V \cdot \omega_k$ is a Lorentz–scalar the amplitude (21) is Lorentz invariant. At this point it is convenient to introduce the dimensionless coupling constants α, α_1 and α_2 which we define as

$$\begin{aligned} \alpha &:= \frac{b}{(2mV)^p}, \\ \alpha_1 &:= \frac{\lambda_1}{4(p+1)m^2(2mV)^p}, \\ \alpha_2 &:= \frac{\lambda_2}{4(2p+1)m^2(2mV)^{2p}}. \end{aligned} \tag{23}$$

This yields

$$w = \frac{\alpha_1}{\sqrt{\alpha_1^2 - \alpha_2}}, \tag{24}$$

and

$$iP(k^2, m) = \sum_{n=0}^{\infty} \left[C_n^{1/2p}(w)\right]^2 \times \frac{\left[(m^p\alpha_1)^2 - m^{2p}\alpha_2\right]^n (2pn+1)^{2pn-2}}{D_k^{2pn+1}(\mathbf{k}^2 + M_n^2)^{pn}} \, i\Delta_F(k^2, M_n). \tag{25}$$

The amplitude (25) shall be referred to as *modified solitary meson propagator*. For $p = 1$ one gets the amplitude for the propagation of pseudoscalar fields, $p = 1/2$ describes scalar particles. The series (25) converges rapidly, depending on the mass the subsequent terms diminish by two (π) or three (ω) orders of magnitude and in practical calculations it is sufficient to use $n_{max} = 4$.

3.2 Proper Normalization

The propagator (25) contains the arbitrary constant D_k which can depend on the energy ω_k and the coupling constants and is fixed by the conditions [6]

- all amplitudes must be Lorentz invariant,
- D_k must be dimensionless,
- all self–scattering diagrams must be finite,
- the fields have to vanish for $\lambda_1, \lambda_2 \to 0$.

Whereas the first three conditions are evident the last one requires to recall:

> If a particle has no interaction then there is no way to create or measure it and the amplitude for such a process vanishes. The field exists solely because of its interaction.

The proper normalization constant is a powerful tool to avoid the problem of regularization which arises in conventional models. In a $\lambda\Phi^4$–theory for example, which is described by setting $\lambda_2 = 0$ and $p = 1$, one gets infinite results calculating the first correction to the two–point function $iP(k^2, m)$. A proper normalization, i.e. using the smallest power

$$D_k \sim (\omega_k V)^2,$$

makes the result finite. A different situation occurs in models including massive spin–1 bosons. Such a case, with or without self–interaction, is harder to regularize due to the additional momentum dependence which arises from the tensor structure in Minkowski space. Nevertheless, the vector mesons ρ

and ω are important ingredients in every boson exchange model. A minimum power proper normalization to solve this problem is

$$D_k \sim (\omega_k V)^4.$$

In summary, we satisfy the above stated four conditions with

$$D_k = \left\{ 1 + \left[\left(\frac{m^2}{\lambda_1} \right)^{\frac{2}{p}} + \left(\frac{m^2}{\lambda_2} \right)^{\frac{1}{p}} \right] (\omega_k V)^2 \right\}^{\kappa} \tag{26}$$

$$\text{where:} \quad \begin{cases} \kappa = 1 & \text{for scalar and pseudoscalar mesons.} \\ \kappa = 2 & \text{for vector mesons.} \end{cases}$$

3.3 The Benefits of OSBEP

With its proper normalization, the solitary meson propagator now is completely determined and can be applied in a boson exchange potential. In conventional models a renormalized Feynman propagator is used to describe the meson propagation. Additionally, an empirical form factor is attached to each vertex to achieve convergence in the scattering equation. In a model with solitary mesons as excess particles the solitary meson propagator (21) should be used instead of the Feynman propagator. Due to the proper normalization, the solitary meson propagator already carries a strong decay with increasing momentum and thus offers the possibility to forgo the form factors. Therefore, proper normalization not only cures the problem to regularize the meson self–energy but simultaneously provides a meson propagator which is able to substitute the form factors and thus partly rejects the phenomenological character from the boson exchange picture.

Additionally, comparing the properly normalized solitary meson propagators to the Bonn–B form factors, we find an empirical scaling relation for the meson self–interaction coupling constants (23). We regarded the simple case $\lambda_2 = 0$ to obtain [1]

$$\begin{aligned} & \alpha(m) = \alpha_\pi \cdot \left(\frac{m_\pi}{m} \right)^{\frac{1}{2}} && \text{for scalar fields,} \\ \text{and:} \quad & \frac{\alpha(m)}{\sqrt{\kappa}} = \frac{\alpha_\pi}{\sqrt{\kappa_\pi}} \cdot \left(\frac{m_\pi}{m} \right) && \text{for pseudoscalar and vector fields.} \end{aligned} \tag{27}$$

Thus, the pion self–interaction coupling constant α_π is the only parameter to describe the meson dynamics. This connection between masses and coupling constants can be anticipated in a model which is motivated by QCD and thus puts physical significance into the parameter α_π.

Together with the meson–nucleon coupling constants the model contains a total number of nine parameters (see Table 1) which are adjusted to obtain a good fit to *np* scattering phase shifts and deuteron data (see Table 2 and Figure 1). The agreement with scattering observables (Figure 2) is excellent and the goal to achieve a description of experimental data which is comparable to the Bonn–B potential is accomplished.

Table 1. OSBEP parameters

	π	η	ρ	ω	σ_0	σ_1	δ
S^P	0^-	0^-	1^-	1^-	0^+	0^+	0^+
$\frac{g_\beta^2}{4\pi}$	13.7	1.3985	1.1398	18.709	14.147	7.8389	1.3688

$\alpha_\pi = 0.428321$ $\qquad$ $f_\rho/g_\rho = 4.422$

Table 2. Deuteron Properties

	Bonn–B[a]	OSBEP	Exp.
E_B (MeV)	2.2246	2.22459	2.22458900(22)
μ_d	0.8514[b]	0.8532[b]	0.857406(1)
Q_d (fm^2)	0.2783[b]	0.2670[b]	0.2859(3)
A_S (fm$^{-1/2}$)	0.8860	0.8792	0.8802(20)
D/S	0.0264	0.0256	0.0256(4)
r_{RMS} (fm)	1.9688	1.9539	1.9627(38)
P_D (%)	4.99	4.6528	—

[a] Data from [4]

[b] Meson exchange current contributions not included

4 The Quest for Off–Shell Effects

Concerning nucleon–nucleon scattering, boson exchange models and inversion potentials show excellent agreement with experimental data. The results of the OSBEP and Bonn–B models are shown in Figure 1, the inversion potentials reproduce the phase shifts by construction. The next step is to apply

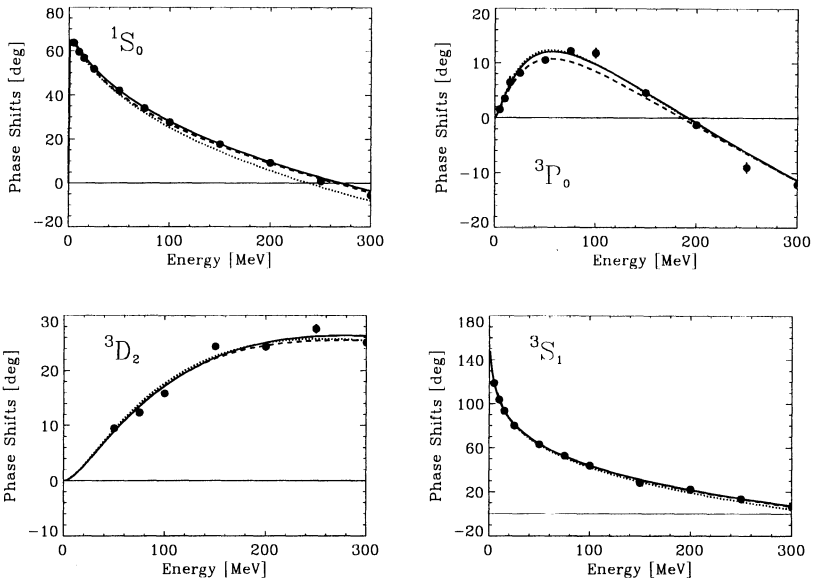

Fig. 1. Selected *np* phase shifts: Arndt SM95 (circles), Nijmegen PWA (dashed), Bonn–B (dotted) and OSBEP (full).

both potential models in more complex reactions to find out whether the absent off–shell information in the inversion potentials would lead to a breakdown of the model in situations where the off–shell part of the scattering amplitude contributes. Three of such processes have been considered and shall be reviewed her: Application of model potentials in $(p, p\gamma)$ Bremsstrahlung [9], calculations of triton binding energy [10] and — most recently — usage of boson exchange and inversion potentials in an in–medium, full–folding optical potential model for nucleon–nucleus scattering [11].

The strategy to compare boson exchange and inversion potentials is as follows. We take some model potential t–matrix $t_{mod}(k, k')$ with its characteristic off–shell (i.e. $k \neq k'$) behavior, calculate the phase shifts from the on–shell informations $t_{mod}(k, k)$, use these model phase shifts to calculate an inversion potential $V_\ell(r)$, as described in Section 2, which in turn yields a t–matrix $t_{inv}(k, k')$ where the off–shell behavior is uniquely defined by the restriction [5]

$$\int_a^\infty r|V_\ell(r)|\, dr < \infty \qquad \text{for} \qquad a \geq 0. \tag{28}$$

Therefore, any on–shell difference of inversion potentials will lead to off–shell differences of the t–matrix. On the other hand, the off–shell behavior of the model t–matrix and the t–matrix obtained from inversion will in general be entirely different, at least for large momenta. Therefore, comparing

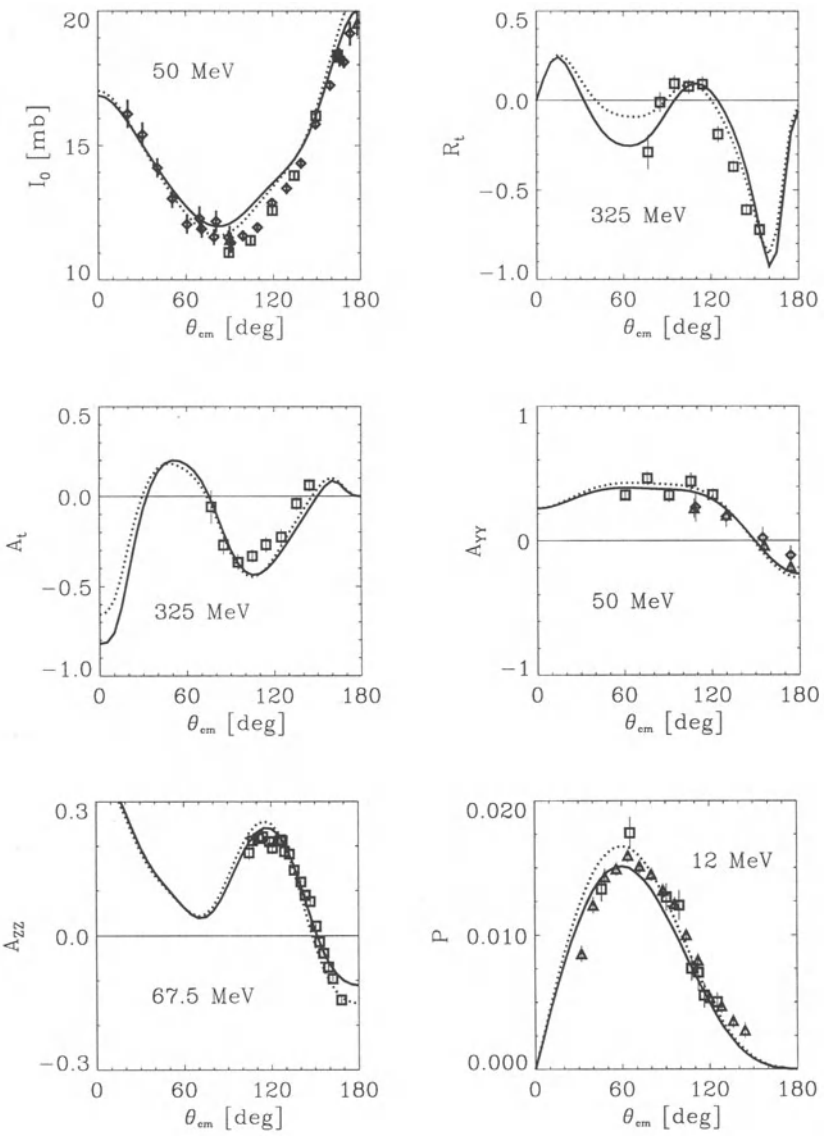

Fig. 2. Observables of np scattering. Kinetic laboratory energy is denoted, experimental data are taken from the VPI–SAID program. We show theoretical predictions from OSBEP (full) and Bonn–B (dotted).

$t_{mod}(k,k')$ and $t_{inv}(k,k')$ in off–shell sensitive reactions works as a tool to test whether off–shell differences of on–shell equivalent t–matrices manifest themselves in the calculation of observable data.

4.1 Cross Sections for $(p, p\gamma)$ Bremsstrahlung

In Figure 3, the theoretical $(p, p\gamma)$ cross sections for several potentials are shown. In detail, Jetter et al. [9] calculated cross sections using the boson exchange potentials Paris and Bonn–B [1] as well as inversion potentials from the Nijmegen PWA [12] and phase shifts from the Bonn–B potential. Two kind of calculations for $(p, p\gamma)$ cross sections were applied. First, an on–shell approximation which is shown as upper curve in Figure 3 and clearly misses the data, second an exact off–shell calculation which is represented by the lower curve. Obviously, using the exact calculation all potentials are consistent with the data, boson exchange models leading to equivalent results as inversion potentials. Additionally, as a surprising result the cross section for $(p, p\gamma)$ Bremsstrahlung, which was assumed to be sensitive to the off–shell behavior of the t–matrix, can not distinguish between the original Bonn–B potential (dashed line) and the on–shell equivalent but off–shell different inversion potential (dotted) obtained from Bonn–B model phase shifts! Consequently, nothing can be learned about the off–shell properties of the NN scattering amplitude from $(p, p\gamma)$ Bremsstrahlung.

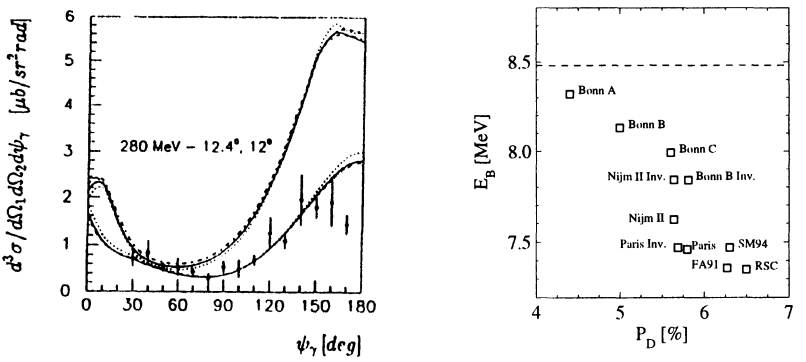

Fig. 3. Left figure: Theoretical $(p, p\gamma)$ cross sections from various boson exchange and inversion potentials. The lower curves show the results for an exact calculation whereas the upper curves represent an on–shell approximation. The lines are Nijmegen PWA inversion (solid), Paris (dash–dotted), Bonn–B (dashed) and an inversion potential from Bonn–B phase shifts (dotted). Right figure: Triton binding energy versus deuteron D–state probability for various potentials. Note the large differences in both entities for the genuine and inversion Bonn–B potential, whereas Paris original and Paris inversion show similar results.

4.2 Triton Binding Energies

Analogue to $(p, p\gamma)$ Bremsstrahlung calculations, a number of potentials were applied to compute binding energies of ^{3}H [10]. As representative examples we consider model and inversion potentials for the Paris and Bonn–B potentials. The results follow the well–known correlation between the deuteron D–state probability and the binding energy $E_B(^3\mathrm{H})$ which is shown in Figure 3 for various models. All of the model predictions underestimate the experimental value of 8.48 MeV, a circumstance which will be discussed below. For the Bonn–B and Paris potential the exact values are listed in Table 3. Note that for the Paris original and inversion potential the triton binding energies are the same whereas for Bonn–B a significant difference arises. The reason can be seen from an argument pointed out by Machleidt [13]. The on–shell t–matrix is related to the central and tensor potential by the approximate relation

Table 3. Deuteron D–State Probabilities and Triton Binding Energies

	Paris	Paris (inv.)	Bonn–B	Bonn–B (inv.)
P_D	5.77 %	5.69 %	4.99 %	5.81 %
$E_B(^3\mathrm{H})$	7.47 MeV	7.47 MeV	8.14 MeV	7.84 MeV

$$t(k,k) \approx V_C(k,k) - \int d^3\mathbf{k}'\, V_T(k,k') \frac{M}{k'^2 - k^2 - i\epsilon} V_T(k',k). \qquad (29)$$

Thus, for the genuine Bonn–B and the Bonn–B inversion potential, which are on–shell equivalent, the *sum* of Born term and integral term in (29) is equal, while the respective terms themselves may be different. The deuteron D–state probability on the other hand is dominantly determined by the tensor potential

$$P_D \approx \int_0^\infty \int_0^\infty k^2 dk\, k'^2 dk' \, \frac{V_T(k,k')}{-E_B(^2\mathrm{H}) - \frac{k^2}{M}} \Psi_0(k), \qquad (30)$$

where $\Psi_0(q)$ is the deuteron S–wave. Thus, two on–shell equivalent potentials may indeed lead to different D–state probabilities and triton binding energies due to differences in the tensor potential parts. Obviously, this is the case for the Bonn–B original and inversion potential. This can be understood from the fact that inversion potentials are first of all local functions of r in coordinate space since the scattering phase shifts as functions of k build a one–dimensional manifold (see Section 2). However, the microscopic boson exchange potentials, which are naturally formulated in momentum space,

are not necessarily local and this deviation may account for the differences in the tensor potential. Comparing the results for the Bonn–B and Paris potentials, one finds that the non–locality of the Paris potential obviously can be well represented by an on–shell equivalent local potential, whereas the non–locality of the Bonn–B potential produces a significant decrement of the D–state probability. This arises from the fact that the tensor force in the Paris potential is local, whereas the tensor potential in the Bonn–B potential is not. Thus, the nonlocality of the other potential contributions essentially play no role in the calculation of the triton binding energy.

After all, the calculation of triton binding energies shows some sensitivity to the non–local structure of potentials. Unfortunately, there is an ongoing discussion about the influence of three–body forces and relativistic corrections on the triton binding energy so that none of the above results can be favored. Further work on this field seems desirable.

4.3 Nucleon–Nucleus Scattering

Embedded in an in–medium full–folding optical potential model various boson exchange and inversion potentials have been applied to calculate observables of nucleon–nucleus scattering [11]. In Figure 4 we show the results obtained for the differential cross section and analyzing power for $^{40}\mathrm{Ca}(p,p)$ scattering at 500 MeV using the Paris potential together with inversion potentials from Paris model phase shifts and phases from the Arndt SM94 PWA [14]. The conclusions are twofold: As in the case of $(p,\, p\gamma)$ Bremsstrahlung, the genuine Paris and Paris inversion potential results can not be distinguished by the experiment and thus no off–shell sensitivity can be found in the analysis of elastic nucleon–nucleus scattering. Additionally, a new effect occurs comparing the inversion potentials from SM94 phase shifts and the Paris potential. The SM94 inversion potential, which by construction fits the elastic NN data much better than the Paris potential, yields significant better results for the cross section and the analyzing power. Conclusively, an improvement in the description of on–shell data also yields better results in nucleon–nucleus scattering.

5 Summary and Outlook

As described in Section 2 and 3, quantum inversion and boson exchange potentials rest on entirely different footings. Whereas the latter are derived from some microscopic model, as the model of solitary mesons, leading to a momentum space potential with — in general — nonlocal behavior, the inversion potentials are obtained model–independently from the Gel'fand–Levitan or Marchenko algorithms. Since elastic NN scattering data enter the inversion potentials via the phase shifts $\delta_\ell(k)$ as a one–dimensional manifold, inversion potentials are local, energy–independent functions in coordinate space. This

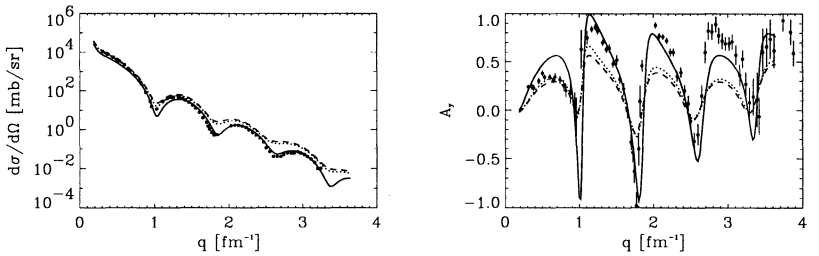

Fig. 4. Differential cross section (left) and analyzing power (right) for ^{40}Ca(p,p) at 500 MeV. We show results for SM94 inversion (solid), genuine Paris potential (dotted) and Paris inversion (dashed).

fundamental difference could be expected to produce significant deviations in the description of processes where the off–shell part of the t–matrix, which does not enter the phase shifts, contributes.

Surprisingly, the application of boson exchange and inversion potentials in the calculation of $(p, p\gamma)$ Bremsstrahlung cross sections and nucleon–nucleus scattering observables produced equivalent results for the boson exchange potentials an their local counterparts. Additionally, in the case of nucleon–nucleus scattering it turned out that an improvement of the description of on–shell data also yields better results for off–shell observables.

The only difference in the comparison of boson exchange versus quantum inversion potentials occurred in the calculation of triton binding energies. It turned out that the usage of local potentials enhances the D–state probability with respect to their non–local on–shell equivalents, leading to a lower triton binding energy. This effect could be traced back to differences in the tensor part of the potential which can differ for local and non–local potentials. Unfortunately, neither boson exchange nor quantum inversion potentials can be favored in this context due to the persistent uncertainty concerning the effect of three–body forces and relativistic corrections on the triton binding energy.

To our disappointment, the study of the above reactions thus is not suitable to put boson exchange potentials to a comparative test. Therefore, as a future prospect, the application of boson exchange and inversion potentials in meson–nucleon and meson–meson scattering seems promising to test the concept of quantum inversion as well as the applicability of NN potential models in a wider range of hadron–hadron interactions. In this context, the OSBEP model can be expected to show interesting results. In contrast to conventional boson exchange potentials where the form factors in nucleon–nucleon and meson–nucleon interactions are different, the concept of proper normalization in OSBEP remains unchanged. Thus, the OSBEP model may be able to describe both interactions consistently with a very small number of parameters.

Acknowledgements

Supported in part by FZ Jülich, COSY Collaboration, Grant Nr. 41126865.

References

[1] M. M. Nagels, T. A. Rijken, and J. J. de Swart, Phys. Rev. D **17**, 768 (1978); M. Lacombe, B. Loiseau, J. M. Richard, R. Vinh Mau, J. Coté, P. Pirès, and R. de Tourreil, Phys. Rev. C **21**, 861 (1980); R. Machleidt, K. Holinde, and Ch. Elster, Physics Reports **149**, 1 (1987).

[2] T. H. R. Skyrme, Nucl. Phys. **31**, 556 (1962); S. Weinberg, Phys. Rev. Lett. **18**, 188 (1967); J. Wambach, in *Quantum Inversion Theory and Applications*, edited by H. V. von Geramb (Lecture Notes in Physics, Springer, New York, 1994); C. Ordónez, L. Ray, and U. van Kolck, Phys. Rev. Lett. **72**, 1982 (1994); C. M. Shakin, Wei-Dong Sun, and J. Szweda, Phys. Rev. C **52**, 3353 (1995).

[3] L. Jäde and H. V. von Geramb, LANL e-print archive nucl-th/9604002, submitted to Phys. Rev. C.

[4] R. Machleidt, Adv. in Nucl. Phys. **19**, 189 (1989).

[5] H. Kohlhoff and H. V. von Geramb, in *Quantum Inversion Theory and Applications*, Proceedings of the 109th W. E. Heraeus Seminar, Bad Honnef 1993, edited by H. V. von Geramb (Lecture Notes in Physics, Springer, New York, 1994); M. Sander, C. Beck, B. C. Schröder, H.-B. Pyo, H. Becker, J. Burrows, H. V. von Geramb, Y. Wu, and S. Ishikawa, in *Conference Proceedings, Physics with GeV-Particle Beams* (World Scientific, Singapore 1995).

[6] P. B. Burt, *Quantum Mechanics and Nonlinear Waves* (Harwood Academic, New York, 1981).

[7] C. Itzykson and J. B. Zuber, *Quantum Field Theory* (Mc. Graw-Hill, New York 1980).

[8] L. Jäde and H. V. von Geramb, LANL preprint server, nucl-th/9510061 (1995).

[9] M. Jetter and H. V. von Geramb, Phys. Rev. C **49**, 1832 (1994).

[10] B. F. Gibson, H. Kohlhoff, and H. V. von Geramb, Phys. Rev. C **51**, R465 (1995).

[11] H. F. Arellano, F. A. Brieva, M. Sander, and H. V. von Geramb, to appear in Phys. Rev. C **54** (1996).

[12] V. Stoks and J. J. de Swart, Phys. Rev. C **48**, 792 (1993).

[13] R. Machleidt and G. Q. Li, LANL e-print server, nucl-th/9301019 (1993).

[14] R. A. Arndt, I. I. Strakovsky and R. L. Workman, Phys. Rev. C **50**, 2731 (1994).

Inversion Potentials for Meson–Nucleon and Meson–Meson Interactions

M. Sander and H.V. von Geramb

Theoretische Kernphysik, Universität Hamburg,
Luruper Chaussee 149, D–22761 Hamburg, Germany

Abstract. Two–body interactions of elementary particles are useful in particle and nuclear physics to describe qualitatively and quantitatively few– and many–body systems. We are extending for this purpose the quantum inversion approach for systems consisting of nucleons and mesons. From the wide range of experimentally studied two–body systems we concentrate here on πN, $\pi\pi$, K^+N, $K\pi$ and $K\overline{K}$. As input we require results of phase shift analyses. Quantum inversion Gelfand–Levitan and Marchenko single and coupled channel algorithms are used for Schrödinger type wave equations in partial wave decomposition. The motivation of this study comes from our two approaches: to generate and investigate potentials directly from data by means of inversion and alternatively use linear and nonlinear boson exchange models. The interesting results of inversion are coordinate space informations about radial ranges, strengths, long distance behaviors, resonance characteristics, threshold effects, scattering lengths and bound state properties.

1 Introduction

It is a paradigm of particle and nuclear physics to describe complex many–body systems in terms of two–body interactions or two–body t–matrices. The formulation of a two–body interaction is therefore a central goal for generations of physicists, both of the experimental and theoretical community. Roughly speaking, we separate these efforts of finding two–body interactions into groups which orient themselves very closely on data, whereas the other extreme follows a fundamental approach. In another contribution to this conference we have dwelled upon the need to follow both approaches [1].

Encouraged by the tremendous success of the inverse scattering method for fixed angular momentum in application to nucleon–nucleon interactions we extend our study in this contribution to meson–nucleon and meson–meson systems in the framework of the Gelfand–Levitan and Marchenko theory. A comprehensive description of our mathematical and numerical framework can be found elsewhere [2,3] and we shall concentrate here solely on the presentation and interpretation of results which are a small fraction of all results contained in the thesis [4]. In particular we study πN, $\pi\pi$, K^+N, $K\pi$ and $K\bar{K}$ scattering. As experimental input for the inversion algorithms we used phase shift analyses of Arndt et al. for πN [5] and K^+N [6], of Froggatt et al. for $\pi\pi$ [7] and of Estabrooks et al. for $K\pi$ [8]. We limit ourselves to

subinelastic and subreaction threshold data. An effective range parameterization is used for the $K\bar{K}$ system [9]. A critical and comprehensive assessment of the data can be found in [4].

For the two–body system the relativistic Schrödinger equation

$$-f_\ell''(k,r)+\left(\frac{\ell(\ell+1)}{r^2}+2\mu(s)V_\ell(r)\right)f_\ell(k,r)=k^2 f_\ell(k,r) \tag{1}$$

is assumed to be valid. The CM parameters are given by

$$k^2=\frac{m_2^2(T_{Lab}^2+2m_1T_{Lab})}{(m_1+m_2)^2+2m_2T_{Lab}}. \tag{2}$$

or

$$k^2=\left(\frac{s-m_1^2-m_2^2}{2\sqrt{s}}\right)^2-\frac{m_1^2m_2^2}{s} \tag{3}$$

with

$$s=M_{12}^2=\left(\sqrt{k^2+m_1^2}+\sqrt{k^2+m_2^2}\right)^2=(m_1+m_2)^2+2m_2T_{Lab}, \tag{4}$$

m_1, m_2 are the masses of the projectile and the target and T_{Lab} is the kinetic energy in the laboratory. The experimental data are given either as a function of T_{Lab} or the Mandelstam variable s. As reduced mass $\mu(s)$ we use either the non–relativistic reduced mass

$$\mu=\frac{m_1m_2}{m_1+m_2} \tag{5}$$

or the reduced energies [10]

$$\mu(s)=\frac{1}{2}\frac{dk^2(s)}{d\sqrt{s}}=\frac{1}{2}\frac{s^2-(m_1^2-m_2^2)^2}{2s^{3/2}}. \tag{6}$$

This expression (6) is generally approximated by the low–energy limit or the conventional non–relativistic reduced mass. Any of these options is to be motivated by the application of the interaction potentials in other contexts. Depending on the choice of the reduced mass, we obtain different inversion potentials. The potential is in any case local and energy independent but dependent on the channel quantum numbers (ℓSJT). Our numerical algorithm guarantees that insertion of the potential in eqn. (1) reproduces the input phase shifts $\delta(k)$ better than 0.02°.

The simplicity of our potential operator may be surprising in view of the non–locality implied by results from meson exchange models. It is also our opinion that the actual potential should be non–local, but we understand that the inversion potential represents a local equivalent yielding the same on–shell two–body t–matrix for the full operator. The local potential permits to compute off–shell t–matrices with a Lippmann–Schwinger equation with

the implication that a non–local potential may yield a different off–shell continuation than a local potential. This difference in the off–shell domain can become important in few– and many–body systems or in the interaction regions of two–body wave–functions. For nucleon–nucleon systems we have put much effort in attempts to clarify this point and find no evidence for differences in observables [1,4]. This is a very surprising result and it is the purpose of this study to initiate a comparison of strictly equivalent local on–shell potentials with their non–local counterparts in the realm of meson–nucleon and meson–meson interactions.

2 πN Scattering

Partial wave phase shifts of the πN system are determined by an analysis of elastic and charge exchange scattering $\pi^+ p \to \pi^+ p, \pi^- p \to \pi^- p$ and $\pi^- p \to \pi^0 n$. They form a complete set of observables entering a partial wave analysis with isospin $T = \frac{1}{2}$ and $\frac{3}{2}$ [5]. The notation for the isospin and angular momentum channels is $\ell_{2T,2S}$. We used the SM95 analysis of Arndt et al. for channels $\ell \leq 3$ [4,5].

πN p–Wave Resonances

The most prominent resonances are the $\Delta(1232)$ in the P_{33} and the $N(1440)$ Roper resonance in the P_{11} channels. The phase shifts for these resonances are shown in the left part of Fig. 1. We factorize the S–matrix into a *resonant* and a *non–resonant* part $S(k) = S_r(k)S_p(k)$. For the resonant part we use

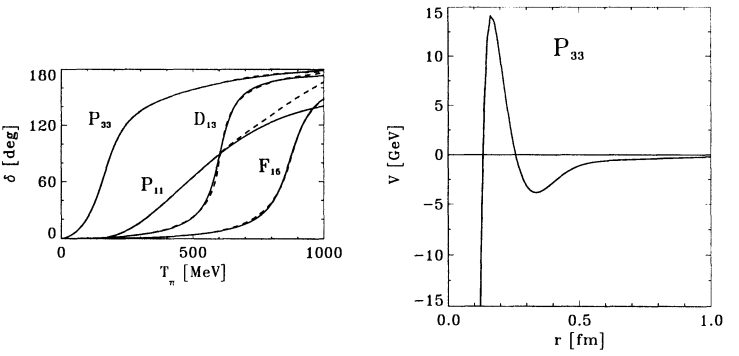

Fig. 1. Left: πN real phase shifts in the resonant channels (dashed) and their reproduction by the inversion potentials (full line).
Right: πN P_{33} potential from quantum inversion.

Table 1. πN resonance parameters used in the inversion scheme.

πN channel	Re(k_r) [fm^{-1}]	Im(k_r) [fm^{-1}]	Mass [MeV]	Width [MeV]	Name
P_{11}	1.8200	−0.6200	1381	159	N(1440)
P_{33}	1.0665	−0.2440	1212	102	Δ(1232)
D_{13}	2.2900	−0.1050	1514	93	N(1520)
F_{15}	2.8520	−0.1230	1674	72	N(1680)

a resonance and an auxiliary pole parameterization [11]

$$S_r(k) = \frac{(k+k_r)(k-k_r^*)}{(k-k_r)(k+k_r^*)} \frac{(k+k_h)(k-k_h^*)}{(k-k_h)(k+k_h^*)}, \tag{7}$$

which contains the right amount of zeros and poles for a decomposition into Jost functions. The rest $S_p(k)$ of the S–matrix is parameterized in our usual parameterization scheme for $\delta_p(k)$ in connection with the symmetric Padé approximant for the exponential function [3].

In Table 1 are summarized the relevant parameters for this decomposition using SM95 [5]. As shown in Fig. 1 (left) this reproduces the input phase shifts very well for $T_\pi \leq 500$ MeV. In Fig. 1 (right) we show the inversion potential for the P_{33} channel with a repulsive well, enabling tunneling for the pion–nucleon system, with a very strong short range attraction, which yields the Δ(1232) quasi bound state. The long range part of this potential, not visible in Fig. 1, behaves like a Yukawa tail with a strength $Y = 650.0$ [MeVfm] and $\mu = 1.77$ [fm^{-1}], see also section 5. The relative distance of the centers of mass in the strong attractive region is unexpectedly small, $r \leq 0.25$ fm. In view of the large radii of the charge form factor of the pion and the nucleon, approximately 0.54 fm for the pion and 0.7 fm for the nucleon, this relative distance implies more than 90% overlap of the intrinsic structures before the strong attractive potential simulates a phase transition of the pion–nucleon quark content into the 3–quark content of the Δ. Ultimately such explanation must be confirmed by QCD calculations. We decline and warn from a far reaching interpretation of this potential with its strength and radial dimensions.

πN Scattering Lengths and πNN Coupling Constants

From the πN potentials in the $T = \frac{1}{2}, \frac{3}{2}$ s–channels we find the scattering lengths $a_1 = 0.178\,[m_\pi^{-1}]$, $a_3 = -0.088\,[m_\pi^{-1}]$. For a comparison with several other predictions see Table 2. These results may be used in the Goldberger–Miyazawa–Oehme sum rule [16]

$$\frac{f^2_{\pi NN}}{4\pi} = \frac{(m_\pi^2-\mu^2)(m_N+m_\pi)}{6m_N m_\pi}(a_1-a_3) - \frac{m_\pi^2-\mu^2}{8\pi^2}\int_0^\infty \frac{\sigma_{\pi^-p}-\sigma_{\pi^+p}}{\sqrt{q^2+m_\pi^2}}dq \tag{8}$$

Table 2. πN s–wave scattering lengths from several models and experimental analyses together with predictions for the πNN coupling constant obtained from the GMO sum rule.

Model	a_1 $[m_\pi^{-1}]$	a_3 $[m_\pi^{-1}]$	$f^2_{\pi NN}/4\pi$	Ref.
SM95 Inversion	0.178	−0.088	0.0766	
KH80	0.173	−0.101	0.079	[12]
$\pi^- p$ 1s state	0.185	−0.104	0.081	[13]
Pearce et al.	0.151	−0.092	0.072	[14]
Schütz et al.	0.169	−0.085	0.074	[15]

to obtain a model independent estimate for the πNN coupling constant. Using the simplified form of this sum rule [17]

$$\frac{f^2_{\pi NN}}{4\pi} = 0.19 m_\pi (a_1 - a_3) - (0.025 \text{ mb}^{-1})\mathcal{J}, \tag{9}$$

where the integral

$$\mathcal{J} = \frac{1}{4\pi^2}\int_0^\infty \frac{\sigma_{\pi^- p} - \sigma_{\pi^+ p}}{\sqrt{q^2 + m_\pi^2}} dq \tag{10}$$

has the VPI value $\mathcal{J} = -1.041$ mb, we find

$$\frac{f^2_{\pi NN}}{4\pi} = 0.0766, \qquad \text{or} \qquad \frac{g^2_{\pi NN}}{4\pi} = 13.84, \tag{11}$$

which is fully consistent with the value of 13.75 ± 0.15 given in [5].

$\pi^- p$ Atoms

The Coulomb attraction between π^- and p causes a bound system called pionic hydrogen $A_{\pi p}$. Additionally, the hadronic interaction between the two constituents distorts the short range interaction and changes the pure Coulomb spectrum. Decay channels $\pi^- p \to \pi^0 n$ and $\pi^- p \to \gamma n$ allow a rapid decay.

The hadronic shift of the $3p \to 1s$ transition and the total $1s$ width has recently been measured at PSI [13]. To analyze this experiment we use quantum inversion for the determination of the hadronic potentials. Inelasticities, Coulomb and other isospin breaking effects are supposed to be not included in the SM95 phase shift analysis [5]. Using the S_{11} and S_{31} phase shifts shown in Fig. 2, we obtain the hadronic potentials $V_{11}(r)$ and $V_{31}(r)$, Fig. 3 (left). The inversion algorithm uses only the nonrelativistic reduced mass $\mu = 121.50$ MeV based upon the $\pi^\pm$ and p masses, consistently with the phase shift analysis.

In the next step we apply a rotation of these potentials in isospin space from good isospin states into particle eigenstates. This yields the potential matrix $V^{ij}(r)$ of the coupled radial Schrödinger equation

$$f_i'' + k_i^2 f_i = \sum_{j=1}^{2} 2\mu_i V^{ij} f_j, \quad i = 1(2) \text{ for } \pi^- p\ (\pi^0 n) \tag{12}$$

for the $\pi^- p \leftrightarrow \pi^0 n$ system. The potential matrix contains the isospin rotation coefficients and the Coulomb attraction

$$V^{11} = V^{\pi^- p} = \frac{2}{3} V_{11} + \frac{1}{3} V_{31} - \frac{e^2}{r}, \tag{13}$$

$$V^{12} = V^{21} = -\frac{\sqrt{2}}{3}(V_{11} - V_{31}), \tag{14}$$

$$V^{22} = V^{\pi^0 n} = \frac{2}{3} V_{31} + \frac{1}{3} V_{11}. \tag{15}$$

The hadronic part of this matrix is shown on the right side of Fig. 3. The reduced masses we used are $\mu_1 = 121.50$ MeV and $\mu_2 = 118.02$ MeV. In Table 3 we signal this choice with the parameter $x = -1$. This mass difference introduces an additional isospin breaking effect. Since this issue is of central importance for the pion–pion system in the next section we investigate this point in further details also here and distinguish the alternative calculation with $\mu_1 = \mu_2 = 121.50$ MeV and $x = +1$. Generally it is assumed that charge and mass isospin–breaking effects should have a small impact on the lifetime and width of $A_{\pi p}$ or the eigenchannel phase shifts.

The bound states of the $\pi^- p$ system can be found as resonances in the energetically open $\pi^0 n$ channel, showing a partial width $\Gamma_{ns}^{\pi^- p \to \pi^0 n}$ deduced from the elastic cross section

$$\sigma(\pi^0 n \to \pi^0 n) = \frac{\pi}{k_2^2} |1 - S_{22}|^2. \tag{16}$$

Results for the ground state are given in Table 3. To account for the full experimental width one has to correct the partial width with the Panofsky ratio $P = 1.546 \pm 0.009$ [13]

$$\Gamma_{ns} = \left(1 + \frac{1}{P}\right) \Gamma_{ns}^{\pi^- p \to \pi^0 n}. \tag{17}$$

To show the effect of isospin breaking caused by different reduced masses in channel 1 and 2, we repeated this calculation with $\mu_2(\pi^0 n)$ set equal to $\mu_1(\pi^- p)$. These results are also included in Table 3 with $x = +1$. Furthermore we have accounted for the γn decay by the introduction of a phenomenologic imaginary Gaussian potential $W(r) = W_{11} = -9 \exp(-4r^2)$ in eqn. (12), where we replace $V_{11} \to V_{11} + iW_{11}$. The point Coulomb potential is replaced by double folded Gaussian charge distributions for the pion and nucleon

$$\frac{e^2}{r} \longrightarrow \frac{e^2\Phi(1.13\,r)}{r}.$$

All results are shown in Table 3. They agree well with the experimental values, and the small isospin breaking effects from the mass difference confirm our assumption and establish an excellent support of the inversion approach.

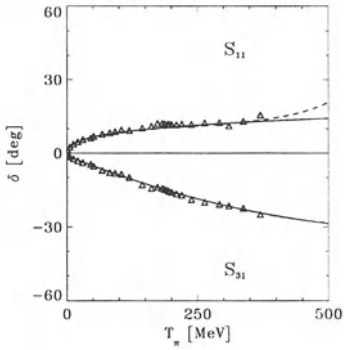

Fig. 2. πN SM95 [5] (dashed line) and KH80 [12] (triangles) data with reproduction by inversion potentials (solid line) for the πN S_{11} and S_{31} channels.

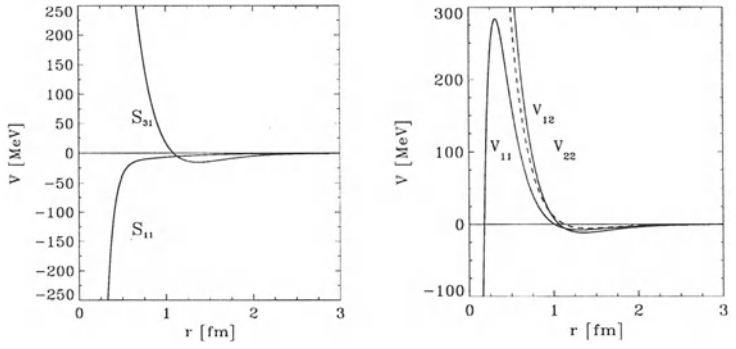

Fig. 3. πN inversion potentials using SM95 phase shifts (left), and the potential matrix (right).

Table 3. Hadronic shift of the $1s$ level, with respect to the pure Coulombic reference energy $E^C_{1s} = 3234.9408$ [eV], and partial widths $\Gamma^{\pi^- p \to \pi^0 n}_{1s}$. These partial widths have to be multiplied with 1.647 to account for the Panofsky ratio to obtain the total widths. This yields a typical value ~ 0.862 [eV] to be compared with the experimental value $\Gamma_{1s} = 0.97 \pm 0.10 \pm 0.05$ [eV]. The strength of the imaginary part in the last entry W_{11} is adjusted to reproduce the experimental value.

	Point Charge Coulomb		Gaussian Charge Coulomb		
x	Shift [eV]	FWHM [eV]	Shift [eV]	FWHM [eV]	
-1	-7.13259	0.5187	-7.01055	0.5144	
$+1$	-7.29821	0.5250	-7.16746	0.5230	
$\mu(s)$	-7.26334	0.5317	-7.13259	0.5266	
	Shift $= -7.127 \pm 0.046$ [eV], $\Gamma^{\pi^0 n}_{1s} = 0.590$ [eV]				Sigg [13]
-1	-7.23259	0.9763	-7.12387	0.9763	$V_{11} + iW_{11}$
Shift $= -7.127 \pm 0.028 \pm 0.036$ [eV], $\Gamma_{1s} = 0.97 \pm 0.10 \pm 0.05$ [eV]					Sigg [13]

3 $\pi\pi$ Scattering

$\pi\pi$ phase shifts come from the analysis of final state interactions in $\pi N \to \pi\pi N$ systems or the K_{e4}–decay $K^- \to \pi^+\pi^- e\bar{\nu}$. Here we use results of the CERN–Munich experiment [7] $\pi^- p \to \pi^+\pi^- n$ for all channels with $\ell \leq 3$. The scattering is purely elastic up to $M_{\pi\pi} = 987.3$ MeV where a coupling $\pi^+\pi^- \leftrightarrow K\bar{K}$ becomes dominant. In addition to the experimental data of Froggatt et al. [7] we use data from meson exchange models [18] and chiral perturbation theory χPT [19]. Notation for the isospin and angular momentum channels uses δ^T_ℓ or V^T_ℓ. The inversion results are shown in Fig. 4.

Similar to the $\pi^- p$ system there exists pionium $A_{\pi\pi}$ which is formed by $\pi^-\pi^+$ Coulomb attraction and decays by charge exchange into the open $\pi^0\pi^0$ channel. The coupled channel system is equivalent to eqn. (12) replacing $p \to \pi^+$ and $n \to \pi^0$. We assume the same approach and rotate the good isospin potentials into particle states [22] which reduces to the same form as given by eqn. (13) – (15), simply replace $V_{11} \to V^0_0$ and $V_{31} \to V^2_0$. Phase shift analyses and inversion use a single mass $\mu = m_{\pi^+}/2$ without Coulomb effects. This assumtion guarantees good isospin $T = 0$ and 2. With the purpose to display uncertainties in the phase shifts we used three sources and distinguish a set of three potentials for V^0_0 and V^2_0 respectively. They are shown in Fig. 4 (right), of which the V^0_0 potential is of particular interest. Similar to the πN P_{33} channel potential we find here a potential barrier and a very strong short range attraction. Such potential may be able to support a potential resonance similar to the Δ–resonance in the πN P_{33} channel, but here in the $\ell = 0, T = 0$ channel the resonance width is expected larger than for $\ell = 1$ since the resonance conditions are more delicate due to the centrifugal barrier. The radial dimensions and potential strenghts are quite comparable.

It is obvious to ask if the implied great width resonance supported by this potential can be identified with the isoscalar σ meson which OBE potential require and which is of general interest [23,24,25,26]. It is intended to study this resonance in more details by our OSBEP approach and use also other experimental information. A first glance on this investigation is given by simply using different reduced masses in eqn. (12). This changes effectively the strength of V_0^0 within a few % but causes a dramatic change of the eigenchannel phase shifts which can be identified with the $T = 0$ isospin state. In Fig. 5 we show three cases of different choices of μ_i. Fig. 5 (top left) $\mu_1 = \mu_2 = m_{\pi+}/2$ without Coulomb potential. This confirmes the original input phase shifts used for the inversion. (top right) $\mu_1 = m_{\pi+}/2$, $\mu_2 = m_{\pi^0}/2$ which are the correct reduced masses in the nonrelativistic limit. As expected, the eigenchannel phase δ_0^2 remains unchanged, whereas δ_0^0 is now far off the data. (bottom) $\mu_1 = \mu_2 = m_{\pi^0}/2$ is a further step, and we observe little change for δ_0^2 but a dramatic effect for δ_0^0. This investigation is supposed to show that the strength of the potential enters very sensitively and changes the δ_0^0 phase in a wide range quite untypical for a resonance. The effects upon the lifetime of pionium has already been studied and we observe a dramatic change of lifetime compared between what is given in Table 4 and [22]. This change requires a deeper understanding since the hypothetical σ–meson is producing the medium–range NN attraction. Medium effects of this resonance should be of particular importance and we are presently studying this aspect in microscopic optical potentials for nucleon–nucleus scattering.

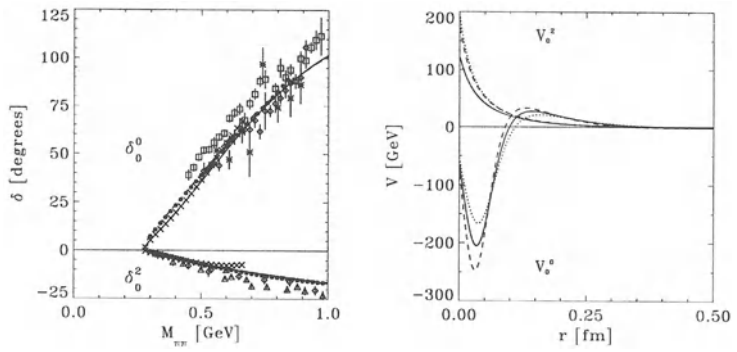

Fig. 4. Left: $\pi\pi$ $\ell = 0$ phase shifts from χPT (crosses) and the reproduction by the inversion potentials (full line), from the analysis by Froggatt (dots) and the reproduction by the inversion potentials (dashed).
Right: $\pi\pi$ $\ell = 0$ inversion potentials based on phase shifts from χPT (full line), the analysis by Froggatt (dashed) and meson exchange (dotted).

Table 4. $A_{\pi\pi}$properties from inversion potentials. The Point Coulomb ground state reference energy $E^C_{1s} = 1.85807248$ [keV]. (x=+1) $\equiv \mu_1 = \mu_2 = m_{\pi+}/2$.

x	E_{1s} [keV]	Shift [eV]	τ [10^{-15} sec]	FWHM [eV]	Reference
+1	1.8638814	−5.809	1.97	0.3481	Froggatt
$\mu(s)$	1.8636070	−5.538	2.05	0.3337	Froggatt
+1	1.8635114	−5.439	1.89	0.3627	Lohse
$\mu(s)$	1.8632880	−5.216	2.03	0.3385	Lohse
+1	1.8616174	−3.545	3.22	0.2128	χPT
$\mu(s)$	1.8614390	−3.367	3.37	0.2031	χPT
	Predictions from experimental analysis and other models				
	1.858		$2.90^{+\infty}_{-2.10}$		Afanasyev [20]
	1.865	−7.0	3.20		Efimov [21]

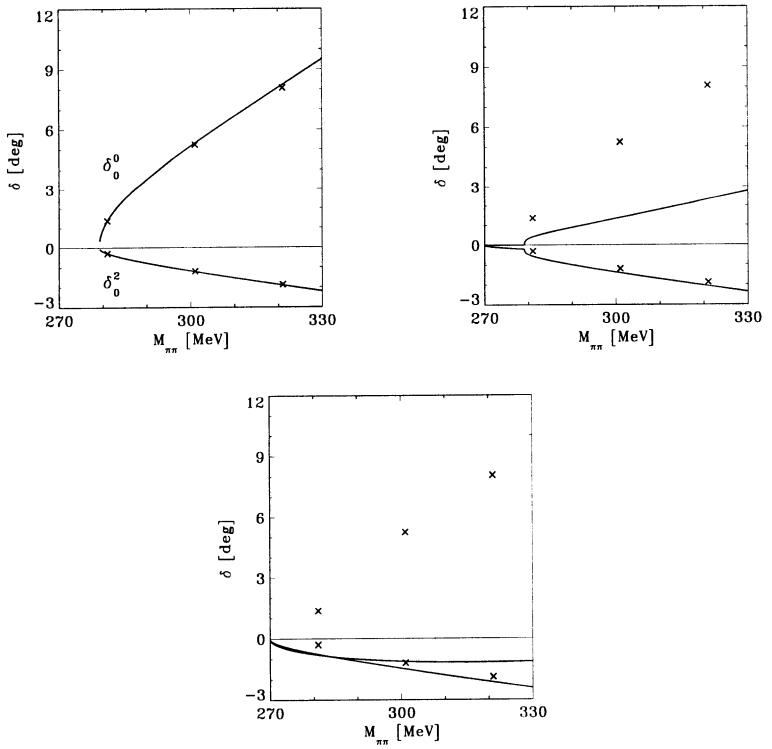

Fig. 5. Eigenchannel phase shifts. More details given in the text.

Table 5. K^+N s–wave scattering lengths from several models and experiment.

Modell	a_0 $(T=0)$ [fm]	a_0 $(T=1)$ [fm]	Ref.
SP92	0.00	−0.33	[6]
Inversion	0.00	−0.33	
Meson Ex. (A)	0.03	−0.26	[27]
Meson Ex. (B1)	−0.15	−0.32	[27]

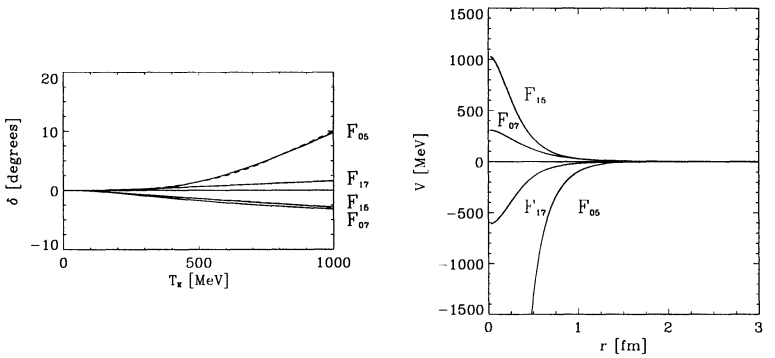

Fig. 6. Left: K^+N $\ell = 3$ phase shifts from the analysis SP92 [6] (dashed) and their reproduction by the respective inversion potentials (full line).
Right: K^+N $\ell = 3$ inversion potentials.

4 K^+N, $K\pi$ and $K\bar{K}$ Scattering

K^+N Scattering

Kaons introduce strangeness into the inversion algorithm where the configurations K^+N, K^0N with $S = +1$ and $K^-N, \bar{K}^0N$ with $S = -1$ are allowed in KN scattering. The $S = -1$ channels show strong resonance effects whereas the the $S = +1$ channels are smooth. Phase shift analyses are restricted by Arndt in SP92 [6] to the K^+N system. In Fig. 6 we show the result for $\ell = 3$, the nomenclature used is $\ell_{T,2J}$, $J = \ell \pm \frac{1}{2}$. The results show little structure in the radial dependencies. Undoubtedly the range of the potential is longer than for the πN system. The long range part of the interaction is discussed in section 5. We calculated K^+N s–wave scattering lengths from inversion potentials and compare them with predictions of the phase shift analysis and models. They are summarized in Table 5. Predictions from meson exchange models [27] agree either with the $T = 0$ or 1 scattering lengths.

Table 6. $K\pi$ s–wave scattering lengths from different theoretical models and experimental analyses.

Model	a_0^1 $[m_\pi^{-1}]$	a_0^3 $[m_\pi^{-1}]$	Ref.
Estabrooks	0.331	−0.138	[8]
Inversion	0.340	−0.147	
Meson Ex.	0.23	−0.064	[18]
χPT	0.17	−0.05	[28]
Quark model	0.23	−0.077	[29], [30]

$K\pi$ scattering

Suitable informations for $K\pi$ scattering come from final state interaction analyses of the reactions $K^\pm p \to K^\pm \pi^+ n$, and $K^\pm p \to K^\pm \pi^- \Delta^{++}$. The notation for channel identification is δ_ℓ^{2T}, where $T = \frac{1}{2}$ or $\frac{3}{2}$. Well known resonances in this system are $K^*(892)$ and $K_0^*(1430)$. The phase shift analysis starts at $M_{K\pi} = 0.73$ GeV and remains elastic up to 1.3 GeV [8]. There is a gap between threshold, $M_{K\pi} = 0.63$ GeV, and the first data points. We bridged this gap with a smooth extrapolation with $\lim_{k\to 0} \delta_\ell^{2T}(k) = \mathcal{O}(k^{2\ell+1})$ [4].

Our scattering lengths, see Table 6, agree well with estimates from dispersion relations ($0.22 \geq a_0^1 \geq 0.045$, $-0.10 \geq a_0^3 \geq -0.165$) [31] and the experimental values [8], but they are 1.4 to 3 times larger than predictions from various models. To solve this puzzle, more data between the $K\pi$ threshold and $M_{K\pi} = 730$ MeV are needed.

$K\not{K}$ Scattering

There exist no phase shift analyses for this system, and we have to rely upon an effective range expansion by Kaminski and Lesniak [9]. Their expansion may be disputed since they neglect inelasticities. This describes briefly the experimental situation with the implication that our analysis represents only some qualitative features.

We are using two sets of parameters from [9] in the effective range expansion

$$k \cot \delta_K(k) = \frac{1}{\mathrm{Re}\ a_K} + \frac{1}{2} R_K k^2 + V_K k^4 \tag{18}$$

whose values are given in Table 7. The phase shifts $\delta_0(M_{KK})$ from this parameterization are shown in Fig. 7, together with the inversion potentials which reproduce the effective range expansion with high precision. There exists a claim from lattice QCD that the short range attractive interaction has an explanation in a non–vanishing propagator structure [32].

Table 7. $K\bar{K}$ isoscalar scattering lengths from [9] and their reproduction by inversion potentials.

Modell	Re a_K [fm]	R_K [fm]	V_K [fm^3]
Set 1	−1.73	0.38	−0.66
Inversion	−1.73	0.38	
Set 2	−1.58	0.20	−0.83
Inversion	−1.58	0.20	

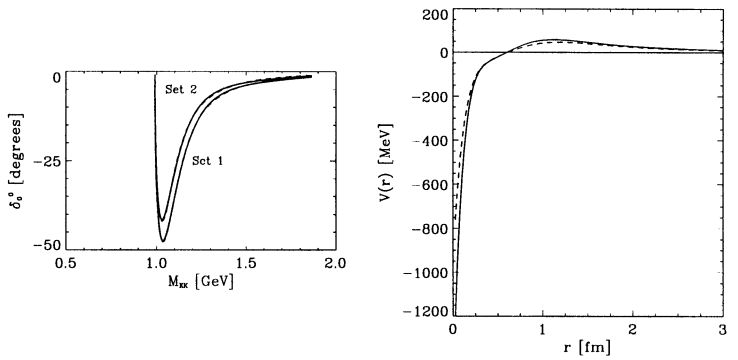

Fig. 7. Left: $K\bar{K}$ $\ell = 0$ real isoscalar phase shifts calculated from the effective range expansion (dashed) using the parameters given by Kaminski and Lesniak [9] and their reproduction by the inversion potentials (full line).
Right: $K\bar{K}$ $\ell = 0$ real isoscalar potentials from quantum inversion based on the two sets of parameters given by Kaminski and Lesniak [9], set 1: full line, set 2: dashed.

5 Long Range Behaviors

In the display of inversion potentials we restricted ourselves to the big effects at distances between 0–2 fm and emphasized the short range domain. Actually, the most reliable information is the long range part of the potentials which can be parameterized in terms of a Yukawa potential with a range parameter given by the Compton wave length of an exchanged particle. For the pion–nucleon system we have also dwelled upon the coupling constant. In Table 8 are summarized the long range Yukawa parameters $V(r) = Ye^{-\mu r}/r$ which we extracted from our inversion potentials in the $\ell = 0$ channels. We find that the exchanged masses in pp, $K\bar{K}$ and K^+N may be interpreted as one–pion, two–pion and one–σ_1 exchange respectively. From the microscopic point of view, the propagators of a dominant pseudoscalar or scalar s–channel exchange transform into a Yukawa–like potential tail. In πN, πK and $\pi\pi$ scattering this interpretation is not valid, since here s– and t–channel

graphs contribute and thus a transformation into coordinate space does not lead to a Yukawa with a physical mass of an exchange particle. A more detailed discussion of this table and its implications can be found in [4].

Table 8. Yukawa parameters. The mass of the exchanged particle is given by $\mu = \frac{mc}{\hbar}$.

	Y [MeVfm]	μ [fm^{-1}]	m [MeV]
pp	14.4	0.684	134.97
K^+N	1325.85	2.9436	580.85
$K\bar{K}$	1923.59	1.316	259.68
πN	111.84	1.61	317.70
πK	638.1	1.87	368.4
$\pi\pi$	1081.28	2.219	437.87

6 Summary and Conclusions

With this contribution we show that the rich sources of phase shift analyses for general hadronic systems can successfully be used to obtain a qualitative and sometimes quantitative understanding of the interaction in terms of a simple local potential. The ranges and strengths of these potentials are often determined by the masses of the scattered particles and the spin–isospin dependence of the partial waves. This dependence can often be understood in terms of a boson exchange picture and ultimately may be related to the underlying QCD dynamics. The latter aspect is most obvious in the p–wave resonanves of the πN system. With this first attempt of using quantum inversion to study the realm of hadronic interactions we establish encouragement to look for alternative equations of motion which should account better for the relativistic kinematics which is definitely important for the lighter hadronic systems or any extension towards higher energy. Various relativistic wave equations have been studied and applied in recent years when treating hadrons with quarks as their constituents.

Acknowledgements

Supported in part by KFA Jülich, COSY Collaboration 41126865.

References

[1] L. Jäde, M. Sander and H.V. von Geramb, *these conference proceedings*

[2] K. Chadan and P.C. Sabatier, *Inverse Problems in Quantum Scattering Theory, 2nd. Edition*, Springer, Berlin (1989)
[3] H.V. von Geramb and H. Kohlhoff, in: H.V. von Geramb (ed.), *Quantum Inversion Theory and Applications*, Lecture Notes in Physics 427, Springer, Berlin (1994); H. Kohlhoff and H.V. von Geramb, *ibid.*
[4] M. Sander, PhD Thesis, University of Hamburg (1996)
[5] R.A. Arndt, I.I. Strakowsky, R.L. Workman and M.M. Pavan, Phys. Rev. **C52**, 2120 (1995)
[6] J. S. Hyslop, R. A. Arndt, L. D. Roper and R. L. Workman, Phys. Rev. **D46**, 961 (1992)
[7] C.D. Froggatt and J. L. Petersen, Nucl. Phys. **B129**, 89 (1977)
[8] P. Estabrooks et al., Nucl. Phys. **B133**, 490 (1978)
[9] R. Kaminski and L. Lesniak, Phys. Rev. **C51**, 2264 (1995)
[10] B.L.G. Bakker and P.J. Mulders, Adv. Nucl. Phys. **17**, 1 (1986)
[11] V.I. Kukulin, V.M. Krasnopol'sky und J. Horáček, *Theory of Resonances*, Academia, Prague (1989)
[12] R. Koch and E. Pietarinen, Nucl. Phys. **A336**, 331 (1980)
[13] D. Sigg et al., Phys. Rev. Lett. **75**, 3245 (1995)
[14] B.C. Pearce and B.K. Jennings, Nucl. Phys. **A528**, 655 (1991)
[15] C. Schütz, J.W. Durso, K. Holinde and J. Speth, Phys. Rev. **C49**, 2671 (1994)
[16] M.L. Goldberger, H. Miyazawa and R. Oehme, Phys. Rev. **99**, 986 (1955)
[17] R.L. Workman, R.A. Arndt and M.M. Pavan, Phys. Rev. Lett. **68**, 1653 (1992)
[18] D. Lohse, J.W. Durso, K. Holinde and J. Speth, Nucl. Phys. **A516**, 513 (1990)
[19] J. Gasser and H. Leutwyler, Phys. Lett. **125B**, 325 (1983)
[20] L.G. Afanasyev et al., Phys. Lett. **B308**, 200 (1993); L.G. Afanasyev et al., Phys. Lett. **B338**, 478 (1994)
[21] G.V. Efimov, M.A. Ivanov and V.E. Lyubovitskii, Sov. J. Nucl. Phys. **44**, 296 (1986)
[22] M. Sander, C. Kuhrts and H.V. von Geramb, Phys. Rev. **C53**, R2610 (1996)
[23] N.A. Törnqvist and M. Roos, Phys. Rev. Lett. **76**, 1575 (1996)
[24] N. Isgur and J. Speth, Phys. Rev. Lett. **77**, 2332 (1996); N.A. Törnqvist and M. Roos, *ibid.*, 2333 (1996)
[25] M. Harada, F. Sannino and J. Schechter, Los Alamos e–print archive hep–ph/9609428; N.A. Törnqvist and M. Roos, *ibid.* hep–ph/9610527
[26] S. Ishida et al., Los Alamos e–print archive hep–ph/9610359
[27] R. Büttgen, K. Holinde, A. Müller–Groeling, J. Speth and P. Wyborny, Nucl. Phys. **A506**, 586 (1990)
[28] V. Bernard, N. Kaiser and U.–G. Meissner, Phys. Rev. **D43**, R2757 (1991)
[29] T. Barnes, E.S. Swanson and J. Weinstein, Phys. Rev. **D46**, 4868 (1992)
[30] Z. Li, M. Guidry, T. Barnes and E.S. Swanson, Bulletin Board hep–ph/9401326
[31] A. Karabarbounis and G. Shaw, J. Phys. **G6**, 583 (1980)
[32] H. R. Fiebig, H. Markum, A. Mihály, K. Rabitsch and C. Starkjohann, Nucl. Phys. B (Proc. Suppl.) **47**, 394 (1996)

Fixed-Energy Inversion of Polarisation-Corrected Electron-Atom Scattering Phase-Shifts into Effective Potentials

Barnabás Apagyi[1], Péter Lévay[1], and Werner Scheid[2]

[1] Department of Theoretical Physics, Institute of Physics, Technical University of Budapest, H–1521 Budapest, Hungary
[2] Institut für Theoretische Physik der Justus-Liebig-Universität, Giessen, Germany

Abstract. The modified Newton-Sabatier method is applied to invert electron-atom scattering phase-shifts into effective potentials. The phase-shifts are corrected for the dipole polarisation interaction of the form $-\alpha/2r^4$. Polarisation phase shifts are calculated by the method of Holzwarth by using Mathieu functions of the second kind. The inversion potentials are compared with the potentials determined earlier by inverting the corresponding total phase-shifts. Examples involving synthetic as well as experimental phase-shifts show that the new method is capable of determining electron-atom potentials from a substantially smaller set of data at the cost of a prior determination of the underlying complex polarisation phase-shifts.

1 Introduction

Charge induced dipole interaction plays an important role in various fields of physics where charged particle interacts with polarisable neutral target. For example, the presence of the polarisation interaction is the cause of the well known Ramsauer-Townsend effect making low energy electron scattering by inert gas almost transparent.

The induced electric dipole interaction may cause a severe problem in performing phase-shift analysis of measured electron-atom differential cross sections. The long range nature of the interaction requires treating so many partial waves that an accurate phase-shift analysis can exhaust the capacity of the largest computers to date. The appearance of great number of total phase-shifts η_l may hinder the accomplishment of fixed-energy inversions as well. It is the aim of this paper to develop a modified scattering method which enables us of using only few polarisation corrected phase shifts in the phase-shift analysis or the inversion procedure.

The problem raised by the great number of phase-shifts can be solved by dividing the region of the interaction into two parts; an interior part, where only the internal forces are dominating the scattering process by the core potential $V_c(r \leq r_0)$, and an outer part where only the electric charge induced dipole polarisation interaction of the form $V_0(r \geq r_0) = -\alpha/2r^4$ plays a role with α being the (calculable) dipole polarisability of the target atom (molecule). Then one can apply the modified scattering theory to derive

phase-shifts corrected for the polarisation effect. The polarisation corrected phase-shifts corresponding to the potential of smaller range have contributions from much fewer partial waves than the total phase-shifts. However, as it becomes clear in the next section, the polarisation corrected phase-shifts may become complex also in the case of real core potentials V_c. It means that the simple effective range theory is not applicable and the exact treatment is unavoidable in this case.

It is well known from the work[1] of Holzwarth that there exists a transition point r_t beyond which the relative wave function achieves a spherical waveform characteristic of the free motion with wave number k. Depending on the scattering energy $E = k^2/2$ and the polarisability $\alpha = f^2$, the transition point $r_t = \sqrt{f/k}$ can be larger than the size r_0 of the neutral target. For example, in the case of the electron-argon atom scattering for which $\alpha = 11.07$ au and $r_0 = 3.7$ au, it can be shown[1] that at E=0.1 eV scattering energy $r_t = 6.23$ au. Between the transition point and the target radius the use of polarisation functions is unavoidable. Because of the long range nature of the polarisation potential, however, one should employ the polarisation functions also beyond the transition point. The simple consideration above makes it possible to develop a modified method by invoking properly treated polarisation functions which replace the spherical functions in the physically important region.

The knowledge of the true scattering potential is of primary interest since it determines the over-all behaviour of the cross section. There are two ways to get information about the interaction acting between projectile and target. One is the direct method in which a priori model assumptions are introduced in potential forms with free parameters. The other is the inverse scattering method which neither makes pre-assumptions about the functional form of the potential nor contains fitting parameters. We shall apply the Newton-Sabatier inverse scattering method[2] as modified by Münchov and Scheid[3] to obtain information about the electron-argon atom potential in the transition region. The inverse scattering method uses as input experimentally determined phase-shifts and gives as output the corresponding unique potential. The modified inverse scattering method[3] has the basic assumption that the potential is known beyond a certain distance and it agrees with the reference potential.

To our best knowledge the modified Newton-Sabatier inversion method with polarisation reference potential on the basis of complex Mathieu functions has not yet been applied to atomic scattering processes. The modified method contains so called technical parameters which have been introduced in order to make the original method feasible to treat realistic cases. However the results are in principle independent of these parameters. To control this statement in the practice, in each case a consistency test is performed by recalculating the phase-shifts from the inversion potentials and comparing them with the input ones.

The organization of this paper is as follows. Section 2 contains the theoretical background with a brief discussion of the Mathieu functions which determine the asymptotical behaviour of the scattering solution. Then the modified Newton-Sabatier inversion method will be exhibited using polarisation potential as a reference potential. In Sect. 3 inversion examples will be presented using synthetic phase-shifts due to long-ranged (r^{-4}) potentials and the realistic electron-argon atom scattering phase-shifts measured[4] at scattering energy of 12 eV. A short summary is given in Sect. 4.

2 Theory

2.1 Polarisation-corrected phase-shifts

Let us consider a charged particle scattered off a neutral atomic target with an electric dipole polarisability of $\alpha = f^2$. The scattering process at the energy $E = k^2/2$ is determined by an effective (dimensionless) potential $U(\rho) \equiv V(r)/E$ which can be split into two parts as ($\rho = rk$)

$$U(r) = U_c(r) + U_0(r), \tag{1}$$

a core potential U_c which has a range $\rho_0 = r_0 k$ approximately determined by the charge radius of the target, and the polarisation potential

$$U_0(\rho \geq \rho_0) = -\frac{\alpha/2}{Er^4} = -\frac{(kf)^2}{\rho^4} \tag{2}$$

which, depending on the magnitudes of the polarisability and energy, may have a much larger range than the core potential. (Atomic units are used throughout the paper.)

The scattering process is described by the radial Schrödinger equation

$$\rho^2[d^2/d\rho^2 + 1 - U(\rho)]\varphi_l^U(\rho) = l(l+1)\varphi_l^U(\rho), \tag{3}$$

with the physical boundary conditions imposed on the wave function,

$$\varphi_l^U(0) = 0, \quad \text{and} \quad \varphi_l^U(\rho \to \infty) = A_l^U \sin(\rho - \frac{\pi}{2}l + \eta_l), \tag{4}$$

where η_l denotes the total phase shift and A_l^U stands for a normalisation constant.

Beyond the core radius r_0 the wave function can be written[1,5,6] as

$$\varphi_l^U(\rho \geq \rho_0) = A_l^U[\cos\delta_l\, \Phi_l^{(1)}(\rho;k,f) - \sin\delta_l\, \Phi_l^{(2)}(\rho;k,f)], \tag{5}$$

with δ_l being the "polarisation corrected" phase shift.

The functions $\Phi_l^{(1)}$ and $\Phi_l^{(2)}$ are two linearly independent solutions of Eq. (3) with potential (2) in the region $\rho \geq \rho_0$, and are fixed by the boundary conditions

$$\Phi_l^{(1)}(\rho \to \infty; k, f) \propto \sin(\rho - l\pi/2 + \eta_l^0(k, f)), \tag{6a}$$

$$\Phi_l^{(2)}(\rho \to \infty; k, f) \propto -\cos(\rho - l\pi/2 + \eta_l^0(k, f)), \tag{6b}$$

together with

$$\Phi_l^{(1)}(\rho; k, f = 0) = \rho j_l(\rho), \tag{7a}$$

$$\Phi_l^{(2)}(\rho; k, f = 0) = \rho n_l(\rho). \tag{7b}$$

Equations (4-6) imply that

$$\eta_l = \delta_l + \eta_l^0 \tag{8}$$

where the polarisation corrected phase shifts δ_l contribute appreciable only in those partial waves where the "core" potential $U - U_0$ is effective ($l \leq l_{max}$). Since the core potential has the range r_0, the polarisation corrected phase-shifts should be known only upto $l_{max} \sim kr_0$ if one wants to determine U_c (in the presence of the polarisation potential $U_0(r)$) from the set $\delta_0, \delta_1, ...\delta_{l_{max}}$.

The functions $\Phi_l^{(1)}$ and $\Phi_l^{(2)}$ which can be called the regular and irregular polarisation functions are related to the Mathieu functions of the second kind[7] $P_l^{(i)}$ $(i = 1, 2)$ in the following way:[1]

$$\Phi_l^{(i)} = \sqrt{kr} P_l^{(i)}. \tag{9}$$

By this relation the polarisation functions can be defined on the whole axis of r $(0 \leq r \leq \infty)$ corresponding to the various representations known for the Mathieu functions. One may use, for example, the ascending power series representation

$$\Phi_l^{\binom{1}{2}}(r; k, f) = \sqrt{kr} P_l^{\binom{1}{2}} = \sqrt{kr} \sum_{n=-\infty}^{\infty} C_n(\tau)(r/\sqrt{f/k})^{\pm(\tau+2n)} \tag{10a}$$

which is important in theoretical considerations, or the Bessel product series representation

$$\Phi_l^{\binom{1}{2}}(r; k, f) = \sqrt{kr} P_l^{\binom{1}{2}} = \sqrt{\pi kr/2} \sum_{n=-\infty}^{\infty} (-1)^n C_n(\tau) \begin{pmatrix} J_{(\tau+n)}(a) \\ Y_{(\tau+n)}(a) \end{pmatrix} J_n(b), \tag{10b}$$

which is useful for practical calculations. In Eqs. (10) J_ν and Y_ν are the Bessel and Neumann functions of order ν, respectively, a (b) is the greater (lesser) of kr or f/r, C_n and τ are the expansion coefficients and the characteristic exponent, respectively.

Inserting Eq. (10a) into Eq. (3) with potential (2), one gets the recurrence relations

$$C_n[(\tau + 2n)^2 - (l + 1/2)^2] + kf[C_{n+1} + C_{n-1}] = 0 \tag{11}$$

for the expansion coefficients $C_n(\tau) = C_{-n}(-\tau)$ which can be evaluated if τ, the characteristic exponent, is known. The characteristic exponent τ

can be determined by the condition that the system of linear homogeneous equations (11) for the coefficients $C_n(\tau)$ has a nontrivial solution, that is, its determinant (the Hill-determinant) $\Delta_l(\tau)$ should vanish,

$$\Delta_l(\tau) = 0. \tag{12}$$

This condition leads to an analytical expression (see. e.g. Ref. 8) for the calculation of τ in terms of the Hill-determinant $\Delta_l(\tau = 0)$ belonging to $\tau = 0$:

$$\sin^2 \frac{\pi}{2}\tau = \frac{1}{2}\Delta_l(\tau = 0). \tag{13}$$

Comparing the asymptotical form of the polarisation functions $\Phi^{(i)}$ given by Eqs. (6) with the power series representation of Eq. (10a), the following relation between the polarisation phase shifts $\eta_l^0 = \eta_l^0(kf)$ and the characteristic exponents $\tau = \tau(kf)$ can be established

$$\tau = l + 1/2 - 2\eta_l^0/\pi. \tag{14}$$

Insertion of this expression into Eq. (13) leads to an equation from which the polarisation phase shifts can be calculated

$$\sin 2\eta_l^0 = (-1)^{l+1}[\Delta_l(\tau = 0) - 1]. \tag{15}$$

A method for evaluating the Hill determinant and the expansion coefficients is given in the Appendix.

From equation (15) it is clear that the polarisation phase-shifts η_l^0 are real only if $0 \leq \Delta_l \leq 2$. The conditions that η_l^0 be real are as follows: $kf \leq 0.69, 1.67, 3.25, 5.76, 9.10$ in the partial waves $l = 0, 1, 2, 3, 4$, respectively. Holzwarth has also shown[1] that at low scattering energies (or high partial waves), Eq. (15) provides the well known effective range results[7]

$$\eta_l^0 \approx \pi(kf)^2/((2l+3)(2l+1)(2l-1)). \tag{16}$$

Since the polarisation phase-shifts η_l^0 corresponding to the background potential $U_0(r)$ may become complex but $\eta_l = \delta_l + \eta_l^0$ is always real for a *real* total potential U, the relation

$$\mathrm{Im}\,\delta_l = -\mathrm{Im}\,\eta_l^0 \tag{17}$$

must hold for energies below the inelastic threshold. Since η_l^0 can be calculated without using the polarisation functions, condition (17) provides a sensitive test for the calculation of the Mathieu functions when applied to get the polarisation corrected phase-shifts δ_l by matching the logarithmic derivatives of the internal solution ϕ_l^U to the outer solution expressed by the polarisation functions as given by Eqs. (5).

From the power series representation, Eq. (10a), of the polarisation functions one can expect that the values $r_t \equiv \sqrt{f/k}$ play the role of a 'transition point' below which, for $r < r_t$, the functions begin to oscillate heavily with

respect to the variable f/r and only beyond the transition point, for $r > r_t$, they achieve a spherical waveform[1]. [Another physical meaning of r_t can be established from the relation: $V_0(r_t) = -E$ or $U_0(\rho_t) = -1$.] Therefore the use of the polarisation functions can be expected to be crucial in the region beween the transition point and the atomic charge radius $r_t \geq r \geq r_0$. Nevertheless, because of the long range nature of the potential U_0, the use of the polarisation functions is also unavoidable if $r_t < r_0$ happens, i.e., when the transition point is smaller than the target radius.

2.2 Inverse scattering at fixed energy

We shall apply the modified Newton-Sabatier method to invert phase shifts into potential at fixed energy. The basic equation of the Newton-Sabatier inversion method can be written in the form[2]

$$\varphi_l^U(\rho) = \varphi_l^{U_0}(\rho) - \sum_{l'=0}^{\infty} c_{l'} L_{ll'}(\rho) \varphi_{l'}^U(\rho) \tag{18}$$

with the matrix elements

$$L_{ll'}(\rho) = \int_0^\rho \varphi_l^{U_0}(\rho') \varphi_{l'}^{U_0}(\rho') d\rho' / \rho'^2 \tag{19}$$

where the functions $\varphi_l^{U_0}(\rho)$ and the reduced reference potential U_0 are known and related to each other by the radial Schrödinger equation

$$\rho^2 [d^2/d\rho^2 + 1 - U_0(\rho)] \varphi_l^{U_0}(\rho) = l(l+1) \varphi_l^{U_0}(\rho). \tag{20}$$

For the elastic scattering treated in this work we assume that $U_0(\rho)$ is a polarisation potential for $\rho \geq \rho_0$ as given by Eq. (2). According to this assumption, the reference potential is most conveniently chosen as

$$U_0(\rho) = \begin{cases} -(kf)^2/\rho_0^4 & \text{for } \rho \leq \rho_0, \\ -(kf)^2/\rho^4 & \text{for } \rho \geq \rho_0. \end{cases} \tag{21}$$

The reference solutions $\varphi_l^{U_0}$ satisfy also the boundary conditions

$$\varphi_l^{U_0}(0) = 0, \quad \text{and} \quad \varphi_l^{U_0}(\rho \to \infty) = \sin(\rho - \frac{\pi}{2} l + \tilde{\eta}_l^0), \tag{22}$$

where the known reference phase-shifts are denoted by $\tilde{\eta}_l^0$.

The solution functions denoted by $\varphi_l^U(\rho)$ in Eq. (18) satisfy the Schrödinger equation (3) with the boundary conditions (4).

Newton[2] has shown that the potential $U(\rho) = V(r)/E$ can be calculated from the equation

$$U(\rho) = U_0(\rho) + \Delta U(\rho), \tag{23}$$

where

$$\Delta U(\rho) = -\frac{2}{\rho}\frac{d}{d\rho}\sum_{l=0}^{\infty} c_l^U \varphi_l^{U_0}(\rho)\varphi_l^U(\rho)/\rho. \tag{24}$$

The modification of the above procedure has been motivated by the need that the method should be applicable to realistic cases when only few measured phase-shifts are available. The modification makes use of the fact that in most cases of physics the potential U is known beyond a given finite distance, say r_0. In the case of electron-atom scattering this form is just the induced dipole polarisation potential $-(\alpha/2r^4)$. As proven by Münchow and Scheid[3] the condition

$$U(\rho) = U_0(\rho) \quad \text{for} \quad \rho \geq \rho_0 \tag{25}$$

makes the solution for $U(\rho)$ unique by selecting out of the infinite many solutions of the Newton-Sabatier method the only one possessing the physical asymptotics.

By using Eq. (25), the solutions φ_l^U of the Schrödinger equation (3) can be written for $\rho \geq \rho_0$ in terms of the regular and irregular Mathieu-function solutions of the second kind $\Phi_l^{(1)}$ and $\Phi_l^{(2)}$ as shown in Eq. (5). The polarisation corrected phase-shifts δ_l are the input quantities for the inverse problem.

The solution of the Newton equations (18) proceeds in two steps after one truncates the summations of l to the first $l_{max}+1$ terms where l_{max} is the largest contributing angular momentum of the input phase-shifts δ_l. First one uses equations (18) at $N \geq 2$ points $\rho = \rho_1, \rho_2, \ldots \rho_N$ with $\rho_i \geq \rho_0$ in order to determine the $2(l_{max}+1)$ unknowns c_l and A_l^U by a least-squares method. Then, with the repeated use of equations (18) for $\rho < \rho_0$ one can calculate the potential $U(\rho)$ via Eqs. (23) and (24). In practice, the procedure is preceded by a transformation of the given phase-shifts δ_l to new phase-shifts δ_l^B in order to reduce the problem to the case where the potential is simply the constant $U(\rho) = -(kf)^2/\rho_0^4$ for $r \geq r_0 = \rho_0/k$. In this case the reference potential U_0 becomes a constant and therefore one may use in Eq. (18) the simple Bessel functions. The usage of the complicated Mathieu solutions is thus limited solely to the calculation of the transformed phase-shifts δ_l^B.

3 Results

In all the following examples we set the reference potential U_0 as given by Eq. (2) and explore the possibility of saving computational expenses by correcting the total phase shifts for the polarisation interaction. The results obtained by inverting the small set of polarisation-corrected phase-shifts will always be compared with those having got earlier[6] by inverting the much larger set of total phase-shifts.

3.1 An analytical potential model

As a first attempt to apply the modified Newton-Sabatier method with polarisation functions to atomic scattering, let us consider the following model potential[6,8]

$$EU(\rho) = V(r) = -e^{-2r}/2r - \frac{1/2}{(r^2+0.474)^2} - i(e^{-3r/2} - e^{-2r})/2r. \quad (26)$$

This potential has all the typical features of electron-atom scattering potentials; it has an attractive screened Coulomb part of range $r_0 \sim 0.5$ au, a long-range polarisation part, and a short-ranged absorption part to account for possible inelastic processes. Let us study the scattering at the energy of $E = 4.5$ au $= 122.4$ eV ($k = 3$ au). Since $\alpha = f^2 = 1$ for the present model, $r_t = \sqrt{f/k} = 0.58$ au $\sim r_0$ so that the internal and transition regions overlap. Moreover, the input polarisation phase-shifts become complex in the partial waves $l = 0, 1$ since $kf = 3$ (see section 2.1) which means that the biggest corrections for the polarisation effect can be expected in the first two partial waves.

This is demonstrated in Table 1 which shows the various phase-shifts relevant to the present calculation. The total phase-shifts η_l have been computed by matching the asymptotical wave function composed from a linear combination of Bessel and Neumann functions to the inner solution at the matching radius of 2.5 au. Those phase-shifts were used earlier[6] to reconstruct the complex potential given by Eq. (26). The input polarisation-corrected phase-shifts δ_l^{in} listed in the fourth and fifth columns of Table 1 have been obtained by matching the asymptotical wave functions, given by Eq. (5), to the inner solutions at a smaller radius of 2 au. Those 2×9 phase-shifts have been used as input for the present inversion calculation which has been carried out using the code BICPOL[11]. The output phase-shifts δ_l^{out} shown in the sixth and seventh columns of Table 1 have been obtained from the inversion potential (dashed lines in Fig. 1) by solving the Schrödinger equation. The last two columns of Table 1 exhibit the differences $\Delta_l = \delta_l^{in} - \delta_l^{out}$ which clearly show also the benefit of the new method.

Figure 1 shows as full lines the complex inversion potentials obtained earlier[6] by inverting the 2×30 total phase shifts η_l. Also shown are as dashed lines, the inversion potentials obtained presently by using the 2×9 polarisation-corrected phase-shifts δ_l^{in} of Table 1 as input data for the inversion calculation, outlined in sect. 2. It can be seen from Fig. 1 that the two inversion methods give practically the same results although the input set of phase-shifts are quite different. The technical parameters of the earlier calculation have been $l_{max} = 29$, $\rho_i = 35, 36, 37$, $r_0 = 2.5$ au. Those of the present calculation with polarisation functions are $l_{max} = 8$, $\rho_i = 7, 7.5, 8$, $r_0 = 2$ au. Contrary to the substantially smaller set of phase shifts, the polarisation-corrected inversion method has resulted in almost the same complex potentials as the conventional method which employs a much larger set of (total)

Table 1. Total phase-shifts, Re η_l and Im η_l, given by the long-range potential of Eq. (26). Polarisation-corrected phase-shifts, Re δ_l^{in} and Im δ_l^{in}, defined by Eq. (5), used as input data for the inversion calculation. Polarisation-corrected phase-shifts, Re δ_l^{out} and Im δ_l^{out}, obtained back using the inversion potential shown by dashed lines in Fig. 1. Differences Δ_l between input/output phase-shifts.

l	Re η_l	Im η_l	Re δ_l^{in}	Im δ_l^{in}	Re δ_l^{out}	Im δ_l^{out}	Re Δ_l	Im Δ_l
0	0.5493	0.0410	1.3522	-1.6500	1.3520	-1.6500	0.0002	0.0000
1	0.2916	0.0348	-0.4494	0.4915	-0.4494	0.4913	0.0000	0.0002
2	0.1364	0.0219	-0.2647	0.0227	-0.2647	0.0226	0.0000	0.0001
3	0.0673	0.0136	0.0072	0.0119	0.0072	0.0118	0.0000	0.0001
4	0.0359	0.0083	0.0539	0.0059	0.0538	0.0056	0.0001	0.0003
5	0.0207	0.0051	0.0285	0.0020	0.0284	0.0018	0.0001	0.0002
6	0.0127	0.0031	0.0094	0.0005	0.0094	0.0004	0.0000	0.0001
7	0.0083	0.0019	0.0027	0.0001	0.0027	0.0001	0.0000	0.0000
8	0.0057	0.0011	0.0008	0.0000	0.0008	0.0000	0.0000	0.0000
9	0.0041	0.0007						
19	0.0005	0.0000						
29	0.0001	0.0000						

phase-shifts. This result suggests the applicability of the method in other field of scattering theory as, e.g., in phase-shift analyses.

3.2 Inversion of experimental phase-shifts of e-Ar scattering at E=12 eV

The results of the preceding subsection are encouraging enough to apply the modified Newton-Sabatier method to invert polarisation-corrected phase-shifts obtained from electron scattering experiments. As an example one chooses electron scattering by argon atom because the polarisability of an inert-gas atom is in general weaker than that of other systems. The polarisability of the Ar-atom is $f^2 = \alpha = 11.07$ au.

The experimental phase shifts of e-Ar scattering at E=12 eV has been determined by Williams[4]. In the second column of Table 2 the measured total phase-shifts η_l^{exp} are listed as given by Williams[4] ($l \leq 3$) together with the effective range total phase-shifts of Eq. (16) for (≥ 4) which were used also in the phase-shift analysis by Williams. The third and fourth columns of Table 2 contain the polarisation phase-shifts η_l^0 which are complex for $l = 0, 1$.

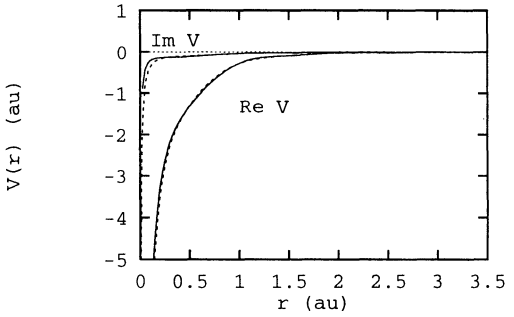

Fig. 1. Real and imaginary part (solid lines) of the inversion potential using input phase-shifts generated by the 2×30 phase-shifts η_l listed partially in Table 1. Dashed lines exhibit the inversion potentials obtained by the 2×9 input polarisation-corrected phase-shifts δ_l^{in} listed in Table 1.

This is because $k = 0.94$ au, $f = 3.3$ so that $kf = 3.1$ (see section 2.1). The input data for the inversion calculation are the polarisation-corrected phase-shifts $\delta_l^{in} = \eta_l^{exp} - \eta_l^0$ which are listed in the fifth and sixth columns of Table 2. The last two columns of Table 2 show the phase-shifts δ^{out} calculated back from the inversion potential (dashed lines) of Fig. 2. The differences between the input/output phase-shifts are small being in general one percent in the relevant partial waves, and this reflects the consistency of the inversion procedure.

The inversion potential of the e-Ar scattering system is shown in Fig. 2 at 12 eV scattering energy as dashed lines. Comparison is made with the inversion potential (solid lines) determined earlier[6] by using the full set of 30 total phase-shifts of η_l^{exp}. The potentials compare well showing the reliability of the present method.

The inversion potential obtained from the total phase-shift without correcting for the long range polarisation potential is per definitionem real. The inversion potential determined by the present method using a set of *complex* polarisation-corrected phase-shifts has a calculated imaginary part which is almost zero. This confirms the consistency of the present method since a scattering potential at an energy below the inelastic threshold should be real. The very small amount of Im V can be considered to originate from the numerical instability of the inversion procedure involving polarisation functions.

Let us discuss the main structures of the inversion potential shown in Fig. 2. It has an atractive part with a minimum value of about -2.8 au at a distance of $r \approx 1.2$ au. At smaller distances the potential is of repulsive nature which can be interpreted as a manifestation of the Pauli-principle. These structures are very stable with respect to variation of the

Table 2. Experimental input phase-shifts η_l^{exp} of electron scattering by Ar-atom measured at energy E =12 eV by Williams (Ref. 4), corresponding polarisation phase-shifts η_l^0, and input polarisation corrected phase-shifts δ_l^{in}. Recalculated phase-shifts δ_l^{out} using the inversion potential shown in Fig. 2 as dashed lines.

l	η_l^{exp}	Re η_l^0	Im η_l^0	Re δ_l^{in}	Im δ_l^{in}	Re δ_l^{out}	Im δ_l^{out}
0	-1.2180	-0.7854	1.7350	-0.4326	-1.7350	-0.4047	-1.7427
1	-0.6260	0.7854	-0.6757	-1.4114	0.6757	-1.3956	0.6618
2	1.1910	0.5578	0.0000	0.6332	0.0000	0.6288	0.0035
3	0.1180	0.1081	0.0000	-0.0099	0.0000	0.0722	-0.0005
4	0.0441	0.0453	0.0000	-0.0012	0.0000	0.0316	0.0028
5	0.0237	0.0248	0.0000	-0.0003	0.0000	0.0158	0.0009
10	0.0032	0.0032	0.0000				
20	0.0004	0.0004	0.0000				
30	0.0001	0.0001	0.0000				

technical parameters which have been for the present case $r_0 = 5.3$ au, $\rho_i = 5.5, 6.2, 6.9, 7.6$, $l_{max} = 5$ (dashed lines), and for the earlier calculation $r_0 = 10$ au, $\rho_i = 25, 26, 27$, $l_{max} = 21$ (solid lines).

From the earlier and present investigation of the electron argon-atom scattering one can confirm that these structures do really exist in the e-Ar system at the scattering energy of 12 eV. These structures are not artifacts due to neglect of proper treatment of polarisation functions as it has been surmised in Ref. 6 where the calculation of complex polarisation functions has not yet been possible. Thus the discovery of these structures can be considered as a model independent support derived from experiment[4] for the pseudopotential theories[12] which construct very similar potentials just obtained for $s-, p-, d-$wave electron scattering by atoms. The repulsive core appearing at short distances may be thus interpreted as a manifestation of the Pauli principle in coordinate space preventing the electron from merging in the electron-cloud of the argon atom.

4 Summary

The application of the modified Newton-Sabatier inversion method[3] has been extended to invert polarisation-corrected phase-shifts arising in electron scattering by atomic target. It has been shown how the effect of the long range

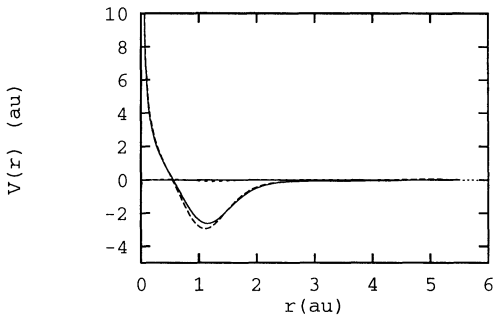

Fig. 2. Inversion potentials obtained by using experimental phase-shifts derived from electron–Ar-atom scattering at scattering energy of 12 eV.

polarisation interaction can be taken into account by using Mathieu function solutions.

The method has been applied first to synthetic phase-shifts derived from known model potential with polarisation tail (r^{-4}). Then the first application of the method to e-Ar scattering at E=12 eV has been carried out with the result of an effective potential which is attractive at small distances but has a repulsive core for $r < 0.5$ au (see Fig. 2), in accordance with the Pauli principle and pseudopotential theories.[12]

The present method of the polarisation phase-shift calculation can be applied also in the case of phase-shift analyses of differential cross-section data. The resulting experimentally determined polarisation-corrected phase-shifts can subsequently be used in the inversion calculation as outlined in section 2 to get model independent information about the electron-atom interaction in the core region.

Acknowledgment This work has been supported by MTA/DFG (76/1995) and OTKA (T17179).

Appendix

Starting from the recurrence relation given by Eq. (11) the coefficients $C_n(\tau) = C_{-n}(-\tau)$ can be calculated by the continued fractions

$$C_n/C_{n-1} = -kf/[(2n+\tau)^2 - (l+1/2)^2 + kfC_{n+1}/C_n], \qquad (A1)$$

$$C_{-n}/C_{-(n-1)} = -kf/[(-2n+\tau)^2 - (l+1/2)^2 + kfC_{-(n+1)}/C_{-n}], \quad (A2)$$

by starting at large values of $n = n_0$ for which

$$C_{n_0}/C_{n_0-1} = -kf/[(2n_0+\tau)^2 - (l+1/2)^2], \quad (A3)$$

and

$$C_{-n_0}/C_{-(n_0-1)} = -kf/[(-2n_0+\tau)^2 - (l+1/2)^2]. \quad (A4)$$

The desired ratios for the coefficients can be calculated up to C_1/C_0 and C_{-1}/C_0. As normalization one fixes $C_0(\tau) = 1$.

The Hill-determinant entering Eqs. (11) and (A1) can be evaluated by its n_0th approximate value Δ_{n_0} as follows. One starts with the relations

$$D_1^0 = 1 - a_1 a_0, \quad D_2^0 = D_1^0 - a_2 a_1, \quad D_1^1 = 1, \quad D_2^1 = D_1^1 - a_2 a_1. \quad (A5)$$

with

$$a_n = kf/[4n^2 - (l+1/2)^2] \quad (A6)$$

to be used in the recurrence relations

$$D_n^0 = D_{n-1}^0 - a_n a_{n-1} D_{n-2}^0, \quad n = 3, 4, .. \quad (A7)$$

$$D_n^1 = D_{n-1}^1 - a_n a_{n-1} D_{n-2}^1, \quad n = 3, 4, .. \quad (A8)$$

from which the n_0th approximate value of the Hill-determinant can be calculated as

$$\Delta_{n_0} = D_{n_0}^1 (2D_{n_0}^0 - D_{n_0}^1). \quad (A9)$$

References

[1] N. A. W. Holzwarth, J. Math. Phys. **14**, 191 (1973).

[2] R. G. Newton, J. Math. Phys. **3**, 75 (1962); P. C. Sabatier, J. Math. Phys. **7**, 1515 (1966).

[3] M. Münchow and W. Scheid, Phys. Rev. Letters **44**, 1299 (1980); K.-E. May, M. Münchow and W. Scheid, Phys. Letters **141** B, 1 (1984); K.-E. May and W. Scheid, Nucl. Phys. A **466**, 157 (1987).

[4] J. F. Williams, J. Phys. B: At. Mol. Phys. **12**, 265 (1979).

[5] D. B. Khrebtukov, J. Phys. A: Math. Gen. **26**, 6357 (1993).

[6] B. Apagyi and P. Lévay, Lecture Notes in Physics, **427**, 252 (1993).

[7] J. Meixner and F. W. Schäfke, *Mathieusche Funktionen und Sphäroidfunktionen* (Springer-Verlag, Berlin, 1954).

[8] P. M. Morse and H. Feshbach, *Methods of Theoretical Physics* (McGraw-Hill, New York, 1953) p. 556.

[9] T. F. O'Maley, L. Spruch, and L. Rosenberg, J. Math. Phys. **2**, 491 (1961).

[10] G. Staszewska, J. Phys. B: At. Mol. Opt. Phys. **22**, 913 (1989).

[11] B. Apagyi and G. Endrédi, BICPOL inversion code, unpublished (1996).

[12] G. B. Bachelet, D. R. Hamann, and M. Schlüter, Phys. Rev. B **26**, 4199 (1982); B. Plenkiewicz, P. Plenkiewicz, P. Baillargeon, and J.-P. Jay-Gerin, Phys. Rev. A **36**, 2002 (1987).

Pion Nucleus Interaction from Inverse Scattering Theory and a Test of Charge Symmetry

S. Jena

Department of Physics, Utkal University Bhubaneswar-751004, India

Abstract. Phase shifts derived from experimental cross section data on the elastic scattering of π^+ and π^- on low mass, zero spin and zero isospin nuclei are used to obtain model independent pion-nucleus potentials with a modified fixed energy inverse scattering formalism. No systematic difference between the π^+ and π^- potentials suggests the absence of any charge symmetry violating effect in the pion-nucleus interaction.

1 Introduction

Studies of pion-nucleus interaction have been of much theoretical and experimental interest [1,2]. They have been useful to obtain information on the isospin structure of the nucleus, to learn about the off-shell behaviour of the hadronic interaction or to study the applicability of multiple scattering theories etc. Since the pions have zero spin, many of the complications of spin dependent effects present in the nucleon-nucleus interaction play no role provided that we are careful to choose nuclei also with zero spin. Pion-nucleus interaction also provides interesting possibility for studying the charge symmetry violation in strong interaction, since the pionic projectiles are available in the charge conjugate states of π^+ and π^- .

In recent years a large amount of pion-nucleus data, both elastic and inelastic, has bcome available [3-6] in the literature. Most theoretical descriptions of the pion-nucleus scattering have been formulated in terms of an optical potential. Such potentials usually contain several free parameters which are optimised to give the best fit to the scattering data. However, with such models, potentials as different as the Kisslinger potential [7] and the Laplacian potential [8] can provide equally good fits to the scattering data and to the pionic atom data. The inherent bias already built into the model from the beginning may mask the true information content of the experimental data. Therefore, there have been several attempts to obtain model independent local potentials directly from the scattering data without the explicit use of a model for the interaction.

Compared with the trivial problem of deducing the cross section from a given potential, the inverse problem of deducing the potential using the given cross section data is entirely nontrivial. Formal methods [9] have been known

for quite some time, but practical methods applicable to specific problems [10,11] were developed only in the early 1980's. The inverse scattering problem is related to the spectral theory of a Sturm-Liouville eigenvalue problem. In connection with the Schrödinger equation two alternative procedures have been suggested; these correspond to taking either the energy or the angular momentum as the spectral variable. The first method developed by Gelfand and Levitan with its variant form due to Marchenko [12] yields the potential at a fixed angular momentum, when the phase shift for that particular partial wave is known for all energies from the scattering data. The second method relates to finding the potential from a set of partial wave phase shifts at a fixed energy. The formal solution to the problem has been given quite some time back by Newton [9], Sabatier [10] and others [13,14], however the first practical application of the formalism has been pointed out by Scheid and his coworkers [15,16] who derived the nucleus-nucleus potentials from the corresponding phase shifts derived with the use of some standard potentials. In our earlier works [17,18] we have discussed a modified form of the Newton-Sabatier formalism for the calculation of the potential from the phase shifts at a fixed energy and have applied the method to the inversion of phases of elastic $\pi^- - {}^4\mathrm{He}$ scattering. The purpose of this contribution is to discuss briefly the general procedure of calculating potentials for a set of phase shifts at a fixed energy, where both the phase shifts and the potentials may be complex. A novel method for extracting the partial wave phase shifts from the elastic differential cross section data is pointed out. The application of the formalism to the scattering of $\pi^{\pm}$ on ${}^4\mathrm{He}$ and ${}^{12}\mathrm{C}$ is presented. The potentials for the π^+ and π^- with the $I = 0$ nucleus ${}^4\mathrm{He}$ is used to discuss the charge symmetry in strong interactions.

2 The Inversion Procedure

The interaction of charged pions with the nucleus contains the Coulomb interaction term $V_C(r)$ which has an infinite range and a short range nuclear potential $V_N(r)$, the only restriction on the unknown part $V_N(r)$ being that it decreases faster than $r^{-3/2}$ for large r [3], and, as we know, this is not a stringent condition in the case of strong interaction potentials. Let us introduce a dimensionless coordinate

$$\rho = kr = \left(\frac{2\mu E}{\hbar^2}\right)^{1/2} r, \tag{1}$$

where μ is the reduced mass of the pion-nucleus system, and E is the centre of mass energy. Assuming a spherically symmetric potential $V(r)$ for the pion, the Schrödinger equation for the l'th partial wave can be written as

$$\rho^2 \left(\frac{d^2}{d\rho^2} + 1 - U(\rho)\right) \phi_l(\rho) = l(l+1)\phi_l(\rho), \tag{2}$$

where

$$U(\rho) = \frac{V(r)}{E}, \quad V(r) = V_N(r) + V_C(r), \tag{3}$$

and

$$\phi_l(\rho) = r\psi_l(r), \tag{4}$$

where $\psi_l(r)$ is the wave function for the l'th partial wave. Let $\phi_l^0(\rho)$ be the wave function when the nuclear part of the interaction is switched off, so that $\phi_l^0(\rho) = F_l(\rho)$, the regular solution of the Coulomb problem.

Outside the range of the nuclear interaction, i.e., for $\rho > \rho_0$ the nuclear part of the potential may be neglected and then the wave function in this region can be expressed as a linear combination of the regular and irregular Coulomb wave functions $F_l(\rho)$ and $G_l(\rho)$

$$\phi_l(\rho) = A_l[\cos\delta_l F_l(\rho) + \sin\delta_l G_l(\rho)] = A_l T_l(\rho), \quad \text{for} \rho > \rho_0. \tag{5}$$

The unknown amplitudes A_l are to be determined as discussed below. The nuclear phase shifts δ_l are extracted from the experimental cross section data after properly subtracting the Coulomb effects [18]. The phase shifts are, in general complex.

Let us define a kernel

$$K(\rho, \rho') = \sum_{l=0}^{\infty} c_l \phi_l(\rho)\phi_l^0(\rho'). \tag{6}$$

It has been shown by Newton [19] and by Coudray and Coz [20] that, if one defines the potential as

$$U(\rho) = U_C(\rho) - \frac{2}{\rho}\frac{d}{d\rho}[\rho^{-1}K(\rho, \rho)], \tag{7}$$

the kernel $K(\rho, \rho')$ turns out to be the unique solution of the Gelfand- Levitan linear integral equation

$$K(\rho, \rho') = g(\rho, \rho') - \int_0^{\infty} d\rho''(\rho'')^{-2}K(\rho, \rho'')g(\rho'', \rho') \tag{8}$$

where

$$g(\rho, \rho') = \sum_{l=0}^{\infty} c_l \phi_l^0(\rho)\phi_l^0(\rho'). \tag{9}$$

The wave function $\phi_l(\rho)$ then satisfies the integral equation

$$\phi_l(\rho) = \phi_l^0(\rho) - \int_0^{\rho} d\rho'(\rho')^{-2}K(\rho, \rho')\phi_l^0(\rho'). \tag{10}$$

Substituting $K(\rho, \rho')$ from Eqn. (6) into the Eqn. (10) above, we get a set of coupled equations

$$\phi_l(\rho) = \phi_l^0(\rho) - \sum_{l'=0}^{\infty} c_{l'} L_{ll'}(\rho)\phi_{l'}(\rho), \tag{11}$$

where the matrix $L_{ll'}$ is given by

$$L_{ll'}(\rho) = \int_0^{\rho} \phi_l^0(\rho')\phi_{l'}^0(\rho')(\rho')^{-2}d\rho'. \tag{12}$$

Equation (11) can be rewritten as

$$\sum_{l'=0}^{\infty} \left[\delta_{ll'} T_{l'}(\rho)A_{l'} + L_{ll'}(\rho)T_{l'}(\rho)b_{l'}\right] = F_l(\rho), \tag{13}$$

where we have introduced a new set of coefficients $b_l = c_l A_l$. Solving the set of linear equations (13) at two radial distances $\rho = \rho_1, \rho_2 (> \rho_0)$ provides the unknown coefficients A_l and b_l, and hence the coefficients c_l. From these the kernel $K(\rho, \rho)$ and the nuclear part of the potential are obtained using the equations (6) and (7) respectively.

In potential problems the number of significant phase shifts is roughly $L = kr_0$. Normally the phase shifts become negligibly small for partial waves of value somewhat higher than L. In the work of May, Münchow and Scheid [15] summation series in Eqn. (13) is truncated at the value of $l' = L$ for computational reasons, even though theoretically an infinite number of partial wave phase shifts contain all the required information for reproducing the true interaction. In this work, the eqn. (13) at more than two values of ρ are considered, which in effect over-determines the solution. The solutions are then optimised by a standard procedure described in Ref. [15]. However, in that procedure the total number of coefficients c_l calculated from the equivalent of eqn. (13) is only equal to L. As a result, the series for $K(\rho, \rho)$ of eqn. (6) is truncated at the value of $l' = L$. Unfortunately, even though the phase shifts for $l > L$ may be negligible, the coefficients $c_l\,(l > L)$ may not be small. This has earlier been demonstrated by Sabatier [20]. Thus the truncation of the series for $K(\rho, \rho)$ at $l = L$ will introduce a considerable amount of error in the value for the potential. In an earlier work [17] we have presented a prescription for calculating c_l's for $l > L$. Including more number of coefficients in the series sum for the potential naturally increases the accuracy in the reproduction of the actual potential.

3 Phase Shifts and Potentials for $\pi^{\pm}$

The differential elastic cross section data for $\pi^{\pm} - {}^4$He at several incident pion energies below the $\Delta(3,3)$ threshold [21-24] have been analysed using the conformal mapping technique [18] to extract the partial wave phase shifts. The ambiguities of complex phase shift analysis are taken care of by minimising the chi-square for a fit to the differential cross section data. Phase shifts for

the first ten partial waves upto the angular momentum state $L = 9$ are used for the inversion. Partial waves for $L > 9$ are seen to contribute insignificantly to the cross section in the energy region considered. The real and imaginary parts of the potentials for $\pi^+ - {}^4\mathrm{He}$ and $\pi^- - {}^4\mathrm{He}$ at incident pion energies of 51 MeV, 60 MeV, 68 MeV and 75 MeV are shown in Figs. 1(a-d). Fig. 2 shows a comparison of the typical $\pi^+ - {}^{12}\mathrm{C}$ inversion potential at 50 MeV with the corresponding Laplacian Potential. Details of the potentials at other incident energies and for other pion-nucleus system have been reported elsewhere [18,25].

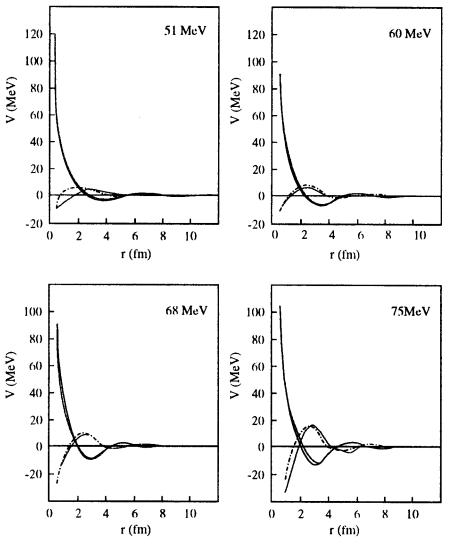

Fig. 1. (a)-(d): Nuclear part of the $\pi^{\pm} - {}^4$ He optical potential obtained by inversion. The solid line and the dashed line represent the real part of the inversion potential for π^- and π^+ respectively. The dotted curve and the dash-dotted curve are twice the negative of the imaginary part of the inversion potential forπ^- and π^+ respectively. Only one of the curves is shown when there is an overlap between the former two or the later two.

As is seen from Fig. 1 and Fig. 2, the inversion formalism yields pion-nucleus potentials which conforms to our knowledge about this interaction from earlier phenomenological models. However, the phenomenological and the inversion potentials differ in their details. General features seen in the pion-nucleus potentials for both ^{4}He and ^{12}C are:

(i) the interaction is attractive at large radii, becoming repulsive at shorter distances.

(ii) The strength of the attractive part of the real potential, as well as imaginary potential increases with increasing incident energy. This conforms to the observed fact that the inelastic scattering is higher at higher energies.

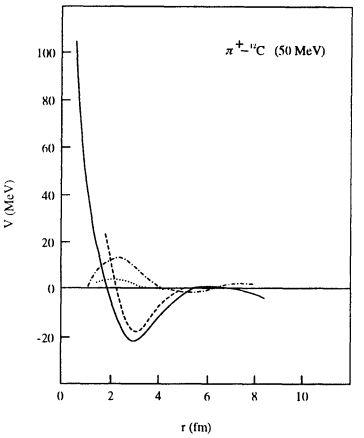

Fig. 2. Figure 2. $\pi^{+} - {}^{12}C$ optical potential at 50 MeV. The solid curve is the real part of the inversion potential. The dashed curve is the real part of the Laplacian potential. The dash-dotted curve is twice the negative of the imaginary part of the Laplacian potential. The dotted curve is twice the negative of the imaginary part of the inversion potential.

(iii) The radius of the repulsive core decreases with energy.
(iv) The inversion potential is more spread out towards the nuclear surface. This could probably serve as a test for the inversion potential in the calculation of pionic absorption by nuclei, which is predominantly a surface effect.

The oscillations in the potential at large distance could be due to the truncation of the infinite series of Eqn. (13), or may be ascribed to some physical phenomenon, similar to the Friedel oscillations in the effective electrostatic interaction between ions in a solid [26,30]. A clear understanding of this feature is still lacking.

4 Test of Charge Symmetry

Owing to the existence of two pions of opposite charges, pion- nucleus interaction provides unique possibility of studying the charge symmetry breaking in nuclear interaction. The observed difference, if any, between the Coulomb corrected cross sections for π^{+} and π^{-} scattering on nuclei with zero isospin can be interpreted as a manifestation of different masses and widths of $\Delta(3,3)$ isobar states excited in the respective processes. Masterson et al. [27] claim to have discovered such charge symmetry breaking effect in the elastic scattering of $\pi^{\pm}$ on d, ^{3}He and H. Their observed estimates of the splittings of $\Delta(3,3)$ states are in suitable agreement with predictions of models [28] which take into account the different quark composition of $\Delta(3,3)$ resonances. Nevertheless the evidence is not yet conclusive, there remain some doubt concerning the conclusion on charge symmetry breaking [29]. These doubts arise from

the fact that for any firm conclusion about charge symmetry breaking one must calculate the hadronic amplitude with very high precision. The matter is complicated by the presence of Coulomb correction, for which doubts still exist regarding the accuracy of the methods in use. Since the model independent pion-nucleus potentials calculated in this work have taken into consideration the Coulomb effects, they provide us a suitable tool to compare for any violation of charge symmetry. From the Figs. 1(a-d) it is noted that there is no significant difference between the hadronic part of the potentials for π^+ and π^-. Even though we have not shown in the graphs the errors bars in the potentials due to the uncertainties in experimental cross section, at the present stage of the experimental accuracy, they are expected to be larger than any slight differences between the two potentials. However no firm conclusion can be drawn, since the effect of charge symmetry breaking is expected, any way, to be very small. Considering the smallness of the effects of the charge symmetry violation, it would have been appropriate to determine accurately the uncertainties in the potentials, so as to be able to specify within what limits charge symmetry is obtained. However, at the present state of the inverse scattering algorithm, there is no specified procedure to estimate the propagation of errors in the phase shifts from different partial waves to the final inversion potentials. Much more work in this direction is needed to get expected answers from such analyses. It has been shown by Khankhasayev et al. [29] that for a mass difference of 6 MeV and a difference in width of 8 MeV for Δ^{++} and Δ^-, the difference between hadronic phases for scattering of π^+ and π^- on ^4He at 75 MeV amounts to a mere 0.72°. Such a difference in hadronic phases may be detected in phase shift analysis, if the differential cross section of elastic scattering is measured with 1-2% precision.

In conclusion we can state that the present study gives us the confidence that the inverse scattering theory has reached a stage where it can directly be applied to complex physical systems to provide us with model independent interactions reliably.

References

[1] T. Erison and W. Weise: *Pions and Nuclei* (Clarendon Press, Oxford, 1988).
[2] W. Kluge, Rep. Prog. Phys. **54** (1991) 1251.
[3] D. Mariow et al., Phys. Rev. **C30** (1984) 1662.
[4] M.W. Rawool-Sullivan et al., Phys. Rev. **C49** (1994) 627.
[5] T. Takahashi et al., Phys. Rev. **C51** (1995) 2542.
[6] B. Brinkmoller et al., Phys. Rev. **C44** (1991) 2031.
[7] L.S. Kisslinger, Phys. Rev. **98** (1955) 761.
[8] G. Faldt, Phys. Rev. **C5** (1972) 400.
[9] R.G. Newton, ,Scattering theory of waves and particles (McGraw Hill, New York, 1966).

[10] K. Chadan and P.C. Sabatier, Inverse Problems in Quantum Scattering Theory (Springer Verlag, 1989).
[11] H.V. von Geramb (Ed.), Quantum Inversion Theory and Applications (Springer Verlag, 1994).
[12] Z.S. Agranovich and V.A. Marchenko, The inverse problem of scattering theory (Gordon and Breach, N.Y., 1963).
[13] C. Coudray, Lett. Nuovo Cim. **19** (1977) 319.
[14] P.J. Redmond, J. Math. Phys. **5** (1964) 1547.
[15] K.E. May, M. Munchow and W. Scheid, Phys. Lett. **B141** (1984) 1.
[16] K.E. May and W. Scheid, Nucl. Phys. **A466** (1987) 157.
[17] B. Deo, S. Jena and S. Swain, J. Phys. **A17** (1984) 2767.
[18] B. Deo, S. Jena and S. Swain, Phys. Rev. **C32** (1985) 1247
[19] R.G. Newton, J. Math. Phys. **3** (1962) 75.
[20] C. Coudray and M. Coz, Ann. Phys. (N.Y) **61** (1970) 488.
[21] F. Binon et al., Nucl. Phys. **A298** (1978) 499.
[22] K.M. Crowe et al., Phys. Rev. **180** (1969) 1349.
[23] M.L. Scott et al., Phys. Rev. **C9** (1974) 1198.
[24] B. Brinkmoller and H.G. Schlaile, Phys. Rev **C48** (1993) 1973.
[25] S. Jena and S. Swain, to be published (Utkal University Preprint No. 1-Phy/96).
[26] B. Apagyi, Private communication.
[27] T.G. Masterson et al., Phys. Rev. **C26** (1982) 2091.
[28] R.P. Bickerstaff and A.W. Thomas, Phys. Rev. **D25** (1982) 1869.
[29] M. Kh. Khankhasayev, F. Nichitiu and G. Sapozhnikov, Phys. Lett. **B175** (1986) 261.
[30] W.A. Harrison, Solid State Theory (McGraw Hill, 1970).

NN Potentials with Explicit Momentum Dependence Obtained from Generalized Darboux Transformations

F. Korinek[1], H. Leeb[1], M. Braun[2] and S. A. Sofianos[2]

[1] Institut für Kernphysik, Technische Universität Wien, Wiedner Hauptstraße 8-10/142, A-1040 Wien, Austria
[2] Department of Physics, University of South Africa, P.O. Box 392, Pretoria 0001, South Africa

Abstract. Using recently developed inversion techniques based on generalized Darboux transformations we constructed, in uncoupled channels, momentum dependent potentials having a momentum independent term and one term linear in the square of the momentum. Varying the momentum dependent term of these potentials we created via inversion sets of potentials that are phase equivalent up to at least 2 GeV to the commonly used Nijmegen and Paris nucleon–nucleon potentials. These sets of potentials offer us the possibility to study the sensitivity of the triton binding energy on the momentum dependence of the NN-force.

1 Introduction

In recent decades much effort has been made to construct nucleon–nucleon (NN) potentials which can describe two–nucleon scattering data as well as many–body observables. In the absence of an appropriate solution within QCD, realistic NN-potentials are still based on the meson–exchange picture. This theory, originally introduced by Yukawa [1], yields an explicit momentum dependent NN-interaction which in configuration space is reflected by a nonlocality. Several potentials have thus been developed [2], [3], [4] which reproduce the NN scattering data in the elastic region, below $E \approx 300$ MeV, equally well. Nevertheless the momentum dependence of these potentials differs significantly in strength and range because the two-body data do not provide any information on it.

The presence of nonlocality in the NN-force is important in studying many–nucleon observables where the off-shell characteristics of the momentum dependent part of the potential are manifested. The interplay between the momentum dependence and the sensitivity of the observables to the off-shell behaviour of the NN force cannot be studied by simply comparing the existing realistic potentials alone since they are only phase equivalent below the pion production threshold and yield different phase shifts beyond $E \approx 300$ MeV which affect the results in many–body calculations.

To investigate the effects stemming from the nonlocality itself we used recently developed inversion techniques [5], [6] to construct sets of potentials

having a different momentum dependence and are phase equivalent up to at least 2 GeV. The inversion scheme is based on Darboux transformations of a specific Sturm–Liouville equation [7], [8], [9] and offers the possibility to construct various momentum dependent interactions in uncoupled channels [10]. We mention here that, to the best of our knowledge, there are no Darboux transformations dealing with the nonlocality of the NN-potential in coupled channels.

Other mathematical solutions of the inverse scattering problem based on the Gel'fand–Levitan or the Marchenko integral equations were given in Refs. [11] and [12]. In recent years these methods have been used by the Hamburg group to construct NN interactions from experimental data [13], [14], [15], [16]. However the inversion scheme used generates only local, momentum independent potentials. Although the equations of Marchenko and Gel'fand–Levitan have been generalized to include energy-dependent interactions [17], [18], [19], [20] they have not yet been applied to experimental nucleon–nucleon scattering data.

In what follows we shall briefly recall in Sect.2 the generalized Darboux transformations and describe the method of constructing phase equivalent momentum dependent potentials. In Sect.3 we shall present and discuss our results for the three–nucleon binding energy.

2 Formalism

2.1 The Darboux transformation

The recently developed inversion scheme based on Darboux transformations [5], [9], [21] can be used to construct potentials depending linearly on energy. Within this method one considers Sturm–Liouville equations of the form

$$\left\{ \frac{\mathrm{d}^2}{\mathrm{d}r^2} - \frac{\lambda^2 - \frac{1}{4}}{r^2} + \kappa^2 - U(r) \right\} \psi(\Theta, r) = \Theta^2 h(r) \psi(\Theta, r) \,, \tag{1}$$

where $U(r)$ is a local spherically symmetric potential, $h(r)$ is a suitably chosen function, and λ, κ , and Θ are in general complex constants. For convenience we introduce the vectors

$$X^{\mathrm{T}} = \left(\frac{W\left[\eta_0(\gamma, r), f_0^-(\alpha_1, r)\right]}{\gamma^2 - \alpha_1^2}, \ \ldots \ , \frac{W\left[\eta_0(\gamma, r), f_0^-(\alpha_N, r)\right]}{\gamma^2 - \alpha_N^2} \right) \,, \tag{2}$$

$$\varphi_0^{\mathrm{T}}(r) = (\varphi_0(\beta_1, r), \ \ldots \ , \varphi_0(\beta_N, r)) \,,$$

and the matrix Y

$$Y := (Y_{ij}) = \left(\frac{W\left[\varphi_0(\beta_i, r), f_0^-(\alpha_j, r)\right]}{\beta_i^2 - \alpha_j^2} \right) \,, \tag{3}$$

where $\varphi_0(\beta_i, r)$ and $\eta_0(\gamma, r)$ are regular solutions while $f_0^-(\alpha_j, r)$ is a Jost solution of the Sturm–Liouville equation (1) with the potential $U_0(r)$ at the Θ-values $\{\alpha_i,\ \beta_i\}$, $i = 1, \cdots, N$ and γ. The pairs $\{\alpha_i, \beta_i\}$ and the variable γ can be chosen arbitrarily. For the Wronskian the standard definition

$$W[\varphi(r), f(r)] = \varphi(r)f'(r) - \varphi'(r)f(r) \tag{4}$$

is used. With these definitions a Darboux transformation is written [5]

$$\eta_2(\gamma, r) = \eta_0(\gamma, r) - X^{\mathrm{T}} Y^{-1} \varphi_0(r)\,. \tag{5}$$

It is straightforward to show that $\eta_2(\gamma, r)$ is also a regular solution of the Sturm–Liouville equation (1) with the potential

$$U_2(r) = U_0(r) - 2\sqrt{h(r)}\frac{\mathrm{d}}{\mathrm{d}r}\frac{1}{\sqrt{h(r)}}\frac{\mathrm{d}}{\mathrm{d}r}\ln(\det Y)\ . \tag{6}$$

From the asymptotic behaviour of $\eta_2(\gamma, r)$ one obtains the analytic expression of the S-matrix associated with the potential $U_2(r)$

$$S_2(k) = S_0(k)\prod_{i=1}^{N}\frac{(k-\beta_i)(k+\alpha_i)}{(k+\beta_i)(k-\alpha_i)}\ , \qquad \mathrm{Im}\,\beta_i < 0,\ \mathrm{Im}\,\alpha_i < 0\ . \tag{7}$$

Here $S_0(k)$ is the S-matrix corresponding to the potential $U_0(r)$. The relationships (5) - (10) represent an inversion scheme. Its application requires the determination of a set of $\{\alpha_i, \beta_i\}$ values of the S-matrix (10) to describe the input data. Given the rational representation of the S-matrix (10) the potential is then evaluated via (6).

2.2 Momentum dependent potentials

The meson–exchange model yields an explicit momentum dependence for realistic nucleon–nucleon potentials. Frequently used NN-potentials, like the Nijmegen [2] or Paris [3], include this dependence in the central component as follows

$$V(r, \mathbf{p}^2) = V^{(\mathrm{a})}(r) + \frac{\mathbf{p}^2}{m}V^{(\mathrm{b})}(r) + V^{(\mathrm{b})}(r)\frac{\mathbf{p}^2}{m}\ . \tag{8}$$

Here, $\mathbf{p}$ is the momentum operator and m is the nucleon mass.

The Darboux transformations can be applied to these potentials by choosing in (1) $\kappa = 0$ and

$$h(r) = -1 + U_{\mathrm{E}}(r)\,. \tag{9}$$

Then Θ corresponds to a wave number, $\gamma = k$, and we get the special case of a radial Schrödinger equation with a potential which depends linearly on the center of mass energy E

$$V(r, E) = \frac{\hbar^2}{m}U(r) + E\,U_{\mathrm{E}}(r)\ . \tag{10}$$

The energy dependence is conceptually different from the momentum dependence. However, for two–body scattering there exists a one-to-one relationship between momentum and energy dependent potentials. This can be obtained if we use the off-shell transformation

$$\psi(\mathbf{r}) = \phi(\mathbf{r}) \frac{1}{\sqrt{1 + 2V^{(\mathrm{b})}(r)}}, \tag{11}$$

where $\psi(\mathbf{r})$ and $\phi(\mathbf{r})$ are the physical wave functions of the Schrödinger equation with momentum and energy dependent potentials, respectively. Since $V^{(\mathrm{b})}(r)$ vanishes asymptotically, $\psi(\mathbf{r})$ and $\phi(\mathbf{r})$ have the same asymptotic behaviour which implies that the phase shifts are the same for both potentials. Inserting (12) into the Schrödinger equation and comparing the corresponding equations for the energy and the momentum dependent potentials one can easily derive the relations

$$U(r) = \frac{m}{\hbar^2} \frac{V^{(\mathrm{a})}(r)}{1 + 2V^{(\mathrm{b})}(r)} - \left(\frac{\nabla V^{(\mathrm{b})}(r)}{1 + 2V^{(\mathrm{b})}(r)} \right)^2 \tag{12}$$

and

$$U_{\mathrm{E}}(r) = \frac{2V^{(\mathrm{b})}(r)}{1 + 2V^{(\mathrm{b})}(r)} \,. \tag{13}$$

The inversion procedure which takes into account the momentum dependent interaction requires firstly to fix the momentum dependent part $V^{(\mathrm{b})}(r)$ and thus the function $h(r)$. The two–nucleon scattering data cannot provide any information about the momentum dependence. Secondly, one has to define an arbitrary but reasonable potential $U_0(r)$ and to determine the S-matrix $S_0(k)$. The inversion scheme is then implemented by determining a set $\{\alpha_i, \beta_i\}$, $i = 1, \cdots, N$ to reproduce the given S-matrix. As outlined above the evaluation of the potential $U(r) \equiv U_2(r)$ is straightforward and yields, via (13), the momentum independent term $V^{(\mathrm{a})}(r)$ of the NN-potential.

3 Results and discussions

Our main concern is to study the importance of the off-shell effects generated by the momentum dependent term of the NN-potential and not to create a new potential. For this purpose we apply our inversion scheme to data generated by realistic NN-potentials which enable us to consider phase shifts at energies far beyond the pion production threshold. With this scattering information and the method described in Sect.2 various sets of phase equivalent potentials having different momentum dependencies can be determined.

In the present work we endeavoured to construct via inversion a set of potentials with different momentum dependencies which are phase equivalent up to at least 2 GeV to the Nijmegen potential [22]. In these calculations we

used the momentum dependent part of the Nijmegen potential $V^{(b)}(r)$ but with an additional factor λ, i.e.,

$$V_\lambda^{(b)}(r) = \lambda V_{\text{Nijm}}^{(b)}(r)\,. \tag{14}$$

For several λ-values the corresponding momentum independent term $V_\lambda^{(a)}(r)$ has been obtained via inversion using the Nijmegen phase shifts. The results for the $^1S_0$ channel are displayed in Fig.1a. The most evident difference between the potentials is the depth at $r \approx 0.8$ fm which varies systematically with λ. This reflects the interplay between the momentum dependent and momentum independent parts of the potentials. By increasing the strength of $V_\lambda^{(b)}(r)$ the behaviour of $V_\lambda^{(a)}(r)$ at short distances has less influence on the phase shifts. However to obtain reliable and stable potentials for $r \gtrsim 0.5$ fm one has to use phase shifts at even higher energies than 2 GeV. When the momentum dependence becomes very strong ($\lambda \gtrsim 1.5$) the potential term $V_\lambda^{(a)}(r)$ becomes negative in the vicinity of the origin. This behaviour can be eliminated by including phase shifts at even higher energies (beyond 4 GeV). Nevertheless this is not necessary since it plays no role as the wave function in this region is to all practical purposes zero. We would like to remark that for $r \gtrsim 5.0$ fm we use $V_\lambda^{(a)}(r) = V_{\text{Nijm}}^{(a)}(r)$ in order to avoid numerically generated small oscillations in the asymptotic region.

Qualitatively similar results were obtained in our previous calculations based on the Paris $^1S_0$ potential. The results for the latter are displayed in Fig.1b for comparison purposes. In this case the variation of the depth at $r \approx 0.8$ fm is even greater which is due to the fact that the Paris potential has a stronger momentum dependence. The same λ-dependence is also found for the p-waves. This is shown in Fig.2 where the results for the Nijmegen $^3P_0$ and the $^3P_1$ channels are given.

As already mentioned above the inverted potentials for different λ-values are phase-equivalent in the sense that the deviation of the phase shifts generated from the inverted potentials from that of the original Nijmegen (or Paris) potential is less than $0.1°$ in the whole range from $0 - 2$ GeV. These differences stem from the rational parametrisation of the S-matrix as well as from numerical noise.

To study the influence of the momentum dependence on the triton binding energy E_t we employed in our calculations the Integro Differential Equation Approach (IDEA) [10], [23]. The method, based on hyperspherical harmonics expansion, is fast and efficient in bound state calculations. For our studies it is sufficient to limit ourselves to a three–channel calculations including the $^1S_0$ and the $^3S_1 - ^3D_1$ partial waves. Since at present no inversion method exists to determine momentum dependent potentials for coupled channels we used different well-established local nucleon–nucleon potentials for the $^3S_1 - ^3D_1$ channel. More specifically we employed the Reid Soft Core (RSC) [24], the Super Soft Core (SSC) [25], the Gogny-Pires-de Tourreil (GPDT) [26], the

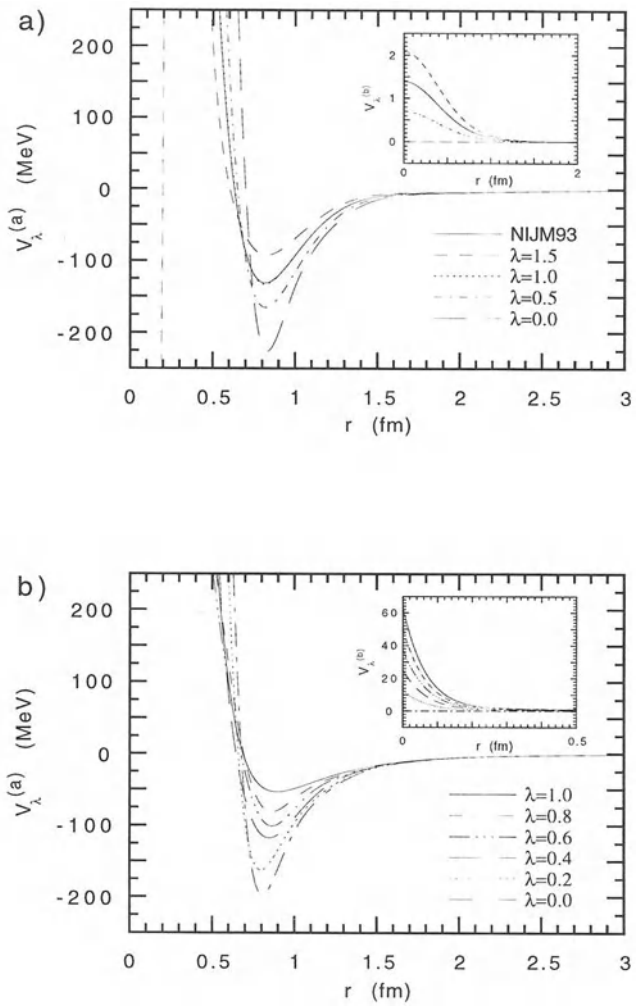

Fig. 1. The momentum independent component $V_\lambda^{(a)}(r)$ obtained by inversion and scaling of $V^{(b)}(r)$ for different λ values for the $^1S_0$ channel of the Nijmegen (a) and Paris (b) potential. The inserts show the $\lambda V^{(b)}(r)$.

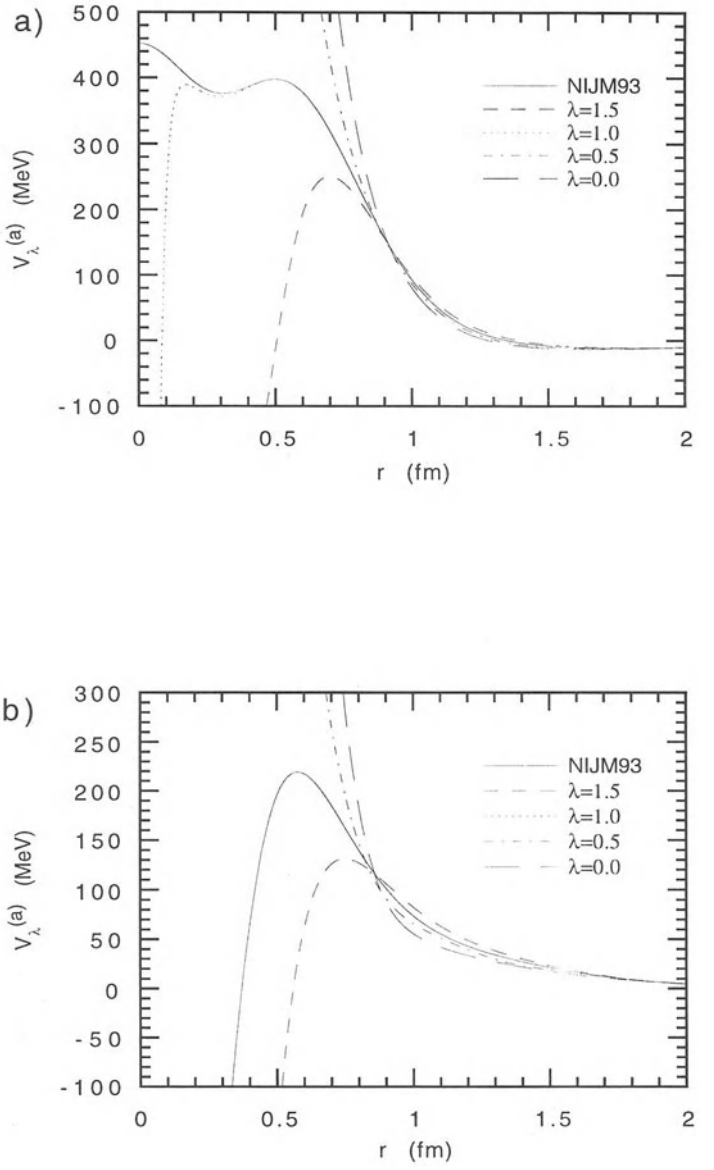

Fig. 2. Same as in Fig.1 but for the $^3P_0$ wave (a) and the $^3P_1$ wave (b).

Argonne (AV14) [27], and the local version of the Nijmegen potential (NIJM) [22].

The differences $E_t(\lambda)-E_t(\lambda = 0.0)$ in MeV obtained for the triton binding energy using as input the $V^{(b)}(r)$ and the $^1S_0$ phase shifts of the Nijmegen potentials and the aforementioned $^3S_1-^3D_1$ interactions are shown in Fig.3a. It is seen that the ΔE_t could be up to about 0.3 MeV for all potentials used. The slightly different sensitivity of E_t to the GPDT potential, comes as no surprise since this potential has a soft core which is responsible for the differences found in few-nucleon calculations as compared to the other potentials. The results obtained when the $V^{(b)}(r)$ and the $^1S_0$ phase shifts are those of the Paris potential are shown in Fig.3b. The effects are similar to the ones obtained for the Nijmegen potentials. However the maximum deviation is of the order of 0.15 MeV with a tendency to become less at $\lambda \approx 1.0$.

Important differences in the triton binding energy can also be obtained by varying the range of nonlocality. This has been shown in our previous calculations [10] where by varying the range of $V^{(b)}(r)$ we obtained differences ΔE_t up to 0.25 MeV.

In conclusion we found that the uncertainty in the velocity dependent part and in the nonlocality range has considerable effects on the triton binding energy. These effects can be exploited to improve the existing NN interaction and thus reducing the discrepancies found between different potential models in describing nuclear data.

Acknowledgements: Financial support from the Austrian FWF, project number P10467-PHY, and from the Foundation for Research Development of South Africa is greatly appreciated.

References

[1] H. Yukawa, Proc. Phys.-Math. Soc. Japan **17** (1935) 48.
[2] M.M. Nagels, T.A. Rijken and J.J. de Swart, Phys. Rev. **D 17** (1978) 768.
[3] M. Lacombe, B. Loiseau, J.M. Richard, R. Vinh Mau, J. Côté, P. Pirès and R. de Tourreil, Phys. Rev. **C 21** (1980) 861.
[4] R. Machleidt, K. Holinde and Ch. Elster, Phys. Rep. **149** (1987) 1.
[5] W.A. Schnizer and H. Leeb, J. Phys. **A 26** (1993) 5145.
[6] H. Leeb and D. Leidinger, Few–Body Systems, Suppl. **6** (1992) 117.
[7] H. Cornille, J. Math. Phys. **17** (1976) 2143; **18** (1977) 1855.
[8] B.V. Rudyak, A. Suzko and B.N. Zakhariev, Phys. Scr. **29** (1984) 515;
A. Suzko, Phys. Scr. **31** (1985) 447;
B.V. Rudyak and B.N. Zakhariev, Inverse Problems **3** (1987) 125.
[9] W.A. Schnizer and H. Leeb, J. Phys. **A 27** (1994) 2605.
[10] F. Korinek, H. Leeb, M. Braun, S.A. Sofianos, R.M. Adam, Nuclear Physics **A**, in press (1996).
[11] I.M. Gel'fand and B.M. Levitan, Am. Math. Soc. Transl. **1** (1955) 253;
B.M. Levitan, *Generalized Translation Operators and Some of the Applications* (Davey, New York, 1964).

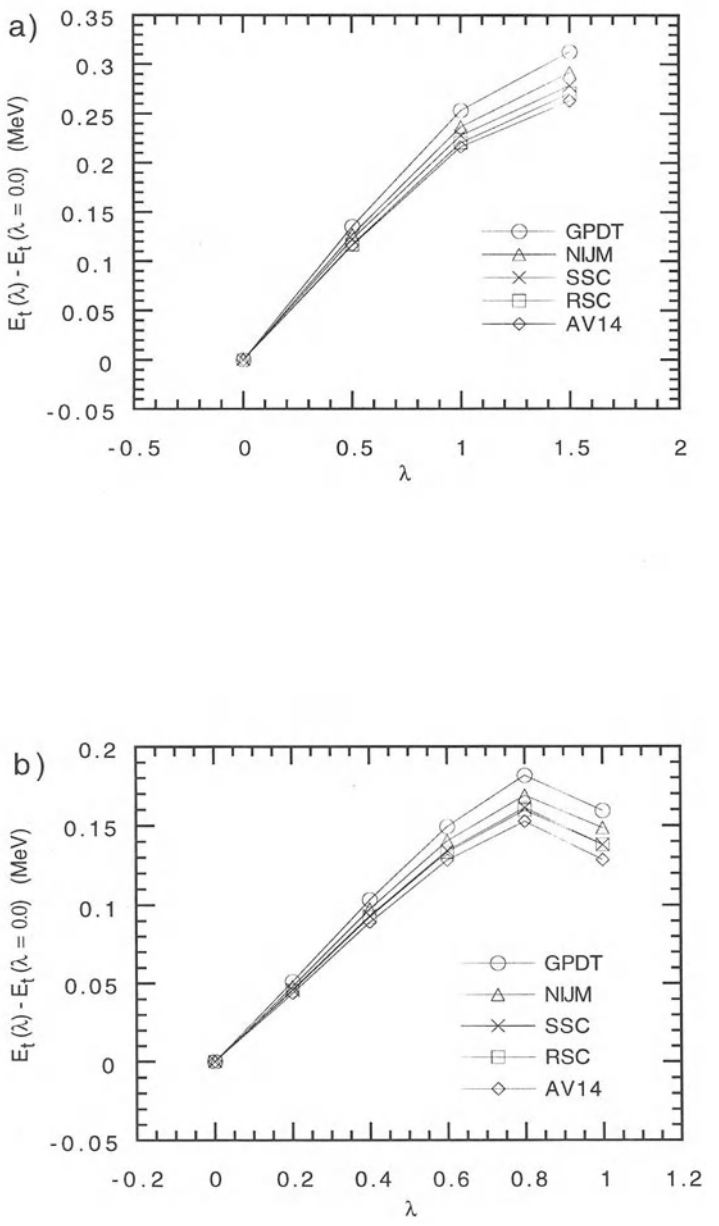

Fig. 3. The difference $E_t(\lambda) - E_t(\lambda = 0.0)$ in the triton binding energy obtained with different $^3S_1 - ^3D_1$ potentials for the Nijmegen (a) and Paris (b) $^1S_0$ potential.

[12] Z.S. Agranovich and V.A. Marchenko, *The Inverse Problem of Scattering Theory* (Gordon and Breach, New York, 1963).
[13] M. Coz, H.V. von Geramb and J.H. Lumpe, Z. Phys. **A 328** (1987) 259.
[14] J. Kuberczyk, M. Coz, H.V. von Geramb and J.D. Lumpe, Z. Phys. **A 328** (1987) 265.
[15] Th. Kirst, K. Amos, L. Berge, M. Coz and H.V. von Geramb, Phys. Rev. **C 40** (1989) 912.
[16] H. Kohlhoff and H.V. von Geramb, *Proc. Conf. on Quantum Inversion Theory and Applications*, Bad Honnef, 1993, ed. H.V. von Geramb (Springer, Berlin, 1994) p. 314.
[17] V.I. Mal'cenko, Am. Math. Soc. Transl. **75** (1966) 227.
[18] M. Jaulent and C. Jean, Commun. Math. Phys. **28** (1972) 177.
[19] M. Jaulent, Ann. Inst. Henri Poincare **17** (1972) 363;
M. Jaulent, C. R. Acad. Sc. Paris **280** (1975) 1467.
[20] M. Jaulent and C. Jean, Lett. Math. Phys. **6** (1981) 183;
M. Jaulent and C. Jean, J. Math. Phys. **23** (1981) 258.
[21] H. Leeb, *Proc. Conf. on Quantum Inversion Theory and Applications*, Bad Honnef, 1993, ed. H.V. von Geramb (Springer, Berlin, 1994) p. 241.
[22] V.G.J. Stoks, R.A.M. Klomp, C.P.F. Terheggen and J.J. de Swart, Phys. Rev. **C 49** (1994) 2950.
[23] M. Fabre de la Ripelle, Few–Body Syst. **1** (1986) 181;
M. Fabre de la Ripelle, H. Fiedeldey and S.A. Sofianos, Phys. Rev. **C 38** (1988) 449.
[24] R.Reid, Ann. Phys. **50** (1968) 411.
[25] R. de Tourreil and D.W.L. Sprung, Nucl. Phys. **A 201** (1973) 193.
[26] D. Gogny, P. Pires and R. de Tourreil, Phys. Lett. **B 32** (1970) 591.
[27] R.B. Wiringa, R.A. Smith and T.L. Ainsworth, Phys. Rev. **C 29** (1984) 1207.

Unitarity and the Scattering Phase Shifts for Inversion Studies

H. Huber[2,1], D. R. Lun[1], L. J. Allen[1], and K. Amos[1]

[1] School of Physics, University of Melbourne, Parkville, Victoria 3052 Australia.
[2] Institut für Kernphysik, Technische Universität Wien,
Wiedner Hauptstrasse 8-10/142, A-1040 Wien, Austria

1 Introduction

The first requirement in application of most global inverse scattering methods [1] seeking (local) interaction potentials from scattering data, is to specify the scattering phase shifts, δ_ℓ, or, equivalently, the S matrix, $S_\ell \equiv e^{2i\delta_\ell}$. With fixed energy inverse scattering problems, knowledge of those phase shifts for all physical values of the angular momentum ℓ allow application of the Newton–Sabatier scheme as modified by Scheid and his collaborators [2]. Other approaches, such as the Lipperheide–Fiedeldey methods [3], require specification of the phase shift function, $\delta(\lambda)$, for all values of the (complex) angular momentum variable, λ $(= \ell + 1/2)$, to provide unique determination of the Schrödinger potential. The starting point with all global inverse scattering methods then is to specify those phase shifts, first at the physical values and then, by interpolation, for all values of the angular momentum variable. But no technique exists to do so unambiguously. Most commonly S matrix fitting procedures (to cross–section data) are used and usually, therewith, aspects of ill-posedness are ignored as are ambiguities due to local minima in the n-parameter hypersurface associated with such procedures.

Our aim has been to obtain phase shifts by a more global means, namely by using the unitarity (generalized flux) theorem in application to real cases. Below the first nonelastic threshold and for the scattering of spinless particles (or if one simply ignores any spin dependent attributes in the scattering), this theorem translates to an integral equation to determine the phase function $(\varphi(\theta))$ of the scattering amplitude $f(\theta) = \sqrt{\frac{d\sigma}{d\Omega}(\theta)}\, \exp(i\varphi(\theta))$. A solution to that integral equation not only exists but also, under particular conditions [4], it is unique. Furthermore, with one of those conditions (hereafter defined as the Martin condition) being valid, an iterative method of Newton [5] gives that solution. When conditions for uniqueness and stability of solution by an iterated fixed point method are not met, a numerical procedure has been proposed [6]. But whatever be the chosen method of solution, the cross section data $\frac{d\sigma}{d\Omega}(\theta)$ must be known at all (real) scattering angles. With actual data sets then, interpolation and extrapolation must be used.

For scattering in which spin–orbit interactions are important, the generalized flux theorem leads to coupled integral equations for two unknown phase functions [7], and while there are still conditions for uniqueness of the solution as well as of the stability of fixed point methods of solution, those conditions are now rather complex.

2 Generalized (unitarity) flux equations

For simplicity, the spinless particle case is outlined herein with the spin–$\frac{1}{2}$ particle scattering from spin 0 extensions alluded to in discussion. The differential cross section for the scattering of spinless particles is given in terms of a scattering amplitude,

$$f(x) = \frac{1}{k} A(x) e^{i\varphi(x)} \ , \tag{1}$$

where $x = \cos(\theta)$, by

$$\frac{d\sigma}{d\Omega} = |f(x)|^2 = \frac{1}{k^2} A^2(x) \ . \tag{2}$$

The magnitude and phase of the scattering amplitude may be extracted from the measured differential cross section, under the constraint that the scattering function is unitary [1] as the generalized unitarity theorem (flux conservation),

$$\mathcal{I}m[f(\theta)] = \mathcal{I}m[f(\mathbf{k_f}, \mathbf{k_i})] = \left(\frac{k}{4\pi}\right) \int f^*(\mathbf{q}, \mathbf{k_f}) f(\mathbf{q}, \mathbf{k_i}) \ d\Omega_q \ , \tag{3}$$

leads to an equation that specifies the phase in terms of the complete (0 to 180°) cross section, viz.

$$\sin\varphi(x) = \int\int \frac{A(y)A(z)\cos[\varphi(y) - \varphi(z)] \ dy \ dz}{2\pi A(x)(1 - x^2 - y^2 - z^2 + 2xyz)^{1/2}} \ . \tag{4}$$

Therein the region of integration is the interior of an ellipse. From the scattering amplitude, the scattering function is obtained by

$$S_\ell - 1 = e^{2i\delta_\ell} - 1 = ik \int_0^\pi f(\theta) \ P_\ell(\theta) \ \sin(\theta) d\theta \ , \tag{5}$$

which in turn identifies the phase shifts, δ_ℓ.

Usually, solutions of (4), or its equivalent, have been sought with iteration schemes based on the contraction mapping principle [1], [4]. That approach also defines an existence condition for a solution and for its global uniqueness as well. In application though we have found difficulties with it. The physical circumstances considered [8] did not meet the domain criteria and

the solutions found were not stable. Thus we considered a modification of the Newton iteration method.

In brief, our modified Newton method [8] considers an operator F acting on functions φ according to

$$F[\varphi] = \sin(\varphi(x)) - \int\int \frac{A(y)A(z)\cos[\varphi(y) - \varphi(z)]\, dy\, dz}{2\pi A(x)(1 - x^2 - y^2 - z^2 + 2xyz)^{1/2}} \,. \tag{6}$$

The Fréchet derivative F' of F is given by

$$\begin{aligned} F'_{\varphi}(h) = {} & \cos(\varphi(x))h(x) \\ & +2\int \left(\int H(x,y,z)\ \sin[\varphi(y) - \varphi(z)]dz \right) h(y)dy \,. \end{aligned} \tag{7}$$

Then, if one can solve the linear functional equation,

$$F(\varphi^n) + F'_{\varphi^n}(\varphi^{n+1} - \varphi^n) = 0 \,, \tag{8}$$

for $\varphi^{(n+1)}$, and if the sequence φ^n converges, its limit is a solution of (4).

The scattering amplitudes for a spin–$\frac{1}{2}$ particle elastically scattered from a spin–0 target have the form

$$f_{\tau'\tau}(\mathbf{k}', \mathbf{k}) = \chi^{\dagger}_{\tau'}\ (g(\theta) + \sigma \cdot \mathbf{n}\ h(\theta))\chi_{\tau}, \quad \mathbf{n} = \frac{\mathbf{k} \times \mathbf{k}'}{|\mathbf{k} \times \mathbf{k}'|} \,, \tag{9}$$

where χ_τ are Pauli spin functions with spin projections $\tau = \pm 1$, and $\mathbf{k}$, $\mathbf{k}'$ are the incoming and outgoing momenta of the projectile ($|\mathbf{k}| = |\mathbf{k}'| = k$). The non-spin-flip and spin-flip amplitudes, $g(\theta)$ and $h(\theta)$ respectively, are defined conventionally by the partial wave expansions,

$$\begin{aligned} g(\theta) &= \frac{1}{2ik} \sum_{\ell=0}^{\infty} [(\ell + 1)S_{\ell+} + \ell S_{\ell-} - (2l + 1)]\, P_\ell(\cos\theta) \,, \\ h(\theta) &= \frac{1}{2k} \sum_{\ell=1}^{\infty} [S_{\ell+} - S_{\ell-}]\, P^1_\ell(\cos\theta) \,. \end{aligned} \tag{10}$$

Therein $\ell\pm$ denote the values $j = \ell \pm 1/2$ and the expansions can be recast in terms of scattering phase shifts since they are given by $\delta_{\ell\pm}(k) = [1/(2i)]\ \ln(S_{\ell\pm}(k))$. It is convenient to choose spin quantization parallel to $\mathbf{n}$ as then transversity amplitudes,

$$f_{\pm,\pm}(\theta) = A_{\pm}(z)\exp(i\Phi_{\pm}) = g(\theta) \pm h(\theta), \quad f_{\mp,\pm}(\theta) = 0 \,, \tag{11}$$

have magnitude functions, $A_{\pm}(x)$, $[x = \cos(\theta)]$, that can be determined from the unpolarized differential cross section $d\sigma/d\Omega$ and the polarization $P(\theta)$ since

$$A^2_{\pm}(x) = \frac{d\sigma}{d\Omega}(1 \pm P) = (|g|^2 + |h|^2)\left(1 \pm \frac{2Re(gh^*)}{(|g|^2 + |h|^2)}\right) \,. \tag{12}$$

Then if $A_{\pm}(r)$ can be specified for all scattering angles, the unitarity condition[7] constitutes two coupled equations for the phase functions $\Phi_{\pm}(\theta)$. Martin conditions exist again but not only are they now quite complicated [7] but also they are rarely satisfied by actual data. Nevertheless the Fréchet derivative approach may be used still to give solutions.

3 Natural ambiguities of the phase functions

Without spin–orbit coupling, the natural ambiguity of a phase function is its complex conjugate, $\varphi'(\theta) = \pi - \varphi(\theta)$. That is a special case of the set possible with spin–orbit coupling as are considered in the following discussion. If the uniqueness conditions are satisfied, the phase function solution of the problem specified by the data set $(\frac{d\sigma}{d\Omega}(\theta), P(\theta))$ is $\Phi^{(1)} \equiv \{\Phi_+^{(1)}(\theta), \Phi_-^{(1)}(\theta)\}$. There is also then a solution to the 'mirrored' problem specified by the data set $(\frac{d\sigma}{d\Omega}(\theta), -P(\theta))$ and which we designate by $\tilde{\Phi}^{(1)}$.

Natural ambiguities to those solutions exist, identified by application of the complex conjugate, the Minami, and the combination of the complex conjugate and Minami transformations. The complex conjugation transform equates to changing the signs of all of the phase shifts, $\delta_{\ell\pm}$, one obtains from the phase functions $\tilde{\Phi}^{(1)}$ (and from $\Phi^{(1)}$ for the 'mirrored' problem) which are given by

$$\Phi^{(2)} = \begin{pmatrix} \Phi_+^{(2)} \\ \Phi_-^{(2)} \end{pmatrix} = \begin{pmatrix} \pi - \tilde{\Phi}_-^{(1)} \\ \pi - \tilde{\Phi}_+^{(1)} \end{pmatrix} , \tag{13}$$

and similarly for $\tilde{\Phi}^{(2)}$. The Minami transform is effected by an interchange of phase shift sets by $\delta_{\ell\pm} \Leftrightarrow \delta_{(\ell+1)\mp}$ or by specification of the new phase functions, $\Phi^{(3)}$, by

$$\Phi^{(3)} = \begin{pmatrix} \Phi_+^{(3)} \\ \Phi_-^{(3)} \end{pmatrix} = \begin{pmatrix} \tilde{\Phi}_-^{(1)} - \theta \\ \tilde{\Phi}_+^{(1)} + \theta \end{pmatrix} \tag{14}$$

and similarly for $\tilde{\Phi}^{(3)}$. A fourth possible solution results from the combination of transforms whence we find the phase functions $\Phi^{(4)}$ (and similarly $\tilde{\Phi}^{(4)}$) from

$$\Phi^{(4)} = \begin{pmatrix} \Phi_+^{(4)} \\ \Phi_-^{(4)} \end{pmatrix} = \begin{pmatrix} \pi - \Phi_+^{(1)} - \theta \\ \pi - \Phi_-^{(1)} + \theta \end{pmatrix} . \tag{15}$$

These natural ambiguities need be understood since the combination of complex conjugation and Minami transformation gives a new phase function set $\Phi_{\pm}^{(4)}$ and $\tilde{\Phi}_{\pm}^{(4)}$ for the original and the mirrored data sets respectively, and hence different sets of phase shifts to fit measured data equally well.

4 Application to nucleon–α scattering

Our interest with low energy $n - \alpha$ and $p - \alpha$ data stems from the fact that much of it lies below the first nonelastic scattering threshold (24 MeV) and for which, therefore, the physical S function is unitary. The nucleon–α scattering system below threshold is of interest also given the simplicity one assumes with the target structure. The closed s–shell configuration one favors to describe the alpha particle, encourages belief that the inherent 5–body problem can be assessed in diverse ways, ranging from its representation by effective real local and phenomenological optical model potential to treatment as a microscopic optical model interaction defined by folding an appropriate effective two–nucleon (NN) g matrices with the density matrix elements of the alpha particle.

4.1 Ignoring spin–orbit coupling

The cross–section data at various energies below threshold from neutron–α scattering have been analyzed using interpolated and extrapolated values to specify the magnitudes $A(\theta)$ at all scattering angles [6] for use in solving the phase function equations. The results for four energies are shown in Fig. 1. These scatterings of neutrons from α particles below threshold do not satisfy the Martin constraint condition. Such is only met if the underlying interaction is very weak. This is demonstrated in Fig. 2 wherein the Martin condition,

$$(1 - 0.79)^{\frac{1}{2}} \leq M(x) \leq 0.79 \tag{16}$$

where

$$M(x) = \int\int \frac{A(y)A(z)}{2\pi A(x)} [1 - x^2 - y^2 - z^2 + 2xyz]^{-\frac{1}{2}} dy\, dz\ , \tag{17}$$

for the scattering of 14.9, 16.4, and 23.7 MeV neutrons from alpha particles are shown by the solid, small dashed, and long dashed curves respectively. They all peak in the vicinity of $x = -0.3$ and at a value clearly in excess of the Martin limit of 0.79. In fact, that value is exceeded over most if not all scattering angles ($1 \geq x \geq -1$). But by using our method with Fréchet derivatives to linearize the problem, by iteration we have found convergent solutions which are displayed in Fig. 3. Therein the converged phase functions for the 14.9, 16.4, 20.0 and 23.7 MeV neutron–α cross sections are displayed by the solid, small dashed, dotted and long dashed curves respectively. From these phase functions, via Legendre integrations we find phase shifts that produce excellent fits the measured cross–section data [6].

To achieve stable results, however, it was necessary to apply the GCV [9] process to minimize fluctuation of the results between iterations; fluctuations that could occur as the complex conjugate phase function intersects with the desired solution and the numerical procedure may track from that desired solution to its complex conjugate at scattering angles near to the intersection point.

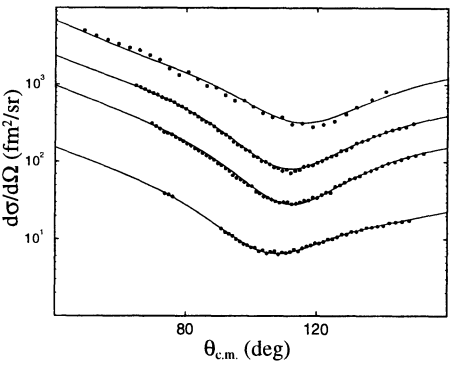

Fig. 1. The neutron–α cross sections at 14.9, 16.4, 20.0, and 23.7 MeV and the results from our unitarity analyses. The cross sections have been enhanced by factors of 30, 10, 5 and 1 respectively for visualization.

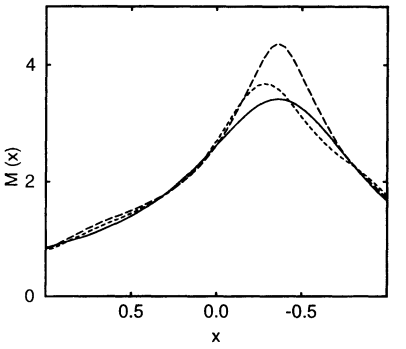

Fig. 2. The functions $M(x)$ as given by Eq. (17) for 14.9, 16.4 and 23.7 MeV neutron–α cross sections.

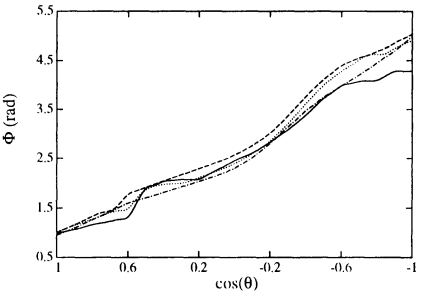

Fig. 3. The phase function solutions for neutron–α scattering derived using the cross sections in Fig. 1 and ignoring spin–orbit coupling.

4.2 Including spin–orbit coupling – 1 MeV case

For convenience, to specify the data at all scattering angles we have used the phase shifts for 1 MeV neutron–α scattering as given by the optical model analysis that was made by Satchler *et al.* [10]. Not only does this give a good fit to the actual measured data but also provides us with the 'exact' phase functions against which we can compare the results of our unitarity based analysis.

Our first (of two) guesses for the initial phase functions was to assume the linear form (in $x = \cos(\theta)$) and the Fréchet solutions we identify as $\Phi^{(1)}$. From those phase functions, by Legendre integration of the associated complex scattering amplitude, we obtained (recalculated) phase shifts that agree extremely well (to 1 part per thousand) for the important low ℓ partial waves of the optical model calculation values of Satchler *et al.*[10]. The initial phase functions and the final results are displayed in Fig. 4 by the dashed and the solid curves respectively. The changes wrought by the iterative method of solution are significant as seen by the variation in cross section and polarization for this scattering given in Fig. 5. Therein the cross section and polarization shown by the dashed curves are the result of using the phase shifts extracted from the initial phase function guess and used in the partial wave summations, while those displayed by the solid curves are the results found using the final (4^{th}) iterate. The latter coincide very precisely with the calculated results of Satchler *et al.* [10]; the input to our calculations.

The second starting phase guess functions were those given by the complex conjugation and Minami transformation of the initial guesses above. The solution for the phase functions are defined as $\Phi_{\pm}^{(4)}$. The phase shifts then extracted by Legendre integration of the resultant scattering amplitudes also compare accurately (for low ℓ) with the complex conjugated, Minami transformed set of Satchler *et al.*[10]. In Fig. 6, the + and − phase functions are shown in the top and bottom segments respectively. The initial guess variations are shown by the dashed lines while the results of our calculations are shown by the solid curves. The symmetry lines between the two solution sets are shown by the small dashed curves. Those symmetry lines also pertain to the two other possible solutions of the coupled nonlinear equations for the phase functions. In this case, the solutions $\Phi_{+}^{(1)}$ and $\Phi_{+}^{(4)}$ intersect near 25° for the scattering angle at which point numerical problems with ambiguity of solution could result. With *GCV* smoothing between iterations[9], the process converged to the 'exact' results. There is no such concern with the Φ_{-} phase solutions though as the trial guesses and final results for $\Phi_{-}^{(1)}$ and $\Phi_{-}^{(4)}$ do not cross.

Two more phase functions for the scattering amplitudes of the data set $\{\frac{d\sigma}{d\Omega}(\theta), P(\theta)\}$ are associated with the phase functions $\Phi^{(2)}$ and $\Phi^{(3)}$, and which are given by the complex conjugate and the Minami transform of the solution with the mirror problem data set $\{\frac{d\sigma}{d\Omega}(\theta), -P(\theta)\}$, i.e. $\tilde{\Phi}^{(1)}$, respectively. The mirror problem was solved using the same linear initial conditions.

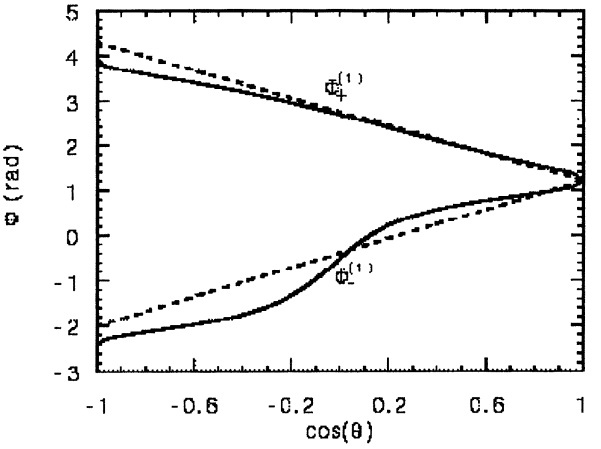

Fig. 4. The initial and final, $\Phi^{(1)}$, phase functions for 1 MeV neutron–α scattering and based upon the optical potential 'data' of Satchler *et al.* [10]. The initial guess functions are displayed by the dashed curves while the solid curves portray the results of our calculations.

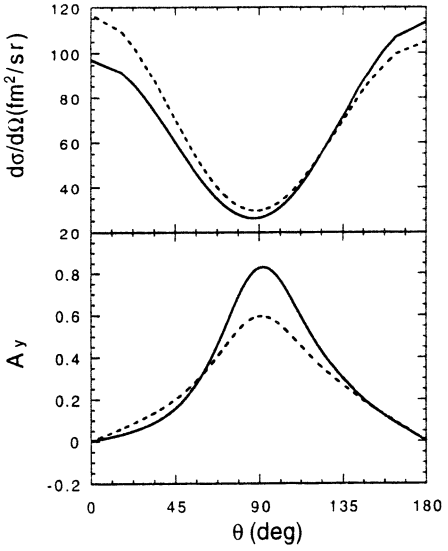

Fig. 5. The differential cross sections (top) and polarizations (bottom) for 1 MeV $n - \alpha$ scattering as calculated from the phase shifts specified by using the initial guess (straight line) phase function (dashed curves) and from the phase shifts found using the phase function solution of the generalized flux equation (solid curves).

The result is quite different from the phase function found when either the complex conjugation or the Minami transform is made upon the Satchler phase shifts. In those cases the phase functions we identify as $\tilde{\Phi}^{(2)}$ and $\tilde{\Phi}^{(3)}$ respectively. Then by using these phase functions for the 'data' set, a quite distinctive set of phase shifts result, which when used in the appropriate partial wave summations give equivalent fits to the cross section and polarization of the optical potential calculation. The inversion potentials associated with each set will be quite different then as well.

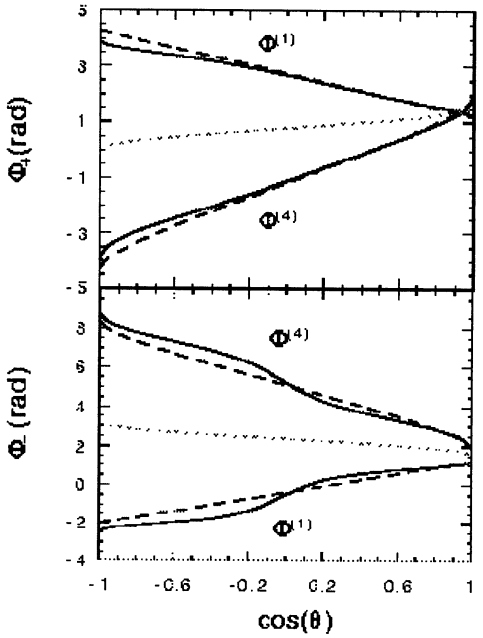

Fig. 6. The (+) (top) and (−) (bottom) phase solutions of $\Phi^{(1)}$ and $\Phi^{(4)}$ as labeled. The starting (guess) phase functions are portrayed by the dashed lines while the final solutions are shown by the solid curves.

References

[1] R. G. Newton, *Scattering of Waves and Particles*, (Springer, 1982); K. Chadan and P. C. Sabatier. *Inverse Problems in Quantum Scattering Theory* 2^{nd} Edition (Berlin, Springer, 1989).

[2] K.-E. May, M. Münchow, and W. Scheid, Phys. Lett. **141B**, 1 (1984); B. Apagyi, A. Schmidt, W. Scheid, and H. Voit, Phys. Rev. C **49**, 2608 (1994).

[3] K. Amos and M. T. Bennett, submission to these lecture notes; and references cited therein.

[4] A. Martin, Nuovo Cim. **A59**, 131 (1969).

[5] R. G. Newton, J. Math. Phys. **9**, 2050 (1968).

[6] N. Alexander, K. Amos, B. Apagyi, and D. R. Lun, Phys. Rev. C **53**, 88 (1996); H. Huber, D. R. Lun, L. J. Allen, and K. Amos, Phys. Rev. A **54**, 1363 (1996).

[7] R. Alvarez–Estrada and B. Carreras, Nucl. Phys. **B54**, 237 (1973); R. F. Alvarez–Estrada, B. Carreras, and G. Mahaux, Nucl. Phys. **B88**, 289 (1975).

[8] D. R. Lun, L.J.Allen, and K. Amos, Phys. Rev. A **50**, 4000 (1994).

[9] P. Craven and G. Wahba, Numerische Mathematik **31**, 377 (1979).

[10] G. R. Satchler, L. W. Owen, A. J. Elwyn, G. L. Morgan, and R. L. Watson, Nucl. Phys. **A112**, 1 (1968).

Potential Reversal and Reflectionless Impurities in Periodic Structures

V. M. Chabanov[1], B. N. Zakhariev[1,2], S. A. Sofianos[2], M. Braun[2]

[1] Laboratory of Theoretical Physics, Joint Institute for Nuclear Research Dubna, 141980, Russia

[2] Department of Physics, University of South Africa, P.O. Box 392, Pretoria, 0001, South Africa

Abstract. We demonstrate that the application of the supersymmetric (SUSY) transformation to a periodic potential in one dimension, which creates a bound state below the lowest allowed band, results in the unexpected phenomenon of potential reversal. This does neither alter other characteristics of the spectrum nor does it result in a reflection of Bloch waves.

1 Introduction

The reflectionless potentials of the soliton type are widely known (Lamb 1980). One way to create them is by inserting a bound state in the spectrum with the aid of the inverse scattering formalism (Chadan and Sabatier 1977, Zakhariev and Suzko 1990) or using supersymmetric (SUSY) transformations (Witten 1981, Andrianov et al. 1984, Sukumar 1985, Baye 1987, Andrianov et al. 1993)

The inverse problem has been considered in the past by various authors (Levitan 1984, Newton 1985, Firsova 1985, Marchenko (1977), Firsova 1987, Roberts 1990) in order to study impurities in periodic potentials. Zakhariev and Pashnev (1994) shown that adding a soliton–like potential in these systems will not necessarily result in transparency, as the boundaries between allowed and forbidden bands will be distorted by bumps in the region where the potential is acting. These bumps act as effective potential barriers that give strong reflection.

For a periodic potential there exist bands in the spectrum that allow the propagation of Bloch waves. One can define analogues of the exponential and sinusoidal solutions for the free particles. From their linear combinations one can construct general solutions on any finite segment of the system. Such solutions, for different periodic potentials on distinct intervals, can be smoothly matched with the solutions for an arbitrary potential (Zakhariev 1992). It is natural that a partial reflection of moving Bloch waves at those matching points will occur. It is possible that bound states under each allowed band could be generated by an arbitrarily small attractive potential perturbation, such as it is the case of free motion on the whole axis (Zakhariev Pashnev 1994). Similarly, we expect that a bound state could be generated over each

allowed band by an arbitrarily small repulsive addition to the potential and thus creating 'overturned potential wells' pressed into forbidden bands.

In this work we want to create a bound state in the lower forbidden band of a periodic potential while keeping the band structure unaltered. For this we shall employ two types of periodic potentials the first being the so–called Dirac comb which is a sum of δ–barriers,

$$V_0(x) = \sum_{n=-\infty}^{\infty} v_0 \delta(x - na)\,, \tag{1}$$

and the second of the form

$$V_0(x) = v_n \cos(\pi x)^{2n}, \tag{2}$$

where n is an integer and v_n is chosen to normalize the potential in the range $[-0.5, +0.5]$. Thus the limit of this potential for $n \to \infty$ is the Dirac comb with $v_0 = 1$, We shall study the behaviour of these one–dimensional potentials upon application of the SUSY transformation.

2 Formalism

With the aid of the SUSY approach a bound state can be inserted in the spectrum which conserves the asymptotic behaviour of Bloch waves. The SUSY method has been described elsewhere (Witten 1981, Andrianov et al. 1984, Sukumar 1985, Baye 1987, Andrianov et al. 1993) and thus we shall only briefly recall it here for convenience and to demonstrate our points. In this method the initial hamiltonian H is factorized

$$H = A^+ A^- + \epsilon = -\frac{d^2}{dx^2} + V_0(x)\,, \tag{3}$$

where ϵ is the so called factorization energy. In this expression, A^- is a first order differential operator,

$$A^- = -\frac{d}{dx} + W(x), \tag{4}$$

A^+ is its Hermitian conjugate, and $W(x)$ can be obtained by solving the equation

$$A^- \psi^- = \left[-\frac{d}{dx} + W(x)\right] \psi^- = 0\,. \tag{5}$$

Here ψ^- is the solution of the Schrödinger equation for the hamiltonian H at the energy ϵ with

$$A^- = -\frac{d}{dx} + \frac{d}{dx} \ln \psi^-. \tag{6}$$

The solutions for the supersymmetric partner $H_1 \equiv A^- A^+ + \epsilon$ can be found by employing a Darboux transformation (Schnizer and Leeb (1990)),

$$H_1 = -\frac{d^2}{dx^2} + V_0(x) - 2\frac{d^2}{dx^2}\ln\psi^- \,. \tag{7}$$

Indeed, let ψ_E^- be an eigenfunction of H at the energy E. Then $\psi_E^+ \equiv A^-\psi_E^-$ is the solution of the Schrödinger equation with H_1 at the same energy

$$H_1(A^-\psi_E^-) = A^-A^+(A^-\psi_E^-) + \epsilon(A^-\psi_E^-) = A^-H\psi_E^- = EA^-\psi_E^- \,. \tag{8}$$

At the factorization energy ϵ the solution ψ^+ can be obtained by solving the first order differential equation

$$A^+\psi^+ = \left[\frac{d}{dx} + \frac{d}{dx}\ln\psi^-\right]\psi^+ = 0 \tag{9}$$

which is equivalent to

$$\psi^+ = \frac{1}{\psi^-} \,. \tag{10}$$

Let the factorization energy $\epsilon < E_1$, where E_1 denotes the lower border of the first allowed band of H. Choosing ψ^- to have no knots and to diverge asymptotically, then ψ^+, according to (10), does not possess knots and vanishes as $|x| \to \infty$. Furthermore, it is easy to see that for all energies $E > E_1$ the solution ψ_E^+ behaves at large x as a freely propagating Bloch–wave i.e. without reflection. In other words the SUSY transformation $H \to H_1$ adds a ground state to the spectrum of the periodic potential without affecting, except from a phase change, the propagation of Bloch–waves.

From the expression for the transformed potential one can see the reversal of the potential,

$$\begin{aligned} V_1(x) &= V_0(x) - 2\frac{d^2}{dx^2}\ln\psi^-(x) \\ &= -V_0(x) + 2\epsilon + 2\left\{\frac{[\psi^-(x)]'}{\psi^-(x)}\right\}^2 , \end{aligned} \tag{11}$$

where we have used the expression for $[\psi^-(x)]''$ obtained from the Schrödinger equation. We notice that V_0 finally appears with a minus sign. In our case V_0 is the comb of the singular δ–functions and therefore the remaining terms, finite at all x, are not sufficient to compensate for the reversal of the δ–peaks,

$$V_1(x) = -\sum_{n=-\infty}^{\infty} v_0\delta(x-na) + 2\epsilon + 2\left\{\frac{[\psi^-(x)]'}{\psi^-(x)}\right\}^2 . \tag{12}$$

It should be emphasized that Eq. (11) is valid also for an arbitrary one–dimensional potential. However, the sign change of V_0 could be hidden by the additional term, thus our model reveals the peculiar reversal effect resulting from the addition of a bound state to the spectrum.

It is noted that the SUSY transformation keeps unaltered the absolute value of the reflection and transmission coefficients. Indeed, let $\psi_E^-(x)$ be a

solution of Schrödinger equation at energy E obeying the asymptotic condition

$$\psi_E^-(x) \sim \exp(-ikx) + r(k)\exp(ikx), \qquad x \to \infty . \tag{13}$$

From this one can easily obtain the asymptotic expression for the solution coresponding to the transformed potential

$$\psi_E^+(x) = -[\psi_E^-(x)]' + [\ln \psi^-(x)]'\psi_E^-(x) , \tag{14}$$

where

$$\psi^-(x) \sim \exp(\kappa x), \qquad x \to \infty, \quad \kappa = |\epsilon|^{1/2} , \tag{15}$$

and

$$\psi_E^+(x) = \exp(-ikx) + \frac{\kappa - ik}{\kappa + ik} r(k)\exp(ikx), \qquad x \to \infty \tag{16}$$

where we normalized $\psi_E^+(x)$ to a unit amplitude of the wave incident from the right.

3 Results

The above formalism has been applied to the periodic potentials described by Eqs. (1) and (2) and the results obtained are given in Fig. 1 and Fig. 2 respectively.

In Fig. 1 a) the effects of SUSY transformation that creates a bound state in the lower forbidden band for the Dirac comb consisting of potential–barriers (spikes) are shown. The potential strength was taken to be $v_0 = 1$ and the bound state energy was chosen to be $\mathcal{E} = -1$ in dimensionless units. It is seen that the 'δ–barriers' turn into 'δ–wells'. The cusps in the potential are due to the derivative terms of Eq. (12). The well between 0 and 1 creates a bound state at the given energy. The corresponding bound state wave function is also shown. Such a reversal of the δ–barriers by creation of a bound state conserves the reflection characteristics of the system.

The dependence of such transformations on the sign of the potential barrier v_0 is shown in Fig. 1 b). The strength in this case is chosen to be $v_0 = -0.5$ while the bound state energy is $\mathcal{E} = -1$. The potential is reversed and the bound state wave function is spread over an extended region in contrast with the previous case where the wave function is rather localized close to the binding well.

In Fig. 2 we consider periodic potentials of the form (2) with different values of n. The strength v_n is chosen to normalize the potential in the range $[-0.5, +0.5]$. In Fig. 2 a) the transformation of the initial potential with $n = 1$ and with $\mathcal{E} = -1$ is considered. It is seen that the reversal in the potential results in this case in a phase shift of the periodic potential. In Fig. 2 b) we present the results with $n = 8$. The increase in n results in a potential repulsion concentrated at specific points. The SUSY transformation results in a reversal of these repulsive pulses. In Fig. 2 c) n is chosen to be $n = 32$ and the repulsive pulses become narrower resembling the spikes of the Dirac comb but with limited strength.

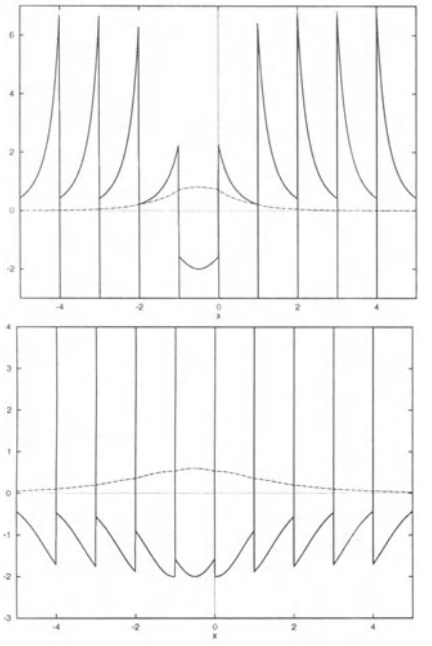

Fig. 1. The modified potentials $V_1(x)$ (——) obtained by inserting a bound state at $\mathcal{E} = -1$ in the lower forbidden band of a Dirac comb and by applying a single SUSY transform: (a) repulsive δ–wells with $v_0 = +1$ (b) attractive δ–wells with $v_0 = -0.5$. The bound state wave functions are indicated by $- \cdot - \cdot -$.

4 Conclusion

The use of SUSY transformations in one–dimensional periodic structures could result in a potential reversal which is a rather general phenomenon. This has been explicitly demonstrated by using two examples, namely, the Dirac comb potential and periodic potentials constructed from even powers of $\cos(\pi x)$ inserting a bound state below the lowest forbidden band of periodic structures without altering the reflection characteristics of the system. So, impurities introduced into a periodic potential which, do not generate reflection of the Bloch waves can have the drastic changes in the potential.

Acknowledgements

Two of the authors (B.N.Z and V.M.C) gratefully acknowledge financial support from the Russian Funds for Fundamental Research (RFFR), the Soros Fund. B.N.Z also aknowledge support from the Foundation for Research Development (FRD) and the University of South Africa.

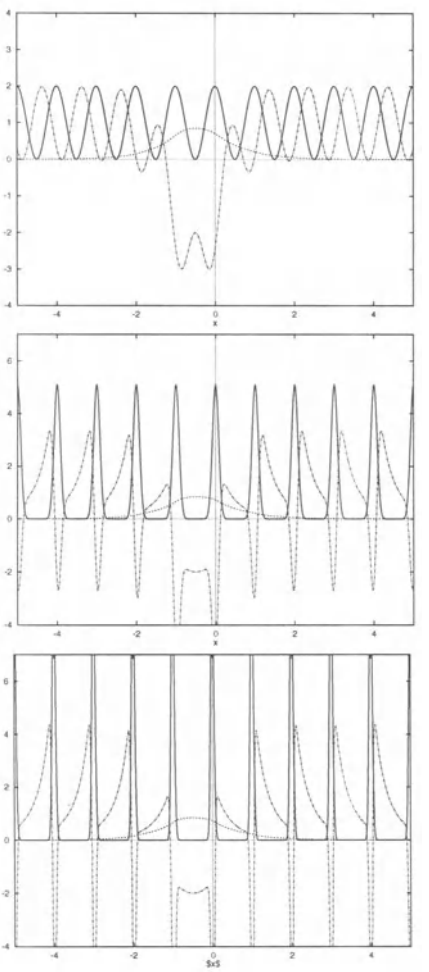

Fig. 2. The initial (——) and modified (– · – · –) potentials $V_0(x)$ and $V_1(x)$ obtained by inserting a bound state at $\mathcal{E} = -1$ in the lower forbidden band of a periodic potential of the form $V(x) = v_n \cos(\pi x)^{2n}$, v_n chosen to make $\int_{-0.5}^{0.5} V(x)dx = 1$, for a) $n = 1$, b) $n = 8$, and c) $n = 32$. The corresponding bound state wave functions are indicated by the broken line (– – –).

References

Andrianov A. A., Borisov N. V. and Ioffe M. V. (1984), *Phys. Lett.* **105A**, 19.
Andrianov A. A., Ioffe M. V. and Spiridonov V. P. (1993), *Phys. Lett.* **A 174**, 273.
Baye D. (1987), *Phys. Rev. Lett.* **58**, 2738.
Chadan K. and Sabatier P. C. (1977), *Inverse Problems in Quantum Scattering Theory*, Springer, New York.
Firsova N. E. (1985), *Theor. Math. Phys.* **62**, 130.

Firsova N. E. (1987), *Math. Sborn.* **58**, 351.
Lamb G. L. Jr (1980), *Elements odf soliton theory*, John Willey & Sons, New York.
Leeb H. (1994), in *Quantum Inversion Theory and Applications*, Vol. 427 of *Lecture Notes in Physics*, ed. H.V. von Geramb, pp. 241-251, Springer-Verlag, Berlin, 1994.
Levitan B. M. (1984), *Sturm-Liouville Inverse Problems*, Nauka, Moscow.
Marchenko V. A. (1986), *Sturm–Liuville Operators and Applications*, Birkhauser, Basel.
Newton R. G. (1985), *J. Math. Phys.* **26**, 311.
Roberts T. M. (1990), *Inverse Probl.* **6**, 797.
Sukumar C. V. (1985), *J. Phys.* A **18**, 2917; *J. Phys.* A **18**, 2937.
Witten E. (1981), *Nucl. Phys.* **B188**, 513.
Zakhariev B. N. and Suzko A. A. (1990) *Direct and Inverse Problems*, Springer, New York.
Zakhariev B. N. (1992), *Sov. J. Part. & Nucl.* **23**, 603.
Zakhariev B. N. and Pashnev A. I. (1994), *Commun. JINR P4-94-496*, Dubna.

The Method of the Weakly Conjugate Operator

Anne Boutet de Monvel[1] and Marius Mantoiu[2]

[1] Institut de Mathématiques de Jussieu, CNRS UMR 9994,
Laboratoire de Physique mathématique et Géométrie, case 7012,
Université Paris 7 Denis Diderot, 2 place Jussieu, F-75251 Paris Cedex 05
[2] Institut mathématique de l'académie roumaine, Bucarest, Roumanie

Abstract. We present an improvement of the Kato-Putnam theorem. We apply this to the spectral theory of some classes of generalized differential operators.

1 Introduction

For the spectral analysis of self-adjoint operators on a Hilbert space, methods relying on the positivity of a commutator are some of the strongest tools. When trying to show that an operator H has no singular spectrum (in some region of the real axis), one is led to look for a second operator A such that the commutator is positive in a suitable sense. There are two main versions of this strategy, which we review briefly.

First, in the Kato-Putnam approach (Kato 1968, Putnam 1967), B has to be positive and injective (this is a rather mild positivity assumption). On the other hand, A has to be H-bounded. As it is well-known, this limits drastically the range of applications. Another shortcoming is the globality: one gets purely absolutely continuous spectrum on the whole real axis, hence operators which also have some singular spectrum are out of reach.

A partial improvement is the second approach, due to Mourre (Mourre 1981, Amrein, Boutet de Monvel, Georgescu 1996). Here regularity assumptions are not longer made on A, but on the commutator $B \equiv \mathrm{i}[H, A]$ (it is sufficient that it be H-bounded). This will work in more realistic situations, because cancellations usually appear when commuting. There is also a condition on the second commutator $[B, A]$, which we will not discuss here. Let us now state the positivity assumption. A *strict Mourre estimate* must hold:

$$E(J)\mathrm{i}[H, A]E(J) \geq aE(J) \tag{1}$$

where E is the spectral measure of H, a a strictly positive constant and J a Borel subset of $\mathbb{R}$. The main consequence is that the spectrum of H in J is purely absolutely continuous.

A great advantage is the fact that (1) is local on the spectrum of H. A second one is the following extension: consider the weaker form of (1) where a compact operator is added in the right-hand side (this is the full Mourre

estimate, much easier to check in concrete cases). The only new fact in the conclusion is the possible appearance in J of some discrete spectrum. The main difficulty in this version is to get the strict positivity. Anyway, this does not contain the Kato-Putnam theory.

Our intention is to present a commutator criterion which is in somehow intermediate between those described above. We call it *the method of the weakly conjugate operator* in agreement to the fact that Mourre's approach is sometimes called the method of the conjugate operator. The term "weakly" refers to the positivity requirement. This point of view, we are closer to the Kato-Putnam theory, on which it improves. Unfortunately, our analysis is also global. As we explained, the main point is that we impose regularity on "the weakly conjugate operator" A (which may be quite singular in applications) only in an indirect way, making assumptions on the commutators $[H, A]$ and $[[H, A], A]$.

The abstract results are exposed in the second chapter. A more primitive version is to be found in (Boutet de Monvel, Kazantseva, Mantoiu 1996), together with applications to Schrödinger operators (which can be recovered as very special cases of the chapters 3 and 4). In (Boutet de Monvel, Kazantseva, Mantoiu 1996) a technical point caused some problems: We had to impose that $\mathrm{i}[H, A]$ be H-bounded in operator sense, and this was quite disagreeable in applications, where it is more natural to consider boundedness in form-sense; this was almost catastrophic for second-order elliptic operators. In order to remedy this, we are obliged to adopt the strategy indicated in (Boutet de Monvel, Georgescu 1992). Namely, in the first stage (Theorem 2.1) we deal with the case of a bounded operator R. The case of an unbounded operator is dealt with by transferring informations between the operator we study, H and its resolvent $R = (\lambda_0 - H)^{-1}$, which must be bounded. This is how we get Theorem 2.2 which only works if λ_0 is real, so we have to impose that H has a spectral gap. This is verified in most of the applications we have in view. The proof of Theorem 2.1 is another version of the so called "method of differential inequalities", also used by Mourre. In fact, in contrast with the approach in (Boutet de Monvel, Kazantseva, Mantoiu 1996), we adopt the more refined techniques developed in (Boutet de Monvel, Georgescu, Mantoiu 1993), (Boutet de Monvel, Georgescu 1992) (see also (Amrein, Boutet de Monvel, Georgescu 1996)), in order to allow some improvements in our main estimates. We also give a result (Proposition 2.1) on the generality of the method, which is a variant of Proposition 5.2 from (Boutet de Monvel, Georgescu 1992).

We may apply this method to quite anisotropic and this is its main merit. We begin with operators of the form $H = H_0 + V$ in $\mathcal{H} = L^2(\mathbb{R}^N)$, where V is a multiplication operator and H_0 the convolution by a suitable symbol h.

We allow large classes of V's which are not H_0-compact. One of the possible behaviors for V is to have radial limits (depending on the direction) with a certain rate of convergence, depending on h. But we are not limited

to this (quite anisotropic) situation. In the forth and fifth chapters we treat second-order, elliptic operators. The interest of the results is two-fold. First, the coefficients of the main term may diverge or vanish both locally and at infinity. Even in the uniformly elliptic case, they are allowed not to have radial limits. Second, the perturbations may also behave quite anisotropically. The Schrödinger operator $H = \Delta + V$ (Δ = the laplacian) is a particular case, for which we generalize the results obtained in (Boutet de Monvel, Kazantseva, Mantoiu 1996).

2 The abstract results

In this section we shall prove some abstract assertions which, in applications, go much beyond the Kato-Putnam theory. It is convenient to start with the case of a bounded operator (we shall explain why in detail later on).

Let R be a bounded, self-adjoint operator in a complex, separable Hilbert space $\mathcal{H}$, with scalar product $\langle \cdot, \cdot \rangle$ and norm $|| \cdot ||$. Let also $\{\mathcal{W}(t) \mid t \in \mathbb{R}\}$ be a strongly continuous unitary representation of $(\mathbb{R}, +)$ into $\mathcal{H}$, with infinitesimal generator A. We denote by $D(A)$ the domain of A equipped with its graph-norm. Setting $\mathcal{W}(t)T = W(-t)TW(t)$, for all $T \in B(\mathcal{H})$ and $t \in \mathbb{R}$, one gets a representation of $(\mathbb{R}, +)$ by automorphisms of the C^*-algebra $B(\mathcal{H})$. In general this is not C_0-group of $B(\mathcal{H})$, because the map $t \mapsto \mathcal{W}(t)T \in B(\mathcal{H})$ is only strongly continuous. We shall give a suitable meaning to the commutator $[R, A]$.

Definition 2.1 We write $R \in C^1(A; \mathcal{H})$ if one of the following equivalent conditions is fulfilled:

(i) The map $\mathbb{R} \ni t \mapsto \mathcal{W}(t)R \in B(\mathcal{H})$ is strongly C^1.

(ii) The sesquilinear form

$$D(A) \times D(A) \ni (f, g) \mapsto \mathrm{i}\langle f,\, RAg\rangle - \mathrm{i}\langle Af,\, Rg\rangle \in \mathbb{C}$$

is continuous when on $D(A)$ we consider the topology of $\mathcal{H}$.

Under the above circumstances, the strong derivative $\frac{\mathrm{d}}{\mathrm{d}t}|_{t=0}\mathcal{W}(t)R$ will be denoted by S. It is a self-adjoint, bounded operator in $\mathcal{H}$, associated by the Riesz lemma to the extension to $\mathcal{H} \times \mathcal{H}$ of the form introduced in (ii), so we will sometimes writes suggestively (but somewhat informally) $S = \mathrm{i}\,[R, A]$.

Definition 2.2 A is *weakly conjugate* to R if $R \in C^1(A; \mathcal{H})$ and $S > 0$.

By $S > 0$ we mean that S is positive and injective or, equivalently, that $\langle f, Sf\rangle > 0$ for all $f \in \mathcal{H} \setminus \{0\}$. This is also the positivity assumption used by Kato and Putnam. But now A is allowed to be unbounded.

The possible lack of surjectivity of S will be compensated by the introduction of two extra spaces, which we use in the proof of Theorem 2.1.

Definition 2.3 (a) $\mathcal{S}$ denotes the completion of $\mathcal{H}$ for the norm $||f||_{\mathcal{S}} \equiv \langle f, Sf\rangle^{1/2}$,

(b) $\mathcal{S}^*$ is the completion of $S\mathcal{H}$ in the norm $||g||_{\mathcal{S}^*} \equiv \langle g, S^{-1}g\rangle$.

It is easy to check that $\mathcal{S}^* \hookrightarrow \mathcal{H} \hookrightarrow \mathcal{S}$, where $\mathcal{Y} \hookrightarrow \mathcal{X}$ means that $(\mathcal{X}, \mathcal{Y})$ is a *Friedrichs couple*, i.e. that $\mathcal{X}$ and $\mathcal{Y}$ are Hilbert spaces and that $\mathcal{Y}$ is embedded continuously and densely into $\mathcal{X}$. The second embedding is obtained by duality, identifying $\mathcal{H}$ with its adjoint $\mathcal{H}^*$ (the topological anti-dual). It is also easy to see that $\mathcal{S}$ and $\mathcal{S}^*$ stay in duality with respect to the scalar product of $\mathcal{H}$; each of them will be identified to the other's adjoint. Obviously, $S \in B(\mathcal{H})$ extends to an unitary operator: $\mathcal{S} \to \mathcal{S}^*$.

There is one more condition to impose. Let us make the assumption that W is a *C_0-group in the Friedrichs couple* $(\mathcal{H}, \mathcal{S}^*)$, i.e. all the operators $W(t)(t \in \mathbb{R})$ leave $\mathcal{S}^*$ invariant. Then one gets a C_0-group in $\mathcal{S}^*$ by restriction and, afterwards, a C_0-group in $\mathcal{S}$ by duality, setting $W_{\mathcal{S}}(t) = (W(-t)\mid_{\mathcal{S}^*})^*$. For simplicity, we denote them all by the same letter W. Their infinitesimal generators will also be all denoted by A. But it is convenient to distinguish between their domains, written $D(A; \mathcal{K})$, where $\mathcal{K} = \mathcal{H}$, $\mathcal{S}$ or $\mathcal{S}^*$. With a suitable interpretation, $\mathcal{W}(t)T = W(-t)TW(t)$ is an element of $B(\mathcal{S}, \mathcal{S}^*)$ for any $T \in B(\mathcal{S}, \mathcal{S}^*)$ and $t \in \mathbb{R}$. Then $\{\mathcal{W}(t) \mid t \in \mathbb{R}\}$ is a representation of $(\mathbb{R}, +)$ by $*$-automorphisms of the $*$-Banach space $B(\mathcal{S}, \mathcal{S}^*)$. We shall work under the hypothesis $S \in C^1(A; \mathcal{S}, \mathcal{S}^*)$ which, in analogy with Definition 2.1, means equivalently

(i) either that the application $\mathbb{R} \ni t \mapsto \mathcal{W}(t)S \in B(\mathcal{S}, \mathcal{S}^*)$ is strongly C^1

(ii) or that the sesquilinear form $(f, g) \mapsto i\langle f, SAg\rangle - i\langle Af, Sg\rangle$ is continuous when on $D(A; \mathcal{S})$ one considers the norm-topology of $\mathcal{S}$.

This gives meaning to the second-order commutator

$$\mathrm{i}[S, A] = \mathrm{i}[\mathrm{i}[R, A], A] \in B(\mathcal{S}, \mathcal{S}^*) \ ,$$

either as the strong derivative at $t = 0$ in (i) or as the symmetric operator assigned to the extension to $\mathcal{S} \times \mathcal{S}$ of the sesquilinear form in (ii).

The relevant information we shall get for R is some uniform estimate on its resolvent. This will be expressed by means of some Banach spaces which we describe now. Recall that $\mathcal{C} \equiv D(A; \mathcal{S}^*)$ is endowed with a Hilbert structure by the graph-norm:

$$||g||_{\mathcal{C}} \equiv \left(||g||^2_{\mathcal{S}^*} + ||Ag||^2_{\mathcal{S}^*}\right)^{1/2}.$$

Then $(\mathcal{S}^*, \mathcal{C})$ is a Friedrichs couple. We assign to it a certain real interpolation space. For the significant facts about real interpolation we refer to (Triebel 1978). See also (Amrein, Boutet de Monvel, Georgescu 1996) and (Boutet de Monvel, Georgescu, Mantoiu 1993), where self-contained treatments are given, as well as applications to a refined form of the Mourre theory.

Definition 2.4 We set

$$\mathcal{E} \equiv (\mathcal{S}^*, \mathcal{C})_{\frac{1}{2},1} = \left\{ g \in \mathcal{S}^* \;\middle|\; \|g\|_{\mathcal{E}} \equiv \int_0^1 \frac{\mathrm{d}t}{t^{3/2}} \|W(t)g - g\|_{\mathcal{S}^*} < \infty \right\} .$$

In order to give some insight, let us also consider the well-known complex interpolation spaces $(\mathcal{S}^*, \mathcal{C})_\theta$, with $\theta \in [0,1]$. Then, one has the following continuous, dense embeddings ($0 < \theta_2 < \frac{1}{2} \leq \theta_1 < 1$):

$$\mathcal{C} = (\mathcal{S}^*, \mathcal{C})_1 \hookrightarrow (\mathcal{S}^*, \mathcal{C})_{\theta_1} \hookrightarrow \mathcal{E} \hookrightarrow (\mathcal{S}^*, \mathcal{C})_{\theta_2} \hookrightarrow \mathcal{S}^* = (\mathcal{S}^*, \mathcal{C})_0 .$$

Hence, $\mathcal{E}$ is slightly smaller than $(\mathcal{S}^*, \mathcal{C})_{\frac{1}{2}}$. For further use, it is convenient to give a description of the adjoint of $\mathcal{E}$. Let us set

$$(\mathcal{C}^*, \mathcal{S})_{\frac{1}{2},\infty} = \left\{ f \in \mathcal{C}^* \;\middle|\; \|f\|_{\mathcal{E}^*} = \sup_{t \in (0,1)} \left[\frac{1}{\sqrt{t}} \|W(t)f - f\|_{\mathcal{C}}^* \right] < \infty \right\} .$$

Then $(\mathcal{C}^*, \mathcal{S})_{\frac{1}{2},\infty}$ may be identified to the adjoint of $\mathcal{E}$ (and it will be denoted by $\mathcal{E}^*$). Set $(\mathcal{E}^*)^\circ$ for the closure of $\mathcal{S}$ in the Banach space $\mathcal{E}^*$. Then $(\mathcal{E}^*)^\circ$ is a closed subspace of $\mathcal{E}^*$. One has $((\mathcal{E}^*)^\circ)^* = \mathcal{E}$ and the following continuous, dense embeddings are true for $0 < \theta_2 \leq \frac{1}{2} < \theta_1 < \infty$:

$$\mathcal{S} = (\mathcal{C}^*, \mathcal{S})_1 \hookrightarrow (\mathcal{C}^*, \mathcal{S})_{\theta_1} \hookrightarrow (\mathcal{E}^*)^\circ \hookrightarrow (\mathcal{C}^*, \mathcal{S})_{\theta_2} \hookrightarrow \mathcal{C}^* = (\mathcal{C}^*, \mathcal{S})_0 .$$

Theorem 2.1 *Assume that A is weakly conjugate to R and that $S = \mathrm{i}[R, A] \in C^1(A; \mathcal{S}, \mathcal{S}^*)$. There exists a constant C such that, for all $\lambda \in \mathbb{R}$, $\mu > 0$ and $f \in \mathcal{E}$:*

$$|\langle f, (R - \lambda \mp \mathrm{i}\mu)^{-1} f \rangle| \leq C \|f\|_{\mathcal{E}}^2 . \tag{2}$$

Proof.

(i) For any $f \in \mathcal{H}$, $\lambda \in \mathbb{R}$, $\mu > 0$ and $\varepsilon > 0$ one has the identities

$$\mp \mathrm{Im}\langle f, (R - \lambda \mp \mathrm{i}\mu \mp \mathrm{i}\varepsilon S) f \rangle = \mu \|f\|^2 + \varepsilon \|f\|_{\mathcal{S}}^2,$$

which give

$$\|(R - \lambda \mp \mathrm{i}\mu \mp \mathrm{i}\varepsilon S) f\| \geq \mu \|f\| \tag{3}$$

and

$$\|f\|_{\mathcal{S}}^2 \leq \frac{1}{\varepsilon} \|\langle f, (R - \lambda \mp \mathrm{i}\mu \mp \mathrm{i}\varepsilon S) f \rangle\| . \tag{4}$$

From (3) and from $(R - \lambda \mp \mathrm{i}\mu \mp \mathrm{i}\varepsilon S)^* = R - \lambda \pm \mathrm{i}\mu \pm \mathrm{i}\varepsilon S$ it follows that $R - \lambda \mp \mathrm{i}\mu \mp \mathrm{i}\varepsilon S : \mathcal{H} \to \mathcal{H}$ are linear homeomorphisms. Let us set

$$G_\varepsilon^\pm \equiv G_\varepsilon^\pm(\lambda, \mu) = (R - \lambda \mp \mathrm{i}\mu \mp \mathrm{i}\varepsilon S)^{-1} .$$

We immediately get from (3) and (4) the inequalities

$$||G_\varepsilon^\pm|| \leq \frac{1}{\mu} \tag{5}$$

$$||G_\varepsilon^\pm g||_{\mathcal{S}} \leq \frac{1}{\sqrt{\varepsilon}} \left|\langle g, G_\varepsilon^\pm g\rangle\right|^{1/2}, \quad g \in \mathcal{H} \supset \mathcal{S}^* \tag{6}$$

$$||G_\varepsilon^\pm||_{\mathcal{S}^* \to \mathcal{S}} \leq \frac{1}{\varepsilon} \ . \tag{7}$$

Since $(G_\varepsilon^\pm)^* = G_\varepsilon^\mp$, one uses sometimes the notations $G_\varepsilon \equiv G_\varepsilon^+$ and $G_\varepsilon^* \equiv G_\varepsilon^-$.

(ii) It is convenient to put the condition $f \in \mathcal{E}$ in a more tractable form. For $\varepsilon > 0$ and $f \in \mathcal{S}^*$, let us set

$$f_\varepsilon = \frac{1}{\varepsilon} \int_0^\varepsilon W(\tau) f d\tau \ . \tag{8}$$

It is shown easily that $f_\varepsilon \in \mathcal{C}$, the application $\varepsilon \mapsto f_\varepsilon \in \mathcal{S}^*$ is C^1 in norm and

$$\int_0^1 \left\{ ||f_\varepsilon'||_{\mathcal{S}^*} + ||Af_\varepsilon||_{\mathcal{S}^*} + \left\| \frac{f_\varepsilon - f}{\varepsilon} \right\|_{\mathcal{S}^*} \right\} \frac{\mathrm{d}\varepsilon}{\sqrt{\varepsilon}} \leq C||f||_{\mathcal{E}}^2 < \infty \ . \tag{9}$$

In particular, this yields

$$||f_\varepsilon - f||_{\mathcal{S}^*} \to 0 \text{ for } \varepsilon \to 0 \ . \tag{10}$$

(iii) We set

$$F_\varepsilon \equiv F_\varepsilon(\lambda, \mu; f) = \langle f_\varepsilon, G_\varepsilon f_\varepsilon \rangle \ ,$$

where $\lambda \in \mathbb{R}$, $\mu > 0$, $\varepsilon > 0$, $f \in \mathcal{E}$ and f_ε is given by (8). One has

$$F_\varepsilon' = \langle f_\varepsilon' - Af_\varepsilon, G_\varepsilon f_\varepsilon \rangle + \langle G_\varepsilon^* f_\varepsilon, f_\varepsilon' + Af_\varepsilon \rangle - i\varepsilon \langle G_\varepsilon^* f_\varepsilon, [S, A] G_\varepsilon f_\varepsilon \rangle \ .$$

The arguments needed to make a rigorous proof out of this formal calculation are similar to those appearing in the usual Mourre theory. See for example Lemma 3.4 in (Boutet de Monvel, Georgescu, Mantoiu 1993). By (6) we get

$$\frac{1}{C}|F_\varepsilon'| \leq \frac{1}{\sqrt{\varepsilon}} (||f_\varepsilon'||_{\mathcal{S}^*} + ||Af_\varepsilon||_{\mathcal{S}^*}) |F_\varepsilon|^{1/2} + ||[S, A]||_{\mathcal{S} \to \mathcal{S}^*} |F_\varepsilon| \ . \tag{11}$$

(iv) Using the version of Gronwall's lemma proved in (Boutet de Monvel, Georgescu, Mantoiu 1993, Appendix B) and (9), we conclude from (11) that the limit $F_0 = \lim_{\varepsilon \to 0} F_\varepsilon$ exists and it satisfies

$$\begin{aligned} |F_0| &\leq C \left\{ |F_1| + \left[\int_0^1 \frac{\mathrm{d}\varepsilon}{\sqrt{\varepsilon}} (||f_\varepsilon'||_{\mathcal{S}^*} + ||Af_\varepsilon||_{\mathcal{S}^*}) \right]^2 \right\} \\ &\leq C\{|F_1| + ||f||_{\mathcal{E}}^2\} \ . \end{aligned} \tag{12}$$

It is easy to bound $|F_1|$ by means of (7) and (8):

$$\begin{aligned} |F_1| \leq ||G_1||_{\mathcal{S}^* \to \mathcal{S}} ||f_1||_{\mathcal{S}^*}^2 &\leq C \left[\int_0^1 ||W(\tau) f||_{\mathcal{S}^*} d\tau \right]^2 \\ &\leq C||f||_{\mathcal{S}^*}^2 \leq C||f||_{\mathcal{E}}^2 \ , \end{aligned}$$

so that (12) reads simply

$$|F_0| \leq C||f||_{\mathcal{E}}^2 \ . \tag{13}$$

(v) To finish the proof, we need only to show that F_0 is the right object, i.e. that $\langle f_\varepsilon, G_\varepsilon(\lambda,\mu)f_\varepsilon\rangle \to \langle f, (R-\lambda\mp i\mu)^{-1}f\rangle$ for $\varepsilon \to 0$. For this, we write

$$\begin{aligned}|\langle f_\varepsilon, G_\varepsilon f_\varepsilon\rangle - \langle f, G_0 f\rangle| \leq\ & ||f_\varepsilon - f||_{\mathcal{S}^*}||G_\varepsilon||_{\mathcal{S}^*\to\mathcal{S}}||f_\varepsilon||_{\mathcal{S}^*} \\ & + ||f_\varepsilon||_{\mathcal{S}^*}||G_\varepsilon - G_0||_{\mathcal{S}^*\to\mathcal{S}}||f_\varepsilon||_{\mathcal{S}^*} \\ & + ||f_\varepsilon||_{\mathcal{S}^*}||G_0||_{\mathcal{S}^*\to\mathcal{S}}||f_\varepsilon - f||_{\mathcal{S}^*} \ .\end{aligned}$$

But

$$||G_\varepsilon(\lambda,\mu)||_{\mathcal{S}^*\to\mathcal{S}} \leq C||G_\varepsilon(\lambda,\mu)|| \leq \frac{C}{\mu} \tag{14}$$

by (5). In addition, the second identity of the resolvent and (14) yield

$$\begin{aligned}||G_\varepsilon - G_0||_{\mathcal{S}^*\to\mathcal{S}} &\leq ||G_\varepsilon||_{\mathcal{S}^*\to\mathcal{S}} \cdot ||\varepsilon S||_{\mathcal{S}\to\mathcal{S}^*} \cdot ||G_0||_{\mathcal{S}^*\to\mathcal{S}} \\ &\leq C\frac{\varepsilon}{\mu^2} \to 0 \text{ for } \varepsilon \to 0 \ .\end{aligned} \tag{15}$$

The convergence now follows from (10) and (15). This and (13) imply one of the estimates (2). The other one is obtained in the same way. □

Remark 2.1 We get from (2) a large class of R-smooth operators, as well as the absence of the singular spectrum. Since our interest lies in the unbounded case, we stated explicitly only the estimate (2), from which Theorem 2.2 will be deduced.

Let us study now a self-adjoint, unbounded operator H in $\mathcal{H}$. We suppose that it has a spectral gap and fix a real number λ_0 not belonging to its spectrum. We intend to apply Theorem 2.1 to $R \equiv (\lambda_0 - H)^{-1}$, which is self-adjoint and bounded. The Sobolev scale associated to H is denoted by $\{\mathcal{G}^s\}_{s\in\mathbb{R}}$, with the convention that $\mathcal{G}^2$ is the operator domain and $\mathcal{G}^1$ the form-domain. $\mathcal{G}^{-s}$ is identified to $(\mathcal{G}^s)^*$ and the duality form of the couple $(\mathcal{G}^s, \mathcal{G}^{-s})$ will also be denoted by $\langle\cdot,\cdot\rangle$. Note the embeddings $\mathcal{G}^1 \hookrightarrow \mathcal{H} \hookrightarrow \mathcal{G}^{-1}$. H extends to a symmetric element of $B(\mathcal{G}^1, \mathcal{G}^{-1})$. We adapt Definition 2.2:

Definition 2.5 The self-adjoint operator A is *weakly conjugate (in form-sense)* to H if $H \in C^1(A; \mathcal{G}^1, \mathcal{G}^{-1})$ and $B \equiv i[H, A] > 0$.

The class $C^1(A; \mathcal{G}^1, \mathcal{G}^{-1})$ is defined in the same way as $C^1(A; \mathcal{H})$, replacing $B(\mathcal{H})$ by $B(\mathcal{G}^1, \mathcal{G}^{-1})$. We have to impose that e^{itA} leave $\mathcal{G}^1$ invariant. It follows that $\mathcal{W}(t)H = e^{-itA}He^{itA}$ (with a suitable interpretation) is well-defined as an element of $B(\mathcal{G}^1, \mathcal{G}^{-1})$. Since $B \in B(\mathcal{G}^1, \mathcal{G}^{-1})$ is positive, we can define the Hilbert space $\mathcal{B}$ as the completion of $\mathcal{G}^1$ in the norm $||f||_{\mathcal{B}} = \langle f, Bf\rangle^{1/2}$. Its adjoint $\mathcal{B}^*$ may be identified with the completion of $B\mathcal{G}^1$ in $||g||_{\mathcal{B}^*} = \langle g, B^{-1}g\rangle^{1/2}$. $(\mathcal{B}, \mathcal{G}^1)$ and $(\mathcal{G}^{-1}, \mathcal{B}^*)$ are Friedrichs couples, but in general $\mathcal{B}$ and $\mathcal{B}^*$ are not comparable to $\mathcal{H}$. B extends to a unitary operator:

$\mathcal{B} \to \mathcal{B}^*$. We must also impose that $W(\,\cdot\,) = \mathrm{e}^{\mathrm{i}\,\cdot A}$ is a C_0-group in the spaces $\mathcal{B}$ and $\mathcal{B}^*$. This has a standard meaning, since, for instance, W is a C_0-group in $\mathcal{G}^{-1}$ and $(\mathcal{G}^{-1}, \mathcal{B}^*)$ is a Friedrichs couple. The interest is twofold. First, it gives the framework for defining the class $C^1(A; \mathcal{B}, \mathcal{B}^*)$ in an already familiar way. Second, it allows to introduce $\mathcal{A} = D(A; \mathcal{B}^*)$, which is a Hilbert space with the graph-norm $||g||_{\mathcal{A}} \equiv (||g||^2_{\mathcal{B}^*} + ||Ag||^2_{\mathcal{B}^*})^{1/2}$. For the Friedrichs couple $(\mathcal{B}^*, \mathcal{A})$, there are real interpolation spaces to define. We shall be interested into

$$\mathcal{F} \equiv (\mathcal{B}^*, \mathcal{A})_{\frac{1}{2},1} = \left\{ g \in \mathcal{B}^* \;\middle|\; ||g||_{\mathcal{F}} = \int_0^1 \frac{\mathrm{d}t}{t^{3/2}} ||W(t)g - g||_{\mathcal{B}^*} < \infty \right\} .$$

The remarks following Definition 2.4 have an obvious counterpart here. In particular, the identification $\mathcal{F}^* = (\mathcal{A}^*, \mathcal{B})_{\frac{1}{2},\infty}$ is available. $(\mathcal{F}^*)^\circ$ is the closure of $\mathcal{B}$ in $\mathcal{F}^*$. We can now state our main result.

Theorem 2.2 *Let H be a self-adjoint operator having a spectral gap. Suppose that it admits a weakly conjugate operator (in form-sense) A, such that $B = \mathrm{i}[H, A] \in C^1(A; \mathcal{B}, \mathcal{B}^*)$. Then*

(a) $|\langle f, (H - \lambda \mp \mathrm{i}\mu)^{-1} f)| \leq C||f||^2_{\mathcal{F}}$, *with C uniform in $\lambda \in \mathbb{R}$, $\mu > 0$ and $f \in \mathcal{F}$.*

(b) *Let $\mathcal{K}$ be an arbitrary Hilbert space. Then any element of $B((\mathcal{F}^*)^\circ, \mathcal{K})$ is H-smooth.*

(c) *H has purely absolutely continuous spectrum.*

Proof. Note that $(H - \lambda \mp \mathrm{i}\mu)^{-1} \in B(\mathcal{G}^{-1}, \mathcal{G}^1) \subset B(\mathcal{B}^*, \mathcal{B}) \subset B(\mathcal{F}^*, \mathcal{F})$, hence (a) makes sense. The point is that we cannot expect an estimate uniform in μ in the Banach space $B(\mathcal{G}^{-1}, \mathcal{G}^1)$. Since (b) and (c) follow straightforward from (a), we are left with the task of deducing (a) from Theorem 2.1. This is done if the following implications are proved (we preserve all the notations introduced previously):

(i) $H \in C^1(A; \mathcal{G}^1, \mathcal{G}^{-1}) \Rightarrow R \in C^1(A; \mathcal{H})$,

(ii) $B > 0 \Rightarrow S > 0$,

(iii) $B \in C^1(A; \mathcal{B}, \mathcal{B}^*) \Rightarrow S \in C^1(A; \mathcal{S}, \mathcal{S}^*)$,

(iv) $||(R - \lambda \mp \mathrm{i}\mu)^{-1}||_{\mathcal{E} \to \mathcal{E}^*} \leq C_1 \Rightarrow ||(H - \lambda \mp \mathrm{i}\mu)^{-1}||_{\mathcal{F} \to \mathcal{F}^*} \leq C_2$,

with constants C_1, C_2 independent of λ and μ.

We shall argue formally, for the sake of brevity. The missing technicalities are easy to supply. The main remark is that $S = RBR$. This gives at once (i) and (ii) (here the assumption $H \in C^1(A; \mathcal{G}^2, \mathcal{G}^{-2})$ suffices, but this will not be enough further on). R (considered as an element of $B(\mathcal{H}, \mathcal{G}^2)$) extends to an isometry: $\mathcal{S} \to \mathcal{B}$. In fact, it is a unitary operator (which we will denote by the same letter) because its range contains $\mathcal{G}^2$, which is dense in $\mathcal{B}$. By duality and the remark that R is symmetric in a suitable sense, R is unitary from $\mathcal{B}^*$ to $\mathcal{S}^*$ (it is a restriction of $R \in B(\mathcal{G}^{-2}, \mathcal{H})$). In addition, $R \in B(\mathcal{A}, \mathcal{C})$, hence $R \in B(\mathcal{C}^*, \mathcal{A}^*)$ too. To see this, write

$$||Rf||_{\mathcal{C}}^2 = ||Rf||_{\mathcal{S}^*}^2 + ||ARf||_{\mathcal{S}^*}^2$$
$$\leq 2(||Rf||_{\mathcal{S}^*}^2 + ||RAf||_{\mathcal{S}^*}^2 + ||[R,A]f||_{\mathcal{S}^*}^2) \ .$$

But $||Rf||_{\mathcal{S}^*}^2 + ||RAf||_{\mathcal{S}^*}^2 = ||f||_{\mathcal{A}}^2$ and $\mathrm{i}[R,A] = S = RBR \in B(\mathcal{B}^*, \mathcal{S}^*)$ by the next line:

$$\mathcal{B}^* \hookrightarrow \mathcal{G}^{-1} \xrightarrow{R} \mathcal{G}^1 \hookrightarrow \mathcal{B} \xrightarrow{B} \mathcal{B}^* \xrightarrow{R} \mathcal{S}^* \ . \tag{16}$$

Now, by real interpolation, $R \in B(\mathcal{F}, \mathcal{E}) \cap B(\mathcal{E}^*, \mathcal{F}^*)$. We also get (iii) if we write

$$\mathrm{i}[S,A] = \mathrm{i}[R,A]BR + RB\mathrm{i}[R,A] + R\mathrm{i}[B,A]R$$
$$= 2RBRBR + R\mathrm{i}[B,A]R \ .$$

The second term is obviously in $B(\mathcal{S}, \mathcal{S}^*)$. For the first one, the same follows from $BR \in B(\mathcal{S}, \mathcal{B}^*)$ and from (16). In order to prove (iv), one needs a formula relating the resolvent of H to the resolvent of R. We start with the identity

$$(H-z)^{-1} = -R + (\lambda_0 - z)(H-z)^{-1}R \tag{17}$$

which gives for $|z-\lambda_0| \cdot ||R|| < 1$

$$(H-z)^{-1} = -\frac{1}{\lambda_0 - z} R\Big[R - \frac{1}{\lambda_0 - z}\Big]^{-1} \tag{18}$$

This extends by holomorphy to any z non-real. By inserting (17) in (18) we get

$$(H-z)^{-1} = -R - R\Big[R - \frac{1}{\lambda_0 - z}\Big]^{-1} R \ .$$

We finish the proof by writing

$$||(H - \lambda \mp \mathrm{i}\mu)^{-1}||_{\mathcal{F} \to \mathcal{F}^*} \leq$$
$$\leq ||R||_{\mathcal{F} \to \mathcal{F}^*} + ||R||_{\mathcal{E}^* \to \mathcal{F}^*} \cdot \Big\|(R - \frac{1}{\lambda_0 - \lambda \pm \mathrm{i}\mu})^{-1}\Big\|_{\mathcal{E} \to \mathcal{E}^*} \cdot ||R||_{\mathcal{F} \to \mathcal{E}} \ . \square$$

Remark 2.2 For operators not having a spectral gap, there is a weaker result, which was proved in (Boutet de Monvel, Kazantseva, Mantoiu 1996). Let us say that A is *weakly conjugate to H in operator sense* if $H \in C^1(A; \mathcal{G}^2, \mathcal{H})$ (obvious meaning) and if $B = \mathrm{i}[H,A]$ (which is in $B(\mathcal{G}^2, \mathcal{H})$ and extends to a symmetric element of $B(\mathcal{G}^1, \mathcal{G}^{-1})$) satisfies $\langle f, Bf\rangle > 0$ for all $f \in \mathcal{G}^1 \setminus \{0\}$. This is stronger than the weak conjugation in form-sense. If one supplies the assumption $B \in C^1(A; \mathcal{B}, \mathcal{B}^*)$, the conclusion of Theorem 2.2 remains true. The point is that the proof of Theorem 2.1 admits an obvious unbounded version if $B \in B(\mathcal{G}^2, \mathcal{H})$. The critical point is step (i), which has no suitable counterpart if one assumes only $B \in B(\mathcal{G}^1, \mathcal{G}^{-1})$.

Remark 2.3 In applications, the space $\mathcal{F}$ is usually quite intricate, so we shall not mention explicitly the resolvent estimates. For the case of Schrödinger operators, we described in (Boutet de Monvel, Kazantseva, Mantoiu 1996) a space which is embedded in $\mathcal{A}$ and which is very explicit. Some scattering results are also available (see Corollaries 1.1, 1.2 and their consequences 2.1 and 2.2 in (Boutet de Monvel, Kazantseva, Mantoiu 1996)). They have finer counterparts here, but, since in applications they give transparent assertions only for situations which are close to the Schrödinger case, we give up stating them.

Finally, we come to the generality of the method of the weakly conjugate operator. In (Boutet de Monvel, Georgescu 1992) it was shown that if the spectrum of H on the real, open interval I is purely absolutely continuous and of constant multiplicity, Mourre's method surely applies locally on I, i.e. there is a self-adjoint operator A satisfying (1) for any compact subset J of I. In addition, A can be chosen such that the successive commutators $[H, A]$ and $[[H, A], A]$ are bounded. In our global case, we must deal with the possible change of multiplicity. We need that this does not happen to wildly.

Proposition 2.1 *Assume that H is a self-adjoint operator on $\mathcal{H}$, with purely absolutely continuous spectrum equal (up to a set of Lebesgue measure 0) to a countable union of disjoint open intervals $\{\sigma_j\}_{j\in\mathbb{N}}$ on which H has constant multiplicity m_j $(0 \leq m_j \leq \infty)$. Then H admits a weakly conjugate operator A such that $H \in C^1(A; \mathcal{H})$ and $B = \mathrm{i}[H, A] \in C^1(A; \mathcal{B}, \mathcal{B}^*)$.*

Proof. Under the stated conditions, H is unitarily equivalent to an operator of the form $\bigoplus_{j\in\mathbb{N}} Q_j$, acting in the Hilbert space $\bigoplus_{j\in\mathbb{N}} L^2(\sigma_j, d\lambda; \mathcal{H}_j)$. Here $\mathcal{H}_j$ is a m_j-dimensional Hilbert space, $d\lambda$ denotes the Lebesgue measure and Q_j is the multiplication operator by the variable in $L^2(\sigma_j, d\lambda; \mathcal{H}_j)$. For any j, choose $F_j : \sigma_j \equiv (a_j, b_j) \to (0, \infty)$ a C^∞-function, with all the derivatives bounded by 1, such that

$$\int_{a_j}^{c} \frac{\mathrm{d}\lambda}{F_j(\lambda)} = \infty = \int_{c}^{b_j} \frac{\mathrm{d}\lambda}{F_j(\lambda)} \tag{19}$$

$(c \in (a_j, b_j)$ is not important). Then the operator defined on $C_0^\infty(\sigma_j)$ by

$$A_j = \frac{\mathrm{i}}{2}\Big(F_j \frac{\mathrm{d}}{\mathrm{d}\lambda} + \frac{\mathrm{d}}{\mathrm{d}\lambda} F_j\Big) \tag{20}$$

is essentially self-adjoint. By denoting its closure also by A_j, we check easily that $Q_j \in C^1(A_j, L^2(\sigma_j, \mathrm{d}\lambda; \mathcal{H}_j))$ and $B_j \equiv \mathrm{i}[Q_j, A_j] = F_j > 0$. We need to have $B_j \in C^1(A_j; \mathcal{B}_j, \mathcal{B}_j^*)$, where $\mathcal{B}_j$ is the completion of $L^2(\sigma_j, \mathrm{d}\lambda; \mathcal{H}_j))$ in the norm $||f||_{\mathcal{B}_j} = ||F_j^{1/2} \cdot f||$.

For this, one has to check up that $|\langle f, \mathrm{i}[B_j, A_j]g\rangle| \leq C||f||_{\mathcal{B}_j} \cdot ||g||_{\mathcal{B}_j}$, for all $f, g \in L^2(\sigma_j, \mathrm{d}\lambda; \mathcal{H}_j))$ i.e. $|\langle f, F_j' \cdot F_j \cdot g\rangle| \leq C||F_j^{1/2} f|| \cdot ||F_j^{1/2} g||$. This is obviously fulfilled with $C \equiv \sup_{\lambda\in\Omega} |F_j'(\lambda)|$. By performing direct sums and transforming back to the initial representation we get our result. □

3 Perturbations of Convolution Operators

We apply now the abstract method developed previously to some operators of the form

$$H = H_0 + V = h(P) + V(Q) \tag{21}$$

acting in the Hilbert space $\mathcal{H}(\mathbb{R}^N) \equiv L^2(\mathbb{R}^N; \mathrm{d}x)$, where $\mathrm{d}x$ is the Lebesgue measure. We denoted by Q the position observable and by $P = -i\nabla$ the corresponding momentum. $\varphi(Q)$ will be the usual multiplication operator by the Borel function φ. The convolution operator $\psi(P)$ is, by definition, unitarily equivalent to $\psi(Q)$ by $\mathcal{F}$, the Fourier transform: $\psi(P) = \mathcal{F}^{-1}\psi(Q)\mathcal{F}$. For the spaces of test functions and distributions on $\mathbb{R}^N$, we use the standard notations: $\mathcal{D}(\mathbb{R}^N)$, $\mathcal{S}(\mathbb{R}^N)$, $\mathcal{S}^*(\mathbb{R}^N)$, $\mathcal{D}^*(\mathbb{R}^N)$.

In our choice of weakly conjugate operator we are guided by the desire to preserve form (21) after commutation. The reason is that there are some effective criteria of positivity for such operators. Consider a real, symmetric, bilinear form γ on $\mathbb{R}^N$ and denote by the same letter the linear, symmetric operator: $\mathbb{R}^N \to \mathbb{R}^N$ assigned to it. We define the self-adjoint operator

$$A_\gamma = \frac{1}{2}\{\gamma(P,Q) + \gamma(Q,P)\} = \gamma(P,Q) + \frac{i}{2}\operatorname{Tr}(\gamma) \ . \tag{22}$$

Here Tr denotes the trace and $(\cdot,\cdot)$ the scalar product in $\mathbb{R}^N$, with $|\cdot|$ the corresponding norm. The unitary group generated by A_γ is given by

$$[W_\gamma(t)f](x) = \mathrm{e}^{t/2\operatorname{Tr}(\gamma)} f(\mathrm{e}^{t\gamma}x)$$

for all $t \in \mathbb{R}$, $x \in \mathbb{R}^N$ and $f \in \mathcal{H}(\mathbb{R}^N)$. It leaves $\mathcal{S}(\mathbb{R}^N)$ invariant. The notations $D_\gamma\varphi \equiv \gamma(x, \nabla\varphi)$ and $D_\gamma^2\varphi \equiv D_\gamma(D_\gamma\varphi)$ are convenient. At least formally

$$B \equiv \mathrm{i}[H, A_\gamma] = (D_\gamma h)(P) - (D_\gamma V)(Q) \ . \tag{23}$$

Definition 3.1 The function $\varphi : \mathbb{R}^N \to \mathbb{R}$ is called *γ-attractive* (resp. *γ-repulsive*) if $D_\gamma\varphi \geq 0$ (resp. $D_\gamma\varphi \leq 0$). If the first inequality is strict almost everywhere, φ will be called *γ-superattractive*.

γ-attractivity is equivalent to the fact that the application $t \mapsto \varphi(\mathrm{e}^{t\gamma}x)$ is increasing.

Definition 3.2 We say that the functions φ, $\psi : \mathbb{R}^N \to [0,\infty)$ *form a compatible couple* if $\mathcal{S}(\mathbb{R}^N) \subset \mathrm{fm}[\varphi(Q)] \cap \mathrm{fm}[\psi(P)]$ ($\mathrm{fm}(T)$ is the form-domain of T) and for every $f \in \mathcal{S}(\mathbb{R}^N)$

$$\langle f, \varphi(Q)f\rangle \leq \langle f, \psi(P)f\rangle \ . \tag{24}$$

We shall state later some conditions implying (24). For the moment, let us make an assertion which mainly stresses the assumptions that one must verify, and barely deserves the name of proposition since (iv) and (v) are left in rather implicit form:

Proposition 3.1 *Let $h : \mathbb{R}^N \to \mathbb{R}$ a smooth function which is polynomially bounded and $V : \mathbb{R}^N \to \mathbb{R}$ a Borel function such that $V(Q)$ is $h(P)$-small in form-sense,* i.e. *$V(Q)$ is $h(P)$-bounded in the sense of forms, with a subunitary bound. Assume that there is a real, symmetric, bilinear form γ on $\mathbb{R}^N$ such that*

(i) *h is γ-superattractive*
(ii) $D_\gamma h \leq C(1 + |h|)$
(iii) $|D_\gamma^2| \leq C D_\gamma h$

(we will say that h is γ-admissible*) if* (i), (ii) *and* (iii) *are true)*

(iv) $(|D_\gamma V|, (1-\delta) D_\gamma h)$ *is a compatible couple for some $\delta > 0$*
(v) $(|D_\gamma^2 V|, C D_\gamma h)$ *is a compatible couple for some finite C.*

Then the self-adjoint operator $H = h(P) + V(Q)$ has no singular spectrum.

Proof. H is self-adjoint as a form-sum, with form-domain $\mathcal{G}^1 \equiv D(|h(P)|^{1/2})$. $\mathcal{S}(\mathbb{R}^N)$ is dense in $\mathcal{G}^1$ (even $\mathcal{FD}(\mathbb{R}^N)$ is dense in $\mathcal{G}^1$, just because $h \in L^\infty_{\mathrm{loc}}(\mathbb{R}^N)$). We shall get the conclusion by taking $A = A_\gamma$ in Theorem 2.2. Since a form-calculation on $\mathcal{S}(\mathbb{R}^N)$ gives

$$W_\gamma(-t) h(P) W_\gamma(t) = h(\mathrm{e}^{t\gamma} P) \ ,$$

in order to check that $\mathcal{G}^1$ is left invariant by W_γ, we need only to show that

$$|h(\mathrm{e}^{t\gamma} x)| \leq c(t) |h(x)|$$

for all $t \in \mathbb{R}$ and $x \in \mathbb{R}^N$. This is done by writing

$$h(\mathrm{e}^{t\gamma} x) = h(x) + \int_0^t \frac{\mathrm{d}}{\mathrm{d}\tau} h(\mathrm{e}^{\tau\gamma} x) \mathrm{d}\tau = h(x) + \int_0^t (D_\gamma h)(\mathrm{e}^{\tau\gamma} x) \mathrm{d}\tau$$

and by using (ii) and the standard form of Gronwall's lemma. It is easy to get (23) as forms on $\mathcal{S}(\mathbb{R}^N)$ and by means of (iv) and (ii) we obtain

$$\delta (D_\gamma h)(P) \leq B \leq (2-\delta)(D_\gamma h)(P) \leq C(1 + |h(P)|) \ . \tag{25}$$

(i), (25) and the fact that $\mathcal{S}(\mathbb{R}^N)$ is dense in $\mathcal{G}^1$ show that

$$H \in C^1(A_\gamma; \mathcal{G}^1, \mathcal{G}^{-1})$$

and that B is positive and nondegenerate as a form defined on $\mathcal{G}^1$. It also follows that the norms $||f||_B = \langle f, Bf \rangle^{1/2}$ and

$$||f||'_{\mathcal{B}} \equiv ||(D_\gamma h)(P)^{1/2} f||$$

are equivalent. The second one will be preferred to define the Hilbert space $\mathcal{B}$ by completion. $\mathcal{B}^*$ will be the completion of $B\mathcal{G}^1$ in the norm

$$||g||'_{\mathcal{B}^*} \equiv ||(D_\gamma h)(P)^{-1/2} g|| \ .$$

For simplicity, the accents will be dropped. In order to finish, we need only to prove that W_γ is a C_0-group in the Friedrichs couple $(\mathcal{G}^1, \mathcal{B}^*)$ and that $B \in C^1(A_\gamma; \mathcal{B}, \mathcal{B}^*)$. This is done by the same type of arguments as above, taking (iii) and (v) into account. □

Remark 3.1 Condition (iv) can be replaced by the requirement that V is γ-repulsive. This is a generalization of Lavine's result on Schrödinger operators (where $h(x) = |x|^2$ and γ the identity in $\mathbb{R}^N$), which seems to be difficult to obtain by other methods. But note that, in order to verify the property $B \in C^1(A_\gamma; \mathcal{B}, \mathcal{B}^*)$ in a simple way, one needs the equivalence between $||\cdot||_{\mathcal{B}}$ and $||\cdot||'_{\mathcal{B}}$ and this requires an extra condition on V. This and the assumption (v) make the γ-repulsive case less attractive than one could have hoped. But there is a simple, though not trivial situation which is easy to deal with. We say that V is *γ-homogeneous of degree* 0 if $D_\gamma V = 0$. This means that V does not change when $e^{t\gamma}$ is applied to its argument. In this case, the conditions (iv) and (v), which were left in an implicit form for the moment, are trivially satisfied.

Remark 3.2 Actually, the choice

$$A_\gamma^{a,b} = \frac{1}{2}[\gamma(P-a, Q-b) + \gamma(Q-b, P-a)]$$

with $a, b \in \mathbb{R}^N$ is also available and we get

$$B \equiv \mathrm{i}[h(P) + V(Q), A_\gamma^{a,b}] = \gamma(P-a, (\nabla h)(P)) - \gamma(Q-b, (\nabla V)(Q)) \ ,$$

which also has the form (21). Hence, our results will have more general counterparts, since a and b are at our disposition.

Example 3.1 We give now an example which will show both the usefulness of more general γ's than identity and the efficiency of Proposition 3.1 to deal with symbols h which are not bounded from below. Take $h(x_1, x_2) = \frac{x_1 \cdot x_2}{\langle x \rangle^2}$, where the notation $\langle x \rangle \equiv (1 + |x|^2)^{1/2}$ will be systematically used. Then $(\partial_1 h)(x_1, x_2) = \frac{x_2}{\langle x \rangle^2}[1 - 2\frac{x_1^2}{\langle x \rangle^2}]$ and $(\partial_2 h)(x_1, x_2) = \frac{x_1}{\langle x \rangle^2}[1 - 2\frac{x_2^2}{\langle x \rangle^2}]$. The only positive combination of the form $D_\gamma h$ is obtained by taking $\gamma = \left(\begin{smallmatrix} 0 & 1 \\ 1 & 0 \end{smallmatrix}\right)$:

$$x_2 \cdot \partial_1 h + x_1 \cdot \partial_2 h = \langle x \rangle^{-4}[x_1^2 + x_2^2 + (x_1^2 - x_2^2)^2] > 0 \text{ for } (x_1, x_2) \neq 0 \ .$$

In fact, h is γ-admissible. For any bounded, Borel function $v : \mathbb{R} \to \mathbb{R}$ we set $V(x_1, x_2) \equiv v(x_1^2 - x_2^2)$ in order to obtain a function which is γ-homogeneous of degree 0. Then, by the Remark 3.1 the self-adjoint operator

$$H = h(P) + V(Q) = \frac{P_1 \cdot P_2}{\langle P \rangle^2} + v(Q_1^2 - Q_2^2)$$

has purely absolutely continuous spectrum. Many examples of this type may be given. However, the cases $h(x_1, x_2) = x_1 \cdot x_2$ and $h(x_1, x_2) = x_1^2 - x_2^2$ are not covered. There is no γ satisfying both (i) and (ii).

Example 3.2 There is a situation not included in Proposition 3.1, but easy to deal with, when some monotony is involved. Rather than formulating a general but easy result, we will show a typical example. Take $h(x) = \frac{x_1}{\langle x \rangle}$. Then $(\partial_1 h)(x) = \langle x \rangle^{-3}[1 + x_2^2 + \ldots + x_N^2] > 0$ and one checks easily that Theorem 2.2 applies with $A = Q_1$ and $H = \frac{P_1}{\langle P \rangle} + V$, where V is a bounded function or, more generally, a bounded map from $\mathbb{R}$ to $B[\mathcal{H}(\mathbb{R}^{N-1})]$. We believe that this example and others of this kind cannot be covered by Mourre's method or by the Kato-Putnam theory.

We come back now to the assumptions (iv) and (v) of Proposition 3.1. Suppose that φ, ψ are two positive functions defined on $\mathbb{R}^N$, such that $\mathcal{S}(\mathbb{R}^N) \subset \mathrm{fm}[\varphi(Q)] \cap \mathrm{fm}[\psi(P)]$ and ψ vanishes on a negligible set. Suppose also that the operator $\varphi^{1/2}(Q) \cdot \psi^{-1/2}(P)$ extends to a bounded operator in $\mathcal{H}(\mathbb{R}^N)$, with norm ≤ 1. Then, for $g = \psi^{1/2}(P)f$, with $f \in \mathcal{S}(\mathbb{R}^N)$, one has $\psi^{-1/2}(P)g = f \in D[\varphi^{1/2}(Q)]$ and

$$||\varphi^{1/2}(Q) \cdot \psi^{-1/2}(P)g|| = ||\varphi^{1/2}(Q)f|| \leq ||g|| = ||\psi^{1/2}(P)f||.$$

This means exactly that (φ, ψ) is a compatible couple and leads us to search for couples (F, G) such that $F(Q)G(P) \in B[\mathcal{H}(\mathbb{R}^N)]$. We recall the definition of some classical spaces, restricting ourselves strictly to the information needed and sending for more comprehensive presentations to (Simon 1979) and (Triebel 1978). $\mu[\Omega]$ denotes the Lebesgue measure of Ω.

Definition 3.3 $L^p_{\mathrm{w}}(\mathbb{R}^N) \equiv \left\{\varphi : \mathbb{R}^N \to \mathbb{C} \;\middle|\; \mu[\{x \mid |\varphi(x)| > t\}] \leq Ct^{-p}\right\}$, $p \in [1, \infty)$.

$L^p_{\mathrm{w}}(\mathbb{R}^N)$ is a quasi-Banach space with the quasi-norm

$$||\varphi||_{L^p_{\mathrm{w}}} \equiv \sup_{t>0}\left\{t\mu[\{x \mid |\varphi(x)| > t\}]^{1/p}\right\}$$

called *the Marcinkiewicz space of order p (or the weak-L^p space).*

If $p \neq 1$, it is Banachizable. We set $L^\infty_{\mathrm{w}}(\mathbb{R}^N) \equiv L^\infty(\mathbb{R}^N)$. Although $L^p_{\mathrm{w}}(\mathbb{R}^N)$ is only slightly bigger than $L^p(\mathbb{R}^N)$ ($p \neq \infty$), there are common functions in $L^p_{\mathrm{w}}(\mathbb{R}^N)$ which are in none of the spaces $L^q(\mathbb{R}^N)$ ($|\cdot|^{-\frac{N}{p}}$ is an example). The relevance of Definition 3.3 in our context is given by the next result, taken from (Simon 1979).

Lemma 3.1 *Let $F \in L^p_{\mathrm{w}}(\mathbb{R}^N)$, $\mathcal{F}G \in L^{p'}_{\mathrm{w}}(\mathbb{R}^N)$, $p \in (2, \infty]$, $1/p + 1/p' = 1$. Then $F(Q) \cdot G(P) \in B[\mathcal{H}(\mathbb{R}^N)]$ and there is a constant c, depending only on p and N, such that*

$$||F(Q) \cdot G(P)|| \leq c||F||_{L^p_{\mathrm{w}}} \cdot ||\mathcal{F}G||_{L^{p'}_{\mathrm{w}}}.$$

Note that $\mathcal{F}G \in L^{p'}_{\rm w}(\mathbb{R}^N)$ with $p' \in (1,2)$ implies $G \in L^{p}_{\rm w}(\mathbb{R}^N)$, but the converse is false. It seems that the value of the constant c is unknown. Combining Proposition 3.1 with Lemma 3.1, we get

Theorem 3.1 *Let γ be a real, symmetric, bilinear form on $\mathbb{R}^N$. Suppose that $h : \mathbb{R}^N \to \mathbb{R}$ is polynomially bounded, γ-admissible, $\mathcal{F}[(D_\gamma h)^{-1/2}] \in L^{p'_1}_{\rm w}(\mathbb{R}^N)$ and $\mathcal{F}[(D_\gamma h)^{-1/2}] \in L^{p'_2}_{\rm w}(\mathbb{R}^N)$ for two values $p'_1, p'_2 \in [1,2)$. Let $V : \mathbb{R}^N \to \mathbb{R}$ a Borel function, such that $V(Q)$ is small in form-sense with respect to $h(P)$, $D_\gamma V \in L^{p_1/2}_{\rm w}(\mathbb{R}^N)$ and $D^2_\gamma V \in L^{p_2/2}_{\rm w}(\mathbb{R}^N)$, where p_j is the exponent conjugate to p'_j, $j = 1,2$. Then, if $||D_\gamma V||_{L^{p_1/2}_{\rm w}}$ is small enough, $H = h(P) + V(Q)$ has purely absolutely continuous spectrum.*

Remark 3.3 An explicit condition implying that $V(Q)$ is small in form-sense with respect to $h(P)$ is the existence of a $p_0 \in (2,\infty)$ such that $\mathcal{F}(|h|^{-1/2}) \in L^{p'_0}_{\rm w}(\mathbb{R}^N)$ where $\frac{1}{p_0} + \frac{1}{p'_0} = 1$, and $V \in L^\infty(\mathbb{R}^N) + L^{p'_0/2}_{\rm w}(\mathbb{R}^N)$, with a small $L^{p'_0/2}_{\rm w}(\mathbb{R}^N)$-component.

Example 3.3 We consider the case $h(x) = |x|^b$, where $a \equiv b/2 \in (0,N)$. We take $\gamma = 1$, hence $A_\gamma \equiv A$ is the generator of dilations. One has $D_\gamma h = bh$ and $D^2_\gamma h = b^2 h$. The Fourier transform of $h^{-1/2} = |\cdot|^{-a}$ is proportional to $|\cdot|^{-N+a}$, hence in $L^{N/N-a}_{\rm w}(\mathbb{R}^N)$. Then $H = |P|^b + V(Q)$ has purely absolutely continuous spectrum for $N > b$ if V satisfies the following conditions:

(i) $V = V_1 + V_2$, with $V_1 \in L^\infty(\mathbb{R}^N)$, $V_2 \in L^{N/b}_{\rm w}(\mathbb{R}^N)$, $||V_2||_{L^{N/b}_{\rm w}}$ small,

(ii) $D_\gamma V \in L^{N/b}_{\rm w}(\mathbb{R}^N)$, with $||D_\gamma V||_{L^{N/b}_{\rm w}}$ small,

(iii) $D^2_\gamma V \in L^{N/b}_{\rm w}(\mathbb{R}^N)$.

The main interest in this kind of results is the fact that V does not have to vanish at infinity. Some insight is given by the fact that $|\cdot|^{-b} \in L^{N/b}_{\rm w}(\mathbb{R}^N)$. Then, the next conditions imply (i), (ii) and (iii):

(i′) V has radial limits (depending on the direction), to which it converges as $\frac{C_0}{r^b}$, with C_0 small enough ($r = |x|$ is the radial distance),

(ii′) $\partial_r V \leq \frac{C_1}{r^{b+1}}$, with C_1 sufficiently small,

(iii′) $\partial^2_r V \leq \frac{C}{r^{b+2}}$, for finite C.

Of course, (i), (ii) and (iii) allow a more general behavior, both at infinity and (especially) locally.

Example 3.4 Let us consider briefly another case, where the choice $\gamma \neq 1$ is very natural. Take into account the decomposition $\mathbb{R}^N = Y \oplus Z$, where Y and Z are proper subspaces of $\mathbb{R}^N$. Set $x = (x^Y, x^Z) \in \mathbb{R}^N$, with $x^Y \in Y$ and $x^Z \in Z$ and take $\gamma = \pi^Y$, the orthogonal projection on Y ($\pi^Y x = x^Y$). We shall suppose that h admits the splitting $h(x) = h^Y(x^Y) + h^Z(x^Z)$. By identifying $\mathcal{H}(\mathbb{R}^N)$ with the Hilbert tensor product $\mathcal{H}(Y) \otimes \mathcal{H}(Z)$, $h(P)$ may be written as $h^Y(P^Y) \otimes 1^Z + 1^Y \otimes h^Z(P^Z)$, where, for instance, $P^Y = -\mathrm{i}\nabla^Y$ is the momentum corresponding to the euclidean space Y and 1^Y the identity

in $\mathcal{H}(Y)$. The operator $A_Y \equiv A_{\pi Y}$ is given by $A_Y = A^Y \otimes 1^Z$, where A^Y is the generator of dilatations in $\mathcal{H}(Y)$.

The advantage now is that the conditions in the Z-variable are very mild. Setting $H = h^Y(P^Y) \otimes 1^Z + 1^Y \otimes h^Z(P^Z) + V(Q^Y, Q^Z)$ (Q^Y is the position observable in Y), one has $\mathrm{i}[H, A_Y] = (D^Y h^Y)(P^Y) \otimes 1^Z - (D^Y V)(Q^Y, Q^Z)$, where $D^Y \equiv D_{\pi Y} = (x^Y, \nabla^Y \cdot)$.

Let us concentrate only on the hypothesis (iv) in Proposition 3.1, assuming that $D^Y h^Y > 0$ and that V is factorized: $V(x) = V^Y(x^Y) \cdot V^Z(x^Z)$, for any $V^Z \in L^\infty(Z)$ (in fact, $V^Z(Q^Z)$ may be replaced by any bounded operator W^Z in $\mathcal{H}(Z)$). Then $(D^Y V)(Q) = (D^Y V^Y)(Q^Y) \otimes V^Z(Q^Z)$ and in order to have $\mathrm{i}[H, A_Y] > 0$ one might impose

$$||V^Y||_{L^\infty} \cdot |(D^Y V^Y)(Q^Y)| < (D^Y h^Y)(P^Y)$$

(inequality between operators acting in $\mathcal{H}(Y)$). In particular, one might use Lemma 3.1 in the euclidean space Y and ask further conditions only on h^Y and V^Y. The discussion can be carried over to the other hypothesis in Proposition 3.1 and the factorizability of V may be by-passed. A typical circumstance is to have radial limits only for directions inside Y. The present approach is particularly well-suited to the case of Schrödinger-type operators, where $h(x) = |x|^2$. In this way, we can generalize some of the results of (Boutet de Monvel, Kazantseva, Mantoiu 1996), by using Lemma 3.1 instead of the point-wise estimate $|P^Y|^2 \geq (\frac{N_Y - 2}{2})^2 |Q^Y|^{-2}$, valid for N_Y (the dimension of Y) ≥ 3.

4 Second-Order Elliptic Differential Operators. The Unperturbed Case

Let us now turn to the case of second-order differential operators with variable coefficients. We shall deal first with the unperturbed operator, written formally $H_a \equiv \sum_{j,k=1}^N P_j a_{jk}(Q) P_k$, where a is a suitable, locally integrable matrix function. We shall write $a \geq 0$ if

$$\int_{\mathbb{R}^N} \sum_{j,k=1}^N a_{jk}(x) \overline{\xi_j(x)} \xi_k(x) \mathrm{d}x \geq 0 \tag{26}$$

for any $\xi \equiv (\xi_1, \ldots, \xi_N) \in \mathcal{D}(\mathbb{R}^N)^N$. Then the next quadratic form makes sense on $\mathcal{D}(\mathbb{R}^N)$:

$$q_a^{(0)}(f) \equiv \int_{\mathbb{R}^N} \sum_{j,k=1}^N a_{jk}(x) \overline{(\partial_j f)(x)} (\partial_k f)(x) \mathrm{d}x$$

and is positive. We set $a > 0$ if in (26) one has equality only if there is a j such that $\xi_j = 0$. This implies that $q_a^{(0)}$ is non-degenerate. Note that, for

instance, the constant matrix $a \equiv \begin{pmatrix} 1 & 0 \\ 0 & 0 \end{pmatrix}$ is > 0. Now, assume that $q_a^{(0)}$ is closable and positive, set $||f||_{D_a} \equiv (q_a^{(0)}(f)+||f||^2)^{1/2}$ and D_a the completion of $\mathcal{D}(\mathbb{R}^N)$ under the norm $||\cdot||_{D_a}$. Identifying $\mathcal{H}(\mathbb{R}^N)$ with its adjoint, we have the continuous, dense embeddings $D_a \hookrightarrow \mathcal{H}(\mathbb{R}^N) \hookrightarrow D_a^*$. $q_a^{(0)}$ extends to a closed form $q_a : D_a \to [0,\infty)$. Under the hypothesis $a > 0$ we also put $||f||_{\dot{D}_a} \equiv q_a^{(0)}(f)$, $\dot{D}_a$ being completion of $\mathcal{D}(\mathbb{R}^N)$ with respect to $||\cdot||_{\dot{D}_a}$ and $\dot{q}_a$ the closed extension of $q_a^{(0)}$ to $\dot{D}_a$. $(\dot{D}_a, D_a)$ and $(D_a^*, \dot{D}_a^*)$ are Friedrichs couples. A unique self-adjoint, positive operator H_a is assigned to q_a such that $D(H_a^{1/2}) = D_a$ and $q_a(f) = ||H_a^{1/2} f||^2$ for all $f \in D_a$. It extends to a symmetric element of $B(D_a, D_a^*)$ and, if $a > 0$, to a symmetric element of $B(\dot{D}_a, \dot{D}_a^*)$. Next, we establish our conventions on ellipticity.

Definition 4.1 The operator H_a will be called

(i) *weakly elliptic* if a is a locally integrable matrix function, $a \geq 0$ and $q_a^{(0)}$ is closable,

(ii) *elliptic* if there exist two continuous functions $\rho_1, \rho_2 : \mathbb{R}^N \to (0,\infty)$ such that $\rho_1 \leq a \leq \rho_2$ (here $\rho_1(x)_{jk} \equiv \rho_1(x) \cdot \delta_{jk}$ for any $x \in \mathbb{R}^N$, $j,k \in 1,\ldots,N$ and $a \leq b$ means $b - a \geq 0$),

(iii) *uniformly elliptic* if in (ii) one can take ρ_1 and ρ_2 strictly positive constants.

For subsequent use we will need following criterion of closability, taken from (Röckner, Wielens 1985):

Lemma 4.1 *The quadratic form $q_a^{(0)}$ is closable if there is a closed, negligible set $\Omega \subset \mathbb{R}^N$ such that for any compact subset K of $\mathbb{R}^N \setminus \Omega$ there exists a finite constant δ_K such that $a(x) \geq \delta_K \cdot 1$ almost everywhere on K.*

This shows in particular that elliptic $\Rightarrow$ weakly elliptic. Our purpose is to find conditions under which H_a has purely absolutely continuous spectrum. The examples we shall cover are to be compared with the following result, taken from (Davies 1989).

Lemma 4.2 *Let H_a be elliptic. If $\alpha(x)$ is the smallest eigenvalue of $a(x)$ which satisfies $\lim_{|x|\to\infty} \frac{\alpha(x)}{|x|^2} = \infty$, then H_a has a compact resolvent, hence its spectrum is purely discrete.*

For the weakly conjugate operator we make the choice (3.2). We need the notation $\{\gamma, a\} \equiv \gamma \cdot a + a \cdot \gamma$ and $\Gamma(a) \equiv \{\gamma, a\} - D_\gamma a$. The second one reads in coordinates:

$$\Gamma(a)_{jk} = \sum_{l=1}^{N} (\gamma_{jl} \cdot a_{lk} + a_{jl} \cdot \gamma_{lk}) - \sum_{m,n=1}^{N} \gamma_{mn} x_m \partial_n a_{jk} \ .$$

Theorem 4.1 *Assume that:*

(a_1) H_a *is weakly elliptic,*

(a_2) $\Gamma(a)$ *and* $\Gamma^2(a) \equiv \Gamma[\Gamma(a)]$ *are locally integrable,*

(a_3) $0 < \Gamma(a) \leq Ca$,

(a_4) *for any* $\xi, \eta \in \mathcal{D}(\mathbb{R}^N)^N$

$$\left|\int_{\mathbb{R}^N} \sum_{j,k} \Gamma^2(a)_{jk} \cdot \overline{\xi_j} \cdot \eta_k \mathrm{d}x\right| \leq C\Big(\int_{\mathbb{R}^N} \sum_{j,k} \Gamma(a)_{jk} \cdot \overline{\xi_j} \cdot \xi_k \mathrm{d}x\Big)^{1/2} \times$$
$$\times \Big(\int_{\mathbb{R}^N} \sum_{j,k} \Gamma(a)_{jk} \overline{\eta_j} \cdot \eta_k \mathrm{d}x\Big)^{1/2} .$$

Then H_a *has purely absolutely continuous spectrum.*

The proof is a straightforward verification of the hypothesis of Theorem 2.2 and has some points in common with the proof of Proposition 3.1. We shall not give further details here. Note the identifications $B = H_{\Gamma(a)}$, $\mathrm{i}[B, A_\gamma] = H_{\Gamma^2(a)}$, $\mathcal{G}^1 = D_a$, $\mathcal{G}^{-1} = D_a^*$, $\mathcal{B} = \dot{D}_{\Gamma(a)}$ and $\mathcal{B}^* = \dot{D}^*_{\Gamma(a)}$.

We give now some examples showing that absolute continuity of the spectrum is compatible with a quite wild behavior of the coefficients both locally and at infinity.

Example 4.1 $a_{jk} = a \cdot \delta_{jk}$, with $a = a_0(M + \sin\varphi)$, where $\varphi : \mathbb{R}^N \to \mathbb{R}$ is a smooth function, $a_0 : \mathbb{R}^N \to [0, \infty)$ a locally integrable function, homogeneous of degree $\beta \in \mathbb{R}$, strictly positive a.e., such that $q_a^{(0)}$ is closable. M is a positive constant. We take $\gamma = 1$ if $\beta < 2$ and $\gamma = -1$ if $\beta > 2$. The reason is that, for $\gamma = 1$, one has (set $\tilde{\varphi} = (x, \nabla\varphi)$ and $\tilde{\tilde{\varphi}} = (\tilde{\varphi})^{\sim} = (x, \nabla(x, \nabla\varphi))$)

$$\Gamma(a) = a_0\{(2-\beta)M + (2-\beta)\sin\varphi - \tilde{\varphi} \cdot \cos\varphi\}$$

and

$$\Gamma^2(a) = a_0\{(2-\beta)^2 M + [(2-\beta)^2 - \tilde{\varphi}^2]\sin\varphi + [\tilde{\tilde{\varphi}} - 2(2-\beta)\tilde{\varphi}]\cos\varphi \ .$$

The conclusion is that H_a *will have purely absolutely continuous spectrum if* $\beta \neq 2$, $\tilde{\varphi}$ *and* $\tilde{\tilde{\varphi}}$ *are bounded,* M *is big enough and* $q_a^{(0)}$ *is closable.*

If $\varphi = 0$, M may be any positive number. Let us write $a_0(x) = |x|^\beta \psi(\frac{x}{|x|})$ and suppose that $0 < c_1 \leq \psi(\omega) \leq c_2 < \infty$ for any $\omega \in S^{N-1}$, the unit sphere in $\mathbb{R}^N$. Then, in order to have $a \in L^1_{\mathrm{loc}}$ and the closability of $q_a^{(0)}$, it is enough that $\beta > -N$ (if $\beta > 0$, one takes $\Omega = 0$ in Lemma 3.1). If φ is a radial function, its constraints read: $\varphi'(r) \leq \frac{C}{r}$ and $\varphi''(r) \leq \frac{C}{r^2}$. Hence, for instance, we may allow $\varphi(r) = \ln r$ for big r. This shows that in the uniformly elliptic case ($\beta = 0$), a needs not have radial limits. However, if these limits exist, they may depend on the direction (take ψ nonconstant). Instead of $\sin\varphi$ we can set $\theta \circ \varphi$, with θ smooth and θ, θ', θ'' bounded. It is remarkable that β

may be non-null. The case $\beta > 2$ shows that in Lemma 4.2. the condition "H_a is elliptic" cannot be removed. It also shows an interesting effect. Take $\beta > 2$ and add to a any positive, C^∞-perturbation b with compact support, such that $b(0) \neq 0$. Then, by Lemma 4.2, H_{a+b} will have purely discrete spectrum.

In conclusion, if one has only weak ellipticity, the local behavior is very important and the spectral properties are very sensitive to perturbations. The annulations and singularities may occur also in nontrivial subspaces of $\mathbb{R}^N$. Write for example $\mathbb{R}^N \cong \mathbb{R}^{N_1} \times \ldots \times \mathbb{R}^{N_m} \ni x = (x_1, \ldots, x_m)$ and $a_0(x) = |x_1|^{\beta_1} \ldots |x_N|^{\beta_m} \cdot \psi_0(\frac{x}{|x|})$, where $\beta_j \in \mathbb{R}$, ψ_0 is smooth and $0 < c_1 \leq \psi(\omega) \leq c_2 < \infty$ for any $\omega \in S^{N-1}$. If $\beta_j > -N_j$, then a is locally integrable and $q_a^{(0)}$ is closable (take $\Omega = \{x \mid \exists j \text{ such that } \beta_j < 0 \text{ and } x_j = 0\}$ in Lemma 4.1). The only extra restriction is $\beta \equiv \sum_{j=1}^m \beta_j \neq 2$.

Example 4.2 $a_{jk} = \delta_{jk} \cdot a$, with $a(x) = \langle x \rangle^\beta \psi(\frac{x}{|x|})\{M + \sin\varphi(x)\}$. If φ and ψ are smooth, $0 < c_1 \leq \psi(\omega) \leq c_2 < \infty$ for all $\omega \in S^{N-1}$ and M is not too small (this depends on φ; any way, $M > 1$ is always enough), then H_a will be elliptic. For $\gamma = 1$, we have

$$\Gamma(a) =$$

$$\Big(2 - \beta\frac{|x|^2}{\langle x\rangle^2}\Big)\langle x\rangle^\beta \psi\Big(\frac{x}{|x|}\Big)[M + \sin\varphi(x)] - \langle x\rangle^\beta \psi\Big(\frac{x}{|x|}\Big)\tilde{\varphi}(x)\cos\varphi(x) \ .$$

If $\beta < 2$, then H_a has purely absolutely continuous spectrum if M is sufficiently big and $\tilde{\varphi}$, $\tilde{\tilde{\varphi}}$ are bounded. For $\beta = 2$, the same conclusion is obtained for $\varphi = 0$. If $\beta > 2$, the quantity $2 - \beta\frac{|x|^2}{\langle x\rangle^2}$ has opposite signs around 0 and infinity and there is no positivity. In fact, by Lemma 4.2, H_a has purely discrete spectrum.

Example 4.3 $a_{jk} = \delta_{jk} \cdot a_j$, with a_j a homogeneous function of degree β_j, such that H_a is weakly elliptic (some oscillations may also be added). If we work with $\gamma_{jk} = \delta_{jk}$, then we need $\beta_j < 2$ for all j, while $\gamma_{jk} = -\delta_{jk}$ requires $\beta > 2$ for all j. But with $\gamma_{jk} = \delta_{jk} \cdot \gamma_j$, the conditions are $\sum_{k=1}^N \beta_k \cdot \gamma_k < 2\gamma_j$ for any j and very often this is a gain. For instance, if $N = 2$, $\beta_1 = 3$ and $\beta_2 = 1$ we require $3\gamma_1 + \gamma_2 < 2\gamma_2$ and this has plenty of solutions (e.g. $\gamma_2 = 0$ and $\gamma_1 < 0$).

5 Second-Order Elliptic Differential Operators. The Perturbed Case

We add now some perturbations to H_a. The operators we have in view have the form

$$H(a, b, V) \equiv H_a + H^b + V(Q) \ , \tag{27}$$

where $V(Q)$ is the multiplication by the Borel function $V : \mathbb{R}^N \to \mathbb{R}$ and H^b is defined by

$$H^b \equiv \frac{1}{2}\{(b(Q), P) + (P, b(Q))\} \ . \tag{28}$$

Here $b \equiv (b_1, \ldots, b_N) : \mathbb{R}^N \to \mathbb{R}^N$ is locally integrable and (28) has an obvious meaning as a quadratic form on $\mathcal{D}(\mathbb{R}^N)$. We shall worry later about conditions making $H(a, b, V)$ a well-defined, self-adjoint operator in $\mathcal{H}(\mathbb{R}^N)$. For the moment, remark that formal calculations give

$$B \equiv \mathrm{i}[H(a, b, V), A_\gamma] = H(\Gamma(a), b_\gamma, -D_\gamma V) \tag{29}$$

and

$$\mathrm{i}[B, A_\gamma] = H(\Gamma^2(a), (b_\gamma)_\gamma, D_\gamma^2 V) \ ,$$

where $(b_\gamma)_j = (\gamma \cdot b - D_\gamma b)_j = \sum_{k=1}^N \gamma_{jk} b_k - \sum_{l,n=1}^N \gamma_{ln} x_l \partial_n b_j$, for any $j \in \{1, \ldots, N\}$. Hence, we need positivity criteria for operators as (29). Suppose first that an inequality of the form

$$H_\rho \geq W(Q) \tag{30}$$

is proved, with $\rho, W : \mathbb{R}^N \to [0, \infty)$ Borel functions, such that $\rho(x) > 0$ a.e. and H_ρ is weakly elliptic (H_ρ is a brief notation for $H_{\rho \cdot 1}$). Then, if $|b| \leq \sqrt{\rho \cdot W}$, we shall have

$$\langle f, H_\rho f\rangle \geq |\langle f, H^b f\rangle| \tag{31}$$

for any $f \in \mathcal{D}(\mathbb{R}^N)$, by a simple application of the Cauchy-Schwarz inequality:

$$\begin{aligned}\left|\frac{1}{2}\{\langle f, (b, P)f\rangle + \langle f, (P, b)f\rangle\}\right| &\leq \left|\sum_{j=1}^N \langle \frac{b_j}{\sqrt{\rho}} f, \sqrt{\rho} P_j f\rangle\right| \\ &\leq \langle f, H_\rho f\rangle^{1/2} \langle f, \frac{|b|^2}{\rho} f\rangle^{1/2}\end{aligned}$$

and it remains only to use (30). Hence, we need only conditions on ρ and W which entails (30). We shall use an easy generalization of an argument from (Faris 1978).

Lemma 5.1 *Let $\rho : \mathbb{R}^N \to \mathbb{R}$ such that $\frac{\rho}{|x|^2}$ and $\frac{\tilde{\rho}}{|x|^2}$ are locally integrable ($\tilde{\rho} \equiv (x, \nabla\rho)$). Assume that H_ρ is weakly elliptic and that $M(\rho) \equiv \frac{1}{2}[N - 2 + \inf(\tilde{\rho}/\rho)] > 0$. Then*

$$H_\rho \geq M(\rho)^2 \frac{\rho(Q)}{|Q|^2} \ . \tag{32}$$

Proof. For any $j, k \in \{1, \ldots, N\}$ we set $J_{jk} = Q_j P_k - Q_k P_j = P_k Q_j - P_j Q_k$, the (j, k)-component of the angular momentum. Some simple calculations show the decomposition of H_ρ into the sum of a radial and an angular term:

$$H_\rho = H_\rho^{\mathrm{rad}} + H_\rho^{\mathrm{ang}} = (P,Q)\frac{\rho(Q)}{|Q|^2}(Q,P) + \frac{1}{2}\sum_{j,k=1}^{N} J_{jk}\frac{\rho(Q)}{|Q|^2}J_{jk} \ .$$

Let us use the relation

$$0 \leq (A - \mathrm{i}B)^*(A - \mathrm{i}B) = A^*A + B^*B - \mathrm{i}(A^*B - B^*A)$$

for $A = \frac{\sqrt{\rho}(Q)}{|Q|}(Q,P)$ and $B = \beta\frac{\sqrt{\rho}(Q)}{|Q|}$. Then $A^*A = H_\rho^{\mathrm{rad}} \leq H_\rho$ and $\mathrm{i}(A^*B - B^*A) = \sum_{j=1}^{N} \mathrm{i}[P_j, \beta\frac{Q_j}{|Q|}\rho(Q)]$. This gives $H_\rho \geq \beta\big[N - 2 + \beta + \frac{\tilde{\rho}(Q)}{\rho(Q)}\big]\frac{\rho(Q)}{|Q|^2}$ and one gets (32) by taking $\beta = M(\rho)$. □

The next result relies on Theorem 2.2, on the considerations above and on some routine verifications. We use notations introduced before.

Theorem 5.1 *Assume that H_a satisfies* (a_1)-(a_2)-(a_3)-(a_4) *from Theorem* 4.1 *and*

(a_5) *There exists a function $\rho : \mathbb{R}^N \to [0,\infty)$, strictly positive a.e., such that $\frac{\rho}{|x|^2}$ and $\frac{\tilde{\rho}}{|x|^2}$ are locally integrable, $M(\rho) > 0$ and $\Gamma(a) \geq \rho \cdot 1$.*

Let also $b : \mathbb{R}^N \to \mathbb{R}^N$ and $V : \mathbb{R}^N \to \mathbb{R}$ be locally integrable functions such that for positive constants α_1, α_2, β_1, β_2, γ_1, γ_2 with $\alpha_1 + \alpha_2 < 1$ and $\beta_1 + \beta_2 < 1$ one has:

(b_1) *H^b is bounded in form-sense with respect to H_a, with relative bound α_1,*

(b_2) $|b_\gamma| \leq \beta_1 M(\rho)\frac{\rho}{|x|}$,

(b_3) $|(b_\gamma)_\gamma| \leq \gamma_1\frac{\rho}{|x|}$,

(c_1) *$V(Q)$ is bounded in form-sense with respect to H_a, with relative bound α_2 ,*

(c_2) $|D_\gamma V| \leq \beta_2 M(\rho)^2\frac{\rho}{|x|^2}$,

(c_3) $|D_\gamma^2 V| \leq \gamma_2\frac{\rho}{|x|^2}$.

Then $H(a,b,V)$, defined as a form-sum, is self-adjoint and has purely absolutely continuous spectrum.

There is also a γ-repulsive version with respect to V. One can make (b_1) and (c_1) explicit in the same spirit as above. It is sufficient that $a \geq \sigma \cdot 1$, where σ has the same properties as ρ,

(b_1') $b = b^{(1)} + b^{(2)}$, with $\frac{|b^{(1)}|}{\sqrt{\sigma}} \in L^\infty(\mathbb{R}^N)$ and $|b^{(2)}| \leq \alpha_1 M(\sigma)\frac{\sigma}{|x|}$, and

(c_1') $V = V^{(1)} + V^{(2)}$, with $V^{(1)} \in L^\infty(\mathbb{R}^N)$ and $|V^{(2)}| \leq \alpha_2 M(\sigma)^2\frac{\sigma}{|x|^2}$.

We shall try now to convince the reader that the conditions imposed on the coefficients are rather mild, especially in what concerns their long-distance behavior. Let us come back to Example 4.1:

$$a_{jk}(x) = \delta_{jk} \cdot |x|^\beta \psi\Big(\frac{x}{|x|}\Big)[M + \sin\varphi(x)] \ ,$$

where $\beta \in (-N, 2) \cup (2, \infty)$, $0 < c_1 \leq \psi(\cdot) \leq c_2 < \infty$ and $\tilde{\varphi}$, $\tilde{\tilde{\varphi}}$ are bounded. If M is big enough, one may take $\sigma(x) = d_1|x|^\beta$ and $\rho(x) = d_2|x|^\beta$ for two positive constants d_1 and d_2. Since $M(\rho) = M(\sigma) = \frac{N-2+\beta}{2}$, we are restricted to $\beta \in (2-N, \infty) \setminus \{2\}$. The conditions on b and V reads now:

(b_1'') $b = b^{(1)} + b^{(2)}$, with $|b^{(1)}| \leq \delta_1 r^{\beta/2}$, $|b^{(2)}| \leq \delta_2 r^{\beta-1}$

(b_2'') $|\partial_r b| \leq \delta_3 r^{\beta-2}$

(b_3'') $|\partial_r^2 b| \leq \delta_4 r^{\beta-3}$

(c_1'') $V = V^{(1)} + V^{(2)}$, with $|V^{(1)}| \leq \delta_5$ and $|V^{(2)}| \leq \delta_6 r^{\beta-2}$

(c_2'') $|\partial_r V| \leq \delta_7 r^{\beta-3}$

(c_3'') $|\partial_r^2 V| \leq \delta_8 r^{\beta-4}$

where $\delta_1, \ldots, \delta_8$ are suitable constants and we set $r = |x|$. Note that, if β is large enough, the coefficients are allowed to diverge at infinity. From the estimate $|\partial_r \varphi| \leq \delta r^\alpha$ with $\alpha < -1$ it follows that φ has radial limits $\varphi(\infty \cdot \omega) \equiv \lim_{r \to \infty} \varphi(r \cdot \omega)$ for any $\omega \in S^{N-1}$ (the unit sphere in $\mathbb{R}^N$) to which it converges as $r^{\alpha+1}$. The limits may depend on ω. This works for V if $\beta \in (2-N, 2)$ and for b if $\beta \in (0, 1)$. Even more anisotropy is permitted by the more clever choices $\sigma(x) = d_1|x|^\beta \psi(\frac{x}{|x|})$. If the coefficients of the main term behave very different in different directions (like $|x_1|^{\beta_1} \ldots |x_N|^{\beta_N}$ for example), the same is allowed for b and V. Important local singularities are also available.

There are cases where it is enough to use arguments as above only in a proper subspace Y of $\mathbb{R}^N$, in some analogy with Example 3.4. The behavior of the coefficients b and V in the Y-variable will be restricted as already explained, but there will be only very mild conditions along $Y^\perp$. We will not develop this here. The important case where $a_{jk} = \delta_{jk}$ (Schrödinger operators) was described in detail from this point of view in (Boutet de Monvel, Kazantseva, Mantoiu 1996). However we did not include a first-order term there.

Note added in proof

After we proved the abstract results of Chapter 2 (which improve on those in (Boutet de Monvel, Kazantseva, Mantoiu 1996) we learned of (Combes, Hislop, Mourre 1996) in which a version of Theorem 2.1 is obtained.

References

Amrein W.O., Boutet de Monvel A., Georgescu V. (1996): *C_0-Groups, Commutator Methods and Spectral Theory of N-Body Hamiltonians*, Progress in Math. **135** (Birkhäuser, Basel)

Boutet de Monvel-Berthier A., Georgescu V. (1992): Some Developments and Applications of the Abstract Mourre Theory, in "Méthodes semi-classiques", vol. 2 (Colloque international, Nantes, juin 1991), Astérisque **210**, 27–48

Boutet de Monvel A., Georgescu V., Mantoiu M. (1993): Locally Smooth Operators and the Limiting Absorption Principle for N-Body Hamiltonians, Reviews in Math. Physics **5**, 105–189

Boutet de Monvel A., Kazantseva G., Mantoiu M. (1996): Some Self-adjoint Operators without Singular Spectrum, Helv. Phys. Acta **69**, 13–25

Combes J.-M., Hislop P.D., Mourre E. (1996): Spectral Averaging, Perturbation of Singular Spectrum and Localisation, Trans. Amer. Math. Soc. (to appear)

Davies E.B. (1989): *Heat Kernels and Spectral Theory* (Cambridge University Press, Cambridge)

Faris W. (1978): Inequalities and Uncertainty Principles, J. Math. Phys. **19**, 461–466

Kato T. (1968): Smooth Operators and Commutators, Studia Math. **31**, 535–546

Mourre E. (1981): Absence of Singular Continuous Spectrum for Certain Self-adjoint Operators, Comm. Math. Phys. **78**, 391–408

Putnam C. (1967): *Commutation Properties of Hilbert Space Operators and Related Topics*, (Springer Verlag, Berlin, New York)

Röckner M., Wielens N. (1985): Dirichlet Forms-Closability and Change of Speed Measure, in "Infinite Dimensional Analysis and Stochastic Processes", Albeverio S. ed., Research Notes in Mathematics **124** (Pitman), 119–144.

Simon B. (1979): *Trace Ideals and Applications*, Lecture Notes (Cambridge University Press, Cambridge).

Triebel H. (1978): *Interpolation Theory, Function Spaces, Differential Operators* (VEB Deutscher-Verlag, Berlin)

Solutions to the Hierarchy of the Periodic Toda Lattices

L. Trlifaj

Institute of Physics, Na Slovance 2, Praha 8 - 18040
Czech Republic

Abstract. The hierarchy of the periodic Toda lattices is derived by means of the Appelle transformation. Members of the hierarchy are determined by equations of motion, by Hamiltonians and Lax pairs. Only two- and three-particle systems besides the basic Toda lattice are solved by quadratures in accordance with the Stäckel theorem. Other members of the hierarchy assume the solving of the polynomial equation, the degree of which is higher than four.

1 Introduction

The periodic Toda lattice describes the motion of $g+1$ point masses on the circle or on the line with periodic repetition under the influence of an exponential force. This motion is characterized by (utmost) $g+1$ conserved quantities which are in mutual involution with respect to the usual Poisson bracket. Any of the quantities can be taken as a Hamiltonian, in this simple way one constructs a hierarchy. The systematic way of constructing a hierarchy for the finite (but open) Toda lattices was given in 1.

We make use of the Appelle transformation 2 when constructing a hierarchy. Any member of the hierarchy of the periodic Toda lattices is determined by the equations of motion, which we write down also in the Hamiltonian form. It is easy then to derive the Lax pair for each of the members. The proof of the explicit integrability is made easy by the auxiliary discrete Hill's equation i.e. by the matrix L, which is common to the whole hierarchy. Consequently particle momenta for different members of the hierarchy depend on the location in the lattice in the same way, they differ only by the time dependence, which is, however, independent on this location. The two- and three-particles ($g = 1, 2$) periodic Toda systems are integrated by means of quadratures for any member of the hierarchy in accordance with the Stäckel theorem, 3, 4. Other systems of the hierarchy cannot be integrated by means of quadratures as they assume, that the polynomial equation, the degree of which is higher than four,has to be solved.

2 The Appelle Transformation

The equations of motion for the basic periodic Toda lattice read 5

$$\dot{a}_n = a_n(b_n - b_{n+1}) \ , \qquad \dot{b} = 2(a_{n+1}^2 - a_n^2) \ , \tag{1}$$

where

$$a_n = a_{n+g+1} = \tfrac{1}{2}\exp[\tfrac{1}{2}(q_n - q_{n+1})], \quad b_n = \tfrac{1}{2}p_n = b_{n+g+1},$$
$$\text{as} \quad q_n = q_{n+g+1}, \quad p_n = p_{n+g+1} \quad (n = -\infty, \ldots, +\infty) \ . \tag{2}$$

The Lax pair, which corresponds to (1), is

$$\dot{L} = BL - LB, \quad L\psi = \lambda\psi \ . \tag{3}$$

The explicit form of the second equation

$$a_n\psi(n+1) + b_n\psi(n) + a_{n-1}\psi(n-1) = \lambda\psi(n) \quad (n = -\infty, \ldots, +\infty) \tag{4}$$

the auxiliary discrete function $\psi(n)$ satisfies is a discrete version of the periodic Hill's equation with the spectral parameter λ. Therefore L and B in the first equation are formally represented by infinite matrices of which the elements with indices equal modulo $g+1$ are equal. Their only nonzero elements are

$$L_{n,n-1} = a_{n-1}, \ L_{n,n} = b_n,$$
$$L_{n,n+1} = a_n, \ B_{n+1,n} = -B_{n,n+1} = a_n, \ B_{n,n} = 0 \ . \tag{5}$$

If one assumes that λ is a time-independent parameter, the time evolution of $\psi(n)$ is given by the following equation

$$L[\dot{\psi} - B\psi] = \lambda[\dot{\psi} - B\psi] \ . \tag{6}$$

There are two independent solutions of (4) (as well as of (6)) $\alpha(n, N)$ and $\beta(n, N)$, which are defined by the boundary conditions

$$\alpha(N, N) = 0 = \beta(N+1, N), \ \alpha(N+1, N) = 1 = \beta(N, N) \ . \tag{7}$$

They are polynomials in λ of the degree $l-1$ and $l-2$ respectively for $n = N + l$ $(l > 1)$. We introduce 3-by-3 matrix

$$\Omega(n, N) =$$

$$\begin{bmatrix} \beta^2(n,N) & \beta(n,N)\alpha(n,N) & \alpha^2(n,N) \\ 2\beta(n,N)\beta(n+1,N) & \beta(n+1,N)\alpha(n,N)+\beta(n,N)\alpha(n+1,N) & 2\alpha(n,N)\alpha(n+1,N) \\ \beta^2(n+1,N) & \beta(n+1,N)\alpha(n+1,N) & \alpha^2(n+1,N) \end{bmatrix} \tag{8}$$

which obeys the equation

$$\Omega(n+1, N) = V(n)\Omega(n, N) \tag{9}$$

according to (4). The 3-by-3 matrix V(n) is

$$V(n) = \begin{bmatrix} 0 & 0 & 1 \\ 0 & -\frac{a_n}{a_{n+1}} & 2\frac{\lambda - b_{n+1}}{a_{n+1}} \\ \frac{a_n^2}{a_{n+1}^2} & -\frac{a_n(\lambda - b_{n+1})}{a_{n+1}^2} & \frac{(\lambda - b_{n+1})^2}{a_{n+1}^2} \end{bmatrix} . \tag{10}$$

Eq. (9) corresponds to a discrete Appelle transformation 2 of (4) as any of the elements in the first row of (8) satisfies a third-order linear difference (recurrence) relation,which results from (9). Columns of (8) represent also three independent solutions of (9).

Some simple relations follow from the form (8) and (9), respectively:

$$\Omega(n,n) = 1, \ \det \Omega(n,N) = \frac{a_N^3}{a_n^3},$$
$$\Omega(n,N) = V(n-1)V(n-2)\dots V(N) \quad (n > N) . \tag{11}$$

One of the three different eigenvalues of $\Omega(n,N)$ is $\frac{a_N}{a_n}$. If $n = N+g+1$ the 3-by-1 eigenmatrix, which belongs to the unit $(\frac{a_N}{a_N})$ eigenvalue, is

$$\tilde{T}(N) = \left(\frac{\alpha(N+g+1,N)}{a_N} , \frac{\alpha(N+g+2,N) - \beta(N+g+1,N)}{a_N} , \frac{\alpha(N+g+2,N+1)}{a_{N+1}} \right) . \tag{12}$$

The product $\Omega(n,N)T(N)$ is a solution of (9), but

$$\Omega(n+g+1,n)\Omega(n,N)T(N) = \Omega(n+g+1,N)T(N) =$$
$$\Omega(n+g+1,N+g+1)\Omega(N+g+1,N)T(N) = \Omega(n,N)T(N) \tag{13}$$

due to the last relation in (11). In other words

$$T(n) = \Omega(n,N)T(N) \tag{14}$$

as a function of the discrete coordinate n satisfies (9), it is its periodic solution, $T(n+g+1) = T(n)$. The elements of $T(n)$ are polynomials in λ, their root forms read

$$\tilde{T}(N) =$$
$$2^{g+1}\Big(\prod_{l=1}^{g}[\lambda - \mu_l(n)], \ a_n^{-1}\prod_{l=1}^{g+1}[\lambda - \nu_l(n)], \ \prod_{l=1}^{g}[\lambda - \mu_l(n+1)]\Big) =$$
$$2^{g+1}\Big(\sum_{l=0}^{g}(-1)^{g-l}\tau_{g-l}(n)\lambda^l, \ a_n^{-1}\sum_{l=0}^{g+1}(-1)^{g-l+1}\gamma_{g-l+1}(n)\lambda^l,$$
$$\sum_{l=0}^{g}(-1)^{g-l}\tau_{g-l}(n+1)\lambda^l\Big) . \tag{15}$$

$\tau_l(n)$ and $\gamma_l(n)$ respectively are elementary symmetric functions of roots $\mu_l(n)$ and $\nu_l(n)$ respectively, $\tau_0(n) = \gamma_0(n) = 1$.The 3 by 3 matrix J

$$J = \begin{bmatrix} 0 & 0 & 2 \\ 0 & -1 & 0 \\ 2 & 0 & 0 \end{bmatrix} \tag{16}$$

builds up invariants for solutions of (9) as

$$a_n^2 \tilde{\Omega}(n,N) J \Omega(n,N) = a_N^2 J \ . \tag{17}$$

The expression

$$a_n^2 \tilde{T}(n) J T(n) =$$

$$-2^{2g+2} \prod_{l=1}^{2g+2} (\lambda - \lambda_l) = -2^{2g+2} \sum_{l=0}^{2g+2} (-1)^l \sigma_{2g-l+2} \lambda^l \tag{18}$$

is thus a constant polynomial of the degree $2g+2$ according to (15). This polynomial is equal to

$$-F^2(\lambda) + 4 = -[\alpha(n+g+2,n) + \beta(n+g+1,n)]^2 + 4 \tag{19}$$

as far as with respect to (4) and (7) the relation

$$a_n \alpha(n+g+2, n+1) = -a_{n+1} \beta(n+g+2, n) \tag{20}$$

and the Wronskian relations for $\alpha(n)$ and $\beta(n)$ are used. This means that only $g+1$ roots from $\lambda_1, .., \lambda_{2g+2}$ are independent. We assume for the sake of simplicity, that there are no multiple roots (i.e. $\lambda_l \neq \lambda_l'$), which is, in general, possible (see 5 e.g.). The roots μ_l $(l = 1, ..., g)$ introduced in (15) lie within those intervals of λ, for which $F^2(\lambda) > 4$, as then only both sides of (18) possess the same (negative) sign. One arrange them in such a way, that

$$\lambda_1 < \lambda_2 \leq \mu_1(n) < \lambda_3 < ... < \lambda_{2g-1} < \lambda_{2g} \leq \mu_g(n) \leq \lambda_{2g+1} < \lambda_{2g+2} \ . \tag{21}$$

According to (14) $T_1(n) = a_n^{-1} \alpha(n+g+1, n)$ is a quadratic form of $\alpha(n,N)$ and $\beta(n,N)$, so that it can be written as a product of two solutions $\chi_\pm(n,N)$ of (4)

$$\chi_\pm(n,N) = 2^{-1}[a_n \alpha(N+g+1,N]^{-\frac{1}{2}} \times$$
$$\{2\alpha(N+g+1,N)\beta(n,N) + [\alpha(N+g+2,N) - \beta(N+g+1,N)]\alpha(n,N)$$
$$\pm (\sqrt{F^2(\lambda)-4}).\alpha(n,N)\} \ . \tag{22}$$

Since $T_1(n)$ is periodic

$$\chi_\pm(n+g+1,N) = P^{\pm 1}(\lambda) \chi_\pm(n,N) \ . \tag{23}$$

Solutions $\chi_\pm(n,N)$ are the well-known Bloch solutions of (4) (see 5 e.g.). One determines $P(\lambda)$ from comparison of $\chi_\pm(N+g+1,N)$ with $\chi_\pm(N,N)$, i.e.

$$2P(\lambda) = F(\lambda) \mp \sqrt{F^2(\lambda)-4} \ . \tag{24}$$

In the allowed bands of real λ, for which $F^2(\lambda) < 4$, (22) represent bounded complex functions for any n. In the forbidden bands characterized by $F^2(\lambda) > 4$, (22) are unbounded and real functions. Parameter λ plays, indeed, role of the spectral parameter.

3 The Time Evolution and the Hierarchy

We have still to determine the time dependence of the special solution (14). Since $T(n)$ is periodic and does not depend on the boundary conditions of type (7), its time-evolution equation reads unlike (6),

$$\dot{T}(n) = W(n)T(n) \tag{25}$$

where the 3×3 matrix $W(n)$ must be still determined. (25) is compatible with (9) and (18) if

$$\dot{V}(n) + V(n)W(n) - W(n+1)(n) = 0 \tag{26}$$

and

$$W(n) = \begin{bmatrix} f_n & g_n & 0 \\ \frac{-2a_n}{a_{n+1}} g_{n+1} & \frac{\dot{a}_n}{a_n} & 2g_n \\ 0 & \frac{a_n}{a_{n+1}} g_{n+1} & -f_n - \frac{2\dot{a}_n}{a_n} \end{bmatrix} \tag{27}$$

At the same time the time derivatives of a_n and b_n are given by f_n's and g_n's,

$$\begin{aligned} 2\dot{a}_n &= -(f_n + f_{n+1})a_n - \frac{2a_n(\lambda - b_{n+1})}{a_{n+1}} g_{n+1} \\ \dot{b}_{n+1} &= -a_n g_n + (\lambda - b_{n+1}) f_{n+1} + \frac{(\lambda - b_{n+1})^2}{a_{n+1}} g_{n+1} + \frac{a_{n+1}^2}{a_{n+2}} g_{n+2} \ . \end{aligned} \tag{28}$$

There are an infinite number of ways to fulfil (28). We limit ourselves to polynomials in λ. They are characterized and thus classified by the maximum chosen power of f_n. If its power is k, the maximum power of g_n is $k-1$. The coefficients f_n, g_n and a_n, b_n must be calculated directly from (28) for $k = 1, 2$. $k = 1$ defines the basic Toda lattice. When $k \geq 3$, we write

$$\begin{aligned} f_n &= \lambda^k + \sum_{l=1}^{k-2} r_{k-l}^l(n) + \rho_k(n), \\ g_{n+1} &= -a_{n+1}\{\lambda^{k-1} + \sum_{l=0}^{k-2} R_{k-l}(n)\lambda^l\} \ . \end{aligned} \tag{29}$$

Comparing coefficients at the same powers of λ in (28) one obtains

$$\begin{aligned} R_2(n) &= b_{n+1}, r_2(n) = 2a_n^2, r_3(n) = 2a_n^2(b_n + b_{n+1}), \\ R_{p+1}(n) &= b_{n+1}R_p(n) + \frac{1}{2}[r_p(n) + r_p(n+1)], (k-1 \geq p \geq \lambda), \\ r_{p+1}(n+1) - r_{p+1}(n) &= [r_p(n+1) - r_p(n)]b_{n+1} + 2a_{n+1}^2 R_p(n+1) \\ &\quad -2a_n^2 R_p(n-1), (k-2 \geq p \geq 2) \ , \end{aligned} \tag{30}$$

$$\rho_k(n+1) =$$

$$- b_{n+1}r_{k-1}(n) + a_{n+1}^2 R_{k-1}(n+1) - a_n^2 R_{k-1}(n-1) - b_{n+1}^2 R_{k-1}(n) \quad (31)$$

$$\frac{\dot{a}_n}{a_n} = -b_{n+1}R_k(n) - \frac{1}{2}[\rho_k(n) + \rho_k(n+1)],$$
$$\dot{b}_n = -b_{n+1}\rho_k(n+1) - a_{n+1}^2 R_k(n+1) + a_n^2 R_k(n-1) - b_{n+1}^2 R_k(n) \ . \quad (32)$$

The recurrence relations (30) for a chosen k can be solved in an algorithmic way, preferably using a computer. If we use (30) without the limitation and take them as an infinite system, then

$$\frac{\dot{a}_n}{a_n} = -\frac{1}{2}\dot{q}_{n+1} + \frac{1}{2}\dot{q}_n = -\frac{1}{2}R_{k+1}(n) + \frac{1}{2}R_{k+1}(n-1),$$
$$\dot{b}_n = \frac{1}{2}\dot{p}_n = \frac{1}{2}r_{k+1}(n-1) - \frac{1}{2}r_{k+1}(n) \ . \quad (33)$$

These equations give the equations of motion for the members of the hierarchy classified by k. According to these equations

$$\dot{q}_n = \frac{\delta\mathcal{H}(k)}{\delta p_n} = \frac{1}{2}\frac{\delta\mathcal{H}(k)}{\delta b_n} = R_{k+1}(n-1) + \text{const.},$$
$$\dot{p}_n = -\frac{\delta\mathcal{H}(k)}{\delta q_n} = -\frac{1}{2}a_n\frac{\delta\mathcal{H}(k)}{\delta a_n} + \frac{1}{2}a_{n-1}\frac{\delta\mathcal{H}(k)}{\delta a_{n-1}},$$
$$\text{i.e.} \quad a_n\frac{\delta\mathcal{H}(k)}{\delta a_n} = 2r_{k+1}(n-1) + \text{const.} \quad (34)$$

We determine the Hamiltonian $\mathcal{H}(k)$ which corresponds to the k-th member of the hierarchy by applying the well-known theorem for homogenous functions, since $r_{k+1}(n)$ and $R_{k+1}(n-1)$ are known as homogenous forms. Therefore

$$\mathcal{H}(k) = 2k\sum_n [b_n R_{k+1}(n-1) + r_{k+1}(n)] = 2k\sum_n R_{k+2}(n) \quad (35)$$

from (30) and the periodicity of the lattice.

One can also easily show that $\mathcal{H}(k)$ are mutually in involution to different k with respect to the Poisson brackets. There are $g+1$ constant and independent $\mathcal{H}(k)$. They are proportional to the traces over one period $Tr(L^{k+1})$ as these traces are constants and homogeneous forms in a_n's and b_n's.

The Lax pair

$$L = B(k)L - LB(k), L\psi = \lambda\psi \quad (36)$$

for the hierarchy can be derived in a similar way, the common quantity L makes it easy. We have

$$\dot{b}_n = 2B_{n,n+1}(k) - 2B_{n-1,n}(k) = \frac{1}{2}r_{k+1}(n) - \frac{1}{2}r_{k+1}(n-1),$$

$$\text{i.e.} \quad \mathrm{B_{n,n+1}(k)} = -\frac{1}{4}\mathrm{r_{k+1}(n)},$$

$$\dot{a}_n = a_{n+1}B_{n,n+2}(k) - a_{n-1}B_{n-1,n+1}(k) + [b_{n+1} - b_n]B_{n,n+1}(k) = \frac{a_n}{2}[R_{k+1} - R_{k+1}(n-1), \quad (37)$$

and for $S_{n,n+p}(k) = a_n \ldots a_{n+p-1}B_{n,n+p}(k)$, $(p > 2)$, we get

$$S_{n,n+p}(k) - S_{n-1,n-1+p}(k) = (b_n - b_{n-1+p})S_{n,n-1+p}(k) + a_n^2 S_{n+1,n-1+p}(k) - a_{n-2+p}^2 S_{n,n-2+p}(k). \quad (38)$$

These difference equations are solved in a similar way to (30). The result of the calculation is that $S_{n,n+p}(k)$, i.e. $B_{n,n+p}(k)$, are zero for $p \geq k+1$. This result follows from the formulae in the paper 6 which are based on the strictly triangular parts of L^k.

4 The Integration and the Conclusion

Now, we perform the integration of equations of motion (33) in an analogical way to the integration of the basic $(k = 1)$ Toda lattice since the matrix L is fixed for the whole hierarchy.

We proceed in four steps. It follows from both (8) and (9) that

$$b_n = -\sum_{l=1}^{g} \mu_l(n) + \frac{1}{2}\sum_{l=1}^{2g+2} \lambda_l \ . \quad (39)$$

As far as there are g independent roots $\mu_l(n)$ $(l = 1, \ldots, g)$ for a fixed n, we have to determine the dependence of $\mu_{l'}(n')$ for $n \neq n'$ and $l \neq l'$ on these $\mu_l(n)$. But this problem is common to the whole hierarchy. Its solution for the basic Toda lattice is known as the Jacobi inverse problem. So we use it in the sequel. We give only final formulae (see e.g. 5, 7 and 8). The Riemann surface of the hyper elliptic curve 7

$$\mathcal{Y}^2 = R(\lambda) = \prod_{l=1}^{2g+2} (\lambda - \lambda_l) \quad (40)$$

is realized by cross-connecting two copies of the λ-plains which are cut along $(\lambda_{2l-1}, \lambda_l)$ $(l = 1 \ldots, g+1)$. On this surface, one takes a closed contour α_l $(l = 1 \ldots, g)$ which surrounds the cut $(\lambda_{2l+1}, \lambda_{2l+2})$ on the upper sheet. One uses also a second set of similar contours, β_l, that start at λ_2 and go on the upper sheet of S as far as λ_{2l+1}, cross the lower sheet and end at λ_2. One introduces a base of the Abelian differentials (of the first kind)

$$\omega_j = \sum_{l=0}^{g-1} c_{jl}\lambda^l R^{-\frac{1}{2}}(\lambda)d\lambda \quad (j = 1, \ldots, g) \tag{41}$$

normalized by

$$\int_{\alpha_l} \omega_j = -i\pi\delta_{jl} \ , \tag{42}$$

so that c_{jl} are real. The matrix (τ_{jl}) defined by

$$\int_{\beta_j} \omega_l = \tau_{jl} \quad (j, l = 1, \ldots, g) \tag{43}$$

is also real and symmetric, a negative-definite matrix. The multi-dimensional Riemann function

$$\theta(\overline{u}) = \sum_{m_1,\ldots,m_g}^{\infty} exp[2\sum_{j=1}^{g} m_j u_j + \sum_{j,l=1}^{g} m_j \tau_{jl} m_l] \tag{44}$$

$$\overline{u} = (u_1, \ldots, u_g) \in C^g \tag{45}$$

is then well-defined, too. We also introduce two vectors $\overline{c}$ and $\overline{d}(t)$ besides $\overline{u}$ by

$$\overline{c} = (c_1, \ldots, c_g) = -(\int_{\infty}^{\infty'} \omega_1, \ldots, \int_{\infty}^{\infty'} \omega_g) \ , \tag{46}$$

where the point corresponding to the point ∞ on the other sheet is denoted by ∞'. The time dependence of $\overline{d}(t)$ is determined later on. The solution of the Jacobi problem reads (see 5 and 7)

$$b_n(t) = b\sum_{j=1}^{g} c_{j\,g-1}\frac{d}{du_j} b_n\{\theta(n\overline{c} + \overline{d}(t))\theta^{-1}((n+1)\overline{c} + \overline{d}(t))\} \ , \tag{47}$$

where b is a constant and one differentiates with respect to the argument u_j defined in (45). Inserting (15) in the first row of (25), and taking into account (18), one obtains

$$\dot{\mu}_l(n) = \prod_{l\neq j=1}^{g} [\mu_l(n) - \mu_j(n)]^{-1} R^{\frac{1}{2}}(\mu_l(n)) a_n^{-1} g_r(\mu_l(n)) \ . \tag{48}$$

Here, we stress the dependence of g_n on $\mu_l(n)$ since g_n is a polynomial in $\lambda = \mu_l(n)$ according to (29). Now, the time derivative of $\overline{d}(t)$ follows from 5, 7, and is given by the equations

$$\overline{d}(t) = \pm \sum_{l=1}^{g} \dot{\mu}_l(n) \sum_{s=0}^{g-1} c_{j\,s} \mu_l^s(n) R^{-\frac{1}{2}}(\mu_l(n)) =$$

$$\sum_{s=0}^{g-1} c_{j\,s} \sum_{l=1}^{g} \frac{\mu_l^s(n)}{\prod_{l\neq j=1}^{g}[\mu_l(n) - \mu_j(n)]} \{\mu_l^{k-1}(n) + \sum_{m=0}^{k-2} R_{l-m}(n-1)\mu_l^m(n)\} \tag{49}$$

according to (48) and (29). The sum in the last expression

$$M(r,g) = \sum_{l=1}^{g} \frac{\mu_l^s(n)}{\prod_{l\neq j=1}^{g}[\mu_l(n) - \mu_j(n)]} = \frac{V(r,g)}{V(g-1,g)} \tag{50}$$

equals $S(r-g+1)$ for $r \geq g-1$, and vanishes otherwise. Here, $V(g-1,g)$ denotes the Vandermond's determinant

$$V(g-1,g) = \begin{vmatrix} \mu_1^{g-1}(n) \ldots & 1 \\ \ldots & \ldots \\ \mu_g^{g-1}(n) \ldots & 1 \end{vmatrix} \tag{51}$$

and $V(r,g)$ is the modified Vandermond's determinant in which the column $(\mu_1^{g-1}(n), \ldots, \mu_g^{g-1}(n))$ is replaced by $(\mu_1^r(n), \ldots, \mu_g^r(n))$. $S(m)$, $(m = r-g+1)$ is a symmetric function,

$$S(m) = \sum_{l_1+l_2+\ldots+l_g=m} \mu_1^{l_1}(n) \ldots \mu_g^{l_g}(n) \quad (S(0) = 0) \ , \tag{52}$$

which can be expressed by means of $\tau_j(n)$ from (15). But $\tau_j(n)$ $(j = 1, \ldots, g)$ can be expressed by means of different a_m's and b_m's, and finally by the elementary symmetric functions τ_j, $(j = 1, \ldots, 2g)$ from (18). However, the dependence on a_m's and b_m's is eliminated in (49), so that (49) can easily be integrated,

$$d_j(t) = -\sum_{s=0}^{g-1} c_{j\,s} \Lambda_s t + d_j(0) \quad (j = 1, \ldots, g) \ , \tag{53}$$

where Λ_s are determined by the elementary symmetric $\tau_j(n)$, i.e. by constants of motion.

We demonstrate the integrability for the periodic two-particle system and the $k = 4$ member of the hierarchy. Then

$$d_j(t) = \frac{1}{4} P E c_{j0} t + d_j(0) \quad (j = 1, \ldots, g) \ , \tag{54}$$

where P and E are constants of motion which are proportional to the total momentum and energy of the system.

In general, there are three possibilities:

1) The basic Toda lattice, when $\sum_{j=1}^{g} c_{j,g-1} \frac{d}{du_j} = \frac{d}{dt}$ and $p_n = \dot{q}_n$. The last equality then allows a simple integration in (21), one obtains explicit formulae for p_n and q_n.

2) The periods of the lattice are $g = 1$ and $g = 2$. Then we use the relation $a_n^2 a_{n+1}^2 = \frac{1}{4}$ and $a_n^2 a_{n+1}^2 a_{n+2}^2 = \frac{1}{8}$, respectively, and eliminate a_{n+1}^2 and a_{n+2}^2, respectively, from the lowest constant Hamiltonians, conserved quantities (the total energy etc.) of the system in which one inserts (21) for b_n. Such expressions are equations of degree two and three, respectively, for some unknown a_n^2. They can therefore explicitly be solved. The calculated values along with (21) for b_n are inserted in $R_{k+1}(n-1)$ and thus also determine

$$q_n(t) = \int_0^t dt R_{k+1}(n-1) + \dot{q}_n(0) + q_n(0)$$

by quadrature. The integration of the two and three particle system is reduced to quadratures. This conclusion agrees with the theorems of Liuville and Stäckel of the classical mechanics (see also 3, 4). Nevertheless, unlike the classical case, Hamiltonians in which not only quadratic moments of motion appear, are admitted.

3) The integration of the remaining Toda lattice assumes that the equations of degree higher than four are to be solved. As is well-known, this is not possible in general. Therefore, these lattices are integrable only in principle, but not explicitly.

References

Ashok D., and Susumo O. (1989), Ann. Phys.(N.Y.) **158**, 215.
Appelle M. (1882), Comptes Rendus Acad. Sci. Paris **91**, 212.
Levi-Civita T., and Amaldi U. (1927): *Lezioni di Mecanica Razionale,* Vol.II, Bologna 1927.
Pars L.A. (1964): *A Treatise on Analytical Dynamics,* Heinemann, London 1964.
Toda M. (1981): *Theory of Nonlinear Lattices,* Springer Vlg., Berlin, 1981.
Kadoma Y., and Ye J. (1996), Physics **D 91**, 324.
Date E., and Tanaka S. (1976), Prog. Theor. Phys. Suppl. **59**, 107.
Dubrovin B.A. (1981), Uspekhi Mat. Nauk **36**, 11.

Spectrum Generating Algebras and Dynamic Symmetries in Scattering

F. Iachello

Center for Theoretical Physics, Sloane Laboratory
Yale University, New Haven, CT 06520-8120 USA

Abstract. The role of spectrum generating algebras and dynamic symmetries in the study of scattering processes is briefly reviewed.

1 Introduction

Spectrum generating algebras (SGA) and dynamic symmetries (DS) have been extensively used in the study of bound state problems. Two notable examples are: (i) the study of collective states in nuclei (interacting boson model) with spectrum generating algebra $U(6)$[1] and (ii) the study of rotations and vibrations of molecules (vibron model) with spectrum generating algebra $U(4)$[2]. In general, it has been found that, for bound state problems in ν dimensions with a finite number of states, a convenient SGA is $U(\nu+1)$. The two examples mentioned above correspond to $\nu = 5$ and $\nu = 3$ respectively. In the SGA approach to bound states, the Hamiltonian, H, and other operators, T, are expanded onto elements of a Lie algebra, $G_\alpha \in \mathcal{G}$,

$$H = f(G_\alpha) \quad , \quad T = g(G_\alpha) \; , \tag{1}$$

and all states are assigned to an irreducible representation [N] of $\mathcal{G}$. ([N] is the total boson number in the interacting boson model and the total vibron number in the vibron model.) A dynamic symmetry is then that situation in which H is only a function of the Casimir operators, C_i, of $\mathcal{G}$ and of a chain of subgroups of $\mathcal{G} \supset \mathcal{G}' \supset \cdots$,

$$H = f(C_i) \quad . \tag{2}$$

When a dynamical symmetry is present, all observables can be calculated in explicit analytic form. In particular, the energies of the quantum states are given explicitly in terms of the quantum numbers that characterize the states, through energy formulas. A typical example of these formulas is the

$SO(4)$ dynamic symmetry of the vibron model wherein the energy levels are given by

$$E(N,\omega,L,M_L) = E_o + A\,\omega(\omega+2) + BL(L+1), \tag{3}$$

with ω, L, M_L being the quantum numbers that characterize the states.

In contrast to bound states, scattering states have not been investigated much in terms of SGA and DS. Apart from some early (1967) work by Zwanzinger [3] who investigated the scattering states of the Coulomb potential by making use of the dynamic symmetry introduced by Pauli in 1926, not much work was done on this problem until the suggestion by the author of this article in 1981 that an appropriate SGA for scattering states in ν dimensions could be the non-compact version $U(\nu,1)$ of $U(\nu+1)$. Since then, a considerable amount of work has been done on the subject. This article is a brief review of this work.

2 The general scheme

In its original formulation, SGAS for scattering were constructed by analytic continuation of SGA for bound states. Thus, starting from $\mathcal{G} = U(\nu+1)$, it was suggested that, for scattering in ν dimensions, $\mathcal{G}^* = U(\nu,1)$ be taken as SGA. For problems with rotational invariance in ν dimensions, the algebra $\mathcal{G}^*$ must contain the rotation algebra $SO(\nu)$. A general scheme for scattering would then be provided by the lattice of algebras

$$\begin{array}{ccccc} & & U(\nu)\oplus U(1) & & (I) \\ & \nearrow & & \searrow & \\ U(\nu,1) & & & & SO(\nu), \\ & \searrow & & \nearrow & \\ & & SO(\nu,1) & & (II) \end{array} \tag{1}$$

where the notation, direct sum $\oplus$, appropriate to algebras has been used, rather than that appropriate to groups, direct product $\otimes$. (Also, for large ν, additional chains could be present.) The two chains would then provide two dynamic symmetries. Corresponding to each dynamic symmetry, there would be an explicit form for the observables in terms of quantum numbers. In scattering theory, the observable is the cross section, which can be obtained from a knowledge of the S-matrix. This quantity thus assumes here the leading role.

The general scheme (2.1) was explicitly worked out in 1982 by the author, together with Alhassid and Gürsey[4] in the case of one-dimensional problems, $\nu = 1$, where $\mathcal{G}^* = U(1,1)$. The two chains in (2.1) correspond in this case to potentials of the Pöschl-Teller type (Chain I) and of the Morse type (Chain II). For these two potentials, the S-matrix (or, in $\nu = 1$ dimension, the reflection and transmission amplitudes) can be computed in explicit form. From the S-matrix one can obtain the cross sections (or, in $\nu = 1$ dimensions, the reflection, R, and transmission, $T = 1 - R$, coefficients.) The result is, for the Pöschl-Teller potential:

$$R = \frac{1 + \cos\left(2\pi\sqrt{v + \frac{1}{4}}\right)}{\mathrm{ch}\,(2\pi\sqrt{\epsilon}) + \cos\left(2\pi\sqrt{v + \frac{1}{4}}\right)} = 1 - T \quad , \quad (I) \tag{2}$$

where v is the potential strength in dimensionless units, $v = (2\mu\ d^2/\hbar^2)\ V_0$, ϵ the energy in the same dimensionless units, $\epsilon = (2\mu\ d^2/\hbar^2)E$, and the potential is $V(x) = V_0\left[\mathrm{th}^2(x/d) - 1\right]$. For the Morse potential, one has obviously

$$R = 1 \quad , \quad T = 0 \quad , \qquad (II) \tag{3}$$

for any ϵ, and the potential is $V(x) = V_0\left[e^{-2x/d} - 20^{-x/d}\right]$. Although the result (2.2) is illuminating, it is not very useful from the general point of view. The reason is that, in one dimensional, the lattice of algebras (2.1) is

$$\begin{array}{lll} & U(1) \oplus U(1) & (I) \\ \nearrow & & \\ U(1,1) & & , \\ \searrow & & \\ & SO(1,1) & (II) \end{array} \tag{4}$$

and the two routes (I) and (II) contain the algebras $U(1)$ and $SO(1,1)$ which are isomorphic, since they are trivially composed of one single element. One cannot therefore study the transition from one chain to the other.

The case of particular interest and importance is obviously the case $\nu = 3$. The bound state part of the 3-dimensional problem has been extensively discussed in terms of $U(4)$. The two chains

$$\begin{array}{ccccc} & & U(3) & & \\ & \nearrow & & \searrow & \\ U(4) & & & & SO(3) \supset SO(2) \\ & \searrow & & \nearrow & \\ & & SO(4) & & \end{array} \quad \begin{array}{c} (I) \\ \\ \\ \\ (II) \end{array} , \tag{5}$$

correspond to potentials of the Pöschl-Teller (or truncated harmonic oscillator) type and of the Morse type. Both these chains are of interest in molecular physics. One may suggest that the chains appropriate to scattering are:

$$\begin{array}{ccccc} & & U(3) \oplus U(1) & & \\ & \nearrow & & \searrow & \\ U(3,1) & & & & SO(3) \supset SO(2) \\ & \searrow & & \nearrow & \\ & & SO(3,1) & & \end{array} \quad \begin{array}{c} (I) \\ \\ \\ \\ (II) \end{array} . \tag{6}$$

The general scheme corresponding to this case, i.e. how to construct S-matrix for both chains(I) and (II) and for the intermediate situation between (I) and (II) has not been investigated up to now. It remains one of the challenges of algebraic scattering theory.

3 Special cases. The Euclidean connection

Although the general scheme remains to be explored, special approaches have been developed. In particular, an approach based on the generalization of Coulomb-like problems has been fully exploited and its corresponding S-matrices have been found. This approach is based on pseudo-orthogonal algebras $SO(n,m)$ and on their corresponding dynamic symmetries. To be precise, the approach starts from the non-compact algebra $SO(2,\nu)$, where ν is the number of space degrees of freedom, and considers the dynamic symmetry associated with the chain[5,6]

$$SO(2,\nu) \supset SO(2) \oplus SO(\nu) \supset \cdots \tag{1}$$

The quantum number associated with $SO(2)$, called v, represents a parameter $v = 0, \pm 1, \pm 2, \cdots$, while $SO(\nu)$ is associated with usual rotations in ν dimensions. By expanding the asymptotic states of $SO(2,\nu)$ into those of $E(2) \oplus E(\nu)$, when E denotes the Euclidean algebra, it is possible to construct S-matrices. The results of this construction, called Euclidean connection, are[5]:

(i) $v = 1$, $SO(2,1)$.

The reflection amplitude, $\mathcal{R}(k)$, is given by

$$\mathcal{R}(k) = \frac{\Gamma\left(v + \frac{1}{2} + if(k)\right)}{\Gamma\left(v + \frac{1}{2} - if(k)\right)} e^{iv[\gamma_+(k) - \gamma_-(k)]} e^{i\phi(k)} . \tag{2}$$

Here $\gamma_+(k), \gamma_-(k)$ and $\phi(k)$ are arbitrary real functions of k, while the function $f(k)$ is obtained from the relation between the Hamiltonian, H, and the Casimir operator of $SO(1,2), C$,

$$H = h\left[-\left(C + \frac{1}{4}\right)\right] , \tag{3}$$

Since, for scattering states, the energy associated with the wave is $E_k = k^2$ (apart from the scale factor $\hbar^2/2\mu$), and, for the continuous representations, the Casimir operator of $SO(2,2)$ can be written as $-\left(C + \frac{1}{4}\right) = f^2(k)$, one has

$$k^2 = h\left[f(k)\right] \tag{4}$$

which determines $f(k)$ once the function h is known.
(ii) $\nu = 2$, $SO(2,2)$.

The S-matrix here is given by

$$S_m(k) = \frac{\Gamma\left[(m + v + 1 + if(k))/2\right] \Gamma\left[(m - v + 1 + if(k))/2\right]}{\Gamma\left[(m + v + 1 - if(k))/2\right] \Gamma\left[(m - v + 1 - if(k))/2\right]} e^{i\phi(k)}, \tag{5}$$

where $\phi(k)$ is an arbitrary real function and m is the two-dimensional angular momentum.
(iii) $\nu = 3$, $SO(2,3)$

The S-matrix here is given by

$$S_\ell(k) = \frac{\Gamma\left[\left(\ell + v + \frac{3}{2} + if(k)\right)/2\right]\ \Gamma\left[\left(\ell - v + \frac{3}{2} + if(k)\right)/2\right]}{\Gamma\left[\left(\ell + v + \frac{3}{2} - if(k)\right)/2\right]\ \Gamma\left[\left(\ell - v + \frac{3}{2} - if(k)\right)/2\right]} e^{i\phi(k)}, \quad (6)$$

where ℓ is the ordinary 3-dimensional angular momentum. The cross section is given as usual by

$$\frac{d\sigma}{d\Omega} = \mid g(k,\theta) \mid^2 ,$$

$$g(k,\theta) = \Sigma_\ell (2\ell + 1)\ \frac{S_\ell(k) - 1}{2ik}\ P_\ell(\cos\theta) . \quad (7)$$

Although the case $\nu = 1$ is not of particular interest, since $\mid \mathcal{R} \mid = 1$, i.e. the wave is entirely reflected, the structure of $\nu = 2$ and $\nu = 3$ is interesting. Even considering $\phi(k) = 0$, Eqs. (3.5) and (3.6) give a class of exactly solvable S-matrices which depend on one parameter v. By specifying the function $f(k)$, one can construct S-matrix models which can be used to study experimental data. Some work in this direction was done by Wu[7] and by Amado and other[8].

The approach was also generalized to any n and m by Frank and others[9] with the result

$$S_\ell(k) = \frac{\Gamma\left(\frac{1}{2}\left[\ell + v + (n+m-2)/2 + if(k)\right]\right)}{\Gamma\left(\frac{1}{2}\left[\ell - v + (n+m-2)/2 - if(k)\right]\right)} \times$$

$$\times \frac{\Gamma\left(\frac{1}{2}\left[\ell + v + (n+m-2)/2 + if(k)\right]\right)}{\Gamma\left(\frac{1}{2}\left[\ell - v + (n+m-2)/2 - if(k)\right]\right)} e^{i\phi(k)} . \quad (8)$$

The method of Euclidean connection, which is based on the mathematical concept of expansion and contraction of Lie algebras, has stimulated further work in this direction[10,11]. Eq. (3.8) also shows the generic result that all S-matrices based on orthogonal algebras are ratios of Γ- functions.

4 Special cases. Coulomb-like problems

The method of Euclidean connection can be used also to construct S-matrices for Coulomb-like problems. The starting point here is the degeneracy group of scattering states of the Coulomb potential in ν dimensions ($\nu \geq 2$), $SO(1,\nu)$. By expanding the asymptotic states of $SO(1,\nu)$, onto the Euclidean states of $E(\nu)$ it is possible to construct Coulomb-like S-matrices[5,6]. The resultes

of the construction are:

The S-matrix is given by

$$S_m(k) = \frac{\Gamma\left(m + \frac{1}{2} + if(k)\right)}{\Gamma\left(m + \frac{1}{2} - if(k)\right)} e^{i\phi(k)} , \tag{1}$$

where $\phi(k)$ is again an arbitrary function of k and $f(k)$ is obtained from the relation between H and C.

(ii) $\nu = 3$, $SO(1,3)$.

The S-matrix is given by

$$S_\ell(k) = \frac{\Gamma\left(\ell + 1 + if(k)\right)}{\Gamma\left(\ell + 1 - if(k)\right)} e^{i\phi(k)} . \tag{2}$$

In the actual Coulomb case, $\phi(k) = 0$ and

$$f(k) = \frac{\beta\mu}{\hbar^2 k} , \tag{3}$$

$\beta = Z_1 Z_2\, e^2$ and μ is the reduced mass. One may note that the S-matrices of this section can be obtained from those of the previous section by setting $v = 1/2, \phi = 2\ell n 2\ f(k)$, and using the duplication formula for the Γ-functions,

$$\Gamma(z)\ \Gamma(z + \frac{1}{2}) = 2^{1-2z}\ \pi^{1/2} \Gamma(2z). \tag{4}$$

In summary, the method of Euclidean connection allows one to construct S-matrices of the Coulomb-type in any number of dimensions.

$SO(3,1)$ S-matrices have found use in the study of heavy-ion collisions. The point here is to consider, as a model of heavy-ion scattering, one in which the S-matrix is given by

$$S_\ell(k) = \frac{\Gamma\left(\ell + 1 + iv(\ell,k)\right)}{\Gamma\left(\ell + 1 - iv(\ell,k)\right)} , \tag{5}$$

where $v(\ell, k)$, called the algebraic potential, contains the 'potential' information. The potential $v(\ell, k)$ is taken as a combination of a Coulomb and a short-range interaction,

$$v(\ell, k) = v_\ell(\ell, k) + v_s(\ell, k) \ . \tag{6}$$

Both Coulomb and short-range interactions are parametrized in some way and the corresponding cross sections are calculated. This method has proven to be of some use, although, as discussed in Sect. 7, the main interest is to deal with multichannel scattering.

5 Algebraic potentials and inverse scattering

As mentioned in the previous section, the potential $v(\ell, k)$ is obtained by an appropriate parametrization of the data. However, both from the point of view of finding a suitable form $v(\ell, k)$ and, vice versa, from the point of view of determining the 'true' configuration space potential, it is of interest to consider the relation between $v(\ell, k)$ and the potential $V(r)$. This relation can be easily obtained in the semiclassical, eikonal and Born approximations. In the semiclassical approximation, the relation is somewhat complex in form. It is discussed in Ref.[12] and it will not be reported here. In Born approximation, the relation is[13]

$$v(\ell, k) \approx -\frac{2\mu k}{\hbar^2 \psi(\ell + 1)} \int_0^\infty r^2 V(r) j_\ell^2(kr) dr \ , \tag{1}$$

where ψ is the digamma function. In eikonal approximation, the relation is

$$v(\ell, k) \approx -\frac{\mu}{2\hbar^2 \ \psi(\ell + 1)} \int_{-\infty}^{+\infty} V(b, z) dz \ ; \ kb = \ell + \frac{1}{2} \ . \tag{2}$$

The relation between $V(r)$ and $v(\ell, k)$ can also be obtained, in general, by solving the inverse scattering problem. Much work in this direction has been done, in particular by Scheid, Zielke and others[14]. For real potentials, the inversion procedure is rather straightforward, while for complex potentials it may lead to ambiguities. The algebraic method here could be of use, in the sense of providing the scattering amplitude for and ℓ and k and thus of serving as an intermediate step between the data and the potential in configuration space.

6 Scattering of particles with spin

The algebraic approach for spinless particles, discussed in the previous sections, can be generalized to include scattering of particles with spin. The simplest generalization is that in which the algebra of the relative notion, $\mathcal{G}_{\mathcal{R}}$, is coupled to the spin algebra, $SU_S(2)$. This method allows one to treat, among other problems, that of scattering of spin-1/2 particles, or, in general of spin-S particles in the presence of spin-orbit interactions, $\mathbf{L}\cdot\mathbf{S}$. This method was introduced by the author in 1986[15] but it has not been used in practice. When applied to the special cases of Sects. 3 and 4, it leads to the $SO(2,3)$ S-matrix for scattering of spin -1/2 particles[15]

$$S_{\ell,j=\ell\pm\frac{1}{2}}(k) = \frac{\Gamma\left[\left(\ell+u^{(\pm)}+3/2+if(k)\right)/2\right]}{\Gamma\left[\left(\ell+u^{(\pm)}+3/2-if(k)\right)/2\right]}\times$$

$$\times\frac{\Gamma\left[\left(\ell-u^{(\pm)}+3/2+if(k)\right)/2\right]}{\Gamma\left[\left(\ell-u^{(\pm)}+3/2-if(k)\right)/2\right]}\,e^{i\phi(k)}\,, \tag{1}$$

where

$$u^{(+)} = u_c + \ell\, u_s\,,$$

$$u^{(-)} = u_c - (\ell+1)u_s\,. \tag{2}$$

The case of $SO(1,3)$ was also treated. The algebraic description of this case is in terms of

$$SO(1,3)\oplus SU_S(2) \supset SO_L(3)\oplus SU_S(2) \supset SU_J(2)\,, \tag{3}$$

where the orbital, L, and spin, S, angular momenta are coupled to total J. In this case both diagonal, $\mathbf{L}\cdot\mathbf{S}$, and non diagonal interactions were considered[15].

Recently, another very interesting approach to problems with spin has been introduced by Lévay and Apagyi[16]. Instead of considering the algebraic structure $\mathcal{G}_R\oplus\mathcal{G}_S$ these authors treat scattering in terms of a single algebraic structure but consider non-standard realizations of this algebra. In particular, they consider the case $\mathcal{G}\equiv SO(3,1)$ and obtain the S-matrix (reflection amplitude)

$$\mathcal{R}_j(k) = (-)^{n_j} \frac{\Gamma(j+1-ik)\ \Gamma(\frac{1}{2}+ik)}{\Gamma(j+1+ik)\ \Gamma(\frac{1}{2}-ik)} , \tag{4}$$

with $n_j = 0$ for $j = \ell + \frac{1}{2}$, $n_j = 1$ for $i = \ell - \frac{1}{2}$. This S-matrix is a generalization of the S-matrix for scattering from a Pöschl-Teller potential. It should be noted that, since

$$SO(3,1) \neq SO(2,1) \oplus SO(3) , \tag{5}$$

i.e. $SO(3,1)$ cannot be split into the direct sum of $SO(2,1)$ and $SO(3)$, the result of Ref.[16] is new. Its further generalization could be useful in heavy-ion scattering when one of the colliding ions has spin=1/2. The method of Lévay and Apagyi is also related to the method discussed in the following section for relativistic scattering.

7 Relativistic scattering

Spectrum generating algebras and dynamic symmetries can, in principle, be used to attack relativistic problems in the context of relativistic quantum mechanics. For bound state problems, a considerable amount of work has been done in this direction by Barut, Bohm and others[17]. This work, however, focuses on Coulomb-like problems and makes use of infinite-component wave equations. A general scheme for finite component wave equations, as, for example, the Dirac equation, has not been worked out yet. The logic of this general scheme should be that of coupling the SGA that describes the space part, $\mathcal{G}_R$, with that describing the internal (spin) degrees of freedom, $\mathcal{G}_S$,

$$\mathcal{G} = \mathcal{G}_R \oplus \mathcal{G}_S . \tag{1}$$

The algebra $\mathcal{G}$ can then be analytically continued in order to describe scattering. The analytic continuation would involve only the space part $\mathcal{G}_R$,

$$\mathcal{G}^* = \mathcal{G}_R^* \oplus \mathcal{G}_S . \tag{2}$$

The explicit construction of such a scheme, both from bound state and scattering problems remains a challenge. So far, only a special case has been

discussed, that of a Dirac particle in Coulomb field (Coulomb-Dirac problem)[18]. (This problem has also been solved by converting the first order Dirac equation into a second order equation and using the methods of previous section[19].) For this problem, one can use the algebraic structure of the space part in spherical coordinates,

$$\begin{array}{ccccc} \mathcal{G}_R = & SO(2,1) & \oplus & SO(3) & \\ & \downarrow & & \downarrow & \\ & \text{radial part} & & \text{orbital part} & \end{array} , \tag{3}$$

together with the algebraic structure of the internal part,

$$\begin{array}{ccccc} \mathcal{G}_S = & SO(2,1) & \oplus & SO(3) & \\ & \downarrow & & \downarrow & \\ & \rho - \text{matrices} & & \sigma - \text{matrices(spin)} & \end{array} . \tag{4}$$

Since the algebras $\mathcal{G}_R$ and $\mathcal{G}_S$ are in this case identical, they can be combined in an obvious way. The orbital, L, and spin, S, parts are combined as

$$\begin{array}{ccccccc} SO(3) & \oplus & SO(3) & \supset & SO(3) & \supset & SO(2) \\ \downarrow & & \downarrow & & \downarrow & & \downarrow \\ \{L_1, L_2, L_3\} & & \{\sigma_1, \sigma_2, \sigma_3\} & & \{J_1, J_2, J_3\} & & \{N_3\} \end{array} , \tag{5}$$

while the radial, M, and ρ-parts can be combined as

$$\begin{array}{ccccccc} SO(2,1) & \oplus & SO(2,1) & \supset & SO(2,1) & \supset & SO(2) \\ \downarrow & & \downarrow & & \downarrow & & \downarrow \\ \{\mu_1, \mu_2, \mu_3\} & & \{i\rho_1, i\rho_2, i\rho_3\} & & \{N_1, N_2, N_3\} & & \{N_3\} \end{array} . \tag{6}$$

Use of the Euclidean connection, produces, after some lengthy manipulations, the S-matrix for Coulomb-Dirac scattering in 3-dimensions,

$$S_{\kappa j}(k) = \exp\left[-i\pi(\lambda - \ell)\right] \left(\frac{-\kappa - i\eta\mu/k}{\lambda - i\eta\epsilon/k} \right) \frac{\Gamma(\lambda + 1 - i\eta\epsilon/k)}{\Gamma(\lambda + 1 + i\eta\epsilon/k)} , \tag{7}$$

where ℓ is the orbial angular momentum, j the total angular momentum, $\kappa = (j + \frac{1}{2})$ for $\ell = j - \frac{1}{2}$ and $-(j + \frac{1}{2})$ for $\ell = j + 1/2$, $\lambda = (\kappa^2 - \eta^2)^{1/2}$, η the usual Sommerfeld parameter $\eta = Ze^2$, and ϵ the relativistic energy $(k^2 - \eta^2)^{1/2}$.

Another case that can be solved algebraically, although not reported in the literature, is that of a relativistic spin-0 particle in a Coulomb field (Coulomb-Klein-Gordon-problem). For this problem, there is no internal part, and one can use only the algebraic structure of $\mathcal{G}_R$ to give the S-matrix for Coulomb-Klein-Gordon scattering in 3-dimensions,

$$S_\ell(k) = \frac{\Gamma(\ell + 1 - i\eta\epsilon/k)}{\Gamma(\ell + 1 + i\eta\epsilon/k)} , \tag{8}$$

which is a simple generalization of (4.2) and it reduces to it for small momenta, $k \ll \mu$.

The Coulomb-Dirac algebraic scattering theory could be extremely useful in analyzing scattering of high energy protons off nuclei (Dirac phenomenology). The idea here could be that of considering scattering models in which the S-matrix is given by

$$S_{\kappa j}(k) = \exp\left[-i\pi(\lambda - \ell)\right] \left(\frac{-\kappa - iv(\lambda, k)}{\lambda - iv(\lambda, k)\frac{\epsilon}{\mu}} \right) \times$$

$$\times \frac{\Gamma\left(\lambda + 1 - iv(\lambda, k)\frac{\epsilon}{\mu}\right)}{\Gamma\left(\lambda + 1 + iv(\lambda, k)\frac{\epsilon}{\mu}\right)} . \tag{9}$$

The Coulomb-Dirac problem could also be generalized by doing the step leading from Eq.(3.6) to Eq.(4.2) backwards. This will produce a wider class of S-matrices with an additional parameters , v.

8 Scattering of composite particle

Although the use of SGA's and dynamic symmetries sheds some new light on one-particle scattering theory, it is not particularly useful, since the Schrodinger or Dirac equation for a single particle in a potential V can be easily solved with other means. An area where algebraic scattering theory can be of extreme interest is instead that of scattering of composite particles. In this case, the problem becomes a many-channel scattering problem of difficult numerical solution. An algebraic reaction theory was suggested by the author[15] and has been implemented in several cases.

For multichannel scattering, the algebraic S-matrix takes on the form[13]

$$S = K^{1/2}\, M\, K^{-1/2}\,, \tag{1}$$

where K is a diagonal matrix with the channel momenta, k_α, along its diagonal and M is the algebraic Jost matrix. For Coulomb-like problems, the algebraic Jost matrix has the form

$$M = \frac{\Gamma(\ell + 1 + iv)}{\Gamma\ell + 1 - iv)} \tag{2}$$

where the argument of the Γ-function is now a matrix. For n channels, v is a $n \times n$ matrix, called a potential matrix. In order to calculate S, one first finds the matrix Z which diagonalizes $K^{1/2}\, v\, K^{-1/2}$. Since the matrices inside the Γ-functions in the numerator and denominator of (8.2) commute, the S-matrix is given by

$$S = Z\, D\, Z^{-1} \tag{3}$$

where D is a diagonal matrix whose diagonal elements are

$$D_{\alpha\alpha'} = \frac{\Gamma(\ell + 1 + i\lambda_\alpha)}{\Gamma(\ell + 1 - i\lambda_\alpha)}\, \delta_{\alpha\alpha'}\,, \tag{4}$$

where the $\lambda'_\alpha s$ are the eigenvalues of $K^{1/2}\, v\, K^{-1/2}$.

Algebraic reaction theory, at least for spinless particles, has been extensively investigated, especially in connection with heavy-ion scattering. For such a case, the S-matrix has been written as[13]

$$S^\ell_{\alpha\alpha'}(k) = k_\alpha^{1/2} \left[\frac{\Gamma(\ell + 1 + iv(\ell, k))}{\Gamma(\ell + 1 - iv(\ell, k))}\right]_{\alpha\alpha'} k_{\alpha'}^{-1/2}\,, \tag{5}$$

with $v(\ell, k)$ written as a sum of a Coulomb and short-range interaction

$$v_{\alpha\alpha'}(\ell, k) = v^c_{\alpha\alpha'}(\ell, k) + v^s_{\alpha\alpha'}(\ell, k)\,. \tag{6}$$

The quantities v^c and v^s are then appropriately parametrized and cross sections are calculated.

The application of algebraic reaction theory to nuclear reactions has received considerable attention, especially by Lichtenthaler, and others[21] and by Ventura, Zuffi and others[22]. Examples are shown in the accompanying paper by Ventura.

9 Internal symmetry

Although the use of algebraic methods reduces the complexity of coupled channel problems to a $n \times n$ matrix diagonalization, there still remains the problem of obtaining the potential matrices, v^c and v^s. When the number of channels becomes moderately large, $n \approx 20 - 30$, this is still a formidable problem. Spectrum generating algebras and dynamic symmetries can be useful here too, since one can exploit the internal symmetry of the colliding particles. The basic point is that the coupling between different channels is induced by transition operators, T, acting on the internal coordinates of the colliding objects. In the algebraic approach, these transition operators become elements of the Lie algebra that describes the internal structure. For example, in the collision between two heavy nuclei, the transition operators can be taken to be elements of $U(6)$, the algebra of the interacting boson model, while in the collision between two molecules, the transition operators can be taken to be elements of $U(4)$, the algebra of the vibron model. Thus, for collisions between two objects, A and B, one has the combined structure

$$\mathcal{G} = \mathcal{G}_A \oplus \mathcal{G}_R \oplus \mathcal{G}_B \ , \tag{1}$$

where $\mathcal{G}_A$ and $\mathcal{G}_B$ describe the internal structure of the two objects and $\mathcal{G}_R$ is the algebra of the relative motion. This approach reduces the number of parameters considerably. For example, in nuclei, multipole excitations with multipolarity λ would produce an algebraic potential matrix which can be written as[13]

$$v_{\alpha' j', \alpha j}(k) = v_\lambda(J,k) \sqrt{\frac{2\lambda+1}{4\pi}} \, (-)^{j'} \begin{pmatrix} j' & \lambda & j \\ 0 & 0 & 0 \end{pmatrix} \beta_\lambda \langle \alpha' j' \parallel G_\lambda \parallel \alpha j \rangle \ . \tag{2}$$

In this expression, G_λ is a generator of $U(6)$ with multipolarity λ and β_λ is the strength of the interaction, while $v_\lambda(J,k)$ is one of the expressions of Sect. 4 which parametrizes the scattering process. This potential matrix is thus obtained in terms of only one parameter, β_λ, instead of $n(n-1)/2$ required if each entry in the potential matrix is taken as a free parameter.

Internal symmetries can be (and have been) also used in scattering, separately from the algebraic approach, in a mixed scheme in which the relative motion is treated in one of the usual approximations, while the internal degrees of freedom are treated algebraically. A particularly useful and interesting approximation is the eikonal approximation. In this approximation, the scattering amplitude between some initial and final state is given by

$$A_{fi}(q) = \frac{k}{2\pi i} \int d^2b \, e^{i\mathbf{q}\cdot\mathbf{b}} \langle f \mid e^{i\chi(\mathbf{b})} - 1 \mid i \rangle \,, \tag{3}$$

where $\mathbf{q} = \mathbf{k}' - \mathbf{k}$ is the momentum transfer and $\chi(\mathbf{b})$ the eikonal phase. This phase depends on the interaction between the incoming particle and the target. If the target is described algebraically, one is led, alfter some manipulation, to the evaluation of a matrix element, which, schematically, can be written as

$$\langle \text{Irrep of } \mathcal{G} \mid e^{i\alpha G_\alpha} \mid \text{Irrep of } \mathcal{G} \rangle \,, \tag{4}$$

where Irrep of $\mathcal{G}$ denotes an irreducible representation of $\mathcal{G}$. This matrix element is nothing but a group element of $\mathcal{G}$. This matrix element is nothing but a group element of $\mathcal{G}$, i.e. a generalization of the familiar Wigner $\mathcal{D}$-matrices

$$\mathcal{D}^J_{MM'}(\theta_1,\theta_2,\theta_3) = \langle J, M \mid e^{i\sum_u \theta_u J_u} \mid J, M' \rangle \,. \tag{5}$$

Algebraic methods are obviously very useful in the evaluation of these matrix elements. A large literature exists on this subject, which initiated with the work of Ginocchio, Amado, Bijker, Mengoni and others and has continued up to recently. This work has dealt with both nuclear and molecular physics by considering scattering of high energy protons off nuclei[23] and of high-energy electrons off molecules[24-26]. This mixed approach has received considerable attention, but it is somewhat outside the scope of this article and it will not be reviewed in detail.

10 Conclusions

Contrary to the case of bound state problems, the algebraic approach to scattering and reactions has not been fully exploited yet, with the only exception of Coulomb-like problems for spinless particles. Areas where further work is needed are: (i) the study of a general scheme for more than one dimension; (ii) applications of this general scheme to atom-atom and molecule-molecule scattering where Coulomb-like S-matrices are not appropriate; (iii) the study of a general scheme for relativistic scattering; (iv) applications of this general scheme to hadron-hadron collisions; (v) the explicit introduction of spin in reactions which, at the moment, has been treated in the rotating-frame approximation; (vi) applications of this scheme to heavy-ion collisions.

Despite these shortcomings spectrum generating algebras and dynamic symmetries have shed some new light on scattering processes and, as such, have played a role in the study of complex reactions.

This work was supported in part under D.O.E. Contract DE-FG02-91ER-40608.

References

[1] A. Arima and F. Iachello, Ann. Phys. (N.Y.) **99**, 253 (1976); **111**, 201 (1978); **123**, 468 (1979).

[2] F. Iachello, Chem. Phys. Lett. **78**, 581 (1981); F. Iachello and R.D. Levine, J. Chem. Phys. **77**, 3046 (1982).

[3] D. Zwanzinger, J. Math. Phys. **8**, 1858 (1967).

[4] Y. Alhassid, F. Gürsey and F. Iachello, Ann. Phy. (N.Y.) **148**, 346 (1983).

[5] Y. Alhassid, F. Gürsey and F. Iachello, Ann. Phys. (N.Y.) **167**, 181 (1986); J. Wu, F. Iachello and Y. Alhassid, Ann. Phys. (N.Y.) **173**, 68 (1987).

[6] A. Frank and K.B. Wolf, Phys. Rev. Lett. **52**, 1737 (1984).

[7] J. Wu, Ph.D. Thesis, Yale University, (1985) unpublished.

[8] R.D. Amado and D.A. Sparrow, in Nuclear Structure, Reactions and Symmetries, R.A. Meyer and V. Paar, eds., World Scientific Singapore (1987).

[9] A. Frank, Y. Alhassid and F. Iachello, Phys. Rev. **34**, 677 (1986).

[10] E. Celeghini, F. Iachello, M. Tarlini and G. Vitiello, in Group Theoretical Methods in Physics, R. Gilmore, ed., World Scientific, Singapore, p.419, (1987).

[11] P. Freund, in Gürsey Memorial Volume, G. Aksas, C. Saclioglu and M. Serdaroglu, eds., Springer Verlag, Berlin (1996).

[12] M.S. Hussein, M.P. Pato, and F. Iachello, Phys. Rev. **C38**, 1072 (1988).

[13] Y. Alhassid and F. Iachello, Nucl. Phys., **A501**, 585 (1989).

[14] A. Zielke, Doctoral Thesis, Giessen (1993), unpublished; A. Zielke, R. Maass, W. Scheid, and O.L. Weaver, Phys. Rev. **A42**, 1358 (1990); A. Zielke and W. Scheid, J. Phys. A; Math. Gen. **25**, 1383 (1992).

[15] F. Iachello, in Nuclear Structure Reactions and Symmetries, R.A. Meyer and V. Paar, eds., World Scientific, Singapore, (1987) p.455 ; F. Iachello, in Relations between Reactions and Structure in Nuclear Physics, D.H. Feng, M. Vallieres, and B.H. Wildenthal, eds., World Scientific, Singapore, (1987) p.165.

[16] P. Lévay, J. Phys. A: Math. Gen. **28**, 5919 (1995); P. Lévay and B. Apagyi, J. Math. Phys. **36**, 6633 (1995).

[17] A. Barut and A. Böhm, Phys. Rev. **139**, B1107 (1965);
A.O. Barut, Phys. Lett. **26B**, 308 (1968); A.O. Barut, D. Corrigan, and H. Kleinert, Phys. Rev. Lett. **20**, 167 (1969); A.O. Barut, and H. Beker, Phys. Rev. Lett. **50**, 1560 (1983); A. Böhm, M. Löewe and P. Magnollay, Phys. Rev. **D31**, 2304 (1985); **32**, 791 (1985); A. Böhm, Phys. Rev. **D33**, 3358 (1986).

[18] Y. Alhassid, F. Gürsey, and F. Iachello, J. Phys. A: Math. Gen. **22**, L947 (1989).

[19] J. Wu, A. Stalhofen, L.C. Biedenharn, and F. Iachello, J. Phys. A: Math. Gen. **20**, 4637 (1987).

[20] Y. Alhassid, F. Iachello, and B. Shao, Phys. Lett. **B201**, 183 (1988).

[21] R. Lichtenthaler Filho, in Perspectives for the Interacting Boson Model, R.F. Casten et al, eds., World Scientific, Singapore, (1994) p.521; R. Lichtenthaler Filho, A.C.C. Villari, L.C. Gomes, P. Carrilho Soares, Phys. Lett. **B269**, 49 (1991).

[22] R. Lichtenthaler Filho, A. Ventura and L. Zuffi, Phys. Rev. **C46**, 707 (1992); R. Lichtenthaler Filho, D. Pereira, L.C. Chamon, L.C. Gomes, A. Ventura and L. Zuffi, Phys. Rev. **C50**, 3033 (1994).

[23] J. Ginocchio, T. Otsuka and D.A. Sparrow, Phys. Rev. **C33**, 247 (1986).

[24] R. Bijker, R.D. Amado and D.A. Sparrow, Phys. Rev. **A33**, 871 (1986); R. Bijker and R.D. Amado, Phys. Rev. **A34**, 71 (1986); **A46**, 1388 (1992); R. Bijker, R.D. Amado, and L.A. Collins, Phys. Rev. **A42**, 6414 (1990).

[25] Y. Alhassid and B. Shao, **A46**, 3978 (1992); **A46**, 3991 (1992); Y. Alhassid, V. Liu and B. Shao, Phys. Rev. **A48**, 2832 (1992); **A46**, 3865 (1992); Y. Alhassid and H. Attias, Nucl. Phys. **A577**, 709 (1994).

[26] A. Mengoni and T. Shirai, J. Phys. **21**, L567 (1988); Phys. Rev. **A44**, 7258 (1991).

Algebraic Coupled-Channels Formalism for Heavy Ions near the Coulomb Barrier

R. Lichtenthäler Filho[1], M. Vaccari[2], A. Ventura[3], and L. Zuffi[4]

[1] Instituto de Física da Universidade de São Paulo, C. P. 20516, São Paulo, SP, Brazil
[2] ENEA, Dipartimento Innovazione, Divisione Fisica Applicata, Bologna, Italy
[3] ENEA, Dipartimento Energia, Centro Dati Nucleari, Bologna, Italy and INFN, Sezione di Firenze, Italy
[4] Dipartimento di Fisica dell' Università di Milano and INFN, Sezione di Milano, Via Celoria 16, Milano, Italy

Abstract. The algebraic coupled-channels formalism based on SO(3,1) symmetry, originally proposed by Alhassid and Iachello (1989) for the description of heavy-ion reactions in the Fraunhofer diffraction regime, appears to be applicable also to reactions in the Fresnel regime, at the cost of some modifications, whose importance increases with decreasing energy and is crucial in the proximity of the Coulomb barrier.

1 Original Formation of the SO(3,1) Scattering Theory

The algebraic scattering theory of low-energy heavy-ion reactions proposed by Alhassid and Iachello (1989) generalises to many reaction channels the well-known analytic form of the S matrix for nonrelativistic Coulomb scattering of two spinless particles of charges Z_p, Z_t (in units of the electron charge, e) and masses A_p, A_t (in atomic mass units, M):

$$S_l^C = \frac{\Gamma(l+1+i\eta)}{\Gamma(l+1-i\eta)} = e^{2i\sigma_l} \ . \tag{1}$$

Here, $\Gamma(z) = \Gamma^*(z^*)$ is the Euler gamma function of complex argument, so that $\sigma_l = \arg(\Gamma(l+1+i\eta))$ is the Coulomb phase shift corresponding to the orbital angular momentum l , and η is the Sommerfeld parameter:

$$\eta = \frac{\mu Z_p Z_t e^2}{\hbar^2 k} = \sqrt{\frac{A_p A_t}{A_p + A_t}} \sqrt{\frac{Mc^2}{2E}} \alpha Z_p Z_t \ , \tag{2}$$

where $\mu = A_p A_t M/(A_p + A_t)$ is the reduced mass of the system, $\alpha = e^2/(\hbar^2 c)$ is the fine structure constant, k and $E = \hbar^2 k^2/(2\mu)$ are the wave number and energy of relative motion in the centre-of-mass frame, respectively.

The scattering amplitude, as a function of the scattering angle in the c. m. frame, θ, reads

$$f_C(\theta) = \frac{1}{2ik}\sum_{l=0}^{\infty}(2l+1)P_l(\cos(\theta))e^{2i\sigma_l}$$
$$= -\frac{\eta}{2k\sin^2(\frac{\theta}{2})}\exp\left(-i\eta\ln(\sin^2(\theta/2)) + 2i\sigma_0\right), \quad (3)$$

and corresponds to the well-known Rutherford formula, for $\theta \neq 0$.

The functional form (1) can be derived by purely algebraic methods, (Wu 1985), since the Hamiltonian of the problem, at fixed c. m. energy, E, is a simple function of a quadratic Casimir invariant of the SO(3,1) algebra generated by the three components of the orbital angular momentum, $\mathbf{L}$, and the three components of a modified Runge-Lenz vector, $\mathbf{K}$:

$$\mathbf{K} = \frac{1}{k}\left[\frac{1}{2}(\mathbf{P}\times\mathbf{L} - \mathbf{L}\times\mathbf{P}) \pm \eta\mathbf{P}\right], \quad (4)$$

where the linear momentum, $\mathbf{P}$, and the angular momentum, $\mathbf{L}$, are both expressed in units of $\hbar$, and both signs on the right-hand-side of formula (4) are acceptable. The Hamiltonian reads:

$$\hat{H} = -\frac{\hbar^2k^2}{2\mu}\eta^2(\mathbf{L}^2 - \mathbf{K}^2 + 1)^{-1} \quad (5)$$

The most general scattering problem with SO(3,1) symmetry is obtained by replacing in the Runge-Lenz vector (4), in the Hamiltonian (5), and in the S matrix (1) the Sommerfeld parameter, η, with an arbitrary real function of k, $v(k)$, henceforth called the algebraic potential.

Such a simple potential, however, is not fit for describing heavy-ion reactions, which result from a combination of Coulomb and nuclear interactions, $v = \eta + v_N$; owing to the latter, the partial waves of low angular momentum are absorbed from the elastic channel and scattered to reaction channels. The simplest way of producing this effect in the formalism is to make v_N complex and angular momentum dependent:

$$v_N(k,l) = \frac{v_R + iv_I}{1+\exp\left(\frac{l-l_0}{\Delta}\right)}, \quad (6)$$

thus breaking the SO(3,1) symmetry. In order for the S matrix be unitary, it is necessary that $v_I \geq 0$.

As a consequence of formula (6), the reflection coefficient, $|S_l|$, as a function of l, shows a strong absorption profile, since it is 0 for $l << l_0$ and raises to 1 in an interval of size Δ centred on l_0, which plays then the role of a grazing angular momentum.

The dimensionless potential depths, v_R and v_I, the critical angular momentum, l_0, and the diffuseness parameter, Δ, depend, in general, on k.

Simple semiclassical arguments suggest the following dependence (Alhassid and Iachello (1989)):

$$v_j(k) = v_j^{(0)} + v_j^{(1)} k \; ; (j = I, R) \tag{7}$$

$$\Delta(k) = d^{(1)} k \; ; \tag{8}$$

$$l_0(k) = r_0 \sqrt{k^2 - k_B^2}, \quad (k > k_B), \tag{9}$$

where $v_{R,I}^{(0,1)}$, $d^{(1)}$ and r_0 are constant. In Eq. (9), k_B is the wave number corresponding to the energy of the Coulomb barrier in the centre-of-mass frame (Broglia and Winther (1991)):

$$E_B \equiv \frac{\hbar^2 k_B^2}{2\mu} = \frac{Z_p Z_t e^2}{r_B}\left(1 - \frac{a}{r_B}\right) , \tag{10}$$

where the diffuseness parameter, a, is of the order of 0.63 fm, and the barrier radius, r_B, is given, to a good approximation, by the formula (Broglia and Winther (1991))

$$r_B = [1.07(A_p^{1/3} + A_t^{1/3}) + 2.72]\,\mathrm{fm}. \tag{11}$$

Inclusion of reaction channels in the algebraic formalism is simple if all the channel spins are zero. The S matrix at given orbital momentum, L (the same for all channels), becomes a $n \times n$ matrix, where n is the number of reaction channels explicitly taken into account (Alhassid and Iachello (1989)):

$$S_{\alpha\beta}^L = k_\alpha^{1/2} \left[\frac{\Gamma(L+1+iV(L,k))}{\Gamma(L+1-iV(L,k))}\right]_{\alpha\beta} k_\beta^{-1/2} \; (\alpha, \beta = 1, \ldots, n) . \tag{12}$$

In the argument of the gamma functions, $L + 1$ multiplies the $n \times n$ identity matrix, and V , the $n \times n$ potential matrix, is symmetrical, because of invariance under time reversal. The channel wave number, k_α , is connected with the entrance value, k_1, by the reaction Q-value of channel α:

$$\frac{\hbar^2 k_\alpha^2}{2\mu_\alpha} = \frac{\hbar^2 k_1^2}{2\mu_1} + Q_\alpha \; , \tag{13}$$

where the reduced mass, μ_α, might differ from μ_1, if α were a rearrangement (nucleon transfer) channel.

The gamma functions of matrix argument are $n \times n$ matrices, too, defined through their integral representation

$$\Gamma(Z) = \int_0^\infty \exp[(Z-1)lnt - t]dt \; , \tag{14}$$

provided the matrix exponential in the integrand exists and the integral converges.

As a consequence of Eq. (14), the recurrence relation $\Gamma(Z+1) = Z\Gamma(Z)$ holds for matrix arguments, too. Moreover, the Γ matrices are easily dealt with in a representation where their argument is diagonal, since $(\Gamma(Z))_{ij} = \Gamma(Z_{ii}\delta_{ij})$, for $Z_{ij} = Z_{ii}\delta_{ij}$.

In order for S be unitary, its spectral norm, $||S||$, should not exceed unity

$$||S|| = \sqrt{\max \lambda_{S^+S}} \leq 1 , \tag{15}$$

where λ_{S^+S} denotes a generic eigenvalue of S^+S.

If some reaction channel has nonzero spin. as is the case for inelastic scattering, formula (12) cannot be applied any more, since L is no longer a multiple of the $n \times n$ identity matrix, but a diagonal matrix with different L_α's in different channels, so that L and V do not commute; neither do the gamma matrices, whose ratio is not defined any more.

In order to reduce the multichannel problem with spin to a spinless one, that makes it possible to use formula (12) for the S matrix, Alhassid and Iachello (1989) resort to an algebraic version of the rotating frame approximation, introduced in the traditional coupled-channels approach by Tanimura (1987), studied in detail by Esbensen, Landowne, and Price (1987), and valid, in the form outlined below, when the spin of the entrance channel is zero, i. e. for even-even projectiles on even-even targets. This approximation requires, in configuration space, the description of the reaction in a rotating frame with the $z-$axis along the separation vector, $\mathbf{r}$, of the interacting ions. In that frame, the interaction potential conserves the projection of the channel spin along the z-axis, s_0. The centrifugal potential is not diagonal with respect to s_0, but it can be replaced with a channel-independent barrier, $J(J+1)/(2\mu_\alpha r^2)$, where J is the total angular momentum. If the interaction potential is expanded in multipoles, only the $\mu = 0$ component of each multipolarity, λ, is effective and the coupled- channels equations have the same structure as in the spinless case.

If only target excitations are explicitly taken into account, the off-diagonal elements of the potential matrix, V, can be written in the simple form (Alhassid and Iachello (1989)):

$$V^J_{\alpha' s', \alpha s} = \frac{1}{\sqrt{4\pi}} \Sigma_\lambda \, v_\lambda(J,k) \hat{\lambda} (-1)^{s'} \begin{pmatrix} s' & \lambda & s \\ 0 & 0 & 0 \end{pmatrix} \beta_\lambda \hat{s}' < s' || G_\lambda || s > \ . \tag{16}$$

Here, s' is the spin of the exit channel, α', and s the spin of the entrance channel, α, and $\hat{\lambda} \equiv \sqrt{2\lambda+1}$; v_λ is the algebraic form factor for a transition of multipolarity λ, while β_λ is a normalization factor playing the role of a deformation. The reduced matrix element of the transition operator, G_λ, is defined in the following version of the Wigner-Eckart theorem:

$$< s'm' || G^\lambda_\mu || sm > = (s\lambda m\mu | s'm') < s' || G_\lambda || s > \ . \tag{17}$$

The diagonal matrix elements have the form already introduced in the one-channel case:

$$V^J_{\alpha s \alpha s} = \frac{v_{\alpha R}(k) + i v_{\alpha I}(k)}{1 + \exp(\frac{l - l_{0\alpha}}{\Delta_\alpha})} + \eta_\alpha \ , \tag{18}$$

where η_α is the Sommerfeld parameter in channel α. At this point, a choice has to be made for the transition form factors, v_λ: the analytic formulae adopted by Alhassid and Iachello (1989) mimic in angular momentum space the expressions commonly adopted in configuration space. In fact, the nuclear form factor is

$$v^N_{\alpha\beta}(l,k) = -\left[\frac{d}{dl}\frac{u_R(k) + i u_I(k)}{1 + \exp[(l - l_0)/\Delta}\right]_{\alpha\beta} , \tag{19}$$

and the Coulomb form factor is

$$v^{C\lambda}_{\alpha\beta} = \frac{3 v^C_0 \eta_\alpha}{2l+1} \begin{cases} (l/l_{0C})^{\lambda+1}, & l \leq l_{0C} \\ (l_{0C}/l)^\lambda, & l \geq l_{0C} \end{cases} \tag{20}$$

In the off-diagonal form factors (19) the geometric parameters $l_{0\alpha\beta}$ and $\Delta_{\alpha\beta}$ are taken to be the arithmetic mean of the corresponding values in channels α and β;

$$l_{0\alpha\beta} = \frac{1}{2}(l_{0\alpha} + l_{0\beta}) \ ; \ \Delta_{\alpha\beta} = \frac{1}{2}(\Delta_\alpha + \Delta_\beta) \ . \tag{21}$$

2 Elastic and Inelastic Scattering Near the Coulomb Barrier

The formalism described in the previous section was originally applied to light heavy-ion reactions, such as $^{16}O + {}^{24}Mg$ at $E = 27.8$ MeV (Alhassid and Iachello (1989)), well above the Coulomb barrier, estimated from formulae (10-11) of the order of 15.0 MeV for this system. The Sommerfeld parameter from formula (2) is $\eta \simeq 8.9$ and the elastic and inelastic angular distributions show large oscillations typical of the Fraunhofer diffraction pattern, expected on condition that

$$p \equiv 2\eta \cos^2(\frac{\theta_g}{2}) < 1 \ , \tag{22}$$

where the grazing angle, θ_g, is connected with the sum, R, of the two nuclear radii by the formula

$$R = \frac{\eta}{k}(1 + \csc(\frac{\theta_g}{2})) \ . \tag{23}$$

The formalism summarized in Section 1 allows satisfactory reproduction of experimental angular distributions in the Fraunhofer regime, characteristic of light heavy-ion reactions above the Coulomb barrier. For heavier systems above the barrier, the high value of η may break condition (22) for the validity of the Fraunhofer regime, and , as soon as $p > 1$, one observes a transition to the Fresnel diffraction regime, which is a fortiori valid at smaller E, thus at higher η, near, or below the Coulomb barrier.

When $E \leq E_B$, however,the form factors for elastic and inelastic scattering may require important modifications. For instance, the simple Woods-Saxon form (6) of the nuclear potential yields oscillations at backward angles in the elastic cross sections, not seen in experimental data. As for inelastic scattering, the cusp point of the Coulomb form factor (20) moves towards $l_{0C} = 0$ when E approaches E_B, and causes unrealistic oscillations in the inelastic angular distribution, even in the absence of a nuclear excitation.

In order to find a more suitable analytic form for the nuclear potential near the Coulomb barrier, one can exploit the fact that the inverse scattering problem, of determining the potential from a given S matrix, rather complicated in configuration space, is easy to solve in angular momentum space (Lichtenthäler et al. (1991)), in the representation where the S matrix is diagonal, by expanding the matrix elements, $S^L_{\alpha\alpha}$, given by formula (12), in a Taylor series around a first-guess potential, $v^0_{L\alpha}$. To first order in the expansion:

$$v_{L\alpha} = v^0_{L\alpha} - i\frac{\ln(S^L_{\alpha\alpha}/S^{0L}_{\alpha\alpha})}{\psi(L+1+i\eta_\alpha+iv^0_{L\alpha})+\psi(L+1-i\eta_\alpha-iv^0_{L\alpha})}\,, \qquad (24)$$

where

$$S^{0L}_{\alpha\alpha} = \frac{\Gamma(L+1+i\eta_\alpha+iv^0_{L\alpha})}{\Gamma(L+1-i\eta_\alpha-iv^0_{L\alpha})}\,, \qquad (25)$$

and $\psi(z) = \frac{d}{dz}\ln\Gamma(z)$ is the digamma function. For high partial waves, with $L \geq 2L_{g\alpha}$, where $L_{g\alpha}$ is the grazing angular momentum in channel α, $v^0_{L\alpha} \simeq 0$ and Eq. (25) reduces to pure Coulomb scattering. Iterative solution of eqs. (24-25) converges quickly for $|S^L_{\alpha\alpha}| < 1$. After obtaining $v_{L\alpha}$ in the representation where the S matrix is diagonal, one goes back to the original representation, by applying to the diagonal potential matrix, $v_{L\alpha}$, the inverse of the similarity transformation that diagonalised the S matrix. A word of caution is necessary, since the presence of the complex logarithm in Eq. (24) makes the relation between S and v multivalued and further restrictions are required in order to determine v uniquely. The adopted restrictions are:

$$(i)\ \lim_{L\to\infty} v_{L\alpha} = 0\,;$$
$$(ii)\ |Im(\ln(S^{L+1}_{\alpha\alpha}) - Im(\ln(S^L_{\alpha\alpha}))| < 2\pi$$

An extensive analysis of elastic angular distributions for the $^{16}O + ^{63}Cu$ system at twelve laboratory energies, ranging from 39 MeV, just below the Coulomb barrier, to 64 MeV (Lichtenthäler et al. (1994)) made use of a simple Woods-Saxon potential with energy independent parameters in configuration space in order to reproduce the elastic scattering cross section, and to determine accordingly the elastic S matrix in angular momentum space. The algebraic potential in L-space was then obtained by iterative solution of eqs. (24-25).

The main results of the analysis were the following: while the imaginary part of the algebraic potential, at fixed energy, is positive for $L = 0$ and goes quickly to zero for $L > L_g$, in such a way that it can be approximated roughly by a Woods-Saxon shape in L-space, the real part bends down to negative values for $L \leq L_g$: the higher the laboratory energy, the more enhanced the bending.

The interpretation of this effect is that there is a repulsive term in the potential that makes the nuclear deflection function, $\Theta(L) = 2\frac{d}{dl}\delta_R(L)$ positive for $L \leq L_g$, where δ_R is the real part of the nuclear phase shift. At higher angular momenta, $L > L_g$, the real potential becomes positive, goes through a maximum and then decreases exponentially with increasing L, as expected for an attractive potential.

The behaviour of v_N as a function of L obtained in the inversion procedure outlined above lends itself to the following parametrization:

$$v_N(k, L) = v^0(k, L) + \alpha[v^0(k, L)]^2, \quad (|v^0| < 1), \tag{26}$$

with

$$v^0(k, L) = v_R(k) f_R(k, L) + i v_I(k) f_I(k, L), \tag{27}$$

and

$$f_j(k, L) = \frac{1}{1 + \exp\left(\frac{L - L_{0j}}{\Delta_j}\right)} \quad (j = R, I) \tag{28}$$

are Woods-Saxon forms with different L_0 and Δ for the real and imaginary part of the potential (R and I, respectively), and α is an expansion parameter.

The real part of the potential:

$$Re(v_N) = v_R(k) f_R(k, L) - \alpha^2 v_I^2(k) f_I^2(k, L) \tag{29}$$

thus receives a negative contribution from the square of the first-order imaginary part, which can be interpreted as a reflection in the imaginary well.

If α is set to unity, for simplicity's sake, formula (26) has six adjustable parameters, namely two depths, two grazing angular momenta and two diffuseness parameters, that allowed Lichtenthäler et al. (1994) to obtain a very accurate reproduction of the algebraic potentials derived by inversion of the elastic S matrix at twelve laboratory energies of $^{16}O + {}^{63}Cu$.

Plotting the real and imaginary nuclear potentials versus energy in the laboratory frame, E_{lab}, reveals an interesting behaviour in the real part, which goes through a maximum at $E_{lab} \simeq 43$ MeV, and, after a small decrease, remains constant up to the highest energy taken into account in the analysis, $E_{lab} = 64$ MeV. This maximum in the real potential is necessary for reproducing the principal diffraction maximum of the experimental elastic cross section at intermediate angles, clearly seen above the Coulomb barrier. As for the imaginary potential, it steadily increases with increasing E_{lab}.

This trend of $Re(v_N)$ versus E_{lab} recalls the threshold anomaly of the real optical potential used in the Schrödinger equation in configuration space,

where the effect is explained by means of a dispersion relation that connects the real and the imaginary optical potential, and is a consequence of the principle of causality. To test the algebraic potential for a possible dispersion relation, we have made a linear approximation to $Im(v_N)(E_{lab})$, shown in Fig.1, computed $Re(v_N)(E_{lab})$ according to the dispersion formulae of Mahaux et al. (1986) and plotted it (the solid curve in Fig.1) in comparison with the twelve values that reproduce the experimental elastic cross sections. The discrepancy between 'experimental' and calculated $Re(v_N)$ seems to increase with increasing energy, but might be due, at least in part, to the fact that we approximated $Im(v_N)$ in $l-$space with a simple Woods-Saxon form,neglecting there second order effects , which are included in $Re(v_N)$. Therefore, the problem requires, and deserves, further investigation.

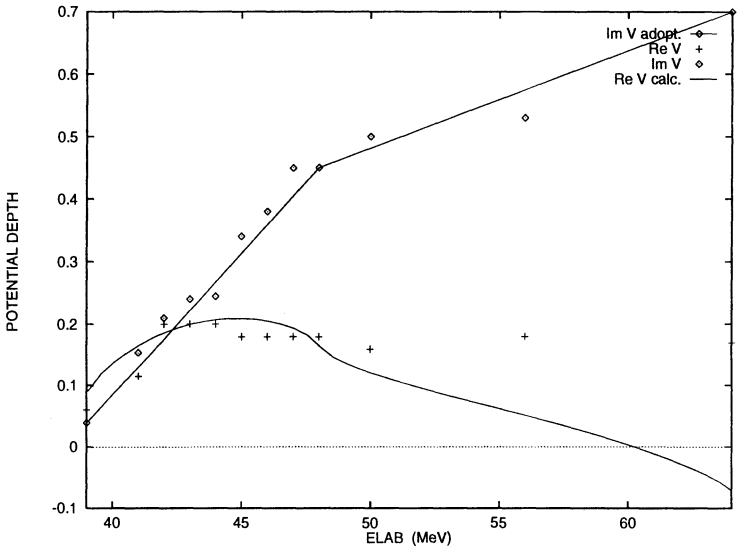

Fig. 1. Algebraic potential vs lab. energy

We come now to the treatment of inelastic scattering: at energies below and near the Coulomb barrier, the dominant role is played by Coulomb excitation, of multipolarity $\lambda = 2$, while the main effect of the nuclear interaction is to reduce the Coulomb scattering cross section at large angles. Being in a region of large η's, we assume that a semiclassical approach to Coulomb scattering makes sense, and try to derive from it a simple analytic formula for the Coulomb form factor.

The trajectory of relative motion of the two ions is thus approximated by a hyperbola of eccentricity $\epsilon > 1$, connected with the scattering angle in the centre-of-mass frame, θ, by the relation

$$\frac{\theta}{2} = \arcsin\left(\frac{1}{\epsilon}\right) . \tag{30}$$

The distance of closest approach of the two ions is a simple function of ϵ

$$b = \frac{Z_p Z_t e^2}{2E}(1+\epsilon) , \tag{31}$$

and the characteristic collision time can be estimated by means of the relation

$$\tau_c = \frac{b}{v_{rel}} = \sqrt{\frac{\mu}{2E}} b . \tag{32}$$

The collision time is essential in determining an upper bound to the energy, E_f, of the states of the target, initially at energy E_i, that can be sizeably excited during the collision, namely those states for which the adiabaticity parameter

$$\xi = \frac{E_f - E_i}{2\hbar}\tau_c = \frac{-Q\tau_c}{2\hbar} \tag{33}$$

does not exceed unity, $Q\,(= E_i - E_f)$ being the reaction Q-value.

All the above quantities are thus simple functions of ϵ, which, in turn, is connected with the orbital angular momentum, L in units of $\hbar$, by the following formula, valid for L (and η) $>>$ 1:

$$\sqrt{L(L+1)} \simeq L + \frac{1}{2} = \eta\sqrt{\epsilon^2 - 1} \tag{34}$$

where η is the Sommerfeld parameter.

A qualitative estimate of the amplitude of Coulomb transition with multipolarity λ from state ψ_i to state ψ_f is given by Broglia and Winther (1991):

$$|\chi_{i\to f}(\theta,\xi)| = \frac{2\pi}{(\lambda+\frac{1}{4})^{3/2}} \frac{Z_p e}{\hbar v_{rel}} \frac{|<\psi_f||G_\lambda||\psi_i>|}{\hat{s}_f} \frac{\sqrt{f_c(\theta,\xi)}}{b^\lambda} . \tag{35}$$

Here, $<\psi_f||G_\lambda||\psi_i>$ is the reduced matrix element of an electric multipole operator, s_f is the spin of the final state, and the adiabatic cutoff function, $f_c(\theta,\xi)$, can be approximated with a simple exponential:

$$f_c(\theta,\xi) \simeq \exp(-a_\lambda \xi) , \tag{36}$$

where, for the most important multipolarity of transition to the low-lying states of the target, $\lambda = 2$, $a_2 \simeq 3.45$.

At this point, we assume that the Coulomb form factor is proportional to $|\chi_{i\to f}/ <\psi_f||G_\lambda||\psi_i>|$ and express it as a function of L, since both ξ and b depend on L through the inverse of formula (34):

$$\epsilon = \sqrt{1 + \frac{\left(L+\frac{1}{2}\right)^2}{\eta^2}} . \tag{37}$$

We thus obtain for the Coulomb form factor, v_C, as a function of E and L:

$$v_C(E,L) = v_C^0(E)\frac{\exp\left[\frac{a_\lambda}{8}\frac{\eta Q}{E}\left(1+\sqrt{1+\frac{(L+\frac{1}{2})^2}{\eta^2}}\right)\right]}{1+\sqrt{1+\frac{(L+\frac{1}{2})^2}{\eta^2}}}, \tag{38}$$

where

$$v_C^0(E) = \frac{2\pi}{(\lambda+1/4)^{3/2}}\frac{1}{\hat{s}_f}\frac{Z_p e}{\hbar v_{rel}}\left(\frac{2E}{Z_p Z_t e^2}\right)^\lambda . \tag{39}$$

One should remember, in any case, that formulae (35–37) give only a rough estimate of the modulus of the Coulomb transition amplitude; that is why we take the freedom of adjusting a_λ in Eq. (36) and $v_C^0(E)$ in Eq. (38) on experimental data of inelastic scattering.

In order to check the angular momentum dependence of the proposed Coulomb form factor (38), we have performed coupled-channels calculations of pure Coulomb excitation in heavy ion reactions by means of the ECIS94 code (Raynal (1994)): Fig.2 shows the $L-$dependence of formula (38) in comparison with the $|S_{\alpha L,\alpha L}|$ matrix element corresponding to a pure Coulomb excitation of the 2_1^+ state of ^{64}Zn, bombarded with ^{16}O at $E_{lab} = 46$ MeV, with multipolarity $\lambda = 2$ and third component $\mu = 0$. The two functions are arbitrarily normalized to 1 at $L_c = 30$, while the Sommerfeld parameter in the elastic channel is $\eta \simeq 21$.

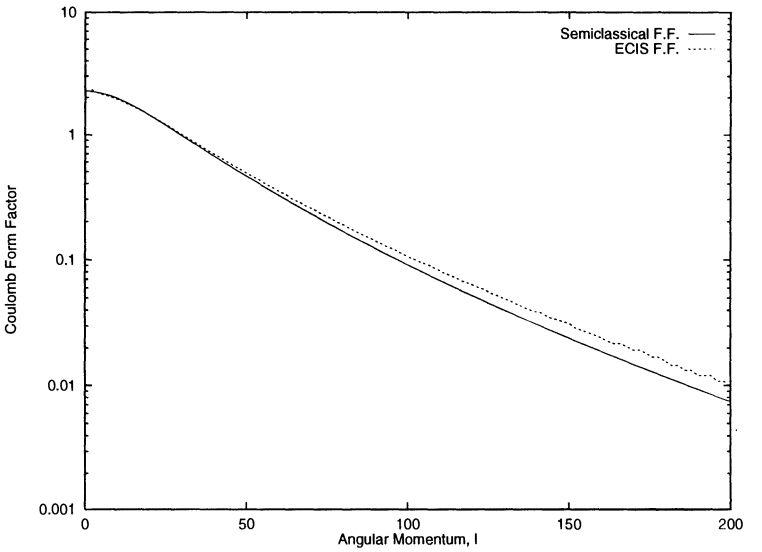

Fig. 2. Coulomb form factor vs angular momentum

As mentioned in Section 1, the algebraic version (16) of the rotating frame approximation cannot be applied to systems with nonzero spin in the entrance channel, e. g. odd-mass targets, like ^{65}Cu, considered by Lichtenthäler et al. (1992), who suggested a more general approximation, where, in the arguments of the gamma matrices, the orbital angular momenta, L_α, are replaced with the total angular momentum, J, only in the kinetic matrix, $L+1 \rightarrow J+1$, but not in the potential matrix, whose elements are, instead of (16),

$$V_{\alpha L,\beta L'} = \frac{1}{\sqrt{4\pi}} \Sigma_\lambda (-1)^{J-s_\alpha} i^{L'-L-\lambda} \hat{L}\hat{L}'\hat{s}_\beta (LL'00|\lambda 0) \qquad (40)$$
$$\times\ W(LL's_\alpha s_\beta|\lambda J) v^\lambda_{\alpha\beta} < s_\beta \| G_\lambda \| s_\alpha > ,$$

where W is a Racah coefficient.

The scattering amplitudes are written in the form (Satchler (1983)):

$$f_{\beta m_\beta,\alpha m_\alpha}(\theta) = \frac{\sqrt{4\pi}}{2ik_\alpha} \Sigma_L \Sigma_{L'} \Sigma_J (Ls_\alpha 0 m_\alpha | J m_\alpha) \qquad (41)$$
$$\times\ (L's_\beta m' m_\beta | J m_\alpha)(\hat{S}^J_{\beta L',\alpha L} - \delta_{\alpha\beta}\delta_{LL'}\delta_{s_\alpha s_\beta})$$
$$\times\ \exp(i\sigma_{\alpha L} + i\sigma_{\beta L'}) Y^{m'}_{L'}(\theta) .$$

Here, the z-axis has been chosen in the direction of the incident beam; moreover, $m' = m_\alpha - m_\beta$, and

$$\hat{S}^J_{\beta L'\alpha L} = \frac{S^J_{\beta L',\alpha L}}{\exp i(\sigma_{\alpha L} + \sigma_{\beta L'})} . \qquad (42)$$

When the spin of the entrance channel is different from zero, the elastic S matrix element, $S^J_{\alpha L,\alpha L}$, computed in the present approximation, does not match exactly the Coulomb S matrix, $S^C_{\alpha L,\alpha L} = \exp(2i\sigma_{\alpha L})$, at high J, and formula (42) would introduce spurious terms in the sum over partial waves (41). These spurious terms are avoided by replacing formula (42), for $\beta = \alpha$, with

$$\hat{S}^J_{\alpha L,\alpha L} = \frac{S^J_{\alpha L,\alpha L}}{S^C_{\alpha J,\alpha J}} , \qquad (43)$$

where

$$S^C_{\alpha J,\alpha J} = \frac{\Gamma(J+1+i\eta_\alpha)}{\Gamma(J+1-i\eta_\alpha)} . \qquad (44)$$

3 Results, Comments and Outlook

The formalism described in the previous sections is applied, to an increasing degree of complexity, to elastic and inelastic scattering of ^{16}O projectiles by Ni and Cu targets: in the case of nickel, the experimental data, recently published by Chamon et al. (1996), refer to laboratory energies in the 34–37

MeV interval, below the Coulomb barrier of the system, so that the only sizeable reaction, in addition to elastic scattering, is inelastic scattering to the 2_1^+ state of the Ni target, where Coulomb excitation of multipolarity $\lambda = 2$ plays a dominant role. The main effect of the nuclear interaction is to reduce the cross sections at backward angles, as shown by Chamon et al. (1996) in their coupled-channels analysis of the data performed by means of the ECIS code (Raynal (1994)).

Since the spin of the entrance channel is zero, it is possible to resort to the algebraic version of the rotating frame approximation, outlined in Section 1, thus reducing the problem to a simple and fast two-channels calculation, whose results are shown in the following figures for different nickel isotopes and incident energies, as a function of the scattering angle in the c.m. frame. As usual, the elastic cross sections are relative to the Rutherford cross section at the same angle, $\sigma/\sigma_R(\theta)$. The fits to the experimental data have comparable accuracy to ECIS and are simpler and faster to obtain. A few preliminary results of the analysis, still in progress, are shown in the following figures for ^{58}Ni (Figs. 3, 4) and for ^{60}Ni (Figs. 5, 6), at $E_{lab} = 35.9$ MeV.

It is to be pointed out that the diagonal terms of the potential matrix contain small, but significant nuclear contributions, which include, in their real part, the second-order effects shortly described in Section 2. As expected, inelastic scattering is dominated by Coulomb excitation, and is thus a good test of the semiclassical approach of Section 2, which, in spite of its extreme simplification, seems to work remarkably well.

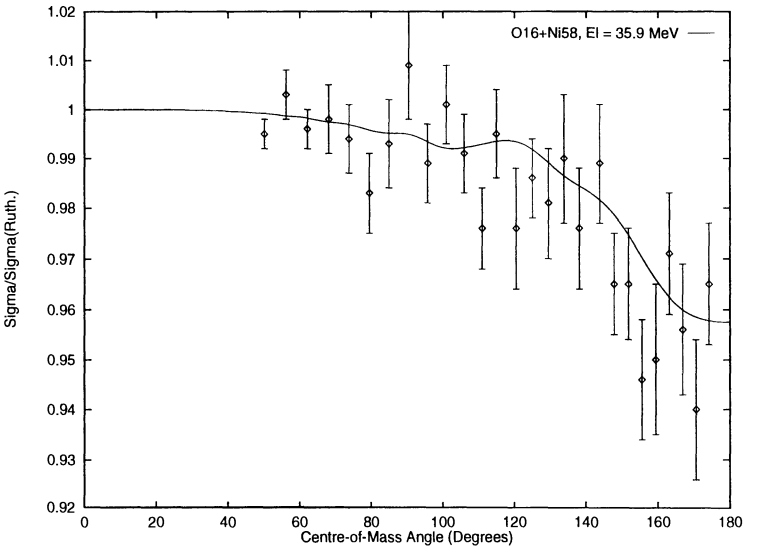

Fig. 3. $^{16}O + {}^{58}Ni$: Elastic scattering at Elab = 35.9 MeV

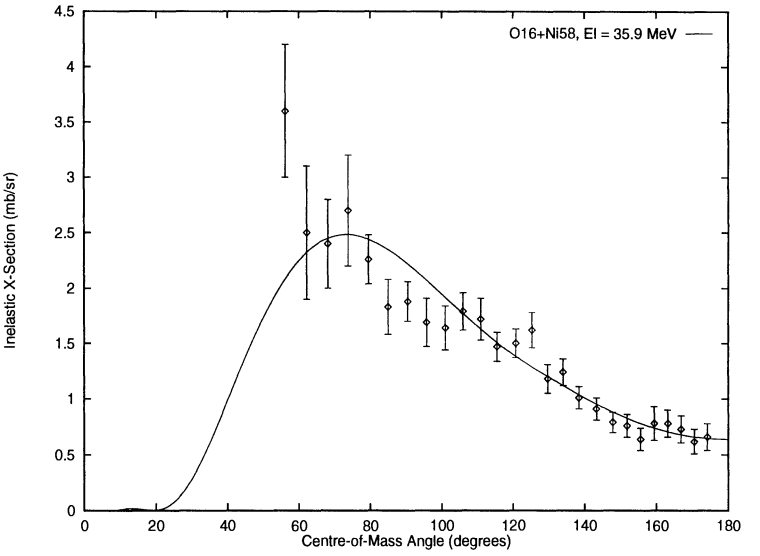

Fig. 4. $^{16}O + {}^{58}Ni$: Inelastic scattering at Elab = 35.9 MeV

A fundamental ingredient of its success is the Q-value dependence in the adiabatic cutoff function of formula (38). The Q-value dependence of the off-diagonal terms of the potential matrix had been overlooked in the original formulation given by Alhassid and Iachello (1989), but its importance in reproducing the results of traditional coupled-channels calculations was already pointed out by Alonso et al. (1992) in their algebraic calculations of multiple transfer of nucleon pairs for the system $^{112}Sn + {}^{120}Sn$ at bombarding energies around the Coulomb barrier.

A second set of coupled-channels calculations refers to the already quoted system, $^{16}O + {}^{63}Cu$, measured by Pereira et al. (1989) at incident energies between 39 and 64 MeV. Here, the $s = 3/2$ spin of ^{63}Cu prevents us from using the rotating frame approximation of Section 1, and we resort to the more general isocentrifugal approximation of Section 2.

The analysis is complicated by the fact that the measured inelastic cross sections are due to cumulative excitation of five low-lying levels of ^{63}Cu, not resolved in the experiments. It is thus necessary to resort to a realistic structure model of odd-mass nuclei, and to compute, within its framework, the E2 transition matrix elements among the five excited states and the ground state. The most suitable model is, in our opinion, the Interacting Boson-Fermion Model (Iachello and Van Isacker (1991)), that exploits an underlying Spin(5) Bose-Fermi symmetry of the Hamiltonian describing the low-lying excitations of ^{63}Cu. Form and parameters of the Hamiltonian used in the present analysis are briefly discussed by Lichtenthäler Filho(1994). It is worth pointing out that this is a successful example of simultaneous algebraic

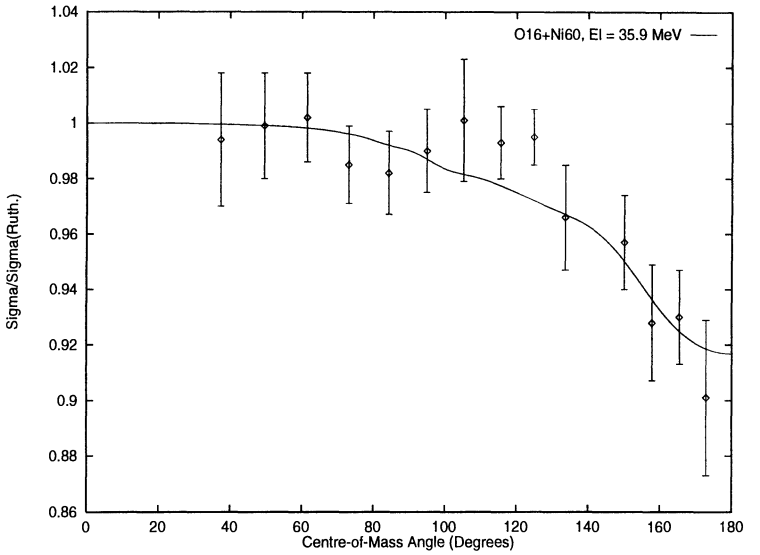

Fig. 5. $^{16}O + {}^{60}Ni$: Elastic scattering at Elab = 35.9 MeV

description of relative motion of interacting ions, based on SO(3,1) symmetry, and of internal excitation of the target, based on Spin(5) symmetry.

As shown in the following Figs.7,8, referring to $E_{lab} = 46$ MeV, both elastic and cumulative inelastic scattering to the five lowest-lying levels of ^{63}Cu are satisfactorily reproduced. The analysis was performed at twelve bombarding energies and the comparison of calculated and experimental cross sections presented elsewhere (Lichtenthäler Filho(1994)).

The same experiment (Pereira et al. (1989)) provided, in addition to elastic and inelastic scattering, also data on proton transfer from the ^{16}O projectile to the ^{63}Cu target, so as to form the ^{64}Zn isotope, either in its ground state, or in the 2_1^+ state, at $E^* = 0.992$ MeV , and on fusion.

The inclusion of nucleon transfer channels in the formalism is not difficult, at least in the no recoil approximation, following semiclassical arguments analogous to Coulomb excitation, and discussed in detail by Broglia and Winther (1991). The following Figs.9,10 show preliminary calculations of one proton transfer, again at $E_{lab} = 46$ MeV. The calculations of proton transfer are in progress, and will be presented elsewhere, together with the relevant formalism.

Once a realistic description of quasielastic reactions, including nucleon transfer, is obtained, also the fusion cross section should be reproduced in our algebraic coupled-channels calculations, so as to get a global overview of heavy ion reactions in the proximity of the Coulomb barrier.

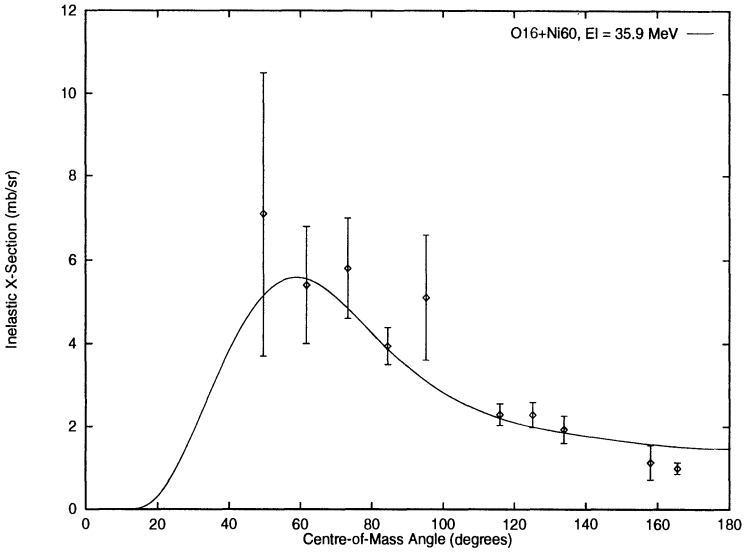

Fig. 6. $^{16}O + {}^{60}Ni$: Inelastic scattering at Elab = 35.9 MeV

The formalism discussed in the present work is applied to the Fresnel diffraction regime, characterized by large values of the Sommerfeld parameter, and might require modifications for light heavy-ion reactions, in the Fraunhofer regime. In that case, however, deeper microscopic insight into excitation and relative motion of nucleon clusters, characteristic of the structure and reactions of light nuclei, might lead to a considerable improvement of the algebraic scattering theory (Cseh (1996)).

As a final remark, we would like to point out that a rigorous treatment of spin degrees of freedom is highly desirable, in order to make the algebraic coupled-channels formalism fully competitive with the traditional one. An interesting perspective is provided by recent studies of nonstandard matrix realizations of SO(n,1) generators, where spin is explicitly taken into account (Lévay (1995), Lévay and Apagyi (1995)).

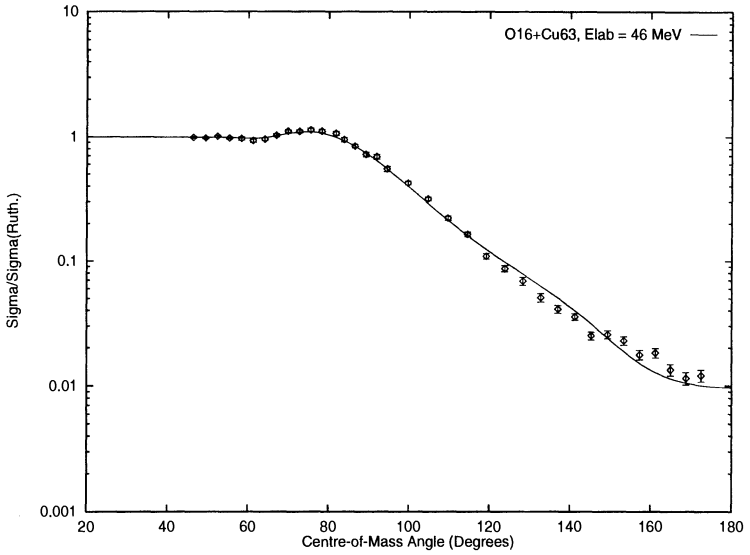

Fig. 7. $^{16}O + {}^{63}Cu$: Elastic scattering at Elab = 46 MeV

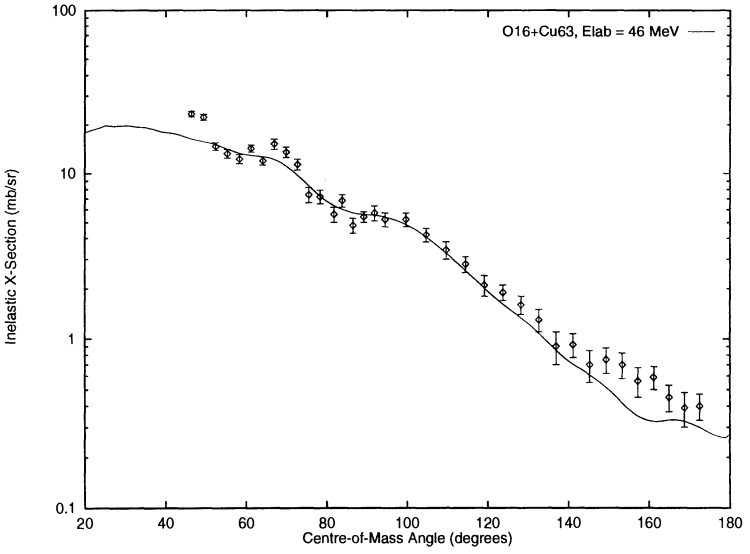

Fig. 8. $^{16}O + {}^{63}Cu$: Inelastic scattering at Elab = 46 MeV

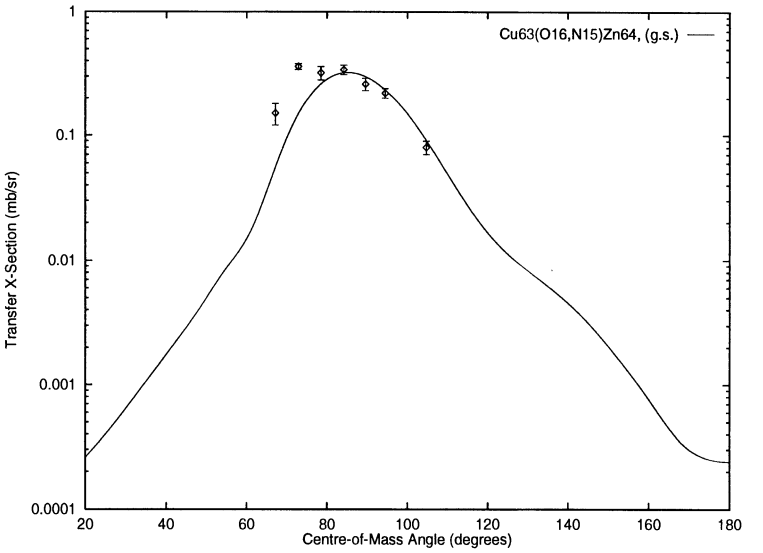

Fig. 9. $^{16}O + {}^{63}Cu$: Proton transfer to the 0_1^+ state of ^{64}Zn

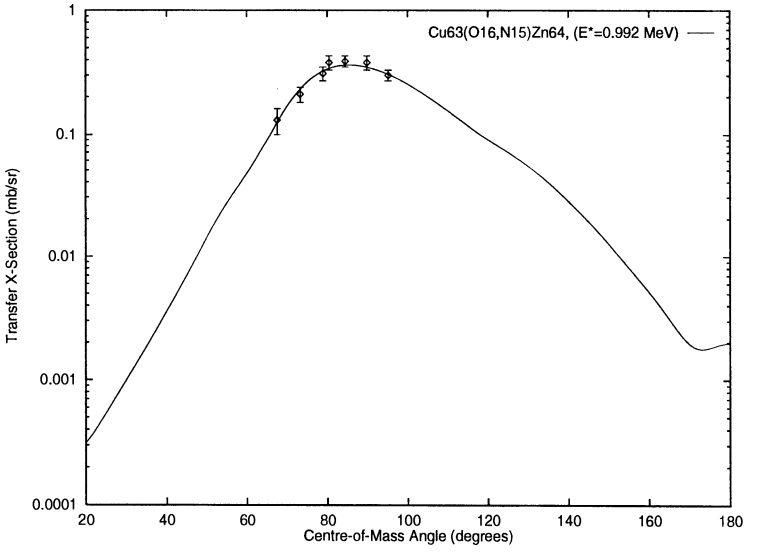

Fig. 10. $^{16}O + {}^{63}Cu$: Proton transfer to the 2_1^+ state of ^{64}Zn

Acknowledgement

It is a pleasure to thank dr. L. C. Chamon for providing us with the experimental data quoted in the present work.

References

Alhassid Y., Iachello F. (1989): Algebraic Approach to Heavy-Ion Reactions. Nucl. Phys. **A 501**, 585–604

Alonso C.E., Gallardo M.I., Lozano M.,Vitturi A. (1992) Algebraic Description of Multistep Processes in Very-Heavy-Ion Reactions. Nucl. Phys. **A 540**, 261–274

Broglia R. A., Winther A. (1991): *Heavy Ion Reactions.* (Addison-Wesley, New York)

Chamon L.C., Pereira D., Rossi Jr E.S., Silva C.P., Dias H., Losano L., Ceneviva C.A.P. (1996): Isotopic dependence of the ion-ion potential in the Systems $^{16}O + {}^{58,60,62,64}Ni$. Nucl. Phys. **A 597**, 253–268

Cseh J. (1996): Algebraic Scattering Theory and Light Heavy-Ion Reactions. these Proceedings

Esbensen H., Landowne S., Price C. (1987): Comment on "Reduction of Coupled Equations for Heavy Ion Reactions". Phys. Rev. **C 36**, 1216–1217

Iachello F., Van Isacker P. (1991): *The Interacting Boson-Fermion Model.* (Cambridge University Press, Cambridge)

Lévay P. (1995): Scattering Potentials with LS-Terms from First-Order Casimir Operators. J. Phys. **A 28**, 5919–5929

Lévay P. and Apagyi B. (1995): Modified Symmetry Generators Related to Solvable Scattering Problems. J. Math. Phys. **36**, 6633–6646

Lichtenthäler Filho R., Villari A. C. C., Gomes L. C., Carrilho Soares P. (1991): An Algebraic Optical Potential for Heavy Ion Collisions. Phys. Lett. **B 269**, 49–53

Lichtenthäler Filho R., Ventura A., and Zuffi L. (1992): Spin Formalism in the Algebraic Scattering Theory for Heavy Ions. Phys. Rev. **C 46**, 707–710.

Lichtenthäler R., Pereira D., Chamon L.C., Gomes L.C., Ventura A., Zuffi L. (1994): Second Order Effects in the Algebraic Potential for Havy-Ion Systems near the Coulomb Barrier. Phys. Rev. **C 50**, 3033–3036

Lichtenthäler Filho R. (1994): The Algebraic Scattering theory and its Application to Heavy-Ion Reactions, in:*Perspectives for the Interacting Boson Model*, edited by R.F. Casten et al., 521–528 (World Scientific, Singapore)

Mahaux C., Ngô H., Satchler G.R., (1986): Causality and the Threshold Anomaly of the Nucleus-Nucleus Potential. Nucl. Phys. **A 449**, 354–394

Pereira D., Ramirez G., Sala O., Chamon L.C., Rocha C.A., Acquadro J.C., Tenreiro (1989): Effect of the Threshold Anomaly on the Fusion Cross Sections for the Systems $^{16}O + {}^{63,65}Cu$. Phys. Lett. **B 220**, 347–350

Raynal J. (1994): Notes on ECIS94. (unpublished)

Satchler G.R. (1983): *Direct Nuclear Reactions* (Clarendon,Oxford)

Tanimura O. (1987): Reduction of Coupled Equations for Heavy Ion Reactions. Phys. Rev. **C 35**, 1600-1602

Wu J. (1985): *Group Theory Approach to Scattering* (Ph. D. Thesis, Yale university, unpublished)

Algebraic Scattering Theory and Light Heavy-Ion Reactions

J. Cseh

Institute of Nuclear Research of the Hungarian Academy of Sciences,
Debrecen, Pf. 51. Hungary-4001

Abstract. The similarities and differences between the Algebraic Scattering Theory and the (Semimicroscopic) Algebraic Cluster Model are discussed. Based on this comparison suggestions are made for new kind of applications and for an alternative formulation of the scattering model.

1 Introduction

The basic problems of scattering theory and of cluster studies of bound and quasibound states show remarkable similarities. As a consequence the methods applied in the two fields are also close to each other. Recently algebraic approaches have been applied in both areas. In this contribution the similarities as well as the differences between these group theoretical models are discussed, and based on this comparison, new ways are suggested for the extension and application of the Algebraic Scattering Theory.

In *scattering theory* we are interested in describing the relative motion of two interacting particles (A and B). Their distance vector changes from minus infinity to plus infinity. The energy spectrum of the system is continuous.

When the interaction shows a dynamic symmetry, i.e. when the Hamiltonian of the system commutes with the elements of a Lie-algebra (G_R) (Schiff 1968) the problem can be solved by purely group theoretical methods. One obtains a closed formula for the scattering matrix, which provides us with the cross section.

If the two particles do not have any internal degrees of freedom, we have a single channel problem. If the particles have internal degrees of freedom, then we are faced with a multichannel problem. If group theoretical models (with group structure G_A and G_B, respectively) can be applied for the description of the internal degrees of freedom, then a completely algebraic treatment of the coupled channel problem can be given.

An Algebraic Scattering Theory (AST) of this kind has been developed and applied in the last 13 years (Alhassid et. al. 1983, Wu et. al. 1987, Alhassid and Iachello 1989), and it is presented in the previous contribution to the present volume (Ventura 1996).

In *cluster studies* we are interested in describing the relative motion of two interacting particles (A and B). Their distance remains finite either per-

manently (bound states) or for a considerable time (quasi-bound states). The energy spectrum of the system is discrete.

When the interaction shows a dynamic symmetry, i.e. when the Hamiltonian of the system commutes with the elements of a Lie-algebra (G_R) the problem can be solved by purely group theoretical methods. One obtains a closed formula for the energy eigenvalues, and other physical quantities can also be calculated in a simple way.

If the particles do not have any internal quantum numbers, we have a problem with a single degree of freedom, and the group structure of the model is G_R. If the clusters have internal quantum numbers (e.g. due to their composite nature) we are faced with the problem of coupled degrees of freedom. When group theoretical models (with group structure G_A and G_B, respectively) can be applied for the description of the internal degrees of freedom, then we have an algebraic description in terms of a model with $G_A \otimes G_R \otimes G_B$ group structure.

A group theoretical description of this kind, called Semimicroscopic Algebraic Cluster Model (SACM) has been developed and applied in the last five years (Cseh 1992, Cseh and Lévai 1994). (For a review of the present situation see (Cseh et. al. 1996, Cseh 1996).)

Similar approaches are applied successfully to two-body problems in other branches of physics as well: two-atomic molecules (Iachello and Levine 1995, Frank and van Isacker 1994), and two-quark systems (Iachello et. al. 1991). In the case of the rotational-vibrational motion of a molecule there is no need to treat any internal degrees of freedom, in the case of quark systems there are internal quantum numbers, but there is no composite internal structure. (A comparison of the algebraic models of the three fields is given in (Iachello et. al. 1995).)

In the scattering problem the relevant irreducible representations are of infinite dimension due to the continuous spectrum. Therefore G_R is non-compact, e.g. $SO(3,1)$. On the other hand, for the description of the discrete spectrum in the cluster problem one applies the finite dimensional irreducible representations of a compact group $U(3)$ in nuclear physic, and $O(4)$ in molecular and hadron specroscopy.

Exact dynamic symmetries, as they are defined above, hold only for very special interactions, like e.g. Coulomb force and harmonic oscillator interaction, therefore, they are not very helpful in describing realistic problems. The algebraic approach, however, which relies on a symmetry is useful not only for systems with exact dynamic symmetry, but also for systems with approximate (broken) symmetries. The way of treating the symmetry breaking in the scattering theory and in the cluster model is different, as discussed more in detail below.

In what follows first brief summaries of the AST and of the SACM are presented in Sections 2 and 3, respectively, which are needed for the analysis of the similarities and differences of their contents and methods. This

comparison suggests some new type of applications of the AST. They are mentioned in Section 4. In Section 5. a possible alternative way of constructing algebraic scattering theories is discussed. The basic concept for that comes also from the algebraic treatment of the bound state problems. Finally some conclusions are drawn in Section 6.

2 Algebraic Scattering Theory

Here we review very briefly the concepts and formulae relevant for our comparison with the cluster model. The notations of Alhassid and Iachello (1989) are followed, and spinless particles are considered.

The basic task of the scattering theory is the derivation of the cross section.

2.1 Single-channel scattering

The differential cross section is obtained in terms of the scattering amplitude:

$$\frac{d\sigma}{d\Omega} = |f(k,\Omega)|^2 \ , \tag{1}$$

and for central interactions the scattering amplitude is given in a partial wave expansion:

$$f(k,\theta) = \frac{1}{2ik}\sum_{l=0}^{\infty}(2l+1)[S_l(k)-1]P_l(cos\theta) \ . \tag{2}$$

The Coulomb problem has an exact $SO(3,1)$ dynamic symmetry, i.e. the Hamiltonian can be written in terms of a Casimir invariant of this group:

$$H = -\frac{\mu(Z_1 Z_2 e^2)^2}{2(C_2+1)} \ , \tag{3}$$

where μ is the reduced mass, and C_2 is the second order Casimir operator with the eigenvalues:

$$\langle C_2 \rangle = \omega(\omega+2) \ ; \qquad \omega = -1 + i\frac{Z_1 Z_2 e^2}{k} \tag{4}$$

for the continuous unitary representations, labeled by the wave number k. The $S_l(k)$ scattering matrix can be obtained in a purely algebraic way (Wu et. al. 1987):

$$S_l = \frac{\Gamma(l+1+i\eta)}{\Gamma(l+1-i\eta)} \ , \tag{5}$$

here Γ denotes Euler's Gamma-function, and η is the Sommerfeld parameter:

$$\eta = \frac{\mu Z_1 Z_2 e^2}{\hbar^2 k} \ . \tag{6}$$

For more general interactions the symmetry does not hold, and one is not able to derive simple formulas, like (5). If, however, the Coulomb force is still an important part of the interaction, like e.g. in case of heavy-ion reactions, one can try a similar description. Dealing with this situation of *symmetry breaking* in the scattering process in the AST the following generalisation is carried out. The *fuctional form of the S matrix (5) is left unchanged*, but the Sommerfeld parameter of the problem with an exact symmetry is *substituted by a generic function* $v(l,k)$, called algebraic potential:

$$S_l = \frac{\Gamma(l+1+iv(l,k))}{\Gamma(l+1-iv(l,k))} \ . \tag{7}$$

For the description of heavy-ion reactions one takes:

$$v(l,k) = \eta + v_S(l,k) \ , \tag{8}$$

where the short-range part is:

$$v_S(l,k) = \frac{v_R(k) + iv_I(k)}{1 + exp[(l - l_0(k))/\Delta(k)]} \ . \tag{9}$$

Here R refers to real, and I means imaginary.The algebraic potential parametrizes the interaction in the similar way in the angular momentum (l) space, like the optical potential does in the the real (r) space.

2.2 Multichannel scattering

The differential cross section from channel α to α' is given by:

$$\left(\frac{d\sigma}{d\Omega}\right)_{\alpha\to\alpha'} = \frac{k_{\alpha'}}{k_\alpha}|f_{\alpha\alpha'}(k,\Omega)|^2 \ . \tag{10}$$

After the partial wave expansion:

$$f_{\alpha\alpha'}(k,\theta) = \frac{1}{2i[k_{\alpha'}k_\alpha]^{1/2}} \sum_{l=0}^{\infty}(2l+1)[S^l_{\alpha\alpha'}(k) - \delta_{\alpha\alpha'}]P_l(cos\theta) \ . \tag{11}$$

The S matrix is still given in terms of the Γ functions:

$$S^l = K^{1/2}\frac{\Gamma(l+1+iv)}{\Gamma(l+1-iv)}K^{-1/2} \ , \tag{12}$$

but now the argument is a matrix. K is a diagonal matrix with the momenta k_α along its diagonal.The algebraic potential contains again two parts corresponding to the Coulomb and strong interactions:

$$v_{\alpha\alpha'}(l,k) = v^C_{\alpha\alpha'}(l,k) + v^S_{\alpha\alpha'}(l,k) \ . \tag{13}$$

3 The Semimicroscopic Algebraic Cluster Model

Here we review very briefly the concepts and formulae of the SACM relevant for our comparison with the Algebraic Scattering Theory. We consider only the problem of two clusters. More detailed presentation of the model can be found in Refs. (Cseh and Lévai 1994, Cseh et. al. 1996, Cseh 1996).

In cluster studies we are interested in determining the energy spectra and dynamic properties (e.g. electromagnetic transition rates) of cluster systems.

3.1 Structureless clusters

Closed shell nuclei, like ^{4}He or ^{16}O, may form this kind of clusters, which remain unchanged in the low-energy region. The joint conclusion of several experimental and theoretical studies is that some collective bands in ^{20}Ne can be considered, to a good approximation, as a core-plus-alpha-particle configuration.

When the internal degrees of freedom of the clusters do not play any role, we have to deal only with their relative motion. If the intercluster force shows a dynamic symmetry then the eigenvalue problem of the energy has an analytic solution. That is the case for the harmonic oscillator force, when the Hamiltonian is:

$$H_{HO} = \gamma(C^{(1)}_{U3} + \frac{3}{2}) = \gamma(n + \frac{3}{2}) \ , \tag{14}$$

where $C^{(1)}_{U3}$ is the linear Casimir operator of the $U(3)$ group, having the physical meaning of the number operator of oscillator quanta, and γ gives the energy of the oscillator quanta. Then the energy eigenvalue is:

$$E = \gamma(n + \frac{3}{2}) \ . \tag{15}$$

The spectrum of the harmonic oscillator is too simple, for the description of atomic nuclei we need more realistic interaction. For light nuclei the harmonic oscillator plus quadrupole-quadrupole interaction turned out to be a reasonable approximation:

$$H = H_{HO} + \chi Q \cdot Q \ . \tag{16}$$

Recalling that the (algebraic) Q operator is related to the second order Casimir operator of $SU(3)$, and to the angular momentum L by:

$$C^{(2)}_{SU3} = 2Q \cdot Q + \frac{3}{4} L \cdot L \ , \tag{17}$$

and taking into account that $L \cdot L$ is the Casimir operator of $SO(3)$, one can write:

$$H = \gamma C^{(1)}_{U3} + \frac{1}{2}\chi C^{(2)}_{SU3} + \frac{3}{8}\chi C^{(2)}_{SO3} \ . \tag{18}$$

The eigenvalues of this Hamiltonian can still be obtained in a closed form by purely algebraic methods:

$$E = \gamma n + \frac{1}{2}\chi n(n+3) + \frac{3}{8}\chi L(L+1) \ , \tag{19}$$

due to the fact that the Hamiltonian is expressed in terms of the invariant operators of a subgroup-chain:

$$U(3) \supset SU(3) \supset SO(3) \ . \tag{20}$$

A more general algebraically solvable interaction emerges if we allow the parameters of H to be more general, but keep the same operators:

$$H = \gamma C_{U3}^{(1)} + \delta C_{SU3}^{(2)} + \beta C_{SO3}^{(2)} + \epsilon \ , \tag{21}$$

$$E = \gamma n + \delta n(n+3) + \beta L(L+1) + \epsilon \ . \tag{22}$$

This formula can describe the energy spectrum of the cluster bands in ^{20}Ne reasonably well, as it is shown in Fig. 1. (The parameters are in MeV: γ=14.577, δ=−0.464, β=0.156, ϵ=−64.00.) In the geometrical picture this interaction corresponds to a shifted anharmonic potential (Hess 1996).

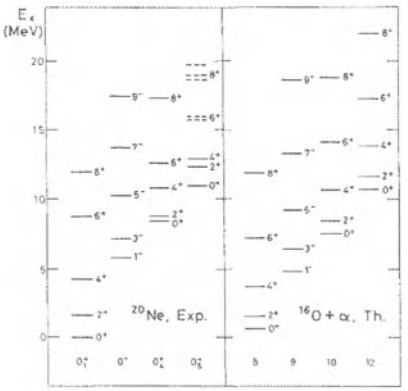

Fig. 1. Experimental states of ^{20}Ne in comparison with the model calculation in terms of an $U(3)$ dynamic symmetry. The dashed lines indicate uncertain assignments. The quantum numbers in the model spectrum are the numbers of oscillator quanta in the relative motion.

In the algebraic cluster model the *symmetry breaking* is described by *changing the functional form of the Hamiltonian*, and expanding it *in terms of the invariant operators of a chain of nested subgroups.* This is a very *special breaking* of the exact symmetry that still allows *purely algebraic solution* of the eigenvalue problem.

Finally one can embed the $U(3)$ symmetry group into a larger group, e.g. $U(4)$ (Iachello 1981), thus the complete chain of subgroups is:

$$U(4) \supset U(3) \supset SU(3) \supset SO(3) \ . \tag{23}$$

The advantage of the embedding is that then the whole spectrum of the problem can be characterised by a single irrep of $U(4)$, which is called dynamical group of the system.

More general symmetry breaking interactions can also be introduced. Then the Hamiltonian matrix is calculated by group theoretical means, and diagonalised numerically.

This treatment of the symmetry breaking is usual in the algebraic structure models (see e.g. Iachello and Arima 1987).

The model space of the SACM is constructed microscopically, i.e. it is free from the Pauli forbidden states as well as from the spurious excitations of the center of mass. The exclusion of the forbidden states can be carried out by following different procedures (Cseh and Lévai 1994, Katō 1988). A simple way is to make an intersection between the cluster model basis (23) and the basis of the fully antisymmetric shell model (Elliott 1958). This procedure is justified by the equivalence of the Hamiltonians of the shell model and of the cluster model. In the harmonic oscillator limit it was proved by Wildermuth and Kanellopoulos (Wildermuth and Kanellopoulos 1958), but is is valid also for more general interactions corresponding to the (21) (specially broken) dynamic symmetry (Cseh et. al. 1996). Furthermore, this Hamiltonian gives the rotational (i.e. quadrupole collective) bands of light nuclei in terms of the spherical shell model (Elliott 1958). Thus we can say that for light nuclei the $U(3)$ (specially broken) dynamic symmetry provides us with the common intersection of the three basic structure models: the collective, the shell and the cluster models. By this we mean that to the extent the $U(3)$ quantum numbers are valid, the states have pure shell model and pure cluster model configurations at the same time, and in addition show well-defined quadrupole deformation.

3.2 Coupled degrees of freedom

In the SACM we describe the internal structure of the clusters by the Wigner-Elliott shell model, having a $U^{ST}(4)$ symmetry in the spin-isospin space, and a $U(3)$ symmetry in the spatial part. Therefore, the model of a two-cluster configuration has a group structure:

$$U_{C_1}^{ST}(4) \otimes U_{C_1}(3) \otimes U_{C_2}^{ST}(4) \otimes U_{C_2}(3) \otimes U_R(4)$$
$$\supset U_C^{ST}(4) \otimes U_C(3) \otimes U_R(3) \supset U_C^S(2) \otimes U(3)$$
$$\supset U_C^S(2) \otimes O(3) \supset U(2) \supset O(2)\ , \tag{24}$$

where C and R stand for cluster and relative motion, respectively. A simple Hamiltonian corresponding to the (specially broken) dynamic symmetry of (24) is:

$$H = \epsilon + \gamma_R n_\pi + \delta_R C^{(2)}_{SU_R(3)} + \delta_C C^{(2)}_{SU_C(3)} + \delta C^{(2)}_{SU(3)} + \beta L^2 + \xi L \cdot S. \tag{25}$$

This gives a reasonable description of several light nuclei.

One of the main advantages of the algebraic method in cluster studies (too) is that complex spectra can be treated relatively easily. E.g. the ground-state region of the ^{24}Mg nucleus and the very highly excited molecular resonances observed in the ^{12}C+^{12}C reactions can be described in a unified way, i.e. as eigenstates of the same Hamiltonian in the same model space.

Further unification in the description of the experimental data can be reached by applying the concept of the multichannel (or multiconfigurational) dynamic symmetry (Cseh 1994, Cseh 1996). This composite symmetry emerges due to the fact that a realistic interaction can be constructed which corresponds to a (specially broken) $U(3)$ dynamic symmetry, and is invariant under the transformations between different cluster configurations. Therefore, the (specially broken) $U(3)$ dynamic symmetry provides us not only with the common intersection between the collective, shell and cluster models, but also with the intersections of various cluster configurations. This allows us to describe different cluster configurations e.g. ^{24}Mg+^{4}He in the low-energy region of ^{28}Si, and ^{12}C+^{16}O in the high-energy region in a unified way, based on the same Hamiltonian.

Detailed applications of the Semimicroscopic Algebraic Cluster Model are presented in (Cseh et. al. 1992).

4 Heavy-Ion Scattering: Requirements and Possibilities

In this section we consider the possibilities of combining the algebraic methods of the scattering theory and of the cluster model. Our way of thinking is governed by the requirements of the reactions of light heavy-ions.

4.1 Continuous spectrum in terms of the algebraic potential matrix

In the description of the multichannel scattering the appearance of particle spin gives rise to further complications in the formalism. Then in addition to the orbital angular momentum l one also has the channel spin j, and only their vectorial sum is conserved: $J = L + j$. By applying the rotating

frame approximation (Alhassid and Iachello 1989), i.e. replacing $l(l+1)$ by $J(J+1)$ the unpolarised cross section becomes the same as that calculated for the spinless case. The approximation is good, when $j \ll J$ for the values of J that are important in the scattering process.

In the spin-dependent case the algebraic potential matrix corresponding to (9) becomes: $v_{\alpha' j', \alpha j}(J,k)$. When the number of open channels is moderately large, the number of strength parameters is also large (Lépine-Szily et. al. 1990). It can be decreased considerably by applying structure models for the description of the internal degrees of freedom of the colliding particles. Then the algebraic potential matrix can be expressed in terms of a smaller number of parameters (partly belonging to the structure model). For practical reasons so far only the target was considered to have internal degrees of freedom in the applications of the AST, while the projectile was taken to be structureless.

The algebraic potentials in different channels are related to each other by the excitation operators of the internal structure, which in the algebraic structure models are usually taken as the generators of the internal algebra G_A: $Q_\lambda = \beta_\lambda G_\lambda$, where β_λ's are deformation parameters. Then the algebraic potential matrix is:

$$v_{\alpha' j', \alpha j}(J,k) = \Sigma_\lambda v_\lambda(J,k) \left[\frac{2\lambda+1}{4\pi}\right]^{\frac{1}{2}} (-)^{j'} \begin{pmatrix} j' & \lambda & j \\ 0 & 0 & 0 \end{pmatrix} \beta_\lambda \langle \alpha' j' || G_\lambda || \alpha j \rangle \ . \tag{26}$$

So far the Interacting Boson Model (IBM) of $U(6)$ group structure (Iachello and Arima 1987), and the Interacting Boson Fermion Model of $U(6) \otimes U(m)$ group structure (Iachello and Van Isacker 1991) have been applied in practical calculations (Lichtenthäler and Gomes 1994). In particular, ^{16}O scattering was considered on medium heavy targets, like Cu isotopes.

A starightforward extension of the method towards lighter targets can be carried out by applying the $G_A = U^{ST}(4) \otimes U(3)$ shell model for the description of the internal structure of the targets, like in the SACM. (For light nuclei the shell model is also applicable relatively easily, and it is considered to be a better approximation than the simple IBM.) This possibility seems to be interesting in light of the fact that extensive experimental studies on reactions of light heavy-ions have been carried out.

4.2 Discrete spectrum

The energy-dependence of the cross sections of light heavy-ions shows evidence not only for continuous spectra, but also for discrete ones. In other words resonances (i.e. quasibound states) are superimposed on the continuous background.

In the traditional differential equation description these resonances are analysed by writing the S matrix as a sum of a slowly varying direct part and a Breit-Wigner term corresponding to the resonance (Sanders et. al. 1981, Maas and Scheid 1992):

$$S = S^{DIR} + S^{RES} \ , \tag{27}$$

$$S^{RES} = iexp[i(\phi_{nucl} + \sigma_{in} + \sigma_{out} + \phi)] \frac{\Gamma_{in}^{1/2} \Gamma_{out}^{1/2}}{E_0 - E - i\Gamma/2} \ . \tag{28}$$

The purely algebraic treatment of the resonances is available at present only for special interactions in one dimensional problems (Alhassid et. al. 1985). Since the resonances are decaying states that do not conserve the flux, their algebraic description is given in terms of nonunitary representations of noncompact groups. This area of the representation theory is less developed than that of the unitary representations of compact groups. Therefore, it is not clear if realistic interactions of three dimensional problems can be dealt with in this way in the near future.

From the viewpoint of the practical needs, however, one could apply an analysis based on the sum of a direct plus resonant term of the S matrix, like in the traditional approach. The first part could be obtained from the coupled channel algebraic calculation. As for the second part, the situation is a bit more complicated. From the SACM one can obtain the spectrum of the (quasi)bound states, i.e. energies and spin-parities. One can also determine cluster spectroscopic factors from this model (Katō 1988, Cseh et. al. 1991). However, in order to get partial and total resonance widths one has to apply geometrical methods, e.g. those of the R-matrix theory. Therefore, from the viewpoint of the methodology it is not a pure group theoretical treatment, rather it is a combination of algebraic and geometric tools. Nevertheless, from the pragmatical viewpoint of describing the heavy-ion resonances it seems to have some advantages. The algebraic description can account for more coupled channels than the geometric one, as well as for a more complete discrete spectrum. Therefore, the combination of these two methods for the treatment of the direct plus resonant term of the heavy-ion reactions seems to be promising as well. Especially if we take into account the fact, that no systematic description in terms of any method is available at present for the treatment of these two aspects of the heavy-ion scattering.

This method of splitting the S matrix into a direct plus resonant term is similar in spirit to the work of Lichtenthäler and Gomes (1994), who carried out an analysis in terms of a direct term combined with a Regge pole. In that treatment the angular momentum is extended into a complex plane, instead of the energy, as mentioned here. The novel feature of the present proposal in this respect is the combination of the algebraic description of the scattering and discrete spectrum, which would enable us to take into account a large number of quasibound states.

5 An Alternative Algebraic Approach to Scattering

In this section we return to the continuous part of the spectrum. As a starting point, let us recall, how the symmetry breaking is treated in the AST on one hand side, and in the SACM, on the other.

For the exact dynamic symmetry, when the Hamiltonian is expressed in terms of the Casimir invariant of a single Lie algebra, both the scattering matrix and the energy eigenvalues are obtained in a closed form by purely group theoretical means. The more realistic cases, however, which correspond to the breaking of the symmetries, were handled in different ways.

In the scattering theory the functional form of the S matrix was unchanged (with respect to the exact symmetry), but the arguments of the Γ functions were generalised. Instead of having the Sommerfeld parameter, corresponding to the exact symmetry, one introduces the more general algebraic potential. The algebraic potential does not have any relation to the subgroups of the original symmetry group.

In the cluster model, as well as in other algebraic models of bound states, the description of the symmetry breaking is different. The functional form of the Hamiltonian is changed. In particular, an expansion is carried out in terms of the generators of the dynamical group, like that of $U(4)$ of Section 3. In simple cases it is a polynomial expansion, but in some models more complicated functions are also applied. In this expansion an important limiting case emerges, when the generators of the dynamical group appear in such a special combination that they form the Casimir invariants of a chain of nested subgroups. This is the case of the specially broken dynamic symmetry, when we still have a closed formula for the solution of the eigenvalue problem, obtained in a purely algebraic way. This kind of (specially broken) dynamic symmetry proved to be very important in structure studies in many respects. (One aspect is discussed in Section 3, that is the interrelations of different descriptions, i.e. algebraic and geometric, and connecting various models, associated with different physical pictures, like quadrupole collective model, shell model, cluster model of different cluster configurations.)

An interesting question is whether or not this latter kind of symmetry breaking can be useful in scattering studies as well. This would result in an algebraic scattering model based on an S matrix having more complex functional form than that of Eq. (5). The Coulomb part, however, would remain the same, with the Sommerfeld parameter in the arguments of the Γ functions. A further question is whether the S matrix expressed in terms of the invariant operators plays an important role, or in other words, if the specially broken dynamic symmetry in the spirit of the structure models is reflected also in the S matrix.

The treatment proposed here is somewhat similar to that applied in the description of barion scattering (Dover and Feshbach 1990). There the scattering matrix was written as a linear combination of the quadratic and cubic Casimir operator of the flavour $SU(3)$ group. The essential difference is that the spatial degrees of freedom were not described in an algebraic way. Here we suggest the expansion of the S matrix in terms of the invariants (or in general in terms of the generators) of the symmetry groups (and their subgroups) describing both the internal and the spatial degrees of freedom.

In searching for the appropriate functional form of the S matrix the following things could guide us. i) For given algebraic potentials the S matrix should approximate that of the AST. ii) The phase shifts corresponding to various simple potentials can be derived in the geometric description, by applying approximation (e.g. Born, semiclassical, eikonal) methods. Similar phase shifts should be obtained from the algebraic treatment when the S matrix has the proper functional form. iii) The functional forms of the S-matrix, corresponding to exact dynamic symmetries other than $SO(3,1)$, may also give hints. iv) The locations of the poles of the S-matrix put strong constraints on the functional form, as well.

As for the AST with other (approximate) dynamic symmetries, the $U(3,1)$ case (Wu 1985) seems to be especially interesting. First, because it is the noncompact extension of the compact $U(4)$ group applied in the study of the discrete spectrum of the two-body problem. Second, because it has the $U(3)$ group as a subgroup. In the cluster model the Pauli forbidden states could be excluded due to the application of the $U(3)$ basis, and the same procedure might have importance in some reaction processes as well.

6 Conclusions

The algebraic methods proved to be very useful in the description of systems of coupled degrees of freedom. In studying the low-energy reactions of heavy-ions we have typically this kind of problems. In addition to accounting for the scattering process, one has to deal also with the effects of the structures of the colliding nuclei. By algebraic methods we can describe both the continuous and the discrete spectrum of the two-(composite)-body systems. The two aspects are treated in the framework of the Algebraic Scattering Theory and of the (Semimicroscopic) Algebraic Cluster Model, respectively.

In this contribution we have discussed the possibilities of combining the methods of these two models, from the viewpoint of the requirements of heavy-ion scattering. In particular, we have considered three issues. i) The application of the Wigner-Elliott shell model for the description of the internal structure of the colliding nuclei. In this way we can establish a relation between the elements of the multichannel algebraic potential matrix of light heavy-ions. ii) Description of the continuous and discrete spectrum in terms of an S matrix split into two parts corresponding to the direct and resonant contributions. They can be determined from the AST and from the SACM, respectively. iii) Construction of an alternative algebraic approach to the scattering problem. In this description the symmetry breaking corresponding to the general interactions is not introduced via the generalisation of of the algebraic potential (Sommerfeld parameter for the Coulomb problem). Instead, the functional form of the S matrix could be generalised.

Acknowledgments

This work was supported by the OTKA Grant No. T14321 and by the US-Hungarian Joint Fund (NO. 345/93).

References

Alhassid Y., Gürsey F., and Iachello F. (1983) : Phys. Rev. Lett. **50** 873
Alhassid Y., Iachello F., Levine R. D. (1985) : Phys. Rev. Lett. **54** 1746
Alhassid Y., Iachello F., (1989) : Nucl. Phys. **A501** 585
Cseh J., Lévai G., Katō K. (1991) : Phys. Rev. **C43** 165
Cseh J. (1992) : Phys. Lett. **B281** 173
Cseh J., Scheid W. (1992) : J. Phys. **G18** 1419; Lévai G., Cseh J., Scheid W. (1992) : Phys. Rev. **C46** 548; Varga K., Cseh J. (1993) : Phys. Rev. **C48** 602; Cseh J., Lévai G., Scheid W. (1993) : Phys. Rev. **C48** 1724; Cseh J., Gupta R. K., Scheid W. (1993) : Phys. Lett. **B299** 205; Cseh J. (1993) : J. Phys. **G19** L97; Fülöp Zs., Lévai G., Somorjai E., Kiss Á. Z., Cseh J., Tikkanen P., Keinonen J. (1996) : Nucl. Phys. **A604** 286; Lévai G., Cseh J. (1996) : Phys. Lett. **B381** 1; Algora A., Cseh J. (1996) : J. Phys. **G22** L39
Cseh J. (1994) : Phys. Rev. **C50** 2240
Cseh J., Lévai G. (1994) : Ann. Phys. (N.Y.) **230** 165
Cseh J. (1996) : *X Int. Conf. on Symmetries in Science* Bregenz, Austria, 1996
Cseh J., Lévai G., Hess P. O., Pál K. F., Varga K., Scheid W. (1996) : *XXI Int. Coll. on Group Theoretical Methods in Physics* Goslar, Germany, 1996
Dover C. B., Feshbach H. (1990) : Ann. Phys. (N.Y.) **198** 321
Elliott J. P. (1958) : Proc. Roy. Soc. **A245** 128; 562
Frank A., Van Isacker P. (1994) : *Algebraic Methods in Molecular and Nuclear Structure Physics* John Viley and Sons Inc., New York
Hess P. O. (1996) : talk at the present conference; Hess P. O., Lévai G., Cseh J. (1996) : Phys. Rev. C, in press
Iachello F. (1981) : Phys. Rev. **C23** 2778
Iachello F., Arima A. (1987) : *The Interacting Boson Model* Cambridge University Press, Cambridge
Iachello F., van Isacker P. (1991) : *The Interacting Boson Fermion Model* Cambridge University Press, Cambridge
Iachello F. Mukopadhyay N. C. Zhang L. (1991) : Phys. Lett. **B256** 295
Iachello F., Levine R. D. (1995) : *Algebraic Theory of Molecules* Oxford University Press, Oxford
Iachello F. Cseh J., Lévai G. (1995) : A. P. H. NS Heavy Ion Physics **1** 91
Katō K., Fukatsu K., Tanaka H., (1988) : Prog. Theor. Phys. **80** 663
Lépine-Szily A., Obuti M. M., Lichtenthäler Filho R., Oliviera J. M. Jr., Villari A. C. C. (1990) : Phys. Lett. **B243** 23; Lépine-Szily A., Oliviera J. M. Jr., Fachinni P., Lichtenthäler Filho R., Obuti M. M., Sciani W., Steinmayer M. K., Villari A. C. C. (1992) : Nucl. Phys. **A539** 487
Lichtenthäler R., Ventura A., Zuffi L. (1992) : Phys. Rev. **C46** 707; Lichtenthäler R., Pereira D., Chamon L. C., Gomes L. C., Ventura A., Zuffi L. (1994) : Phys. Rev. **C50** 3033

Lichtenthäler R., Gomes L. C. (1994) : Phys. Rev. **C50** 3163
Maas R., Scheid W. (1992) : J. Phys. **G18** 707
Sanders S. J., Paul M., Cseh J., Geesman D. F., Henning W., Kovar D. G., Kozub R., Olmer C., Schiffer J. P. (1980) : Phys. Rev. **C21** 1810
Schiff L. I. (1968) : *Quantum Mechanics* McGraw-Hill, New York
Ventura A., in this volume
Wildemuth K., Kanellopoulos Th. (1958) : Nucl. Phys. **9** 596
Wu J. (1985) : PhD thesis, Yale University
Wu J., Iachello F., Alhassid Y., (1987) : Ann. Phys. (N.Y.) **173** 68, and references therein

Geometrical Relation of the SACM

P.O.Hess*

Instituto de Ciencias Nucleares, UNAM, Circuito Exterior, C.U., A.P. 70-543, 04510 México D.F., Mexico
e-mail: HESS@ROXANNE.NUCLECU.UNAM.MX

Abstract. A geometrical mapping of the semimicroscopic algebraic cluster model (SACM) is given. The geometrical variables are the relative radius vector, the quadrupole deformation parameters β and γ and the orientation of the deformed nucleus in the molecular system. The position of the minimum of the nuclear molecular potential is determined by the minimal number of π-bosons, describing the relative motion. This minimal number is determined by the implementation of the Pauli- principle. Applications to simple systems ($^{16}O+\alpha$, $^{12}C+\alpha$ and $^{28}Si+^{28}Si$) are presented.

1 Introduction

The Semimicroscopic Algebraic Cluster Model (SACM) (Cseh et al. 1992, Cseh et al. 1994, Cseh et al. 1996a) is very successful in describing in a unified way the low lying collective states and the high lying molecular resonances within a nucleus. The main physical inputs are: i) the transformation of a many body particle state to a two cluster system, ii) describing the relative motion via spin one π and scalar σ bosons (with the total number of bosons conserved) and iii) taking into account the Pauli principle by requiring, for example, a minimal number of π bosons. The second input is a method to introduce a cutoff in the model which restricts the number of π bosons between 0 and a maximal number. The last one can be understood looking at the following example: The ^{20}Ne nucleus can be considered as a $^{16}O+\alpha$ cluster system. While the ^{20}Ne has in total 20 oscillation quanta, the sum of the oscillation quanta of ^{16}O and α sum up to only 12. In order to take into account the Pauli principle, i.e., that antisymmetrization does not annihilate the state, one has to require that the relative motion contains *at least* the number of oscillation quanta needed to sum up to 20. Thus, in the example considered, the minimal number of relative quanta is 8. For a detailed description of the SACM see Ref. (Cseh et al. 1992, Cseh et al. 1994, Cseh et al. 1996a). Up to now, this model was applied to light systems only because the spin-orbit interaction can be neglected.

One difficulty of an algebraic model is its interpretation in geometrical terms. This did led in the past to some activity in relating algebraic models to their geometrical counterparts, as for example the IBA-I model (Iachello et

* work supported by CONACyT, no. E120-550/95

al. 1987) with its geometrical one (Eisenberg et al. 1987). This mapping can be found in Ref. (Kirson et al. 1985, Leviatan et al. 1988) and is related very much with what we will present here. The question is if the SACM can also be related to a geometrical interpretation and how the condition of minimal number of π bosons is reflected.

In this contribution we give a short review of the geometrical interpretation of the Semimicroscopic Algebraic Cluster Model. The detailed analysis is given elsewhere (Hess et al. 1996). We will show that the minimal number of π bosons is related to the position of the molecular potential minimum. The mapping will be applied to the systems $^{16}O+\alpha$, $^{12}C+\alpha$ and $^{28}Si+^{28}Si$. The simplest system is the first one which consists of two spherical clusters. The second one has a strongly oblate deformed and one spherical cluster. The last example is a symmetric system with two oblate deformed clusters. The results of $^{28}Si+^{28}Si$ are new and not published in Ref. (Hess et al. 1996). This system plays an important role in understanding the structure of ^{56}Ni (Cseh 1996b) which obtained a boost of interest after the publishing of new experimental data (Kraus et al. 1995).

2 Geometrical Relation of the SACM

2.1 Definition of the Potential and the Trial State

The geometrical potential is defined as the expectation value of the Hamiltonian of the SACM with respect to some trial state which depends on parameters yet to be related to physical variables as the distance of the two clusters

$$V(\boldsymbol{\alpha}) = < \boldsymbol{\alpha} \mid \hat{H}_{mic} \mid \boldsymbol{\alpha} > \tag{1}$$

As a trial state we take a similar form as the coherent state proposed in Ref. (Kirson et al. 1985, Leviatan et al. 1988) with the difference to exclude all states which have a number of π bosons less than the minimal one (n_o):

$$\begin{aligned} \mid \boldsymbol{\alpha} > &= \mathcal{N}_{N,n_o}(\boldsymbol{\alpha}\cdot\boldsymbol{\pi}^\dagger)^{n_o}\,[\sigma^\dagger + (\boldsymbol{\alpha}\cdot\boldsymbol{\pi}^\dagger)]^N \mid 0> \\ &= \frac{N!}{(N+n_o)!}\mathcal{N}_{N,n_o}\frac{d^{n_o}}{d\gamma^{n_o}}\,[\sigma^\dagger + \gamma(\boldsymbol{\alpha}\cdot\boldsymbol{\pi}^\dagger)]^{N+n_o} \mid 0>|_{\gamma=1} \quad . \end{aligned} \tag{2}$$

In the compact form of the second line the γ value has to be set equal to 1 after the differentiation has been carried out. The normalization factor can be directly calculated and gives (Hess et al. 1996)

$$\begin{aligned} \mathcal{N}^{-2}_{N,n_o} &= N!n_o!(\boldsymbol{\alpha}\cdot\boldsymbol{\alpha})^{n_o}\,[1+(\boldsymbol{\alpha}\cdot\boldsymbol{\alpha})]^N \\ &\quad *_2F_1(-n_o,-N;1;\frac{(\boldsymbol{\alpha}\cdot\boldsymbol{\alpha})}{1+(\boldsymbol{\alpha}\cdot\boldsymbol{\alpha})}) \quad . \end{aligned} \tag{3}$$

For the creation and annihilation operators we use a co- and contravariant notation, i.e., that the annihilation operator is given by π^m and the creation operator by $\pi^\dagger_m$. The co- and contravariant component of, e.g., the annihilation operator are related via $\pi^m = (-1)^{1-m}\pi_{-m}$.

The expectation value of any operator $\mathbf{O}$, which is a function of the π and σ bosons, is easily calculated via

$$\begin{aligned} &< \boldsymbol{\alpha} \mid \mathbf{O} \mid \boldsymbol{\alpha} >= \\ &\mathcal{N}^2_{N,n_o}\left[\frac{N!}{(N+n_o)!}\right]^2 \frac{d^{n_o}}{d\gamma_1^{n_o}}\frac{d^{n_o}}{d\gamma_2^{n_o}} \\ &* < 0 \mid [\sigma + \gamma_1(\boldsymbol{\alpha}\cdot\boldsymbol{\pi})]^{N+n_o}\mathbf{O}[\sigma^\dagger + \gamma_2(\boldsymbol{\alpha}\cdot\boldsymbol{\pi}^\dagger)]^{N+n_o} \mid 0 > \ . \end{aligned} \tag{4}$$

We give here the result for the most important building blocks of any interaction which can appear in the Hamiltonian of the SACM:

$$\begin{aligned} < \boldsymbol{\alpha} \mid \sigma^\dagger\pi_m \mid \boldsymbol{\alpha} > &= (N+n_o)\alpha_m\mathcal{N}^2_{Nn_o}\frac{(N!)^2}{(N+n_o)!} \\ &\quad *\frac{d^{n_o}}{d\gamma_1^{n_o}}\frac{d^{n_o}}{d\gamma_2^{n_o}}\gamma_2\ [1+\gamma_1\gamma_2(\boldsymbol{\alpha}\cdot\boldsymbol{\alpha})\ ]^{N+n_o-1}, \\ < \boldsymbol{\alpha} \mid \sigma^\dagger\sigma \mid \boldsymbol{\alpha} > &= N^2\frac{\mathcal{N}^2_{Nn_o}}{\mathcal{N}^2_{(N-1)n_o}}, \end{aligned}$$

$$\begin{aligned} &< \boldsymbol{\alpha} \mid \ [[\boldsymbol{\pi}^\dagger \times \boldsymbol{\pi}^\dagger]^{[S_1]} \times \ [\boldsymbol{\pi}\times\boldsymbol{\pi}]^{[S_2]}]^{[S_3]}_m \mid \boldsymbol{\alpha} > \\ &\quad = (N+n_o)(N+n_o-1)\ [\ [\boldsymbol{\alpha}\times\boldsymbol{\alpha}]^{[S_1]} \times \ [\boldsymbol{\alpha}\times\boldsymbol{\alpha}]^{[S_2]}]^{[S_3]}_m\mathcal{N}^2_{Nn_o} \\ &\qquad *\frac{(N!)^2}{(N+n_o)!}\frac{d^{n_o}}{d\gamma_1^{n_o}}\frac{d^{n_o}}{d\gamma_2^{n_o}}(\gamma_1\gamma_2)^2\ [1+\gamma_1\gamma_2(\boldsymbol{\alpha}\cdot\boldsymbol{\alpha})]^{N+n_o-2}\ . \end{aligned} \tag{5}$$

The boson vacuum $\mid 0 >$ has an internal structure related to the two clusters. There is the total number of oscillation quanta (n_{C_k}) in cluster number k, the $SU(3)$ irrep of each cluster denoted by $(\lambda_{C_k}, \mu_{C_k})$, the total (λ, μ), the angular momentum L_C, its projection M_C and the other quantum numbers related to multiplicity indices.

$$\mid 0 > \rightarrow \mid n_{C_1}(\lambda_{C_1},\mu_{C_1}), n_{C_2}(\lambda_{C_2},\mu_{C_2})\rho_C(\lambda_C,\mu_C)\kappa_C L_C, M_C = L_C > \ . \tag{6}$$

This is important for determining the expectation value of the algebraic quadrupole operator of each cluster $Q^a_m(k)$ (equal to the Elliott quadrupole operator (Elliott 1958)) with respect to the trial state. We use the relation given in Ref. (Castaños 1988):

$$< Q^a_m(k) >= \sqrt{\frac{5}{\pi}}(n_{C_k} + \frac{3}{2}(A_k - 1))\alpha_{2m}(k)\ . \tag{7}$$

where $\alpha_{2m}(k)$ is the quadrupole deformation variable in the molecular system (Eisenberg et al. 1987).

2.2 Relation of α_m to r_m

Up to now, the potential depends on some parameters α_m $(m = -1, 0, +1)$ which still have to be related to the relative distance vector r_m written here in spherical components. It is done by defining it as the expectation value of the microscopic distance operator $\mathbf{r}_m$

$$< \boldsymbol{\alpha} \mid \mathbf{r}_m \mid \boldsymbol{\alpha} >= r_m \ . \tag{8}$$

In order to take into account the cutoff, introduced by the use of the σ bosons, the microscopic distance operator has to be modified in such a way that in removing the cutoff it tends to the usual definition. It also should take into account that for $N = 0$ the expectation value is equal to the average position of a state with n_o oscillation quanta. This is given by (Hess et al. 1996)

$$r_o = \sqrt{\frac{\hbar}{m\omega} n_o} \tag{9}$$

where r_o is the absolute value of a vector $r_{o,m}$ and is one of the main results of the geometrical mapping. With this the modified microscopic distance operator is given by (Hess et al. 1996)

$$\mathbf{r}_m = \sqrt{\frac{\hbar}{2m\omega}} \frac{(\pi_m^\dagger \sigma + \sigma^\dagger \pi_m)}{\sqrt{< 0 \mid \sigma^\dagger \sigma \mid 0 >}} + r_{o,m} \ . \tag{10}$$

calculating its expectation value with respect to the trial state and set it equal to r_m we get, for the large N limit, a relation of α_m with $(r_m - r_o)$, namely

$$\alpha_m \approx \sqrt{\frac{m\omega}{2N\hbar}} (r_m - r_{o,m}) \ . \tag{11}$$

Note that $\alpha_m \sim \frac{1}{\sqrt{N}}$. Due to this, all N-dependence is removed from the mapping of any operator, e.g., the number operator for the π-bosons, in the large N limit, is mapped to $N(\boldsymbol{\alpha} \cdot \boldsymbol{\alpha}) = \frac{m\omega}{2\hbar}(r - r_o)^2$. Now we have all elements together in order to get the potential out of the SACM.

3 Applications

The first system we discuss is $^{16}O + \alpha$ and consists of two spherical clusters. The only relevant degree of freedom is the radial distance of both clusters. As an Hamiltonian of the SACM we used

$$\mathbf{H} = \epsilon + \gamma \mathbf{n}_\pi + \eta \mathbf{C}_2(n_\pi, 0) + \beta \mathbf{L}^2 \tag{12}$$

with $\epsilon = -63.998MeV$, $\gamma = \hbar\omega = 3.185MeV$, $\eta = -0.4641MeV$ and $\beta = 0.1562MeV$. The model parameters were obtained using the new, standardized Hamiltonian of the SACM (Cseh et al. 1996). There, the γ parameter is related to the $\hbar\omega$ of the united system.

Proceding in the calculation of the expectation value we obtain for the potential

$$V(r) = -63.998 + 1.9078(r - r_o)^2 - 0.0118(r - r_o)^4 \ . \tag{13}$$

This is a very simple potential and is dominated by the structure of a harmonic oscillator. Assuming as a kinetic energy the usual one ($-\frac{\hbar^2}{2\mu}\Delta$, with μ as the reduced mass) we can estimate the expected position of the first excited 1^- state. Of course, this should be seen as a rough estimation in order to see if the potential has the expected properties. As a result we get for the energy of the first excited 1^- state the value of about $7MeV$. This has to be compared with the first observed one, which is at about $5.8MeV$ (Lederer et al. 1978). We can also compare the deduced average distance (r_o) of the two clusters with an estimation where we suppose a sharp surface of the two clusters. We obtain for r_o the value $\approx 5fm$ (the minimal number of π bosons is 8) compared to $4.9fm$ of the estimation. We see that all values fall into the right ballpark and thus gives us the confidence that the potential obtained makes sense.

The next sytem we discuss is $^{12}C + \alpha$ which consists of one deformed and one spherical cluster, which is the next complicated case. The Hamiltonian is given by (Hess et al. 1996)

$$\begin{aligned}\mathbf{H} = &-29.416 + 13.921\mathbf{n}_\pi - 0.5738\mathbf{n}_\pi(\mathbf{n}_\pi + 3) - 0.0896\mathbf{C}_2(\lambda, \mu) \\ &+0.5422\mathbf{K}^2 + 0.2038\mathbf{L}^2 \ .\end{aligned} \tag{14}$$

The mapped potential will now depends, additionally to r, on the deformation of the cluster and the orientation of its symmetry axis to the molecular z-axis. The latter is defined as being along the radial distance vector. The potential has the form

$$\begin{aligned}V(r) = &-41.925 + (2.0467 + 0.2329\beta_C(3cos^2\theta_{2C} - 1))(r - r_o)^2 \\ &-0.01868(r - r_o)^4 \ .\end{aligned} \tag{15}$$

Taking into account that the ^{12}C cluster is oblate and has a large deformation $\beta = -0.66$ (Jones et al. 1986), the energetically lowest position is at $\theta_{2C} = 0^o$, which agrees well with microscopic calculations (Leander et al. 1975). Also the estimated position of the first excited 1^- state, expanding in r for $\theta_{2C} = 0^o$ and doing the estimation in the same way as done in the last example, is about $7MeV$ which is practically the same as the observed one (Lederer et

al. 1978). The value of r_o is approximately $3.5fm$ ($n_o = 4$) compared to the value $5.7fm$, obtained assuming a sharp surface of the clusters. Again the properties of the potential fall in the right ballpark.

Our last example is $^{28}Si + ^{28}Si \rightarrow ^{56}Ni$. It recently attracted more attention (Cseh 1996b) due to new experimental data (Kraus et al. 1995) which question the interpretation of 28 as a shell closure. The system consists of two oblate deformed clusters and is symmetric. As collective variables we have the internuclear distance coordinate r_m, the orientation of the symmetry axis of each cluster with respect to the molecular z-axis and an additional angle describing the rotation of the symmetry axis of one cluster out of the plane defined by the symmetry axis of the other cluster and the molecular z-axis. Further there are the deformation variables of each cluster.

As an Hamiltonian we use (Cseh 1996b)

$$\begin{aligned}\mathbf{H} = &-334.98 + 10.054\mathbf{n}_\pi - 0.00609\mathbf{C}_{2,C}(\lambda_C, \mu_C) - 0.0312\mathbf{C}_2(\lambda, \mu) \\ &+(0.672 - 0.0153\mathbf{n}_\pi)\mathbf{L}^2,\end{aligned} \tag{16}$$

where (λ_C, μ_C) is the $SU(3)$ cluster irrep (we take the maximal coupling which turns out to be the $(0, 24)$) and $(\lambda, \mu) = (20, 8)$ is the lowest $SU(3)$ irrep of ^{56}Ni (Cseh 1996b).

Calculating its expectation value with respect to the trial state and expressing the variables α_m in terms of r_m and $r_{o,m}$ we obtain a potential whose minimum in the angular variables is such that the two clusters face each other with their flat side, i.e., their symmetry axis are parallel to each other and also parallel to the molecular z-axis. Details of the calculation and the form of the potential will be given elsewhere (Lévai et al. 1996). In deriving the potential we had also to symmetrize the system, which according to Ref. (Hess et al. 1996) modifies the structure near the position r_o of the nuclear molecular potential minimum. Noting that the minimal number of π bosons is 36 (Cseh 1996b) the r_o is $12.2fm$ and the potential has the form

$$\begin{aligned}V = &-361.38 - 1.375(r - r_o)^2 \frac{1 - e^{-0.2422(r-r_o)^2}}{1 + e^{-0.2422(r-r_o)^2}} \\ &-0.0009123(r - r_o)^4 \quad ,\end{aligned} \tag{17}$$

where we took $\hbar\omega = 10.054MeV$, $\hbar c = 197.33MeVfm$ and for the nuclear mass $mc^2 = 938MeV$.

As can be observed, there is a drastic change of structure for the quadratic term in $(r - r_o)$. This is due to the symmetrization and this contribution vanishes at $r = r_o$ while for r very different from r_o it approaches the usual form of the potential as we have encountered it before. The general form of the potential is very flat near $r = r_o$. Therefore, it is hard to make an estimation

of the position of the first excited 1^- state as in the other examples. We can, though, estimate the touching distance, under the assumption that the mass distribution of each cluster is box like and their surface is well defined. We obtain for a deformation of $\beta \approx 0.2$ (Kraus et al. 1995) and the orientation given above the value $8fm$ and for a spherical cluster $9.6fm$. This has to compared with the $12.2fm$ obtained by us. The orientation obtained by the geometrical relation as the lowest in energy agrees very well with microscopic estimations. Calculations for this system within the SACM are still preliminary and the details will be published elsewhere (Lévai et al. 1996).

4 Conclusions

In this contribution we gave a short review of the geometrical relation of the SACM. We applied it to three systems. The first one ($^{16}O + \alpha$) consists of two spherical clusters, the next one ($^{12}C + \alpha$) of one deformed and one spherical cluster and the last one ($^{28}Si + ^{28}Si$) is symmetric and has two oblate deformed clusters. In all systems the potential obtained are reasonable and reflect the microscopic properties quite well, like which orientation is lowest in energy. We could also reproduce qualitatively the position of the minimum of the nuclear molecular potential and of the first excited 1^- state. An important result was that the position r_o of the minimum is related to the minimal number of π bosons required in order to satisfy the Pauli principle.

Detailed derivations of the formulas, given in the text, are available in Ref. (Hess et al. 1996).

References

O.Castaños, J.P.Draayer, Y.Leschber (1988): Z. Phys. **A329**, 33
J.Cseh (1992): Phys. Lett. **B281**, 173
J.Cseh, G.Lévai (1994): Ann. of Phys. **230**, 165
J.Cseh (1996a): see also the contribution in this conference.
J.Cseh (1996b): poster contribution given at the *4. International Conference on Radioactive Nuclear Beams*, Omiya, Japan, june 1996
J. Cseh, G. Lévai (1996): Phys. Lett. **B381**, 1
J.M.Eisenberg, W.Greiner (1987): *Nuclear Models I: Nuclear Theory*, (3rd edition, North-Holland Physics Publishing, Holland)
J.P.Elliott (1958): Proc. R. Soc. London **A245**, 128, 562
P.O.Hess, G.Lévai, J.Cseh (1996): Phys. Rev. **C**, in press
F.Iachello, A.Arima (1987): *The Interacting Boson Model*, (Cambridge Univeristy Press, Cambridge, UK)
K.Jones et al. (1986): Phys. Rev. **C33**, 17
M.W.Kirson et al. (1985): Phys. Rev. Lett. **55**, 2846
G.Kraus et al. (1995): Phys. Scripta **156**, 114
G.Leander, S.E.Larson (1975): Nucl. Phys. **A239**, 93

C.M.Lederer, V.S.Shirley (1978): *Tables of Isotopes*, (7th edition, National Standard Reference System, Wiley and Sons, New York)
G.Lévai, J.Cseh, P.O.Hess (1996): in preparation
A.Leviatan, M.W.Kirson (1988): Ann. Phys. (N.Y.) **188**, 142

Phase-Equivalent Complex Potentials

Daniel Baye[1], Jean-Marc Sparenberg[1], Géza Lévai[2]

[1] Physique Nucléaire Théorique et Physique Mathématique C.P. 229, Université Libre de Bruxelles, B 1050 Brussels, Belgium
[2] Institute of Nuclear Research of the Hungarian Academy of Sciences, P.O. Box 51, 4001 Debrecen, Hungary

Abstract. Potentials providing the same complex phase shifts as a given complex potential but with a shallower real part are constructed with supersymmetric transformations. Successive pairs of transformations eliminate normalizable solutions corresponding to complex eigenvalues of the Schrödinger equation with the full complex potential. With respect to real potentials, a new feature is the occurrence of normalizable solutions with complex energies presenting a positive real part. Removing such solutions provides a way of suppressing narrow resonances but may lead to complicated equivalent potentials with little physical interest. We discuss the singularity of the transformed potential and its relation with the Levinson theorem, the transformation of the Jost function, and the link with the Marchenko approach. The technique is tested with the solvable Pöschl-Teller potential. As physical applications, deep optical potentials for the $\alpha + {}^{16}\mathrm{O}$ and ${}^{16}\mathrm{O} + {}^{16}\mathrm{O}$ scatterings are transformed into l-dependent phase-equivalent shallow optical potentials.

1 Introduction

The optical model (Feshbach 1992; Hodgson 1978) is widely used to analyze the cross sections obtained in heavy-ion scattering. Nucleus-nucleus potentials usually involve a negative imaginary part. However the data analysis is plagued by discrete ambiguities. The deep or shallow nature of optical potentials is a long-standing problem in nuclear physics. In several cases, different complex potentials offer a similar quality of fit for a given collision. Well known examples where very different potentials fit the data in a satisfactory way are provided by the $\alpha + \alpha$ (Ali and Bodmer 1966; Buck et al. 1977), ${}^{12}\mathrm{C} + {}^{12}\mathrm{C}$ (Reilly et al. 1973; Bromley 1978), and ${}^{16}\mathrm{O} + {}^{16}\mathrm{O}$ (Siemssen et al. 1967; Chatwin et al. 1970; Kondō et al. 1989) elastic collisions.

In the seventies, theoretical arguments appeared providing a justification for deep potentials (Neudatchin et al. 1971; Buck et al. 1977). The lowest bound states of the *real* part of such potentials are interpreted in terms of approximate forbidden states, i.e. of states in the relative motion of the colliding nuclei which are not allowed by the Pauli principle (Wildermuth and Tang 1977). These bound states are therefore considered as non-physical. The other bound states can sometimes be interpreted as approximate physical states of the fused nucleus. Microscopic models provide a prescription about the number of forbidden states, which allows a selection of the most

convenient potential depths. With this prescription, accurate phenomenological potentials have been found for example for the $\alpha + \alpha$ (Buck et al. 1977), $\alpha + {}^{16}\mathrm{O}$ (Michel et al. 1983), $\alpha + {}^{40}\mathrm{Ca}$ (Michel and Vanderpoorten 1979), and ${}^{16}\mathrm{O} + {}^{16}\mathrm{O}$ (Kondō et al. 1989) scatterings.

For *real* potentials, the apparent difference between deep and shallow potentials can be exactly eliminated by constructing phase-equivalent potentials (Baye 1987a). Indeed, supersymmetric transformations (Sukumar 1985; Lévai 1994), which are based on a factorization of the Hamiltonian, allow to construct potentials which provide exactly the same phase shifts as a given potential (Baye 1987a, 1987b, 1993, 1994; Ancarani and Baye 1992; Baye and Sparenberg 1994). Deep potentials can be transformed into equivalent shallow potentials by removing their unphysical bound states. The resulting potentials display a singularity at the origin which is unavoidable according to the generalized Levinson theorem (Swan 1963): the variation of the number of bound states is compensated by a variation of the singularity imposed by the fixed difference of phase shifts at zero and infinite energies. The resulting shallow potential usually depends on the angular momentum. An application (Baye 1987a) to the $\alpha + \alpha$ potential of Buck et al. (1977) has shown that it is approximately equivalent to the potential of Ali and Bodmer (1966). More general modifications of a potential are possible, without changing the phase shifts. The bound spectrum can be modified in an arbitrary way (Baye 1993, 1994). The technique is not restricted to removing at each step the nodeless ground state as it was assumed in early works (Baye 1987a, 1987b). In fact, *all* potentials which are phase equivalent to a given real potential can be constructed (Baye and Sparenberg 1994).

However, realistic heavy-ion collisions are not restricted to a single channel. In order to take absorption towards open channels into account, complex optical potentials are used. Recently, it was shown that supersymmetric transformations can also be applied to the construction of potentials which are phase equivalent to a given *complex* potential (Baye et al. 1996; Sparenberg and Baye 1996). In this case, the real part of the potential can be made shallower by removing normalizable solutions of the Schrödinger equation with the complex potential. These complex normalizable solutions do not have a direct physical meaning in the case of a complex potential. They do not imply the existence of any physical bound system. They differ from usual resonances whose wave functions are not square integrable. The method remains very similar to the phase-equivalence problem for real potentials. The main difficulty is here determining normalizable solutions of complex potentials.

In Sect. 2, the supersymmetric-transformation technique is presented in the complex case. In Sect. 3, the singularity of the transformed potential and its relation with the Levinson theorem, the transformation of the Jost function, and the link with the Marchenko equation are discussed. In Sect. 4, the method is applied to a complex Pöschl-Teller potential and to the $\alpha + {}^{16}\mathrm{O}$

and $^{16}O + {}^{16}O$ elastic scatterings. Finally, concluding remarks and prospects are presented in Sect. 5.

2 Derivation of Phase-Equivalent Potentials

For $\hbar^2/2\mu = 1$ (where μ is the reduced mass of the system), the radial Schrödinger equation at orbital momentum l, for any complex energy $E = k^2$, reads

$$\left(-\frac{\mathrm{d}^2}{\mathrm{d}r^2} + V^l(r)\right)\psi^l(k,r) = k^2\psi^l(k,r), \tag{1}$$

where the radial function $\psi^l(k,r)$ vanishes at the origin. The complex effective potential

$$V^l(r) = U^l(r) + \mathrm{i}W^l(r), \tag{2}$$

where W^l is negative, behaves asymptotically as

$$V^l(r) \underset{r\to\infty}{\to} \frac{l(l+1)}{r^2} + \frac{2\eta k}{r}, \tag{3}$$

where $\eta = Z_1 Z_2 e^2/2k$ is the Sommerfeld parameter. This potential is bounded except possibly near the origin. Near $r = 0$, it behaves as

$$V^l(r) \underset{r\to 0}{\to} \frac{\nu^l(\nu^l+1)}{r^2}, \tag{4}$$

where ν^l is a positive integer. For regular potentials, ν^l is equal to l. In the following, we consider singular potentials with $\nu^l \neq l$. The superscript l appearing in the different notations refers to the orbital momentum of the partial wave, which is not affected by the supersymmetric transformations. For simplicity, it is dropped till the end of this section.

Let $\psi_0(k_0,r)$ be a normalizable solution at the complex energy $E_0 = k_0^2$, with $\mathrm{Im}\, k_0 > 0$ and $\int_0^\infty \psi_0^2(k_0,r)\,\mathrm{d}r = 1$. The hamiltonian H_0 in (1), with $V_0(r) \equiv V(r)$, can be factorized as

$$H_0 = A_0^+ A_0^- + E_0 \tag{5}$$

with

$$A_0^\pm = \pm\frac{\mathrm{d}}{\mathrm{d}r} + \frac{\psi_0'(k_0,r)}{\psi_0(k_0,r)}. \tag{6}$$

This factorization is easily verified by a direct calculation in which the fact that $\psi_0(k_0,r)$ satisfies the Schrödinger equation (1) is employed. We are not using in (6) the traditional notation involving the derivative of a logarithm

(Sukumar 1985) in order to avoid ambiguity problems with logarithms of complex numbers. In a complex case, the problem of the zeros of $\psi_0(k_0, r)$ in the denominator of the last term in (6) should not occur because complex solutions are not expected in general to exhibit exact zeros.

The supersymmetric partner of H_0 is defined as (Sukumar 1985)

$$H_1 = A_0^- A_0^+ + E_0 = H_0 - 2\frac{\mathrm{d}}{\mathrm{d}r}\left(\frac{\psi_0'(k_0, r)}{\psi_0(k_0, r)}\right). \tag{7}$$

If $\psi_0(k, r)$ is an eigenfunction of H_0 at energy E (which can be real positive for scattering states but also complex for normalizable solutions), an eigenfunction of H_1 at the same energy is given by

$$\psi_1(k, r) = (E - E_0)^{-1/2} A_0^- \psi_0(k, r) \tag{8}$$

for $E \neq E_0$. The normalization factor is chosen so that $\int_0^\infty \psi_1^2(k, r)\,\mathrm{d}r = 1$ if $\int_0^\infty \psi_0^2(k, r)\,\mathrm{d}r = 1$. The function $\psi_1(k, r)$ can also be written as

$$\psi_1(k, r) = (E - E_0)^{1/2} \frac{\int_0^r \psi_0(k_0, t)\psi_0(k, t)dt}{\psi_0(k_0, r)} \tag{9}$$

by using simple properties of the Wronskian of $\psi_0(k_0, r)$ and $\psi_0(k, r)$ (Baye 1987b; Ancarani and Baye 1992). As shown by (8), the function $A_0^- \psi_0(k_0, r)$ vanishes and energy E_0 does not correspond any more to a normalizable solution for H_1.

In a second step, H_1 is factorized as (Baye 1987a, 1987b)

$$H_1 = A_1^+ A_1^- + E_0 \tag{10}$$

with

$$A_1^\pm = \pm\frac{\mathrm{d}}{\mathrm{d}r} - \frac{\psi_0'(k_0, r)}{\psi_0(k_0, r)} + \frac{\psi_0^2(k_0, r)}{\int_0^r \psi_0^2(k_0, t)\mathrm{d}t}. \tag{11}$$

The supersymmetric partner of H_1 is therefore

$$H_2 = A_1^- A_1^+ + E_0 \tag{12}$$

which corresponds to a potential

$$V_2(r) = V_0(r) - 2\frac{\mathrm{d}}{\mathrm{d}r}\left(\frac{\psi_0^2(k_0, r)}{\int_0^r \psi_0^2(k_0, t)\mathrm{d}t}\right). \tag{13}$$

Although accidental zeros cannot be excluded, the denominator should not vanish in general since the integral $\int_0^r \psi_0^2(k_0, t)\,\mathrm{d}t$ is a complex function. When the modulus of the denominator is very small at some r value, the new potential $V_2(r)$ will present a peak. Such a case does not occur for a real potential where $\int_0^r \psi_0^2(k_0, t)\,\mathrm{d}t$ is an increasing function of r. In (13), the

phase choice for the complex function $\psi_0(k_0, r)$ does obviously not play any role.

Bounded eigensolutions of hamiltonian H_2 at a discrete normalizable-state energy $E_i \neq E_0$ or at a positive energy read

$$\psi_2(k, r) = (E - E_0)^{-1/2} A_1^- \psi_1(k, r). \tag{14}$$

Introducing (9) in (14) leads to an expression of $\psi_2(k, r)$ as a function of the eigensolutions of H_0,

$$\psi_2(k, r) = \psi_0(k, r) - \psi_0(k_0, r) \frac{\int_0^r \psi_0(k_0, t)\psi_0(k, t)\,\mathrm{d}t}{\int_0^r \psi_0^2(k_0, t)\mathrm{d}t}. \tag{15}$$

Here also $\int_0^\infty \psi_2^2(k, r)\,\mathrm{d}r = 1$ when $\int_0^\infty \psi_0^2(k, r)\,\mathrm{d}r = 1$. Since $\psi_0(k_0, r)$ is normalizable, the asymptotic behaviour of $\psi_2(k, r)$ in (15) is identical to the asymptotic behaviour of $\psi_0(k, r)$. Therefore, the potential $V_2(r)$, which does not have a normalizable solution at E_0 but has otherwise the same other eigenenergies as $V_0(r)$, is phase equivalent to $V_0(r)$. Equations (5) to (15) are simple generalizations of the equations derived in the real case (Baye 1987a, 1987b). Notice that complex conjugation does not occur in (13) and (15).

Relation (13) can be iterated. Starting from a solution $\psi_2(k_1, r)$ of H_2 at an energy $E_1 = k_1^2$ where the initial potential V_0 has another normalizable solution, one can transform V_2 into V_4, and so on. The final potential V_{2n} is obtained when n normalizable solutions are removed. As in the real case (Ancarani and Baye 1992), compact formulas based on determinants involving normalizable solutions of the initial potential can be derived. Moreover, adding such solutions, modifying their energy, and any combination of such modifications, can be obtained by generalizing the contents of Baye (1987b, 1993, 1994) and Baye and Sparenberg (1994).

3 Interpretation

3.1 Singularity of the Potential and the Levinson Theorem

Using (9) and a similar equation equivalent to (14) allows us to compare the behaviours of solutions near the origin. Since $\psi_0^l(k, r)$ behaves like $r^{\nu_0^l+1}$, leading terms of series expansions show that $\psi_1^l(k, r)$ behaves like $r^{\nu_0^l+2}$ and $\psi_2^l(k, r)$ behaves like $r^{\nu_0^l+3}$. Consistently, (13) shows that the singularity parameter ν_2^l of potential $V_2^l(r)$ increases by two units with respect to $V_0^l(r)$, i.e.

$$\nu_2^l = \nu_0^l + 2. \tag{16}$$

The strength $\nu^l(\nu^l + 1)$ of the potential singularity at the origin increases at each state removal. Let us explain how successive potentials can provide the

same phase shifts in spite of different numbers of normalizable states with a generalized Levinson theorem.

The Levinson theorem (Newton 1982, Chap. 12) establishes a link between the number n^l of bound states and the phase shift $\delta^l(k)$ of a real regular potential decreasing faster than r^{-2} for r tending towards infinity. It was extended to the Coulomb case (Iwinski et al. 1985) and generalized (Swan 1963) to potentials with a singularity at the origin. Taking into account all these generalizations, a theorem valid for all complex potentials containing a Coulomb term and a r^{-2} singularity at the origin given by (4) can be conjectured (Sparenberg and Baye 1996),

$$\begin{aligned} &|S^l(0)| = |S^l(\infty)| = 1, \\ &\arg S^l(0) = (2n^l + \nu^l - l)\pi, \\ &\arg S^l(\infty) = 0, \end{aligned} \tag{17}$$

where n^l is the number of normalizable solutions and S^l does not include the Coulomb scattering matrix. The theorem may have to be modified in the s wave when a square-integrable state exists at zero energy (Newton 1982), but this case does not occur when the potential contains a Coulomb term (Iwinski et al. 1985).

The phase shifts before and after the supersymmetric transformation share the same Levinson theorem in spite of different n^l values, because of a common sum $2n^l + \nu^l$. As in the real case, the singularity change is unavoidable when phase equivalence is imposed.

3.2 Modification of the Jost Function

For any complex k, the generalized Jost solutions $f^l(\pm k, r)$ are defined as the solutions of Eq. (1) at energy k^2, with the asymptotic behaviours

$$f^l(\pm k, r) \underset{r\to\infty}{\to} \exp\left(i\tfrac{1}{2}\nu^l\pi \pm ikr \mp i\eta\ln(\mp 2ikr)\right) \tag{18}$$

(see Sparenberg and Baye 1996 for details). The Jost function $F^l(k)$ is deduced from the limit

$$f^l(k, r) \underset{r\to 0}{\to} (2\nu^l - 1)!!F^l(k)(-kr)^{-\nu^l}. \tag{19}$$

The k_0 value of a normalizable state satisfies $F^l(k_0) = 0$. The S matrix appearing in (17) is defined for any complex k by

$$S^l(k)S^l_C(k) = F^l(-k)/F^l(k), \tag{20}$$

where S_C is the Coulomb scattering matrix (Newton 1982, Sect. 4.6.1).

The Jost function $F_2^l(k)$ of the transformed potential $V_2^l(r)$ can be deduced from transformations of Jost solutions of $V_0^l(r)$. Let us start from a

Jost solution $f_0^l(k,r)$ of H_0 where V_0 is assumed to be regular. Equation (8) remains valid and provides the transformed Jost solution

$$\tilde{f}_1^l(k,r) = (k^2 - k_0^2)^{-1/2} A_0^- f_0^l(k,r) \tag{21}$$

which is proportional but not identical to the Jost solution of H_1, because it does not satisfy (18). The exact Jost solution $f_2^l(k,r)$ of H_2 is then obtained from $\tilde{f}_1^l(k,r)$ with a similar equation. It can be expanded, using (19) for $f_0^l(k,r)$, as

$$f_2^l(k,r) \underset{r\to 0}{\to} (k^2 - k_0^2)^{-1}(2\nu^l + 3)!! F_0^l(k)(-k)^{-\nu^l} r^{-\nu^l - 2}. \tag{22}$$

Hence, comparing (22) with the definition (19) provides the relation

$$F_2^l(k) = \frac{k^2}{k^2 - k_0^2} F_0^l(k). \tag{23}$$

This equation shows that (i) the zero of the Jost function at k_0 is removed, (ii) a pole appears in the Jost function at $-k_0$, and (iii) the S matrix defined in (20) remains unchanged after the transformation pair, i.e.

$$S_2^l(k) = S_0^l(k). \tag{24}$$

For the singular transformed potential $V_2^l(r)$, the zeros of the Jost function and the poles of the S matrix are not identical. Removing a normalizable solution without modifying the S matrix implies replacing a zero of the Jost function by a pole.

3.3 Marchenko Equation

Equation (13) has the form

$$V_2(r) = V_0(r) - 2\frac{\mathrm{d}}{\mathrm{d}r} K(r,r) \tag{25}$$

with

$$K(r,t) = \frac{\psi_0(k_0,r)\psi_0(k_0,t)}{1 - \int_r^\infty \psi_0^2(k_0,s)\mathrm{d}s}. \tag{26}$$

The kernel $K(r,t)$ satisfies the Marchenko equation

$$K(r,t) + \Omega(r,t) + \int_r^\infty K(r,s)\Omega(s,t)\mathrm{d}s = 0 \tag{27}$$

involving the separable kernel

$$\Omega(r,t) = -\psi_0(k_0,r)\psi_0(k_0,t) \tag{28}$$

in agreement with e.g. Eqs. (V.2.4) in Chadan and Sabatier (1977), when the scattering matrix is not modified. From (21), one can show that Jost solutions transform as physical wave functions according to (15), i.e.

$$f_2(k,r) = f_0(k,r) + \int_r^\infty K(r,t) f_0(k,t) \mathrm{d}t, \tag{29}$$

where we use the orthogonality of solutions at different energies.

4 Applications

4.1 Complex Pöschl-Teller Potential

The Pöschl-Teller potential is defined as

$$V(r) = -\frac{s(s+1)}{\cosh^2 r}, \tag{30}$$

where s characterizes the complex strength of the potential. Analytic solutions are available but only for $l = 0$. The energies of the $l = 0$ normalizable states are given, as in the real case (Flügge 1971), by

$$E_{n+1} = -(s - 1 - 2n)^2, \tag{31}$$

where the positive integer n satisfies

$$2n + 1 < \mathrm{Re}\ s. \tag{32}$$

Normalizable states correspond to zeros in Im $k > 0$ of the Jost function

$$F(k) = \frac{2^{\mathrm{i}k}\sqrt{\pi}\Gamma(1 - \mathrm{i}k)}{\Gamma\left(\frac{1}{2}(2 + s - \mathrm{i}k)\right)\Gamma\left(\frac{1}{2}(1 - s - \mathrm{i}k)\right)}. \tag{33}$$

For Re $s > -1/2$, the poles of the second Γ function in the denominator of (33) lie in Re $k < 0$ and provide normalizable states in Im $k > 0$ if (32) holds.

Let us choose $s = 5.1 + 2\mathrm{i}$ which corresponds to $s(s+1) = 27.11 + 22.4\mathrm{i}$. The zeros of the Jost function are represented by full dots in Fig. 1 for the full complex potential and by open dots on the imaginary axis for its real part. For a complex potential, they are not any more symmetric with respect to this imaginary axis. Three normalizable states labelled N1, N2 and N3 appear in Re $k < 0$. While the energies of N1 and N2 have negative real parts, the energy E_3 of N3 is $3.99 - 0.4\mathrm{i}$. The scattering matrix of this potential is represented by thick lines in Fig. 2 (before and after the transformation). The Levinson theorem (17) leads to different $\delta(0)$ values for the complex potential (three normalizable states) and for its real part (two bound states). The phase δ and modulus $|S|$ respectively present a fast decrease and a minimum near Re E_3.

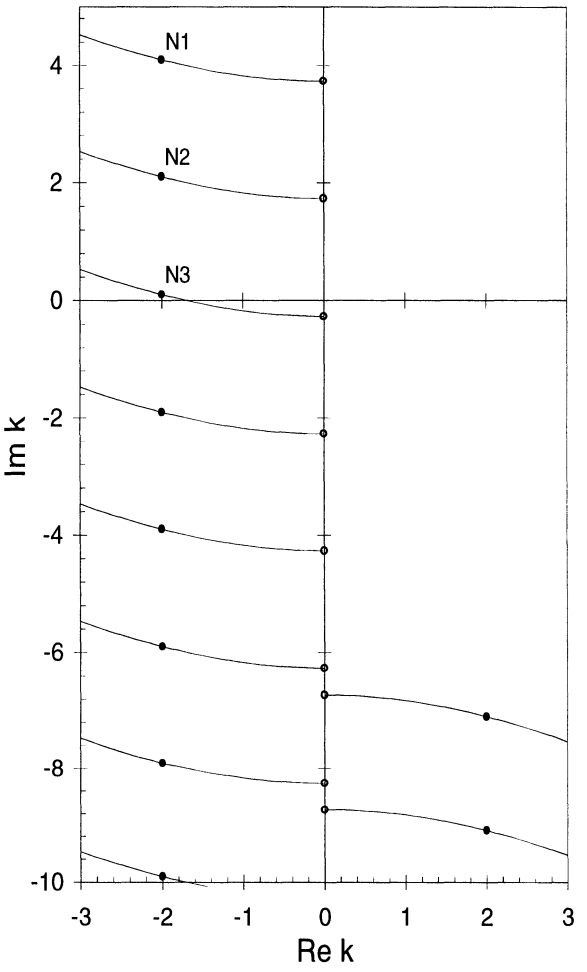

Fig. 1. Zeros of the Jost function of the complex Pöschl-Teller potential with $s = 5.1 + 2i$ (full dots) and of its real part (open dots). Normalizable states are denoted as N1, N2 and N3. Trajectories are calculated for a constant real part (-27.11) and a variable imaginary part of the Pöschl-Teller potential.

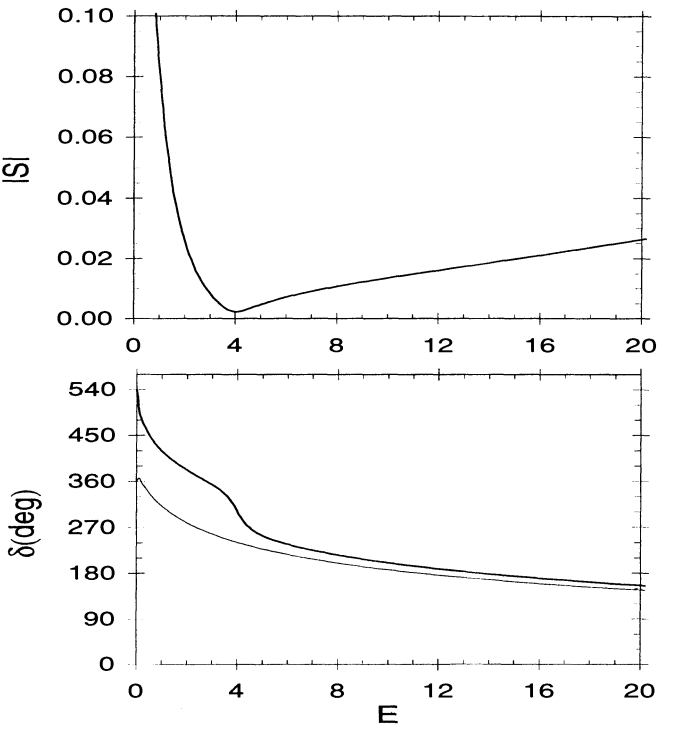

Fig. 2. Scattering matrix $|S|\exp(2i\delta)$ of the complex Pöschl-Teller potential (thick lines). The phase shift obtained with the real part U is represented as a thin line.

The potentials resulting from successive transformations (13) are displayed in Fig. 3. The transformed real parts U_2 and U_4 obtained after removing the normalizable states at energies E_1 and E_2 corresponding to N1 and N2 in Fig. 1, become progressively shallower (l.h.s. of Fig. 3). Each potential U_{2n} exhibits a singularity $2n(2n+1)/r^2$. The imaginary parts are less modified. Their depth is progressively reduced and their range increases. However, removing the solution N3 at energy E_3 leads to a potential which presents strong oscillations (r.h.s. of Fig. 3). These oscillations appear because the third normalizable solution $\psi_0(k_3, r)$ tends to $\exp(ik_3 r)$ which has a large spatial extension with slowly damped oscillations. This situation occurs for k values such that

$$0 < \mathrm{Im}\ k \ll |\mathrm{Re}\ k|. \tag{34}$$

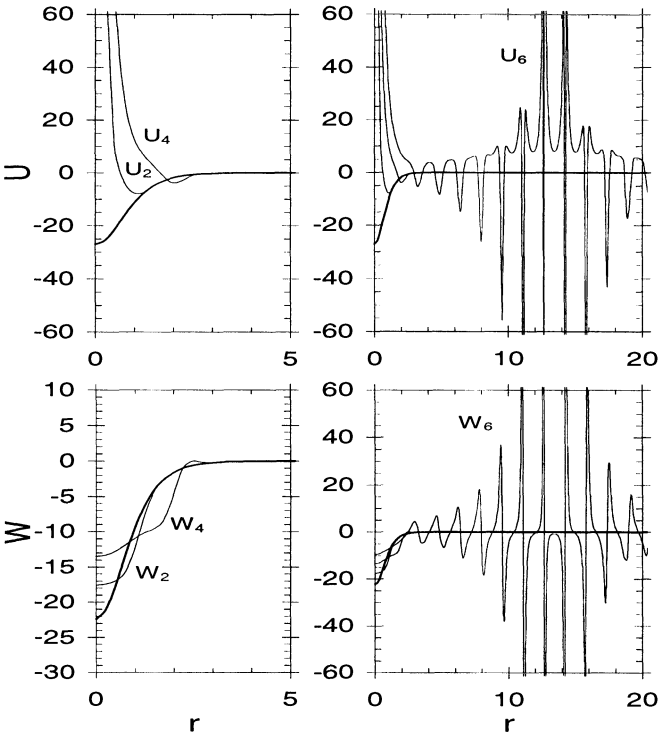

Fig. 3. Potentials $U_{2n} + \mathrm{i}W_{2n}$ obtained by successively removing the "lowest" normalizable states from the Pöschl-Teller potential (thick lines).

Such solutions lead to unpleasant potentials and should not be removed in physical applications (Baye et al. 1996; Sparenberg and Baye 1996).

More detailed information about analytical transformations of the Pöschl-Teller potential are given in another contribution to this conference (Lévai et al. 1996).

4.2 $\alpha + {}^{16}\mathrm{O}$ Scattering

A unique deep potential valid over a broad energy range is available for the $\alpha + {}^{16}\mathrm{O}$ elastic scattering (Michel et al. 1983). Its real part provides an approximate description of the ^{20}Ne spectrum. This implies however that its $\frac{1}{2}(8-l)$ lowest bound states for the even partial waves $l = 0$ to 6 and its $\frac{1}{2}(9-l)$ lowest bound states for the odd partial waves $l = 1$ to 7 be considered

as non physical. Higher bound states and low-energy resonances qualitatively approximate the observed ^{20}Ne spectrum. Removing the unphysical bound states should lead to a shallow potential which has the same physical content as the real part of the potential of Michel et al. (1983). Notice that this real part slightly depends on energy. We shall consider the potential at the lowest energy for which it has been fitted (32.2 MeV).

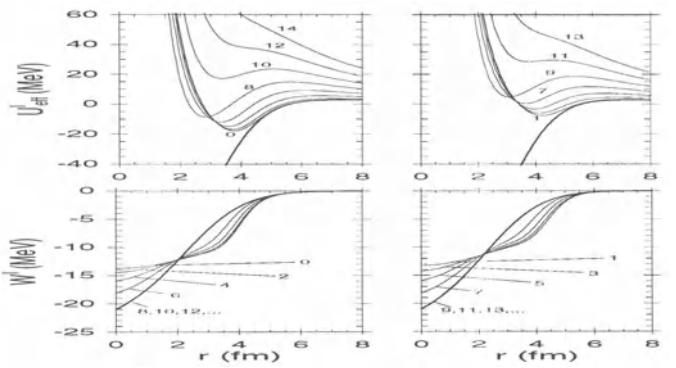

Fig. 4. Shallow effective potentials $U^l_{\rm eff} + {\rm i}W^l$ for $l = 0$ to 14, obtained by removing all non-physical normalizable states from the $\alpha + {}^{16}$O optical potential of Michel et al. (1983) (thick lines).

By successive transformations (13), we remove in each partial wave a number of normalizable solutions equal to the number of unphysical bound states (Baye et al. 1996). The resulting complex effective potentials are shown in Fig. 4. They depend on l but provide exactly the same cross sections as the deep potential. In spite of the fact that the original potential does not depend on parity, the minima of the final effective potentials are clearly different for even and odd partial waves. This can be understood as follows. The effective real parts $U^l_{\rm eff}(r)$ which include the centrifugal term present a singularity of the form $n(n+1)/r^2$ with $n = 8$ for even waves and $n = 9$ for odd waves ($l \leq 9$). The stronger singularity for odd waves pushes the minimum towards larger r values. This odd-even effect is consistent with the fact that positive and negative-parity states belong to different bands in the ^{20}Ne spectrum.

The imaginary parts $W^l(r)$ are also l dependent. Their range is increased by the transformation. Here also, an odd-even effect occurs. The range of W^l for the odd waves is slightly larger than for the comparable even waves.

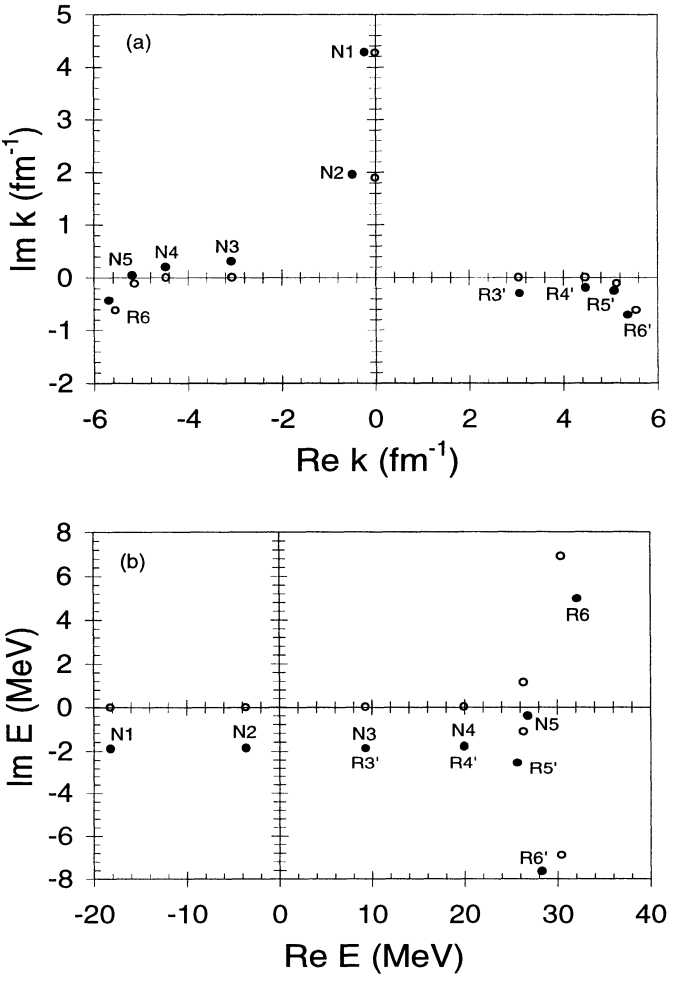

Fig. 5. Poles of the $l = 18$ S matrix for the deep potential of Kondō et al. (1989) at 25 MeV in the complex k and E planes (full dots). The poles of normalizable states (N) or resonances (R) are numbered by increasing real parts of their energy. Empty dots represent the poles of the real part of the effective potential.

4.3 $^{16}O + {}^{16}O$ Scattering

For the $^{16}O + {}^{16}O$ Scattering, deep and shallow optical potentials provide similar fits of excitation functions over the 10 to 35 MeV energy range in the center-of-mass frame. A shallow potential, with Woods-Saxon form factors for both the real and imaginary parts, could be deduced (Siemssen et al. 1967; Chatwin et al. 1970). The real part of the potential of Kondō et al. (1989), which fits elastic scattering data in the same energy range, is deep with non-physical bound states simulating the expected $\frac{1}{2}(24 - l)$ forbidden states.

Supersymmetric transformations are able to transform the deep potential of Kondō et al. (1989) into a shallow one, allowing a comparison with the potential of Chatwin et al. (1970). Such transformations must be performed for each partial wave separately but assume that the potential does not depend on energy. To this end, we freeze the energy dependence of the potential at 25 MeV and focus on the dominant $l = 18$ partial wave at this energy. The $l = 18$ effective potential for $E_{\text{c.m.}} = 25$ MeV is represented below in Fig. 7 ($2n = 0$, thick lines).

Figure 5 displays the first zeros of the $l = 18$ Jost function or poles of the S matrix in the complex k and E planes (full dots). The poles are numbered by increasing real parts of the energy; a letter indicates whether the pole corresponds to a normalizable state (N, Im $k_0 > 0$) or to a resonance (R, Im $k_0 < 0$). Empty dots represent the poles related to the real part of the effective potential. Poles under the real k axis, which correspond to resonances, are calculated with the complex scaling (or complex rotation) method (Ho 1983).

The real part of the potential has two bound states, with a positive-imaginary wave number. The S-matrix poles representing resonances of this real part are symmetric with respect to the imaginary k axis. The first two resonances are very narrow. The negative imaginary part of the potential modifies these properties. Poles become non symmetric and receive an individual physical interpretation (Sparenberg and Baye 1996). Normalizable-state k values (N1 and N2) become complex, with a negative real part. Resonances in the right-hand side of the k plane move away from the real axis and become broader (R3' to R6'). The first three resonances with Re $k < 0$ become square-integrable solutions N3 to N5 with Re E positive. The other resonances remain under the real k axis and become narrower such as R6. Resonance energies are not any more symmetric with respect to the imaginary axis.

Figure 6 compares the phase shifts of the real part of the potential (thin line) and the scattering matrix of the full complex $l = 18$ potential (thick lines). The Levinson theorem (17) is verified in both cases. The phase shift obtained with the real part of the potential starts from 2π at $E = 0$ since this real potential has two bound states. The complex phase shift starts from 5π at $E = 0$ since the complex potential has five normalizable states N1 to N5.

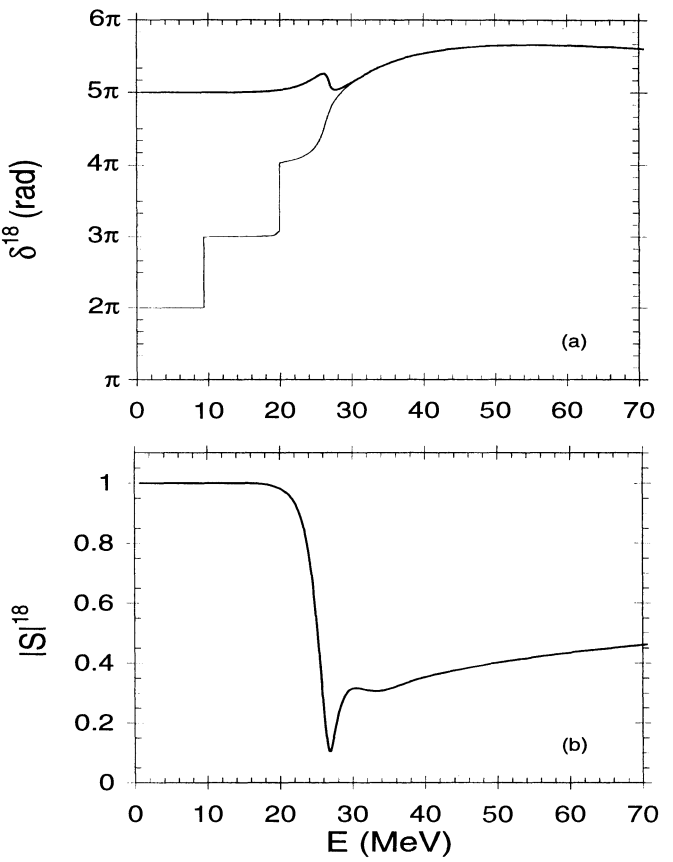

Fig. 6. $l = 18$ phase shift of the real part of the potential of Kondō et al. (1989) (thin line), and scattering matrix $|S|\exp(2i\delta)$ for the full complex potential (thick lines).

For the full complex potential, the influence of the two resonances of the real part disappears. This is due to the fact that the poles N3 and N4 in Fig. 5 are respectively nearly symmetric to R3' and R4' with respect to the k-plane origin. On the other hand, a broad resonance arises from the pole R5', while the associated pole N5 changes into a square-integrable state and leads to a decrease of the phase of the scattering matrix.

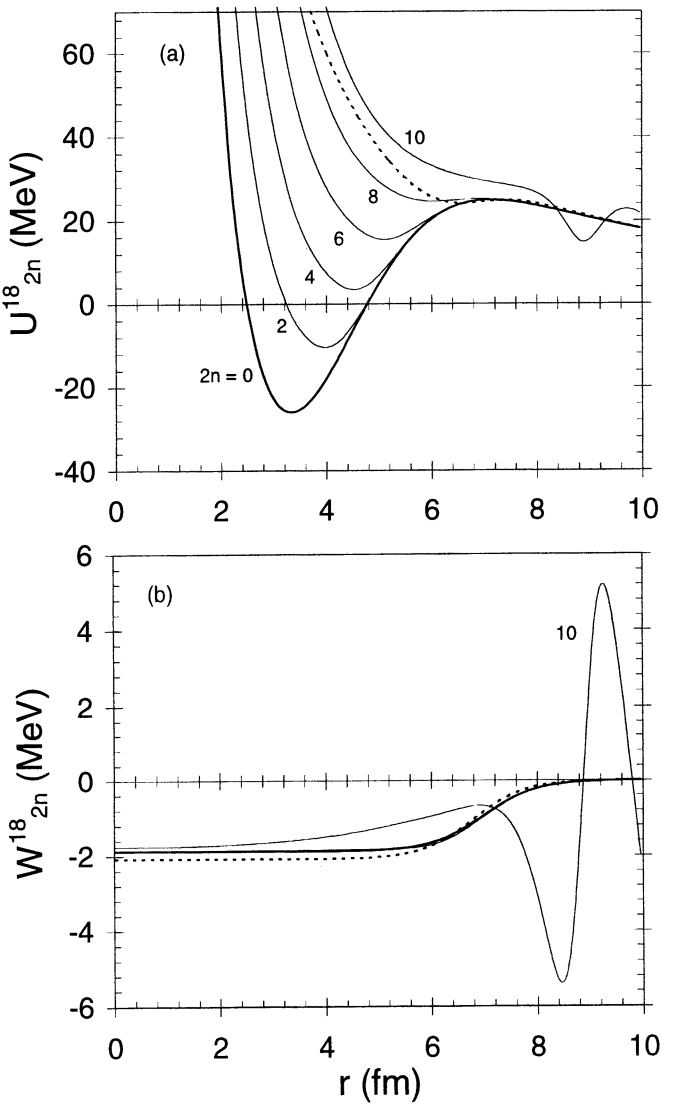

Fig. 7. Real and imaginary parts of the $l = 18$ potential V_0^{18} of Kondō et al. (1989) (thick line), of the phase-equivalent potentials V_2^{18}, ..., V_{10}^{18} (thin lines, labeled by $2n$), and of the shallow potential of Chatwin et al. (1970) (dotted lines). The imaginary potentials W_2^{18} to W_8^{18} are almost indistinguishable from the initial imaginary part.

Potentials V_0^{18}, V_2^{18}, ..., V_{10}^{18} which are phase equivalent to the $l = 18$ potential of Kondō et al. (1989) are shown in Fig. 7 (Sparenberg and Baye 1996). The states are removed according to increasing real parts of the energy (i.e. successively N1, N2, ..., N5 in Fig. 5). For the first four transformed potentials, the comments are identical: the imaginary part of the potential is almost not modified, while the depth of the real part regularly decreases. The last potential V_{10}^{18} is very different. This kind of behaviour has already been met in Sect. 4.1. Figure 7 also shows that the potential singularity at the origin increases at each state removal, in agreement with (16).

In Fig. 7, the supersymmetric partners of the deep potential of Kondō et al. (1989) are compared with the shallow potential of Chatwin et al. (1970) (dotted lines). This last potential is close to potential V_8^{18} obtained by removing four normalizable states from the deep potential, which correspond to the three $l = 18$ forbidden states and to one additional state possibly related to a physical resonance. Similar results are obtained for other partial waves, but with a different number of transformations. By removing all normalizable states which lead to non-oscillating potentials, the resulting supersymmetric partner of the deep potential of Kondō et al. (1989) is very close to the shallow potential of Chatwin et al. (1970) over the whole angular-momentum range considered (see Sparenberg and Baye 1996). Moreover, the effect of supersymmetric transformations on the real part of the potential is almost identical when the energy appearing in the potential of Kondō et al. (1989) is allowed to vary. Consequently, the real part of the supersymmetric partner does not depend on energy in this domain, in agreement with a property of the shallow phenomenological potential. This real part depends on angular momentum but can be simulated over a limited energy range by an l-independent potential.

5 Conclusions

The technique of supersymmetric transformations has been extended to the construction of potentials which are phase equivalent to complex potentials. The formalism for the real case can be used without significant modification except for the replacement of the bound-state wave functions by normalizable solutions of the complex potential.

For complex potentials with a small imaginary part, the removal of the normalizable states leads to potentials whose real part is very close to the potentials obtained after removing bound states from the real part of the original potential. On the contrary the imaginary part undergoes modifications which cannot easily be predicted. A weak imaginary term provides a way of removing narrow resonances from the real part without affecting the rest of the phase shift.

The modification of the Jost function under a pair of supersymmetric transformations clarifies the fact that the collision matrix does not change in

spite of the suppression of a normalizable solution. The role of the singularity in relation with a conjectured generalized Levinson theorem has also been emphasized.

The construction of phase-equivalent potentials should reduce the discrete-ambiguity problem in the optical-model description of nuclear collisions. More general transformations than the removal of bound states can also be considered: moving bound states or adding new states while keeping phase equivalence are also possible. In principle the whole bound spectrum can be modified in an arbitrary way but the resulting potentials would not necessarily be simple enough to allow a useful physical interpretation.

The supersymmetric technique can be applied to other aspects of the inverse problem. An application to the reconstruction of a potential from its phase shifts at fixed angular momentum is in progress.

Acknowledgments

This text presents research results of the Belgian program on interuniversity attraction poles initiated by the Belgian-state Federal Services for Scientific, Technical and Cultural Affairs. This work was also supported by the OTKA grants No. W015140 and T14321 (Hungary). J.-M. S. is Aspirant of the Fonds National de la Recherche Scientifique (Belgium).

References

Ali S., Bodmer A.R. (1966): Nucl. Phys. **80**, 99
Ancarani L.U., Baye D. (1992): Phys. Rev. A **46**, 206
Baye D. (1987a): Phys. Rev. Lett. **58**, 2738
Baye D. (1987b): J. Phys. A **20**, 5529
Baye D. (1993): Phys. Rev. A **48**, 2040
Baye D. (1994): in Quantum Inversion Theory and Applications, ed. von Geramb H.V., Lecture Notes in Physics **427** (Springer, Berlin) p. 127
Baye D., Sparenberg J.-M. (1994): Phys. Rev. Lett. **73**, 2789
Baye D., Lévai G., Sparenberg J.-M. (1996): Nucl. Phys. **A599**, 435
Bromley D.A. (1978): in Nuclear Molecular Phenomena, ed. Cindro N. (North-Holland, Amsterdam) p. 3
Buck B., Friedrich H., Wheatley C. (1977): Nucl. Phys. **A275**, 246
Chadan K., Sabatier P.C. (1977): Inverse Problems in Quantum Scattering Theory (Springer, New York)
Chatwin R.A. , Eck J.S., Robson D., Richter A. (1970): Phys. Rev. C **1**, 795
Feshbach H. (1992): Theoretical Nuclear Physics: Nuclear Reactions (Wiley, New York)
Flügge S., (1971): Practical Quantum Mechanics I (Springer, Berlin) p. 94
Ho Y.K. (1983): Phys. Reports **99** 1
Hodgson P.E. (1978): Nuclear Heavy Ion Reactions (Clarendon, Oxford)
Iwinski Z.R., Rosenberg L., Spruch L. (1985): Phys. Rev. Lett. **54**, 1602

Kondō Y., Robson B.A., Smith R. (1989): Phys. Lett. B **227**, 310
Lévai G. (1994): in Quantum Inversion Theory and Applications, ed. von Geramb H.V., Lecture Notes in Physics **427** (Springer, Berlin) p. 107
Lévai G., Baye D., Sparenberg J.-M. (1996): contribution to this conference
Michel F., Albinski J., Belery P., Delbar T., Grégoire G., Tasiaux B., Reidemeister G. (1983): Phys. Rev. C **28**, 1904
Michel F., Vanderpoorten R. (1979): Phys. Lett. B **82**, 183
Neudatchin V.G., Kukulin V.I., Korotkikh V.L., Korennoy V.P. (1971): Phys. Lett. **34B**, 581
Newton R.G. (1982): Scattering Theory of Waves and Particles, Second Edition (Springer, New York)
Reilly W., Wieland R., Gobbi A., Sachs M.W., Maher J., Siemssen R.H., Mingay D., Bromley D.A. (1973): Nuovo Cim. **13A**, 913
Siemssen R.H., Maher J.V., Weidinger A., Bromley D.A. (1967): Phys. Rev. Lett. **19**, 369
Sparenberg J.-M., Baye D. (1996): Phys. Rev. C **54**, 1309
Sukumar C.V. (1985): J. Phys. A **18**, 2917; 2937
Swan P. (1963): Nucl. Phys. **46**, 669
Wildermuth K., Tang Y.C. (1977): A Unified Theory of the Nucleus (Vieweg, Braunschweig)

Exactly Solvable Models for Two–Dimensional Quantum Systems

A.A. Suzko[1,2]

[1] Bogolubov Laboratory of Theoretical Physics, JINR, 141980, Dubna, Russia
[2] Radiation Physics and Chemistry Problems Institute, Academy of Sciences of Belarus, Minsk.

Abstract. A wide class of two–dimensional exactly solvable models is constructed on the basis of the inverse scattering problem in the adiabatic representation. Exactly solvable models with prescribed spectral properties are constructed by using the generalized method of Bargmann potentials. Two–dimensional potentials are presented within the consistent formulation of both mutually connected inverse problems to which the initial task is reduced: the parametric problem and the multichannel problem for the system of gauge equations. The algebraic technique is elaborated for the reconstruction of time-dependent and time-independent two–dimensional Bargmann potentials and corresponding solutions in a closed analytic form on the basis of the nonstandard parametric inverse problem with scattering data depending on a coordinate variable. Specific examples of exactly solvable models are given within the parametric problem on the entire line and on the half-line. In particular, transparent symmetric and nonsymmetric potentials, parametric family of phase-equivalent potentials, two-dimensional potentials without and with bound states are presented with the corresponding solutions of the parametric problem.

1 Introduction

The solution of complex multidimensional problems is often based on the dimensional reduction procedure of space realized by some partial expansion of the wave function of the original Hamiltonian over the known basis functions (see, for instance, Newton (1966)). In this sense the procedure of the adiabatic representation is a variant of dimensional reduction of space, too, because it leads to two the effective scattering problems in the spaces of a lower dimension, than the original $\mathsf{M} = \mathsf{B} \times \hat{\mathsf{M}}$. One of them is the parametric scattering problem in the space $\hat{\mathsf{M}}$ for the Hamiltonians $h^f(\mathbf{x})$ parametrically dependent on coordinate variables $\mathbf{x}$, belonging to the external space, $\mathbf{x} \in \mathsf{B}$. Another problem is the effective scattering theory in the space B for the system of gauge equations with induced gauge fields, generated by the procedure of adiabatic expansion of the total wave function $\Psi(\mathbf{X}) = \sum \int \Phi_n(\mathbf{x};.) F_n(\mathbf{x})$ over eigenstates $\Phi_n(\mathbf{x};\mathbf{y})$ of the self-adjoint Hamiltonian $h^f(\mathbf{x})$. A consistent solution to both problems provides a complete solution of the initial one. At the same time the method of adiabatic representation is very useful for investigation of many real quantum systems with some degrees of freedom the separation of which is not valid, in so far as it allows one to take into

account the mutual influence of slowly changing external (collective) and rapidly changing internal fields.

The direct scattering problem treated in the adiabatic approach has a long history that dates back to the studies of Born and Oppenheimer(1927), Born and Fock(1928). On the contrary, the inverse problem in the adiabatic approach has been proposed by the author quite recently (Suzko et al.(1989), Vinitsky and Suzko (1990)) and further developed in (Suzko (1993a), Suzko (1993), Suzko (1992), 5, 6). In this way, the premises were created for generation of a wide class of exactly solvable models for multidimensional and multiparticle objects. This method of analytic modelling is based on the consistent formulation in a closed analytic form of both connected problems: the multichannel problem for the system of equations with a covariant derivative and the parametric problem. The main point is that the potential and the basis wave functions have to be found from the scattering data parametrically depending on the spatial variables. After that, it is easily to surmise how the technique of Bargmann potentials and Darboux transformations can be used (Vinitsky and Suzko (1990), Suzko (1992), Suzko (1993a), Suzko (1993)). For this the Jost functions have to be rational, as usual, but parametrically depending on spatial variables through the dependence of spectral characteristics on them. Now this algebraic technique, based on the Gelfand–Levitan (Gelfand and Levitan (1951), Levitan (1984))) and Marchenko methods (Agranovich and Marchenko (1960), Marchenko (1977)), is tested by applying it to a number of specific two-dimensional examples, in particular, transparent symmetric and nonsymmetric potentials, reconstruction of two–dimensional potentials without and with bound states in the parametric problems on the entire line and on the half-line.

Exactly solvable three-body models with two-center spheroidal potentials have been developed in the adiabatic approach (Suzko (1992)) on the basis of the method of generalized algebraic Darboux and Bargmann transformations with some varying parameters (Rudyak, Suzko, Zakhariev (1984), Suzko (1984,1985), Suzko (1986)). Generalized Darboux and Bargmann transformations have been suggested and elaborated to construct a wide class of potentials and corresponding solutions to the Schrödinger equations for variable values of orbital angular momentum L and energy E. It has been shown (Suzko (1984,1985)), the generalized Bargmann transformations with some varying parameters are related to the generalized Darboux transformations (Rudyak, Suzko, Zakhariev (1984) and can be obtained as their superposition. The multichannel generalization of this approach has been given by Suzko (1986) and the analytical relationships were established between different potential matrices and their pertinent solutions with variable values of E and L. In particular cases, when $L = const$ or $E = const$, the obtained relations are transformed into familiar expressions for potentials and solutions of the Darboux–Bargmann transformations.

Later on the method suggested by Suzko (1984,1985) was caught up by Rudyak and Zakhariev (1987) and then, unfortunately, without reference to the origin it was used by Schnizer and Leeb (1990,1993). The studies performed for the Schrödinger equations with some varying parameters allowed us to construct algebraic Bargmann and Darboux transformations (Suzko (1993a), Suzko (1993), Suzko (1996)) for equations with an additional functional dependence $h(r)$ in the right-hand side. Under a certain choice of $h(r)$, these generalized transformations turn into the familiar Bargmann and Darboux transformations with varying (Suzko (1984,1985), Suzko (1986), Rudyak, Suzko, Zakhariev (1984)) and with fixed energy, angular momentum, Coulomb coupling constant and so on.

Based on the generalized multichannel and one-channel technique of - Bargmann potentials for the gauge system of equations and the parametrically dependent equations, the elaborated method of adiabatic representation allows us to generate a wide class of exactly solvable multidimensional models. We will reconstruct the potential $V(\mathbf{x}, \mathbf{y})$ and find the functions of the moving basis by applying the parametric inverse problem with the scattering data $\{\mathcal{S}(\mathbf{x}, k), \mathcal{E}_n(\mathbf{x}), \gamma_n^2\}$ depending on the adiabatic spatial variables. This dependence is determined by solving the inverse problem for the system of equations. When the functional dependence of scattering data on the external coordinate variable is given, the matrix elements of the induced vector and scalar potentials can be constructed and studied in terms of first obtained exact solutions of the parametric problem. The full solution of the original problem is then obtained by solving the system of multichannel equations with respect to the expansion coefficients. The suggested approach permits investigation of the dynamical quantum transition amplitudes by using exact solutions of parametric task for spectral data with prescribed properties (8). Models of this type can be employed to study certain geometric aspects of quantum scattering theory and to seek analytic solutions to nonlinear evolution equations. Thus, the parametric inverse problem is of primary interest by itself and not only as a constituent of the solution of the initial multidimensional problem in the adiabatic approach.

Here we have considered a set of certain examples of exactly solvable parametric models to show how the technique of Bargmann potentials is extended to the two-dimensional quantum systems. For a given functional dependence of spectral characteristics on the external coordinate variable, we reconstruct transparent symmetric and nonsymmetric potentials in another spatial coordinates with the pertinent solutions of the task on the whole axis. Parametric family of phase-equivalent potentials with one and two bound potential curves and their eigenfunctions are constructed. By specifying the functional dependence of spectral data on time through the dependence on it of the parametric adiabatic variable, time-dependent transparent potentials and corresponding basis functions for two-level systems are presented. We give also an example

of reconstruction of two-dimensional potentials in a consistent formulation of the two inverse problems to which the initial problem is reduced.

2 Adiabatic representation

The adiabatic representation method is elaborated on the basis of a consistent formulation of both connected problems: the parametric problem and the multichannel problem for the system of equations with a covariant derivative. In this approach the Hamiltonian H is decomposed into

$$H = h^s \otimes I + h^f, \tag{1}$$

where $h^f \equiv h^f(\mathbf{x})$ is the family of Hamiltonians depending parametrically on the slow variables. The searched wave function $\Psi(\mathbf{X})$ ($\mathbf{X} = \{\mathbf{x}, \mathbf{y}\}$) of the total Hamiltonian is given by the expansion

$$|\Psi(\mathbf{X})>= |n><n|\Psi>= \sum_n \int \Phi_n(\mathbf{x};.)F_n(\mathbf{x}) \tag{2}$$

in the eigenstates $\Phi_n(\mathbf{x};.)$ of the self-adjoint parametric Hamiltonian

$$h^f(\mathbf{x})\Phi_n(\mathbf{x};.) = \mathcal{E}_n(\mathbf{x})\Phi_n(\mathbf{x};.); \tag{3}$$

$$h^f(\mathbf{x}) = -\Delta_{\mathbf{y}} + V(\mathbf{x}, \mathbf{y}).$$

Here (.) stands for the variables $\mathbf{y}$ to be specified in every particular problem. Since the Hamiltonian $h^f(\mathbf{x})$ is self-adjoint, its eigenfunctions form a complete orthonormal set:

$$|n><n| = \delta(\mathbf{y} - \mathbf{y}'); \quad <n \mid m>= \int \Phi_n^\dagger(\mathbf{x};\mathbf{y})\Phi_m(\mathbf{x};\mathbf{y})d\mathbf{y} = \delta_{nm} \quad \forall \mathbf{x}. \tag{4}$$

The symbol $\sum \int$ in (1) denotes summation over the states of the discrete spectrum $\mathcal{E}_n(\mathbf{x}) \in \sigma_d(h^f(\mathbf{x}))$, and integration over the states of the continuous spectrum, $\mathcal{E}_k(\mathbf{x}) \in \sigma_c(h^f(\mathbf{x}))$. If basis functions $\Phi_n(\mathbf{x};\mathbf{y})$ are specified on a compact set of values $\mathbf{y} \in \hat{M}$, all of them are square integrable, and the spectrum is purely discrete, as in the case for the spherical parametrization of space with angular variables $\mathbf{y} \in S^M$. Depending on a specific formulation of the problem, use is made of a compact or noncompact base manifold. Upon substituting the expansion (1) into the initial Schrödinger equation

$$H\Psi(\mathbf{X}) = E\Psi(\mathbf{X}) \tag{5}$$

and using relations of orthonormalization (4), we arrive at the multichannel system of equations for the expansion coefficients $F = \{F_n\}$:

$$[-D^2(\mathbf{x}) + V(\mathbf{x}) - i\partial/\partial t]F(\mathbf{x}) = 0. \tag{6}$$

Here the lengthened derivative is $D(\mathbf{x}) = [\nabla_{\mathbf{x}} - i\mathbf{A}(\mathbf{x})]$ and $\mathbf{A}(\mathbf{x})$ and $V(\mathbf{x})$ is the effective vector and scalar potentials, respectively, matrix elements of which are generated by the basis functions

$$A_{nm}(\mathbf{x}) =< \Phi_n(\mathbf{x};.)|i\nabla_{\mathbf{x}}|\Phi_m(\mathbf{x};.) >, \qquad (7)$$
$$V_{nm}(\mathbf{x}) =< \Phi_n(\mathbf{x};.)|h^f(\mathbf{x})|\Phi_m(\mathbf{x};.) >= \mathcal{E}_n(\mathbf{x})\delta_{nm}.$$

The representation of (1) is invariant with respect to choosing a basis set of functions:

$$|\Psi >= |n >< n|\Psi >= |n > \mathcal{U}^{\dagger}\mathcal{U} < n|\Psi >= |\Phi'(\mathbf{x};.) > F'(\mathbf{x}).$$

Then, at any point $\mathbf{x}$ new basis functions $|\Phi' >$ are related with $|\Phi >$ by the unitary transformation $\mathcal{U}(\mathbf{x})$, and $F(\mathbf{x})$ is replaced by $F'(\mathbf{x})$:

$$|\Phi(\mathbf{x};.) >= |\Phi'(\mathbf{x};.) > \mathcal{U}(\mathbf{x}), \quad F(\mathbf{x}) = \mathcal{U}^{\dagger}(\mathbf{x})F'(\mathbf{x}). \qquad (8)$$

Under this transformation the effective matrices $V(\mathbf{x})$ and $A(\mathbf{x})$ are transformed as gauge scalar and vector fields

$$A'_{\mu}(\mathbf{x}) \to \mathcal{U}A_{\mu}(\mathbf{x})\mathcal{U}^{-1} - i\mathcal{U}^{-1}\partial_{\mu}\mathcal{U}, \quad V'(\mathbf{x}) \to \mathcal{U}V(\mathbf{x})\mathcal{U}^{-1} + i\mathcal{U}^{-1}\partial\mathcal{U}/\partial t \quad (9)$$

in consequence of which the lengthened derivative in (5) is a covariant one.

The matrix elements of the operator A realize the coupling between equations in the system (5) in contrast with ordinary coupled channel methods. Therefore anti-Hermitian operator A is interpreted as the operator of nonadiabacity. Here we assume that $h(\mathbf{x})$ is real, limited and continuous in $\mathbf{x}$. Then the eigenfunctions are real-valued and orthonormal

$$< \phi_n(\mathbf{x}) \mid \phi_m(\mathbf{x}) >= \delta_{nm} \quad \forall \mathbf{x}.$$

After differentiation of this relation we obtain that the nonadiabatic couplings $A_{nm} = -A_{mn}$ are real and antisymmetric in n and m.

Under the unitary condition of gauge transformation $\mathcal{U}$

$$\mathcal{U}(\mathbf{x})\mathcal{U}^{-1}(\mathbf{x}) = 1, \quad \mathcal{U}^{\dagger}(\mathbf{x}) = \mathcal{U}^{-1}(\mathbf{x}), \quad \forall \mathbf{x} \in B. \qquad (10)$$

that follows from the condition of completeness of the sets Φ and Φ' one can annihilate A by the corresponding choice of basis set of functions Φ' and gauge transformation $\mathcal{U}$. Really, the transition to the representation of a fixed basis $|e(\mathbf{y}) >$ with using (12)

$$|\Phi(\mathbf{x};\mathbf{y}) >= |e(\mathbf{y}) > \mathcal{U}(\mathbf{x}) \ , \ \mathcal{U}(\mathbf{x}) =< e(\mathbf{y})|\Phi(\mathbf{x};\mathbf{y}) >, \qquad (11)$$

the definition (7) and (4) allows one to rewrite A in terms of the operator $\mathcal{U}(\mathbf{x})$:

$$A_{\mu}(\mathbf{x}) = i\mathcal{U}^{-1}(\mathbf{x})\partial_{\mu}\mathcal{U}(\mathbf{x}). \qquad (12)$$

It is evident from (9) that the matrix of the gauge field A vanishes in the absence of singularities of $A(\mathbf{x})$, the matrix of the scalar potential can be expressed in the representation of the fixed basis $|e(\mathbf{y})>$. Then the system (5) is reduced to a system of ordinary equations coupled through the effective potential matrix

$$\left\{-\Delta + UV(\mathbf{x})U^{-1} - p^2)\right\}F'(\mathbf{x},\mathbf{p}) = 0 \tag{13}$$

for new coefficients F' connected with F by (12). After that, the standard methods of multichannel inverse problem are applicable to the system of equations (15), provided that the corresponding scattering matrix and information about the states of the discrete spectrum – their positions and normalization constants – are known.

Thus, the inverse scattering problem in the adiabatic approach is formulated by consistently reducing it to a multichannel one for the system of gauge type Eqs.(5) and a parametric one (2).

3 Two-dimensional exactly solvable models in the parametric inverse problem

Now we shall construct a wide class of potentials for which solutions to the parametric Schrödinger equation in a closed analytic form can be found. Based on the parametric statement of the inverse problem (Vinitsky and Suzko (1990), Suzko (1993a), Suzko (1993)) we consider reconstruction of the two-dimensional Bargmann potentials $V(x;y)$. The scattering matrix $S(x;k)$ of the parametric equation

$$\left[-d^2/dy^2 + \overset{\circ}{V}(y) + V(x;y)\right]\Phi(x;y) = \mathcal{E}(x)\Phi(x;y) \tag{14}$$

is defined by the Jost functions $f_{\pm}(x;k)$ dependent on x as the parameter

$$\mathcal{S}(x;k) = f_{-}(x;k)(f_{+}(x;k))^{-1}. \tag{15}$$

From the definition of the Jost functions through the Wronskian for each fixed x

$$f_{\pm}(x;k) = W\{f_{\pm}(x;k,y), \varphi(x:,k,y)\} \quad \forall x$$

it follows that

$$f_{\pm}(x;k) = \lim_{y\to 0} f_{\pm}(x;k,y)$$

and the Jost solutions together with the Jost functions have the property $f^*(x;k,y) = f(x;-k^*,y)$. Normalization functions $\gamma_n^2(x)$ of the potential curves $\mathcal{E}_n(x)$, as usual, are defined in terms of the Jost solutions at $k = i\kappa_n(x)$, $\mathcal{E}_n(x) = -\kappa_n^2(x)$.

$$\gamma_n^{-2}(x) = \int_0^\infty |f(i\kappa_n(x), y)|^2 dy. \tag{16}$$

An algebraic procedure of solution of the parametric inverse problem has been worked out in (Suzko (1993a), Suzko (1993),5, 6). In this papers we suggested to use the Jost functions that are rational and parametrically depending on the spatial variables of x through the dependence of spectral data on them

$$f(x;k) = \overset{\circ}{f}(k) \prod \frac{k - i\alpha(x)}{k + i\beta(x)}. \tag{17}$$

The parametric Jost function (6) defined as a function of the coordinate variable x has N curves $k = i\beta_j(x)$ of simple poles and N curves of simple zeros on the $k = i\alpha_j(x)$. In $\alpha(x)$ there are not only zeros on the imaginary semi-axis corresponding to bound states $Re\kappa_j(x) = 0$, $Im\kappa_j(x) > 0$ but also zeros in the lower half-plane with $Im\nu_j(x) < 0$ (the number of simple poles of β_j equals the total number of κ_j and ν_j). In this case the scattering matrix and spectral function assume the form

$$\begin{aligned} \mathcal{S}(x;k) &= \overset{\circ}{S}(k) \prod \frac{(k + i\alpha(x))(k + i\beta(x))}{(k - i\beta(x))(k - i\alpha(x))}, \\ \rho(x;k) &= \overset{\circ}{\rho}(k) \prod \frac{(k - i\beta(x))(k + i\beta(x))}{(k + i\alpha(x))(k - i\alpha(x))}. \end{aligned} \tag{18}$$

For such $\mathcal{S}(x;k)$ and $\rho(x;k)$ the kernels of integral equations of the parametric inverse problem can be represented as sums of terms with a factorized dependence on the fast variable y: $Q(x;y,y') = \sum_i^N B_i(x;y)\, B_i(x;y')$. When the kernel Q is inserted into the base parametric equation of the inverse problem

$$K(x;y,y') + Q(x;y,y') + \int_{y(0)}^{\infty(y)} K(x;y,y'')Q(x;y'',y')dy' = 0, \tag{19}$$

it is evident that the kernel of the generalized shift $K(x;y,y')$ also becomes degenerate, $K(x;y,y') = \sum_i^N K_i(x;y)B_i(x;y')$ and integral equations (19) become algebraic. Then, the spherically nonsymmetric potential and solutions corresponding to it can be expressed in a closed analytic form in terms of the known solutions and spectral characteristics by using the generalized equations of the parametric inverse problem

$$V^f(x;y) = \overset{\circ}{V}(y) \mp 2\frac{d}{dy}K(x;y,y), \tag{20}$$

$$\Phi(x;k,y) = \overset{\circ}{\Phi}(k,y) + \int_{y(0)}^{\infty(y)} K(x;y,y')\,\overset{\circ}{\Phi}(k,y')dy'. \tag{21}$$

Integration limits in (19), (21) and signs in (20) depend on the particular approach to the inverse problem. Limits from y to ∞ (from y to a) and minus sign correspond to the generalized Marchenko formulation (Pivovarchik and Suzko (1982)) (R-matrix inverse problem Zakhariev and Suzko (1990)). Limits $[0,y]$ and plus sign represent the Gelfand–Levitan approach.

3.1 Exactly solvable models in the generalized Marchenko approach on the semi-axis

For the parametric inverse problem, radial or on a semi-axis, when $\overset{\circ}{V}(x;y) = 0$ the kernel of the basic integral equation (19) in the Marchenko approach

$$Q(x;y+y') = \frac{1}{2\pi}\int_{-\infty}^{\infty}[1-\mathcal{S}(x;k)]\exp[ik(y+y')] + \sum_{n}^{N} M_n^2(x)\exp[-\kappa_n(x)(y+y')] \tag{22}$$

with the Jost functions (6) is rewritten as follows

$$Q(x;y+y') = -i\sum_{n}^{N} Res\ \mathcal{S}(k=ib_n(x))\exp[-b_n(x)(y+y')]$$

$$+\sum_{n}^{N}\{-iRes\ \mathcal{S}(k=i\kappa_n(x))\exp[-\kappa_n(x)(y+y')] + M_n^2\exp[-\kappa_n(x)(y+y')]\}. \tag{23}$$

Following the procedure of constructing phase–equivalent potentials suggested by Zakhariev and Suzko (1990) for the one-dimensional problem and by Suzko (1993a), Suzko (1993) for the parametric problem, one can cancel out the second summation in the right-hand side of (23) if the normalization functions $M_n^2(x)$ are chosen to be equal to $i\ Res\ \mathcal{S}(k)$ at $k = i\kappa_n(x)$

$$\overset{\circ}{M}{}_n^2(x) = i\ Res\ \mathcal{S}(k)|_{k=i\kappa_n(x)}. \tag{24}$$

As a result, we obtain the simpler expression for the kernel $Q(x;y) = \overset{\circ}{Q}(x;y)$

$$\overset{\circ}{Q}(x;y+y') = -i\sum_{n}^{N} Res\ \mathcal{S}(k)|_{k=ib_n(x)} \exp[-b_n(x)(y+y')]$$

$$\equiv \sum_{n}^{N} A_n(x)\exp[-b_n(x)(y+y')], \tag{25}$$

where

$$A_n(x) = \frac{2b_n(x)(b_n(x)+\kappa_n(x))}{(b_n(x)-\kappa_n(x))}$$

$$\prod_{n'\neq n}^{N} \frac{(b_n(x)+\kappa_{n'}(x))(b_n(x)+b_{n'}(x))}{(b_n(x)-b_{n'}(x))(b_n(x)-\kappa_{n'}(x))}. \tag{26}$$

Inserting the kernel $\overset{\circ}{Q}(x;y,y')$ (25) into the parametric equations of the inverse problem (19)–(21) we obtain

$$\overset{\circ}{V}(x;y) = -2\frac{d^2}{dy^2}\ln\det||P(x;y)||; \tag{27}$$

$$\overset{\circ}{f}_{\pm}(x;k,y) =$$

$$\exp(\pm iky) + \sum_{nn'}^{N} A_n(x)P^{-1}_{nn'}(x;y)\frac{\exp[-(b_n(x)+b_{n'}(x)\mp ik)y]}{(b_n(x)\mp ik)} \tag{28}$$

where $P_{nn'}(x;y)$ is defined as follows

$$P_{nn'}(x;y) = \delta_{nn'} + A_n(x)\frac{\exp[-(b_n(x)+b_{n'}(x))y]}{b_n(x)+b_{n'}(x)}.$$

The corresponding algebraic formulae for the one–dimensional Bargmann potentials and their solutions (Zakhariev and Suzko (1990)) can be directly obtained if we put $\kappa_n(x) \equiv \kappa_n$ and $b_n(x) \equiv b_n$.

3.2 Parametric family of phase-equivalent potentials

At the second stage we find a family of potentials and solutions for normalizing functions $M_n^2(x)$ that do not obey the condition (24). Since the scattering $\mathcal{S}(x;k)$–function is independent of the choice of the normalization functions $M_n^2(x)$, we have $\mathcal{S}(x;k) = \overset{\circ}{\mathcal{S}}(x;k)$. As a result, when $\overset{\circ}{V}(x;y) \neq 0$, the integral term in the generalized expression for $Q(x;y,y')$

$$Q(x;y,y') = \frac{1}{2\pi}\int_{-\infty}^{\infty}[\overset{\circ}{\mathcal{S}}(x;k) - \mathcal{S}(x;k)]\,\overset{\circ}{f}(x;k,y)\,\overset{\circ}{f}(x;k,y')$$
$$+\sum_{n}^{N} M_n^2(x)\,\overset{\circ}{f}(i\kappa_n(x),y)\,\overset{\circ}{f}(i\kappa_n(x),y')$$
$$-\sum_{n^o}^{N^o}\overset{\circ}{M}{}^2_{n^o}(x)\,\overset{\circ}{f}(i\kappa_{n^o}(x),y)\,\overset{\circ}{f}(i\kappa_{n^o}(x),y') \qquad (29)$$

vanishes. Since, on the other hand, both $V(x;y)$ and $\overset{\circ}{V}(x;y)$ possess the same potential curves (curves of bound states) $\mathcal{E}_n(x)$ and different normalization factors $M_n^2(x)$ and $\overset{\circ}{M}{}^2_n(x)$, respectively, we find

$$Q(x;y,y') = \sum_{n}^{N}(M_n^2(x) - \overset{\circ}{M}{}^2_n(x))\,\overset{\circ}{f}(i\kappa_n(x),y)\,\overset{\circ}{f}(i\kappa_n(x),y'). \qquad (30)$$

And similarly, the kernel of the generalized shift $K(x;y,y')$ is written as

$$K(x;y,y') = -\sum_{n}^{N}(M_n^2(x) - \overset{\circ}{M}{}^2_n(x))f(i\kappa_n(x),y)\,\overset{\circ}{f}(i\kappa_n(x),y'). \qquad (31)$$

Inserting $K(x;y,y')$ and $F(x;y,y')$ into the basic parametric Marchenko Eqs.(19)–(21) we derive the following relations for the Jost potential and solutions

$$V(x;y) = \overset{\circ}{V}(x;y) + 2\frac{d^2}{dy^2}\ln\det P(x;y); \qquad (32)$$

$$f_{\pm}(x;k,y) = \overset{\circ}{f}_{\pm}(x;k,y) -$$
$$-\sum_{nm}^{N}(M_n^2 - \overset{\circ}{M}{}^2_n)\,\overset{\circ}{f}(i\kappa_n(x),y)P^{-1}_{nm}(x;y)\int_y^{\infty}\overset{\circ}{f}(i\kappa_m(x),y')\,\overset{\circ}{f}_{\pm}(k,y')dy'.$$

The explicit dependence on fast variables is defined by the Jost solutions (28) determined at $k = i\kappa_n(x)$, i.e. on the level-energy curves depending on the parametric variable x. Here we employed the notation

$$P_{nm}(x;y) = \delta_{nm} + (M_n^2(x) - \overset{\circ}{M}{}^2_n(x))\int_y^{\infty}\overset{\circ}{f}(i\kappa_n(x),y')\,\overset{\circ}{f}(i\kappa_m(x),y')dy'.$$

Since $\mathcal{S}(x;k)$ from (7) corresponding to the two-dimensional potentials $V(x;y)$ (32) is independent of the normalizations $M_n^2(x)$, $\mathcal{S}(x;k) = \overset{\circ}{\mathcal{S}}(x;k)$ the formula (32) represents a parametric family of phase-equivalent potentials depending on N parameters in the addition to the parametric spatial variable x. Among them there is a potential with the condition (24).

3.3 Bargmann potential with a single potential curve

Bargmann potential in the simple case, when the scattering $\mathcal{S}(x,k)$–matrix has two pole lines $k = i\kappa(x)$ and $k = i\beta(x)$, is presented on figure 1. Assume that

$$f(x;k) = \frac{k - i\kappa(x)}{k + i\beta(x)}; \quad Im\{\kappa(x)\} = Im\{\beta(x)\} = 0,$$

i.e.,

$$\mathcal{S}(x,k) = \frac{(k + i\kappa(x))(k + i\beta(x))}{(k - i\kappa(x))(k - i\beta(x))}.$$

One pole curve corresponds to the zeros on the $k = i\kappa(x)$ of the parametric Jost function $f_+(x;k))$, the other pole curve corresponds to the poles on the $k = i\beta(x)$ of the parametric Jost function $f_-(x;k)$. We have necessarily $\beta(x) > 0$ (for the Jost function $f_+(x;k)$ to be analytic in the upper half-plane k for all x). When $\kappa(x) > 0$, we have the bound state line (the potential curve of bound state $\mathcal{E}(x) = -\kappa^2(x)$), when $\kappa(x) < 0$, we have no bound states. Factorization of the kernel $Q(x;y,y')$

$$Q(x;y+y') = \frac{1}{2\pi}\int_{-\infty}^{\infty}\left[1 - \frac{(k + i\kappa(x))(k + i\beta(x))}{(k - i\kappa(x))(k - i\beta(x))}\right]\exp[ik(y+y')]$$
$$+ M^2(x)\exp[-\kappa_n(x)(y+y')] \tag{33}$$

is achieved by a special choice of normalization function $M^2(x) \equiv M^2_{\kappa(x)}$. In accordance with (24) we have

$$\overset{\circ}{M}{}^2_n(x) = iRes\ \mathcal{S}(k)|_{k=i\kappa_n(x)} = 2\kappa(x)\frac{(\beta(x)+\kappa(x))}{(\beta(x)-\kappa(x))}. \tag{34}$$

Closing the integration contour by a semicircle of infinite radius in the upper half-plane of complex k in (33) and making use of the residue theorem with account (34), we find

$$Q(x;y+y') = 2\beta(x)\frac{(\beta(x)+\kappa(x))}{(\beta(x)-\kappa(x))}\exp[-\beta(x)(y+y')]. \tag{35}$$

Solving now the parametric Marchenko equations with this kernel, we find the kernel

$$K(x;y,y') = -2\beta(x)\frac{c(x)\exp[-\beta(x)(y+y')]}{1 + c(x)\exp[-2\beta(x)y]}, \tag{36}$$

where $c(x) = (\beta(x)+\kappa(x))/(\beta(x)-\kappa(x))$, determining the potential $V(x,y)$ and the corresponding solution of the parametric Schrödinger equation

$$V(x;y) = -8\beta^2(x)\frac{c(x)\exp[-2\beta(x)y]}{\{1 + c(x)\exp[-2\beta(x)y]\}^2}$$
$$= -2\beta^2(x)\frac{1}{cosh^2[\beta(x)(y-y_o)]}; \tag{37}$$

$$f_{\pm}(x;ky) = \exp(\pm ky)\Big\{1 + \frac{2\beta(x)\exp[-2\beta(x)(y-y_o)]}{(\pm ik - \beta(x))(1+\exp[-2\beta(x)(y-y_o)]}\Big\}. \quad (38)$$

Here we used the substitution $exp(2\beta(x)y_o) = (\beta(x)+\kappa(x))/(\beta(x)-\kappa(x))$. If $\kappa(x) < 0 \ \forall x$, the potential (37) is not deep enough to produce of a bound state curve and the potential in the form (37) corresponds to $\mathcal{S}(x,k)$ with one pole curve on $k = i\beta(x)$. Depending on the particular problem, the pole curves can, in general, behave in different ways, it is only necessary to take into account the condition $\beta(x) > \kappa(x)$ that follows from (34), because the normalization function has to be positive $M^2 > 0$.

In the present case (Fig.1), we specify $\kappa(x))$ and $\beta(x)$ as follows

$$\kappa(x) = \frac{\sqrt{2}\kappa}{\cosh(\kappa x - 13.5)}, \quad \beta(x) = \frac{\sqrt{2}\beta}{\cosh(\beta x - 15)} + 0.3, \quad \kappa = 0.6, \quad \beta = 0.7.$$

The two-dimensional potential and the normalized wave functions $\psi(\kappa(x), y)$ corresponding to $S(x,k)$ with these $\kappa(x)$ and $k = ib(x)$ are presented in Figs.1A and 1B. In complete analogy with the procedure (30)–(32) we can construct a whole family of phase-equivalent potentials differing from each other of the normalization $M^2(x)$ of the potential curve.

3.4 More general model with two potential curves

Let us now present a more complicate case with two potential curves in the problem on the semi-axis. To simplify the problem, we again choose the reference potential $\overset{\circ}{V}(x;y) = 0$. Then the Jost function can be written in the form

$$f(x;k) = \prod \frac{(k+i\beta_1(x))(k+i\beta_2(x))}{(k-i\kappa_1(x))(k-i\kappa_2(x))}. \quad (39)$$

We take the normalizations of bound state wave functions in the form (24). Thereby the potential $V(x,y)$, is determined only by the spectral data $\kappa_i(x)$ and $\beta_i(x)$, $i = 1,2$ and corresponds to one of the phase-equivalent potentials. From normalizations $M_n^2(x)$ being positively definite the conditions $\beta_2(x) \geq \kappa_2(x)$ and $\beta_1(x) \geq \kappa_1(x)$ follow. The spectral data have been chosen in the following way

$$\kappa_1(x) = \frac{\sqrt{2}\kappa_1}{\cosh(\kappa_1 x - 4.8)}, \quad \beta_1(x) = \frac{\sqrt{2}\beta_1}{\cosh(\beta_1 x - 5)} + 0.3,$$

$$\kappa_2(x) = \frac{\sqrt{2}\kappa_2}{\cosh(\kappa_1 x - 5)} + 0.4, \ \beta_2(x) = \frac{\sqrt{2}\beta_2}{\cosh(\beta_2 x - 5)} + 0.5,$$

$$\kappa_1 = 0.6, \ \beta_1 = \kappa_2 = \beta_2 = 0.7.$$

From the relations (27), (28) we obtain the two-dimensional potential $V(x,y)$ Fig.2A and the corresponding normalized wave functions $\psi_{1,2}(x,y)$ Fig.2B,C of the self-energy curves $\mathcal{E}_{12}(x)$. The behaviour of the potential and wave functions becomes more complicated in comparison with the one corresponding to $\mathcal{S}(x;k)$ with two pole curves, presented in Fig.1.

4 Reflectionless potentials in the parametric problem

The simplest case corresponds to reflectionless potentials in one of the spatial variables or in both adiabatic and fast variables. If the reflection function $\mathcal{S}^{ref}$ is chosen to be equal to zero at all energies and at all values of adiabatic variable x, then the integral in the relation for $Q(x;y,y')$ vanishes and only the sum over bound states remains (see the contribution to these Proceedings (8)). In this case the transmission coefficient $\mathcal{S}^{tr}$ whose modulus is equal to 1 is a rational function

$$\mathcal{S}^{tr}(x;k) = \prod \frac{k+i\kappa(x)}{k-i\kappa(x)}. \tag{40}$$

Symmetrical transparent potentials for each fixed value of x and appropriate wave functions are completely defined by the energy levels (5) since the normalization functions can be determined by them

$$\gamma_n^2(x) = iRes\mathcal{S}^{tr}(k)_{/k=i\kappa_n(x)} = 2\kappa_n(x) \prod_{m\neq n} \left|\frac{\kappa_m(x)+\kappa_n(x)}{\kappa_m(x)-\kappa_n(x)}\right|. \tag{41}$$

The relations for the potentials and solutions can be expressed in terms of the normalized eigenfunctions and represented in a more symmetric and convenient form. Following (Calogero and Degasperis (1982), 5), introduce the function

$$\lambda_n(x;y) = \gamma_n(x)\exp(-\kappa_n(x)y).$$

Then the formula for $K(x;y,y')$ can be written as

$$\begin{aligned} K(x;y,y') = &-\sum_n^N \gamma_n(x)\psi_n(x;y)\exp(-\kappa_n(x)y') = \\ &-\sum_n^N \psi_n(x;y)\lambda_n(x;y). \end{aligned} \tag{42}$$

For the normalized eigenfunctions $\psi_n(x;y)$ from (21), we obtain

$$\psi_n(x;y) = \sum_j^N \lambda_j(x;y)A^{-1}_{jn}(x;y) \tag{43}$$

with the matrix $A_{jn}(x;y)$ given by

$$A_{jn}(x;y) = \delta_{jn} + \frac{\lambda_j(x;y)\lambda_n(x;y)}{\kappa_n(x)+\kappa_j(x)}. \tag{44}$$

Finally, the kernel $K(x;y,y')$ and the potential can be represented as

$$K(x;y,y') = -\sum_{n}^{N}\sum_{j}^{N}\lambda_j(x;y)A_{jn}^{-1}(x;y)\lambda_n(x;y),$$

$$V(x;y) = -4\sum_{n}^{m}\kappa_n(x)\psi_n^2(x;y). \tag{45}$$

Note, these relations are obtained for the specific case of zero reflection function $\mathcal{S}^r(x;k) = 0 \ \ \forall x$. The set of time-independent and time-dependent transparent potentials have been constructed in (5, 6, 7) for which the parametric Schrödinger equations have exact solutions. Examples of the reconstruction of potentials that are symmetric and transparent in y with various parameters are presented in Figs.3 and nonsymmetric transparent potentials are presented in these Proceedings (8).

5 Exactly solvable models with time-dependent potentials

Based on the technique of degenerate kernels, we gave a simple example of a two-dimensional exactly solvable model for a two-level system with a periodical dependence of the dynamical variable $x(t)$ on time (Suzko, Velicheva 7). We defined two terms in the following way

$$\mathcal{E}_1 = -1/ch^2(x/3), \ \ \mathcal{E}_2 = -(1/ch(x/2) + 0.25)^2$$

with

$$x(t) = \overset{\circ}{x}\ (1 - a\ cos(\omega t)),$$

where $\overset{\circ}{x} = x(t = 0)$ corresponds to the time-independent case. We reconstruct symmetric transparent potentials and appropriate basis wave functions that are determined by the energy levels due to choosing the normalization functions $\gamma_n^2(x(t))$ in the form (41). The dynamical behaviour of the potentials and the pertinent eigenfunctions is presented for ωt equal to $0, \pi/6, \pi/3, \pi/2, \pi$ in Figs.(3a,b,c,d,f) – (5a,b,c,d,f), respectively, and $a = 1$. Since their behaviour is mirror-symmetric with respect to the line $\omega t \in (0, \pi)$, it is not shown. It is easy to see that the potential and functions change from very simple one-dimensional ones for $\omega t = 0$, Figs.3a – 5a, to quite complicate two-dimensional potentials and functions for all other values of $\omega t \neq 0$. In our case the potential curves have been chosen when $t = 0$, $x(0) = 0$ and $\mathcal{E}_1 = -1$, $\mathcal{E}_2 = -1.5625$. A one-dimensional transparent potential with two bound states and corresponding wave functions are immediately obtained from more general relations Suzko (1993a), Suzko (1993) of the parametric task. When $\omega t \neq 0$, we have two-dimensional potentials and functions. At $\omega t = \pi/2$ and $\omega t = 3\pi/2$, $x(t)$ coincides with $\overset{\circ}{x}$ and we have the two-dimensional time-independent case, while at $\omega t = 2\pi$, the system comes back into the one-dimensional position with the initial states

$|\phi_n(x(t);y) >\equiv |\phi_n(y) >$. Note, the eigenfunctions $\psi_2(x;y)$ are symmetric and $\psi_1(x;y)$ are antisymmetric in y at each fixed values of $x(t)$ as it is required for the problem on the entire axis $-\infty < y < \infty$ with a potential $V(x;y)$ symmetric in y.

Obviously, we can choose another dependence on time, and other initial spectral data with prescribed properties. For instance, the two–dimensional or three–dimensional dependence of spectral characteristics on the parametric adiabatic variables can occur. In our paper from these Proceedings we have presented examples of transparent but nonsymmetric time-dependent potentials. In such a way one may also investigate properties of adiabatically driven quantum systems, Hamiltonians for which are slowly varying functions of time. The transition amplitudes in this case are defined by the matrix elements of an exchange interaction $A(x)$ that can be calculated in terms of analytic basis functions (Suzko, Velicheva 8). The basis wave functions found in this way can be used to study a number of problems in nuclear, atomic, and molecular physics.

So, we have considered certain examples of exactly solvable parametric models to show how the technique of Bargmann potentials is extended to the parametric family of the inverse problems. For a given functional dependence of spectral characteristics on the external coordinate variable, one may derive a large class of exactly solvable multidimensional models on the basis of the parametric inverse problem in the space of a lower dimension.

6 Constructing two–dimensional exactly solvable models in a consistent formulation

Based on the multichannel and one-channel technique of Bargmann potentials for a transformed system of Eqs.(5) and the parametrically dependent Eq.(2), the method of analytic modeling of effective interactions in complicated multidimensional problems and of finding appropriate solutions has been suggested by Vinitsky and Suzko (1990) and developed in (Suzko (1993a), Suzko (1993), 5, 6). The inverse scattering problem for the system of equations (5) consists of several steps: the determination of the S–matrix in terms of known multidimensional amplitudes and subsequent reconstruction of effective vector, A, and scalar, V, potential matrices, as well as solutions. It is solved by using a unitary transformation of the gauge type (9), (10) that reduces the system of Eqs.(5) to a system of ordinary equations coupled through the effective potential matrix (15).

We will analyze the simplest case in which the reconstruction of the matrix of the potential interaction $||V_{ij}(x)||$ is performed with $||\overset{\circ}{V}_{ij}(x)|| = 0$ taken for the reference potential. For reflectionless potential matrices, the matrix elements $Q_{ij}(x,x')$ involves only the sum over the bound states

$$Q_{ij}(x,x') = \sum_{\lambda}^{N} \exp(-\kappa_i^{\lambda} x)\gamma_i^{\lambda}\gamma_j^{\lambda} \exp(-\kappa_j^{\lambda} x). \tag{46}$$

Then the system of integral equations of the inverse problem is reduced to a system of algebraic equations. By employing the results of (Plekhanov, Suzko, Zakhariev (1982), Zakhariev and Suzko (1990)), the expressions for the potential and solution matrices can be written in the explicit form

$$V'_{ij}(x) = 2\frac{d}{dx}\sum_{\nu\lambda} \exp(-\kappa_i^{\nu} x)\gamma_i^{\nu} P^{-1}_{\nu\lambda}(x)\gamma_j^{\lambda} \exp(-\kappa_j^{\lambda} x), \tag{47}$$

$$F'^{\pm}_{jj'}(k,x) = \exp(\pm ik_j x)\delta_{jj'} - \frac{\gamma_j\gamma_{j'} \exp(-\kappa_j x)\int_x^{\infty} \exp(-(\kappa_{j'} \pm ik_{j'})x')dx'}{1 + \sum_i^m (\gamma_i^2/2\kappa_i)\exp(-2\kappa_i x)} \tag{48}$$

where

$$P_{\nu\lambda} = \delta_{\nu\lambda} + \sum_{j'}^{m} \frac{\gamma_{j'}^{\nu}\gamma_{j'}^{\lambda}}{\kappa_{j'}^{\nu} + \kappa_{j'}^{\lambda}} \exp(-(\kappa_{j'}^{\nu} + \kappa_{j'}^{\lambda})x).$$

By diagonalizing the potential matrix with account of $\mathcal{U}^{-1}(x)V'(x)\mathcal{U}(x) = \mathcal{E}(x)$, we get searched scalar $\mathcal{E}(x)$ and vector potentials $A(x)$ by using formula (9), (12).

To reconstruct the two–dimensional potential $V(x,y)$ at the second step from the spectral data $\{\mathcal{E}_i(x), \gamma_i^2(x)\}$, which are functions of the variable x, we make use of the parametric inverse problem (19) – (21), in which $V(x:y)$ and $\psi_i(x;y)$ are reconstructed for the parametric equation (2) at each fixed value of x. The technique of Bargmann potentials for the parametric inverse problem makes it possible to find explicitly the solutions $\psi_i(x,y)$ and the potential $V(x,y)$ in the analytic form within a consistent approach. Figures 6 – 7 show examples of the consistent analytic solution of the full problem for a potentials that are transparent in both variables.

In the case of single bound state (5), we arrive at one of the generalized Eckart potentials

$$V(x;y) = -2\frac{2\kappa(x)\gamma^2(x)\exp(-2\kappa(x)y)}{[1 + (\gamma^2(x)/2\kappa(x))\exp(-2\kappa(x)y)]^2}, \tag{49}$$

This expression can be recast into the simpler form well known in soliton theory

$$V(x;y) = -\frac{2\kappa^2(x)}{\cosh^2[\kappa(x)(y - y_0(x)]} \tag{50}$$

with the aid of the substitution

$$\exp(2\kappa(x)y_0) = \gamma^2(x)/2\kappa(x). \tag{51}$$

The Jost solutions on the trajectory $k = i\kappa(x)$ and at arbitrary values of k are, respectively, given by

$$f(i\kappa(x), y) = \frac{\exp(-\kappa(x)y)}{1 + \exp[-2\kappa(x)(y - y_0(x)]}, \tag{52}$$

$$f_{\pm}(x; k, y) =$$

$$\exp(\pm iky)\Big\{1 - \frac{\exp[-2\kappa(x)(y - y_0(x)]}{(1 + \exp[-2\kappa(x)(y - y_0(x)])(\kappa(x) \mp ik)}\Big\}. \tag{53}$$

The explicit expression for the normalized wave function $\psi(x, y)$ corresponding to the term $\mathcal{E}(x) = -\kappa^2(x)$ for the potential (50) has the form

$$\psi(x, y) = \frac{\sqrt{\kappa(x)/2}}{\cosh[\kappa(x)(y - y_0(x)]}. \tag{54}$$

It can be shown easily that the potential is related to the normalized wave function by the equation

$$V(x; y) = -4\kappa(x)\psi^2(x; y) \tag{55}$$

Note that $y_0(x)$ in equations (50), (52) – (55) is always related to the normalization function $\gamma^2(x)$ by equation (51). If the normalization function is chosen in accordance with (41),

$$\gamma^2(x) = 2\kappa(x),$$

we have $y_0(x) = 0 \ \forall x$, which corresponds to the potential that is not only transparent but also symmetric in y. It is no surprising because it can be seen from (50), for $y_0(x) = 0$, the potential is symmetric with $y = 0$. If the behaviour of the energy curve $\mathcal{E}(x)$ corresponds to the potential $V(x) \equiv \mathcal{E}(x)$,

$$\mathcal{E}(x) = -\frac{2\kappa^2}{cosh^2(\kappa x)}, \tag{56}$$

which appears in equation (5) and which is symmetric and transparent in x (Fig.6), arising under the condition $\gamma^2 = 2\kappa$ and $x_0 = 0$, the relation (50) leads to a transparent two–dimensional potential that is symmetric in both variables (Fig.6a) and possesses one bound state $E = -\kappa^2$. The relations (54) and (53) yield the two–dimensional normalized function of the bound state $\psi(x; y)$ (Fig.6b) corresponding to the potential curve (56), and also the two–dimensional wave functions $f_{\pm}(x; k, y)$ of the continuous spectrum for the parametric problem.

Now we will demonstrate a more complicated example of the consistent analytic solution of the full problem for the potential that is again transparent in both variables x and y but possesses two bound states in contrast with one state of the previous case. Both problems are solved by using the Marchenko

approach adapted to the two–channel system of equations and the parametric Schrödinger equation. We take the values $E_1 = -0.5$ and $E_2 = -1$ for the bound–state energies and $\gamma_1^1 = 2, \gamma_2^2 = 2, \gamma_1^2 = 0.5$ and $\gamma_2^1 = 0.25$ for their normalization factors $\{\gamma_j^\lambda\}$. For these values of parameters we found the reflectionless potential matrix whose elements $V'_{11}(x), V'_{12}(x), V'_{12}(x) = V'_{21}(x)$ and $V'_{22}(x)$ are represented graphically in Fig.7a. The potential curves $\mathcal{E}_1(x)$ and $\mathcal{E}_2(x)$ (Fig.7b) are found by solving the algebraic problem for eigenvalues

$$\mathcal{E}_{1,2}(x) = \frac{1}{2}\left[V'_{11}(x) + V'_{22}(x)\right] \pm \sqrt{(V'_{11}(x) - V'_{22}(x))^2 + 4V'^2_{12}(x)}\Big]. \quad (57)$$

The nonadiabatic connection, accomplished by the matrix element of the effective vector potential $A_{12} = -A_{21}$ is shown in Fig.7c. To reconstruct the two–dimensional potential $V(x, y)$ at the second step we use the parametric inverse problem (41)–(45), in which $V(x; y)$ and basis wave functions $\psi_i(x, y)$ are defined from the spectral data $\{\mathcal{E}_i(x), \gamma_i^2(x)\}$ at each fixed value of x. The potential $V(x, y)$, that is transparent and symmetric in y, is determined only by the potential curves $\mathcal{E}_i(x)$ because of in this case the normalization functions $\gamma_i^2(x)$ are expressed in terms of the level-energy values (41). The two–dimensional potential $V(x, y)$ and the corresponding normalized wave functions $\psi_{1,2}(x, y)$ of the self-energy curves $\mathcal{E}_{12}(x)$ are presented in Figs.(7d) – (7e,f), respectively. The potential symmetric and transparent in y has the structure: the principal peak and several weak rapidly diminishing peaks. In more detail, a number of examples were considered in (5, 6).

7 Conclusions

On the basis of the inverse scattering problem in the adiabatic representation, a wide class of exactly solvable two-dimensional models is constructed by the generalized method of Bargmann potentials for a parametric family of inverse problems and for systems of equations with covariant derivatives. Exactly solvable models with prescribed spectral data are built on the basis of the parametric inverse problem and in a consistent formulation of the two inverse problems to which the initial problem is reduced. This technique is tested by applying it to a number of specific examples on the basis of the parametric inverse problem on the entire line and on the half-line. In particular, two-dimensional potentials are constructed with one and two energy level curves and transparent potentials are presented that are symmetric and nonsymmetric in one or both spatial variables.

Acknowledgments. This work was supported in part by the Foundation of the "Heisenberg-Landau Program" of investigations. The author is grateful to Professor H.Von Geramb and E.P.Velicheva for useful discussions.

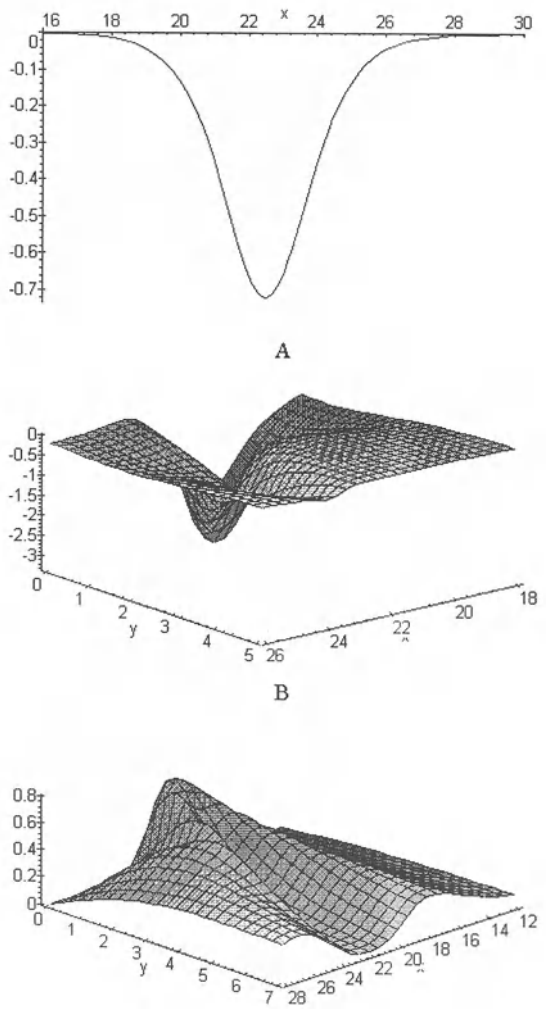

Fig. 1. (**A**) Potential $V(x, y)$ corresponding to $S(x; k)$ with two pole curves in the upper k half-plane, (**B**) the normalized eigenfunction $\psi(x; y)$ at $k = -i\kappa(x)$, the upper curve is the energy-level curve $\mathcal{E}(x) = -\kappa^2(x)$

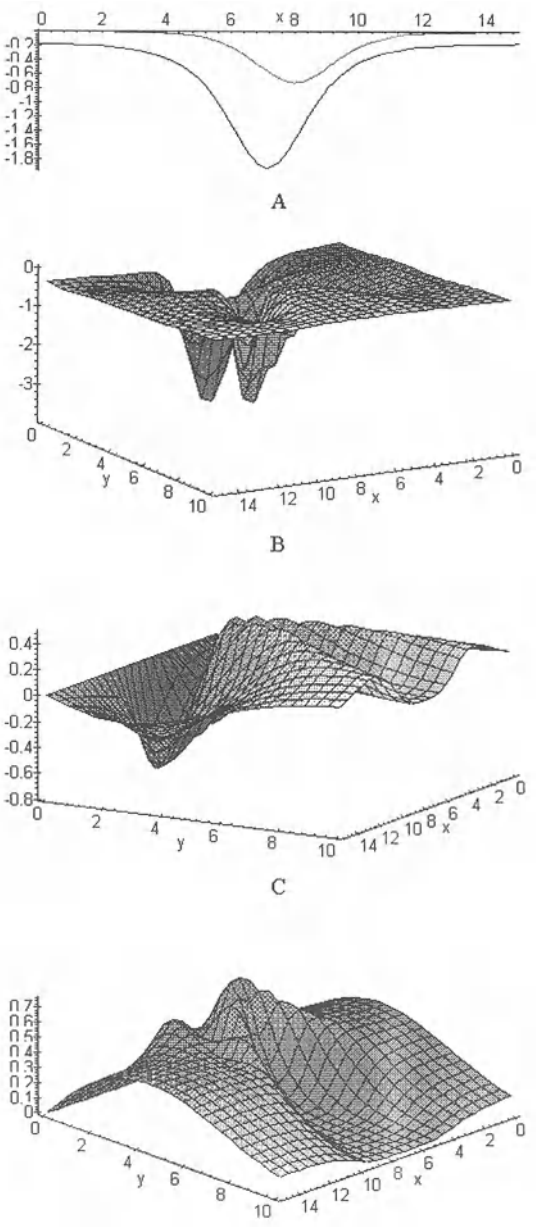

Fig. 2. (**A**) Potential $V(x, y)$ with $\mathcal{S}(x; k)$ with 4 pole curves in the upper k half-plane, (**B,C**) the normalized eigenfunctions $\psi_{1,2}(x; y)$ at $k = -i\kappa_{1,2}(x)$, the energy-level curves $\mathcal{E}_{1,2}(x) = -\kappa_{1,2}^2(x)$ are shown in the upper figure.

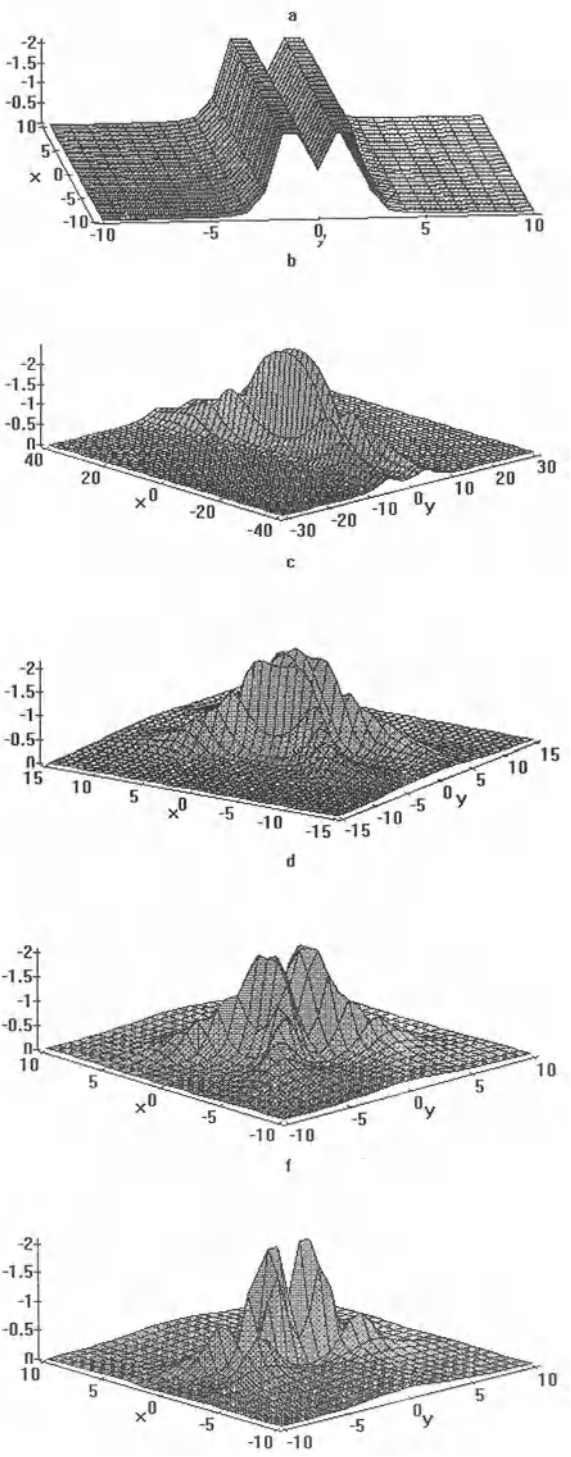

Fig. 3. Potentials $V(x(t), y)$, transparent and symmetrical in y, calculated for different values of ωt: (**a**) $\omega t = 0$, (**b**) $\omega t = \pi/6$, (**c**) $\omega t = \pi/3$, (**d**) $\omega t = \pi/2$, (**f**) $\omega t = \pi$. To achieve a clearer presentation, the potential is inverted.

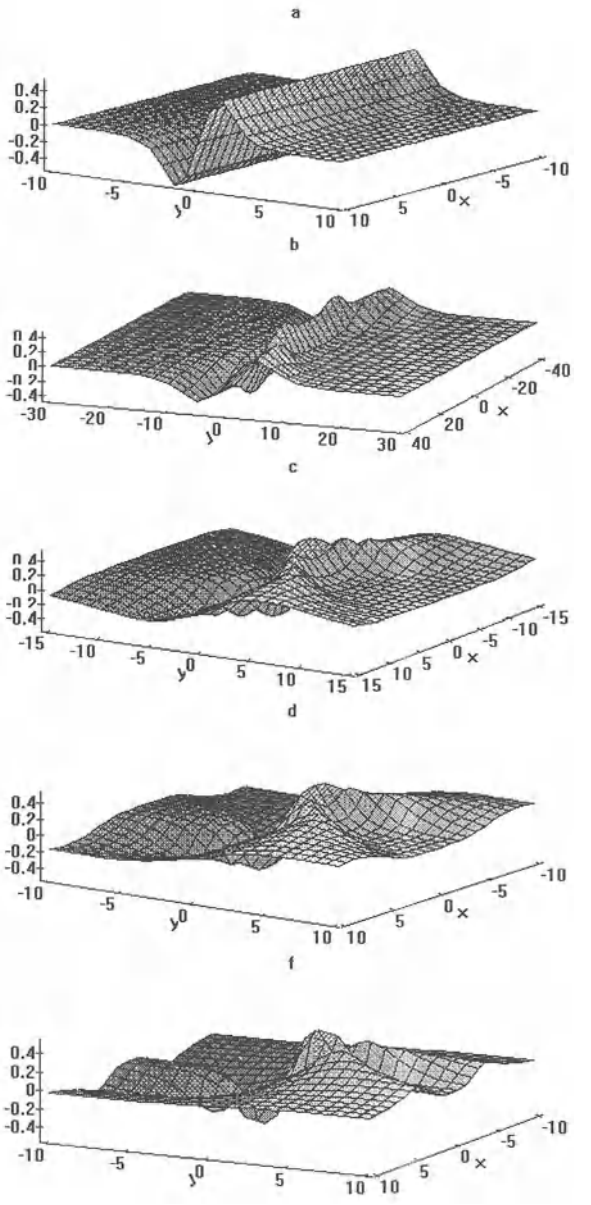

Fig. 4. Eigenfunctions $\phi_1(x(t), y)$ at (a) $\omega t = 0$, (b) $\omega t = \pi/6$, (c) $\omega t = \pi/3$, (d) $\omega t = \pi/2$, (f) $\omega t = \pi$.

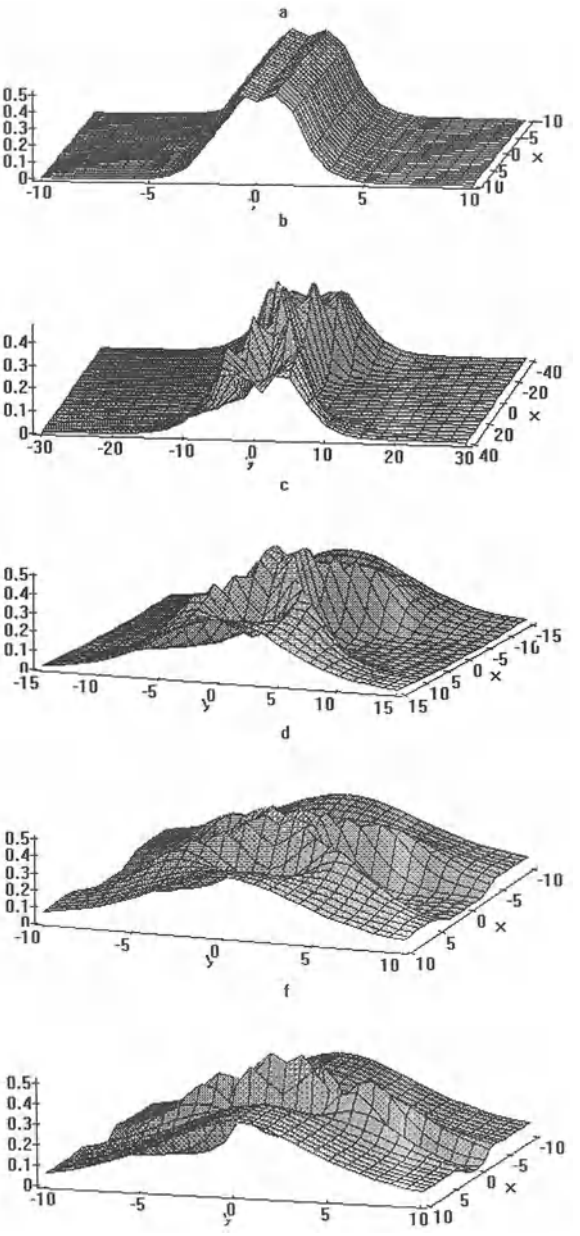

Fig. 5. Eigenfunctions $\phi_2(x(t), y)$ at (a) $\omega t = 0$, (b) $\omega t = \pi/6$, (c) $\omega t = \pi/3$, (d) $\omega t = \pi/2$, (f) $\omega t = \pi$.

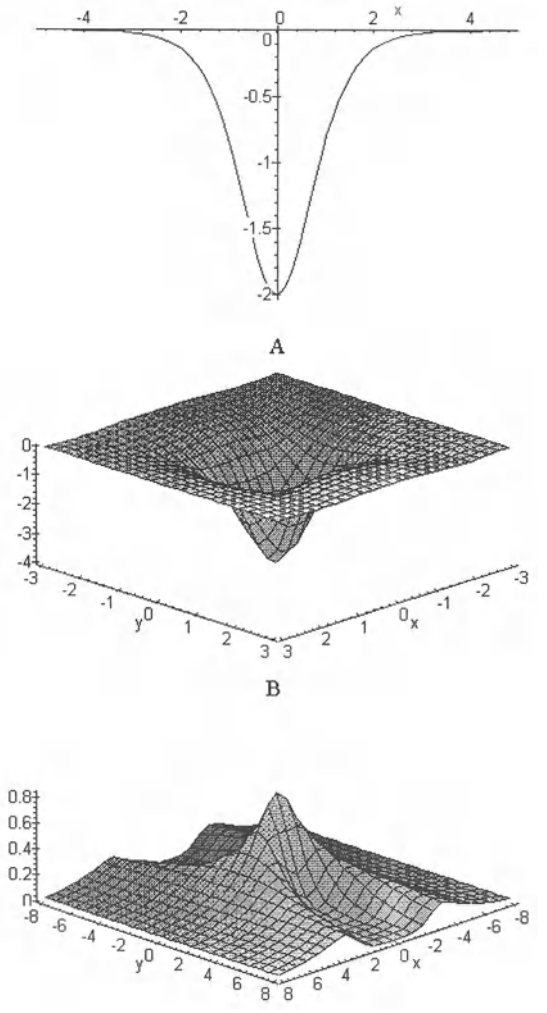

Fig. 6. Two-dimensional potential $V(x;y)$ (**A**) that is reflectionless and symmetric in both coordinate variables x and y. (**B**) Eigenfunction $\psi(x;y)$ at $k = -i\kappa(x)$. Potential curve $\mathcal{E}(x)$ corresponds to one–dimensional potential that is transparent and symmetric in x and which possess a bound state at $E = -1$.

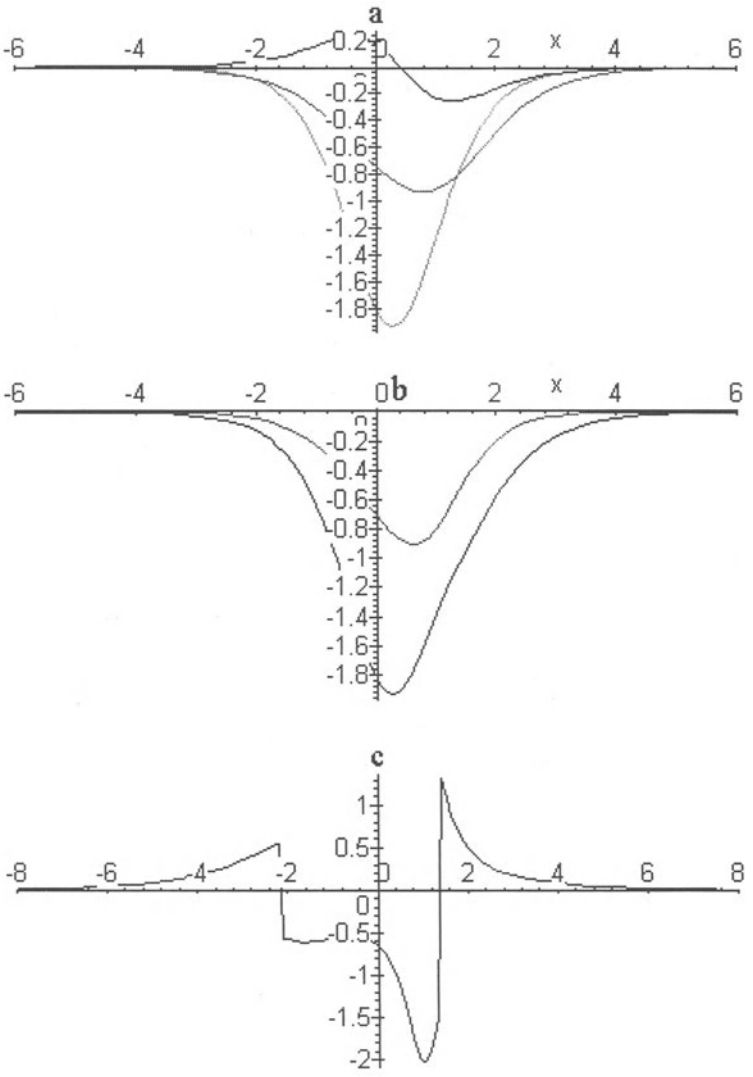

Fig. 7. (a-c) Bargmann potential matrices $V'(x)$ (a) that is reflectionless in x. The energy–level curves (b) $\mathcal{E}_1(x)$ and $\mathcal{E}_2(x)$ and the matrix element $A_{12}(x)$ of the induced vector potential (c)

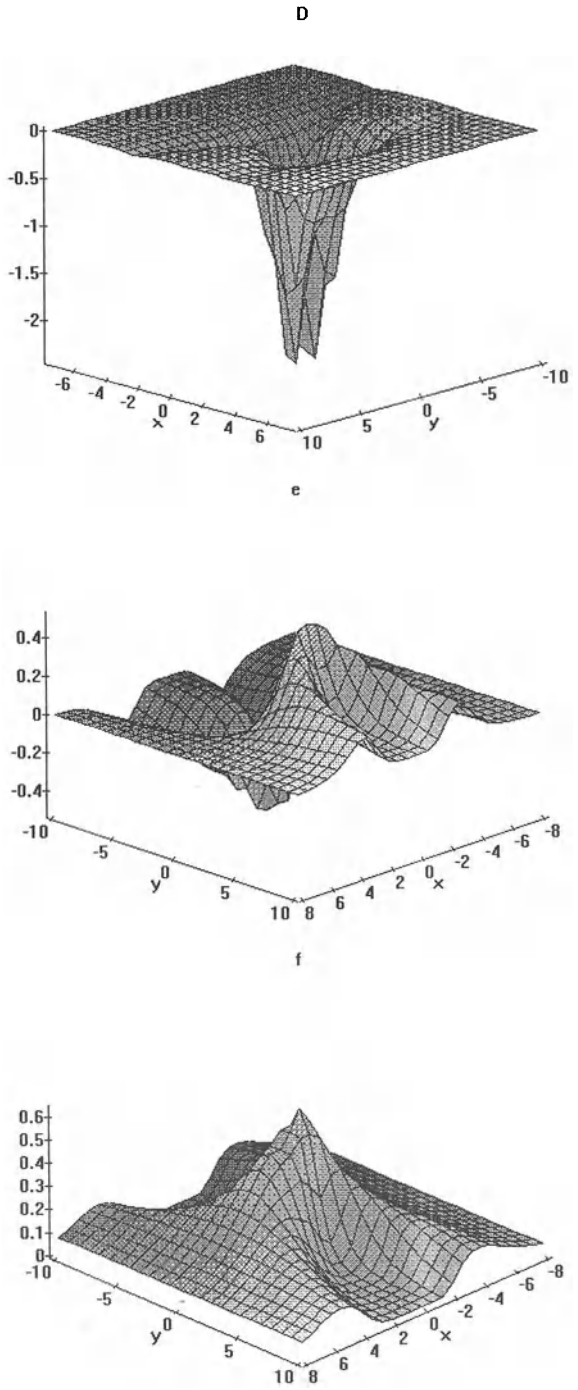

Fig. 8. (continued **Fig.7d-f.**) Two-dimensional potential $V(x;y)$ (**d**) that is reflectionless in both coordinate variables and symmetric in y. Eigenfunctions $\psi_1(x;y)$ and $\psi_2(x;y)$ (**e,f**) correspond to the energy–level curves shown in **Fig.7b**

References

Agranovich Z.S., Marchenko V.A. (1960): *Inverse Scattering Problem* (Kharkov)

Born M., Oppenheimer R. (1927): Ann. d. Phys. **84**, 457

Born M., Fock V. (1928): Zs. Phys. **51**, 165

Calodgero F., Degasperis A. (1982): *Spectral transform and solitons* (North-Holland Publishing Company, Amsterdam-New-York-Oxford).

Chadan K., Sabatier P.C. (1977,1989): *Inverse Problems in Quantum Scattering Theory*, Springer-Verlag, New York, Berlin, Heidelberg.

Gelfand L.M. and Levitan B.M. (1951): On the determination of a differential equation by its spectral function. Izv.Akad.Nauk SSR ser.Math., **15**, 309-360.

Dubovik V.M., Markovski B.L., Suzko A.A., Vinitsky S.I. (1989): Scattering problem for Faddeev equations in adiabatic representation. Phys.Lett., **A142**, 133-138.

Levitan B.M. (1984): *Sturm-Liouville Inverse Problems* (Nauka, Moscow)

Marchenko V.A. (1977): *Sturm-Liouville Operators and their Applications* (Naukova Dumka, Kiev)

Pivovarchik V.N. and Suzko A.A. (1982): In Proc.Inst.Heat and Mass Transfer. *Evolution Methods in Inhomogeneous Media.* (Press, Minsk) 168-177.

Newton R.G. (1966): *Scattering Theory of Waves and Particles*, McGraw-Hill, New York.

Plekhanov E.B., Suzko A.A., Zakhariev B.N. (1982): Multichannel and Multidimensional Bargmann Potentials. Annal.der Phys., **39** No.5, 313-319.

Rudyak B.V., Suzko A.A., Zakhariev B.N. (1984): Exactly Solvable Models (Crum–Krein Transformatios in the (λ^2, E)–Plane. Physica Scripta, **29**, 515-517.

Rudyak B.V., Zakhariev B.N. (1987): New Exactly Solvable Models for the Schrödinger Equation. Inverse Problems, **3**, 125-133.

Schnizer W.A., Leeb H. (1990): *Inverse Methods in Action*, Proc. Int. Meeting, ed. by P.C. Sabatier (Springer-Verlag, New York, Berlin, Heidelberg) 455.

Schnizer W.A., Leeb H. (1993): New Exactly Solvable Models for the Schrödinger Equation from Generalized Darboux Transformatios. J.Phys. **A26**, 5145-5156.

Suzko A.A. (1984,1985): Exactly Solvable Models in the (λ^2, E)–Plane. Physica Scripta, **31**, 447-449;
In Proc. IX European Conference on Few Body Problems in Physics (Tbilisi, August, 1984, Poster section papers) 56-57.

Suzko A.A., (1986): Multichannel Exactly Solvable Models. Physica Scripta, **34**, 5-7.

Vinitsky S.I., Suzko A. A. (1990): Exactly Solvable Multidimensional and Tree-Particle Scattering Problems in the Adiabatic Representation. Sov. J. Nucl. Phys. **52**, 442–451.

Suzko A.A. (1992): Exactly Solvable Tree-Body Models with Two-Center Potentials. Sov. J. Nucl. Phys. **55**, 1359–1365 (translated from Yadernaya Fizika **55**, 2446-2457).

Suzko A.A. (1993a): *Multidimensional and three-body inverse scattering problems in the adiabatic representation"* , Proc. Int.Conf. in *Lecture Notes in Physics, " Quantum Inversion Theory and Applications*, ed. H.V.von Geramb), 1993. **Vol. 427**, (Springer-Verlag, Heidelberg), 67–106.

Suzko A.A. (1993b): Multidimensional and three-particle scattering problems in the adiabatic representation. Phys. Part. Nucl. **24**, 485-516 (translated from Fiz. Elem. Chastits At.Yadra **24**, 1133-1213).

Suzko A.A. (1993c): Supersymmetry and Geometric Nonadiabatic Phases in Diatomic Systems. Physics of Atomic Nuclei **56**, 674–679 (translated from Yadernaya Fizika **56**, 189–201).

Suzko A.A., Velicheva E.P. (1996a): Exactly Solvable Two-Dimensional Models in the Adiabatic Representation. Physics of Atomic Nuclei **59**, 1087–1103 (translated from Yadernaya Fizika **59**, 1132-1148).

Suzko A.A., Velicheva E.P. (1996b): Phys. Part. Nucl. **27** (translated from Fiz. Elem. Chastits At.Yadra **27**, 923-964).

Suzko A.A., Velicheva E.P. (1996c): "Two-dimensional exactly solvable models with time-dependent potentials," *Proc. Intern. Conf. on Quantum Systems: New Trends and Methods.* (Minsk, 4-7, June)

Suzko A.A., Velicheva E.P. (1996d): "Exactly solvable quantum models for investigation of nonadiabatic transitions" *Proc. Intern. Conf. on Inverse and Algebraic Quantum Scattering Theory* (Lake Balaton 96 – Balatonföldvar, 3–7, September).

Suzko, A.A., (1996): "Generalized Algebraic Bargmann–Darboux Transformations". *Proc. Intern. Workshop on Classical and Quantum Integrable Systems* (Dubna 8-12 July, 1996) to be published in Intern. J. Modern Physics (1996) No.12.

Zakhariev B.N., Suzko A.A. (1985,1990): *Potentials and Quantum Scattering: Direct and Inverse Problems* Springer-Verlag, New York, Berlin, Heidelberg.

Exactly Solvable Quantum Models for Investigation of Nonadiabatic Transitions

A.A. Suzko[1] and E.P. Velicheva[2]

[1] Bogolubov Laboratory of Theoretical Physics, JINR, 141980, Dubna, Russia **
[2] Gomel State University, Belarus

Abstract. The generalized technique of Bargmann potentials is applied for the reconstruction of time-dependent and time-independent two–dimensional potentials and corresponding solutions in a closed analytic form on the basis of the inverse scattering problem in the adiabatic representation. Matrix elements of the induced gauge potentials can be constructed and studied in terms of obtained exact solutions. The approach suggested permits investigation of the dynamical quantum transition amplitudes for spectral data with a prescribed dependence on parametric coordinate variables.

1 Introduction

The problem of adiabatically driven quantum systems was posed by Born and Oppenheimer (Born and Oppenheimer(1927)) and Born and Fock (Born and Fock(1928)). Then it has been intensely studied in many works (for references, see Solov'ev(1989), Kvitsinsky and Putterman (1990)) by means of direct methods. We suggest investigation of this problem by the inverse scattering method. The main advantage of the inverse scattering problem is that it permits one to construct a wide class of Hamiltonians for which solutions in a closed analytical form can be found. In our view, the use of exactly solvable models offers good prospects for investigations of many real quantum systems with several degrees of freedom and, in particular, of nonadiabatic transitions.

An algebraic procedure of solution of the time-independent problem with two degrees of freedom was presented in (Suzko (1993), Suzko (1992), Vinitsky and Suzko (1990)) within the inverse scattering problem in the adiabatic approach. The method of adiabatic representation allows one to take into account the mutual influence of slowly changing external and rapidly changing internal fields. This method has been elaborated on the basis of a consistent formulation of both mutually connected problems: the parametric problem and the multichannel problem for the system of equations with a covariant derivative. Generalization of the Bargmann technique to the parametric family of inverse problems allows one to generate a wide class of exactly solvable models, when the functional dependence of scattering data on the external

** Radiation Physics and Chemistry Problems Institute, Academy of Sciences of Belarus, Minsk.

coordinate variable is known. As a result, for a given functional dependence of spectral characteristics $\{\mathcal{E}_n(x), \gamma^2(x), \mathcal{S}(x,k)\}$ on parametric coordinate variables x, potentials $V(x,y)$ and the corresponding solutions of the parametric Schrödinger equation in a closed analytical form can be found. By using the analytic basis functions, the matrix of exchange interactions A can be calculated with a straightforward procedure, and thereafter, the complete solution of the initial problem can be obtained.

In this paper we suggest to use a wide class of exactly solvable models of the parametric problem for studying the transition amplitudes in adiabatically driven dynamical systems, so that its Hamiltonians are slowly varying functions of time. For description of these dynamical systems the method of the adiabatic approximation to quantum mechanics is usually used. The transition amplitudes in this approach are essentially defined by the matrix elements of exchange interactions. By specifying the functional dependence of spectral characteristics on time through the dependence on it of the external dynamical variable, the elements A can be computed in terms of the analytic basis functions.

This paper is focused on the class of transparent potentials that are constructed with their pertinent solutions of the parametric task and give corresponding matrix elements of exchange interaction calculated at different moments of time.

2 The Adiabatic Approximation and Inverse Problem

Consider the system evolving according to the Schrödinger equation

$$i\hbar \frac{d|\Psi(t)>}{dt} = H(x(t))|\Psi(t)> \tag{1}$$

where the Hamiltonian $H(x(t))$ is a slowly varying function of time. If $\phi_n(x(t);y)$ are solutions to the equation

$$H(x(t))|\phi_n(x(t);y)>=\mathcal{E}_n(x(t))|\phi_n(x(t);y)> \tag{2}$$

and form a complete orthonormal set $\{|\phi_n(x(t),y)>\}$ with elements depending on $x = x(t)$ parametrically, then Ψ can be given (see, for instance, 4) by the expansion

$$|\Psi(t,x(t),\mathbf{y})>=\sum_n c_n(t) exp\Big(-\frac{i}{\hbar}\int_0^t \mathcal{E}_n(x(t'))dt'\Big)|\phi_n(x(t);y)>. \tag{3}$$

With account of (2) the system of equations for $c_n(t)$ can be written in the form

$$\dot{c}_n(t) = \sum_m B_{nm}(x(t)) exp\Big[-\frac{i}{\hbar}\int_0^t (\mathcal{E}_n(t') - \mathcal{E}_m(t'))dt'\Big] c_m(t). \tag{4}$$

The matrix elements of exchange interaction

$$B_{nm}(x(t)) =< n|\dot{m} >= A_{nm}(x) \cdot \dot{x}(t), \quad A_{nm}(\mathbf{x}) =< n(x)| \bigtriangledown_x |m(x) > \quad (5)$$

are generated by basis functions $|n >$ of the "instantaneous" Hamiltonian (2). Here, we assume that $H(x(t))$ is real, limited and continuous in t. Then for each t the eigenfunctions are real valued and orthonormal

$$< \phi_n(x) \mid \phi_m(x) >= \delta_{nm} \quad \forall x.$$

So, the nonadiabatic couplings $A_{nm} = -A_{mn}$ in (5) are real and antisymmetric in n and m. The matrix elements (5) of the induced connection A can be computed in terms of the analytic eigenfunctions of equations (2) for a given functional dependence of scattering data $\{\mathcal{E}_n(x), \gamma_n^2(x), \mathcal{S}(x,k)\}$ on the slow coordinate variables $x(t)$ $(\mathcal{E}_n(x(t)) = -\kappa_n^2(x(t)))$. After that the transition amplitudes $c(t)$ can be determined from (4).

In accordance with the general definition of the inverse problem, the parametric inverse problem consists of the reconstruction of the potentials and corresponding solutions from known spectral data $\{\rho(x,k), N^2(x), \mathcal{E}(x)\}$ or the scattering data $\{S(x,k), \gamma_n^2(x), \mathcal{E}_n(x)\}$ parametrically depending on the coordinate variables x. This dependence reflects the peculiarity of the nonstandard parametric inverse problem. Specifying this dependence and employing the methods of inverse scattering problem (Chadan and Sabatier (1977,1989), Zakhariev and Suzko (1990)), we present a wide class of Hamiltonians for which one can construct exactly solvable models and, consequently, derive solutions in a closed analytic form. These Hamiltonians with generalized Bargmann potentials (Suzko (1993)) are defined by the rational Jost functions

$$f(x;k) = \prod \frac{k - i\alpha(x)}{k + i\beta(x)} \quad (6)$$

parametrically depending on the "slow" dynamical variables x through the dependence of spectral parameters on them. The parametric Jost function (6) has N simple poles on the curves $k = i\beta_j(x)$ and N simple zeros on the curves $k = i\alpha_j(x)$ defined as functions of the coordinate variable x. In $\alpha(x)$ there are not only zeros on the imaginary semiaxis corresponding to bound states $\mathrm{Re}\,\kappa_j(x) = 0$, $\mathrm{Im}\,\kappa_j(x) > 0$ but also zeros in the lower half-plane with $\mathrm{Im}\,\nu_j(x) < 0$ (the number of simple poles of β_j equals the total number of κ_j and ν_j). In this case the scattering matrix and spectral function assume the form

$$S(x;k) = \prod \frac{(k + i\alpha(x))(k + i\beta(x))}{(k - i\beta(x))(k - i\alpha(x))}, \quad \rho(x;k) = \prod \frac{(k - i\beta(x))(k + i\beta(x))}{(k + i\alpha(x))(k - i\alpha(x))}. \quad (7)$$

For such $S(x;k)$ and $\rho(x;k)$ the kernels of integral equations of the parametric inverse problem can be represented as sums of terms with a factorized dependence on the fast variable y: $Q(x;y,y') = \sum_i^N B_i(x;y)\ B_i(x;y')$. When the kernel Q is inserted into the base parametric equation of the inverse problem

$$K(x;y,y') + Q(x;y,y') + \int_{y(0)}^{\infty(y)} K(x;y,y'')Q(x;y'',y')dy' = 0, \tag{8}$$

it is evident that the kernel of the generalized shift $K(x;y,y')$ also becomes degenerate: $K(x;y,y') = \sum_i^N K_i(x;y)B_i(x;y')$. As a consequence, the system of integral equations of the inverse problem is reduced to the system of algebraic equations. Then, the spherically nonsymmetric potential and solutions corresponding to it can be expressed in a closed analytic form in terms of the known solutions and spectral characteristics.

3 Transparent Potentials

Let us consider quite a simple example of the use of the suggested technique. Reflectionless (transparent) potentials along the fast variable describe the one-dimensional inverse problem along the whole axis with the zero-th reflection coefficient, $s^{ref} = 0$. The transmission coefficient s^{tr} with the absolute value equal to unity is a rational function. Then $Q(x;y,y')$

$$Q(x;y,y') = \frac{1}{2\pi}\int_{-\infty}^{\infty} s^{ref}(x;k)\exp[ik(y+y')]dk + \sum_n^m \gamma_n^2(x)\exp[-\kappa_n(x)(y+y')], \tag{9}$$

will contain only the contribution of states of the discrete spectrum

$$Q(x;y,y') = \sum_n^m \gamma_n^2(x)\exp[-\kappa_n(x)(y+y')]. \tag{10}$$

Analogously, for $K(x;y,y')$ we have

$$K(x;y,y') = -\sum_n^m \gamma_n^2(x)f(i\kappa_n(x),y)\exp[-\kappa_n(x)y']. \tag{11}$$

For the Jost solutions at $k = i\kappa_n(x)$ we get, from the main equations of the parametric inverse problem, the following system of algebraic equations

$$f(i\kappa_n(x),y) = \sum_j \exp(-\kappa_j(x)y)P_{jn}^{-1}(x;y) \tag{12}$$

with the matrix of coefficients $P_{jn}(x;y)$ parametrically depending on x:

$$P_{nj}(x;y) = \delta_{nj} + \frac{\gamma_n^2(x)\exp[-(\kappa_n(x)+\kappa_j(x))y]}{\kappa_n(x)+\kappa_j(x)}.$$

Upon substituting $f(i\kappa_n(x), y)$ into $K(x;y,y')$ (11) and using main relations of the inverse problem, we get

$$V(x;y) = -2\frac{d}{dy}K(x;y,y) = -2\frac{d^2}{dy^2}\ln\det||P_{nj}(x;y)||, \tag{13}$$

$$f(x;k,y) = \exp(\pm iky) + \int_y^\infty K(x;y,y')\exp(\pm iky')dy' =$$

$$\exp(\pm iky) + \sum_{nj}\gamma_n^2(x)\exp[-\kappa_n(x)y]P_{nj}^{-1}(x;y)\frac{\exp[(-\kappa_j(x)\pm ik)y]}{\kappa_j(x)\mp ik}. \tag{14}$$

Note, symmetrical transparent potentials for each fixed value of x and appropriate wave functions are completely defined by the energy levels (5) since the normalized functions can be determined by the energy levels

$$\gamma_n^2(x) = iRes\mathcal{S}^{tr}(k)_{/k=i\kappa_n(x)} = 2\kappa_n(x)\prod_{m\neq n}\left|\frac{\kappa_m(x)+\kappa_n(x)}{\kappa_m(x)-\kappa_n(x)}\right|. \tag{15}$$

Examples of the reconstruction of time-dependent and time-independent two–dimensional symmetrical potentials and corresponding solutions have been considered in (5, 6, 7). In this paper we will present examples of transparent but nonsymmetric time-dependent potentials and give matrix elements of exchange interaction induced by basis functions of the parametric instantaneous Hamiltonian.

4 Special cases of parametric dependence for two-level sytems

Based on the technique of degenerate kernels, we give a simple example of a two-dimensional exactly solvable model with nonsymmetric transparent potentials for a two-level system with a periodical dependence of the dynamical variable x on time. Let us define two potential curves in the following way

$$\mathcal{E}_1 = -1/ch^2(x/3),\ \ \mathcal{E}_2 = -(1/ch(x/2)+0.25)^2,\ \ \gamma_n^2(x) = 2\kappa_n(x) \tag{16}$$

with

$$x(t) = \overset{\circ}{x}\,(1 - a\ cos(\omega t)),$$

where $\overset{\circ}{x}$ corresponds to the time-independent case.

The dynamical behaviour of the potentials $V(x(t),y)$ and the pertinent normalized eigenfunctions $\phi_n(x(t),y) = \gamma_n(x(t))f(i\kappa_n(x(t),y))$, $n = 1,2$ is

presented for ωt equal to $0, \pi/4, \pi/3, \pi/2, \pi$ in Figs.(1a, b, c, d, e) – (3a, b, c, d, e), respectively, $a = 1$. Since their behaviour is mirror-symmetric with respect to the line $\omega t \in (0, \pi)$, it is not shown in the Figures. It is easy to see that the potential and functions change from very simple one-dimensional ones for $\omega t = 0$, Figs.1a – 3a, to quite complicated two-dimensional potentials and functions for all other values of $\omega t \neq 0$. A one-dimensional transparent potential $V(y)$ with two bound states $\mathcal{E}_1 = -1$, $\mathcal{E}_2 = -1.5625$ and corresponding wave functions $\phi_n(y)$ are immediately obtained from more general relations (13) and (12) of the parametric task (Suzko (1993)). When $\omega t \neq 0$, we have two-dimensional potentials and corresponding functions. At $\omega t = \pi/2$ and $\omega t = 3\pi/2$, $x(t)$ coincides with $\overset{\circ}{x}$ and we have the two-dimensional time-independent case, $V(\overset{\circ}{x}, y), |\phi_n(\overset{\circ}{x}; y) >$, shown in Figs.(1d) – (3d), while at $\omega t = 2\pi$, the system comes back to the one-dimensional position with the initial states $|\phi_n(y) >$.

The behaviuor of the matrix elements of the nonadiabatic coupling $A_{12}(x(t))$ and $B_{12}(x(t))$ calculated at different instants by using (5) and (12) are pictured in Figs.4b – 4e. Naturally, when $\omega t = 0$, A_{ij} and B_{ij} are absent, since the dependence on x vanishes. For $\omega t \neq 0$ all functions $A_{12}(x) = -A_{12}(-x)$ are antisymmetric and all $B_{12}(x) = B_{12}(-x)$ are symmetric with respect to the origin of the coordinates. The behaviour of A is defined by our choice of spectral data and of the dependence of x on time (16). It is evident, $B(x)$ are symmetric functions since they are obtained as the product of both antisymmetric functions: $A(x)$ and $\dot{x}(t)$. Remember that the matrix elements of $A_{12}(x(t)) = -A_{21}(x(t))$ and $B_{12}(x(t)) = -B_{21}(x(t))$ are antisymmtric in the index of the state (here 1 and 2). The tendency of changing A as a function of ωt is the following: the amplitude of changing of A is the larger, the smaller the ωt. When ωt is small, the second pick to the right of the origin is comparable with the first pick. With increasing ωt, the second pick is decreasing. From our point of view this behaviour of the exchange interaction A can be explained by the mutual influence of eigenstates. At small values of ωt the potential curvers are close to each other on a larger interval than at large values of ωt. It is interesting to note, at $\omega t = \pi$ the matrix elements $B_{12}(x) = 0$ in spite of the adiabatic coupling $A_{12}(x) \neq 0$.

Obviously, another parametric dependence of the spectral characteristics can be chosen, and other initial spectral data corresponding not only to the one– but also to two– or three-dimensional dependence on the extra coordinate variables can occur. In particular, for the special case of parametric variation, the spectral characteristics may be taken in a factorized form as in (Kvitsinsky and Putterman (1990))

$$\mathcal{E}_n(x) = x\widetilde{\mathcal{E}_n}, \qquad \Phi_n(x, y) = x^{n/4}\widetilde{\Phi_n}(x^{1/2}y) \tag{17}$$

where $x = x(t)$ and $\widetilde{\mathcal{E}_n}$ and $\widetilde{\Phi_n}(y)$ are eigenvalues and eigenfunctions of the time-independent task. In the last paper, transition amplitudes were evaluated for the class of Hamiltonians

$$H(x) = -\frac{\hbar^2}{2m}\triangle_y + xV(x^{1/2}y) \tag{18}$$

with the restriction that the time-independent Hamiltonian $\widetilde{H} = H(x = 1)$ has a purely discrete spectrum. In general, the potentials with spectral characteristics satisfying (17) can be only infinite.

At the same time our approach permits one to consider a much larger class of Hamiltonians with known discrete and continious parts, whose particular case is operators with spectral data in a factorized form like (17). In the latter case behaviour of potentials and functions is very simple in comparison with the previous Figs.(1) – (3). Only infinitely deeper potentials can possess energy curves which go to infinity as $x \to \infty$.

5 Conclusions

In conclusion, we would like to note that this approach allows one to construct a very wide class of two-dimensional exactly solvable models with time-dependent and time-independent potentials. We have presented an example of the two–dimensional time-dependent transparent potentials with their basis functions for two-level systems. We applied these exact wave functions for calculating the matrix elements of nonadiabatic couplings determining the transition amplitudes. In fact, we can trace the behaviour of the matrix elements of exchange interaction (5) at any moment of time and recommend our approach for the investigation of the Landau–Zener transitions and level crossing problems.

Acknowledgments. This work was supported in part by the Foundation of the "Heisenberg-Landau Program" of investigations.

References

Born M., Oppenheimer R. (1927) Ann. d. Phys. **84**, 457

Born M., Fock V. (1928) Zs. Phys. **51**, 165

Solov'ev E.A. (1989): Usp. Fiz. Nauk. **157**, 437–476

Kvitsinsky Andrei A., Putterman Seth (1990): Exponentially suppressed transitions in an adiabatically driven system with a discrete spectrum. Phys. Rev. **A42**, 6303–6307

Suzko A.A. (1993): Phys. Part. Nucl. **24**, 485 *Multidimensional and three-body inverse scattering problems in the adiabatic representation"* , Proc. Int.Conf. in *Lecture Notes in Physics, " Quantum Inversion Theory and Applications*, ed. H.V.von Geramb), 1993. **Vol. 427**, (Springer-Verlag, Heidelberg), 67-106

Suzko A.A. (1992): Exactly Solvable Tree-Body Models with Two-Center Potentials. Sov. J. Nucl. Phys. **55**, 1359–1365; Supersymmetry, Geometric Nonadiabatic Phases in Diatomic Systems. Yad. Fiz. **56**, 189–201

Vinitsky S.I.,Suzko A. A. (1990): Exactly Solvable Multidimensional and Tree-Particle Scattering Problems in the Adiabatic Representation. Sov. J. Nucl. Phys. **52**, 442–451.

Chadan K., Sabatier P.C. (1977,1989): *Inverse Problems in Quantum Scattering Theory* (Springer-Verlag, New York, Berlin, Heidelberg)

Zakhariev B.N., Suzko A.A. (1990): *Potentials and Quantum Scattering: Direct and Inverse Problems* (Springer-Verlag, New York, Berlin, Heidelberg)

Hwang J.T., Pechukas Ph. (1977): The Adiabatic Theorem in the Complex Plane and the Semiclassical of Nonadiabatic Transition Amplidudes. J. Chem. Phys. **67**, 4640–4653

Suzko A.A., Velicheva E.P. (1996): Exactly Soluble Two-Dimensional Models in the Adiabatic Representation. Physics of Atomic Nuclei **59**, 1087–1103

Suzko A.A., Velicheva E.P. (1996): Exactly Solvable Models and Investigation of Level Crossing. Phys. Part. Nucl. **27**, 923

Suzko A.A., Velicheva E.P. (1996): *Proc. Intern. Conf. on Quantum Systems: New Trends and Methods.* (Minsk, 4-7, June)

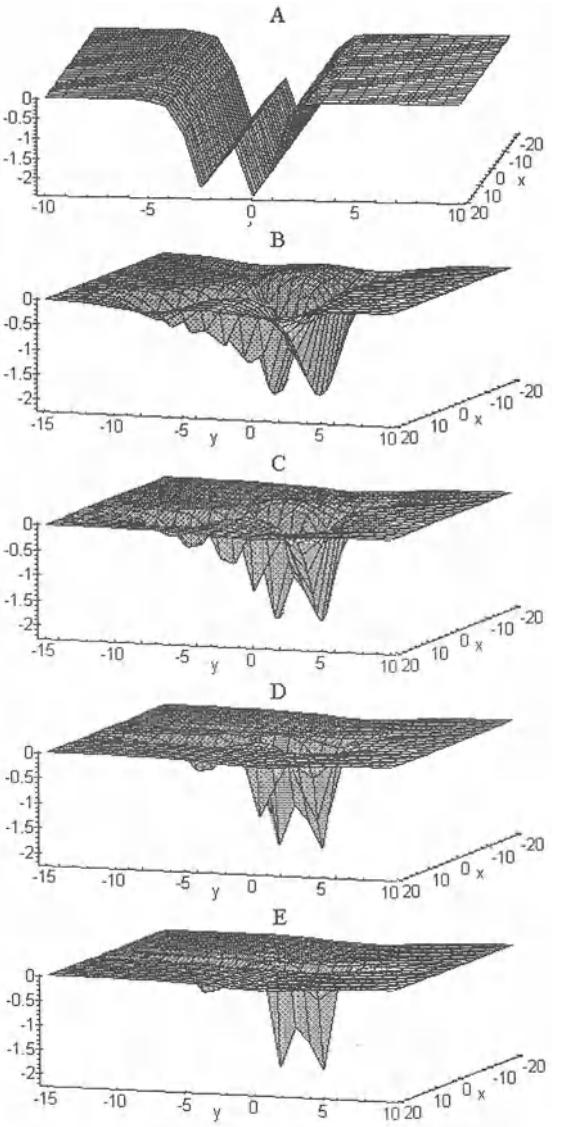

Fig. 1. Potentials $V(x(t), y)$ calculated for different values of ωt: (a) $\omega t = 0$, (b) $\omega t = \pi/4$, (c) $\omega t = \pi/3$, (d) $\omega t = \pi/2$, (e) $\omega t = \pi$.

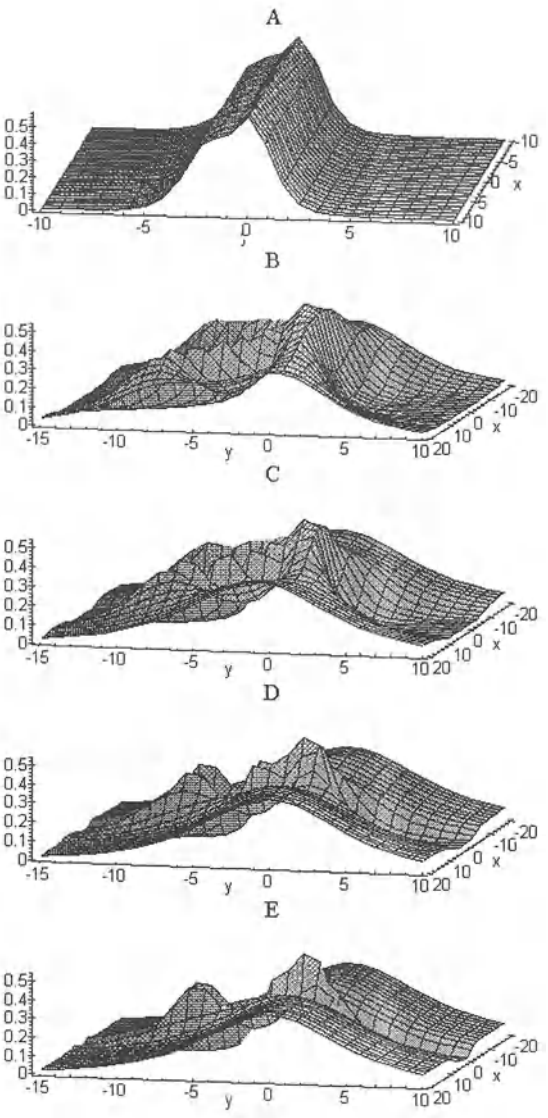

Fig. 2. Eigenfunctions $\phi_1(x(t), y)$ at (a) $\omega t = 0$, (b) $\omega t = \pi/4$, (c) $\omega t = \pi/3$, (d) $\omega t = \pi/2$, (e) $\omega t = \pi$.

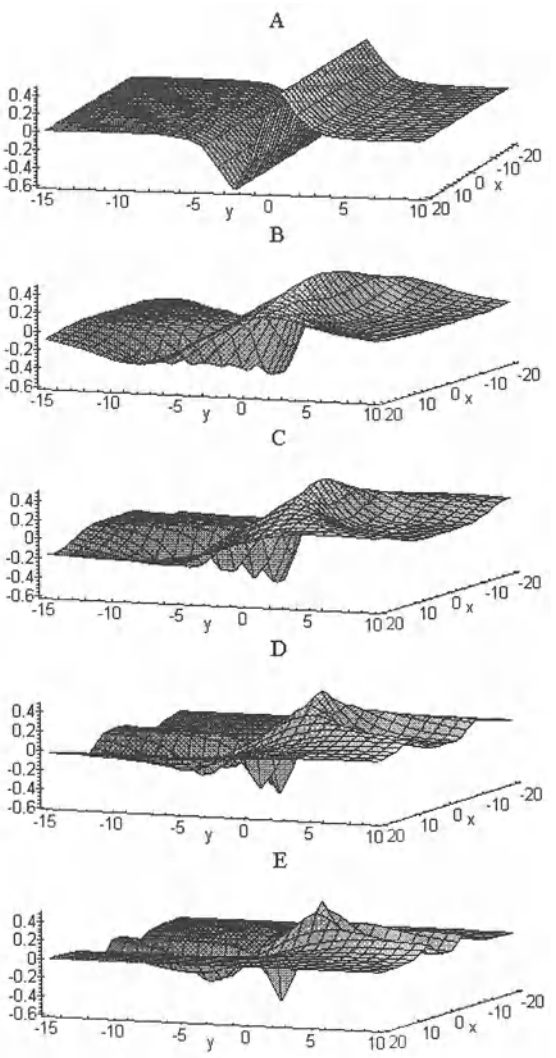

Fig. 3. Eigenfunctions $\phi_2(x(t), y)$ at (a) $\omega t = 0$, (b) $\omega t = \pi/4$, (c) $\omega t = \pi/3$, (d) $\omega t = \pi/2$, (e) $\omega t = \pi$.

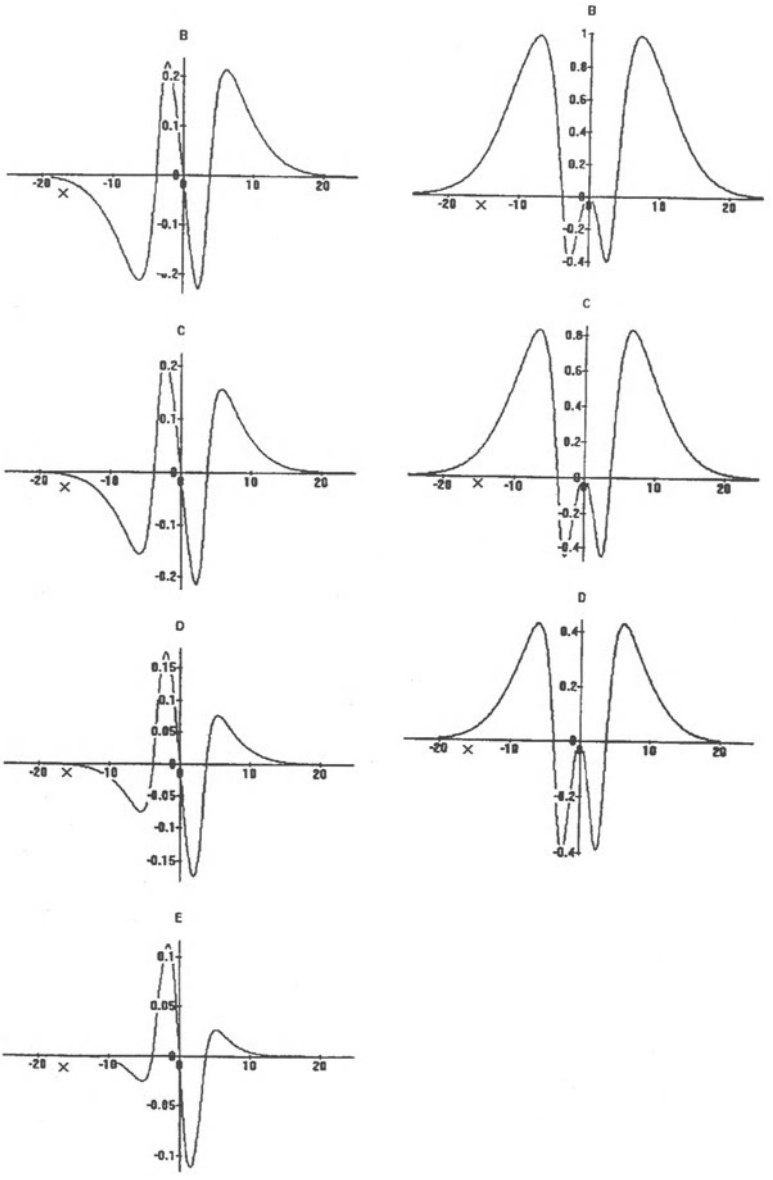

Fig. 4. Matrix elements of exchange interactions $A_{12}(x)$ (the left column) and $B_{12}(x)$ (the right column) calculated for different values of ωt: (b) $\omega t = \pi/4$, (c) $\omega t = \pi/3$, (d) $\omega t = \pi/2$, (e) $\omega t = \pi$.

Modified Symmetry Generators for $SO(3,2)$ and Algebraic Scattering Theory

Péter Lévay[1], Barnabás Apagyi[1], and Werner Scheid[2]

[1] Department of Theoretical Physics, Institute of Physics, Technical University of Budapest, H–1521 Budapest, Hungary
[2] Institut für Theoretische Physik der Justus-Liebig-Universität, Giessen, Germany

Abstract. Based on a realization found previously for the Lie-algebra of the group $SO(3,1)$ a new realization for the $SO(3,2)$ algebra is presented. The symmetry generators are matrix-valued differential operators. The matrix-valued nature of the realization is induced by a *finite* dimensional (non-unitary) representation of the *noncompact* $SO(3,1)$ subgroup. The Casimir operators can be calculated, and the quadratic Casimir operator is shown to yield a three dimensional scattering problem with Pöschl-Teller potentials with an LS term, and an *optical* potential. The presence of the optical potential can be traced back to the *noncompact* nature of the $SO(3,1)$ group giving us the inducing representation. It is also pointed out, that the quadratic Casimir can be written in the instructive form of a Laplace-operator incorporating $so(3,1)$-valued gauge-fields. The role played by gauge transformations in deriving new interaction terms is emphasized.

1 Introduction

The aim of this paper is to report on the existence of a nonstandard realization found for the Lie algebra of the group $SO(3,2)$. Such realizations are useful in algebraic scattering theory where the Casimir operator(s) of the noncompact group in question can be related to the Hamilton operator of some scattering problem. Hence finding interesting new coordinate realizations amounts to finding interesting scattering potentials for which the scattering states are described by group theory.

In a previous paper [1] a similar construction for the $SO(3,1)$ case has already been investigated by one of us, with the conclusion that such realizations result in matrix-valued nonlocal interaction terms of LS-type. An interesting $so(3) \simeq su(2)$ gauge structure of such realizations has also been observed, i.e. the modified matrix-valued generators could be written as operators containing covariant derivatives by employing $so(3) \simeq su(2)$ gauge-fields. This result enabled the construction of other solvable scattering potentials by simply gauge transforming the original scattering problem.

In this paper such ideas will be developed for the larger group $SO(3,2)$, which is more suitable for the description of heavy-ion reactions [2]. In particular, we will show in section 1 how to generalize the construction of [1] for the $SO(3,2)$ case. In section 2 we calculate the quadratic Casimir in our

matrix-valued realization and show that in addition to the LS terms well-known from the $SO(3,1)$ case an optical potential appears in the associated scattering problem. The group theoretical characterization of the scattering states is also discussed here. The geometrical meaning of our realization is clarified in section 3 where we indicate the presence of an $so(3,1)$ gauge structure. Our conclusions are left for section 4.

2 A matrix-valued realization for $SO(3,2)$

We start by giving the matrix-valued realization found in [1] for the generators of the algebra of the group $SO(3,1)$,

$$\mathbf{J} = \mathbf{L} + \mathbf{S}, \quad \mathbf{M} = \mathbf{K} + \mathbf{S} \times \mathbf{R}, \tag{2.1}$$

$$\mathbf{L} = \mathbf{R} \times \mathbf{P}, \quad \mathbf{K} = \frac{1}{2}(1 + R^2)\mathbf{P} - \mathbf{R}(\mathbf{RP}). \tag{2.2}$$

Notice that the realization in terms of $\mathbf{J}$ and $\mathbf{M}$ modifies the well-known realization in terms of $\mathbf{L}$ and $\mathbf{K}$ (related to the angular momentum operator and the Runge-Lenz vector after a canonical and a similarity transformation)[1]. The operators of (2.1) and (2.2) satisfy the $so(3,1)$ commutation relations

$$[J_i, J_j] = i\varepsilon_{ijk}J_k, \quad [J_i, M_j] = i\varepsilon_{ijk}M_k, \quad [M_i, M_j] = -i\varepsilon_{ijk}J_k. \tag{2.3}$$

Our task is to find a similar realization for the Lie-algebra of $SO(3,2)$. In this spirit first we try to find the standard $SO(3,2)$ generators (i.e. the analogues of the operators $\mathbf{L}$ and $\mathbf{K}$), and then add matrix-valued modifications to them. In order to do it we consider the $SO(3,2)$ invariant line element

$$ds^2 = -dX_1^2 - dX_2^2 - dX_3^2 + dX_4^2 + dX_5^2, \quad (-\mathbf{X}^2 + X_4^2 + X_5^2 = 1).$$

Introducing the coordinates

$$\mathbf{X} = \frac{2}{1 - R^2}\mathbf{R}, \quad X_4 = \frac{1 + R^2}{1 - R^2}v_1 \quad X_5 = \frac{1 + R^2}{1 - R^2}v_2, \tag{2.4}$$

we obtain the line element

$$ds^2 = \frac{4}{(1 - R^2)^2}d\mathbf{R}^2 - \left(\frac{1 + R^2}{1 - R^2}\right)^2 d\chi^2 = g_{\mu\nu}dy^\mu dy^\nu, \tag{2.5}$$

where $(y_1, y_2, y_3, y_4) \equiv (R_1, R_2, R_3, \chi)$, and $v_1 = \cos\chi$, $v_2 = \sin\chi$

Now we can obtain $SO(3,2)$ generators corresponding to infinitesimal transformations preserving the metric (2.5), by writing the usual ($SO(3,2)$ generators

$$\varepsilon_{jkm}L_m = -i(X_j\frac{\partial}{\partial X_k} - X_k\frac{\partial}{\partial X_j}), \quad V = -i(X_4\frac{\partial}{\partial X_5} - X_5\frac{\partial}{\partial X_4}), \quad (2.6a)$$

$$B_j = -i(X_j\frac{\partial}{\partial X_4} + X_4\frac{\partial}{\partial X_j}), \quad D_j = -i(X_j\frac{\partial}{\partial X_5} + X_5\frac{\partial}{\partial X_j}), \quad (2.6b)$$

(j,l,k=1,2,3), in terms of the coordinates (R_1, R_2, R_3, χ),

$$\mathbf{L} = \mathbf{R} \times \mathbf{P}, \quad V = v_3, \quad (2.7a)$$

$$\mathbf{B} = \mathbf{K}v_1 - \frac{2}{1+R^2}\mathbf{R}v_2v_3, \quad \mathbf{D} = \mathbf{K}v_2 + \frac{2}{1+R^2}\mathbf{R}v_1v_3, \quad (2.7b)$$

where $\mathbf{K}$ is defined as in equation (2.2). Here $v_3 \equiv -i\partial/\partial\chi$, hence the operators of Eqs. (2.7) are first order differential operators. One can calculate the quadratic Casimir, and finds

$$C(SO(3,2)) = \mathbf{L}^2 + V^2 - \mathbf{B}^2 - \mathbf{D}^2 = \frac{1}{\sqrt{g}}\partial_\mu(\sqrt{g}g^{\mu\nu}\partial_\nu). \quad (2.8)$$

Moreover by employing the similarity transformation $T(R) = \sqrt{\frac{1-R^2}{1+R^2}}$ one can relate our $SO(3,2)$ Casimir to the $SO(3,1)$ Casimir $C(SO(3,1)) = \mathbf{L}^2 - \mathbf{K}^2$ as follows

$$T^{-1}C(SO(3,2))T = C(SO(3,1)) + (V^2 - \frac{1}{4})\left(\frac{1-R^2}{1+R^2}\right)^2 - \frac{5}{4}. \quad (2.9)$$

By choosing scattering states for which the eigenvalue of the operator V (the potential strength parameter in [2]) is $\frac{1}{2}$ the $SO(3,2)$ Casimir describes all the scattering phenomena obtained for the $SO(3,1)$ Casimir. (E.g. Coulomb scattering after a canonical transformation. See equation (54) of [3].) In this way we managed to clarify the geometrical meaning of the $SO(3,2)$ generators and to substantially simplify the analysis given in [2]. Moreover, we have also found a new (2.7) form for the generators of the $SO(3,2)$ algebra.

Looking at this $SO(3,2)$ realization one can see that a straightforward way to modify it is to replace the $SO(3,1)$ generators $(\mathbf{L}, \mathbf{K})$ in (2.7) by the modified ones $(\mathbf{J}, \mathbf{M})$ of (2.1), and to add possible further modifications to them. The commutation relations that are to be satisfied are

$$[J_m, J_n] = i\varepsilon_{mnk}J_k, \quad [J_m, \mathcal{B}_n] = i\varepsilon_{mnk}\mathcal{B}_k, \quad [J_m, \mathcal{D}_n] = i\varepsilon_{mnk}\mathcal{D}_k, \quad (2.10a)$$

$$[V, \mathcal{B}_n] = i\mathcal{D}_n, \quad [V, \mathcal{D}_n] = -i\mathcal{B}_n, \quad (2.10b)$$

$$[\mathcal{B}_m, \mathcal{B}_n] = [\mathcal{D}_m, \mathcal{D}_n] = -i\varepsilon_{mnk} J_k, \quad [\mathcal{B}_m, \mathcal{D}_n] = -i\delta_{mn}. \tag{2.10c}$$

We have found the following set of modified $SO(3,2)$ generators satisfying the aforementioned commutation relations

$$\mathbf{J} = \mathbf{L} + \mathbf{S}, \quad V = v_3, \tag{2.11a}$$

$$\mathcal{B} = v_1\mathbf{M} - v_2 \frac{2}{1+R^2}\mathbf{R}(v_3 - \mathbf{TR}) - v_2\mathbf{T}, \tag{2.11b}$$

$$\mathcal{D} = v_2\mathbf{M} + v_1 \frac{2}{1+R^2}\mathbf{R}(v_3 - \mathbf{TR}) + v_1\mathbf{T}, \tag{2.11c}$$

where $\mathbf{M}$ is defined as in (2.2), and the matrices $\mathbf{S}$ and $\mathbf{T}$ form a *finite dimensional* irreducible representation of the $so(3,1)$ algebra. Notice that since the algebra $so(3,1)$ is noncompact these representations are *nonhermitian*. In this paper we employ the simplest choice

$$S_j \equiv \begin{pmatrix} \frac{1}{2}\sigma_j & 0 \\ 0 & \frac{1}{2}\sigma_j \end{pmatrix}, \quad T_j \equiv \begin{pmatrix} 0 & \frac{i}{2}\sigma_j \\ \frac{i}{2}\sigma_j & 0 \end{pmatrix}. \tag{2.12}$$

We close this section with the important observation that our modified $so(3,2)$ generators are induced by a *nonhermitian* matrix representation of the subalgebra $so(3,1)$, unlike in [1] where the modified $so(3,1)$ generators are induced by a *hermitian* matrix representation of the subalgebra $so(3)$. In the language of induced representations of groups it amounts to saying that the basic difference is the fact that the inducing subgroup $SO(3,1)$ is noncompact for the $SO(3,2)$ case whereas it was compact ($SO(3)$) for the $SO(3,1)$ case.

3 Calculation of the quadratic Casimir operator

In this section we calculate the quadratic Casimir operator for our new (2.11) realization. We have to calculate

$$\mathcal{C}(SO(3,2)) = \mathbf{J}^2 + V^2 - \mathcal{B}^2 - \mathcal{D}^2. \tag{3.1}$$

Straightforward calculation shows that

$$T^{-1}(R)\mathcal{C}(SO(3,2))T(R) =$$

$$\mathcal{C}(SO(3,1)) + \left(\frac{1-R^2}{1+R^2}\right)^2 V^2 - 4\frac{1-R^2}{(1+R^2)^2}(\mathbf{RT})V - \frac{3}{4}, \tag{3.2}$$

where the similarity transformation is the same as in Eq.(2.9), and $\mathcal{C}(SO(3,1))$ $= \mathbf{J}^2 - \mathbf{M}^2$. Employing a coordinate transformation

$$R(r) = \coth\frac{r}{2}, \tag{3.3}$$

and further similarity transformations [1] [2] with the choice (2.12) we get,

$$T^{-1}(R)\mathcal{C}(SO(3,2))T(R) =$$
$$\mathcal{C}(SO(3,1)) + \frac{v^2}{\cosh^2 r} + \frac{iv\sinh r}{\cosh^2 r}\begin{pmatrix} 0 & \sigma\mathbf{n} \\ \sigma\mathbf{n} & 0 \end{pmatrix} - \frac{3}{4}. \tag{3.4}$$

Here $\mathbf{n}$ is defined as $\mathbf{R} \equiv R(r)\mathbf{n}$, v is the eigenvalue (the potential strength) [2] of the operator V, and

$$\mathcal{C}(SO(3,1)) = \frac{\partial^2}{\partial r^2} + \frac{2}{r}\frac{\partial}{\partial r} - \frac{\mathbf{L}^2}{\sinh^2 r} - \frac{\mathcal{M}}{2\sinh^2\frac{r}{2}} - \frac{3}{4}. \tag{3.5}$$

Moreover, the operator $\mathcal{M}$ is defined as [1]

$$\mathcal{M} = \sigma\mathbf{n} + 1. \tag{3.6}$$

From the form of Eqs.(3.4) and (3.5) one can see that it is of the form of a scattering Hamiltonian with a *nonhermitian* matrix-valued interaction term.

In order to characterize the scattering states algebraically one has to recall that $SO(3,2)$ is a group of rank two. This means that two numbers are needed for the labelling of its irreducible representations. These numbers are associated with the eigenvalues of the two Casimir operators characterizing $SO(3,2)$. One of them is of course (3.1), and the other is (see [3] for the details)

$$\mathcal{C}'(SO(3,2)) = (\mathbf{J}V + \mathcal{B}\times\mathcal{D} - \mathcal{D}\times\mathcal{B})^2 - (\mathcal{B}\mathbf{J})^2 - (\mathcal{D}\mathbf{J})^2. \tag{3.7}$$

Let us denote the pair labelling the irrep as (ω,λ). For the labelling of basis vectors within the irrep, we choose extra labels provided by the eigenvalues of other operators commuting among themselves and the Casimir operators. (Recall also that now our differential operators are matrix-valued.) For this purpose we choose the operators J^2, J_3 and V, hence scattering states can be labelled as $|\omega,\lambda;j,m,v,\mu\rangle$ $\mu = 1,2,3,4$ where the equations [4]

$$\mathcal{C}_{\mu\nu}(SO(3,2))|\omega,\lambda;j,m,v,\nu\rangle = (\omega(\omega+3)+\lambda(\lambda+1))|\omega,\lambda;j,m,v,\mu\rangle, \tag{3.8a}$$

$$\mathcal{C}'_{\mu\nu}(SO(3,2))|\omega,\lambda;j,m,v,\nu\rangle = (\omega+1)(\omega+2)\lambda(\lambda+1))|\omega,\lambda;j,m,v,\mu\rangle, \tag{3.8b}$$

$$J^2|\omega,\lambda;j,m,v,\mu\rangle = j(j+1)|\omega,\lambda;j,m,v,\mu\rangle, \tag{3.8c}$$

$$J_3|\omega,\lambda;j,m,v,\mu\rangle = m|\omega,\lambda;j,m,v\rangle, \tag{3.8d}$$

$$V|\omega,\lambda;j,m,v,\mu\rangle = v|\omega,\lambda;j,m,v,\mu\rangle \tag{3.8e}$$

hold. The scattering representations has to be related to the series labelled as [5]

$$\omega = -\frac{3}{2} + ik, \quad k \in \mathbf{C}, \tag{3.9}$$

with the important distinction that the group label k related to the scattering energy must be chosen *complex* in order to account for the appearance of a complex potential [6]. In order to fix the label λ, one has to investigate the properties of the other Casimir operator. The important property we will use is the relation [3]

$$\mathcal{C}'(SO(3,2)) = \frac{15}{16} + \frac{3}{4}\mathcal{C}(SO(3,2). \tag{3.10}$$

From this relation and equations (3.8a,b) it follows that

$$\lambda = \frac{1}{2}. \tag{3.11}$$

Now we write the four component wave function in the form [7]

$$\psi^{\mu}_{k,\frac{1}{2},j,m,v}(\mathbf{r}) = \langle k,\frac{1}{2};j,m,v,\mu|\mathbf{r}\rangle = \begin{pmatrix} f^{(1)}_{k,\frac{1}{2},v}(r)\mathcal{Y}_{\kappa,m}(\mathbf{n}) \\ f^{(2)}_{k,\frac{1}{2},v}(r)\mathcal{Y}_{-\kappa,m}(\mathbf{n}) \end{pmatrix}, \tag{3.12}$$

where $\mathcal{Y}_{\kappa,m}(\mathbf{n})$ are the spinor harmonics and

$$\kappa = \pm\left(j+\frac{1}{2}\right) = \begin{cases} l+1, & \text{for } j = l+\frac{1}{2}, \\ -l, & \text{for } j = l-\frac{1}{2} \end{cases}. \tag{3.13}$$

Using the action [1],[7] of the operators $\mathcal{M}$ and $\sigma\mathbf{n}$ on the spinor harmonics

$$\mathcal{M}\mathcal{Y}_{\kappa,m}(\mathbf{n}) = -\kappa\mathcal{Y}_{\kappa,m}(\mathbf{n}), \tag{3.14}$$

$$\sigma\mathbf{n}\mathcal{Y}_{\kappa,m}(\mathbf{n}) = -\mathcal{Y}_{\kappa,m}(\mathbf{n}), \tag{3.15}$$

we end up with the following form for the Schrödinger equation

$$\left((-\frac{\partial^2}{\partial r^2} - \frac{2}{r}\frac{\partial}{\partial r})\delta_{\alpha\beta} + V_{\alpha\beta}(r)\right) f^{(\beta)}(r) = k^2 f^{(\alpha)}, \tag{3.16}$$

with $\alpha,\beta = 1,2$ and the interaction matrix is

$$V_{\alpha\beta} \equiv \begin{pmatrix} \frac{l(l+1)}{\sinh^2 r} - \frac{\kappa}{2\sinh^2\frac{r}{2}} - \frac{v^2}{\cosh^2 r} & -iv\frac{\sinh r}{\cosh^2 r} \\ -iv\frac{\sinh r}{\cosh^2 r} & \frac{l(l+1)}{\sinh^2 r} + \frac{\kappa}{2\sinh^2\frac{r}{2}} - \frac{v^2}{\cosh^2 r} \end{pmatrix}. \tag{3.17}$$

We have few comments concerning this interaction term. After recalling that $L^2 = \mathcal{M}(\mathcal{M}-1)$ [1] the term $\frac{l(l+1)}{\sinh^2 r} \mp \frac{\kappa}{2\sinh^2 \frac{r}{2}}$ can be written in the form $\frac{\kappa(\kappa \mp 1)}{4\sinh^2 \frac{r}{2}} - \frac{\kappa(\kappa \pm 1)}{4\sinh^2 \frac{r}{2}}$. According to [1] and [8] one can show that these potentials are supersymmetry partners of each other. Moreover, one can easily see that these potentials are arising from the Casimir operator $\mathcal{C}(SO(3,1))$ of the $SO(3,1)$ subgroup. The modification in the interaction term coming from the group $SO(3,2)$ is of the form

$$V_{\alpha\beta}(SO(3,2)) \equiv -\begin{pmatrix} \frac{v^2}{\cosh^2 r} & iv\frac{\sinh r}{\cosh^2 r} \\ iv\frac{\sinh r}{\cosh^2 r} & \frac{v^2}{\cosh^2 r} \end{pmatrix}. \tag{3.18}$$

Notice that this modification is antihermitian, accordingly the eigenvalue k^2 is complex. The presence of such an optical potential can be traced back to the fact that the inducing representation of $SO(3,1)$ is a finite dimensional irreducible but *nonunitary* representation. It should not come as a surprise since $SO(3,1)$ is a *noncompact* group, hence it has no finite dimensional unitary irreducible representations.

4 The $SO(3,1)$ gauge structure of the quadratic Casimir operator

In section 2. we indicated that the quadratic Casimir $C(SO(3,2))$ can be written as the Laplace-Beltrami operator for an appropriately chosen metric. (See Eqs. (2.5) and (2.8).) Based on this result it is an interesting question whether it is possible to identify a similar structure for the modified Casimir $\mathcal{C}(SO(3,2))$. Indeed one can prove that a formula similar to (2.8) is true for $\mathcal{C}(SO(3,2))$. It is

$$\mathcal{C}(SO(3,2)) = \mathbf{J}^2 + V^2 - \mathcal{B}^2 - \mathcal{D}^2 =$$
$$\frac{1}{\sqrt{g}}(\partial_\mu + iA_\mu)(\sqrt{g}g^{\mu\nu}(\partial_\nu + iA_\nu)) + S^2 - T^2, \tag{4.1}$$

where

$$A_\mu = \begin{pmatrix} A_i \\ A_4 \end{pmatrix} = \frac{2}{R^2-1}\begin{pmatrix} (\mathbf{S}\times\mathbf{R})_i \\ \mathbf{TR} \end{pmatrix}. \tag{4.2}$$

It can be shown [3] that the $so(3,1)$-valued vector fields are $SO(3,2)$ symmetric gauge-fields. This means that under the infinitesimal coordinate transformations leaving invariant the line element (2.5) A_μ transforms as a vector field *up to infinitesimal* $SO(3,1)$ *gauge transformations.* (See also [9] and [10] in this respect.)

This result has important consequences concerning algebraic scattering theory. Namely, it follows that the modified generators $\mathbf{J}$, V, $\mathcal{B}$, $\mathcal{D}$ are gauge covariant in the sense that if we make a gauge transformation

$$A_\mu^{\mathcal{U}} = \mathcal{U}^\dagger(\mathbf{R},\chi)A_\mu(\mathbf{R})\mathcal{U}(\mathbf{R},\chi) - i\mathcal{U}^\dagger(\mathbf{R},\chi)\partial_\mu\mathcal{U}(\mathbf{R},\chi), \tag{4.3}$$

they transform as

$$(\mathbf{J}, V, \mathcal{B}, \mathcal{D}) \mapsto \mathcal{U}^\dagger(\mathbf{J}, V, \mathcal{B}, \mathcal{D})\mathcal{U}. \tag{4.4}$$

Hence new realizations for $SO(3,2)$ can be found by gauge transformations. From such new realizations one can derive new interaction terms by transforming the quadratic Casimir as

$$\mathcal{C}(SO(3,1)) \mapsto \mathcal{U}^\dagger\mathcal{C}(SO(3,1))\mathcal{U}. \tag{4.5}$$

In this spirit in [1] for the group $SO(3,1)$ it was shown that the SUSY partner potentials mentioned in section 3 can be regarded as potentials arising from two different Casimir operators related by a suitable $SU(2)$ gauge transformation. The interrelation between SUSY transformations and gauge transformations is a result which deserves further elaboration.

5 Conclusions

In this paper we introduced a new matrix-valued realization for the group $SO(3,2)$. By calculating the Casimir operators we derived an interaction term compatible with the $SO(3,2)$ symmetry. This interaction term is matrix-valued, containing LS terms and an optical potential. The interesting gauge structure of the quadratic Casimir operator was also demonstrated, and the role of gauge transformations for deriving new interaction terms was emphasized.

However, important issues are left to be clarified. Firstly, we did not yet manage to calculate the scattering matrix for the interaction term (3.18). It is true that the form of the S-matrix for $SO(3,2)$ is fixed by group theory [5], however we have to choose the multichannel formalism developed by Alhassid and Iachello [11]. Using the asymptotical behavior of our modified generators one should be able to extract matrix-valued recursion relations for the Jost functions, hence the S-matrix can in principle be found. Secondly, we did not considered here the important possibility of obtaining nonlocal potentials by simply using a canonical transformation $\mathbf{P} \mapsto -\mathbf{R}$, $\mathbf{R} \mapsto \mathbf{P}$ in the quadratic Casimir (3.2). For the $SO(3,1)$ case this program was carried through in [1]. Since $SO(3,1)$ is a subgroup of $SO(3,2)$ we expect these results to recover the ones known from [1] with the choice $v = 0$. Such questions can hopefully be answered in future works.

Acknowledgment This work has been supported by MTA/DFG Grant Nr. (76/1995) and OTKA Grant Nr. (T17179).

References

[1] Lévay P 1996 J. Phys. A: Math. Gen. (submitted for publication).
[2] Zielke A and Scheid W 1993 J. Phys. A: Math. Gen. **26** 2047.
[3] Lévay P in preparation.
[4] Evans N T 1967 J. Math. Phys. **8** 179.
[5] Wu J, Iachello Fand Alhassid Y 1987 Ann. Phys. **173** 68.
[6] Baye D, Levai G and Sparenberg J M 1996 Nucl. Phys. **A599** 435.
[7] Greiner W 1990 *Relativistic Quantum Mechanics*, (Springer-Verlag, New York) pp. 212.
[8] Lévay P 1995 J. Phys. A: Math. Gen. **28** 5919.
[9] Lévay P 1994 J. Phys. A: Math. Gen. **27** 2857.
[10] Forgács P and Manton N S 1980 Commun. Math. Phys. **72** 15.
[11] Alhassid Y and Iachello F 1989 Nucl. Phys. **A501** 585.

Analytical Results on Generating Phase-Equivalent Potentials by Supersymmetry: Removal and Addition of Bound States

Géza Lévai[1], Daniel Baye[2], Jean-Marc Sparenberg[2]

[1] Institute of Nuclear Research of the Hungarian Academy of Sciences, P.O. Box 51, 4001 Debrecen, Hungary
[2] Physique Nucléaire Théorique et Physique Mathématique C.P. 229, Université Libre de Bruxelles, B 1050 Brussels, Belgium

Abstract. Applying the techniques of supersymmetric quantum mechanics we determine closed algebraic expressions for potentials that are phase-equivalent with the generalized Pöschl–Teller potential. Among the examples we discuss the elimination of any single bound state, adding a single bound state at specific energies and eliminating the first few bound states. In our work we applied the abstract mathematical formalism developed recently for the modification of the spectrum of potentials without changing the phase shifts, and adapted it to the case of the generalized Pöschl–Teller potential. We discuss the importance of shape invariance in these procedures and comment on the possibility of deriving similar closed formulas for various other potentials.

1 Introduction

Since its introduction fifteen years ago supersymmetric quantum mechanics (SUSYQM) has evolved into a highly sophisticated method of handling isospectral quantum mechanical systems. Its early applications concerned mainly single transformations by which the ground state of a potential could be removed or a new ground state could be introduced, depending on the solution of the Schrödinger equation used in the process. It was noticed that these manipulations also change the r^{-2}-like singularity of the potentials and modify the phase shifts in a characteristic way (Sukumar 1985). Later it was shown that by using pairs of such transformations one can construct potentials that lead to the same phase shifts as the original potential despite the different number of bound states the two potentials support, and this result was interpreted (Baye 1987) in terms of the generalized Levinson theorem (Swan 1963). The relation of SUSYQM to other methods of analyzing isospectral potentials, such as the inverse scattering theory has also been discussed (Sukumar 1985; Baye 1987, 1994).

More recently the formalism of generating phase-equivalent potentials has been developed to a stage where in principle arbitrary modifications of the energy spectrum are possible (Ancarani and Baye 1992; Baye 1993; Baye and Sparenberg 1994). The final potential and the wavefunctions are expressed

in terms of compact formulas depending on integrals and determinants composed of physical and unphysical solutions of the Schrödinger equation. These expressions can be evaluated by numerical techniques in general.

The generality and compactness of the formulas also raises the question whether it is possible to find examples where the whole procedure can be performed in an analytical way, i.e. whether there are cases where the resulting potential is obtained in a closed algebraic expression. Such investigations are also motivated by the renewed interest in exactly solvable quantum mechanical problems raised also partly by SUSYQM (see, for example, Lévai (1994) and references). Efforts in this direction include the phase-equivalent removal of the ground state of the Coulomb (Amado 1988), Morse and Hulthen (Talukdar et al. 1992) potentials, as well as other transformations of the Coulomb potential (Khare and Sukhatme 1989; Ancarani and Baye 1992). Apart from their aesthetic value, the importance of fully analytical transformations lies in the fact that exact results can be obtained even in critical conditions when the numerical techniques might not be safely controlled. Handling complex potentials can raise such problems, for example (Baye et al. 1996a, 1996b).

In Sect. 2 we briefly review the basic (single and combined) transformations used in SUSYQM. In Sect. 3 these techniques are then applied to the generalized Pöschl-Teller potential (GPT) and analytical transformations are formulated for removing or adding a bound state in the GPT spectrum, as well as for removing the two lowest bound states. Finally, in Sect. 4 we summarize the results and discuss the possibility of applying similar transformations to other types of potentials.

2 The Basic Transformations of SUSYQM

Let us consider the Schrödinger equation (with $\hbar^2/2\mu = 1$)

$$H_0\varphi_0(k,r) = \left(-\frac{\mathrm{d}^2}{\mathrm{d}r^2} + V_0(r)\right)\varphi_0(k,r) = k^2\varphi_0(k,r) \tag{1}$$

and the factorization of the corresponding Hamiltonian

$$H_0 = A_0^+ A_0^- + E_0 \ , \tag{2}$$

where the factorization energy $E_0 = k_0^2$ does not exceed the ground-state energy $E_0^{(0)}$, and

$$A_0^\pm = \pm\frac{\mathrm{d}}{\mathrm{d}r} + \frac{\varphi_0'(k_0,r)}{\varphi_0(k_0,r)} \ . \tag{3}$$

Due to $E_0 \le E_0^{(0)}$ the solutions are nodeless. The supersymmetric partner of H_0 is defined as

$$H_1 = A_0^- A_0^+ + E_0 = H_0 - 2\frac{\mathrm{d}}{\mathrm{d}r}\left(\frac{\varphi_0'(k_0,r)}{\varphi_0(k_0,r)}\right) \ . \tag{4}$$

The properties of $V_0(r)$ and $V_1(r)$ are connected in a characteristic way determined by the nature of solution φ_0, as shown in Table 1 (Ancarani and Baye 1992).

Table 1. Types of solutions and the corresponding SUSY transformations.

Solution φ_0	$\psi_0^{(0)}$	ϕ_0	χ_0	f_0
Fact. energy E_0	$E_0^{(0)}$	$E_0 < E_0^{(0)}$	$E_0 < E_0^{(0)}$	$E_0 < E_0^{(0)}$
$\lim_{r\to 0}\varphi_0$	$r^{\nu+1}$	$r^{-\nu}$	$r^{\nu+1}$	$r^{-\nu}$
$\lim_{r\to\infty}\varphi_0$	$\exp(-k_0^{(0)}r)$	$\exp(k_0 r)$	$\exp(k_0 r)$	$\exp(-k_0 r)$
Transformation (old notation)	T_+^+ (T_1)	T_-^- (T_2)	T_-^0 (T_3)	T_+^0 (T_4)
Spectrum modification	supresses g.s.	adds new g.s ($\nu > 0$ only)	none	none ($\nu > 0$ only)
Singularity mod.	$2(\nu+1)r^{-2}$	$-2\nu r^{-2}$	$2(\nu+1)r^{-2}$	$-2\nu r^{-2}$
Phase shift mod.	$\tan^{-1}(k/k_0^{(0)})$	$-\tan^{-1}(k/k_0)$	$-\tan^{-1}(k/k_0)$	$\tan^{-1}(k/k_0)$

Further potentials can be derived by combining these single SUSY transformations. In particular, three pairs of such transformations can be employed to construct potentials $V_2(r)$ phase-equivalent with $V_0(r)$:

$$V_2(r) = V_0(r) + 2\frac{\mathrm{d}}{\mathrm{d}r}\left(\frac{(\varphi_0(k_0,r))^2}{\beta + \int_r^\infty (\varphi_0(k_0,t))^2 \mathrm{d}t}\right) . \tag{5}$$

It was shown (Baye 1993; Baye and Sparenberg 1994) that the cases correspond to the following choices of β in (5):

$$\beta = \begin{cases} -1, & E_0 \text{ physical for } H_0; \quad T_-^0 T_+^+; \text{ supresses state} \\ \alpha, & E_0 \text{ nonphysical for } H_0; \; T_-^- T_+^0; \text{ adds new state} \\ \frac{\alpha}{1-\alpha}, & E_0 \text{ physical for } H_0; \quad T_-^- T_+^+; \text{ no change} \end{cases} \tag{6}$$

It was also noticed (Baye 1993) that the "no-node condition" for φ_0 is not necessary when pairs of SUSY transformations are applied. The iteration of such dual transformations is also possible (Baye 1993; Baye and Sparenberg 1994).

The elementary transformations can also be iterated (Sparenberg and Baye 1995), in which case the new potential (which is not phase-equivalent with $V_0(r)$) takes the form

$$V_m(r) = V_0(r) - 2\frac{\mathrm{d}^2}{\mathrm{d}r^2}\ln|W(\varphi_0(k_1,r),\ldots,\varphi_0(k_m,r)|\ . \tag{7}$$

3 Phase-Equivalent Partners of the Generalized Pöschl–Teller Potential

Consider the Schrödinger equation

$$\left(-\frac{\mathrm{d}^2}{\mathrm{d}r^2}+V(r)\right)\psi=E\psi \tag{8}$$

with the generalized Pöschl–Teller (GPT) potential

$$V(r)=-\frac{s(s+1)}{\cosh^2 r}+\frac{\lambda(\lambda-1)}{\sinh^2 r}\ , \tag{9}$$

where we assume that s can be complex. We note that although only the s-wave solutions of this potential can be obtained analytically, its second term resembles the centrifugal term, with $l=\lambda-1$ in many respects.

Setting $E=k^2$ the two independent solutions can be expressed in terms of hypergeometric functions as

$$F_1(r)\simeq\frac{(\sinh r)^\lambda}{(\cosh r)^s}\ {}_2F_1(\tfrac{1}{2}(-s+\lambda-\mathrm{i}k),\tfrac{1}{2}(-s+\lambda+\mathrm{i}k);\lambda+\tfrac{1}{2};-\sinh^2 r) \tag{10}$$

and

$$F_2(r)\simeq\frac{(\sinh r)^{1-\lambda}}{(\cosh r)^s}\ {}_2F_1(\tfrac{1}{2}(1-s-\lambda-\mathrm{i}k),\tfrac{1}{2}(1-s-\lambda+\mathrm{i}k);-\lambda+\tfrac{3}{2};-\sinh^2 r)\ . \tag{11}$$

We assume that $\lambda\geq 1$ holds, therefore $F_1(r)$ is regular, while $F_2(r)$ is irregular in the origin. (The $\lambda\leq 0$ choice would simply exchange the role of the two solutions, because they are interrelated via the $\lambda\leftrightarrow 1-\lambda$ transformation which leaves potential (9) invariant.)

Bound states located at

$$E_n=k^2=-(s-\lambda-2n)^2 \tag{12}$$

appear if $\mathrm{Re}(s)>2n+\lambda$ holds, and the corresponding bound-state wavefunctions are expressed in terms of $F_1(r)$ in (10), which in these cases reduces to a form containing a Jacobi polynomial:

$$\psi_n(r)\simeq F_1(r)\simeq(\sinh r)^\lambda(\cosh r)^{2n-s}P_n^{(s-\lambda-2n,\lambda-\frac{1}{2})}(1-\frac{2}{\cosh^2 r})\ . \tag{13}$$

We mention here that normalization factors and other numerical scaling factors do not influence the final form of the derived potentials, therefore we drop them in the following.

3.1 Removal of an Arbitrary Bound State

The phase-equivalent removal of the Nth bound state at E_N requires the application of (5) with $\beta = -1$ and $\varphi_0(k_0, r)$ being the corresponding normalized bound-state wavefunction $\psi_0^{(N)}(r)$ (Baye and Sparenberg 1994). According to (13) it can be written as

$$\psi_0^{(N)}(r) = (\sinh r)^\lambda \sum_{j=0}^{N} c_j \, (\cosh r)^{2j-s} \equiv \frac{(\sinh r)^\lambda}{(\cosh r)^s} p_N(\cosh r) \tag{14}$$

with

$$c_j = \frac{(-)^{N-j}\Gamma(s-\lambda-N+1)\Gamma(s-j+\frac{1}{2})\mathcal{N}_N}{j!(N-j)!\Gamma(s-\lambda-N-j+1)\Gamma(s-N+\frac{1}{2})} \, . \tag{15}$$

Since the wavefunctions are normalized to unity the integration from r to ∞ can be rewritten to one from 0 to r, and the integral can be evaluated by (37):

$$\int_0^r (\psi_0^{(N)}(t))^2 \mathrm{d}t = (\sinh r)^{2\lambda+1} (\cosh r)^{1-2s} G_N(r), \tag{16}$$

where

$$G_N(r) \equiv \sum_{m=0}^{2N} \frac{d_m (\cosh r)^{2m}}{2\lambda+1} \, {}_2F_1(\lambda - s + m + 1, 1; \lambda + \tfrac{3}{2}; -\sinh^2 r) \tag{17}$$

with

$$d_m = \sum_{j=\max(0,m-N)}^{\min(m,N)} c_j c_{m-j} \, . \tag{18}$$

The resulting potential which has bound states at E_n in (12), except for $n = N$ then takes the form

$$V_2(r) = V_0(r) + \frac{2}{\sinh^2 r \cosh^2 r} \left(\frac{(p_N(\cosh r))^2}{G_N(r)} \right)^2 - \left(\frac{\lambda}{\sinh^2 r} - \frac{s}{\cosh^2 r} + \frac{p_N'(\cosh r)}{\cosh r \, p_N(\cosh r)} \right) \frac{4(p_N(\cosh r))^2}{G_N(r)} \, . \tag{19}$$

We note that $V_2(r)$ remains unchanged if the factors not depending on j in (15) are dropped.

3.2 Addition of a New Bound State at Specific Energies

In order to add a new bound state at energy $E = k^2$ one has to apply (5) with $\varphi_0(k,r)$ chosen as an f-type solution of (8) which is irregular at the origin (with $\lambda \geq 2$ at least) and exponentially goes to zero asymptotically. β in (6) now remains arbitrary, representing an additional parameter (α) of the resulting potential. The required unphysical solution of the Schrödinger equation can be expressed in terms of the linear combination of $F_1(r)$ and $F_2(r)$ in Eqs. (10) and (11):

$$f_0(k,r) \simeq (\cosh r)^{ik} (\tanh r)^{1-\lambda}$$

$$\times \, {}_2F_1(\tfrac{1}{2}(s-\lambda+2-\mathrm{i}k), \tfrac{1}{2}(-s-\lambda+1-\mathrm{i}k); 1-\mathrm{i}k; 1-\tanh^2 r) \ , \qquad (20)$$

where $\mathrm{Im}(k) > 0$ has to hold. In order to determine $V_2(r)$ the following type integrals have to be evaluated:

$$I(x(r)) = \int_0^x y^{c-2}(1-y)^{a+b-c}(F(a,b;c;y))^2 \mathrm{d}y \ , \qquad (21)$$

where we have introduced the new $y = 1 - \tanh^2 r$ variable together with the parameters

$$a = \tfrac{1}{2}(s-\lambda+2-\mathrm{i}k), \qquad b = \tfrac{1}{2}(-s-\lambda+1-\mathrm{i}k), \qquad c = 1-\mathrm{i}k \ . \qquad (22)$$

The evaluation of this integral and its expression in terms of a closed formula can be given only in exceptional cases. It can, however, be transformed into further formulas by means of integration by parts. This allows changing some of the parameters, which can open the way to further specific cases. We present a formula in the Appendix, by which the parameters a or b can be increased or decreased by one unit. Direct evaluation of integral (21) is possible when either a or b is a non-positive integer $-N \leq 0$, because the hypergeometric function then reduces to a polynomial form.

From the $b = -N$ choice we get $\mathrm{i}k = -s-\lambda+1+2N$, which means that a new bound state can be introduced at energies $E_N = -(s+\lambda-1-2N)^2$. The $\mathrm{Re}(\mathrm{i}k) < 0$ requirement now yields $\mathrm{Re}(s) - \lambda > 2N+1-2\lambda$, indicating that the original potential may have at least $N-\lambda$ bound states. Due to the $b = -N$ choice the nonphysical f-type wavefunction has the form

$$f(r) \simeq \frac{(\sinh r)^{1-\lambda}}{(\cosh r)^s} p_N(\cosh r) \equiv \frac{(\sinh r)^{1-\lambda}}{(\cosh r)^s} \sum_{j=0}^{N} c_j \, (\cosh r)^{2j} \ , \qquad (23)$$

where

$$c_j = \frac{(-)^j \Gamma(s-j+\frac{1}{2})}{j!(N-j)!\Gamma(s+\lambda-N-j)} \ . \qquad (24)$$

(While reducing (20) to (23) we dropped some unimportant numerical scaling factors which cancel out in the final formulas anyway.) The integration can

then be carried out using an appropriate form of (37) with $x = \sinh^2 r$. Setting coefficients d_m as in (18) we can define

$$G_N(r) = \sum_{m=0}^{2N} \frac{d_m(\cosh r)^{2m}}{2(\lambda+s-m-1)} \; {}_2F_1(s-m+\tfrac{1}{2}, 1; \lambda+s-m; 1/\cosh^2 r) + \alpha(\sinh r)^{2\lambda-3}(\cosh r)^{2s+1} \quad , \tag{25}$$

which can be used to express integral (21) as

$$\int_r^\infty (f_0(k_N, t))^2 \mathrm{d}t = (\sinh r)^{3-2\lambda}(\cosh r)^{-2s-1} G_N(r) - \alpha \tag{26}$$

and the final potential phase-equivalent to (9) as

$$V_2(r) = V_0(r) + \frac{2}{\tanh^2 r}\left(\frac{(p_N(\cosh r))^2}{G_N(r)}\right)^2 - \left(\frac{\lambda-1}{\tanh^2 r} + s - \cosh r \, \frac{p'_N(\cosh r)}{p_N(\cosh r)}\right) \frac{4(p_N(\cosh r))^2}{G_N(r)} \quad . \tag{27}$$

The $a = -N$ choice in (21) leads to $\mathrm{i}k = s - \lambda + 2 + 2N$. This introduces bound states at $E_N = -(s-\lambda+2+2N)^2$ if $\mathrm{Re}(\mathrm{i}k) < 0$ holds. This corresponds to the "continuation" of the GPT spectrum (12) to formally negative quantum numbers ($n = -N$). However, from $\mathrm{Re}(\mathrm{i}k) = \mathrm{Re}(s) - \lambda + 2 + 2N < 0$ $\mathrm{Re}(s) - \lambda < 0$ also follows, which means that (contrary to the previous example originating from $b = -N$) the original $V_0(r)$ potential can not support any bound states, therefore the resulting $V_2(r)$ potential will have only a single bound state. We do not present here the explicit form of $V_2(r)$, only mention that in algebraic terms it is generally similar to the form of the potentials determined previously in this Subsection.

3.3 Removal of the First Few Bound States

Another method of obtaining phase-equivalent partners of the GPT potential is combining two procedures: first removing N states by iterated *single* transformations (which, of course, results an intermediate potential $V_N(r)$ *not* phase-equivalent with the original one), and then restoring the phase-shifts by another sequence of *single* transformation. This requires the application of (7) with the first N physical bound-state solutions in the Wronskian. Since the GPT potential is shape-invariant, this procedure recovers another GPT potential (9) with s and λ replaced with $s-N$ and $\lambda+N$. In the second step the Wronskian of the χ-type unphysical solutions of $V_N(r)$ has to be applied in (7). Here it is essential to set the factorization energies equal to the energies of the bound states removed in the first step, otherwise phase-equivalence is lost.

We illustrate this procedure with the removal of the first two bound states of potential (9). Let us assume that $\psi_i^j \equiv \psi_i(k_j, r)$ $(j = 1, 2)$ are solutions of the Schrödinger equation with potential $V_i(r)$ at $E_j = k_j^2$. Then the second logarithmic derivative of the Wronskian of these two solutions is

$$\frac{\mathrm{d}^2}{\mathrm{d}r^2} \ln W(\psi_i^1, \psi_i^2) \equiv \frac{\mathrm{d}^2}{\mathrm{d}r^2} \ln W = \frac{W''}{W} - \left(\frac{W'}{W}\right)^2 , \tag{28}$$

where the prime here denotes derivation with respect to r and

$$W(\psi_i^1, \psi_i^2) = \psi_i^1 (\psi_i^2)' - (\psi_i^1)' \psi_i^2 . \tag{29}$$

Based on the Schrödinger equation one also obtains the formulas

$$W'(\psi_i^1, \psi_i^2) = \psi_i^1 (\psi_i^2)'' - (\psi_i^1)'' \psi_i^2 = ((k_i^1)^2 - (k_i^2)^2) \psi_i^1 \psi_i^2 \tag{30}$$

and

$$W''(\psi_i^1, \psi_i^2) = ((k_i^1)^2 - (k_i^2)^2)(\psi_i^1 (\psi_i^2)' + (\psi_i^1)' \psi_i^2) . \tag{31}$$

Using the first two bound-state wavefunctions (13) of (9) in this procedure we, indeed, get another GPT potential $V_2(r)$ with parameters $s-2$ and $\lambda+2$. The two χ-type solutions of this to be applied in the second transformation are those in (11) with $ik = (s - \lambda)$ and $(s - \lambda - 2)$:

$$\chi_2^1(r) = (\sinh r)^{\lambda+2} (\cosh r)^{-s+2} \, {}_2F_1(-s + \lambda + 2, 2; \lambda + \tfrac{5}{2}; -\sinh^2 r) \tag{32}$$

and

$$\chi_2^2(r) = (\sinh r)^{\lambda+2} (\cosh r)^{-s+2} \, {}_2F_1(-s + \lambda + 3, 1; \lambda + \tfrac{5}{2}; -\sinh^2 r) . \tag{33}$$

Let us denote the hypergeometric functions appearing in (32) and (33) with $F^1(z)$ and $F^2(z)$, respectively, where $z = -\sinh^2 r$. Then the final $V_4(r)$ potential phase-equivalent with $V_0(r)$ is

$$V_4(r) = V_2(r) + 8 \left[1 + \frac{1}{\sinh^2 r \cosh^2 r} \left(\frac{s - \lambda - 1}{\Delta(-\sinh^2 r)} \right)^2 - \left(\frac{\lambda + 2}{\sinh^2 r} - \frac{s - 2}{\cosh^2 r} - 2 \frac{(F^2(z))'}{F^2(z)} \right) \frac{s - \lambda - 1}{\Delta(-\sinh^2 r)} \right] , \tag{34}$$

where $\Delta(z)$ is formally defined as a logarithmic derivative:

$$\Delta(z) = \frac{\mathrm{d}}{\mathrm{d}z} \ln \left(\frac{F^1(z)}{F^2(z)} \right) . \tag{35}$$

Similar, but more complicated formulas can be obtained after removing more than two of the lowest states. We again stress that this two-step analytical procedure was made possible by the shape-invariant nature of the GPT potential, because this allowed us to get simple closed expressions for the unphysical χ-type solutions of the intermediate potential. It also has to be stressed that this relatively simple process works only if the *lowest* few states are removed, otherwise the same problem of complicated solutions arises.

4 Summary and Conclusions

In this contribution we applied the abstract formalism of supersymmetric quantum mechanics to the specific case of the generalized Pöschl–Teller potential. In particular we explicitly derived closed algebraic expressions for potentials that are phase-equivalent with the GPT potential and the spectra of which are obtained from simple manipulations on the GPT spectrum. The transformed wavefunctions (not discussed here) can also be determined by similar analytic calculations.

First an arbitrary bound state was removed from the spectrum. This required the evaluation of definite integrals containing the square of the corresponding wavefunction. The integrand could always be reduced to polynomial form in this case. This procedure seems to be applicable to other types of potentials as well: preliminary results suggest that it is generalizable to the Ginocchio potential (Ginocchio 1984), which is a member of the Natanzon potential class and contains the Pöschl–Teller potential as a special case.

In the second example we added a new bound state to the GPT spectrum. Here the integrand contained hypergeometric functions, and the integrals could be evaluated only in special cases, which meant that the new bound state could be inserted only at specific energies. This procedure requires an r^{-2}-like attractive singularity of the original potential, therefore it is generalizable only to potentials that have this feature. This forbids similar treatment of a number of potentials (Morse, Hulthen, Rosen–Morse, etc.).

In the third case we followed a two-step procedure to eliminate the lowest states of the GPT potential: the lowest two states were removed in the first step and then the phase shifts were restored in the second one. Instead of integrals here we had to deal with Wronskians composed of solutions of the Schrödinger equation. The shape-invariant nature of the GPT potential played an important role in this case, because it guaranteed that we could use simple compact formulas for the solutions of the intermediate potential. Similar treatment of other radial shape-invariant potentials seems possible.

These analytical transformations can be used, for example, to test numerical methods in situations that might be problematic in terms of numerical techniques. This is the case, for example, for certain types of complex potentials (Baye et al. 1996a, 1996b): our results are applicable to complex potentials without any major modification. Extending this work to further more general potentials could introduce new potential shapes, some of which might be close to realistic potentials that can not be treated analytically.

Appendix

Using recurrence relations of the hypergeometric functions (Abramowitz and Stegun 1970) and integration by parts integral (21) can be written in alternative forms by modifying parameters a or b by one unit:

$$I(x) = \frac{1}{2(a-1)} \left[y^{c-1}(1-y)^{a+b-c}\ {}_2F_1(a-1,b;c;y)\ {}_2F_1(a,b;c;y) \right]_0^x$$
$$- \frac{c-a}{2(a-1)} \int_0^x y^{c-2}(1-y)^{a-1+b-c} ({}_2F_1(a-1,b;c;y))^2 \mathrm{d}y \ . \quad (36)$$

When the hypergeometric functions do not show up in the integrand $I(x)$ can directly be evaluated using a variation of Eq. 3.194.1 due to Gradshteyn and Rhyzik (1965):

$$\int_0^y x^\alpha (1+x)^\beta \mathrm{d}x = \frac{1}{\alpha+1} y^{\alpha+1}(1+y)^{\beta+1}\ {}_2F_1(\alpha+\beta+2,1;\alpha+2;-y) \ , \quad (37)$$

with $\mathrm{Re}(\alpha) > -1$.

Acknowledgments

J.-M. S. is Aspirant of the Fonds National de la Recherche Scientifique (Belgium). This work was also supported by the OTKA grants No. W015140 and F020689 (Hungary).

References

Abramowitz M., Stegun I.A. (1970): Handbook of Mathematical Functions (Dover, New York).
Amado R.D. (1988): Phys. Rev. A **37**, 2277
Ancarani L.U., Baye D. (1992): Phys. Rev. A **46**, 206
Baye D. (1987): J. Phys. A **20**, 5529
Baye D. (1993): Phys. Rev. A **48**, 2040
Baye D. (1994): in Quantum Inversion Theory and Applications, ed. von Geramb H.V., Lecture Notes in Physics **427** (Springer, Berlin) 127
Baye D., Sparenberg J.-M. (1994): Phys. Rev. Lett. **73**, 2789
Baye D., Lévai G., Sparenberg J.-M. (1996): Nucl. Phys. **A599**, 435
Baye D., Sparenberg J.-M., Lévai G. (1996): contribution to this conference
Ginocchio J.N. (1984): Ann. Phys. (N.Y.) **152**, 203
Gradshteyn I.S., Rhyzik I.M. (1965): Table of Integrals, Series and Products (Academic, New York)
Khare A., Sukhatme U. (1989): J. Phys. A **22**, 2847
Lévai G. (1994): in Quantum Inversion Theory and Applications, ed. von Geramb H.V., Lecture Notes in Physics **427** (Springer, Berlin) p. 107
Sparenberg J.-M., Baye D. (1995): J. Phys. A **28**, 5079
Sukumar C.V. (1985): J. Phys. A **18**, 2917; 2937
Swan P. (1963): Nucl. Phys. **46**, 669
Talukdar B, Das U., Bhattacharyya C., Bera K. (1992): J. Phys. A **25**, 4073

Multidimensional Inverse Scattering with Fixed-Energy Data

A.G. Ramm

Department of Mathematics, Kansas State University
Manhattan, KS 66506-2602, USA
ramm@math.ksu.edu

1 Introduction

In this lecture the author reviews his results on multidimensional inverse scattering. References to the works of other authors can be found in [20]. Five topics are briefly discussed:

- 1) property C with constraints and new type of the uniqueness theorems for inverse scattering,
- 2) inversion of noisy discrete fixed-energy 3D scattering data and error estimates,
- 3) variational principles equivalent to inverse scattering problems,
- 4) low-frequency data inversion,
- 5) asymptotic inverse scattering theory for scattering by small inhomogeneities.

Detailed proofs of the results can be found in the cited references. In this paper the emphasis is on the ideas and formulation of the results.
The inverse problems we consider are: inverse potential, geophysical and obstacle scattering *(IPS, IGS, IOS)*. We recall the statements of these problems. Let

$$[\nabla^2 + k^2 - q(x)]\, u = 0 \text{ in } \mathbb{R}^3, \quad k = const > 0 \tag{1.1}$$

$$u = \exp(ik\alpha \cdot x) + A(\alpha', \alpha, k)\frac{\exp(ikr)}{r} + o\left(\frac{1}{r}\right),$$

$$r := |x| \to \infty, \alpha' := \frac{x}{r}, \alpha \in S^2, \tag{1.2}$$

where S^2 is the unit sphere, α is a given unit vector, $A(\alpha', \alpha, k)$ is the scattering amplitude, and $q(x)$ is the potential. We assume that $q \in Q := \{q : q = \overline{q}$ (real-valuedness), $q(x) = 0$ for $|x| \geq a$, $q \in L^\infty\}$, $k > 0$ is fixed. The solution to (1.1)-(1.2) is called the scattering solution. We denote B_a the ball centered at the origin with radius a, $u_0 := \exp(ik\alpha \cdot x)$, $M_k := \{z : z \in \mathbb{C}^3, z \cdot z = k^2\}$, $z \cdot y := \sum_{j=1}^3 z_j y_j$, $M_1 := M$, M_k is a non-compact algebraic variety in $\mathbb{C}^3$, $M \cap \mathbb{R}^3 = S^2$.

The IPS consists of finding $q \in Q$, *given* $A(\alpha', \alpha) := A(\alpha', \alpha, k)$ *for all* $\alpha', \alpha \in S^2$. We fix $k = 1$ without loss of generality.
The general method for a study of inverse scattering problems, based on property C, was introduced in [4] and in [20] a detailed account of this method is given and its many applications are described. (See [4-42]). Later [29-31,38] the author introduced the notion of *property C with constraints* and found several applications of this notion in inverse scattering.
Let us define *property C: let* L_j *be linear partial differential expressions,* $j = 1, 2$, $N_j = N_j(D) := \{w : L_j\ w = 0\ in\ D\}$, $D \subset \mathbb{R}^n$, $n \geq 2$, D *is a bounded domain; consider subsets of* N_j *for which the products* $w_1 w_2$ *are defined,* $w_j \in N_j$; *let* $f \in L^p(D)$, $p \geq 1$, *and assume that the equation*

$$\int_D f(x) w_1 w_2 dx = 0 \quad \forall w_j \in N_j, \tag{1.3}$$

implies $f(x) = 0$. *Then we say that the pair* $\{L_1, L_2\}$ *has property* C.
This definition is rather flexible: we can take $f(x)$ not in $L^p(D)$ but in a different space, including a space of distributions.

The definition of *property C with constraints is similar, but* w_j *in (1.3) runs not through all of* N_j *but through a subset of* N_j *of finite codimension.*

For example, w_j may satisfy finitely many linear constraints:

$$(w_j, h_m) = 0, \quad 1 \leq m \leq M_j < \infty,$$

where (w_j, h_m) is a linear functional on N_j. This functional can be defined by a function or distribution with support in $\overline{D} = D \cup \partial D$.
Let $l_j = \nabla^2 + k^2 - q_j(x)$, $q_j \in Q$.

Theorem 1.1 [29,30,38]. The pair $\{l_1, l_2\}$ **has property** C **with constraints.**

Let A_j be the scattering amplitude corresponding to $q_j, j = 1, 2$. From Theorem 1.1 one derives:

Theorem 1.2 [32,33]. If $q \in Q$, $j = 1, 2$, **and** $A_1(\alpha', \alpha) - A_2(\alpha', \alpha)$ **is a finite rank kernel in** $L^2(S^2)$, **then** $q_1 = q_2$.

Sketch of proof: Let $q_1 - q_2 := p(x)$, $A_1 - A_2 := A$. *Then one proves [20,p.67] that*

$$-4\pi A = \int p(x) u_1(x, \alpha) u_2(x, -\alpha') dx \quad \forall \alpha', \alpha \in S^2. \tag{$*$}$$

If A *is a finite rank kernel, then* $A = \sum_{m=1}^{M} a_m(\alpha) b_m(\alpha')$. *Let* $(\nu_2(\alpha'), b_m(\alpha')) = 0$, $1 \leq m \leq M$, $\nu_1(\alpha)$ *be arbitrary. Multiply* $(*)$ *by* $\nu_1(\alpha)\nu_2(\alpha')$ *and integrate over* $S^2 \times S^2$ *to get*

$$0 = \int_{B_a} p(x) w_1(x) w_2(x) dx, \qquad (**)$$

$$w_1 := \int_{S^2} u_1(x, \alpha) \nu_1(\alpha) d\alpha, \; w_2 := \int_{S^2} u_2(x, -\alpha') \nu_2(\alpha') d\alpha'.$$

The set $\{w_1\}$ *is dense in* $N_1 := \{w : l_1 w = 0 \text{ in } B_a\}$ *in* $L^2(B_a)$ *norm when* ν *run through all of* $L^2(S^2)$, *while the set* $\{w_2\}$ *has codimension* $\leq M$ *in* N_2 *(see [33]). By Theorem 1.1, the set* $\{w_1 w_2\}$ *is total in* $L^2(B_a)$. *Therefore* $(**)$ *implies* $p(x) = 0$.

Note that the classical uniqueness theorem for ISP [20] says: if $A_1(\alpha', \alpha) = A_2(\alpha', \alpha)$ $\forall \alpha', \alpha \in S^2$ and $q_j \in Q$, then $q_1 = q_2$. Thus, Theorem 2 is a far-reaching generalization of the classical uniqueness theorem. Results in [29,30,38] cover also the case of *IOS* for various boundary conditions, and contain results on inverse spectral problems and inverse boundary value problems. *Roughly speaking, it is proved in [29,30,38] that one can drop any finite number of spectral data or boundary data, and uniqueness of the solutions to inverse spectral problems and inverse boundary value problems is still guaranteed.*

Assume that $q = q(r)$, that is, the potential is spherically symmetric, and that all the phase shifts with $\ell > \ell_0$ vanish, where ℓ_0 is an arbitrary large fixed integer. Then, as follows from Theorem 1.2, $q(r) = 0$.

The *IGS* problem consists of finding an inhomogeneity $v(x)$ in the velocity profile from the surface scattering data. The governing equation is

$$[\nabla^2 + k^2 + k^2 v(x)] \, U = -\delta(x - y) \text{ in } \mathbb{R}^3, \quad k = \; const \; > 0, \qquad (1.4)$$

U satisfies the radiation condition, $v(x) \in Q$, $supp \; v \subset \mathbb{R}^3_-$, $\mathbb{R}^3_- := \{x : x_3 < 0\}$. The surface scattering data are the values $U(x, y) := U(x, y, k)$ $\forall x$, $\forall y \in P := \{x : x_3 = 0\}$, $k > 0$ is a fixed constant.

The *IOS* problem consists of finding an obstacle D and the boundary condition on $\partial D := S$ from the scattering amplitude $A(\alpha', \alpha)$, $k > 0$ is fixed. The scattering solution is defined by equation (1.1) in $D' := \mathbb{R} \setminus D$ with $q(x) = 0$, equation (1.2), and the boundary condition:

$$u_N + \sigma(s) u = 0 \text{ on } S := \partial D, \quad \sigma(s) \geq 0, \qquad (1.5)$$

where u_N is the normal derivative, N is the outer unit normal to S, $\sigma(s) \in C(S)$. It is proved in [41] for Liapunov's boundaries and in [43] for Lipschitz's and even less smooth boundaries (see also [44]) that *IOS* has at most one solution. It is proved in [4,20] that *IGS* has at most one solution. We do not give the strongest results from [20] because of the lack of space. For example, in *IPS* and *IOS* the uniqueness results are proved in [20,41] for the data known $\forall \alpha' \in \tilde{S}^2_1$, and all $\alpha \in \tilde{S}^2_2$ where $\tilde{S}^2_j$ are arbitrary small open subsets of

S^2, in *IGS* the surface of data can be given on arbitrary small open subsets of P, the assumptions on $q(x)$ and $v(x)$ can be relaxed, etc.
In section 2 we describe an inversion algorithm for *IPS* and give an error estimate for this algorithm. In section 3 we formulate a variational principle equivalent to inverse scattering problems. In section 4 we outline a low-frequency data inversion in *IGS*. In section 5 an asymptotic theory for scattering by a small inhomogeneity is given. In section 6 two old open problems are stated.

2 Inversion of Noisy Fixed-Energy Discrete Scattering Data

Assume that $A_\delta(\alpha', \alpha)$ is known, $\sup_{\alpha', \alpha \in S^2} |A_\delta - A| < \delta$, so that $A_\delta(\alpha', \alpha)$ is the noisy scattering amplitude measured at a fixed energy ($k = 1$) with $\delta > 0$ being the noise level. We do not assume any statistical properties of the noise. At the end, it will be clear that only the values of A_δ at a discrete set of $\alpha', \alpha \in S^2$ are used in the inversion algorithm. We fix an arbitrary $\xi \in \mathbb{R}^3$ and chose θ', θ such that

$$\theta' - \theta = \xi, \quad |\theta| \to \infty, \quad \theta', \theta \in M. \tag{2.1}$$

This can be done easily and explicitly: choose the coordinates in which $\xi = te_3$, $t > 0$, e_j are unit orthonormal basis vectors, $\theta' = \frac{t}{2}e_3 + y$, $\theta = -\frac{t}{2}e_3 + y$, $y_3 = 0$, $|y| \to \infty$, $y_1^2 + y_2^2 = y \cdot y = 1 - \frac{t^2}{4}$. There are infinitely many y that satisfy these requirements. Let

$$\tilde{q}(\xi) := \int_{\mathbb{R}^3} \exp(-i\xi \cdot x) q(x) dx.$$

Fix arbitrary a_1 and b such that $a < a_1 < b$. Let $N(\delta) := [\frac{|ln\delta|}{ln|ln\delta|}]$, where $[x]$ is the closest to x integer. Define

$$A_{\delta\ell}(\alpha) := (A_\delta(\alpha', \alpha),\ Y_\ell(\alpha'))_{L_2(S^2)},$$

where $Y_\ell(\alpha) := Y_{\ell m}(\alpha)$ are the orthonormal spherical harmonics. Let

$$\hat{A}_\delta(\theta', \alpha) := \sum_{\ell=0}^{N(\delta)} A_{\delta\ell}(\alpha) Y_\ell(\theta'),$$

where the summation is taken over ℓ and also over m, $-\ell \leq m \leq \ell$, $Y_\ell(\theta)$ is naturally defined for all $\theta \in M$. Let $h_\ell(r)$ be the spherical Hankel function normalized so that $h_\ell(r) \sim \frac{\exp(ir)}{r}$ as $r \to \infty$, and let

$$\hat{u}_\delta(x, \alpha) := \exp(i\alpha \cdot x) + \sum_{\ell=0}^{N(\delta)} A_{\delta\ell}(\alpha) Y_\ell(\alpha') h_\ell(r).$$

Define

$$\rho_\delta(\nu) := \exp(-i\theta \cdot x) \int_{S^2} u_\delta(x,\alpha)\nu(\alpha)d\alpha - 1, \quad \theta \in M, \quad \nu \in L^2(S^2),$$

$\mu(\delta) = \exp[-\gamma N(\delta)]$, $\gamma := ln\frac{a_1}{a} > 0$, $\| \rho \| := \| \rho \|_{L^2(B_b \setminus B_{a_1})}$. Let $c > 0$ be a sufficiently large constant, $\xi \in \mathbb{R}$, and θ', θ satisfy (2.1). Consider the variational problem:

$$|\theta| = \sup, \quad \sup |\theta| := \vartheta(\delta), \tag{2.2}$$

$$\| \rho_\delta(\nu) \| + \| \nu \|_{L^2(S^2)} \exp(|Im\theta|b)\mu(\delta) \leq c|\theta|^{-1}. \tag{2.3}$$

Lemma 2.1 $\vartheta(\delta) \geq c_0 \frac{|ln\delta|}{(ln|ln\delta|)^2}, c_0 = const > 0.$

Let $\theta(\delta)$, and $\nu_\delta(\alpha)$ be any approximate solution to (2.2) in the following sense: (2.1) and (2.3) hold and $|\theta(\delta)| \geq \frac{1}{2}\vartheta(\delta)$. Define

$$\hat{q} := -4\pi \int_{S^2} \hat{A}_\delta(\theta'(\delta), \alpha)\nu_\delta(\alpha, \theta(\delta))d\alpha. \tag{2.4}$$

Theorem 2.1 One has

$$|\hat{q} - \tilde{q}(\xi)| \leq c_1 \frac{(ln|ln\delta|)^2}{|ln\delta|}, \tag{2.5}$$

where c_1 can be chosen uniformly for $\xi \in \mathbb{R}^3$ and $q \in \mathcal{K} \subset Q$, where $\mathcal{K}$ is an arbitrary fixed compact subset of Q.

Formula (2.4) gives an inversion algorithm and (2.5) is its error estimate. Since calculation of (2.4) by a cubature formula requires the knowledge of $\hat{A}_\delta(\alpha', \alpha)$ at a discrete set only, formula (2.4) gives inversion procedure for noisy, discrete, fixed-energy, 3-D scattering data.

3 Variational Principles Equivalent to Inverse Scattering Problems

We give here only the variational principle equivalent to *IPS* and refer the reader to [21,42] where similar principles for *IGS* and *IOS* are given.
The basic idea is to use not only the data fitting, but also the basic equation for the scattering solution, namely,

$$u = u_0 - \int_{\mathbb{R}^3} gqudz, \quad g := \frac{\exp(i|x-y|)}{4\pi|x-y|}, \quad k = 1. \tag{3.1}$$

Consider the variational principle:

$$\mathcal{F}(p,f) := \| -4\pi A(\alpha', \alpha) - \int_{B_a} \exp(-i\alpha' \cdot y) f(y,\alpha)dy \|_{L^2(S^2 \times S^2)}$$

$$+ \| f(x,\alpha) - p(x)u_0(x,\alpha) + p(x) \int_{B_a} g(x,z)f(z,\alpha)dz \|_{L^2(B_a \times S^2)}$$

$$= \min \tag{3.2}$$

Theorem 3.1 If $A(\alpha', \alpha)$ **is the scattering amplitude corresponding to a potential** $q \in Q$, **then** $\min \mathcal{F}(p, f) = 0$, **where** min **is taken over** $p \in L^2(B_q)$ **and** $f(x, \alpha) \in L^2(B_a \times S^2)$; $\min \mathcal{F}(p, f)$ **is attained at the pair** $\{q, qu(x, \alpha)\}$ **and only at this pair.** *Here* $q \in Q$ *is the unique potential corresponding to* $A(\alpha', \alpha)$ *and* $u(x, \alpha)$ *is the corresponding scattering solution.*

Remark 3.1 Unfortunately we cannot give any stability results for the solution to (3.2) with noisy data $A_\delta(\alpha', \alpha)$ **in place of the exact data** $A(\alpha', \alpha)$ **in (3.2).**

4 Inversion of Low-Frequency Surface Scattering Data

Consider (1.4) and assume that the data $U(x, y, k), \forall x, y \in P, \ \forall k \in (0, k_0)$ are known, where $k_0 > 0$ is an arbitrary small number. The usual integral equation equivalent to (1.4) (with the radiation condition) is:

$$U = g + k^2 \int_{B_a} g(x, y, k) v(z) U(z, y, k) dz, \quad g := \frac{\exp(ik|k - y|)}{4\pi |x - y|}. \tag{4.1}$$

It is proved in [41] that (4.1) is uniquely solvable for sufficiently small k and the following limit exists:

$$f(x, y) := 16\pi^2 \lim_{k \to 0} \frac{U - g}{k^2} = \int_{B_a} \frac{v(x) dz}{|x - z||z - y|}, \quad x, y \in P. \tag{4.2}$$

The function $f(x, y)$ is known if $U(x, y)$ is known $\forall x, y \in P$. Equation (4.2) is first kind Fredholm equation for $v(z)$. It is proved in [41] that this equation has at most one solution, this solution is found analytically, and necessary and sufficient condition for a function $f(x, y)$ to be representable by the right-hand side of (4.2) are given [20,21,41]. Numerical experiments in solving (4.2) are reported in [20]. The problem is highly ill-posed, but it was possible to identify numerically the support of $v(x)$ from noisy discrete surface data. A number of other geophysical inverse problems were studied by the above methodology (well-to-well exploration, induction logging, etc, see [20,21,41]). However, in many cases it is desirable to get less information about the inhomogeneity $v(x)$, but to get it in a computationally stable and easy (non-intensive computationally) way. Such a way is discussed in the next section.

5 Asymptotic Inverse Scattering Theory for Small Inhomogeneities

Consider *IGS* problem and assume that

$$\begin{gathered} supp\ v := D, \quad diam(D) = d, \\ c_1 d^3 \leq |D| := meas\ D \leq c_2 d^3, \\ \frac{\int_D |v| dx}{|\int_D v dx|} \leq c, \quad \sup |v| \leq c. \end{gathered} \tag{5.1}$$

Given $U(x, y, k)$ for x and y running through some subsets of P and for k fixed or k running through some finite number of wave numbers, we want to find the location of D and get some idea about its geometry and the intensity $v_D := \int_D v dx$.

In [1-3] more general assumptions are made: ∇^2 is replaced by a second-order elliptic operator. Let $(U - g)k^{-2} := f(x, y)$. We suppressed k-dependence in what follows. Equation (4.1) implies

$$f(x, y) \approx g(x, \tilde{z}) g(\tilde{z}, y) v_D, \quad v_D := \int_D v dx \tag{5.2}$$

where $\tilde{z}$ is a point in a neighborhood of D.

Let $\xi_i = (x_i, y_i)$ be a data point, $\hat{g}(\xi_i, z) := g(x_i, z) g(z, y_i), i \in I$, where I is a finite set of indices. By (5.2), $f(\xi)$ is approximately proportional to $\hat{g}(\xi, \tilde{z})$ for some $\tilde{z}$. Let us estimate $\tilde{z}$ by finding global maximum of the correlation coefficient

$$r(z) := \frac{|\sum f(\xi_i) \hat{g}(\xi_i, z)|^2}{\sum |f(\xi_i)|^2 \sum |\hat{g}(\xi_i, z)|^2} = \max, \tag{5.3}$$

where the summation is over $i \in I$. Define

$$z_0 := \int_D z v(z) dz / v_D. \tag{5.4}$$

One can prove [1] the following

Theorem 5.1 Global minimizer $\tilde{z}$ of (5.3) satisfies the following equation.

$$\tilde{z} = z_0 + C(d^{\frac{3}{2}}) \text{ as } d \to 0 \tag{5.5}$$

A similar result holds when the exact data $U(\xi_i)$ are replaced by the noisy data $U(\xi_i) + n_i$, where n_i are independent random variables with zero mean value and variance σ^2 (see [1]).

If v does not change sign then $\tilde{z}$ belongs to the convex hull of D. If, in addition, D is convex, then $\tilde{z} \in D$. If D is centrally symmetric and connected and $v(x) = v(-x)$ in the coordinate system with the origin at the center of symmetry, then $\tilde{z} = C(d^{\frac{3}{2}})$.

We can now describe a very simple practical algorithm for localization of the small inhomogeneity $v(x)$: *calculate $r(z)$ by formula (5.3) and find its global minimizer $\tilde{z}$.* The point $\tilde{z}$ determines the position of D with the error $C(d^{\frac{3}{2}})$ as $d \to 0$. If $\tilde{z}$ is found then an estimate of v_D is calculated by the formula

$$\tilde{v}_D := \frac{Re \sum f(\xi_i) \hat{g}(\xi_i, \tilde{z})}{\sum |\hat{g}(\xi_i, \tilde{z})|^2}, \tag{5.6}$$

which follows from (5.2). One has

Theorem 5.2.

$$\tilde{v}_d = v_d[1 + C(d^{\frac{3}{2}})] \text{ as } d \to 0.$$

One can get additional, useful practically, information about $v(z)$ from the surface scattering date, in particular, one can estimate the first and second moments of $v(z)$. (See [1-2] for details.)
A similar approach can be used in *IPS* ([3]). Assuming that

$$d^2(k^2 + \sup|q(x)|) \ll 1 \text{ and } d \sup|q| \ll k,$$

where $d = diam(supp\ q)$, $supp\ q := D \subset \mathbb{R}^3$, one can give a computationally easy and stable method for locating D, finding $q_D := \int_D q(x)dx$, the intensity of the potential, and its first and second moments.
Let us sketch the method. We have the well-known equations

$$A(\alpha', \alpha) = -\frac{1}{4\pi}\int_D \exp(-ik\alpha' \cdot x)q(x)u(x, \alpha)dx, \tag{5.7}$$

$$U(x, \alpha) = \exp(ik\alpha \cdot x) - \int_D g(x, y, k)q(y)u(y, \alpha)dy, \quad \alpha, \alpha' \in S^2. \tag{5.8}$$

Thus

$$-4\pi A(\alpha', \alpha) =$$

$$\int_D q(z)\exp[ik(\alpha - \alpha')\cdot x]dx - \int_D dx \exp(-ik\alpha\cdot x)q(x)\int_D g(x, y, k)qudy. \tag{5.9}$$

Let

$$x_0 := \int_D xq(x)dx/q_D, \quad \kappa := k^2 + Q, \quad Q := \sup_{x\in\mathbb{R}^3}|q|. \tag{5.10}$$

One can prove that (5.9) implies

$$-4\pi A(\alpha', \alpha) = \exp[ik(\alpha - \alpha') \cdot x_0]q_D[1 + C(\kappa d^2)], \quad d \to 0. \tag{5.11}$$

Thus

$$4\pi|A(\alpha', \alpha)| = |q_D|(1 + \kappa d^2); \quad 0 \le arg[-A(\alpha', \alpha)] := c(\alpha', \alpha) < 2\pi, \tag{5.12}$$

$$c(\alpha', \alpha) = k(\alpha - \alpha') \cdot x_0 + 2\pi n(\alpha', \alpha) + C(\kappa d^2) \tag{5.13}$$

where $n(\alpha', \alpha)$ is an integer.
Let $\beta := \alpha - \alpha'$. If $\alpha, \alpha' \in S^2$ then $|\beta| \le 2$. If β is given, $\beta \in \mathbb{R}^3$, $|\beta| \le 2$, and $\mathcal{P}$, a plane containing the origin, is fixed, then one can find uniquely α, $\alpha' \in S^2 \cap \mathcal{P}$, such that $\beta = \alpha' - \alpha$. Therefore (5.13) can be written as

$$c(\beta, P) = k\beta \cdot x_0 + 2\pi n(\beta, \mathcal{P}) + C(\kappa d^2), \quad |\beta| \le 2. \tag{5.14}$$

From the second equation (5.12) it follows that $c(\beta, \mathcal{P})$ is discontinuous only for those β for which $c(\beta, \mathcal{P}) = 0$ or $c(\beta, \mathcal{P}) = 2\pi - 0$. Suppose the origin is inside $B_a \supset D := supp\ q(x)$ and assume that $x_0 \in B_a$. This will happen, for example, if the ratio $\frac{\int_{B_a}|q|dx}{|\int_{B_a} qdx|}$ is not too large. For instance, if $q(x)$ does not change sign, then this ratio is 1 and $x_0 \in B_a$. Define $\triangle := \pi(ka)^{-1}$ and let $|\beta_2 - \beta_1| < \triangle$. Then $|k(\beta_2 - \beta_1) \cdot x_0| \le ka|\beta_2 - \beta_1| < \pi$. Fix any $\beta_1 \ne \beta_2$ such that $|\beta_1 - \beta_2| < \triangle$. Consider the following three possibilities:

- 1) $-\pi + C(\kappa d^2) < c_2 - c_1 < \pi - C(\kappa d^2)$, where $c_j = c(\beta_j, \mathcal{P}_j)$; then $(\beta_2 - \beta_1) \cdot x_0 = k^{-1}(c_2 - c_1) + C(\kappa k^{-1} d^2)$;
- 2) $c_2 - c_1 > \pi + C(\kappa d^2)$, then $n_2 = n_1 + 1$, $n_j := (\beta_j, \mathcal{P}_j)$; thus $(\beta_2 - \beta_1)x_0 = k^{-1}[c_2 - c_1 - 2\pi + C(\kappa d^2)]$;
- 3) $c_2 - c_1 < -\pi - C(\kappa d^2)$, then $n_2 - n_1 = -1$, and $(\beta_2 - \beta_1)x_0 = k^{-1}[c_1 - c_1 + 2\pi + C(\kappa d^2)]$.

Let us estimate the point x_0 which localizes the support of the potential. Let $\{\beta_j, c_j\}$ be the data. For all pairs j_1, j_2 such that $|\beta_{j_1} - \beta_{j_2}| < \triangle$, $\beta_{j_1} \neq \beta_{j_2}$, consider the equations

$$x \cdot b_l = k^{-1} p_l, \quad 1 \leq l \leq L, \quad b_l := \beta_{j_2} - \beta_{j_1}, \quad p_l := c_{j_2} - c_{j_1} + 2\pi s. \tag{5.15}$$

Index l numerates the pairs $\{j_1, j_2\}$, $s = 0, 1$, or -1 according to which of the possibilities 1), 2) or 3) occurs.
Solve (5.15) for x by solving the system

$$B^t B\tilde{x} = k^{-1} B^t p, \quad p = \begin{pmatrix} p_1 \\ \vdots \\ p_l \end{pmatrix}, \quad B = \begin{pmatrix} b_{11}\ b_{12}\ b_{13} \\ \vdots \\ b_{L1}\ b_{L2}\ b_{L3} \end{pmatrix} \tag{5.16}$$

If the vectors $\frac{\beta}{|\beta|}$, $\beta := \alpha', \alpha$, are distributed uniformly on S^2 and if there are many pairs $\{\beta_{j_1}, \beta_{j_2}\}$, $\beta_{j_1} \neq \beta_{j_2}$, such that $|\beta_{j_1} - \beta_{j_2}| < \triangle$, then one can find $\tilde{x}$ from (5..16).

Theorem 5.3 One has $|\tilde{x} - x_0| = C(kd^2 + k^{-1}Qd^2)$ **as** $d \to 0$.

If $\tilde{x}$ is found, then one estimates the intensity of the potential, q_D, by the formula

$$\tilde{q}_D = q_D[1 + C(d^2k^2 + Qd^2)] \text{ as } d \to 0. \tag{5.17}$$

As above, one can find the first and second moments of $q(x)$ from the scattering data.

6 Open Problems

We mention just two major problems each of which has been open for about half a century:

- 1) *Do the data* $A(\alpha', \alpha_0, k)$ *(or* $A(-\alpha, \alpha, k)$*) determine* $q(x)$ *uniquely?* Here $\alpha_0 \in S^2$ is fixed, α', α run through all of S^2 and k runs through $(0, \infty)$.
- 2) *Do the data* $A(\alpha', \alpha_0, k_0)$ *determine* D *uniquely?*

Here $\alpha_0 \in S^2$ and $k_0 > 0$ are fixed, α' runs through an open subset of S^2, and $D \subset \mathbb{R}^3$ is a bounded domain with a Lipschitz (or smooth) boundary on which the Dirichlet (or Neumann, or Robin) boundary condition is assumed.

References

[1] KATSEVICH A.I. & RAMM A.G., Approximate inverse geophysical scattering on a small body, *SIAM J. Appl. Math.*, **56**, N1, (1996), 192-218.

[2] KATSEVICH A.I. & RAMM A.G., Inverse geophysical and potential scattering on a small body, in the book: Experimental and Numerical Methods for Solving Ill-Posed Inverse Problems: Medical and Nonmedical Applications, vol. SPIE-2570, (1995), 151–162.

[3] KATSEVICH A.I. & RAMM A.G., Approximate solution to inverse scattering problem for potentials with small support,*Math. Meth. in the Appl. Sci.*,**19**, N14, (1996), 1121-1134.

[4] RAMM A.G. Completeness of the products of solutions to PDE and uniqueness theorems in inverse scattering, *Inverse problems*, **3**, (1987), L77-L82

[5] RAMM A.G., A uniqueness theorem for two-parameter inversion, *Inverse Probl.*, **4**, (1988), L7-10.

[6] RAMM A.G., A uniqueness theorem for a boundary inverse problem, *Inverse Probl.*, **4**, (1988), L1-5.

[7] RAMM A.G., Recovery of the potential from fixed energy scattering data. *Inverse Problems*, **4**, (1988), 877-886; **5**, (1989) 255.

[8] RAMM A.G., A simple proof of uniqueness theorem in impedance tomography. *Appl. Math. Lett.*, **1**, N3, (1988), 287-290.

[9] RAMM A.G., Uniqueness theorems for multidimensional inverse problems with unbounded coefficients. *J. Math. Anal. Appl.*, **134**, (1988), 211-253; **139**, (1989), 302; **136**, (1988), 568-574.

[10] RAMM A.G., Numerical method for solving 3D inverse problems of geophysics, *J. Math. Anal. Appl.*, **136**, (1988), 352-356.

[11] RAMM A.G., Multidimensional inverse problems: Uniqueness theorems, *Appl. Math. Lett.*, **1**, N4, (1988), 377-380.

[12] RAMM A.G., Multidimensional inverse scattering problems and completeness of the products of solutions to homogeneous PDE. *Zeitschr. f. angew. Math. u. Mech.*, **69**, (1989) N4, T13-T22.

[13] RAMM A.G., Numerical method for solving 3D inverse problems with complete and incomplete data, In the book: "Wave Phenomena", Springer-Verlag, New York 1989, (eds. L. Lam and H. Morris), 34- 43.

[14] RAMM A.G., Numerical recovery of the 3D potential from fixed energy incomplete scattering data, *Appl. Math. Lett.* **2**, N1, (1989), 101-104.

[15] RAMM A.G., Property C and uniqueness theorems for multidimensional inverse spectral problem, *Appl. Math. Lett.*, **3**, (1990), 57-60.

[16] RAMM A.G., Stability of the numerical method for solving the 3D inverse scattering problem with fixed energy data, *Inverse problems* **6**, (1990), L7-12.

[17] RAMM A.G., Completeness of the products of solutions of PDE and inverse problems, *Inverse Probl.*, **6**, (1990), 643-664.

[18] RAMM A.G., Uniqueness result for inverse problem of geophysics I, *Inverse Probl.*, **6**, (1990), 635-642.

[19] RAMM A.G., Uniqueness theorems for geophysical problems with incomplete surface data. *Appl. Math. Lett.*, **3**, (1990), N4, 41-44.

[20] RAMM A.G., Multidimensional inverse scattering problems, LONGMAN/WILEY, New York, 1992, pp. 1-386.

[21] RAMM A.G., Multidimensional inverse scattering problems, *Mir Publishers*, Moscow, 1994 (Russian), pp. 1-496.

[22] RAMM A.G., Stability of the numerical method for solving 3D inverse scattering problem with fixed energy data, *J.f.die reine und angew. Math*, **414**, (1991), 1-21.

[23] RAMM A.G., Stability of the inversion of 3D fixed-frequency data, *J. Math. Anal. Appl.*, **169**, N2(1992), 329-349.

[24] RAMM A.G., Stability of the solution to 3D fixed-energy inverse scattering problem, *J. Math. Anal. Appl.*, **170**, N1 (1992), 1-15.

[25] RAMM A.G., Finding conductivity from boundary measurements, *Comp.& Math. with Appl.*, **21**, N8, (1991), 85-91

[26] RAMM A.G., Stability estimates in inverse scattering, *Acta Appl. Math.*, **28**, N1, (1992), 1-42.

[27] RAMM A.G., Numerical solution of 3D inverse scattering problems with noisy discrete fixed-energy data, *Appl. Math. Lett.*, **5**, N6, (1992), 15-18.

[28] RAMM A.G., Property C and inverse problems, *ICM-90 Satellite Conference Proceedings, Inverse Problems in Engineering Sciences*, Proc. of a conference held in Osaka, Japan, Aug. 1990, Springer Verlag, New York, 1991, pp. 139-144.

[29] RAMM A.G., Property C with constraints and inverse spectral problems with incomplete data, *J. Math. Anal. Appl.*, **180**, N1, (1993), 239-244

[30] RAMM A.G., Property C with constraints and inverse problems, *J. of Inverse and Ill-Posed Problems*, **1**, N3 (1993), 227-230.

[31] RAMM A.G., Property C and applications.*Math. Comp. Modelling*, **18**, N1, (1993), 1-4.

[32] RAMM A.G., Scattering amplitude is not a finite rank kernel in the basis of spherical harmonics, *Appl. Math. Lett.*, **6**, N5, (1993), 89-92.

[33] RAMM A.G., Scattering amplitude is not a finite-rank kernel, *J. of Inverse and Ill-Posed Problems*, **1**, N4, (1993), 349-354.(with P.Stefanov)

[34] RAMM A.G., Scattering amplitude as a function of the obstacle, *Appl. Math. Lett.*, **6**, N5, (1993), 85-87.

[35] RAMM A.G., Multidimensional inverse scattering: solved and unsolved problems, *Proc. Intern. Confer. on Dynamical Syst.and Applic.*, **Vol.1**, Atlanta, (1994), pp.287-296.(Eds. G.Ladde and M.Sambandham)

[36] RAMM A.G., Stability of the solution to inverse obstacle scattering problem, *J. Inverse and Ill-Posed Problems*, **2**, N3, (1994), 269-275.

[37] RAMM A.G., Stability estimates for obstacle scattering, *J.Math.Anal.Appl.*, **188**, N3, (1994), 743-751.

[38] RAMM A.G., Property C with constraints, *Compt. Rendus, Paris*, ser **1**, **321**, N 11, (1995), 1413-1417.

[39] RAMM A.G., A formula for inversion of boundary data, *J. of Inverse and Ill-Posed Problems*, **3**, N5, (1995), 411-415.

[40] RAMM A.G., Finding potential from the fixed-energy scattering data via D-N map, *J. of Inverse and Ill-Posed Problems*, **4**, N2,(1996), 145-152.

[41] RAMM A.G., Scattering by obstacles, D. REIDEL, Dordrecht, 1986.

[42] RAMM A.G., Numerical method for solving inverse scattering problems, *Doklady of Russian Acad. of Sci.*, **337**, N1, (1994), 20-22

[43] RAMM A.G., Uniqueness theorems for inverse obstacle scattering problems in Lipschitz domains, *Applic. Analysis*, **59**, (1995), 377-383.

[44] RAMM A.G., RUIZ A. Existence and uniqueness of scattering solutions in non-smooth domains, *J. Math. Anal. Appl.*, **201** , (1996), 329-338.

List of Authors

Lecture Notes in Physics

For information about Vols. 1–455
please contact your bookseller or Springer-Verlag

Vol. 456: H. B. Geyer (Ed.), Field Theory, Topology and Condensed Matter Physics. Proceedings, 1994. XII, 206 pages. 1995.

Vol. 457: P. Garbaczewski, M. Wolf, A. Weron (Eds.), Chaos – The Interplay Between Stochastic and Deterministic Behaviour. Proceedings, 1995. XII, 573 pages. 1995.

Vol. 458: I. W. Roxburgh, J.-L. Masnou (Eds.), Physical Processes in Astrophysics. Proceedings, 1993. XII, 249 pages. 1995.

Vol. 459: G. Winnewisser, G. C. Pelz (Eds.), The Physics and Chemistry of Interstellar Molecular Clouds. Proceedings, 1993. XV, 393 pages. 1995.

Vol. 460: S. Cotsakis, G. W. Gibbons (Eds.), Global Structure and Evolution in General Relativity. Proceedings, 1994. IX, 173 pages. 1996.

Vol. 461: R. López-Pen˜a, R. Capovilla, R. Garcı´a-Pelayo, H. Waelbroeck, F. Zertuche (Eds.), Complex Systems and Binary Networks. Lectures, México 1995. X, 223 pages. 1995.

Vol. 462: M. Meneguzzi, A. Pouquet, P.-L. Sulem (Eds.), Small-Scale Structures in Three-Dimensional Hydrodynamic and Magnetohydrodynamic Turbulence. Proceedings, 1995. IX, 421 pages. 1995.

Vol. 463: H. Hippelein, K. Meisenheimer, H.-J. Röser (Eds.), Galaxies in the Young Universe. Proceedings, 1994. XV, 314 pages. 1995.

Vol. 464: L. Ratke, H. U. Walter, B. Feuerbach (Eds.), Materials and Fluids Under Low Gravity. Proceedings, 1994. XVIII, 424 pages, 1996.

Vol. 465: S. Beckwith, J. Staude, A. Quetz, A. Natta (Eds.), Disks and Outflows Around Young Stars. Proceedings, 1994. XII, 361 pages, 1996.

Vol. 466: H. Ebert, G. Schütz (Eds.), Spin – Orbit-Influenced Spectroscopies of Magnetic Solids. Proceedings, 1995. VII, 287 pages, 1996.

Vol. 467: A. Steinchen (Ed.), Dynamics of Multiphase Flows Across Interfaces. 1994/1995. XII, 267 pages. 1996.

Vol. 468: C. Chiuderi, G. Einaudi (Eds.), Plasma Astrophysics. 1994. VII, 326 pages. 1996.

Vol. 469: H. Grosse, L. Pittner (Eds.), Low-Dimensional Models in Statistical Physics and Quantum Field Theory. Proceedings, 1995. XVII, 339 pages. 1996.

Vol. 470: E. Martı´nez-González, J. L. Sanz (Eds.), The Universe at High-z, Large-Scale Structure and the Cosmic Microwave Background. Proceedings, 1995. VIII, 254 pages. 1996.

Vol. 471: W. Kundt (Ed.), Jets from Stars and Galactic Nuclei. Proceedings, 1995. X, 290 pages. 1996.

Vol. 472: J. Greiner (Ed.), Supersoft X-Ray Sources. Proceedings, 1996. XIII, 350 pages. 1996.

Vol. 473: P. Weingartner, G. Schurz (Eds.), Law and Prediction in the Light of Chaos Research. X, 291 pages. 1996.

Vol. 474: Aa. Sandqvist, P. O. Lindblad (Eds.), Barred Galaxies and Circumnuclear Activity. Proceedings of the Nobel Symposium 98, 1995. XI, 306 pages. 1996.

Vol. 475: J. Klamut, B. W. Veal, B. M. Dabrowski, P. W. Klamut, M. Kazimierski (Eds.), Recent Developments in High Temperature Superconductivity. Proceedings, 1995. XIII, 362 pages. 1996.

Vol. 476: J. Parisi, S. C. Müller, W. Zimmermann (Eds.), Nonlinear Physics of Complex Systems. Current Status and Future Trends. XIII, 388 pages. 1996.

Vol. 477: Z. Petru, J. Przystawa, K. Rapcewicz (Eds.), From Quantum Mechanics to Technology. Proceedings, 1996. IX, 379 pages. 1996.

Vol. 479: H. Latal, W. Schweiger (Eds.), Perturbative and Nonperturbative Aspects of Quantum Field Theory. Proceedings, 1996. X, 430 pages. 1997.

Vol. 480: H. Flyvbjerg, J. Hertz, M. H. Jensen, O. G. Mouritsen, K. Sneppen (Eds.), Physics of Biological Systems. From Molecules to Species. X, 364 pages. 1997.

Vol. 481: F. Lenz, H. Grießhammer, D. Stoll (Eds.), Lectures on QCD. VII, 276 pages. 1997.

Vol. 482: X.-W. Pan, D. H. Feng, M. Vallières (Eds.), Contemporary Nuclear Shell Models. Proceedings, 1996. XII, 309 pages. 1997.

Vol. 483: G. Trottet (Ed.), Coronal Physics from Radio and Space Observations. XVII, 226 pages. 1997.

Vol. 484: L. Schimansky-Geier, T. Pöschel (Eds.), Stochastic Dynamics. XVIII, 386 pages. 1997.

Vol. 486: G. Chavent, P. C. Sabatier (Eds.), Inverse Problems of Wave Propagation and Diffraction. XV, 379 pages. 1997.

Vol. 488: B. Apagyi, G. Endrédi, P. Lévay (Eds.), Inverse and Algebraic Quantum Scattering Theory. XV, 385 pages. 1997.

Vol. 489: G. M. Simnett, C. E. Alissandrakis, L. Vlahos (Eds.), Solar and Heliospheric Plasma Physics. VIII, 278 pages, 1997.

Vol. 490: O. Boratav, A. Eden, A. Erzan (Eds.), Turbulence Modeling and Vortex Dynamics. XIV, 652 pages, 1997.

New Series m: Monographs

Vol. m 1: H. Hora, Plasmas at High Temperature and Density. VIII, 442 pages. 1991.

Vol. m 2: P. Busch, P. J. Lahti, P. Mittelstaedt, The Quantum Theory of Measurement. XIII, 165 pages. 1991. Second Revised Edition: XIII, 181 pages. 1996.

Vol. m 3: A. Heck, J. M. Perdang (Eds.), Applying Fractals in Astronomy. IX, 210 pages. 1991.

Vol. m 4: R. K. Zeytounian, Mécanique des fluides fondamentale. XV, 615 pages, 1991.

Vol. m 5: R. K. Zeytounian, Meteorological Fluid Dynamics. XI, 346 pages. 1991.

Vol. m 6: N. M. J. Woodhouse, Special Relativity. VIII, 86 pages. 1992.

Vol. m 7: G. Morandi, The Role of Topology in Classical and Quantum Physics. XIII, 239 pages. 1992.

Vol. m 8: D. Funaro, Polynomial Approximation of Differential Equations. X, 305 pages. 1992.

Vol. m 9: M. Namiki, Stochastic Quantization. X, 217 pages. 1992.

Vol. m 10: J. Hoppe, Lectures on Integrable Systems. VII, 111 pages. 1992.

Vol. m 11: A. D. Yaghjian, Relativistic Dynamics of a Charged Sphere. XII, 115 pages. 1992.

Vol. m 12: G. Esposito, Quantum Gravity, Quantum Cosmology and Lorentzian Geometries. Second Corrected and Enlarged Edition. XVIII, 349 pages. 1994.

Vol. m 13: M. Klein, A. Knauf, Classical Planar Scattering by Coulombic Potentials. V, 142 pages. 1992.

Vol. m 14: A. Lerda, Anyons. XI, 138 pages. 1992.

Vol. m 15: N. Peters, B. Rogg (Eds.), Reduced Kinetic Mechanisms for Applications in Combustion Systems. X, 360 pages. 1993.

Vol. m 16: P. Christe, M. Henkel, Introduction to Conformal Invariance and Its Applications to Critical Phenomena. XV, 260 pages. 1993.

Vol. m 17: M. Schoen, Computer Simulation of Condensed Phases in Complex Geometries. X, 136 pages. 1993.

Vol. m 18: H. Carmichael, An Open Systems Approach to Quantum Optics. X, 179 pages. 1993.

Vol. m 19: S. D. Bogan, M. K. Hinders, Interface Effects in Elastic Wave Scattering. XII, 182 pages. 1994.

Vol. m 20: E. Abdalla, M. C. B. Abdalla, D. Dalmazi, A. Zadra, 2D-Gravity in Non-Critical Strings. IX, 319 pages. 1994.

Vol. m 21: G. P. Berman, E. N. Bulgakov, D. D. Holm, Crossover-Time in Quantum Boson and Spin Systems. XI, 268 pages. 1994.

Vol. m 22: M.-O. Hongler, Chaotic and Stochastic Behaviour in Automatic Production Lines. V, 85 pages. 1994.

Vol. m 23: V. S. Viswanath, G. Müller, The Recursion Method. X, 259 pages. 1994.

Vol. m 24: A. Ern, V. Giovangigli, Multicomponent Transport Algorithms. XIV, 427 pages. 1994.

Vol. m 25: A. V. Bogdanov, G. V. Dubrovskiy, M. P. Krutikov, D. V. Kulginov, V. M. Strelchenya, Interaction of Gases with Surfaces. XIV, 132 pages. 1995.

Vol. m 26: M. Dineykhan, G. V. Efimov, G. Ganbold, S. N. Nedelko, Oscillator Representation in Quantum Physics. IX, 279 pages. 1995.

Vol. m 27: J. T. Ottesen, Infinite Dimensional Groups and Algebras in Quantum Physics. IX, 218 pages. 1995.

Vol. m 28: O. Piguet, S. P. Sorella, Algebraic Renormalization. IX, 134 pages. 1995.

Vol. m 29: C. Bendjaballah, Introduction to Photon Communication. VII, 193 pages. 1995.

Vol. m 30: A. J. Greer, W. J. Kossler, Low Magnetic Fields in Anisotropic Superconductors. VII, 161 pages. 1995.

Vol. m 31: P. Busch, M. Grabowski, P. J. Lahti, Operational Quantum Physics. XI, 230 pages. 1995.

Vol. m 32: L. de Broglie, Diverses questions de mécanique et de thermodynamique classiques et relativistes. XII, 198 pages. 1995.

Vol. m 33: R. Alkofer, H. Reinhardt, Chiral Quark Dynamics. VIII, 115 pages. 1995.

Vol. m 34: R. Jost, Das Märchen vom Elfenbeinernen Turm. VIII, 286 pages. 1995.

Vol. m 35: E. Elizalde, Ten Physical Applications of Spectral Zeta Functions. XIV, 228 pages. 1995.

Vol. m 36: G. Dunne, Self-Dual Chern-Simons Theories. X, 217 pages. 1995.

Vol. m 37: S. Childress, A.D. Gilbert, Stretch, Twist, Fold: The Fast Dynamo. XI, 410 pages. 1995.

Vol. m 38: J. González, M. A. Martín-Delgado, G. Sierra, A. H. Vozmediano, Quantum Electron Liquids and High-T_c Superconductivity. X, 299 pages. 1995.

Vol. m 39: L. Pittner, Algebraic Foundations of Non-Commutative Differential Geometry and Quantum Groups. XII, 469 pages. 1996.

Vol. m 40: H.-J. Borchers, Translation Group and Particle Representations in Quantum Field Theory. VII, 131 pages. 1996.

Vol. m 41: B. K. Chakrabarti, A. Dutta, P. Sen, Quantum Ising Phases and Transitions in Transverse Ising Models. X, 204 pages. 1996.

Vol. m 42: P. Bouwknegt, J. McCarthy, K. Pilch, The W_3 Algebra. Modules, Semi-infinite Cohomology and BV Algebras. XI, 204 pages. 1996.

Vol. m 43: M. Schottenloher, A Mathematical Introduction to Conformal Field Theory. VIII, 142 pages. 1997.

Vol. m 44: A. Bach, Indistinguishable Classical Particles. VIII, 157 pages. 1997.

Vol. m 45: M. Ferrari, V. T. Granik, A. Imam, J. C. Nadeau (Eds.), Advances in Doublet Mechanics. XVI, 214 pages. 1997.

Vol. m 46: M. Camenzind, Les noyaux actifs de galaxies. XVIII, 218 pages. 1997.

Vol. m 48: P. Kopietz, Bosonization of Interacting Fermions in Arbitrary Dimensions. XII, 259 pages. 1997.